

Abstracts *Volume*

MAY 21 to 25, 2018



7th international
MAAR CONFERENCE
— OLOT - CATALONIA - SPAIN

DL GI 743-2018
ISBN 978-84-09-01627-3

Cover Photo: ACGAX. Servei d'Imatges.
Fons Ajuntament d'Olot.
Autor: Eduard Masdeu

Authors: Xavier Bolós and Joan Martí

Abstracts *Volume*

—
MAY 21 to 25, 2018

Scientific Committee

Members

IN ALPHABETICAL ORDER

Patrick BACHÈLERY

Observatoire de Physique du Globe de Clermont-Ferrand
and Laboratoire Magmas et Volcans (France)

Pierre BOIVIN

Laboratoire Magmas et Volcans (France)

Xavier BOLÓS

Univesidad Nacional Autónoma de México (Mexico)

Gerardo CARRASCO

Universidad Nacional Autónoma de México (Mexico)

Shane CRONIN

The University of Auckland (New Zealand)

Gabor KERESZTURI

Massey University (New Zealand)

Jiaqi LIU

Chinese Academy of Sciences (China)

Didier LAPORTE

Laboratoire Magmas et Volcans (France)

Volker LORENZ

University of Wuerzburg (Germany)

José LuíS MACÍAS

Universidad Nacional Autónoma de México (Mexico)

Joan MARTÍ

Consejo Superior de Investigaciones Científicas (Spain)

Károly NÉMETH

Massey University (New Zealand)

Oriol OMS

Universitat Autònoma de Barcelona (Spain)

Michael ORT

Northern Arizona University (USA)

Pierre-Simon ROSS

Institut National de la Recherche Scientifique (Canada)

Dmitri ROUWET

Istituto Nazionale di Geofisica e Vulcanologia (Italy)

Claus SIEBE

Universidad Nacional Autónoma de México (Mexico)

Ian SMITH

The University of Auckland (New Zealand)

Giovanni SOSA

Universidad Nacional Autónoma de México (Mexico)

Gregg VALENTINE

University at Buffalo (USA)

Benjamin VAN WYK DE VRIES

Observatoire de Physique de Globe de Clermont- Ferrand
and Laboratoire Magmas et Volcans (France)

James WHITE

University of Otago (New Zealand)

Local Organizing Committee

Technical *Secretary*

Chair

Xavier BOLÓS

Univesidad Nacional Autónoma de México (Mexico)

Fundació d'Estudis Superiors d'Olot

C/ Joan Pere Fontanella 3, 17800 Olot

(+34) 972 26 21 28

fes@olot.cat

Members

Joan MARTÍ

Consejo Superior de Investigaciones Científicas

Scientific advisor

José Luis MACÍAS

Universidad Nacional Autónoma de México

Scientific advisor

Oriol OMS

Universitat Autònoma de Barcelona

Scientific advisor

Károly NÉMETH

Massey University

Scientific advisor

Marta FONTANIOL

Fundació d'Estudis Superiors d'Olot

Logistical advisor

Marta FIGUERAS

Fundació d'Estudis Superiors d'Olot

Logistical advisor

Jordi CALABUIG

Fundació d'Estudis Superiors d'Olot

Logistical advisor

Xavier PUIG

Parc Natural de la Zona Volcànica de la Garrotxa

Logistical advisor

Ariadna VILLEGAS

Ajuntament d'Olot

Logistical advisor

Presentation

Since the first “International Maar Conference” (IMC) meeting, the series has become one of the most successful discussion forums in volcanology, mainly because it provides a unique opportunity to bring together people from many different volcanological fields (physical volcanologists, sedimentologists, modellers, petrologists, etc), any of whom may become involved in some way in the study of different eruption styles of basaltic volcanism and, in particular, those occurring in monogenetic volcanic fields. Previous IMC meetings have been held in a wide diversity of places (Hungary, Slovakia and Germany) that posed different problems in terms of eruption dynamics, products and landforms in these volcanic areas.

The city of Olot, the main location of the La Garrotxa Volcanic Field, the most recent area in the Quaternary Catalan Volcanic Zone, will provide a unique opportunity for holding a multidisciplinary volcanological forum that will focus on different aspects of maars and monogenetic volcanism. In Olot and its surroundings volcanoes are present in many aspects of local society, as its cultural heritage, local history, architecture or even in its excellent cuisine. People live among volcanoes and they are aware that they represent the most characteristic feature of their region. Protection of all this area and of the volcanoes in particular, has been effective since 1982, when it was declared as a Natural Park (The Garrotxa Volcanic Zone Natural Park) by de Catalan Government.

The Local Organizing Committee and the International Association of Volcanology and Chemistry of Earth's Interior (IAVCEI) are pleased to welcome you to the 7th International Maar Conference (IMC) in Olot (Spain) in May 21- 25, 2018.

Contents

MAY 21 to 25, 2018



Oral Session 1

Monogenetic volcanoes: eruption dynamics, growth, structure and physical modeling

Page 14 - 1. Exploring eruptive and erosional features of monogenetic scoria cones using Principal Component Analysis and machine learning. Gabor Kereszturi, Marie-Noelle Guilbaud, Reddy Pullanagari, Claus Siebe and Sergio Salinas.

Page 16 - 2. A global perspective on Maars: Maar Volcano Location and Shape (MaarVLS). Alison Graettinger, Cody Nichols (KEYNOTE)

Page 18 - 3. Assessing the role of phreatomagmatism in the eruption dynamics of the trachyandesitic maar-like Pavin crater (Massif central, France): constraints from the pyroclasts microtextures. Laurent Arbaret and Jean-Louis Bourdier

Page 20 - 4. Sedimentary features as indicators of hydrogeological conditions controlling initial phreatomagmatic eruption phases of the monogenetic Potrerillo and San Juanito volcanoes in the Ceboruco graben, western Mexico. Javier Agustín-Flores, Claus Siebe, Katrin Sieron, Dolores Ferrés, Karime González-Zuccolotto

Page 22 - 5. Historical phreatomagmatic activity at the summit of Tacaná Volcano, México-Guatemala. José Luis Macías, José Luis Arce, Ricardo Saucedo, Juan Manuel Espíndola, Giovanni Sosa-Ceballos

Page 24 - 6. Tilocálar volcanoes: Effusive, magmatic explosive and phreatic monogenetic activity under compressional control in the northern Chile. Gabriel Ureta, Felipe Aguilera, and Karoly Németh

Page 26 - 7. Pre-historic effusive ring-fracture activity from the southern caldera's rim of Los Humeros volcanic complex and geothermal field, Eastern Mexico, implications for hazards. Carrasco-Núñez, G., Barrios, S., Hernández, J.

Page 28 - 8. Examining the internal structure and the eruption dynamics of Parícutin monogenetic volcano (1943 – 1952, Mexico) inferred from ERT 3D model combined with historical and geological evidences. Xavier Bolós, Gerardo Cifuentes, José Luis Macías, Giovanni Sosa-Ceballos, Denis Ramón Avellán, Alexander Delgado-Torres

Page 30 - 9. Garrotxa Volcanic Field as a Link to Young Martian Volcanism. Kei Kurita, Rina Noguchi, Hiroki Ichikawa, H.Samuel, David Baratoux

Page 32 - 10. Field and experimental analysis of sediment-magma mingling at the 71 Gulch Volcano in the western Snake River Plain, Idaho, USA. Kadie Bennis, Alison Graettinger

Page 34 - 11. A Tale of Two Fluids: Water and Magma in the Shallow Subsurface. Michael Ort, Michaela Kim, Emily S. Anderson, Curtis M. Oldenburg (KEYNOTE)

Page 36 - 12. How the early syn-eruptive crater infill progressively becomes the lower diatreme: Round Butte, Hopi Buttes volcanic field, Navajo Nation, Arizona. Benjamin Latutrie, Pierre-Simon Ross

Page 38 - 13. Kiejo-Mbaka (Rungwe Volcanic Province, Tanzania) monogenetic volcanic field evolution. Claudia Principe, Fatumati Mnzava, Claudio Pasqua

Page 40 - 14. The Stolpen Volcano in the Lausitz Volcanic Field (Eastern Germany) - Studies at the type locality of 'basalt'. Olaf Tietz, Jörg Büchner

Page 42 - 15. Linking experimental cratering models to large maar-diatremes. Károly Németh, Mohammed Rashad Moufti (KEYNOTE)

Page 44 - 16. Magma fragmentation: a review of main (possible) physical and thermodynamics mechanisms. Roberto Sulpizio

Page 46 - 17. Surtsey revisited: Fragmentation and heat transfer studies in the framework of the ICDP project SUSTAIN. Bernd Zimanowski, Ralf F. Büttner, James D.L. White, Magnús T. Gudmundsson

Page 48 - 18. The Mysterious Grooves of Bárcena. Susan W. Kieffer, Eckart Meiburg, Jim Best

Page 50 - 19. Shallow magma diversions during explosive diatreme-forming eruptions. Nicolas Le Corvec, James D. Muirhead, James D. L. White

Page 52 - 20. On the interaction of magma, groundwater and country rocks: two contrasting phreatomagmatic maar-diatreme emplacement models. Volker Lorenz, Stephan Kurszlaukis, Peter Suhr

Page 54 - 21. Exploration of miniature volcanology using rootless cones as natural analogues of huge volcanoes across Earth and Mars. Rina Noguchi, Kei Kurita

Posters *Session 1*

Monogenetic volcanoes: eruption dynamics, growth, structure and physical modeling

- Page 58 - 1. Morphometry of maar lakes of Calatrava Volcanic Field (Spain).** Rafael U. Gosálvez, Montse Morales, Elena González
- Page 61 - 2. Spatial and morphometric analyses of Anaun monogenetic volcanic field (Sredinny Range, Kamchatka).** Dmitry Melnikov, Anna Volynets
- Page 62 - 3. Geomorphology of the Cuelgaperros maar: interferences between its hydromagmatic activity and the fluvial dynamics of the Jabalonriver (Campo de Calatrava Volcanic Field, Spain).** Miguel Ángel Poblete, Salvador Beato, José Luis Marino
- Page 64 - 4. A proposal for a classification of types of hydrovolcanoes based on geomorphic criteria.** Miguel Ángel Poblete, Salvador Beato, José Luis Marino
- Page 66 - 5. A preliminary UAV application on Kula Monogenetic Field (western Anatolia, Turkey).** Göksu Uslular, Çağdaş Sağır, Gonca Gençlioğlu-Kuşcu, Bedri Kurtuluş
- Page 68 - 6. Maar structures in Southern Peru and their application on geothermal resources explorations.** Guillermo Díaz
- Page 70 - 7. Contained sub-surface Kimber-lite explosions in Snap Lake Dyke and CL186, NWT, Canada.** Stephan Kurszlaukis, Alexandrina Fulop
- Page 72 - 8. Monogenetic volcanism at El Hierro Island: the Ventejís-Pico de los moles eruption.** Laura Becerril, Dario Pedrazzi, Domenico Doronzo, Adelina Geyer, Joan Martí
- Page 74 - 9. Maars in the Calatrava Massif. (Campo de Calatrava, Spain).** M^a Elena González, Rafael Becerra, Rafael Ubaldo Gosálvez, Estela Escobar, Javier Dóniz
- Page 76 - 10. The role of phreatomagmatism on scoria cone forming eruptions in the Quaternary Auckland Volcanic Field (New Zealand).** Gabor Kereszturi and Karoly Nemeth
- Page 78 - 11. Lava lakes filling phreatomagmatic craters at Twin Peaks, Hopi Buttes volcanic field, Navajo Nation, Arizona.** Benjamin Latutrie, Pierre-Simon Ross
- Page 80 - 12. Magma ascent dynamics and eruptive mechanisms at monogenetic volcanoes: Wiri Mountain, Auckland Volcanic Field, New Zealand.** Károly Németh, Heather Handley, Jan Lindsay
- Page 82 - 13. Maars of the Arxan-Chaihe Volcanic Field, Inner Mongolia, China.** Bo-Xin Li, Károly Németh
- Page 84 - 14. Structural control on intraplate volcanism in the volcanic fields of Los Encinos and Santo Domingo, San Luis Potosí, México.** Claudia Peredo Mancilla, Vsevolod Yutsis, Xavier Bolós
- Page 86 - 15. Evaluation of the presence of extrusive carbonatites in the Cabezo Segura volcano (Calatrava Volcanic Field, Spain).** Fernando Sarrionandia, Manuel Carracedo-Sánchez, Eneko Iriarte, Jon Errandonea-Martin, José Ignacio Gil-Ibarguch
- Page 88 - 16. Early phreatomagmatic tuffs in the Columbia River flood basalts.** David W. Unruh, John A. Wolff, Klarissa N. Davis
- Page 90 - 17. Analog Experiment for Rootless Eruption.** Rina Noguchi, Ai Hamada, Ayako Suzuki, Kei Kurita
- Page 92 - 18. Fragmentation studies: towards a uniform 'recipe' for characterization of juvenile pyroclasts.** Pierre-Simon Ross, Nathalie Lefebvre, Tobias Dürig, Pier Paolo Comida, Juanita Rausch, Daniela Mele, Bernd Zimanowski, Ralph Büttner, James White
- Page 94 - 19. A new analogue for Maar-diatremes?: Fluidized bed chemical reactors.** Bob Tarff, Simon Day
- Page 96 - 20. Geophysical and geochemical survey across El Hierro (Canary Islands) during the 2011-2012 monogenetic eruption.** Stéphanie Barde-Cabusson, Xavier Bolós, Víctor Villasante Marcos, Helena Albert, Ilazkiñe Iribarren Rodríguez, Natividad Luengo-Oroz, Dario Pedrazzi, Llorenç Planagumà, Joan Martí
- Page 98 - 21. Magnetometric survey of la Joya Honda Maar (México) and surroundings; volcanic implications.** Héctor López Loera, David Ernesto Torres Gaytan, José Jorge Aranda-Gómez

Oral Session 2

Geochemistry and petrology of monogenetic volcanism related magmas

- Page 102 - 1. Felsic rocks within the Michoacán-Guanajuato monogenetic volcanic field; mafic magma-crust interaction?** Giovanni Sosa-Ceballos, Mario Emmanuel Bojjsseaneau-López, Juan Daniel Pérez-Orozco (INVITED TALK)
- Page 104 - 2. Small-scale basaltic systems and the behavior of the mantle.** Ian Smith (KEYNOTE)
- Page 106 - 3. Tolbachik group of volcanoes (Kamchatka): the areal type of volcanic activity.** Anna Volynets, Yulia Kugaenko
- Page 108 - 4. Monogenetic volcanoes in the northernmost volcanic arc of the Colombian Andes.** Hugo Murcia, Carlos Borrero, Károly Németh
- Page 111 - 5. Quaternary monogenetic volcanism in the Chyulu Hills volcanic field, Kenya: compositional variations in time and space.** Elisabeth Widom, Dave Kuentz
- Page 112 - 6. Melt compositions relationships between large polygenetic and adjacent monogenetic edifices: results of melt inclusions study in minerals of two large volcanic centers (Kamchatka).** Maria Tolstykh, Anna Volynets, Maria Pevzner (KEYNOTE)
- Page 114 - 7. Implication of 2 Myr of volcanism at Kīlauea Pt., Kauaʻi for the Origin of Hawaiian Rejuvenated Volcanism.** Michael O. Garcia, Thor Thordarson
- Page 116 - 8. Tephra laminae in the alginite succession of Pula maar recording large explosive eruptions of basaltic volcanoes of the Mio/Pliocene Bakony-Balaton Highland Volcanic Field (Hungary).** Ildikó Soós, Szabolcs Harangi, Károly Németh, Réka Lukács
- Page 118 - 9. Optical and geochemical analysis of the tephra layers from the Hinkelsmaar (Eifel region, Western Germany).** Martina Vögtli, Nikolaus J. Kuhn, Leander Franz, Christian de Capitani, Martin Koziol
- Page 120 - 10. Crystal forensic studies to unravel the nature of pre-eruptive magmatic processes in basalt volcanic fields.** Szabolcs Harangi, Éva M. Jankovics, Tamás Sági, Theodoros Ntaflos (KEYNOTE)
- Page 122 - 11. Application of Response Surface Methodology (RSM) to Instrumental Mass Fractionation (IMF) prediction in stable isotope SIMS analyses.** Carles Fàbrega, David Parcerisa, Frances Deegan, Martin Whitehouse, Valentin Troll, Andrey Gurenko

Posters Session 2

- Page 126 - 1. Magmatic evolution of the South Aegean volcanic arc: evidence from Milos, based on a hot zone model.** Xiaolong Zhou, Pieter Vroon, Klaudia Kuiper, Jan Wijbrans
- Page 128 - 2. Triplex eruption at Ichinsky volcano (Kamchatka) 6500 14C years BP: a shift from monogenetic to polygenetic type of activity.** Anna Volynets, Maria Pevzner, Maria Tolstykh
- Page 130 - 3. Cerro Tujle maar, southeast of the Salar de Atacama Basin, Chile: Morphological, petrographic and geochemical analysis.** Gabriel Ureta, Felipe Aguilera, Károly Németh, Andrew Menzies
- Page 132 - 4. Tephra evidence for the most recent eruption of Laoheishan volcano, Wudalianchi volcanic field, northeast China.** Chunqing Sun, Károly Németh, Tao Zhan, Haitao You, Guoqiang Chu, Jiaqi Liu
- Page 134 - 5. Radiometric dating of Quaternary volcanoes in the western Zacapu lacustrine basin (Michoacán, México) reveals monogenetic clusters.** Nanci Reyes-Guzmán, Claus Siebe, Oryaëlle Chevrel, Marie-Noëlle Guilbaud, Sergio Salinas, Paul Layer

Oral Session 3

Lakes in maar volcanoes: the sedimentary record of paleontology, climate change and hydrochemistry

- Page 138 - 1. Volcanic lakes in Europe: the role of maar lakes in volcanic hazard assessment** Dmitri Rouwet (INVITED TALK)
- Page 140 - 2. Geological and paleontological Pliocene record: introducing the Camp dels Ninots maar (Catalan Coastal Ranges, Spain).** Oriol Oms, Xavier Bolós, Joan Martí, Bruno Gómez de Soler, Gerard Campeny, Jordi Agustí (KEYNOTE)
- Page 143 - 3. High resolution pCO₂ variations in Lake Averno (Italy).** Nathalie Hasselle, Jacopo Cabassi, Franco Tassi, Dmitri Rouwet, Rossella Di Napoli, Alessandro Aiuppa
- Page 144 - 4. Event Sedimentation in Maar Lakes – the Change in Monotony.** Peter Suhr
- Page 146 - 5. Enhanced contribution of ENSO to the East Asian Winter Monsoon in Northeast China since the Mid-Holocene.** Jing Wu, Qiang Liu, Qiaoyu Cui, Deke Xu, Guoqiang Chu, Jiaqi Liu
- Page 149 - 6. Palaeo-environmental impact of last volcanic eruptions in the Iberian Peninsula: preliminary multi-proxy analysis results from Pla de les Preses palaeolake (Vall d'en Bas, La Garrotxa, NE Iberia).** Jordi Revelles, Eneko Iriarte, Walter Finsinger, Francesc Burjachs, Gabriel Alcalde, Maria Saña
- Page 150 - 7. Millennial and centennial-scale climatic variability recorded in the sediments of Laguna Azul (southern Patagonia, Argentina).** Bernd Zolitschka, Stephanie Janssen, Nora I. Maidana, Christoph Mayr, Torsten Haberzettl, Hugo Corbella, Andreas Lücke, Christian Ohlendorf, Frank Schäbitz
- Page 152 - 8. Joya de Yuriria maar (Guanajuato, Mexico): geological, tectonic and paleo-hydrogeological environment.** Pooja Kshirsagar, Norma Maritza Arriaga Hernández, Claus Siebe, Marie Noëlle Guilbaud, Raúl Miranda-Avilés
- Page 154 - 9. The Late Quaternary sediment record from Maar Lake Sihailongwan (northeastern China): diatom-based inferences of limnological and climatic changes.** Patrick Rioual, Guoqiang Chu, Jens Mingram, Martina Stebich, Qiang Liu, Jingtai Han, Jiaqi Liu
- Page 156 - 10. Volcanic Closure of the Alf Valley During the Weichselian Pleniglacial – Witnesses of the Last Glaciation in the. Quaternary Westeifel Volcanic Field (Germany).** Thomas Lange, Luise Eichhorn, Michael Pirrung, Thomas Jahr, Karl-Heinz Köppen, Georg Büchel

Posters Session 3

- Page 161 - 1. Orbital-scale environmental changes during the Late Pliocene in NE Spain: the Camp dels Ninots maar record.** Gonzalo Jiménez-Moreno, Francesc Burjachs, Isabel Expósito, Oriol Oms, Juan José Villalain, Ángel Carrancho, Jordi Agustí, Gerard Campeny, Bruno Gómez de Soler, Jan van der Made
- Page 162 - 2. Water frogs (Anura, Ranidae) from the Pliocene Camp dels Ninots Konservat-Lagerstätte (Caldes de Malavella, NE Spain).** Hugues-Alexandre Blain, Iván Lozano-Fernández, Almudena Martínez-Monzón, Tomas Prikryl, Oriol Oms, Pere Anadón, Pablo Rodríguez-Salgado, Jordi Agustí, Gerard Campeny Vall-Ilosera, Bruno Gómez de Soler
- Page 164 - 3. Macromammal taphonomy of the Camp dels Ninots maar site (Caldes de Malavella, NE Spain).** Francesc García, Isabel Cáceres, Bruno Gómez de Soler, Gerard Campeny, Oriol Oms, Pablo Rodríguez-Salgado, Jordi Agustí
- Page 166 - 4. Research history and main discoveries of the fossil-Lagerstätte Camp dels Ninots maar (Caldes de Malavella, Girona, Spain).** Bruno Gómez de Soler, Gerard Campeny, Jordi Agustí, Pere Anadón, Eduardo Barrón, Xavier Bolós, Hugues-Alexandre Blain, Francesc Burjachs, Isabel Cáceres, Ángel Carrancho, Albert Casas, Julien Claude, Juan Diego Martín-Martín, Isabel Expósito, Marta Fontanals, Francesc García, Mahjoub Himi, Jordi Ibáñez, Gonzalo Jiménez-Moreno, María José Jurado, Lucía López-Polín, Jan van der Made, Joan Martí, Pablo Mateos, Jordi Miró, Elena Moreno-Ribas, Oriol Oms, Tomas Prikryl, Pablo Rodríguez-Salgado, Florent Rivals, Souhila Roubach, Oscar Sanisidr, Juan José Villalain
- Page 168 - 5. Multidisciplinary study of the Hindon Maar Fossil-Lagerstätte, Waipiata Volcanic Field, New Zealand.** Uwe Kaulfuss, Daphne E. Lee, Andrew Gorman, Jennifer M. Bannister, Jon K. Lindqvist, John G. Conran, Dallas C. Mildenhall
- Page 170 - 6. Origin and distribution of silica nodules in the Camp dels Ninots maar (La Selva Basin, NE Spain).** Jordi Miró, Oriol Oms, Juan Diego Martín-Martín, Jordi Ibáñez, Pere Anadón, Jordi Tritlla, Bruno Gomez de Soler, Gerard Campeny
- Page 172 - 7. Early lake sedimentation in the Pliocene Camp dels Ninots maar (Catalan Coastal Ranges, Spain).** Oriol Oms, Alejandro Gil, Sergi Pla-Rabés, Pere Anadón, Jordi Ibáñez, Pablo Rodríguez-Salgado, Esteve Cardellach, Bruno Gómez de Soler, Gerard Campeny, Jordi Agustí
- Page 174 - 8. Palaeoenvironmental reconstruction from the mineralogy of the Pliocene Camp dels Ninots maar lake sediments (Catalan Volcanic Zone, NE Iberia).** Pablo Rodríguez-Salgado, Jordi Ibáñez, Pere Anadón, Bruno Gómez de Soler, Gerard Campeny, Jordi Agustí, Oriol Oms
- Page 176 - 9. Maar sediment in central Vietnam Highland near Pleiku: An archive of regional monsoon intensity?** Arndt Schimmelmann, Hường Nguyễn-Văn, Dương Nguyễn-Thùy, Jan P. Schimmelmann, Antti E.K. Ojala, Nguyệt Nguyễn-Ánh, Quốc Trọng Đỗ, Dương Thùy Nguyễn, Phương Hòa Tạ, Vũ Huỳnh-Kim, Nhi Quỳnh Phạm-Nữ, Bernd Zolitschka, Ingmar Unkel
- Page 178 - 10. Temperature records derived from glycerol dialkyl glycerol tetraethers (GDGTs) from 60 ka to 9 ka in Sihailongwan maar lake, northeastern China.** Zeyang Zhu, Jens Mingram, Jiaqi Liu, Guoqiang Chu, Jing Wu, Qiang Liu

Oral Session 4

Volcanic hazard and risk assessment in monogenetic volcanic fields

Page 182 - 1. Using VOLCANBOX to conduct hazard assessment in monogenetic volcanic fields. Joan Martí, Laura Becerril, Stefania Bartolini (KEYNOTE)

Page 184 - 2. Deception Island, Antarctica: eruptive dynamics and volcanic hazards in a post-caldera monogenetic volcanic field. Dario Pedrazzi, Karoly Németh, Adelina Geyer, Antonio Álvarez-Valero, Gerardo Aguirre-Díaz, Stefania Bartolini

Page 186 - 3. Significance of Holocene monogenetic clusters within the Michoacán-Guanajuato Volcanic Field (México). Claus Siebe, Nanci Reyes, Ahmed Nasser Mahgoub, Sergio Salinas, Harald Böhnel, Marie-Noelle Guilbaud, Patricia Larrea

Page 188 - 4. Cyclic variation in intensity of explosivity during a maar-diatreme eruption on an ocean island volcano: implications for dynamic hazard models. Bob Tarff, Simon Day, Hilary Downes, Ioan Seghedi

Oral Session 5

Natural resources and geotourism development in volcanic areas

Page 192 - 1. Epithermal gold in felsic diatremes. Pierre-Simon Ross, Patrick Hayman, Gerardo Carrasco Núñez (INVITED TALK)

Page 194 - 2. We want you to “put in value the volcanism” in the “Styrian volcano land” (Austria). Ingomar Fritz (KEYNOTE)

Page 196 - 3. Irazú’s Southern Volcanic Field: a place of learning and leisure. Eliecer Duarte

Page 198 - 4. Conservation of the macrovertebrates fossils from fossil-Lagerstätten Camp dels Ninots, as a principal element for disseminate heritage. Souhila Roubach, Elena Moreno-Ribas, Bruno Gómez de Soler, Gerard Campeny

Posters Session 5

Page 203 - 1. Public engagement with the history of life. A new fossil-Lagerstätten heritage site: the Camp dels Ninots maar. Gerard Campeny, Bruno Gómez de Soler, Marta Fontanals, Jordi Agustí, Oriol Oms, Robert Sala

Page 204 - 2. Campo de Calatrava, the largest number of maar lakes in continental Europe. Rafael U. Gosálvez, Montse Morales, Máximo Florín, Elena González

Page 206 - 3. From hydrogeological and geophysical investigations to the hydraulic structure of the Ulmener Maar, West Eifel Volcanic Field, Germany. Sven Philipp, Karl-Heinz Köppen, Thomas Lange

Page 208 - 4. The evidence of Maar-diatreme system in the Madneuli Copper-gold-polymetallic deposit, Lesser Caucasus, Georgia. Nino Popkhadze, Robert Moritz

Page 210 - 5. Perşani Mountains, a small monogenetic volcanic field (Southeastern Carpathians, Romania) with remarkable geodiversity and high geoheritage values. Ildikó Soós, Szabolcs Harangi, János Szepesi, and Károly Németh

Page 212 - 6. Assessment of hydromagmatic geomorphosites in the Campo de Calatrava Volcanic Field (Ciudad Real, Spain). Salvador Beato, Miguel Ángel Poblete, José Luis Marino

Page 214 - 7. A geotouristic route to discover the maars of the Medias Lunas Range (Campo de Calatrava Volcanic Field, Central Spain). Salvador Beato, Miguel Ángel Poblete, José Luis Marino

Page 216 - 8. Monte Preto monogenetic volcano (Fogo, Cape Verde) an exceptional volcanic heritage for the geotourism. Javier Dóniz-Páez, Rafael Becerra-Ramírez, Elena González-Cárdenas, Estela Escobar-Lahoz, Samara Dionis, Vera Alfama

Page 219 - 9. Identification, cataloguing, and preservation of outcrops of geological interest in monogenetic volcanic fields: the case La Garrotxa volcanoes Natural Park. Llorenç Planaguma, Joan Martí, Xavier Bolós

Oral *Session 1*

Monogenetic volcanoes: eruption dynamics, growth, structure and physical modeling.

Conveners

Joan Martí (joan.marti@ictja.csic.es)

Pierre-Simon Ross (Pierre-Simon.Ross@ete.inrs.ca)

Volker Lorenz (vlorenz@geologie.uni-wuerzburg.de)

Xavier Bolós (xavier.bolos@gmail.com)

Dario Pedrazzi (pedrario@gmail.com)

This session invites scientific contributions about growth and distribution of monogenetic volcanoes, their internal structure, the role of substrate geology on eruption diversity, and specially maar-diatremes development.

Small-scale basaltic volcanic systems are the most widespread forms of magmatism on the planet and are expressed at the Earth's surface as fields of small volcanoes which are the landforms resulting from explosive and effusive processes triggered by the rise of small batches of magma. This session is concerned with the growth, geomorphology, eruption dynamics, geodynamic distribution and degradation of this type of volcanism. Monogenetic volcanoes distribution inside a volcanic field depends in each case on their regional and local tectonic controls. The great variety of eruptive styles, edifice morphologies, and deposits shown by monogenetic volcanoes are the result of a complex combination of internal (magma composition, gas content, magma rheology, magma volume, etc.) and external (regional and local stress fields, stratigraphic and rheological contrasts of substrate rock, hydrogeology, etc.) parameters, during the magma transport from the source region to the surface. This is meant to be a multi-disciplinary session and we invite contributions that include different type of methods, such as; field studies, geophysical methods, numerical and analogue modelling of volcanic processes and GIS analysis.

Exploring eruptive and erosional features of monogenetic scoria cones using Principal Component Analysis and machine learning

Gabor Kereszturi¹, Marie-Noelle Guilbaud², Reddy Pullanagari¹, Claus Siebe² and Sergio Salinas³

¹ *Geosciences, School of Agriculture and Environment, Massey University, Palmerston North, New Zealand, g.kereszturi@massey.ac.nz*

² *Departamento de Vulcanología, Instituto de Geofísica, Universidad Nacional Autónoma de México, México D.F., México*

³ *División de Ingeniería en Ciencias de la Tierra, Facultad de Ingeniería, Universidad Nacional Autónoma de México, Cd. de México*

Keywords: cinder cone, monogenetic, machine learning.

Scoria cones are common landforms that populate monogenetic volcanic fields worldwide. These volcanoes are dominantly basaltic to andesitic in composition, and can be the result of a great variety of eruption styles ranging from lava-fountaining to violent Strombolian activities (Martin and Németh, 2006; Valentine and Gregg, 2008). These eruptions are typically small in volume and can under favorable circumstances be influenced by shallow groundwater, producing phreatomagmatic eruptions (Martin and Németh, 2006). However, the dominant portion of the pyroclastic succession of scoria cones consists of scoriaceous coarse ash to lapilli deposits with embedded angular to fluidal blocks/bombs. Hence, the growth of the edifice occurs to the largest extent by fallout from a low and unsteady eruptive column and is mostly ballistic in origin (Riedel et al., 2003), forming conical edifices with a crater on top (Wood, 1980). The geometry of the resultant edifice is often characterized by simple measures of geomorphic attributes (Fig. 1), such as cone height, basal width, crater width and slope angle (Favalli et al., 2009; Guilbaud et al., 2012; Kereszturi et al., 2012). These parameters tend to loosely correlate with age, since weathering and erosion gradually degrade the original edifice, inducing changes to the overall geomorphology of the edifice. However, relative chronology based on morphometry is hampered by the geomorphological diversity of scoria cones due to eruption-related processes, such as grain size dependent angle of repose values and interbedded ash horizons (Kereszturi et al., 2012; 2013) and also to poorly-known climate-related spatial and temporal variations in erosional processes. The influencing factors of scoria cone morphology are often inter-related and hard to de-convolute, leading to equifinality over tens of ky to My time scales (Kereszturi et al., 2013). This issue requires new approaches to test that can quantitatively capture the diversity of scoria cones erupted under different magmatic and environmental settings.

This investigation aims to investigate the impact of eruptive and erosional processes on the geomorphic attributes, as obtained from remote sensing datasets and by using multivariate statistical analyses and machine learning approaches.

The study areas are two volcanic fields, the Michoacán-Guanajuato and Sierra Chichinautzin from the Trans-Mexican Volcanic Belt in central Mexico. These fields were chosen due to their field exposure, abundance of volcanic cones, and high diversity of magma compositions and eruptive styles. This study is based on a compiled database that includes geological maps, chronological, volumetric, topographic, and climate variables related to 77 scoria cones, erupted between 2.6 My and recent. These cones have all been dated by either from historical accounts or by radiometric dating methods (e.g. 40Ar-39Ar, 40K-40Ar, 14C), published in Siebe et al. (2005) and Guilbaud et al. (2011; 2012). The well-established age of the cones allows us to assess the impact of eruption vs. erosion-related controls on the geomorphology of scoria cones. The input data for the present study was optical imagery from Google Earth, geological maps to delineate scoria cones base and crater boundaries, as well as Shuttle Radar Topography Mission (SRTM) Digital Terrain Model data complemented with multispectral Sentinel-2 imagery and climatic variables.

In the last few decades, a tremendous advance has been taken place in the field of remote sensing including image processing and image manipulation tools, such as Principal Component Analysis (PCA). This has also been complemented by a new generation of statistical learning approaches, such as Support Vector Machine, Artificial Neural Network, and Random Forest all of which are designed to address complex issues that cannot be solved using classical parametric approaches, such as linear regression. In this study, we have tested PCA and machine learning approaches to explore geomorphic features of scoria cones (Fig. 1).

The PCA re-projects the data using linear transformation to produce a non-correlating set of variables, called principal components. Based on the de-correlated principal component loadings, we observe that the variables with the strongest influence on the data variability are the crater and cone base diameters along with the volume and height of the edifices. The results also show that the examined two volcanic fields display scoria cones with slightly different geomorphic signatures based on the

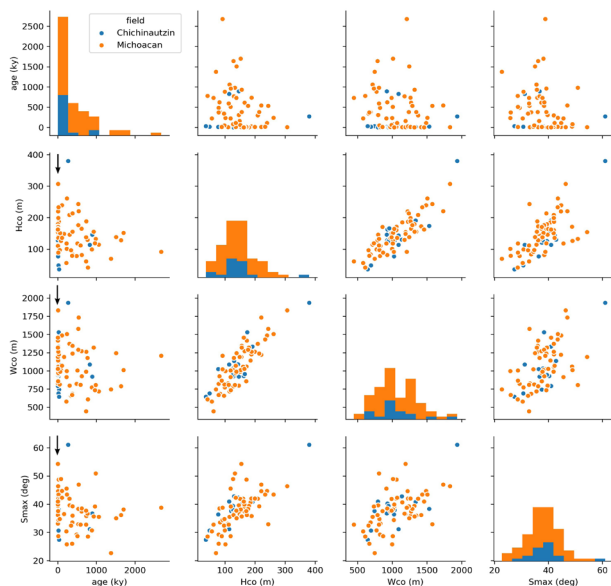


Fig. 1 Pairwise plot of the important geomorphic variables and age for the Sierra Chichinautzin (blue) and Michoacán-Guanajuato (orange). Note the large scatter (black arrow) for Upper Pleistocene to Holocene cones

first two PCA components. Even scoria cones with a similarly young age (<5 ky) show strong dissimilarities that might originate from differences in magma composition and/or eruption styles (product of the dominant particle size or the amount of spatter) between cones from the two volcanic fields.

In this study, the data was analyzed using Support Vector Machine Regression (SVMR). SVMR is well-known non-parametric statistical learning technique that is based on separating hyperplanes applied to the training data (Vapnik, 1995). We used radial basis function kernel based SVMR for non-linear transformation of data that improves predictions accuracy. The results show that the SVMR can provide a robust age model for the cones >1 ky with cross-validated R2 values >0.8. While this preliminary result is promising, this approach still requires some fine-tuning to handle different non-uniform scattering (i.e. heteroscedasticity). This non-uniform scatter confirms the hypothesis that the shape of young cones is largely controlled by eruptive processes (Fig. 1), whereas time-dependent erosional processes control the shape of old cones. Hence, this approach might help to better understand growth and degradation of the most common type of monogenetic volcano on Earth.

References

- Favalli, M., Karátson, D., Mazzarini, F., Pareschi, M.T. and Boschi, E., 2009. Morphometry of scoria cones located on a volcano flank: A case study from Mt. Etna (Italy), based on high-resolution LiDAR data. *J. Volcanol. Geotherm. Res.*, 186(3-4): 320-330.
- Guilbaud, M.-N., Siebe, C., Layer, P. and Salinas, S., 2012. Reconstruction of the volcanic history of the Tacámbaro-Puruarán area (Michoacán, México) reveals high frequency of Holocene monogenetic eruptions. *Bull. Volcanol.*, 74(5): 1187-1211.
- Guilbaud, M.-N., Siebe, C., Layer, P., Salinas, S., Castro-Govea, R., Garduño-Monroy, V.H. and Corvec, N.L., 2011. Geology, geochronology, and tectonic setting of the Jorullo Volcano region, Michoacán, México. *J. Volcanol. Geotherm. Res.*, 201(1-4): 97-112.
- Kereszturi, G., Geyer, A., Martí, J., Németh, K. and Dóniz-Páez, F.J., 2013. Evaluation of morphometry-based dating of monogenetic volcanoes—a case study from Bandas del Sur, Tenerife (Canary Islands). *Bull. Volcanol.*, 75(7): 1-19.
- Kereszturi, G., Jordan, G., Németh, K. and Dóniz-Páez, J., 2012. Syn-eruptive morphometric variability of monogenetic scoria cones. *Bull. Volcanol.*, 74(9): 2171-2185.
- Martin, U. and Németh, K., 2006. How Strombolian is a “Strombolian” scoria cone? Some irregularities in scoria cone architecture from the Transmexican Volcanic Belt, near Volcán Ceboruco (Mexico), and Al Haruj (Libya). *J. Volcanol. Geotherm. Res.*, 155(1-2): 104-118.
- Riedel, C., Ernst, G.G.J. and Riley, M., 2003. Controls on the growth and geometry of pyroclastic constructs. *J. Volcanol. Geotherm. Res.*, 127(1-2): 121-152.
- Siebe, C., Arana-Salinasa, L. and Abrams, M., 2005. Geology and radiocarbon ages of Tláloc, Tlacotenco, Cuauhtzin, Hijo del Cuauhtzin, Teutli, and Ocusacayo monogenetic volcanoes in the central part of the Sierra Chichinautzin, México. *J. Volcanol. Geotherm. Res.*, 141: 225-243.
- Valentine, G.A. and Gregg, T.K.P., 2008. Continental basaltic volcanoes - Processes and problems. *J. Volcanol. Geotherm. Res.*, 177(4): 857-873.
- Vapnik, V.N., 1995: *The Nature of Statistical Learning Theory*, New York: Springer-Verlag, pp. 1-314.
- Wood, C.A., 1980. Morphometric evolution of cinder cones. *J. Volcanol. Geotherm. Res.*, 7(3-4): 387-413.

A global perspective on Maars: Maar Volcano Location and Shape (MaarVLS)

Alison Graettinger, Cody Nichols

University of Missouri Kansas City, Kansas City, Missouri, 64110 USA. graettingera@umkc.edu

Keywords: maar crater shape, distribution, database.

A maar crater is the top of a much larger diatreme structure produced by phreatomagmatic explosions in the subsurface. The size and shape of the crater reflects the growth history of the total structure during an eruption. Maars have been identified around the world with detailed studies of individual sites and the volcanic fields that contain them. Maar research has now reached a point where it is both possible, and necessary, to consider the global population of maars and volcanic fields containing maars.

Global analysis enables the identification of universal characteristics of maars and the identification of exceptional / anomalous subsets of maars. This provides an important perspective to support and inspire future maar research by highlighting knowledge gaps and supporting informed comparisons between volcanic fields. The easiest place to start this analysis is with the morphometry and distribution of morphologically intact maars on Earth using freely available imagery from Google Earth, NASA, and the USGS. A working database, Maar Volcano Location and Shape (MaarVLS) has been developed to initiate the collection of observations for a global catalog of maars and key features.

The preliminary version of the database includes references, the location, size, and shape (primary and secondary diameter, area, perimeter and dimensionless shape parameters), volcanic field type, proximal population estimates, magma composition, elevation, depth, and age of previously documented maars. The data are currently limited by what is available in published work and consequently precise age and composition is lacking. The database is designed to grow and incorporate data as it becomes available in these, and additional areas, such as host substrate lithology, hydrologic data, and spatial statistics of the host volcanic field.

The first version of the MaarVLS database includes 241 maars with mean diameters between 70-5000 m. It is estimated that future versions may reach 400 well-preserved maars. Of the maars studied, 65% host lakes making depth estimates limited, but available depth measurements range 6-340 m. Maars in the database are historic, Holocene and Pleistocene in age, with preserved crater rims (75% complete and visible in satellite imagery). The database includes

maars from 29 countries and 65 volcanic fields (Figure 1). Most maars occur in fields with other volcanic constructs with 56% of the database in monogenetic fields and 42% in complex volcanic fields with larger volcanic constructs (calderas and stratovolcanoes). Most maars are mafic, but the database includes three rhyolitic and seven intermediate composition maars to date.

Maars are typically noncircular in planform shape, and many show polylobate shapes that resemble overlapping circles. Within an individual volcanic field maars range in size (with the largest maar typically no more than two times diameter of the smallest maar in a given field) and shape, including both circular and complex maars. Between 20-50% of maars within a given volcanic field display secondary directions of elongation. That is, maars are not all simple ellipses aligned above a feeder dike.

Crater shape preserves evidence of the growth process, including moving vent positions within the diatreme structure. Crater growth is the result of excavation and subsidence by subsurface explosions and collapse of the crater rim (White and Ross 2011; Valentine and White 2012). The lateral migration of explosion locations is common (Ort and Carrasco-Núñez 2009; Jordan et al. 2013) and necessary to achieve the sizes and shapes observed in the MaarVLS database.

Beyond the superficial characteristics of common size and shape, the database can be used to identify unique populations, such as exceptionally large craters (>3 km) and chains of craters which both represent <5 % of the population. These features represent end member shapes and provide a means to investigate the limits of explosion migration and crater shape. This shape analysis can incorporate both numerical studies and experimental work (Valentine et al. 2015). Shape data can also be integrated into studies of spatial statistics of vents in volcanic fields, and compared against available structural data sets. The distribution of vents, and alignment of vents has been shown to reflect structural controls in some volcanic fields (Mazzarini and D’Orazio 2003; Cebria et al. 2011). The incorporation of the orientation of crater elongation(s) will provide additional insight to the evolution of a crater during an eruption.

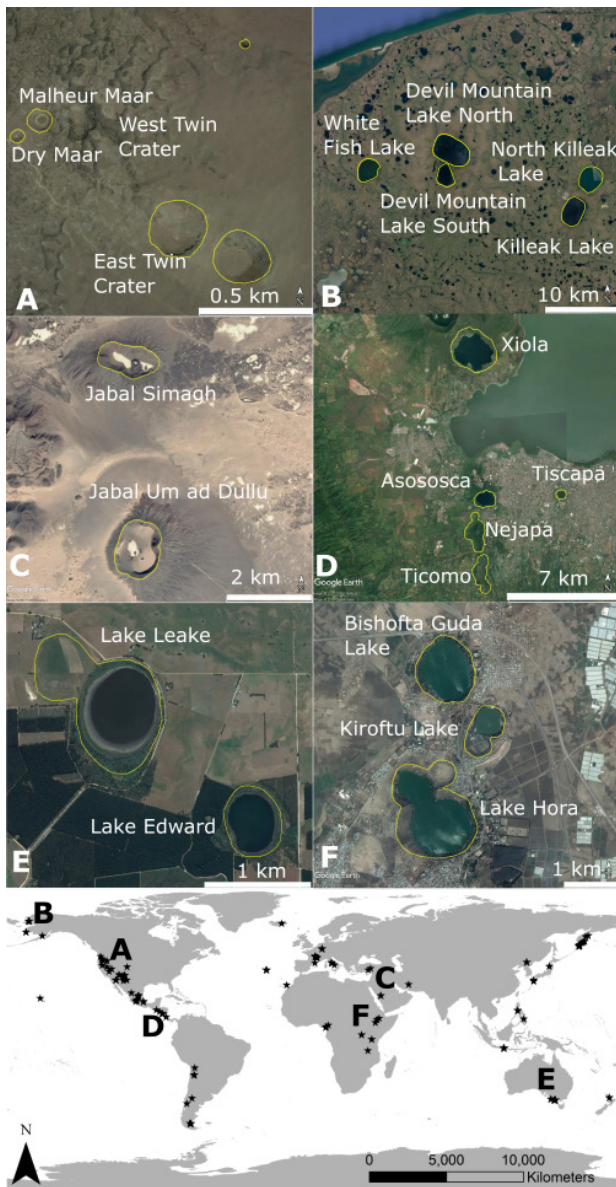


Fig. 1 – Example of maars in the MaarVLS database and map. Crater rims are highlighted. Map indicates location of maars with black stars and letters are next to the location of maars in images above. A) Diamond Craters, USA; B) Espenberg Maars, USA; C) Harrat Kishb, Saudi Arabia; D) Nejapa-Mira Flores Volcanic Field, Nicaragua; E) Newer Volcanic Province, Australia; F) Bishoftu Volcanic Field, Ethiopia.

These initial analyses represent the potential of a catalog like MaarVLS to facilitate future comparative studies, identify knowledge gaps, and enable the identification of unique populations of maars, integrate spatial and morphological studies, and answer fundamental questions about the typical behavior of maars. Future applications of this data will become possible as the database grows through contributions from the community and future research.

Acknowledgements

The database is the product of contributions from numerous undergraduate researchers at the Uni. at Buffalo and UMKC. The database is available at Vhub.org and is maintained; for contributions please contact A. Graettinger.

References

- Carn, S., 2000. The Lamongan volcanic field, East Java, Indonesia: physical volcanology, historic activity and hazards. *Journal of Volcanology and Geothermal Research*, 95: 81-108
- Cebria, J.M., Martin-Escorza, C., Lopez- Ruiz, J., Moran Zenteno, D.J., Martiny, B.M. 2011. Numerical recognition of alignments in monogenetic volcanic areas: Examples from the Michoacan-Guanajuato Volcanic Field in Mexico and Calatrava in Spain. *Journal of Volcanology and Geothermal Research*, 201: 73-82.
- Jordan, S.C., Cas, R.A.F., Hayman, P.C., 2013. The origin of a large (>3 km) maar volcano by coalescence of multiple shallow craters: Lake Purrumbete maar, southeastern Australia *Journal of Volcanology and Geothermal Research*, 254: 5-22
- Ku, Y.-P., Chen, C.-H., Song, S.-R., Iizuka, Y., Shen, J.J.-S., 2009. A 2 Ma record of explosive volcanism in southwestern Luzon: Implications for the timing of subducted slab steepening. *Geochemistry, Geophysics, Geosystems*, 6:6.
- Mazzarini, F., D’Orazio, M., 2003. Spatial distribution of cones and satellite-detected lineaments in the Pali Aike Volcanic Field (southernmost Patagonia): insights into the tectonic setting of a Neogene rift system. *Journal of Volcanology and Geothermal Research*, 125: 291-305.
- Ort, M.H., Carrasco-Núñez, G., 2009. Lateral vent migration during phreatomagmatic and magmatic eruptions at Tecuitlapa Maar, east-central Mexico. *Journal of Volcanology and Geothermal Research*, 181: 67-77.
- Valentine, G.A., White, J.D.L., 2012. Revised conceptual model for maar-diatremes: Subsurface processes, energetics, and eruptive products. *Geology*, 40 (12).
- Valentine, G.A., Graettinger, A.H., Macorps, E., Ross, P.-S., White, J.D.L., Dohring, E., Sonder, I., 2015. Experiments with vertically and laterally migrating subsurface explosions with applications to the geology of phreatomagmatic and hydrothermal explosion craters and diatremes. *Bulletin of Volcanology*, 77: 15.
- White, J.D.L., Ross, P.S., 2011. Maar-diatreme volcanoes: A review. *Journal of Volcanology and Geothermal Research*, 201: 1-29.

Assessing the role of phreatomagmatism in the eruption dynamics of the trachyandesitic maar-like Pavin crater (Massif central, France): constraints from the pyroclasts microtextures

Laurent Arbaret and **Jean-Louis Bourdier**

Institut des Sciences de la Terre d'Orléans, UMR 7327 (CNRS-Université Orléans-BRGM), Orléans, France. Jean-Louis.Bourdier@univ-orleans.fr

Keywords: phreatomagmatism, microtexture, degassing

Pavin volcano in the Massif central (France) is a young (≈ 7 ka) subcircular (≈ 1 km diameter), lake-filled (≈ 90 m deep) monogenetic explosive crater with an erupted volume estimated to 50-75 Mm³ (Bourdier, 1980, Leyrit et al., 2016). The juvenile magma composition is trachyandesitic (≈ 58 wt% SiO₂, Bourdier, 1980). Apart from its differentiated magma composition, Pavin looks much like many young basaltic maars of typical phreatomagmatic origin, such as the Tazenat maar in the neighbouring Chaîne des Puys. This morphological similarity prompts to envision a phreatomagmatic character for the Pavin eruption, i.e. that the eruption was basically driven by interaction at depth of the ascending magma with external water.

Facies analysis of the Pavin pyroclastic deposits at the field scale provides some support to this, notably (1) in proximal areas (< 2 km) the pyroclastic sequence includes at least 2 layers (e.g. in the reference Clidères section of Leyrit et al., 2016) of dominantly fine-grained, poorly sorted, amalgamated surge beds showing evidence of being water-saturated during emplacement, and (2) secondary to dominant pumices, additional juvenile components are dark grey, less vesicular, pyroclasts with surficial morphology akin to that of cauliflower bombs common in basaltic maar deposits. Such low-vesicularity clast population was tentatively interpreted as reflecting some degree of magma quenching by water interaction (Bourdier, 1980 ; Boivin et al., 2010).

Further evidence in the field for a phreatomagmatic origin is not obvious. Instead, (1) the most proximal Pavin deposits are only crudely stratified and lack the typical thin bedding that should reflect the rhythmic character inherent in fuel-coolant interaction processes, and (2) the juvenile pyroclasts are dominantly pumices that do not differ in hand specimen from pumices from purely magmatic (or considered so) explosive eruption. This has led to various assessments of the role of phreatomagmatism in the Pavin eruption, interpreted either as a combination of magmatic degassing and water-magma interaction (Bourdier, 1980, Boivin et al., 2010) or as a typical phreatomagmatic eruption (Leyrit et al., 2016).

The objective of the present study is to re-examine this issue by looking at the Pavin juvenile pyroclasts microtex-

tures at the lapilli (1-2 cm) scale, including bulk vesicularity (density) measurements, and 2D (backscatter SEM) and 3D (microtomography) imaging of selected clasts covering the vesicularity range. Preliminary qualitative results of this on-going study are summarized below :

(1) the juvenile lithologies include macroscopically homogeneous light-yellow pumices (density range 0.4-1.0), homogeneous denser grey lapilli (density range 0.8-2.1), and a significant amount of heterogeneous clasts with grey and light parts, often as irregular stripes.

(2) the vesicle population of pumices is dominated by strongly coalesced, rounded bubbles > 20 μ m. It strongly contrasts with that of the denser grey lapilli where vesicles are angular and poorly connected. Equant microlites < 50 μ m are abundant in the denser grey lapilli and virtually absent in the pumices. This provides a consistent link between the vesicles shape and groundmass crystallinity, the vesicles shape in the dense clasts being controlled primarily by a pre- to syn- microlite population making the groundmass densely crystallized.

(3) a strong fabric of the larger vesicles is present in all lithologies, indicative that most of the vesicle evolution (and growth of the equant microlites) occurred as the magma was deformed during ascension, prior to fragmentation.

(4) a population of spherical bubbles of a few microns is present in all lithologies, as is a population of abundant tiny needle-like microlites about 1 μ m wide. The needle-like microlites show no preferred orientation.

(5) most of the equant and needle-like microlites display frequent open (unfilled by groundmass) transversal cracks.

The occurrence of frequent banded clasts makes it difficult to interpret the denser grey lapilli as having undergone quenching effects, as previously suggested (Bourdier, 1980 ; Boivin et al., 2010). Instead, the vesicle and equant microlite populations observed in the denser grey lapilli, and the banded vesicular-unvesicular textures, are consistent with syn-eruptive outgassing, as observed for instance in the range of juvenile lithologies from vulcanian eruptions like the 1997 eruptions at Montserrat (e.g. Burgisser et al., 2010).

By contrast, the Pavin pumices are devoid of equant microlites and do not show evidence of outgassing, similar in this respect to plinian pumices. The age of the Pavin eruption implies post-eruptive meteoric rehydration of the pumice glass that will not allow to recover pristine residual water content of the pumice glass, preventing precise reconstitution of the degassing and vesiculation processes. The qualitative observations of the pumice microtextures, however, suggest these were formed under virtually closed-system conditions for most of their ascent prior to fragmentation. Therefore, since the pumice component is dominant among the juvenile lithologies, magma degassing might well be the primary control on the eruptive dynamics and explosivity. By contrast, the grey denser lithology and the heterogeneous dense-vesicular, mostly banded clasts would reflect various degrees of outgassing (open-system conditions) for parts of the magma column.

The contribution of magma-water interaction in the eruptive process thus remains elusive from microtextural observations. The ubiquitous population of tiny needle-like microlites, obviously grown under strong ΔT conditions, was not observed in vulcanian (purely magmatic) eruption products (Montserrat 1997, Burgisser et al., 2010 ; Merapi 2010, Drignon et al., 2016), nor in plinian pumices we observed so far. It might reflect contact with external water and would be the only microtextural evidence for this. If this is the case, this would have affected the whole magma, at a late stage of the magma ascent.

In conclusion, our preliminary study of the pyroclasts microtextures do not provide much further evidence for a phreatomagmatic influence in the Pavin eruption. The interpretation of the denser juvenile clasts as quenched magma portions (Bourdier, 1980 ; Boivin et al., 2010) must be discarded. The microtextural evidence is that the Pavin explosive process fundamentally involved magmatic degassing. However, magma-water interaction might be tentatively recorded by late-stage, second-order, microtextural features. It thus might well have assisted the explosive process and increased the energy of the explosive process, leading to the resulting maar-like structure, as suggested by previous statements (Bourdier, 1980 ; Boivin et al., 2010).

Acknowledgements

Y. Le Moigne, M. Gourcerol, C. Daffos, and I. Di Carlo are thanked for assistance in data acquisition.

References

- Boivin, P., Besson, J.-C., Ferry, P., Gourgaud, A., Miallier, D., Thouret, J.-C., Vernet, G., 2010. Update on the eruption of lake Pavin, 7000 years ago. *Revue des Sciences Naturelles d'Auvergne* 74 : 47-56.
- Bourdier, J.-L., 1980. Contribution à l'étude volcanologique de deux secteurs d'intérêt géothermique dans le Mont-Dore : le groupe holocène du Pavin et le massif du Sancy. Unpublished 3^o cycle thesis, Clermont-Ferrand University, 180 p.
- Burgisser, A., Poussineau, S., Arbaret, L., Druitt, T.H., Giachetti, T., Bourdier, J.-L., 2010. Pre-explosive conduit conditions of the 1997 Vulcanian explosions of Soufriere Hills Volcano (Montserrat) : I. pressure and vesicularity distribution. *Journal of Volcanology and Geothermal Research*, 194 : 27-41.
- Drignon, M. J., Tonin, B., Arbaret, L., Burgisser, A., Komorowski, J.-C., Martel, C. and Yaputra, R., 2016. Pre-explosive conduit conditions during the 2010 eruption of Merapi volcano (Java, Indonesia). *Geophysical Research Letters*, DOI 10.1002/2016GL071153.
- Leyrit, H., Zylberman, W., Lutz, P., Jaillard, A., Lavina, P., 2016. Characterization of Phreatomagmatic Deposits from the Eruption of the Pavin Maar (France). In : Sime-Ngando et al. Eds, *Lake Pavin*, Springer, 105-128.

Sedimentary features as indicators of hydrogeological conditions controlling initial phreatomagmatic eruption phases of the monogenetic Potrerillo and San Juanito volcanoes in the Ceboruco graben, western Mexico

Javier Agustín-Flores¹, Claus Siebe¹, Katrin Sieron², **Dolors Ferrés¹**, Karime González-Zuccolotto¹

¹ Instituto de Geofísica, Universidad Nacional Autónoma de México, Ciudad de México, Mexico, dferres@geofisica.unam.mx

² Center of Earth Sciences, Universidad Veracruzana, Xalapa, México

Keywords: Phreatomagmatic eruption, western MVB, Ceboruco volcano

A recent inventory (Siebe and Salinas, 2014) of the monogenetic volcanoes in the Mexican Volcanic Belt (MVB) documents that only 3% (88 volcanoes) of them can be classified as phreatomagmatic. They are located mainly in fluvial, lacustrine, and littoral settings (Kshirsagar et al., 2015, 2016) as documented in other examples around the world. The inventory points out that nearly half of the phreatomagmatic volcanoes in the MVB occur in a littoral setting near the Gulf of Mexico (Sieron et al., 2014). Kshirsagar et al. (2015; 2016) state that the rare occurrence of phreatomagmatic eruptions within other areas of the MVB indicates that optimal conditions for phreatomagmatism are uncommon, despite abundant fluvial and lacustrine settings. They conclude that local and distinct hydrogeological conditions control the occurrence of phreatomagmatic vents.

by the Ceboruco volcano (Fig. 1), a Late Quaternary andesitic to dacitic stratovolcano (Sieron and Siebe, 2008).

Twenty-eight Late Quaternary monogenetic volcanoes in the vicinity of Ceboruco volcano, which range in age from 100,000 to <2,000 years BP, are concentrated along a 2-km wide and 30-km long stripe within the Ceboruco graben, aligned in NW-SE direction. They vary in composition, morphology, and eruptive style.

Strombolian-type activity, with moderate to low explosivity, and dome construction characterized by initial explosive activity followed by lava extrusion dominates. Nevertheless, Sieron and Siebe (2008) already recognized a few explosion craters, whose construction involved phreatomagmatic phases.

Three monogenetic volcanoes were studied in detail: Potrerillo I (basaltic andesite), Potrerillo II (trachydacite), and San Juanito (basaltic andesite); all located within a ~12 km² sub-drainage, hydrological basin, at relatively high altitude, at the western flank of Ceboruco stratovolcano (Fig. 1). The purpose of this study is to examine how the nature and proportion of different types of pyroclasts within the exposed deposits of Potrerillo I, Potrerillo II, and San Juanito, as well as their sedimentary features can explain the initiation and progression of explosion conditions, and the role of explosive magma-water interactions. Despite the lack of systematic hydrogeological information, the diversified and distinct eruptive styles of each eruption center helped to infer the extent of control of the hydrogeological conditions in the studied cases.

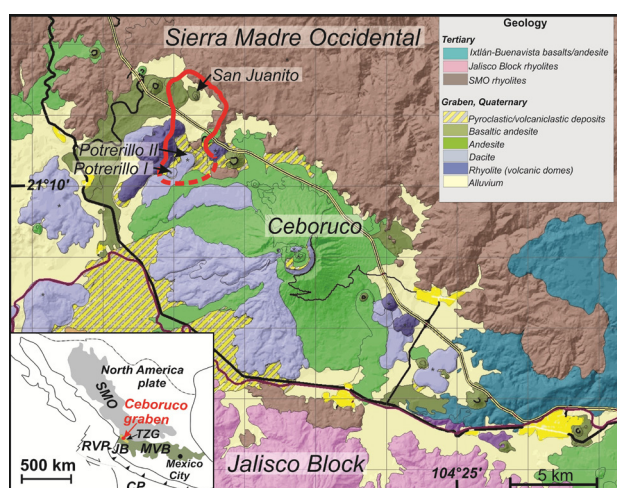


Fig. 1 – Geological map of the central part of the Ceboruco graben showing the three studied monogenetic edifices at the northwestern flank of Ceboruco stratovolcano

The Ceboruco asymmetric graben is a 30-km-long segment of the Tepic-Zacoalco graben system, a region occupied by the western part of the MVB. This volcanic arc is related to the subduction of the oceanic Rivera and Cocos plates beneath the continental North America plate. The area is dominated

Unlike basaltic andesite Potrerillo I, which formed by an entirely dry magmatic eruption, the prevalence of initial, short-lived, weak and dry phreatomagmatic phases is envisaged for Potrerillo II and San Juanito eruptions. Both tephra rings show dominantly atypical, crudely bedded, coarse-grained deposits where the evidence for energetic, diluted pyroclastic density currents is rare (San Juanito) or subordinated (Potrerillo II). Examples of such architectures are frequently documented in ejecta deposits associated to high-silica maar-diatreme/tuff ring eruptions,

but not to less evolved magma compositions. Deposits of both volcanoes exhibit an overall prevalence of “dryness” at the time of deposition. It is hence inferred that during the phreatomagmatic phases low energy explosions that generated dry dense tephra jets dominated. Subordinated transient explosive magmatic activity also occurred. The general cyclic trend from less dry to drier phreatomagmatic peaks indicates intermittence of the phreatomagmatic explosions suggesting changes in the amount of water involved.

It is inferred that the sub-basin drainage where the three volcanoes were emplaced is underlain by a rock-fractured, low storativity, unconfined aquifer with good hydraulic conditions but highly dependent on the distribution of rainfall. Therefore, the variation in the depths of phreatomagmatic explosions, fluctuations in the water involved, and the absence or presence of phreatomagmatic phases in the studied volcanoes are probably highly influenced by the water-bearing conditions (degree of saturation) of the aquifers at the time of the eruption, which in turn depend on the amount and distribution of rainfall. Even when general substrate conditions (assuming a similar substrate in the area near Ceboruco volcano) to trigger phreatomagmatic explosions could be apparently favorable, it is concluded that the intricate interdependency of substrate and climatic conditions other than magma-system properties make them less common than expected in the Ceboruco area.

This study improves our understanding of phreatomagmatic eruptions of different compositions in similar settings. The recognition of associated hazards will allow to define eruptive scenarios of monogenetic eruptions, and help complete the volcanic hazard map of the Ceboruco volcano area.

Acknowledgements

This research was part of the project “Evaluación del peligro volcánico del volcán Ceboruco (Nayarit), con énfasis en su posible impacto sobre la infraestructura de la Comisión Federal de Electricidad” (Convenio CFE-800720929), which was funded by the Comisión Federal de Electricidad.

References

- Kshirsagar, P., Siebe, C., Guilbaud, M.-N., Salinas, S., Layer, P., 2015. Late Pleistocene (~21,000 yr BP) Alberca de Guadalupe maar volcano (Zacapu basin, Michoacán): stratigraphy, tectonic setting, and paleo-hydrogeological environment. *Journal of Volcanology and Geothermal Research*, 304: 214–236.
- Kshirsagar, P., Siebe, C., Guilbaud, M.N., Salinas, S., 2016. Geological and environmental controls on the change of eruptive style (phreatomagmatic to Strombolian-effusive) of Late Pleistocene El Caracol tuff cone and its comparison with adjacent volcanoes around the Zacapu basin (Michoacán, México). *Journal of Volcanology and Geothermal Research*, 318: 114-133.
- Siebe, C., Salinas, S., 2014. Distribution of monogenetic phreatomagmatic volcanoes (maars, tuff-cones, tuff-rings) in the Mexican Volcanic Belt and their tectonic and hydrogeologic environment. IAVCEI-5IMC Conference, Querétaro, Mexico.
- Sieron, K., Capra, L., Rodríguez-Elizarrás, S., 2014. Hazard assessment at San Martín volcano based on geological record, numerical modeling, and spatial analysis. *Natural Hazards*, 70, 275-297.
- Sieron, K., Siebe, C., 2008. Revised stratigraphy and eruption rates of Ceboruco volcano and surrounding monogenetic vents (Nayarit, Mexico) from historical documents and new radiocarbon dates. *Journal of Volcanology and Geothermal Research*, 176, 241-264.

Historical phreatomagmatic activity at the summit of Tacaná Volcano, México–Guatemala

José Luis Macías¹, José Luis Arce², Ricardo Saucedo³, Juan Manuel Espíndola⁴, and Giovanni Sosa-Ceballos¹

¹ Instituto de Geofísica, UNAM, Campus Morelia, 58190 Morelia, Michoacán, México. jlmacias@igeofisica.unam.mx

² Instituto de Geología, UNAM, Coyoacán 04510, Ciudad de México, México

³ Instituto de Geología, Universidad Autónoma de San Luis Potosí, San Luis Potosí, México

⁴ Instituto de Geofísica, UNAM, Coyoacán 04510, Ciudad de México, México

Keywords: Tacaná, historical, phreatomagmatism

The Tacaná Volcanic Complex (TVC) is the northernmost volcanic center of the Central American Volcanic Arc. The complex consists of four volcanic edifices from oldest to youngest: Chichuj, Tacaná, and San Antonio volcanoes, and Las Ardillas dome. Tacaná volcano the highest peak of the complex (4060 m) marks the international border between México and Guatemala. This edifice has been the focus of historical activity documented in 1855, 1949, and 1986 (De la Cruz et al., 1999). The last phreatic explosion was a reminder for scientists and local authorities of the potential threat that Tacaná represents for circa 300,000 inhabitants settled at 35 km around its summit.



Figure 1. Aerial view from the southwest of Tacaná volcano showing the summit dome and a greenish crater-lake of figure 2.

According to Macías et al. (2015), the TVC was constructed along the past 250 ka inside the remains of a ~2 Ma caldera. Tacaná itself started its construction about 50 ka ago through the emission of andesitic and dacitic lava flows and domes with associated pyroclastic density currents. The edifice has been destroyed at least twice during the past 15 ka producing debris avalanche deposits and has generated at least nine explosive events during the past ~8000 years. These number of eruptions is high if we considered that the volcano was practically unknown prior than its 1986 activity.

The summit area of Tacaná holds evidence of explosions craters located at different elevations, one of this is an elongated 80 x 48 m wide crater that contains a greenish lake. It has a variable depth (≤ 20 m) with walls made of pyroclastic deposits as described below. This crater was excavated through andesitic lava flows emitted by Tacaná volcano. This crater represents the venting site of a historic eruption at Tacaná occurred during the last Classic period of the Mesoamerican culture. Here, we present a summary of the deposits associated with this crater.



Figure 2. View from the southeast of the crater-lake produced by a historic eruption of Tacaná volcano. The lake stands at an elevation of 3800 m and has a diameter of ~100 m.

We studied the deposits associated to this crater in circa 50 stratigraphic sections located at elevations between 2500 and 4060 m. The deposits overlie a dark-brown clayed paleosol, dated with the 14C at 850 ± 40 yr B.P. The

deposit is covered at some locations by different paleosols, the youngest of which dated at 205 ± 85 yr B.P. Atop these deposits frequently appear the 1902 ash fallout of Santa María Volcano, Guatemala.



Figure 3 Section at the crater rim of Tacaná volcano that displays the lower paleosol (850 ± 40 yr B.P.), and the bedded deposits on top associated with the historic eruption of Tacaná.

A composite column of these deposits consists, from base to top, of:

- Brown to ochre massive breccia (~5 m) composed of blocks to lapilli angular heterolithic, supported by a fine to medium ash matrix.

- A gray, massive fine ash layer (40 cm) rich in accretionary lapilli and voids.

- Set of multiple gray to ochre thin beds varying in thickness from ~1 m (proximal) to less than 5 cm (distal). These layers show cross (or) parallel bedding and are composed of lapilli set in a medium ash matrix. Some layers are indurated.

- A massive clast-supported layer with reverse grading that varies in thickness from 94 to 10 cm. It consists of lapilli pumice (80 % vol.) and lapilli heterolithic lithics (20 % vol.). Pumice consists of plagioclase + pyroxene + hornblende set in a glassy groundmass. A sample of this pumice yielded a chemical composition of 56 % wt. SiO₂ (basaltic andesite).

- Set of fine gray ash indurated layers with cross to parallel bedding and voids (≤ 16 cm). A charcoal sample taken in distal exposures yielded a new age of 760 ± 30 yr B.P.

Based on our stratigraphic correlation, the characteristic of the deposits, and radiocarbon dates we propose that reactivation of Tacaná occurred around 760 yrs ago. This eruption represents one of the youngest best recorded magmatic events of the volcano. The size of the crater and distribution of the deposits point out that it was larger in magnitude than the phreatic explosions occurred

during the last century. The eruption was triggered by the intrusion of a small magma body of andesitic composition that reached shallow depths through a series of fractures that transect the volcanic edifice.

The results indicate that a small batch of basaltic andesite magma encountered a shallow water table producing a phreatomagmatic explosion that dispersed a proximal breccia around the vent located SW of the Tacaná volcano summit. The eruption was followed by series of explosions that dispersed dilute pyroclastic density currents that were able to drape most of the Tacaná summit. The deposits emplaced by these density currents are wet, rich in clay particles, and contain accretionary lapilli. The phreatomagmatic explosions rapidly finished the available water, then shifting to a dry magmatic event that turned into a sustained low-altitude eruptive column that dispersed a trackable pumice-rich fallout around the vent up to a distance of ~1 km. The eruption ended with another series of phreatomagmatic explosions that dispersed dilute pyroclastic density currents that like reached farthest distances from the vent (~1 km). During the waning phase a thin ash bed covered the deposits.

In terms of hazard, a future explosion as the ~760 yrs B.P. phreatomagmatic event would pose a significant risk to populations settled around the volcano. Several areas on top of the TVC summit are being affected by fumarolic activity and pervasive hydrothermal alteration, and therefore might be prone to collapse.

Acknowledgements

This study was funded by PN 522 CONACYT project to J.L. Macías and the Instituto de Geofísica, Unidad Morelia.

References

- De la Cruz-Reyna S, Armienta MA, Zamora V, Juárez F (1989) Chemical changes in spring waters at Tacaná Volcano, Chiapas, México. *J Volcanol Geotherm Res* 38: 345–353. doi:10.1016/0377-0273(89)90047-4
- Macías, J.L., Arce, J.L., Layer, P., Saucedo, R., and Mora J.C. (2015), Eruptive History of Tacaná Volcano. In: *Active Volcanoes of Chiapas (México): El Chichón and Tacaná*. Edited by T. Scolamacchia and J.L. Macías. Springer Verlag.p. 115-138 DOI 10.1007/978-3-642-25890-9_6.

Tilocálar volcanoes: Effusive, magmatic explosive and phreatic monogenetic activity under compressional control in the northern Chile

Gabriel Ureta¹, Felipe Aguilera^{2,3} and Károly Németh⁴

¹ Programa de Doctorado en Ciencias Mención Geología, Universidad Católica del Norte, Av. Angamos 0610, Antofagasta Chile. gabriel.ureta@ucn.cl

² Centro Nacional de Investigación para la Gestión Integrada de Desastres (CIGIDEN), Chile.

³ Departamento en Ciencias Geológicas, Universidad Católica del Norte, Av. Angamos 0610, Antofagasta, Chile.

⁴ Institute of Agriculture and Environment, Massey University, Palmerston North, New Zealand.

Keywords: phreatomagmatism, phreatic eruption, scoria

Tilocálar volcanoes (Fig. 1) are located at the southeast border of the Salar de Atacama Basin in the Central Andean Volcanic Zone, northern Chile. These are constituted of two monogenetic centers, Tilocálar Norte and Tilocálar Sur, respectively (Fig. 1). Both centers are emplaced in a compressional deformation zone, where it's the more notorious feature is the N-S Tilomonte ridge. The ridge is the surface expression of east vergence blind reverse faults, which fold the upper rock units (González et al., 2009). Tilocálar volcanoes are built over a basement constituted by Ordovician Tambillo Monzogranite and paraconglomerate with intercalations of poorly lithified sandstone, corresponding to the Oligocene-Eocene Tambores Formation, which are covered by Pliocene Tucúcaro Ignimbrite (Gardeweg and Ramírez, 1982).

Tilocálar Norte is located on the frontal limb of the easternmost Tilomonte ridge, and corresponds to a small scoria and spatter cone associated with N-S-trending lava flows (<1 Ma K-Ar whole rock; Gardeweg and Ramírez, 1982) and an isolated small dome, called El Maní dome (Fig. 1b). Four lava flows have been mapped, which cover 3.23 km² area and total bulk volume of 0.53 km³. Maximum extension of lava flows are 3.9 and 1.2 km for north and south flows, respectively. El Maní dome is located 300 m south-western from the emission center, covering 619 m² area and a bulk volume of 3,016 m³. Tilocálar Norte lavas correspond to andesites, trachyandesites and dacites (59.80 to 63.26% wt. SiO₂; Gardeweg and Ramírez, 1982; Ortega, 2008; Hoffmann, 2011), pertaining to metaluminous and a high-K calcalkaline series. However, El Maní dome presents two types of products, dacitic (63.89% wt. SiO₂) and rhyolitic lavas (74.65% wt. SiO₂), which have been related to the mingling between original magma source that generates the Tilocálar lava flows and shallow crustal melts that generated products as Tucúcaro Ignimbrite (76.31% wt. SiO₂), respectively (González et al., 2017).

Tilocálar Sur (Fig. 2) is located on top of the hinge zone of Tilomonte ridge and corresponds to a small scoria cone composed of a succession of pyroclastic fall deposits, E-W-trending lava flows and a broad crater. Tilocálar Sur has an age that varies from 730±50 ka to 460±50 ka

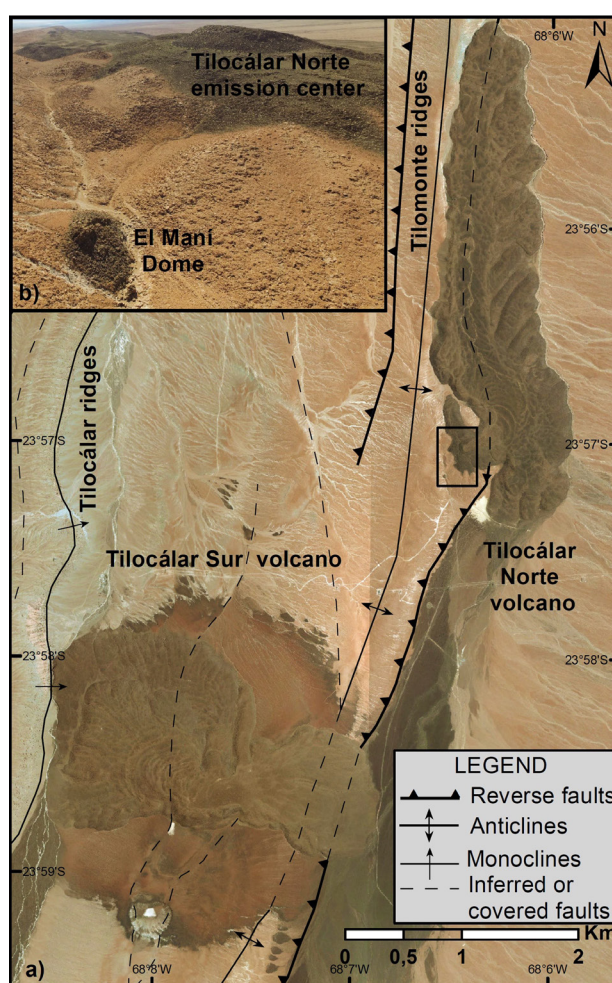


Fig. 1 – a) Location map of Tilocálar volcanoes, northern Chile, based on a satellite image. Outlined box show the position of figure 1b. b) Zoom at El Maní dome and Tilocálar Norte emission center.

(U-Th groundmass; González et al., 2009). The pyroclastic fall deposits are distinguished into two agglutinated andesitic scoria fall units (58.54% wt. SiO₂; Ortega, 2008), which reach up to 6.4 m thickness, an exposed area of 2.2 km² and an exposed bulk volume of 0.3 km³. The lower pyroclastic unit corresponds to a moderately vesicular

black scoriaceous deposit, 5.51 m thickness, which lies over Tucúcaro Ignimbrite, whereas the upper pyroclastic unit is dominated by a succession of moderately vesicular reddish brown scoria deposit, with 0.89 m thickness. Four and two lava flows have been recognized in the north-western and eastern sides, respectively, reaching up to 1.8 and 1.4 km length, respectively. Lava flows cover an area of 3.56 km² and a bulk volume of 0.44 km³, corresponding to basaltic andesites and pyroxene andesites (55.29- 62.25% wt. SiO₂; Gardeweg and Ramírez, 1982; Ortega, 2008; Hoffmann, 2011). The broad crater is located 1.2 km southwest from the Tilocálar Sur volcano (Fig. 2). The crater has a diameter of 288 x 363 m; it is elongated to east-west direction in map view. This crater is surrounded by sandstones, granitoids and tuffs fragments, which are individual rock fragments laying on the ground surface around of the crater rim. Those rock fragments could correspond to pre-existing basement rocks from Tambores and Tambillo formations and Tucúcaro Ignimbrite. Those fragments appear up to 680 m distance to north, north-east and east from the crater, whereas to the southeast, south and southwest, the fragments are present up to 510, 280 and 330 m distance from the explosion crater, respectively. The ejection of the fragments to the west is uncertain due to the presence of alluvial material.

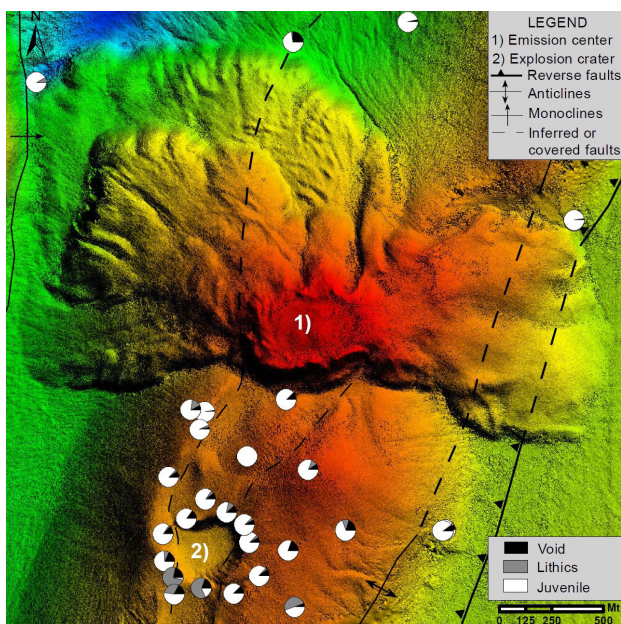


Fig. 2 – Digital Elevation Model (DEM) of the Tilocálar Sur volcano showing the proportions of interstitial material (<0,5 mm; void), wall-rock clasts (lithics) and juvenile pyroclasts (juvenile) proportions

The magma related to Tilocálar volcanoes would have probably migrated along reverse faults and in fold core regions. Furthermore, it is stored in flat portions of reverse faults, which are interconnected by ramp structures (González et al., 2009). These volcanoes exhibit multiple eruptive phases. Tilocálar Norte has been built by a single effusive phase, where diverse lava flows and dome were emitted. Tilocálar Sur was built in three stages, firstly by a mild magmatic volatile-driven explosive phase, related to the emission of agglutinated scoria, followed by an ef-

usive phase (lava flows), and finishing with an explosive phase, which formed an explosion crater, probably related to phreatic activity (as so far no juvenile pyroclasts have been identified that could support direct magma and water interaction, hence phreatomagmatism), produced by the violent expansion of the steam generated from heated groundwater by a near magmatic source. The uprising of fluids seems to be favored by the presence of normal faults, which controls the emplacement of both emission center and explosion crater of Tilocálar Sur volcano (Fig. 2). These normal faults are associated to the extensional zone generated in the hinge zone of the ridge.

Acknowledgements

We thank to Comisión Nacional de Investigación Científica y Tecnología (CONICYT) for the GU Doctoral Grant “Becas de Doctorado Nacional CONICYT - PCHA / Doctorado Nacional / 2016-21161286”, which allows to fund this research. We also thank to Cristóbal González, Diego Jaldin and Diego James for their support during fieldworks.

References

- Gardeweg, M., Ramírez, C. F., 1982. Geología de los volcanes del Callejón de Tilocalar, Cordillera de los Andes-Antofagasta. In: III Congreso Geológico Chileno, A111–A123.
- González, G., Cembrano, J., Aron, F., Veloso, E. E., Shyu, J. B. H., 2009. Coeval compressional deformation and volcanism in the central Andes, case studies from northern Chile (23 S–24 S). *Tectonics* 28, TC6003.
- González, C., Ureta, G., González, R., Aguilera, F., Menzies, A., 2017. Evidencia de mingling en el sistema monogenético del volcán Tilocalar Norte (Región de Antofagasta, Chile): Análisis petrográfico y geoquímico. In: 12 International Center for Earth Science conference, Argentina.
- Hoffmann, C., 2011. Petrografía y geoquímica de los conos del campo de lavas Negros de Aras (23°57′-24°26′ Lat. S. y 67°57′-68°42′ Long. O.) al norte del volcán Socompa, Il región de Antofagasta, Chile. Undergraduate Thesis, Universidad de Concepción.
- Ortega, V., 2008. Estudio petrográfico y petrológico de las rocas de los volcanes Láscar, Tilocalar Norte y Tilocalar Sur. Undergraduate Thesis, Universidad Católica del Norte.

Pre-historic effusive ring-fracture activity from the southern caldera's rim of Los Humeros volcanic complex and geothermal field, Eastern Mexico, implications for hazards

Carrasco-Núñez, G¹, Barrios, S.1, Hernández, J.¹

¹ *Centro de Geociencias, campus UNAM Juriquila. Universidad Nacional Autónoma de México. Institute of Geophysics, UNAM, Campus Morelia, 58190 Morelia, Michoacán, Mexico. gerardoc@geociencias.unam.mx*

Keywords: lava flows, Holocene, monogenetic volcanism, volcanic hazards.

Los Humeros Volcanic Complex (LHVC) is the easternmost active silicic-basaltic caldera volcano of the Trans-Mexican Volcanic Belt. The LHVC was formed during the Pleistocene by two major caldera-collapse events followed by alternated explosive and effusive activity, which culminate and the emplacement of several monogenetic eruptive centers. The first caldera-forming eruption produced the 15-20 km wide Los Humeros Caldera, which was associated with the emplacement of the 115 km³ (DRE) Xaltipan Ignimbrite (Ferriz and Mahood, 1984). This unit was formerly dated at 460 ky (Ferriz and Mahood, 1984), however, it has been recently dated at 164±4.2ka by Carrasco-Núñez et al. (in press). After an intense period of eruptive activity including rhyolitic domes and a series of andesitic to rhyolitic Plinian and sub-Plinian pumice fall deposits (Faby Tuff) dated at 70 ± 23 ka and 74.2 ± 4.5 ka (Carrasco-Núñez et al., in press) a second caldera-forming event occurred at 69 ± 16 ka (Carrasco-Núñez et al., in press), with the emplacement of the rhyodacitic Zaragoza Ignimbrite (15 km³ DRE) and the nested 8-10 km wide Los Potreros Caldera (Ferriz and Mahood, 1984; Carrasco-Núñez and Branney, 2005). After that caldera stage, volcanic activity resumed at about 50 ka with the emplacement of a complex succession of rhyolitic lava domes, followed by an explosive period producing a peculiar contemporaneous explosive alternation both rhyodacitic and basaltic andesite magmas at 7.3 kr (Cuicuiltic member, Dávila & Carrasco-Núñez, 2014), followed by an intense period of trachytic, trachyandesitic, basaltic-andesitic and basaltic lava flows, and dacitic, trachydacitic, andesitic and basaltic pumice and scoria fall deposits emitted by more than 80 monogenetic eruptive centers located in the LHVC (Ferriz and Mahood, 1984; Dávila-Harris and Carrasco-Núñez, 2014; Norini et al., 2015; Carrasco et al., in press; Carrasco-Núñez et al., 2017).

The intense effusive episode occurred during a recent period from late Holocene to pre-historic times, formed a widely distributed lava flow field, which was emplaced mainly through a ring-fracture system associated with the southern caldera rim, with a dominant orientation to the NW, which change to a NE direction. Most of these vents are aligned on those principal orientations, sug-

gesting a volcano-structural caldera control for its emplacement. The source area for this volcanism is related to several dozens of vents, however, there are vents that overlap and form well-defined lava flows that are continuously feed forming compound lava flows, some of them showing reinjection of new magma and sometimes forming important breakouts at the lava fronts. These lavas are aa and blocky flows, which sometimes developed relatively long lava tunnels, as in the case of the upper part of the Texcal lava flow, where they extend for more than 1500m long (Espinaza et al, 2016), indicating a common reinjection of magma in many of these lava flows.

Based on C14 dating, paleomagnetic data (Juárez et al., 2017) and observed compositional variations we confirm that the most recent part of the volcanic field was probably formed in many different pulses but mainly grouped into two main effusive episodes, which apparently occurred in a relatively short time frame. The most recent effusive activity formed the Texcal, Tepeyahualco, and Sarabia lava flows, which corresponds to olivine basalts, trachyandesitic and basaltic andesites, respectively, and erupted around 3,800 yr B.P. A second period of effusive activity produced El Pájaro and El Frijol lava flows, of trachytic and basaltic andesite composition, respectively, erupted at 2,800 yr B.P., time that apparently overlap with the beginning of the settlements of the pre-hispanic city of Cantona, which was built mainly over the Tepeyahualco and Texcal lava flows (Fig. 1).

In addition to this volcanism there are also two olivine-bearing basaltic lava flows emplaced within the caldera, during late Holocene times. One of them is filling the Xalapazco crater that was believed to be originated from phreatomagmatic eruptions like a maar volcano, however, it is now clear that this correspond to a big explosion crater that partially destroyed the Mazataloya crater (Rojas, 2015).

The area around the LHVC was affected by climate changes during the Holocene, which may cause some influence in the communities located nearby (Bhattacharya et al., 2015). However, it is clear that the prehistoric activity of the ring-fracture volcanism of the LHVC

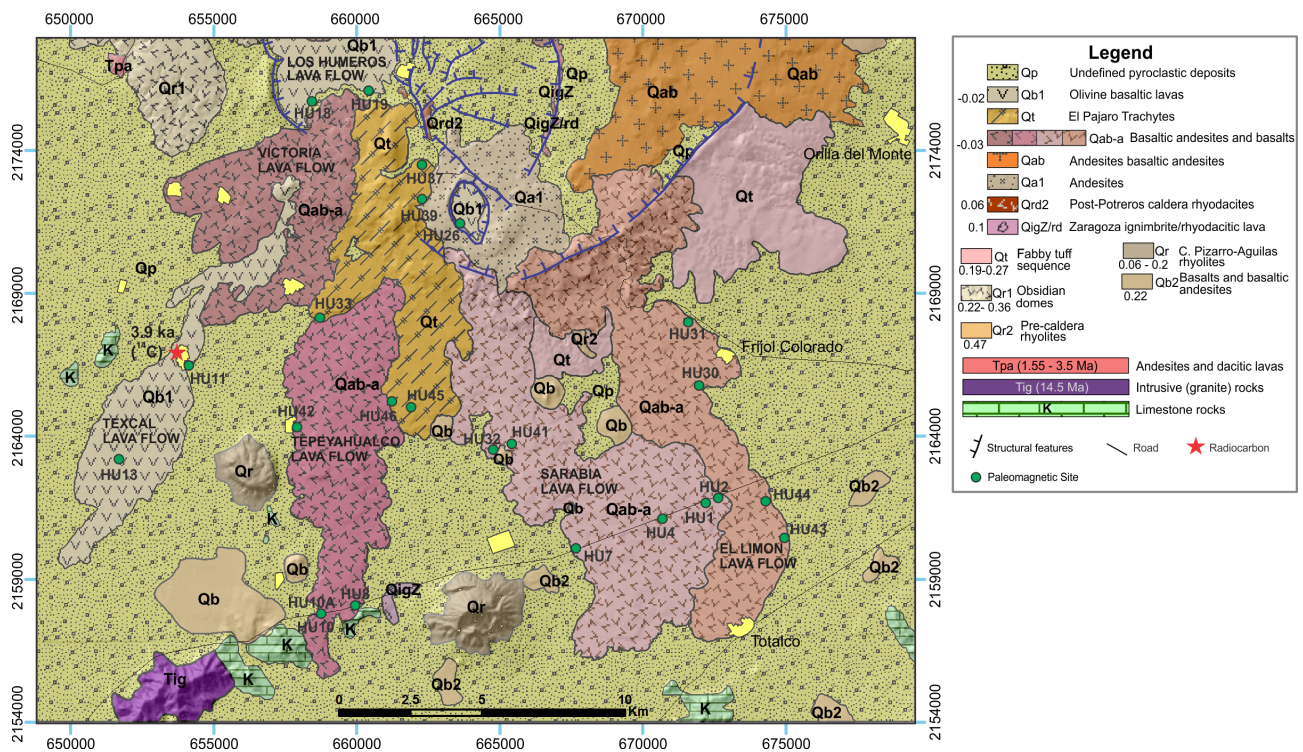


Fig. 1 – Geologic map of the southern rim of Los Humeros caldera and geothermal field showing the distribution of the Holocene/prehistoric ring-fracture lava flows.

occurred in times when the area was already populated, implying that a more likely reason for the abandonment of the Cantona city in the last millennium was related to volcanic activity. Therefore it is important to consider that recurrent activity cannot be discarded in the future

Acknowledgements

This work was funded by P05 project of the Cemie-GEO SENER-CONACYT Consortium No. 2007032, as well as IN-106314 PAPIIT (UNAM) project.

References

Bhattacharya, T., Byrne, R., Böhnell, H., Wogau, K., Kienel, U., Ingram, B.L. and Zimmerman, S., 2015. Cultural implications of late Holocene climate change in the Cuenca Oriental, Mexico. *Proceedings of the National Academy of Sciences*, 112(6): 1693-1698.

Carrasco-Núñez, G., and Branney, M., 2005. Progressive assembly of a massive layer of ignimbrite with normal-to-reverse compositional zoning: the Zaragoza ignimbrite of central Mexico, *Bulletin of Volcanology*, 68: 3-20.

Carrasco-Núñez, G., Hernández, J., De León, L., Dávila, P., Norini, G., Bernal, J.P., Jicha, B., Navarro, M., López, P., 2017b. Geologic Map of Los Humeros volcanic complex and geothermal field, eastern Trans-Mexican Volcanic Belt. *Terra Digitalis* 1(2): 1-11.

Carrasco-Núñez, G., Bernal, J.P., Dávila, P., Jicha, B., Hernández, J., in press. Reappraisal of Los Humeros volcanic complex from U/Th (zircon) and Ar/Ar dating, implications for greater

geothermal potential. *Geochemistry, Geophysics, Geosystems*.

Dávila-Harris, P., and Carrasco-Núñez, G., 2014. An unusual syn-eruptive bimodal eruption: the Holocene Cuicuiltic Member at Los Humeros caldera, Mexico, *Journal of Volcanology and Geothermal Research*, 271: 24-42.

De la Cruz, V., 1983. *Estudio geológico a detalle de la zona geotérmica Los Humeros, Puebla, C.F.E. Mexico*, Internal report, 10/83, pp. 51.

Espinaza, R., 2006. *Field trip guide*. Association for Mexican Cave Studies Bulletin 19: 275-305.

Ferriz, H., and Mahood, G., 1984. Eruption Rates and Compositional Trends at Los Humeros Volcanic Center, Puebla, Mexico, *Journal of Geophysical Research*, 89, B10: 8511-8524.

Juárez, E., Böhnell, H., Nasser Mahgoub, A., Carrasco-Núñez, G., and Pavón-Carrasco, F.J., 2017. Paleomagnetism of Los Humeros caldera, and its contribution to the Holocene succession of lava flows. UGM abstract volumen.

Rojas, E., 2015. Rojas Ortega, E., 2016. Litoestratigrafía, petrografía y geoquímica de la toba Llano, y su relación con el cráter el Xalapazco, Caldera de Los Humeros, Puebla. URL: <https://colecciondigital.cemiegeo.org/xmlui/handle/123456789/509>

Examining the internal structure and the eruption dynamics of Parícutin monogenetic volcano (1943 – 1952, Mexico) inferred from ERT 3D model combined with historical and geological evidences

Xavier Bolós¹, Gerardo Cifuentes¹, José Luis Macías¹, Giovanni Sosa-Ceballos¹, Denis Ramón Avellán¹, Alexander Delgado-Torres¹

¹ *Institute of Geophysics, UNAM, Campus Morelia, 58190 Morelia, Michoacán, Mexico. xavier.bolos@gmail.com*

Keywords: Parícutin eruption, Phreatomagmatism, 3D resistivity model.

Parícutin is one of the most famous monogenetic volcanoes around the world because is the youngest volcano of the Michoacán-Guanajuato Volcanic Field (MGVF) and one of only two monogenetic eruptions occurred in historical times at the Trans Mexican Volcanic Belt: Jorullo (1759-1774) and Parícutin (1943-1952).

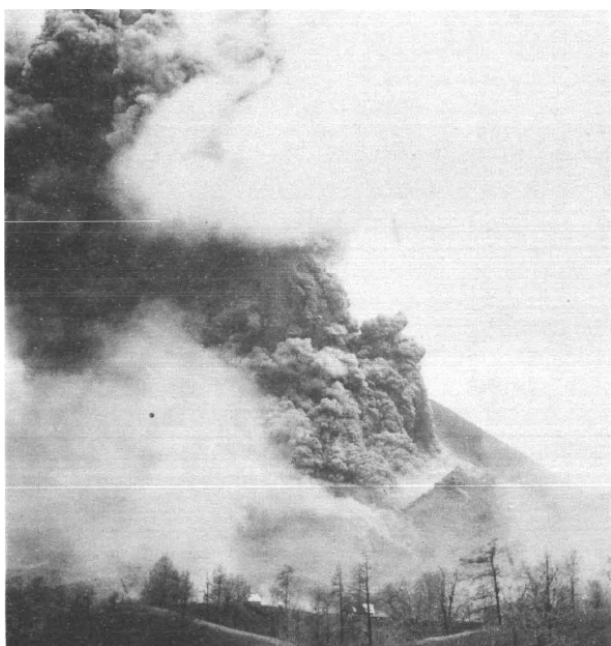


Fig. 1 – Picture of the Parícutin during a violent Strombolian eruption in 1943. Foto by Hugo Brehme.

August 2, 1943. The break in the cone in early afternoon. Huge jets of black ash play from the broken segment of the cone. The rocks, “Los Faroles,” that crown the ridge are beginning to move to the left. One of the craters of Cerro de Jaratiro is in the foreground (Foshag and González, (1956).

MGVF has an area of about ~40,000 km² that contains the largest concentration of monogenetic vents on Earth associated with a subduction-related continental arc, holding more than 1,100 edifices consisting of abundant scoria cones, semi-shield volcanoes with large effusive magma volumes, tens of lava domes, several maars, tuff rings and spatters (Hasenaka and Carmichael, 1985). Moreover, in this volcanic field, there are at least two stratovolcanoes

Tancítaro (3,845 m) and Patamban (3,450 m) despite being poorly studied probably they have an important role to understand magma ascents in this volcanic field.

The eruption of Parícutin volcano started on February 20, 1943, and ended on March 4, 1952 (Wilcox, 1954). It produced ~ 0.7 km³ of lava and 0.89–1.3 km³ of tephra (Fries, 1953) forming a large scoria along the eruptive fissure. The onset of activity was preceded by more than one month of enhanced regional seismicity perceived and described by local people. The volcano started with a fissural eruption in the middle of a cornfield emitting ash, sulfur-rich gases, and incandescent bombs. The main cone grew rapidly, reaching ~150 m in height at the end of the first month. Explosive activity was intense during the first three years (Fig. 1) although it accounts for ~75% of total eruption volume (Fries,1953). Of this, only 10% resides in the cone (Pioli et al., 2008). The remaining tephra extends over tens of km² and the ash was dispersed as far as Mexico City, about 400 km east of the vent (Velasco, 1945).



Fig. 2 – Photography of tephra deposit with cross-bedding inferred as an alternation of PDCs with Strombolian fall-out deposits.

The activity was associated with extensive lava effusions with different vents along the eruptive fissure, mainly during the last six years of the eruption. Lava flows covered the towns of Parícutin and San Juan Parangaricutiro. The activity of Parícutin changes the eruptive style during the eruption producing effusive and Strombolian activity, as well as violent Strombolian eruptions (Fig. 1) producing PDCs provably related to phreatomagmatism.

In the present work, we discuss the temporal events of the eruption insights from new stratigraphic sections that reveal PDCs diluted (Fig. 2) and using historical descriptions and pictures (Fig. 1). Moreover, we have carried out electrical resistivity tomography (ERT) using a non-conventional array in order to get profiles with any geometry. The same methodology was recently successfully implemented in an archaeological Maya pyramid (Chichén Itzá) obtaining a 3D model of its structure and discovering new hidden cameras (René et al., 2017). We applied the same method for the first time in volcanology in order to assess the eruption dynamics and the role of the basement in this area attempting to understand the behavior of the feeder dike and the plumbing system, which until now lacked any detailed geophysical data.



Fig. 3 – Location of the ERT profiles in a non-conventional array around the Parícutin volcanic cone.

We present this analysis in a 3D resistivity model interpreting the main structures observed. We detect high resistivity values corresponding to spatter facies and proximal well-welded pyroclasts. We also found that the main intrusion might be aligned with the orientation of the eruptive fissure. Our data shows that the hydrothermal system is generated by convection of groundwater supplied by the recharge of meteoric water in specific areas of the cone. The main volcanic edifice of Parícutin presents normal faults produced by the overburden of pyroclastic materials deposited during the eruption. The resistivity model suggests that these faults constitute the main pathways whereby hydrothermal fluids rise to the surface through the volcanic cone.

The results obtained in this study will help to explain changes in the explosive behavior during monogenetic eruptions, taking the case study of Parícutin from geo-

logical, geophysical and historical evidence in order to be extrapolated to other volcanoes of similar characteristics lacking direct information of the eruption.

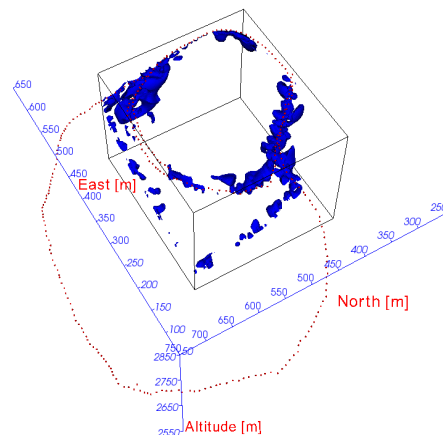


Fig. 4 – Preliminary 3D resistivity model of the Parícutin volcano. Values between 10 000 to 50 000 ohms-m showing the orientation of the feeder dike.

Acknowledgements

This study was partially funded by Instituto de Geofísica, Unidad Morelia. X. Bolós was funded by a UNAM-DGAPA post-doctoral fellowship (2016–2018). We also appreciate the collaboration of the ENES-UNAM students and other colleagues for their collaboration during the field campaign.

References

- Foshag, W.F., González, J., 1956. Birth and development of Parícutin Volcano Mexico. U.S.
- Fries Jr., C., 1953. Volumes and weights of pyroclastic material, lava, and water erupted by Parícutin volcano, Michoacán. EOS Trans. Am. Geophys. Union 34, 603–616.
- Hasenaka, T., Carmichael, I.S.E., 1985. A compilation of location, size, and geomorphological parameters of volcanoes of the Michoacan–Guanajuato volcanic field, central Mexico. Geofis. Int. 24, 577–607.
- Pioli, L., et al., 2008. Explosive dynamics of violent Strombolian eruptions: the eruption of Parícutin Volcano 1943–1952 (Mexico). Earth Planet. Sci. Lett. 271, 359–368.
- René E. et al., 2017. Short Note: Interior Imaging of El Castillo Pyramid, Chichen Itza, Mexico, Using ERT-3D Methods: Preliminary Results, Geofísica Internacional, 56 (2), 219–227, 2017.
- Velasco, A.H., 1945. Estudio de las cenizas del volcán caídas en la ciudad de México. El Parícutin, Estado de Michoacán, pp. 139–145.
- Wilcox, R.E., 1954. Petrology of Parícutin volcano, Mexico. U.S. Geol. Surv. Bull. 965-C, 281–353.

Garrotxa Volcanic Field as a Link to Young Martian Volcanism

Kei Kurita¹, Rina Noguchi², Hiroki Ichikawa³, H.Samuel⁴ and David Baratoux⁴

¹ Earthquake Res. Inst, Univ. of Tokyo, 113-0032 Tokyo, Japan. kurikuri@eri.u-tokyo.ac.jp

² Volcanic Fluid Research Center, Tokyo Institute of Technology, 152-8551 Tokyo, Japan.

³ ELSI, Tokyo Institute of Technology, 152-8551 Tokyo, Japan.

⁴ IRAP, CNRS, Toulouse, France.

⁴ Geosciences Environment, Toulouse, France.

Keywords: martian volcanism, delamination, transient lava field

Introduction

In this presentation we will discuss a probable link between Garrotxa Volcanic Field and the Martian young volcanic field such as lava field of the Central Elysium Planitia. Both volcanism occur at the specific region where the crustal thickness largely changes from extremely thick to thin regions. The structural similarity indicates detailed volcanotectonic understandings in the Garrotxa helps the martian study where material data and geophysical interior data are deadly deficient.

Martian Volcanism

Existence of various styles of volcanism on Mars has been revealed by recent analysis based on the high resolution satellite imagery: Keszthelyi et al., (2000), Platz et al., (2015), Grott et al., (2013), Vaucher et al., (2009), Broz et al., (2017), Peters and Christensen (2017). Although large shield volcanoes such as Olympus Mons are the most well-known volcanic construct there exist planetary-wide distributions of lava fields and small cones. Since these objects are small scale and relatively featureless among the surface geomorphological units their identification has been difficult and there still remain large number of undiscovered volcanic construct on Mars.

One of the surprising results in the martian volcanism is the discoveries of quite recent activity, which indicates the Martian interior is still active enough. Most of the young volcanisms have been identified as small cone fields: Broz et al., 2017 and lava fields: Hartmann et al., 1999, Vaucher et al., 2009. These transient activities are contrasting to the large shield-building volcanism in the points of effusion mass and activity duration and suggesting the formation mechanism seems different. The large shield volcanoes were formed by long-lasting magma effusion over hundreds million years, which are similar to the terrestrial hotspot volcanism. What kind of the internal process is responsible for the transient, more or less monogenetic activity on Mars where no plate tectonics is working is a fundamental issue in martian studies.

Working model for CEP lava field:

To explore the formation mechanism of transient lava field we describe one of the most recent activity occurred at the Central Elysium Planitia. This area is characterized by very smoothed surface indicating of coverage of low

viscosity lava flows. The existence of rootless cones at distant regions from the source (several hundreds kms away) suggests high temperature origin of the magma and fast emplacement process (Noguchi and Kurita, 2015). The interesting point is the location of CEP, which is situated at the boundary of north-south dichotomy. By gravity anomaly and topography variation moho depth is estimated assuming the material densities (Neumann et al., 2004). CEP is located just above the region where the moho depth changes largely from the deep southern hemisphere to the shallow northern hemisphere (Figure 2 right figure). This suggests us a probability of delamination of lower crust to induce volcanism which is proposed for the origin of basaltic volcanism away from the plate boundaries on the Earth (Lustrino 2005, Valera et al., 2011 for recent reference). Tectonically emplaced mafic lower crust at deeper region transforms to eclogite, which is denser than the upper mantle rocks delaminates and drops, which induces adiabatic rise of mantle materials as a compensation flow. This can result in a local melting. Since Mars is much smaller than the Earth the pressure at the base of the crust of southern hemisphere (~70 km) is less than the pressure of basalt-eclogite transition. Because of this eclogite has been considered implausible in the martian interior. Recently higher concentration of iron in the martian basaltic crust has been revealed (Baratoux et al., 2014) and higher concentration of iron is known to reduce the transition pressure, which makes delamination-induced volcanism on Mars plausible (Kurita et al., 2012). This is our working hypothesis for the origin of CEP volcanism. To substantiate the model deficiency of material data as well as internal structure is critical, which is a usual difficulty in the planetary research.

Link to Garrotxa Volcanic Field:

This is a reason why we are so much interested in the origin of Garrotxa Volcanic Field. The Garrotxa is also located just above the transition zone of moho-depth variation (Figure 2 left figure). Seismological and geodetic surveys has revealed absence of lower crustal root (Gunnell et al., 2008) and petrological and volcanotectonic studies discuss the composition of the present lower crustal materials by using xenolith (Bolós et al., 2015). We propose the Garrotxa Volcanic Field as a terrestrial analog for the martian young volcanism for the further study target.

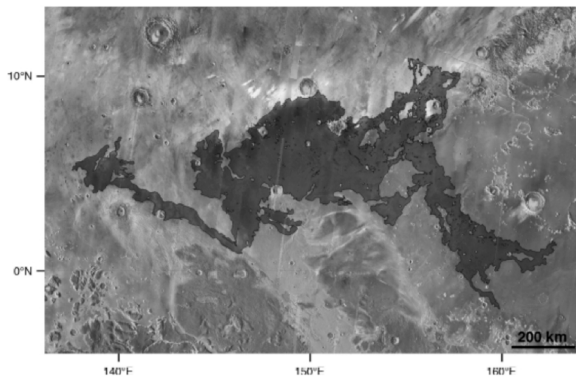


Fig. 1 – The lava field in the Central Elysium Planitia. Most of the lava flows are considered to emanate from the fissures at north-east end of the lava field, Cerberus Fossae (Figure after Jaeger et al., 2010)

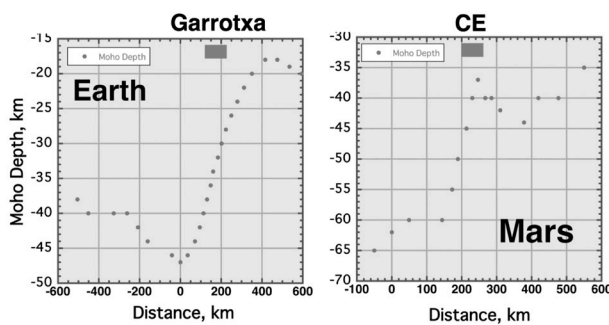


Fig. 2 – Moho depth variation in the eastern Pyrenees, Earth (Diaz and Gallart, 2009) and the CEP, Mars (Neumann et al., 2004)

References

- Baratoux, D., et al., 2014. Petrological constraints on the density of the Martian crust. *Journal Geophys. Res. E.*, 119:1707-1727.
- Bolós, X., et al., 2015. Volcano-structural analysis of La Garrotxa Volcanic Field (NE Iberia): implications for the plumbing system. *Tectonophysics* 642:58-70
- Broz, P., Hauber, E., Wray, J., Michael, G., 2017. Amazonian volcanism inside Valles Marineris on Mars. *Earth Planet. Sci. Lett.*, 473:122-130.
- Diaz, J., Gallart, J., 2009. Crustal structure beneath the Iberian Peninsula and surrounding waters: a new compilation of deep seismic sounding results. *Phys. Earth Planet. Inter.*, 173:181-190.
- Diniega, S., Sangha, S., Browne, B., 2018. Using satellite imagery to identify and analyze tumuli on Earth and Mars. *Earth Planet. Sci. Lett.*, 482: 52-61.
- Grott, M., et al., 2013. Long-term Evolution of the Martian Crust-Mantle System. *Space Science Review* 174: 49-111.
- Gunnell, Y., Zeyen, H., Calvet, M., 2008. Geophysical evidence of a missing lithospheric root beneath the Eastern Pyrenees. *Earth Planet. Sci. Lett.*, 276:302-313.
- Hartmann, W., et al., 1999. Evidence for recent volcanism on Mars from crater counts. *Nature* 397: 586-589.
- Jaeger, W., et al., 2010. Emplacement of the youngest flood lava on Mars: a short turbulent story. *Icarus* 205:230-243.
- Keszthelyi, L., McEwen, A., Thordarson, T., 2000. Terrestrial analogs and thermal models for Martian flood lavas. *Journal Geophys. Res.*, E 105: 15027-15049.
- Kurita, K., Ohmori, S., Noguchi, R., 2012. Delamination-induced magmatism as a source of recent Martian volcanism. *European Planetary Sci. Congress: EPSC2012-680*.
- Lustrino, M., 2005. How the delamination and detachment of lower crust can influence basaltic magmatism. *Earth Science Reviews* 72:21-38.
- Neumann, G., et al., 2004. Crustal structure of Mars from gravity and topography. *Journal Geophys. Res.*, E 109:doi 10.1029/2004JE002262
- Noguchi, R., Kurita, K., 2015. Unique characteristics of cones in Central Elysium Planitia, Mars. *Planet. Space Sci.*, 111:44-54.
- Peters, S., Christensen, P., 2017. Flank vents and graben as indicators of Late Amazonian volcanotectonic activity on Olympus Mons, *Journal Geophys. Res.*, E. 197: DOI 10.1002/2016JE005108.
- Platz, T., Byrne, P., Hiesinger, H., 2015. Volcanism across the inner solar system: an overview. *Geological Society of London Special Paper* 401: 1–56.
- Valera, J., Negredo, A., Jimenez-Munt, I., 2011. Deep and near-surface consequences of root removal by asymmetric continental delamination. *Tectonophysics*. 502: 257-265.
- Vaucher, J., et al., 2009. The morphologies of volcanic landforms at central Elysium Planitia: Evidence for recent and fluid lavas on Mars. *Icarus* 200: 39-51.
- Vaucher, J., et al., 2009. The volcanic history of central Elysium Planitia: Implications for martian magmatism, *Icarus* 204:418-442.

Field and experimental analysis of sediment–magma mingling at the 71 Gulch Volcano in the western Snake River Plain, Idaho, USA

Kadie Bennis, Alison Graettinger

University of Missouri – Kansas City, 5100 Rockhill Rd. Kansas City, Missouri, USA. kadie.bennis@mail.umkc.edu

Keywords: phreatomagmatism, pillow basalt, western Snake River Plain.

Phreatomagmatic eruptions result from the interaction of magma with groundwater, surface water, and/or wet sediment. The resulting deposits exhibit distinctive textures that contain evidence for the environment at the time of eruption, including the presence of and access to water. This evidence includes the distribution of exclusively subaqueous deposits, the geometry and structure of magmatic intrusions (including peperite), and the nature of the host sediment (grain size, porosity, and permeability). 71 Gulch Volcano in the western Snake River Plain, Idaho, USA, is an eroded basaltic fissure that erupted into a lake and preserves excellent examples of sediment–magma mingling and explosive and effusive activity in a shallow lake environment.

The western Snake River Plain (WSRP) is a normal-fault bounded basin located between the northern Rocky Mountains and the northern Basin and Range in southwestern Idaho (Wood 1994; Wood and Clemens 2002). During the Miocene–Pleistocene, Lake Idaho inundated the WSRP, resulting in the interaction of lacustrine sediment and magma within the basin (Wood and Clemens 2002). Volcanic activity during this time produced 400 basaltic vents, many of which interacted with the lake, including 71 Gulch (Németh and White 2009; Figure 1).

71 Gulch is an ideal field site to investigate shallow intrusive and eruptive processes into a shallow lake, because

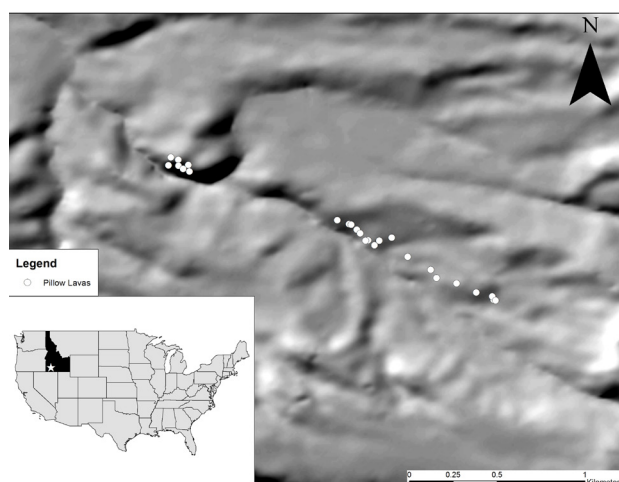


Fig. 1 – Hillshade of 71 Gulch Volcano (star) in reference to Idaho, USA. The white dots represent the locations of pillow lavas. Elevation increases from the west to east.

there are defined subsurface and defined subaqueous exposures. As Lake Idaho drained, the Snake River cut down into the pyroclastic deposits and lacustrine host rocks (Godchaux et al. 1992), which exposed the intrusive to eruptive interface. Further examination showed that deposits at 71 Gulch include shallow (<10 m), intrusive deposits that mingle with the host sediment and, in some instances, the eruptive products on the lake floor.

The purpose of this research is to establish the intrusive and eruptive environment of these deposits with a focus on distinguishing deposits that interacted with groundwater, lake water, or the atmosphere. We aim to define the lake bottom and the water level at the time of the eruption in order to constrain how much water the magma interacted with in both the subsurface and eruptive environment.

A detailed characterization of these deposits involved field work focusing on the distribution and relationships between intrusive, eruptive, and host lithologies, and sample collection for geochemical and microtextural analysis. There are two types of host lithologies at this field site: medium to coarse-grained sandstone and poorly sorted volcanoclastic deposits (ash to block sized particles). The sandstone is gray to beige in color and can exhibit bedding at a scale of tens of centimeters to meters. There are some well-rounded, pebble to cobble-sized lenses within the sandstone near the paleo-lake bottom. The volcanoclastic deposits are palagonitized lapilli tuffs with <0.5 m blocks and rare bombs of basalt.

71 Gulch displays a range of sediment–magma mingling textures in geometry and scale. Figure 2 is an example of such behavior as sandstone protrudes into a basaltic dike, which is shown brecciating into the host sediment to form peperite (Pp). In addition, there is evidence that pillow lavas formed both intrusively (pillowed dikes) and extrusively (pillow stacks on top of lacustrine sandstone). Intrusive, blocky, and fluidal peperite is found throughout the volcanic field, with clasts ranging from <5 cm to approximately 10 cm in size. Blocky peperite tends to occur in localities near tabular dikes. Fluidal peperite occurs near dikes with complex geometries.

The location, relative elevation, and distribution of pillow lavas (Figure 1) were mapped in addition to the location

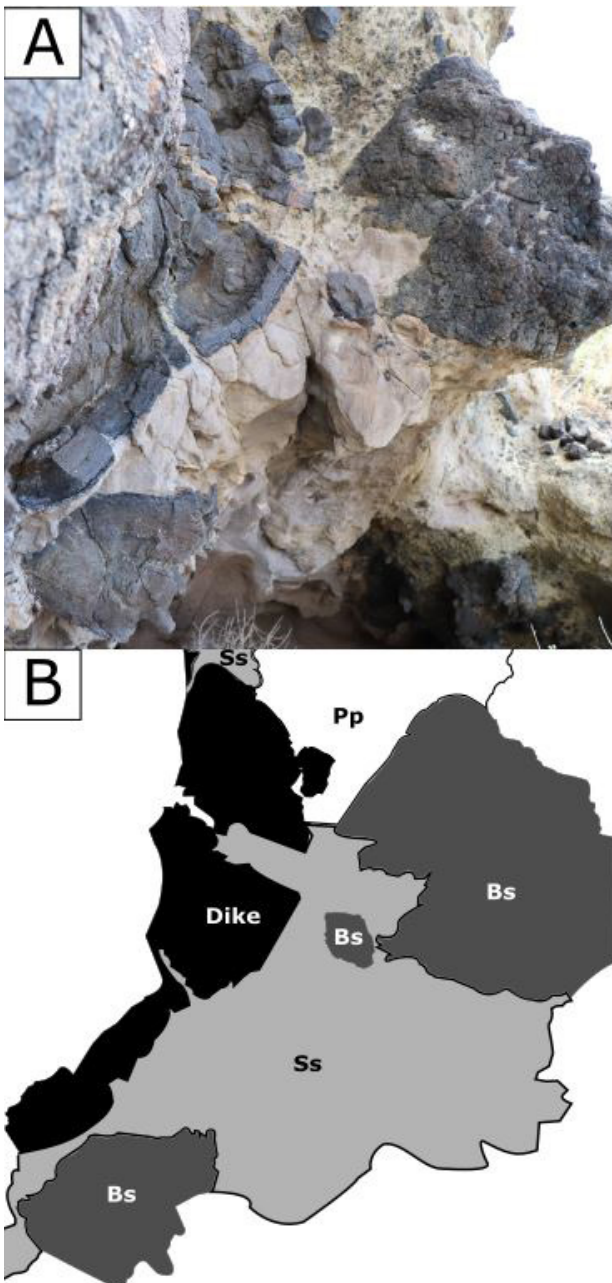


Fig. 2 – An example of a basaltic dike intruding into sandstone (Ss), creating an interface that shows the sandstone protruding into the dike. Some of the basalt (Bs) brecciates into the host sediment near the top, resulting in the formation of peperite (Pp).

of undisturbed lacustrine sediment/eruptive deposits contacts. Based on the pillow basalt with the highest and lowest recorded elevation, the calculated minimum depth of the water is approximately 106 m along a slope of 2.3°. In addition to mapped contacts between eruptive products and undisturbed lake sediments, these data help define the paleo-lake bottom, the water depth, and help constrain the overall paleoenvironment of 71 Gulch in its eruptive state. The presence of high elevation pillow lavas and extensive lapilli tuff-sandstone contacts suggest that 71 Gulch erupted in an entirely subaqueous volcanic environment in contrast with previous descriptions by Németh and White (2009).

Microtextural analyses using thin sections characterized the interface between the sediment and magma at millimeter to centimeter scales. This included noting any protrusions, the exchange of particles/fragments between sediment and magma, the presence and alignment of crystals along the interface, and determining the abundance and distribution of sideromelane and tachylite along this interface.

With the increase in experimental capabilities involving remelted basaltic rock, it is possible to create synthetic sediment-magma interfaces for comparison to these natural examples. Small-scale preliminary tests were conducted and they are important to establish the scale and conditions required to reconstruct sediment-magma mingling in larger experiments in conjunction with experiments investigating phreatomagmatic explosions. Both the natural and the synthetic textures will provide a basis for comparison for future investigations into sediment-magma mingling in the field and laboratory.

References

- Godchaux, M.M., Bonnicksen, B., Jenks, M.D., 1992. Types of phreatomagmatic volcanos in the western Snake River Plain, Idaho, USA. *Journal of Volcanology and Geothermal Research* 52: 1–25.
- Godchaux, M.M., and Bonnicksen, B., 2002. Syneruptive magma-water and posteruptive lava-water interactions in the western Snake River Plain, Idaho, during the past 12 million years, in Bill Bonnicksen, C.M. White, and Michael McCurry, eds., *Tectonic and Magmatic Evolution of the Snake River Plain Volcanic Province: Idaho Geological Survey Bulletin 30: 387-434.*
- Németh, K., White, C.M., 2009. Intra-vent peperites related to the phreatomagmatic 71 Gulch Volcano, western Snake River Plain volcanic field, Idaho (USA). *Journal of Volcanology and Geothermal Research* 183, 30–41.

Wood, S.H., 1994. Seismic expression and geological significance of a lacustrine delta in Neogene deposits of the western Snake River plain, Idaho. *AAPG bulletin* 78: 102–121.

Wood, S.H., Clemens, D.M., 2002. Geologic and tectonic history of the western Snake River Plain, Idaho and Oregon in Bill Bonnicksen, C.M. White, and Michael McCurry, eds., *Tectonic and Magmatic Evolution of the Snake River Plain Volcanic Province: Idaho Geological Survey Bulletin 30: 69-103.*

A Tale of Two Fluids: Water and Magma in the Shallow Subsurface

Michael Ort¹, Michaela Kim¹, Emily S. Anderson¹, Curtis M. Oldenburg²

¹ SESES, Box 4099, Northern Arizona University, Flagstaff, AZ 86011, USA. michael.ort@nau.edu

² Energy Geosciences Division, Lawrence Berkeley National Laboratory, Berkeley CA 94720, USA

Keywords: anisotropy of magnetic susceptibility, groundwater ascent, shallow magma storage.

Phreatomagmatism requires the interaction of water and magma, but how do these two fluids come into contact with each other? We present a study of magma movement within dikes just below the diatreme level and link it to a study of how such magma may heat water, thereby driving the water up into the country rock and diatreme where it can interact with magma at shallow levels.

The Jagged Rocks Dike Complex is in the southern Hopi Buttes Volcanic Field of northern Arizona, USA. Re et al. (2015, 2016) and Muirhead et al. (2016) show that the dike-and-sill system, which extends about 2.5 km in a northwest-southeast trend with several parallel strands and many en-echelon offsets, is the feeder system for a few maar-diatremes. Current exposure, ~350 m below the pre-eruptive surface, reveals the dike cutting through the soft silts of the Upper Triassic Chinle Formation. The Jurassic Moenave Formation, a lithified sandstone, and the Miocene Bidahochi Formation, similar in texture to the Chinle Formation, were the overlying units at the time of eruption (~7 Ma). The Moenkopi Formation, a lithified sandstone, underlies the Chinle Formation.

We studied the rock fabric, using anisotropy of magnetic susceptibility (AMS) and anisotropy of anhysteretic remanent magnetization (AARM) of the dike segments of the northwest sector of Jagged Rocks (Kim, 2017). Zones, based upon vesicle and crystals and groundmass texture, were identified at the margins and the centers of the dikes. The margins are glassy and appear to be chilled, whereas the middles tend to be devitrified and have larger vesicles. Sampling involved drilling 12-15 cores from each zone, called a site (thirty sampled in total). Sites were located on each margin and the middle of the dike at each locality and, in some cases, in two more zones between the margins and middle of the dike.

AMS data are presented as K1, K2, and K3 axes, with K1 being the maximum and K3 the minimum susceptibility. In dikes, the K1 direction is typically parallel to either the elongation of the magnetic grains (shape anisotropy) or the distribution of equant grains within the matrix (distribution anisotropy). In cases of rapid cooling, though, single-domain magnetic grains can have elongations perpendicular to their susceptibility axes. To check for this, we used AARM techniques, which are not affected by this problem. In all cases, the AMS data appear to be interpretable as parallel to the elongation or distribution of grains.

The most striking feature of the AMS results (Fig. 1) is that the K1 axis is typically near horizontal and in the plane of the dike. Most sites have K2 in the plane of the dike, typically near vertical, and K3 is perpendicular to the dike plane (i.e. directed into the country rock). This is interpreted to indicate that flow was within the plane of the dike, as expected, but it was flowing horizontally and not vertically. This is true for the initial flow of the dike segments, as recorded at the margins, and during later flow in the middle of the dikes. Many sites show imbrication of the K1 directions from their two margins that indicate flow was to the northwest along the dikes.

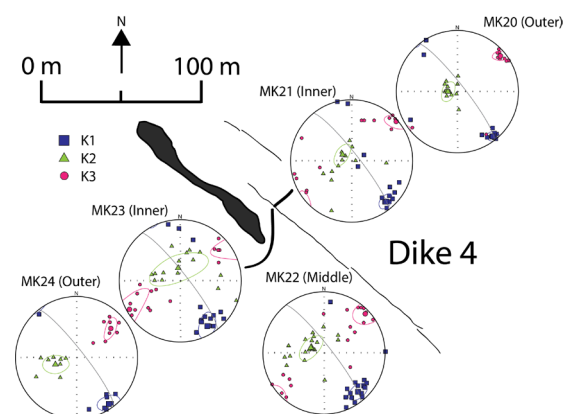


Fig. 1 – AMS data for dike segment 4. K1 and K2 axes are in dike plane (shown as line), with K1 ~ horizontal.

The dikes and sills form massifs of fragmented juvenile and country rock material in several places. Re et al. (2015, 2016) interpret these as underlying maar-diatremes and presumably are where magma ascended. These rocks are fragmental and were not sampled in our study. This leads

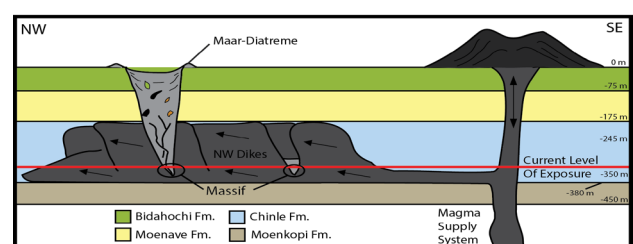


Fig. 2 – Model for how dike-sill complex formed at Jagged Rocks. Current level of exposure is indicated.

us to interpret the dikes and sills as representing magma storage during the eruptions, which indicates that the “footprint” of the maar-diatremes was widespread and significant amounts of magma, and heat, were emplaced in the shallow subsurface. A magnetic survey indicates these intrusions have shallow bottoms (<30 m below current exposure) at the base of the Chinle Formation.

Modern models for maar-diatreme systems include explosions happening at many different levels within the diatremes. This requires that water be present at these levels. Some water can be “thrown” there, moving upward as liquid and vapor through repeated explosions, much as clasts can move upward and downward in the diatremes. However, significant amounts of water will leave the system through explosions and as vapor rising out of the crater. In addition, some maars form in areas where the water table is far below the level at which explosions could throw material out to start forming a crater. How does water get up to shallow enough levels to form the maar? Finally, Jorullo volcano in Mexico produced hot mud flows, pouring out of the ground, for many days early in the eruption. Can magmatic heat lead to water ascent during eruptions, helping to provide water at high levels in diatremes?

Anderson (2017) used the TOUGH2 code to model heat transfer and water movement in vapor and liquid forms during shallow intrusions and eruptions. The base conditions included an eolian sandstone aquifer with overlying limestone, both with fractures in them. Two maars in the San Francisco Volcanic Field of northern Arizona were models for the base conditions. The initial water table was at 345 m depth.

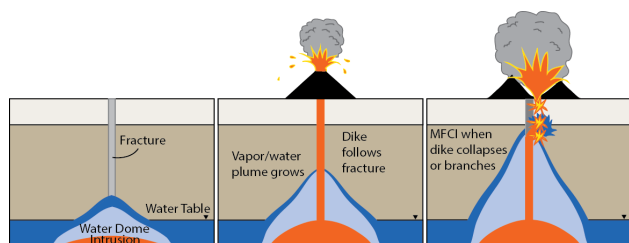


Fig. 3 – Schematic diagram of possible maar-forming eruption. Eruption begins with dry intrusion, but magma body near water table drives up a large quantity of vapor and condensed water, which then interacts with branching or collapsing dikes for phreatomagmatic explosions. This can form a diatreme with repeated events

Results show that, in the absence of a high-permeability zone (a fracture), the water heats, vaporizes, flows upward, and condenses to form a “water dome” above the intrusion, rising to ~265 m within 4.4 days. With a fracture present, the water rises much farther along the fracture, in most cases reaching, or nearly reaching, the surface within days. Water forms a condensation zone around the fracture, extending out 40-60 meters. In many natural systems, more fractures would be present over that distance, creating a more continuous zone of water above the previous water table. Putting an ascending intrusion into the fracture caused the water to move upward fast-

er, but dried out the rock close to the intrusion. Another experiment tested a magma injection below the water table for eight days. This drove a much larger body of water toward the surface. Depth to the water table matters – we used “extreme” depths and found the water could rise close enough to the surface for explosive water-magma interaction. In places with shallower water tables, the water rise is much faster and more water is available at high levels. Such systems might expel hot water, such as at Jorullo, or gas at the surface and would provide abundant water within the diatreme, which is equivalent to a large, high-permeability fracture. This would facilitate magma-water interaction in diatremes and provide a steady source of water to the entire diatreme from base to maar. We suggest that maar-diatremes may have significant magma intrusion/storage systems beneath them and that these can transfer much of their abundant heat to the groundwater, leading to its ascent in fracture zones and diatremes, where it can be involved in phreatomagmatic explosions. Dikes supply magma into the diatreme and unstable conditions there allow the water and magma to come into contact. This may be a more efficient method than explosive transport of non-interactive water to provide abundant water to maar-diatremes.

Acknowledgements

We thank James White, James Muirhead, and Giuseppe Re for extensive discussions.

References

- Anderson, E.S., 2017. An investigation of the role of thermal conditions, hydrologic processes, and country-rock permeability in maar eruptions. MS Geology thesis, Northern Arizona University, 155 p.
- Kim, M., 2017. Flow behavior and emplacement of the northwest dike swarm in the Jagged Rocks Complex, Hopi Buttes Volcanic Field, Arizona. MS Geology thesis, Northern Arizona University, 108 p.
- Muirhead, J.D., Van Eaton, A.R., Re, G., White, J.D.L., Ort, M.H., 2016. Monogenetic volcanoes fed by interconnected dikes and sills in the Hopi Buttes volcanic field, Navajo Nation, USA, *Bulletin of Volcanology* DOI:10.1007/s00445-016-1005-8.
- Re, G., White, J.D.L., Ort, M.H., 2015. Dikes, sills, and stress-regime evolution during emplacement of the Jagged Rocks Complex, Hopi Buttes Volcanic Field, Navajo Nation, USA. *Journal of Volcanology and Geothermal Research*. DOI: 10.1016/j.jvolgeores.2015.01.009.
- Re, G., White, J.D.L., Muirhead, J.D., Ort, M.H., 2016. Subterranean fragmentation of magma during conduit initiation and evolution in the shallow plumbing system of the small-volume Jagged Rocks volcanoes (Hopi Buttes Volcanic Field, Arizona, USA). *Bulletin of Volcanology* DOI 10.1007/s00445-016-1050-3.

How the early syn-eruptive crater infill progressively becomes the lower diatreme: Round Butte, Hopi Buttes volcanic field, Navajo Nation, Arizona

Benjamin Latutrie¹, Pierre-Simon Ross¹

¹ Institut National de la Recherche Scientifique, Centre Eau Terre Environnement, 490 Rue de la Couronne, Québec (QC), G1K 9A9, Canada: Benjamin.Latutrie@ete.inrs.ca

Keywords: diatreme, crater, eruptive processes

The Miocene Hopi Buttes volcanic field (HBVF) in the Navajo Nation (Arizona, USA) provides excellent exposures of maar-diatreme volcanoes (White and Ross, 2011) at different erosion depths, from the maar ejecta ring and crater infill (White, 1991) to the deep diatreme (Lefebvre et al., 2013). The base of the current exposure at Round Butte, in the eastern part of the HBVF, lies ~190 m below the pre-eruptive surface. At this depth, the Round Butte diatreme is ~130 m in diameter and the exposure consists of 30 m high cliffs. The diatreme displays an intriguingly complex history, given its relatively small size. We carried out one month of field work there as part of the first author's PhD project. Geological contacts were mapped on high resolution pictures of the cliffs (Fig. 1). We described and sampled all the units defined during the mapping and then did componentry measurements using the line count method proposed by Lefebvre et al. (2013).

The upper part of the diatreme (syn-eruptive crater infill) is composed of two main bedded pyroclastic units. The older bedded unit is coarse grained (lapilli tuff), diffusively to well bedded, and heterolithic (mixture of juvenile fragments and lithics in sub-equal proportions). It contains a number of megablocks of Bidahochi Formation, the youngest formation in the country rock stratigraphy (Billingsley et al., 2013). The older bedded unit has locally suffered liquefaction and has been invaded by debris jets in many places. The debris jets created "invasive" columns

of non-bedded material, between which domains of early diffusely bedded crater infill are left; we call these "residual columns" (Fig. 1).

The younger bedded unit, mostly consisting of thick, lenticular to planar, lapilli tuff to tuff breccia beds, represents the late syn-eruptive crater infill. The composition mostly ranges from heterolithic to juvenile-rich. The younger bedded unit does not have the disturbed aspect of the older one and is not clearly cut by invasive columns. It was deposited on top of an unconformity where subvertical columns are truncated (Fig. 1). At least on the South face, the late bedded unit was fed by a vent which we informally call the "main vent" (Fig. 1, middle). The upper bedded unit is generally poor in Bidahochi megablocks. Non-bedded pyroclastic rocks are also found at Round Butte. They range in grain size from fine lapilli tuff to tuff breccia and vary in composition from juvenile-rich to heterolithic, with a great diversity of lithics clasts, including some sourced from the Moenkopi Formation ~440 m below the pre-eruptive surface. The non-bedded rocks form invasive columns into the older bedded unit, and sometimes invasive columns emplaced into other invasive columns, a feature typical of lower diatemes (Lefebvre et al., 2013). In the southwest part of the diatreme, a relatively large debris avalanche crops out (Fig. 1, lower left). This deposit shows a succession of Moenave Formation breccias and liquefied Bidahochi Formation, intercalated by a pyro

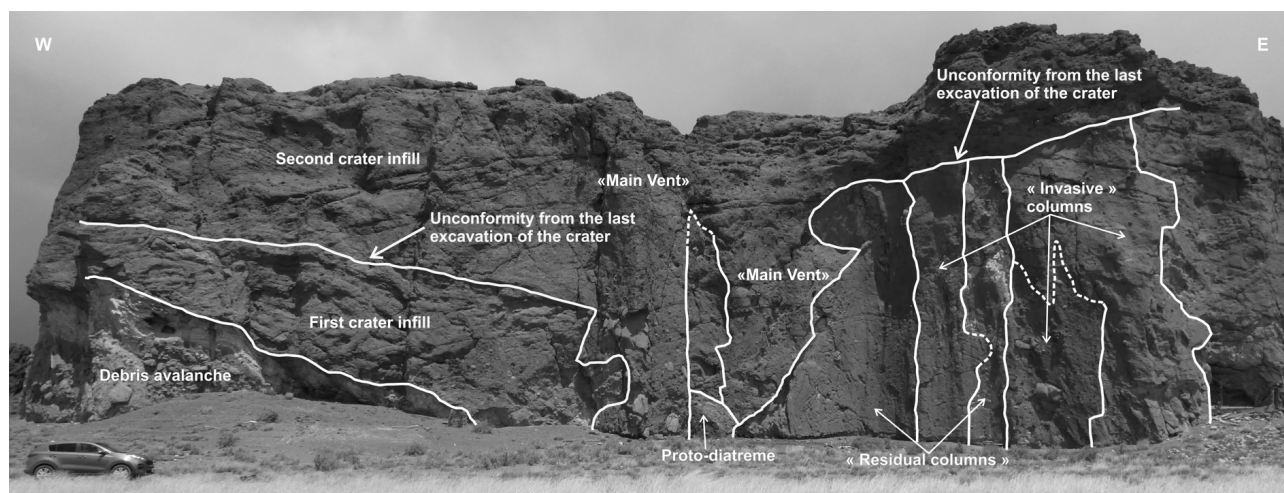


Fig. 1 – South face of Round Butte diatreme in the Hopi Buttes volcanic field. The cliff displays a complex history with two phases of crater infill and the transition between upper and lower diatreme.

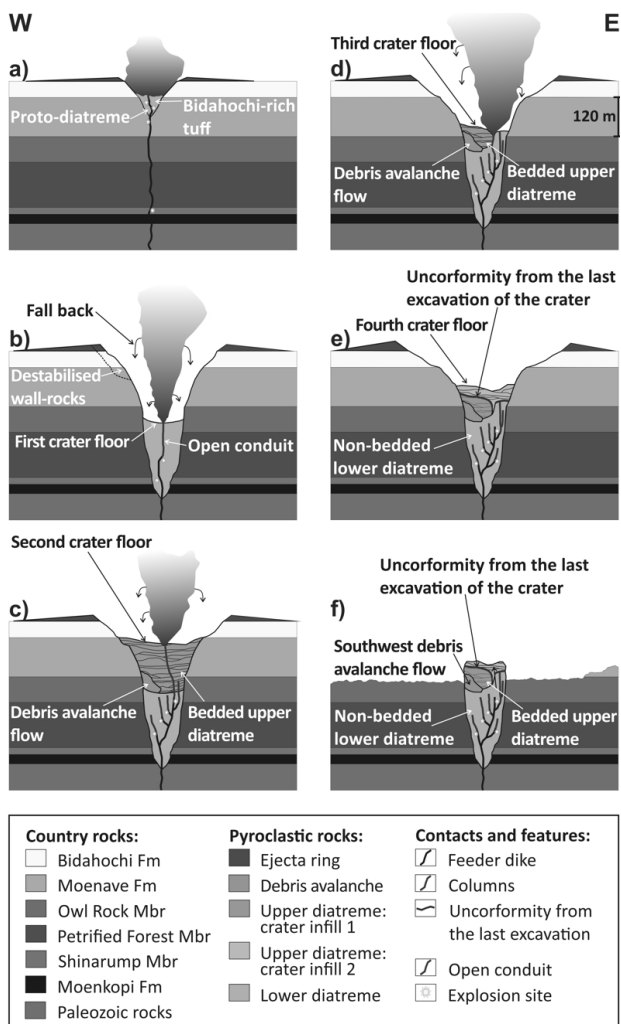


Fig. 2 – Preliminary model displaying the formation of the different units at Round Butte diatreme.

clastic level. Our preliminary model has six steps (Fig. 2).

(a) A dike rises and interacts explosively with a wet substrate. This creates the initial crater and a proto-diatreme, now found preserved locally as a megablock of Bidahochi-rich bedded pyroclastic rock cut by a coherent dike on the South face (Fig. 1, middle).

(b) A phase of intensely explosive activity leads to deep excavation of the country rock, creating a crater deeper than the current lower level of exposure, and probably a significant ejecta ring on top of the initial paleo-surface.

(c) Crater excavation triggers the debris avalanche, emplaced in several stages during which explosive activity continued. The older crater infill is deposited. Megablocks of the Bidahochi Formation are falling repeatedly, leading to lateral enlargement of the crater. The early ejecta ring is also partly recycled, and is now found as lapilli- to megablock-sized fragments of bedded tuff and lapilli tuff in the early crater infill. Continued infilling by pyroclastic material leads to the crater level being higher than the top of the current outcrop. This early crater infill becomes locally liquefied, blurring some of the bedding. Else-

where it is invaded by debris jets (White and Ross, 2011), the passage of which also disturbs bedding, and creates non-bedded invasive columns. Residual columns, with mostly destroyed bedding, are left between the invasive columns. This is how the (bedded) early syn-eruptive crater infill progressively evolves into the (non-bedded) lower diatreme.

(d) Another period of intensely explosive activity leads to the second major excavation phase. This digs into the early bedded pyroclastic rocks and locally exposes the non-bedded pyroclastic rocks at the bottom of the new crater, creating the “unconformity”.

(e) The younger bedded pyroclastic unit is deposited on top of the unconformity and explosive activity ends. Post-eruptive crater infilling might have taken place but is not preserved.

(f) Erosion leads to the current outcrop with typical inverted topography.

Acknowledgements

James D.L. White did the early work on Round Butte and introduced PSR to this fascinating volcano. Pier-Paolo Comida helped us in the field. We thank the Morris family for allowing us to work at Round Butte. Any persons wishing to conduct geological investigations on the Navajo Nation must first apply for, and receive, a permit from the Navajo Nation Minerals Department, P.O. Box 1910, Window Rock, Arizona 86515, USA, telephone 1-928-871-6587.

References

- Billingsley, G.H., Block, D., Hiza-Redsteer, M. 2013. Geologic map of the Winslow 30' x 60' quadrangle, Coconino and Navajo Counties, northern Arizona. US Geological Survey Scientific Investigations, Map 3247, Scale 1:50000.
- Lefebvre, N.S., White, J.D., Kjarsgaard, B. 2013. Unbedded diatreme deposits reveal maar-diatreme-forming eruptive processes: Standing Rocks West, Hopi Buttes, Navajo Nation, USA. *Bulletin of Volcanology* 75:739.
- White, J.D. 1991. Maar-diatreme phreatomagmatism at Hopi Buttes, Navajo Nation (Arizona), USA. *Bulletin of Volcanology* 53:239-258.
- White, J.D., Ross, P-S. 2011. Maar-diatreme volcanoes: a review. *Journal of Volcanology and Geothermal Research* 201:1-29.

Kiejo-Mbaka (Rungwe Volcanic Province, Tanzania) monogenetic volcanic field evolution

Claudia Principe¹, Fatumati Mnzava², Claudio Pasqua³

¹ Institute of Geosciences and Earth Resources, National Researches Council, Via Moruzzi 1, 56124 Pisa, Italy - c.principe@igg.cnr.it

² Tanzania Geothermal Development Company Limited (TGDC).

³ ELC-Electroconclut S.p.A. Via Marostica 1, 20146 Milano, Italy

Keywords: : Kiejo-Mbaka, maar field, cinder cones, geothermal energy

Here we present the results of a geological survey performed during 2017 in the Kiejo-Mbaka area (KM), that is part of the Rungwe Volcanic Province (RVP) in Tanzania. The survey was addressed to the geothermal exploration of this area in the framework of a project of "Surface Exploration and Training in Luhoi and Kiejo-Mbaka Geothermal Areas" (project No 1767-GSE). In order to define the geothermal potential of this area, a geological mapping at the scale of 1:25.000 of an area of approximately 300 km² was performed, integrated by the complete stratigraphy of the volcanic deposits, volcanic facies analysis and volcano-tectonic mapping of a "wide area" of about 600 km².

The Rungwe Volcanic Province (RVP), is part of the East African Rift System (EARS). The RVP is located at the northern end of Lake Nyasa, where the EARS splits up into its Western and Eastern branches around the Tanzanian craton (Fig. 1).

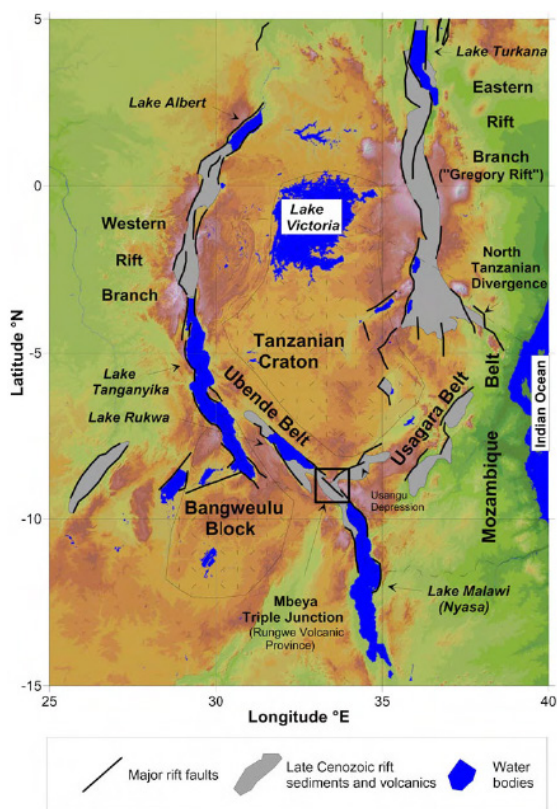


Fig. 1 - Location of RVP (Mbeya Triple Junction) regarding the Basement and the rift structure, on the background of a SRTM DEM. The study area is indicated by the black square (from Delvaux et al., 2010)

The Quaternary volcanism in this area is the southernmost expression of volcanism associated with the current rifting event and is mainly characterized by the alkaline products of the RVP. The RVP consists of three major eruption centers, namely Ngozi, Rungwe, and Kiejo volcanoes and several small monogenetic volcanic edifices. The last eruption of Kiejo volcano occurred in historic times, at about 1,800 A.D. (Harkin, 1960). Three main volcanic activity stages are described in the RVP by previous authors (e.g. Fontijn et al., 2012) as follows: (1) Late Miocene: 9.2-5.4 Ma; (2) Late Pliocene-Early Pleistocene: 3.0-1.6 Ma; (3) Mid-Pleistocene-Recent: since 0.6 Ma.

Monogenetic volcanism resulted to have characterized the great part of the volcanic activity in in KM and to be strongly related to the tectonic and volcano-tectonic history of this area. The volcanic history of the KM area starts in the morphological low resulting from the Livingstone rift faulting. The oldest volcanic activity is represented by the occurrence of a series of phonolitic domes probably corresponding to one rift step fault, which is now covered by subsequent volcanic deposits and sediments. The Late Pliocene rift activity in KM is represented by the Karonga lava flows of basaltic composition that are straightforwardly interpreted as the products of fissural eruptions which occurred along the rift fault. Afterwards there was a period of eruptive stasis, concurrent with the decrease in the level and extension of Nyasa Lake.

Subsequently, the Mbaka faulting episode took place. Afterwards, during a period of ca. 1 Ma (from ca. 2.5 to 1.5 Ma), the Kiejo-Mbaka area experienced three major events: (i) the formation of the Mwakaleli caldera, with the related Katete Ignimbrite emplacement; (ii) the dissemination along the steps of the Mbaka fault of a number of cinder cones with very primitive (olivine-basalt) scoriae and lava deposits; (iii) the construction of the Tukuyu basaltic shield volcano. Along the Mbaka fault-related elements, which are buried by the ignimbritic deposit, there are a number of monogenetic cinder cones and related lava flows of basaltic, olivine-basaltic, and ankaramitic composition. They represent the last magmas that raised along the deep Mbaka fault structural elements. On the other side of the Mbaka river valley, the Tukuyu basalt and olivine-basalt lava flows cover the Nyasa lake sediments filling the southernmost portion of the Mbaka valley and come in contact with the metamorphic basement. After about a million years of rest, volcanic activity re-started in the Kiejo-Mbaka area, with the birth of the Kiejo volcano, dating back up to ca. 0.4 ka. The latest volcanic activity in

the K-M took place with the Sarabwe monogenetic eruption, dated at the 19th century, which seems to be related to the reactivation of the N-S tectonic trend rather than to the continuation of the Kijejo central volcano activity.



Fig. 2 – From Top to bottom: the Kyungululu maar, the nested maar craters at Ibale, and the Ikafu maar,.

Even if a central edifice certainly exists, the dimension of the Kijejo volcanic center has been overestimated into the literature, probably due to its prominent morphological position on the Southern border steps of the Mwakaleli caldera, and because of the superimposition of a number of monogenetic centers. There are a Phonolitic dome and at least five maar craters, three of them aligned on a fault related to the Mbaka trend at the intersection with NS-trending tectonic elements. Twenty maar craters (Fig. 2) was found inside KM. Maar edifices are distributed throughout the prospect, being systematically aligned at the crossing of NS-trending tectonic elements with other tectonic structures. They all belong to the same relatively recent stratigraphic unit that follows the positioning of few cinder cones with related picritic basaltic lavas, at the crossing of N040°-050° elements with the main outcropping step of the Mbaka fault. Maar-related explosion breccia deposits was investigated. From the petrographic point of view, the juvenile fraction of all the sampled maar deposits provides the evidence that no extremely volatile-rich, olivine-melilitic or carbonatitic magmas, are present in the KM maars, differently than in the case described in North Tanzania by Berghuijs & Mattsson (2013). As a matter of fact, KM maar-producing vents emitted basalts. This fact induces to interpret the fragmentation of these deposits, where present, as phreatomagmatic instead of magmatic fragmentation.

Acknowledgements

It's our grateful to thanks all who played their role and made this to happen; just to mention few, we thank the Icelandic International Development Agency (ICEIDA) for financially support and technical guide, the Tanzania Geothermal Development Company (TGDC) for technical support and provision of conducive working environment and the Electroconsult (ELC) for the trust and made us to be part of the team on accomplishing the Kyejo-Mbaka project.

References

- Delvaux D, Kraml M, Sierralta M, Wittenberg A., Mayalla JW, Kabaka K, Makene C (2010): Surface Exploration of a Viable Geothermal Resource in Mbeya Area, Sw Tanzania. Part I: Geology of the Ngozi - Songwe Geothermal System. Proceedings World Geothermal Congress 2010 Bali, Indonesia, 25-29 April 2010.
- Fontijn K, Ernst GGJ, Bonadonna C, Elburg MA, Mbede E, Jacobs P (2012). The 4 ka Rungwe Pumice (SW Tanzania): a wind-still Plinian eruption. Bulletin of Volcanology 73, 1353–1368.
- Harkin, DA (1960): The Rungwe Volcanics at the northern end of Lake Nyasa. Mem Geological Surv. Tanzania, 2, 172 pp.

The Stolpen Volcano in the Lausitz Volcanic Field (Eastern Germany) – Studies at the type locality of ‘basalt’

Olaf Tietz¹ and Jörg Büchner¹

¹ Senckenberg Museum of Natural History Görlitz, 02826 Görlitz, Germany. olaf.tietz@senckenberg.de

Keywords: Basanite, Cenozoic, History of Geoscience

The Stolpen Castle Hill (Fig. 1), which was designated in Germany as a “national geotope” (Goth & Suhr 2007) represents the type locality for the rock name basalt. Agricola had used and published this term the first time in connection with Stolpen in the year 1546 in his publication “De natura fossilium” (Fig. 2). The term basalt stretches back to Antique time, especially to Gaius Plinius Secundus (Pliny the Elder, AD 23–79). Agricola (1546) does not call Pliny, but the content clearly follows Pliny (ca. 77). Violently discussed was considered the term basalt in the early modern period since the first use by Agricola (1546).



Fig. 1 – Stolpen Castle Hill – the type locality for the term “basalt” – with inclined basaltic columns at the western edge.

Various source analyses in antique writings and the find of a new hand written copy from Pliny (ca. 77) in the year 1851 makes it probable, that Pliny had not use the term ‘basalten’, but instead the term ‘basaniten’ (Krafft 1994). It is probably a corruption! Beside this scribal error by the handmade copies of the original manuscript, also the rock type described by Pliny is not clear. Probably it was not basalt in today’s sense, because Pliny does not mention the typical columns, in contrast to Agricola, he described only the strong hardness and the grey colour like iron. Therefore, various other rock types are also considered in the literature, e.g. lydite or greywacke. Also the regional localization of the “basalt” from Pliny in Egypt and/or Ethiopia is not helpful for the determination of the described rock by Pliny; because she is to general and the text translation is ambiguous (it could also mean Egyptian instead of Egypt). Also not the mentioned sculptures and buildings, which Pliny connected with his “basalt”

description, can help, because these objects exist not today or probably only as copy (for the last three topics see among others Humboldt 1790). But the term ‘basaniten’ could also be descended from the ancient landscape Baschan/Basan in Jordan/Syria (Kammerzell 2000, p. 121, footnote 13), and there exists really much basalt! For the reasons mentioned above, it is difficult today to determine the etymologically origin and the rock type, which Pliny has originally meant. Presumably, that can barely satisfactorily clarified today. Nethertheless, Agricola had described a basaltic rock with the use of the term basalt at first time from the Castle Hill Stolpen in Saxony (East Germany).



Fig. 2 – Georgius Agricola (1494–1555) had described the first time the rock basalt from the Stolpen castle hill 1546:

“Super hunc basalten Stolpa arx episcopi Miseni est extracta” (© alamy stock photo).

Since Agricola (1546) many different investigations took place at the basaltic Stolpen Castle Hill, for detail information see the explanation by Büchner et al. (2017). The rock age of the Stolpen basalt is after one K-Ar-isotopic determination $25.3 \pm 0,5$ Ma (Pfeiffer et al. 1984), but K-K isotopic age determinations in the Lausitz Volcanic Field (Büchner et al. 2015) suggests an older age of about 30 Ma. New mineralogical (QAPF) and geochemical (TAS) research into the petrography of the Stolpen lava rock was undertaken by Büchner et al. (2017). The preliminary results reveal that, in the context of present rock nomenclature, the rock at Stolpen Castle Hill is not basalt and is rather best described as basanite with tendencies towards nephelinite, a typical

rock type in the Lausitz Volcanic Field (Fig. 3). Therefore and based on the further demonstrated inhomogeneities in the Stolpen lava rock, the Stolpen Castle Hill is not in a scientific sense a suitable type locality for basalt or basanite. However, outcropping volcanic rocks as well as its scientific historical importance undoubtedly give Stolpen relevance as a type locality for volcanic rocks.

The example of Stolpen poses the question of to what extent historical type localities can be combined with present day rock nomenclature. And furthermore, the question arises whether the definition of type localities for natural rocks makes sense, because these often show transitions and convergences; homogeneous rock bodies occur rarely or not at all in nature.

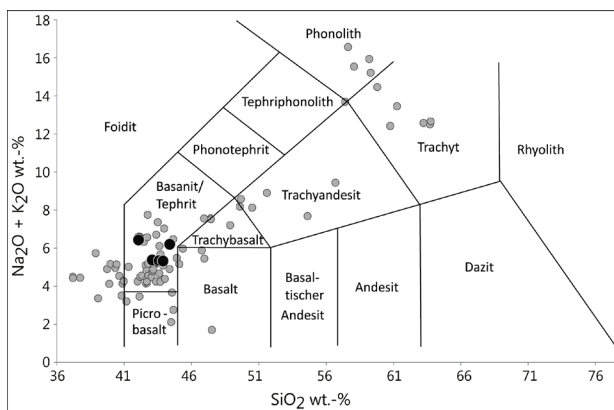


Fig. 3 – TAS diagram of lava rocks from Stolpen Volcano (black) in comparison with the Lausitz Volcanic Field (grey) (Büchner et al. 2017).

References

Agricola, G. 1546. De natura fossilium lib. X. – Basel; H. Froben. In: H. Prescher (ed.): Georgius Agricola: De natura fossilium libri X. Die Mineralien. translated in German and edited by G. Fraustadt in connection with H. Prescher; Gedenkausgabe des Staatlichen Museums für Mineralogie und Geologie zu Dresden, Issue IV, Berlin; VEB Deutscher Verlag der Wissenschaften 1958: pp. 548.

Büchner, J., O. Tietz, L. Viereck, P. Suhr & M. Abratis 2015. Volcanology, geochemistry and age of the Lausitz Volcanic Field. International Journal of Earth Sciences 104: 2057–2083

Büchner, J., O. Tietz, A. Tietz, & T. Scholle 2017. Ist der Basalt ein Sachse? Wissenschaftshistorische, petrographische und geochemische Untersuchungen am Burgberg Stolpen, der Typlokalität für Basalt seit 1546. Berichte der Naturforschenden Gesellschaft der Oberlausitz 25: 127–142

Goth, K. & P. Suhr 2007. “Der Basalt ist ein Sachse”. Der Basaltschlot des Burgberges von Stolpen in der Lausitz. – In: Look E.-R. & L. Feldmann (eds.): Faszination Geologie. Die bedeutendsten Geotope Deutschlands. Schweizerbart; Stuttgart: 88–89

Humboldt, A. von 1790. Zerstreute Bemerkungen über den Basalt der älteren und neueren Schriftsteller. – In: Humboldt, A. v.: Mineralogische Beobachtungen über einige Basalte am Rhein. Schulbuchhandlung; Braunschweig: 9–74

Kammerzell, F. 2000. Aegypto-Germanica: Ägyptischer Wortschatz in westeuropäischer Sprache (Teil 1). – In: Schierholz, S.J. (ed.): Die deutsche Sprache in der Gegenwart. Festschrift für Dieter Cherubim zum 60. Geburtstag. Peter Lang publishing group; Frankfurt, Berlin, Bern, Bruxelles, New York, Oxford, Wien: 115–127

Krafft, F. 1994. Georg Agricola und der Basalt. In: Naumann, F. (ed.): Georgius Agricola – 500 Jahre. Wissenschaftliche Konferenz vom 25.–27. März 1994 in Chemnitz, Freistaat Sachsen. Birkhäuser Verlag; Basel: 105–115

Pfeiffer, L., G. Kaiser & J. Pilot 1984. K-Ar-Datierung von jungen Vulkaniten im Süden der DDR. Freiburger Forschungshefte C 389: 93–97

Plinius, G. S. ca. 77 AD. Naturalis historia. Vol. XXXVI, ch. 58.

Linking experimental cratering models to large maar-diatremes

Károly Németh¹, and Mohammed Rashad Moufti²

¹ Institute of Agriculture and Environment, Massey University, Palmerston North, New Zealand

² Geohazards Research Centre, King Abdulaziz University, Jeddah, Kingdom of Saudi Arabia

Keywords: explosion, excavation, tuff ring

In recent years, scaled analogue experiments have provided valuable insight to our understanding of crater formation (e.g. Graettinger et al 2015 and references therein). These experiments operated with underground explosions without distinguishing the magma fragmentation style associated with the formation of the craters. These experiments introduced the “scaled depth” of an explosion that combines the actual depth with the potential energy associated with the explosion (that roughly linked to magma flux). The scaled depth of an explosion is expressed by a formula of $SD=d/E^{1/3}$, where d is the depth of explosion and E is the energy associated with it. In addition, it has been identified that there is an optimal scaled depth (OSD) that is the ideal depth of an explosion that produces the largest craters and most voluminous eruptive products around the crater. These studies produced important predictions on the lateral and vertical facies distribution on tephra ring pyroclastic successions such as 1) if explosions occur shallower than the OSD, the tephra rings are dominated with thick pyroclastic breccia in proximal rings with little pyroclastic density current deposits (PDC), 2) if the explosions occur around the OSD large volume of tephra produced with thick medial blanket of fall and PDC, and 3) if explosions deeper than the OSD, the deposits will be dominated by PDC deposits.

Here we provide field observations on three large young (<2 Ma) maars from western Saudi Arabia, part of the Cenozoic Alkaline Basaltic Intraplate Province of western Arabia with an aim to test the predictions of experimental cratering in natural examples.

Among the three maars, Al Wahbah (Fig. 1) is the largest and it is located in the Harrat Kishb. Al Wahbah is about 2300X1750 m across today and its crater depth reaches 250 m measuring from the base of the tuff ring succession to the flat floored bottom of the playa lake/salt pan covered crater. The crater margin is irregular shaped and scalloped indicating that the maar might have formed by multiple explosions in multiple locations. Somehow the tuff ring succession however showing great lateral continuity suggesting the tuff ring is rather resulted from processes acted uniformly around the crater. Only one exception can be noted as toward the NW and SE some opposite thickening of deposits can be observed indicating that the formation of the tephra ring might have associated with eruption along a fissure that gradually formed the crater.



Fig. 1 – Al Wahbah maar looking toward the NW.

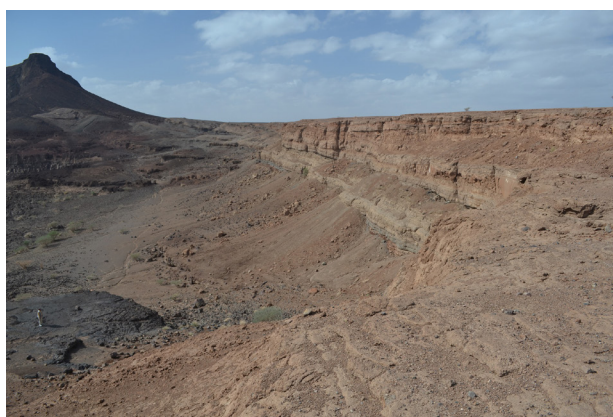


Fig. 2 – Al Wahbah pyroclastic succession in the NW.

Al Wahbah tuff ring is about 40 m thick in most (Fig. 2). The deposits dip outward from the crater in about 18° and can be traced at least 1.5 km away from the present day crater rim in each direction. In the NW however differential erosion stripped the tuff ring about 300 m back from the maar rim where the pre-volcanic Neoproterozoic undeformed dioritic granite and gabbro exposed in the crater wall. The tuff ring sits on two basaltic lava flows (50-60 m). In addition, in the NW the maar cut half a scoria cone that went through an erosion stage prior the maar forming eruption cut it half. Similar, but smaller spatter cone half sections are located in the SE maar wall. All these indicates that immediately before the maar eruption, a chain of spatter and scoria cones sitting on thick lava flows constructed the eruptive environment, hence it is unlikely to had a preexisting crater in the region. Al Wahbah likely erupted in a positive landform-dominated region. The tuff ring succession is dominated by intercalated PDC and pyroclastic breccia dominated deposits inferred to be resulted from pyroclastic debris curtain deposition. The entire succession shows evidences that phreatomagmatic fragmentation was the main energy source to drive the explosive eruptions. The succession is coherent with the prediction that the explosions were

close to OSD or slightly deeper than that. To maintain this a gradual downward shifting of the eruption locus and/or increase of energy release through increasing magma flux were needed to maintain the explosive conditions. This is consistent with Lorenz's (1986) model and requires deep pressurized aquifer and magma interaction.

A similar situation is observed and linked to the preserved pyroclastic succession of Hutaymah maar (Fig. 3) in the Harrat Hutaymah. Hutaymah maar is slightly smaller than Al Wahbah but its proximal succession better preserved (Fig. 4) that is dominated by alternating pyroclastic breccias with PDC deposits. In the tuff ring there is no systematic change in the deposit characteristics other than having a more magmatic fragment enriched upper section suggesting that magma flux in the late stage of the eruption and the exhaustion of water tables to fuel phreatomagmatism shifted the eruption to be more magmatic fragmentation dominated.



Fig. 3 – Hutaymah maar, a slightly smaller version of Al Wahbah.



Fig. 4 – Hutaymah maar pyroclastic succession.

Hutaymah maar is also inferred to formed due to explosions occurred and maintained close to the OSD through the entire eruption.

The third example shown here is from the Jubb (Ni'ayy) maar also part of Harrat Hutaymah. This maar shows differences in comparison to Al Wahbah and Hutaymah maar by having a less deep and pronounced crater. The crater size is slightly smaller than Al Wahbah and Hutaymah and its depth is far shallower. The tuff ring succession dip outward in a gentler angle (10-15°) and in the "crater wall" deposits are PDC-dominated with not a lot of vertical variations indicating explosions deeper than OSD.

The examples from Saudi Arabia show consistency in large scale with experimental data suggesting that each maar must have erupted in explosive conditions close or deeper than the OSD. This also suggests that the phreatomagmatic eruptions were fueled by deep, and potentially pressurized aquifers located in the depth range similar

to the current depth of the craters. In the course of the eruptions explosion locus must have migrated deeper to maintain the OSD conditions.

While these results are promising, linking the scaled experiments with real natural examples is needed for further understanding maar-forming eruptions. The link between experiments and natural examples so far is poorly established. Especially in large maars such as Al Wahbah, the role of crater floor subsidence in the formation of the large "hole-in-the-ground" as a similar process how calderas form may need to be combined with the recent experimental results. The role and effect of the lateral and vertical migration of explosion sites on the resulting facies architecture of the tuff ring around the crater also need to be examined in more robust way prior concluding the volcanic eruption processes formed those large maars.



Fig. 5 – PDC dominated proximal tuff ring succession at Jubb (Ni'ayy) maar.

References

Graettinger, AH, Valentine, GA, Sonder, I, Ross, P-S, White, JDL 2015. Facies distribution of ejecta in analog tephra rings from experiments with single and multiple subsurface explosions. *Bulletin of Volcanology* 77: 66.

Lorenz, V 1986. On the growth of maars and diatremes and its relevance to the formation of tuff rings. *Bulletin of Volcanology* 48: 265-274.

Magma fragmentation: a review of main (possible) physical and thermodynamics mechanisms

Roberto Sulpizio ¹

¹ Dipartimento di Scienze della Terra e Geoambientali, UNIBA, via Orabona 4, 70125, Bari, Italy. roberto.sulpizio@uniba.it

Keywords: magma fragmentation, phreatomagmatism, mechanical strenght.

Historically, three basic models have been proposed for the mechanism of fragmentation. First, in the critical vesicularity model, in which a critical vesicularity determines the fragmentation threshold (Sparks, 1978). Second, in the brittle failure model, in which the liquid magma behaves similar to solid magma, and the bubble walls fail when the maximum stress exceeds the strength of the magma (Alidibirov, 1994; Zhang, 1999). Third, the relaxation time scale model is based on the idea that when strain rates during deformation exceed the inverse relaxation time of melt, $1 / \tau_r$, brittle fragmentation may result (Webb and Dingwell, 1990; Papale, 1999; Ichihara et al., 2002; Gonnermann and Manga, 2003).

There are several lines of evidence that indicate the fixed porosity criteria is not effective, firstly because the fragmentation occurs also in poorly vesicular or not vesicular magmas.

In this framework, it is convenient to consider the Maxwell's equation for viscoelastic media, which indicates the equilibrium conditions between rate of deformation and mechanical strength of magma:

$$\frac{dv}{dz} = k \left(\frac{G_{\infty}}{\mu} \right)$$

where v is velocity at changing depth z , k is a constant, G is the dynamic modulus and μ the magma viscosity. It is evident from the equation that magma fragmentation relates to rate of deformation and elastic vs. viscous characteristics of magma.

In particular, the term dv/dz has the dimension of $1/t$, and it corresponds to a hyperbolic diagram in the G_{∞}/μ vs. t space (Fig. 1).

This diagram demonstrate that every material can be fragmented if the deformation occurs within a characteristic time.

Preexisting bubbles should be important for magmas to react explosively to a rapid acceleration. The stress dis-

tribution around bubbles strongly depends on the vesicularity (Zhang, 1999): larger vesicularity can generate a larger tensile stress under the same overpressure. In other words, the presence of bubbles and thin sets among them deteriorate the mechanical response of a magma, as confirmed in laboratory experiments showing that preexisting bubbles reduce the overpressure required for fragmentation (Martel et al., 2000; 2001; Spieler et al., 2004).

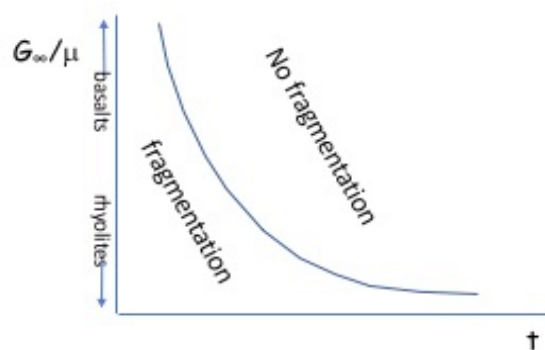


Fig. 1 - Diagram showing the mechanical strength of magma vs. characteristic time of deformation.

When considering also magma-water interaction the response of a (bubbly) fluid to rapid acceleration is still poorly understood. This is because it involves several interacting physical processes and properties, including viscoelasticity, thermo-hydraulics, shock wave propagation, and rock mechanics.

References

Alidibirov, A., Dingwell, D.B. (1996). Magma fragmentation by rapid decompression, *Nature* 380, 146 – 148

Gonnermann, H.M., Manga, M. (2003). Explosive volcanism may not be an inevitable consequence of magma fragmentation, *Nature* 426: 432 – 435.

Ichihara, M., Rittel, D., Sturtevant, B. (2002). Fragmentation of a porous viscoelastic material: implications to magma fragmentation, *J. Geophys. Res.* 107, doi:10.1029/2001JB000591

Martel, C., Dingwell, D.B., Spieler, O., Pichavant, M., Wilke, M. (2000). Fragmentation of foamed silicic melts: an experimental study, *Earth Planet. Sci. Lett.* 178 (2000) 47–58.

Martel, C., Dingwell, D.B., Spieler, O., Pichavant, M., Wilke, M. (2001). Experimental fragmentation of crystal- and vesicle-bearing silicic melts, *Bull. Volcanol.* 63 (2001) 398–405.

Papale, P. (1999). Strain-induced magma fragmentation in explosive eruptions, *Nature* 397: 425 – 428

Sparks, R.S.J. (1978). The dynamics of bubble formation and growth in magmas: a review and analysis, *J. Volcanol. Geotherm. Res.* 3: 1 – 37

Webb, S.L., Dingwell, D.B. (1990). Non-Newtonian rheology of igneous melts at high stresses and strain rates: experimental results for rhyolite, andesite, basalt, and nephelinite, *J. Geophys. Res.* 95: 15695 – 15701

Zhang, Y. (1999). A criterion for the fragmentation of bubbly magma based on brittle failure theory, *Nature* 402: 648 – 650.

Surtsey revisited: Fragmentation and heat transfer studies in the framework of the ICDP project SUSTAIN

Bernd Zimanowski¹, Ralf F. Büttner¹, James D.L. White², and Magnús T. Gudmundsson³

¹ PVL, Universität Würzburg, Pleicherwall 1, D-07070 Würzburg, Germany. zimano@mail.uni-wuerzburg.de

² Department of Geology, University of Otago, Dunedin 9054, New Zealand.

³ Institute of Earth Sciences, University of Iceland, IS-101 Reykjavik, Iceland.

Keywords: phreatomagmatic volcanism, thermal granulation, fragmentation and heat transfer

Surtsey (Vestmannaeyjar, Iceland) is the type example of Surtseyan volcanism (Baldursson and Ingadóttir, 2007). The initial stage of the eruption was submarine and built a 130 m high edifice before emergence of the embryonic island. Abundant and excellent observations were made during the 1963–1967 eruptions but no observations confidently reveal the subaqueous eruption processes, mainly because the 1979 hole did not reach the seafloor. The SUSTAIN drilling program (A New Drill Core at Surtsey Volcano: A Natural Laboratory for Time-Lapse Characterization of Hydrothermal Seawater and Microbial Interactions with Basaltic Tephra) aims to sample the complete succession of a neo-volcanic island from the surface to the underlying oceanic crust. Understanding the internal structure and facies architecture of the type locality of Surtseyan volcanism is a prime aim of the program. Likewise, Surtsey provides a unique reference for thermal granulation experiments that will help test and refine models for explosive magmatic and phreatomagmatic fragmentation and production of airborne ash clouds.

It is not known whether the initial eruptive style was effusive, forming pillow lavas, or explosive, producing pyroclasts (Zimanowski and Büttner 2003), as found in the 1979 drillhole and observed during the explosive period when external water had access to the vent (November 1963–April 1964). Subglacial eruptions have begun at higher pressures without a significant suppression of fragmentation (Gudmundsson et al. 2004), and other subaqueously erupted volcanoes lack evidence of initial pillow lavas. How the onset of fragmentation, submarine transport and tephra deposition from submarine eruptions affected the seafloor, through processes such as scouring and burial are not well understood. In the last 30 years field and experimental work has yielded a greatly improved understanding of volcanic fragmentation mechanisms. Whether Surtsey activity was predominantly phreatomagmatic or involved substantial magmatic-driven explosivity can be clarified with rigorous analysis of deposits and experiments using remelted material from the island. This question has important implications for the potential hazards to air traffic from future Surtseyan-type eruptions.

In summer 2017 the drilling operation was successfully carried out. All the core samples and data need still to be analysed and interpreted, however, now we know, that Surtur is underlain by a diatrema – at least a small one.

The workgroup at the PVL in Würzburg joined the project in April 2017. Meanwhile we got about 80 kg of material, pro-

duced by crushing and homogenizing bombs and blocks sampled on Surtsey in 2016. Melt samples were produced in our experimental induction furnace and analyzed using XRF. The samples produced in steel crucibles with Al₂O₃ inserts were found to well represent the composition of Surtur bombs and lava (Schipper et al. 2015).

Standardized MFCI fragmentation experiments were conducted (Fig 1), as well as isothermal magmatic fragmentation runs (Zimanowski et al. 2015).

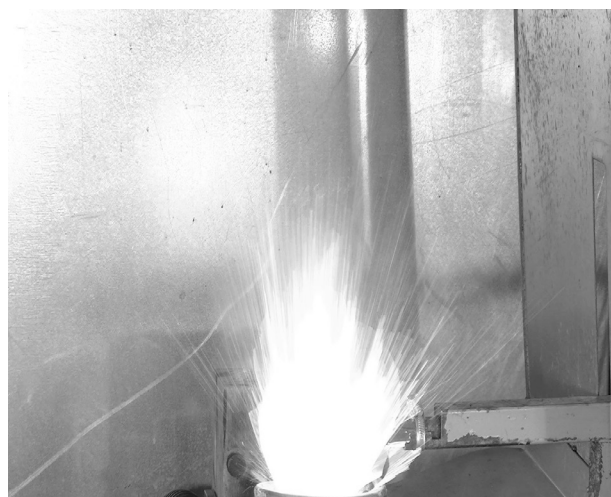


Fig. 1 – Explosive interaction of a Surtsey melt – water premix. Frame width is 60 cm. Expansion velocity approx. 350 m/s

The samples are currently analyzed using SEM and micro-tomography to reveal fingerprint characteristics of the fragmentation processes and fragmentation energetics (Dürig et al. 2012). In the next step the experimental findings will be compared to the characteristics of the natural samples.

Experiments on the production of hyaloclastites by thermal granulation and measurements of the heat transfer have been performed using short term calorimetry (Schmid et al. 2010, Sonder et al. 2011, Schipper et al. 2011, Schipper et al. 2013). These experiments will not only provide typical particles for comparison to natural deposits, but also data on the effective range of heat transfer during the subaqueous eruptive phase and the post eruptive hydrothermal coupling conditions (Fig 2).

Several kg of experimental hyaloclastite have been produced during the quite extensive calorimetric experiments

to serve as fresh and sterile sample material for hydrothermal and micro-biological experiments and will be distributed within the project. Part already has been inserted into one drill hole at Surtsey and is now exposed to the present hydrothermal conditions. Additional experiments using “dirty” coolants and brine are scheduled, once we received information from the measurements during and after the drilling operation. This abstract represents work in progress and we are confident to present additional new findings at the conference.

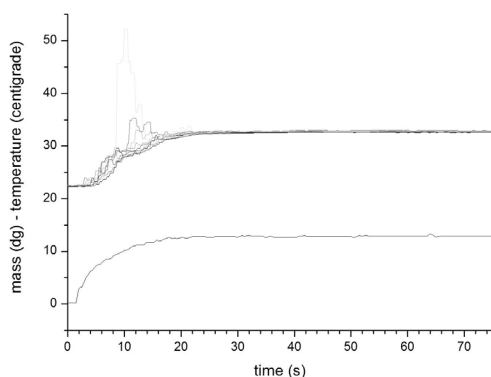


Fig. 2 – Raw data of a cooling experiment in the short term calorimeter. 0,123 kg of melt at 1190°C granulated in 3 kg of water at 22.5 °C.

Acknowledgements

This project is funded by the German Science Foundation (DFG) within the framework of the ICDP Project SUSTAIN, where the drilling operation has been funded from an ICDP grant and a consortium of other funding agencies.

References

- Baldursson, S. and Ingadóttir, Á., 2007. Nomination of Surtsey for the UNESCO World Heritage List, Icelandic Institute of Natural History, Reykjavik.
- Dürrig, T., Dioguardi, F., Büttner, R., Dellino, P., Mele, D., and Zimanowski, B., 2012. A new method for the determination of the specific kinetic energy (SKE) released to pyroclastic particles at magmatic fragmentation: theory and first experimental results. *Bull. Volcanol.* 74, 4: 895.
- Gudmundsson, M. T., Sigmundsson, F., Björnsson, H., and Högnadóttir, T. 2004. The 1996 eruption at Gjalp, Vatnajökull ice cap, Iceland: Efficiency of heat transfer, ice deformation and subglacial water pressure. *Bull. Volcanol.* 66, 1: 46-65.
- Jakobsson, S., and Moore, J. G., 1986. Hydrothermal minerals and alteration rates at Surtsey volcano, Iceland. *GSA Bulletin*, 97: 648–659.
- Jakobsson, S., P., Thors K., Vésteinsson, Á., T., and Ásbjörnsdóttir, L., 2009. Some aspects of the seafloor morphology at Surtsey volcano: the new multibeam bathymetric survey of 2007. *Surtsey Research* 12: 9-20.
- Moore, J.G., 1985. Structure and eruptive mechanisms at Surtsey Volcano, Iceland. *Geological Magazine* 122: 649-661.
- Schmid, A., Sonder, I., Seegelken, R., Zimanowski, B., Büttner, R., Gudmundsson, M., and Oddsson, B., 2010. Experiments on the heat discharge at the dynamic magma-water-interface. *Geophys. Res. Lett.* 37: L20311.
- Schipper, C. I., White, J. D. L., Zimanowski, B., Büttner, R., Sonder, I., and Schmid, A., 2011: Experimental interaction of magma and “dirty” coolants. *Earth Planet. Sci. Lett.* 303: 323-336.
- Schipper, C. I., Sonder, I., Schmid, A., White, J.D.L., Dürrig, T., Zimanowski, B., and Büttner, R., 2013. Vapour dynamics during magma-water interaction experiments: Hydromagmatic origins of sub-marine volcanoclastic particles (limu o Pele). *Geophys. J. Int.* 192 (3): 1109-1115.
- Schipper, C.I., Jakobsson, S.P., White, J.D.L., Palin, M., and Bush-MacInowski, T., 2015. The Surtsey magma series. *Sci. Rep.* 5, 11498, doi: 10.1038/srep11498.
- Sonder, I., Schmid, A., Seegelken, R., Zimanowski, B., and Büttner, R. 2011. Heat source or heat sink: What dominates behavior of non-explosive magma-water interaction? *J. Geophys. Res.* 116: B09203.
- Zimanowski, B. and Büttner, R., 2003. Phreatomagmatic explosions in subaqueous eruptions, in White, J.D.L., Smellie, J.L., and Clague, D. (eds.): *Explosive sub-aqueous volcanism*, AGU Monograph, 140 (ISBN 0-87590-999-X): 51-60.
- Zimanowski, B., Büttner, R., Dellino, P., White, J.D.L., Wohletz, K.H., 2015. Magma-Water Interaction and Phreatomagmatic Fragmentation. In: Sigurdsson, H., Houghton, B., Rymer, H., Stix, J., McNutt, S. (Eds.), *The Encyclopedia of Volcanoes*, pp. 473-484.

The Mysterious Grooves of Bárcena

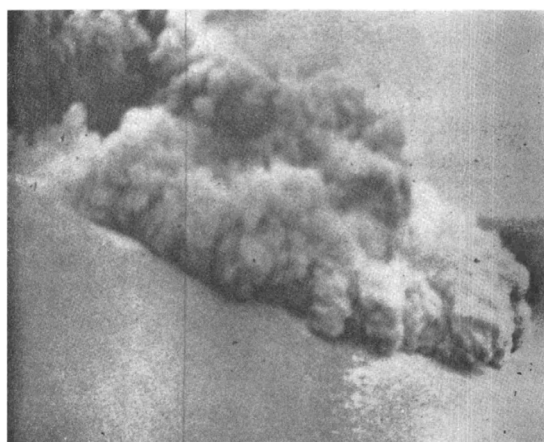
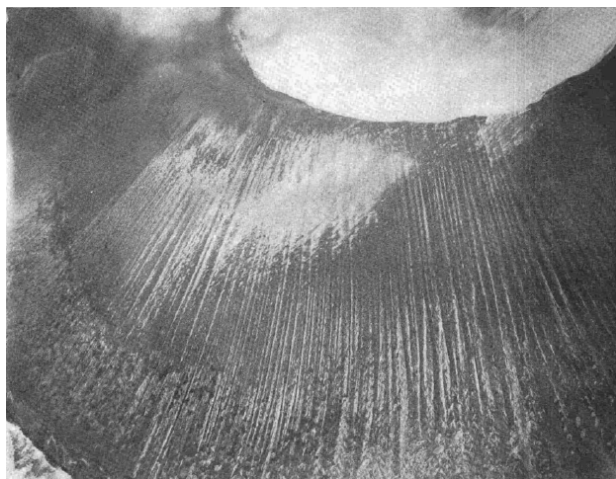
Susan W. Kieffer¹, Eckart Meiburg², Jim Best¹

¹ Department of Geology, University of Illinois at Urbana-Champaign, Urbana, IL61801 USA. s1kieffer@gmail.com

² Department of Mechanical Engineering, University of California, Santa Barbara, CA 93106 USA

³ Departments of Geography and GIS, Mechanical Science and Engineering and Ven Te Chow Hydrosystems Laboratory, University of Illinois at Urbana-Champaign, Urbana, IL 6180, USA.

Keywords: Bárcena, furrows, vortices.



August, 1952, eruption of Bárcena.
Volcanic density flow (tephra avalanche) of August 12, on Bárcena cone. Crater rim upper left corner, south side of Cráter Herrera extreme right center. Unretouched enlargement from a 16 mm duplicate Kodachrome motion picture frame.
(T. HOWELL photo)

Figure 1 (top): Grooves on Bárcena and (bottom) density current on August 12, 1959. From Richards (1959)

In this abstract, we suggest a way in which fields of grooves on a volcano may yield information on the structure of erosive density currents. Three processes may occur: an erosive channeling instability, the Görtler instability, and hydraulic regime changes.

Bárcena Volcano on Isla San Benedicto, about 300 nautical miles (345 miles) west of Mexico, erupted at 0745 on August 1, 1952. As Richards (1959) pointed out, Bárcena has an “index of explosiveness of about 90 per cent, the highest of any known oceanic volcano in the eastern Pacific Ocean.” He estimated that about 300 million cubic meters of tephra and lava were erupted during the whole eruption cycle.

Density currents (called “tephra avalanches” by Richards, 1959) descended the flanks and carved a field of grooves (Fig. 1,2) during Vulcanian eruptions prior to September 12 (Richards, 1959, p. 108). The grooves have widths of 10-20 feet (3-6 m), depths of 3-10 feet (1-3 m), and lengths of 800-1000 feet (240-300 m). From published photos, it appears that the ridges separating the grooves typically have the same or smaller widths, giving an estimated wavelength $\sim O(10\text{ m})$. The lengths are related to changes of slope on the volcano—from steep on the volcanic cone to mild downslope where the cone intersects preexisting topography of Isla San Benedicto. Above the change in slope, the grooves are U-shaped and, in plan view, they are straight. Where the grooves survive the change in slope they are wider and not as deep, with variable lengths less than a few hundred feet ($<O(100\text{ m})$). Where the change of slope is great, the grooves terminate abruptly. Below the change in slope dunes were developed with an orientation of right angles to the flow and with wave lengths up to 11 m (Moore, 1967). In his classic paper on base surges, Moore (1967) compared the Bárcena eruptions to atomic explosions.

Richards (1959) eliminated rain erosion, avalanches of bombs or blocks, and ash landslides from the crater rim by listing seven features that must be explained (see attached figures). Above the change in slope, the furrows (1) begin immediately below the crater rim, (2) are U-shaped; (3) are straight; (4) are parallel and non-coalescing. Below the change in slope they (5) increase in width down slope; (6) display turbulent patterns on the cone; and (7) some show local deposition at the lower ends. He concluded that they were formed by tephra avalanches. The even spacing and parallel alignment of the grooves suggests that their spanwise length scale is reinforced by some instability mechanism that strongly selects this wavelength.

We propose that the grooves were carved by vortices in the boundary layer of a dusty-gas density current(s). Mixtures of particle-laden fluids flowing along the ground are subject to a vortex-producing instability due to differences in concentration and velocity boundary-layer thicknesses (Hall et al., 2008). We refer to this as the “erosive channeling instability,” and dub it the “groovy instability” for short. This instability depends on the relative thicknesses of the velocity and particle concentration boundary layers, δu and δc , respectively. When $L = \delta u / \delta c < 1$, this instability produces vortices that have a wavelength typically about $O(25)$ times the concentration boundary layer thickness. Models of pyroclastic flow structure (Dufek, 2016, his figure 11) suggest that this condition on L is met in many pyroclastic density currents.

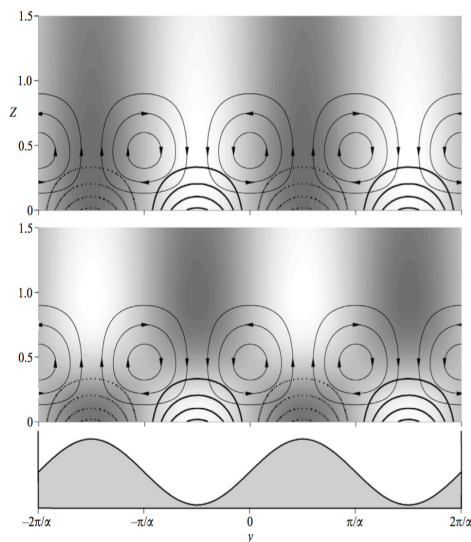


FIGURE 6. Dominant unstable eigenfunction modes for $\alpha_{max} = 0.24$, $Re = Pe = 1000$, $L = 0.5$, $G = 10^{-1}$, $c_p = 10^{-2}$ and $N = 10^{-3}$. The solid and dashed lines depict positive and negative concentration perturbation contours, respectively. Streamlines of the transverse perturbation velocity field are superimposed, with arrows denoting the flow direction. In the top frame, grey shading reflects the perturbation u -velocity, with lighter areas indicating positive values and darker areas negative values. The middle frame shows perturbation shear $\partial u/\partial z$ through grey shading, with lighter areas indicating positive values and darker areas negative values. The shape of the interface perturbation is shown in the bottom frame.

Figure 2: Eigenmodes for the model of Hall et al. (2008). See text for discussion.

The characteristics of flow for $L < 1$, derived from a Navier-Stokes-based linear stability analysis (Hall et al., 2008), in a spanwise cross section are shown in Figure 2. The bottom panel shows the shape of the interface between fluid (liquid water in this case) and underlying sediment that is being eroded by the fluid. In the upper and middle frames, the solid/dashed lines depict perturbations of the particle concentration density: solid lines \Rightarrow an increase in particle concentration above the mean, and dashed lines \Rightarrow a decrease. Reduced particle loading above the peaks results in a lower hydrostatic pressure compared to the troughs, and this creates a spanwise pressure gradient along the interface. This pressure gradient drives a perturbation in flow from the troughs to the peaks: the troughs thus get deeper through erosion and the peaks get higher through sedimentation. This flow results in the formation of counter-rotating streamwise vortices depicted by the closed, nearly circular lines with arrows. The vortices further carve the furrows.

The characteristics of flow for $L < 1$, derived from a Navier-Stokes-based linear stability analysis (Hall et al., 2008), in a spanwise cross section are shown in Figure 2. The bottom panel shows the shape of the interface between fluid (liquid water in this case) and underlying sediment that is being eroded by the fluid. In the upper and middle frames, the solid/dashed lines depict perturbations of the particle concentration density: solid lines \Rightarrow an increase in particle concentration above the mean, and dashed lines \Rightarrow a decrease. Reduced particle loading above the peaks results in a lower hydrostatic pressure compared to the troughs, and this creates a spanwise pressure gradient along the interface. This pressure gradient drives a perturbation in flow from the troughs to the peaks: the troughs thus get deeper through erosion and the peaks get higher

through sedimentation. This flow results in the formation of counter-rotating streamwise vortices depicted by the closed, nearly circular lines with arrows. The vortices further carve the furrows.

Using this theory for the groovy instability, the observed wavelength of $\sim O(10)$ m implies a very thin (~ 0.4 m) particle concentration layer. For density currents it is common to assume that the particle concentration layer ranges from ~ 0.1 - 1.0 of the full height of the flow (excluding the elutriated zone of mixing with the overlying ambient fluid). This would imply an effective flow thickness of 0.4 - 4 meters. This dimension is a small fraction of the visible height of pyroclastic flows that are crowned by dilute material arising from an overriding mixing zone and trailing wake, but appears to be consistent with numerical models such as those of Dufek and Bergantz (2007) or Dufek (2016) in which a thin saltating layer of higher particle concentration develops at the base.

In order to carve grooves that are 1 - 3 meters deep it seems likely that the wavelength of $\sim O(10)$ m was set during the initial eruption(s) and that these grooves thereafter acted as channels for repeated flows before September 12 when they were first observed during air flights (see photo in Figure 1).

The fact that the change of slope plays a role in determining groove properties suggests that the groovy instability and the Görtler instability (due to boundary curvature) may interact.

Richards estimated a velocity of “30 knots or more” (>15 m/s) for an eruption on December 12, much later than the initial activity, and later than the eruptions that carved the grooves. Flows with this velocity are hydraulically supercritical if their depth, d , is $d < \sqrt{2/g} = 23$ m. Because 15 m/s is a lower limit on the velocity, and the calculated flow thickness is less than 23 m, possibly by an order of magnitude, we believe that the flow on the upper part of Bárcena was supercritical. Where the change of slope was gradual, the supercritical conditions could have been maintained for some distance, permitting the grooves to penetrate onto the area of lower slope. Where the change was abrupt, we suggest that the flow decelerated to subcritical conditions through a hydraulic jump with velocities low enough to transition from erosive to depositional conditions resulting in sedimentation and dune formation.

References

- Dufek, J. 2016. The fluid mechanics of pyroclastic density currents. *Annual Rev. Fluid Mech.* 48: 459-485.
- Dufek, J., Bergantz, G.W. (2007) Suspended load and bed-load transport of particle-laden gravity currents: the role of particle-bed interaction. *Theor. Comput. Fluid Dyn.* 21:119-145
- Hall, B, Meiburg, E., Kneller, B. 2008. Channel formation by turbidity currents: Navier-Stokes-based linear stability analysis. *J. Fluid Mech.* 615: 185-210.
- Richards, A.F. 1959. Geology of the Islas Revillagigedo, Mexico 1. Birth and development of Volcán Bárcena, Isla San Benedicto (1). *Bull. Volc. Ser.2.* 22:73-123

Shallow magma diversions during explosive diatreme-forming eruptions

Nicolas Le Corvec¹, James D. Muirhead², James D. L. White³

¹ Laboratoire Magmas et Volcans, Université Clermont Auvergne - CNRS - IRD, OPGC, Clermont-Ferrand, France. nicolas.le_corvec@uca.fr

² Department of Earth Sciences, Syracuse University, Syracuse, New York, USA.

³ Geology Department, University of Otago, Dunedin, New Zealand.

Keywords: Maars, magma propagation, finite element modeling

Recent field and geophysical studies have revealed complex networks of sub-vertical dikes to sub-horizontal sills underlying monogenetic volcanic fields [Richardson et al., 2015; McLean et al., 2017], with the growth of these networks affecting the location and style of eruptive activity. Hazardous vent-site shifts are documented for monogenetic eruptions [Abrams and Siebe, 1994], resulting from lateral magma diversion during growth of dike and sill feeders [Lefebvre et al., 2012; Muirhead et al., 2016]. Magma diversions and transitions in intrusion geometries can be explained by several physical and structural factors, such as mechanical contrasts [Kavanagh et al., 2006], pre-existing fractures [Le Corvec et al., 2013], and stress loading/unloading [Maccaferri et al., 2014]. These diversions can modulate eruptive behavior between explosive and effusive activity (e.g., [Valentine et al., 2015]), where changes in eruption style are hypothesized to result from changes in magma-water ratios [Muirhead et al., 2016], reduced internal magma pressure causing volatile exsolution [White, 1996], and/or a build-up of volatiles at dike-sill junctions [Richardson et al., 2015].

The development of shallow feeder systems is increasingly recognized as playing an important role in modulating explosive eruptive activity [Re et al., 2015]; however, no studies to date have modelled how topographic and material changes resulting from explosive, crater-forming

eruptions influence the development of underlying feeder systems. Here we utilize, for the first time, finite element modeling to analyze the evolution of stress states during explosive excavation and filling of gravitationally loaded country rock during maar-diatreme volcanism. This methodology allows us to test how local stress fields, and therefore magma propagation, respond to the mechanical changes produced by excavation of maar-diatreme structures that are common in mafic and kimberlite volcanic fields (Fig. 1).

We use finite element models through COMSOL Multiphysics® to investigate the effects of diatreme excavation for single-explosion craters and infilling on the local state of stress (Fig. 1). These stress changes are expected to affect the geometry of surrounding intrusions, which form normal to the least compressive stress.

Diatreme formation is a complex process that occurs during kimberlite and basaltic phreatomagmatic eruptions [Brown and Valentine, 2013; Kurszlaukis and Lorenz, 2017]. Furthermore excavation of vents, with or without infilling, occurs during explosive eruptions of other styles (e.g., vulcanian and plinian eruptions). The stress changes examined here are expected also to take place in a variety of volcanic settings and eruptive scenarios, including on other planetary bodies, though typically imposed on different pre-eruption topography. Here we show that stress

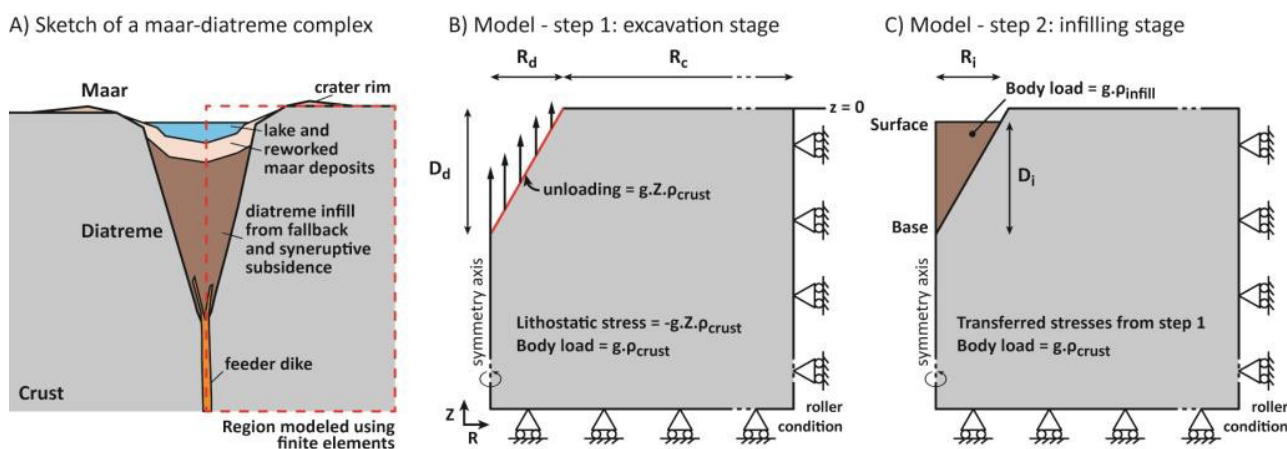
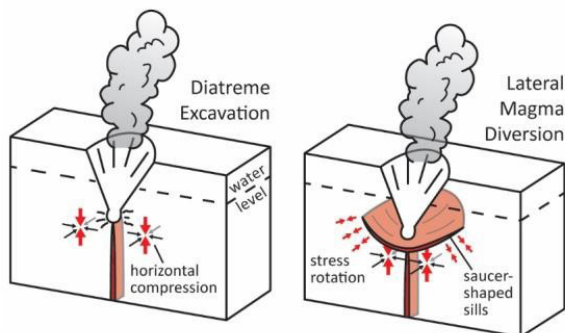


Fig. 1 – Finite element model (FEM) configuration. A) Sketch of a maar-diatreme complex. The dotted red square represents the area modeled numerically using an axisymmetric axis. B) The initial step models the excavation stage. The model is gravitationally loaded with a lithostatic pre-stress and a body load. A vertical load acting on the diatreme's wall represents the mass of rock excavated. C) The second step models the infilling stage. The initial stress conditions and geometry are transferred from the initial step. The diatreme is filled with either 25, 50 or 75% of the total diatreme volume.

states resulting from explosive excavation of country rock and diatreme infilling provide a novel mechanism to explain sill transitions and saucer-shaped sill formation in crust immediately enclosing diatremes (Fig. 2a). Modeled stress fields in this study, and resulting intrusion geometries, provide new insights into processes controlling diatreme development, and support recent models of diatreme growth proposed by [Valentine et al., 2017]. Overall, modeled stress states reveal a critical feedback between explosive maar-diatreme vent excavation, infilling, and development of geometrically complex magma networks. Phases of explosive excavation encourage magma to stall in sills below the excavated structure, allowing for lateral changes in the position of fragmentation zones early in the diatreme's history rather than progressive deepening, whereas subsequent infilling should promote magma ascent to shallower levels within the diatreme (Fig. 2b). Horizontal compression in the upper diatreme drives lateral magma diversions, encouraging explosive diatreme widening and growth at shallow depths. Compressional stresses resulting from increasing infill volumes during continued diatreme growth are expected to promote sill-driven lateral quarrying, nest-diatreme formation, and larger explosive activity in well-developed

examples:

a) Proto-diatreme (excavation stage)



b) Developing diatreme (infilling stage)

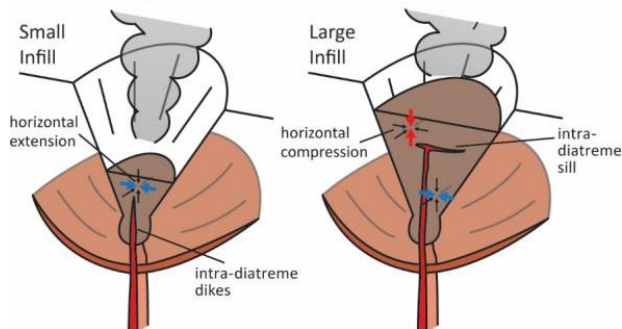


Fig. 2 – Sketch of a maar-diatreme eruption and formation of the magmatic plumbing system during a) the proto-diatreme (aka excavation stage) and b) developing diatreme (aka infilling stage). The colored arrows represent the orientation of the minimum compressional stress (σ^3), the blue and red colors represent the differential tectonic stress, extensional and compressional, respectively.

References

- Abrams, M. J., and C. Siebe (1994), Cerro Xalapaxco: an unusual tuff cone with multiple explosion craters, in central Mexico (Puebla), *Journal of Volcanology and Geothermal Research*, 63(3), 183-199, doi:[http://dx.doi.org/10.1016/0377-0273\(94\)90073-6](http://dx.doi.org/10.1016/0377-0273(94)90073-6).
- Brown, R. J., and G. A. Valentine (2013), Physical characteristics of kimberlite and basaltic intraplate volcanism and implications of a biased kimberlite record, *GSA Bulletin*, 125(7-8), 1224-1238, doi:[10.1130/B30749.1](https://doi.org/10.1130/B30749.1).
- Kavanagh, J. L., T. Menand, and R. S. J. Sparks (2006), An experimental investigation of sill formation and propagation in layered elastic media, *Earth and Planetary Science Letters*, 245(3-4), 799-813.
- Kurszlauskis, S., and V. Lorenz (2017), Differences and similarities between emplacement models of kimberlite and basaltic maar-diatreme volcanoes, *Geological Society, London, Special Publications*, 446(1), 101-122, doi:[10.1144/sp446.5](https://doi.org/10.1144/sp446.5).
- Le Corvec, N., T. Menand, and J. Lindsay (2013), Interaction of ascending magma with pre-existing crustal fractures in monogenetic basaltic volcanism: an experimental approach, *Journal of Geophysical Research: Solid Earth*, 118(3), 968-984, doi:[10.1002/jgrb.50142](https://doi.org/10.1002/jgrb.50142).
- Lefebvre, N. S., J. D. L. White, and B. A. Kjarsgaard (2012), Spatter-dike reveals subterranean magma diversions: Consequences for small multivalent basaltic eruptions, *Geology*, 40(5), 423-426, doi:[10.1130/g32794.1](https://doi.org/10.1130/g32794.1).
- Maccaferri, F., E. Rivalta, D. Keir, and V. Acocella (2014), Off-rift volcanism in rift zones determined by crustal unloading, *Nature Geosci*, 7(4), 297-300, doi:[10.1038/ngeo2110](https://doi.org/10.1038/ngeo2110).
- McLean, C. E., N. Schofield, D. J. Brown, D. W. Jolley, and A. Reid (2017), 3D seismic imaging of the shallow plumbing system beneath the Ben Nevis Monogenetic Volcanic Field: Faroe-Shetland Basin, *Journal of the Geological Society*, 174(3), 468-485, doi:[10.1144/jgs2016-118](https://doi.org/10.1144/jgs2016-118).
- Muirhead, J. D., A. R. Van Eaton, G. Re, J. D. L. White, and M. H. Ort (2016), Monogenetic volcanoes fed by interconnected dikes and sills in the Hopi Buttes volcanic field, Navajo Nation, USA, *Bulletin of Volcanology*, 78(2), 11, doi:[10.1007/s00445-016-1005-8](https://doi.org/10.1007/s00445-016-1005-8).
- Re, G., J. D. L. White, and M. H. Ort (2015), Dikes, sills, and stress-regime evolution during emplacement of the Jagged Rocks Complex, Hopi Buttes Volcanic Field, Navajo Nation, USA, *Journal of Volcanology and Geothermal Research*, 295, 65-79, doi:<http://dx.doi.org/10.1016/j.jvolgeores.2015.01.009>.
- Richardson, J. A., C. B. Connor, P. H. Wetmore, L. J. Connor, and E. A. Gallant (2015), Role of sills in the development of volcanic fields: Insights from lidar mapping surveys of the San Rafael Swell, Utah, *Geology*, 43(11), 1023-1026, doi:[10.1130/G37094.1](https://doi.org/10.1130/G37094.1).
- Valentine, G. A., A. H. Graettinger, É. Macorps, P.-S. Ross, J. D. L. White, E. Döhring, and I. Sonder (2015), Experiments with vertically and laterally migrating subsurface explosions with applications to the geology of phreatomagmatic and hydrothermal explosion craters and diatremes, *Bulletin of Volcanology*, 77(3), 15, doi:[10.1007/s00445-015-0901-7](https://doi.org/10.1007/s00445-015-0901-7).
- Valentine, G. A., J. D. L. White, P.-S. Ross, A. H. Graettinger, and I. Sonder (2017), Updates to Concepts on Phreatomagmatic Maar-Diatremes and Their Pyroclastic Deposits, *Frontiers in Earth Science*, 5(68), doi:[10.3389/feart.2017.00068](https://doi.org/10.3389/feart.2017.00068).
- White, J. D. L. (1996), Impure coolants and interaction dynamics of phreatomagmatic eruptions, *Journal of Volcanology and Geothermal Research*, 74(3), 155-170, doi:[https://doi.org/10.1016/S0377-0273\(96\)00061-3](https://doi.org/10.1016/S0377-0273(96)00061-3).

On the interaction of magma, groundwater and country rocks: two contrasting phreatomagmatic maar-diatreme emplacement models

Volker Lorenz¹, Stephan Kurszlaukis² and Peter Suhr³

¹ *Physical Volcanological Laboratory, Institute of Geography and Geology, University of Würzburg, 97070 Würzburg, Germany. vlorenz@geologie.uni-wuerzburg.de*

² *De Beers Canada, 1601 Airport Road NE, Suite 300, Calgary, Alberta, T2E 6Z8, Canada.*

³ *Senckenberg Naturhistorische Sammlungen Dresden, Königsbrücker Landstr. 159, 01109 Dresden, Germany*

Keywords: maar-diatreme, emplacement models, phreatomagmatism

At present, there exist two partially diverging models on the phreatomagmatic emplacement of maar-diatreme volcanoes in subaerial continental environments - with both models having evolved in some aspects since they were first published.

The early model (Lorenz 1986) assumes that the majority of the phreatomagmatic explosions occurred in the root zone of the maar-diatreme volcano. If eruptions were able to pierce the crater floor, they deposited tephra inside the maar crater, on the tephra ring surrounding the maar crater and in distal environments. Growth of both diatreme and maar crater in diameter and depth and of thickness of the surrounding tephra ring is considered to be controlled by a restricted amount of available groundwater (frequently in hydraulically active fracture zones), that is depleted by eruptions, and by consequent formation of a cone of depression of the groundwater table. The incremental ejection of relatively large amounts of fragmented country rocks per unit eruption results in repeated mass deficiencies in the root zone and consequent collapse, subsidence and growth of the overlying diatreme, maar crater and tephra ring (Kurszlaukis and Lorenz 2017; Lorenz et al. 2017). Phreatomagmatic explosions inside the diatreme have also been considered possible (Lorenz and Kurszlaukis 2007), but occur mostly along the margin of the pipe and play only a limited role.

A revised phreatomagmatic emplacement model was published by Valentine and White (2012) and subsequently followed by a series of papers dealing with additional details of the model (Graettinger and Valentine 2017, and references therein; Valentine et al. 2017, and references therein). In this revised model, based on energy relationships of deep and shallow explosions and the assumption that groundwater was irregularly distributed inside diatremes, it was suggested that dykes could intrude to all intra-diatreme levels. These dykes interact with water where it is available and - with the exception of a few 100 m below the crater - could explode only non-eruptively and form failed tephra jets in all deeper levels of the diatreme. At the site of such non-eruptive explosions, the dyke magma, country rocks and tephra would get fragmented phreatomagmatically and juvenile and acciden-

tal pyroclasts could get transported for possibly a few 100 m upwards, but still contained within the diatreme, by such tephra jets. As a consequence, tephra jets would transport part of the previously and newly fragmented tephra higher upwards. Some country rock clasts of high level origin would get circulated downwards along the margins of the tephra jets. Only at depths of ~100 to ~200 m, rarely deeper, below the maar crater floor there exists the possibility of eruptive explosions. As a consequence of these near-surface eruptive explosions, ejected country rocks would be dominated by country rock clasts from near-surface horizons whereas country rock clasts from deeper rocks would have a much smaller chance to get ejected because of their dependence on numerous random non-eruptive explosions and the consequent complex "stop and go" lift process.

The two models differ quite remarkably in a number of aspects, of which we will discuss here only a few. The revised model requires the diatreme to contain almost at any intra-diatreme level groundwater largely derived from wet tephra deposited on the crater floor and also introduced into the diatreme from surrounding fracture zones and from below by failed tephra jets. In order for the many non-eruptive explosions to happen inside the diatreme, dykes have to intrude along rather dry parts of the diatreme tephra until they reach sufficient water and explode phreatomagmatically. Thus, dry and wet tephra volumes have to alternate vertically and horizontally inside diatremes in order for a series of dykes to reach the near-surface level of eruptive explosion potential. In order to allow this random "stop and go" transport mechanism and to make use of alternating volumes of dry and wet tephra, quite a number of dykes are required, the more the larger the diatreme is in size. The study of many diatremes, especially large ones, and their tephra deposits, however, does not show such large numbers of intra-diatreme dykes, it also does not show many intra-diatreme dykes fragmented by adjacent non-eruptive explosions. In case large numbers of dykes would not be considered to be required for the "stop and go" process then a smaller number of dykes has to get restarted in its intrusive activity after their non-eruptive explosions and form irregularly shaped and possibly differently oriented dyke continua-

tions or even plugs. And in any case the water available in the tephra for the many non-eruptive and eruptive explosions would be required to get recharged repeatedly.

The lack of large amounts of clasts in tephra rings derived from country rocks surrounding lower diatreme levels could also be largely due to the fact that lower rock levels of a cone shaped diatreme make up for a relatively smaller volume of the available pre-eruptive country rock volume than higher levels of medium and large sized diatremes of equivalent thickness. And in case of unstable walls, maar craters get larger in diameter during the eruptions than the diameter of the uppermost diatreme level, with this process also contributing an even larger proportion of near-surface country rock clasts to the tephra ring.

Another problem arises from the fact that diatreme tephra is usually rather badly sorted. In case they would be cool enough and water-saturated at intermediate and deep intra-diatreme levels their permeability will have decreased or almost been lost due to increasing overburden and consequent compaction. Would the contact of intruding dykes with such water-saturated, partially compacted and badly sorted tephra allow regularly phreatomagmatic explosions at depths of 1000 to 2000 m? One also has to consider that inside the lower end of cone-shaped diatremes the intruding dykes would cause elevated temperatures and the additional frequent injection of hot tephra by failed tephra jets would possibly prevent availability of liquid H₂O.

Until the horseshoe-shaped crater of Surtur 2, Surtsey/Iceland, stayed open to the Atlantic sea, the crater was involved in phreatomagmatic eruptions. However, once the subaerial tephra-ring of the crater closed, the basaltic magma rose, erupted and formed a lava lake and lava flows (Thorarinsson 1965). Obviously, the tephra ring below the sea level did not allow seawater to penetrate the subaqueous tephra wall and prevented continuation of phreatomagmatic eruptions – as seems typical, for the evolution of most basaltic volcanic islands that are covered by a shield volcano.

The revised model suggests that eruptive explosions are restricted to the uppermost several 100 m within a diatreme. However, the diatremes of the Missouri River Breaks, Montana, contain about 1000 m of bedded tephra and are surrounded in part by subsided large former near-surface country rock slabs (Hearn 1968; Delpit et al. 2014). Therefore, during the eruptive activity and deposition of the many tephra beds on the crater floor, there must have occurred ongoing syn-eruptive subsidence of these tephra beds and of the surrounding country rock slabs as well. This impressive syn-eruptive subsidence can only have been possible, if a mass deficiency had been caused repeatedly due to explosive quarrying below – possibly, at a syn-eruptively increasing depth finally well below 1000 m – resulting in tephra ejection also from below the bedded tephra. Tephra deposition in a steep-walled, diatreme-deep open crater should not have been possible because the Tertiary and underlying Mesozoic sediments had not been really indurated yet (Delpit et al. 2014).

Future studies should investigate more details of diatremes, as, e.g., presence of intra-diatreme dykes, transition from dykes into tephra jet feeder conduits within small and large diatremes, including bedded tephra levels, structural features and paleohydrogeology of surrounding country rocks, the potential for sufficient groundwater and recharge of diatreme tephra with groundwater. In addition, experiments should be performed with badly sorted water saturated tephra - under various pressures as are typical for the different intra-diatreme levels - with injected basaltic melt in order to learn about the feasibility of generating MFCLs inside the fill of the different diatreme levels.

References

- Delpit, S., Ross, P.S., Hearn, B.C. 2014. Deep-bedded ultramafic diatremes in the Missouri River Breaks volcanic field, Montana, USA: 1 km of syn-eruptive subsidence. *Bulletin of Volcanology* 76(7): 1–22.
- Graettinger, A.H., Valentine, G.A. 2017. Evidence for the relative depths and energies of phreatomagmatic explosions recorded in tephra rings. *Bulletin of Volcanology* 79(12): 88.
- Hearn, B.C. Jr. 1968. Diatremes with kimberlitic affinities in north-central Montana. *Science* 159: 622–625.
- Kurszlaukis, S., Lorenz, V. 2017. Differences and similarities between emplacement models of kimberlite and basaltic maar-diatreme volcanoes. *Geological Society, London, Special Publications* 446(1): 101–122.
- Lorenz, V. 1986. On the growth of maars and diatremes and its relevance to the formation of tuff-rings. *Bulletin of Volcanology* 48: 265–274.
- Lorenz, V., Suhr, P., Suhr, S. 2017. Phreatomagmatic maar-diatreme volcanoes and their incremental growth: a model. *Geological Society, London, Special Publications* 446(1): 29–59.
- Thorarinsson, S. 1965. The Surtsey eruption. Course of events and the development of the new island, Surtsey Research Progress Report 1: 51–55.
- Valentine, G.A., White, J.D.L., Ross, P.S., Graettinger, A., Sonder, I. 2017. Updates to concepts on phreatomagmatic maar-diatremes and their pyro-clastic deposits. *Frontiers in Earth Science* 5: 68. doi:10.3389/feart.2017.00068

Exploration of miniature volcanology using rootless cones as natural analogues of huge volcanoes across Earth and Mars

Rina Noguchi¹ and Kei Kurita²

¹ Volcanic Fluid Research Center, School of Science, Tokyo Institute of Technology, 2-12-1, Ookayama, Meguro-ku, Tokyo 152-8551, Japan. r-noguchi@ksvo.titech.ac.jp

² Earthquake Research Institute, the University of Tokyo, 1-1-1, Yayoi, Bunkyo-ku, Tokyo, 132-0031, Japan.

Keywords: miniature volcanology, rootless cone, Mars.

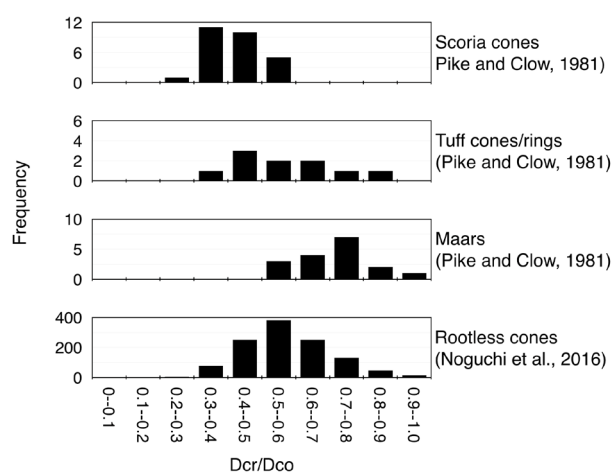
Recent study is skeptical about the arguments for a widely accepted value: magma:water mass ratio. Amount of explosion experiments have been conducted and found the specific mass ratio of magma and water contributes to make the maximum change efficiency from thermal to mechanical energy (Sheridan and Wohletz, 1983). However, White and Valentine, 2016 is skeptical for concept of the magma:water mass ratio as a fundamental role of phreatomagmatic eruption considering further experiments (e.g., Zimanowski et al., 1997; 0.03-0.04 for the optimal magma:water mass ratio, though Sheridan and Wohletz, 1983 showed as 0.1 to 0.3) and many factors such as system geometry. Furthermore, it is unclear that how to apply the magma:water mass ratio for natural volcanoes.



Fig. 1 – Examples of rootless cone in Myvatn, Iceland.

To resolve these issues, we focus on rootless cones which are formed by pure molten fuel coolant interaction in nature. Rootless cones are sub hundreds meter scale of pyroclastic cones which are formed by explosive interactions of molten lava and water-saturated sediments (e.g., Fagents and Thordarson, 2007). When lava drainage systems (such as lava tube) are formed on water-saturated sediments, explosions occur due to rapid vaporization of water. Since most of volatiles in lava should be degassed when it appeared on subaerial, the formation of rootless cones (hereafter rootless eruption) is considerable as pure molten-fuel coolant interaction. Rootless cones are not unique to the Earth — they also exists on Mars (e.g., Greeley and Fagents, 2001). Thanks to absent of ocean, vegetation, and thick atmosphere, significant amount of high-resolution visible images have been collected. Therefore we can analyze rootless cones complementa-

ry between Earth and Mars. In this study, we characterize rootless eruptions from several points include geomorphometrical and material analyses. Through these analyses, we aim to quantify the effect of external water in explosive volcanic eruptions across Earth and Mars.



2 –Ratio of the crater and the bottom diameter (Dcr/Dco) of several terrestrial pyroclastic cones.

In geomorphometrical analysis, we focus on a classical value: ratio of bottom and crater diameter of cones (Dcr/Dco; Wood, 1980). Using aerial photos and satellite images, we measured diameters of rootless cones. Fig.2 shows Dcr/Dco for several types of pyroclastic cones include rootless cones. For Dcr/Dco, it has been known that small in scoria cones and large in tuff rings/cones and maars (e.g., Frey and Jarosewich, 1982). In the case of rootless cones, the ratio has wide range as cover other pyroclastic cones which were formed by several magma:water conditions, though their size (i.e., the bottom diameter) is significantly smaller in both case of Earth and Mars. This tendency supports our idea to use rootless cones as natural analogs of general volcanoes.

Statistical analysis of ash-size grains tells us rootless eruptions are type of which bridges magmatic and phreatomagmatic eruptions (Noguchi et al., in preparation). Fig.3 shows result of cluster analysis for samples from several eruption types, using component proportions of statistically determined grain types. The grain type was

determined based on cluster analysis use multivariate parameters of grain shape and transparency. Samples from rootless eruptions were categorized several clusters; some with phreatomagmatic samples, and others with magmatic samples. This result may suggest some fragmentation processes (such as magmatic vaporization and MFCI) are common and its degree of contribution make difference across these eruption type.

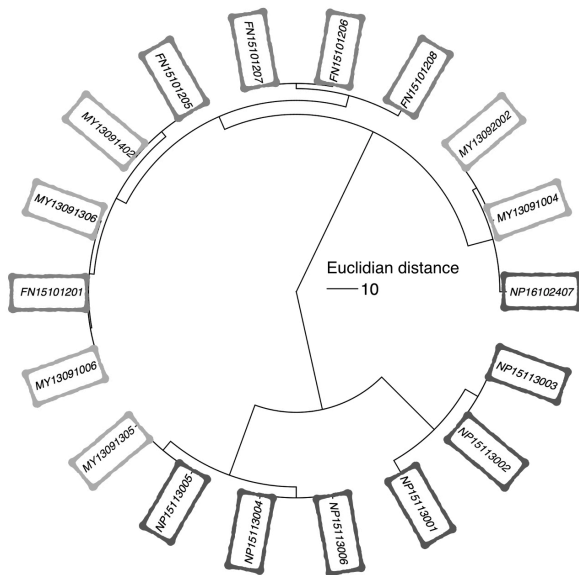


Fig. 3 – Dendrogram for sample clustering by percentages of the grain type based on the cluster analysis (modified Noguchi et al., in preparation). Samples were collected from Funabara scoria cone (FN), Nippana tuff ring (NP), and rootless cones in Myvatn (MY).

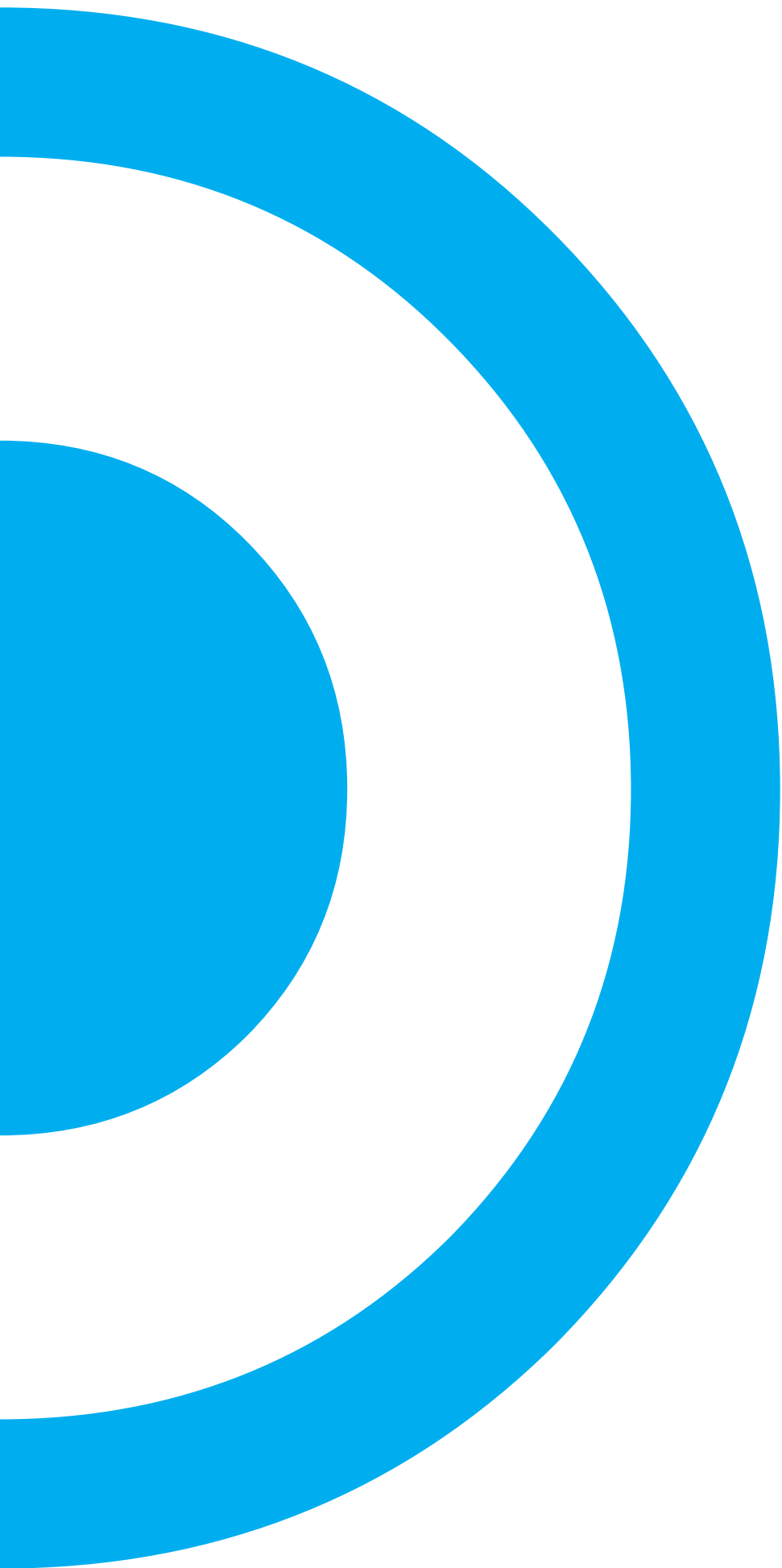
Our geomorphometrical and material analyses found that rootless cones can be the cross-sectional type between pyroclastic cones which are formed by magmatic and phreatomagmatic eruptions. By using rootless eruptions as the scale between magmatic and phreatomagmatic eruptions, we can extract the fragmentation process and quantify the influence of external water.

Acknowledgements

Volcanic ash samples were taken thanks to Y. Suzuki, K. Nemeth, A. Hoskuldsson, A. Einarsson, T. Saruya, E. Gjellerow, and A. Fridriksson. The cluster analysis was helped by H. Hino. This study was supported by the Izu Peninsula Geopark Promotion Council, the Sasakawa Scientific Research Grant from The Japan Science Society (25-602), the Joint Usage/ Research Center program No. 2015-B-04 from the Earthquake Research Institute, the University of Tokyo, and KAKENHI No.17H02063.

References

- Brož, P. and E. Hauber, 2012. A unique volcanic field in Tharsis, Mars: pyroclastic cones as evidence for explosive eruptions. *Icarus* 218, 88–99.
- Brož, P. and E. Hauber, 2013, Hydrovolcanic tuff rings and cones as indicators for phreatomagmatic explosive eruptions on Mars, *J. Geophys. Res.*, 118, 1-20, doi:10.1002/jgre.20120.
- Fagents, S.A. and T. Thordarson, 2007, Rootless volcanic cones in Iceland and on Mars, In: *The Geology of Mars*, Cambridge University Press, Cambridge, 151-177.
- Frey, H. and M. Jarosewich, 1982, Subkilometer Martian volcanoes: properties and possible terrestrial analogs, *J. Geophys. Res.*, 87, 9867-9879.
- Greeley, R. and S.A. Fagents, 2001, Icelandic pseudocraters as analogs to some volcanic cones on Mars, *J. Geophys. Res.*, 106, E9, 20527-20546, doi:10.1029/2000JE001378.
- Noguchi, R., Á. Höskuldsson, and K. Kurita, 2016, Detailed topographical, distributional, and material analyses of rootless cones in Myvatn, Iceland. *J. Volcanol. Geotherm. Res.*, 318, 89–102.
- Noguchi, R., H. Hino, N. Geshi, S. Otsuki, and K. Kurita, New classification method of volcanic ash samples using statistically determined grain types, in preparation.
- Pike, R. J., and G.D. Clow, 1981, Revised classification of terrestrial volcanoes and catalog of topographic dimensions, with new results of edifice volume (No. 81-1038). US Geological Survey.
- Sheridan, M.F. and K.H. Wohletz, 1983, Hydrovolcanism: basic considerations and review, *J. Volcanol. Geotherm. Res.*, 17, (1), 1–29.
- White, J.D. and G.A. Valentine, 2016, Magmatic versus phreatomagmatic fragmentation: Absence of evidence is not evidence of absence, *Geosphere*, 12(5), 1478–1488.
- Wood, C.A., 1980, Morphometric evolution of cinder cones, *J. Volcanol. Geotherm. Res.*, 7, 387-413.
- Zimanowski, B., K. Wohletz, P. Dellino, and R. Büttner, 2003, The volcanic ash problem, *J. Volcanol. Geotherm. Res.*, 122, 1–5.



Posters *Session 1*

Monogenetic volcanoes: eruption dynamics, growth, structure and physical modeling.

Conveners

Joan Martí (joan.marti@ictja.csic.es)

Pierre-Simon Ross (Pierre-Simon.Ross@ete.inrs.ca)

Volker Lorenz (vlorenz@geologie.uni-wuerzburg.de)

Xavier Bolós (xavier.bolos@gmail.com)

Dario Pedrazzi (pedrario@gmail.com)

This session invites scientific contributions about growth and distribution of monogenetic volcanoes, their internal structure, the role of substrate geology on eruption diversity, and specially maar-diatremes development.

Small-scale basaltic volcanic systems are the most widespread forms of magmatism on the planet and are expressed at the Earth's surface as fields of small volcanoes which are the landforms resulting from explosive and effusive processes triggered by the rise of small batches of magma. This session is concerned with the growth, geomorphology, eruption dynamics, geodynamic distribution and degradation of this type of volcanism. Monogenetic volcanoes distribution inside a volcanic field depends in each case on their regional and local tectonic controls. The great variety of eruptive styles, edifice morphologies, and deposits shown by monogenetic volcanoes are the result of a complex combination of internal (magma composition, gas content, magma rheology, magma volume, etc.) and external (regional and local stress fields, stratigraphic and rheological contrasts of substrate rock, hydrogeology, etc.) parameters, during the magma transport from the source region to the surface. This is meant to be a multi-disciplinary session and we invite contributions that include different type of methods, such as; field studies, geophysical methods, numerical and analogue modelling of volcanic processes and GIS analysis.

Morphometry of maar lakes of Calatrava Volcanic Field (Spain)

Rafael U. Gosálvez¹, Montse Morales¹ and Elena González¹

¹ GEOVOL Research Group, Departmente of Geography and Land Planning, UCLM, Campus Ciudad Real, 13071 Ciudad Real, Castilla-La Mancha, España. RafaelU.Gosalvez@uclm.es

Keywords: Calatrava Volcanic Field, Maar lake, Morphometry.

Recent study is skeptical about the arguments for a wide. The aim of this paper is to approach a morphometric analysis of the maars lakes of Calatrava Volcanic Field (CVF), located in Spain. The morphometric parameters proposed by Head et al. (1981), Sheridan and Wohletz (1983), Fisher and Schmincke (1984), Cas and Wright (1987) and De la Nuez et al. (1997) for the study of volcanic craters and explosion have been applied to 27 maars lake of CVF (Gosálvez, 2011). A series of parameters proposed by Dóniz-Páez (2009) have been added for monogenic basaltic volcanoes (pyroclastic cones) of Tenerife whose use has been adapted here to the maars lakes analyzed in CVF. The morphometric parameters have been calculated through a Geographical Information System (QGIS 2.14.20). The obtaining of these morphometric parameters serves to characterize the maars lake of CVF identified in this work and to define the most common hydrovolcanic or hydrovolcano-type building of CVF. The results obtained are shown in Table 1 where the descriptive statistics are presented. With all these values you can establish the average hydromagmatic vent capable of accumulating temporary water in CVF, whose dimensions are shown in Fig. 1.

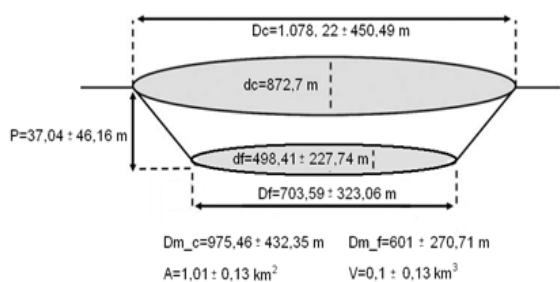


Fig. 1 – Average dimensions of maars lakes in Calatrava Volcanic Field. (Dc= Larger diameter of crater; dc = Minor diameter of crater; Dm_c = Average diameter of crater; Ec = Elongation of crater; Df = Larger diameter of bottom of crater; df = smaller diameter of the bottom of crater; Dm_f = Average diameter of the bottom of crater; Ecf = Elongation of the bottom of crater P = Maximum depth; A = Area of crater and V = Volume of maar).

A tool that has also been applied are the diagrams that relate different morphometric parameters. These diagrams were proposed by Head et al. (1981) and have been used subsequently by various authors such as Fisher and Schmincke (1984) and Cas and Wright (1987) and in Spain by De la Nuez et al. (1993 and 1997). Of all those that have

been proposed, two have been used here, one that relates the radius of the crater and the height / depth (Fig. 2) and the one that relates the radius of the crater and the volume of maar lake (Fig. 3). According to Fig. 2, analyzed maars lake correspond to hydrovolcanic buildings, presenting crater radii (Rc) between 100 and 1000 m and depths (H) of craters between 5 and 100 m. Some of them are close to the definition of boiler buildings due to their size.

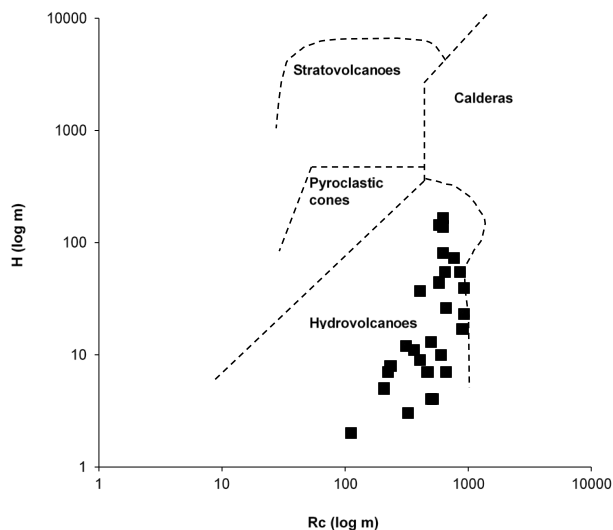


Fig. 2 – Logarithmic diagram radio (Rc) / Depths (H) of maars lakes analyzed from CVF. Source: Head et al., 1981.

Considering Figure 3, most of maar lakes analyzed correspond to maars s.s., possessing volumes less than 0.1 km³ and radius of crater between 100 and 1000 m. As for the maars lakes classified as rings of tuffs and, above all, those included in the areas of cones of tuffs, the diagram does not serve in this case to correctly classify the hydrovolcanic vent. This is because the geomorphological context where the hydromagmatic eruption occurs has not been taken into account. The maars lakes located in the ordovician quartz saws generate vents that dislodge large volumes, which leads to interpreting them as rings or cones of tuffs, when in reality they are deep maars with deposits of underdeveloped tuffs or even channeled towards depressed topographic areas (paleo valleys, piedmont, etc.). The morphometric analysis allows to conclude that the maars lakes studied in CVF are related to the hydromag-

matic activity that has been developed in this volcanic field during the recent Cenozoic, while it has allowed to distinguish the presence of different hydrovolcanic morphologies.

References

Cas, R.A.F., Wright, J.V. 1987. Volcanic Successions: Modern and Ancient. geological approach to

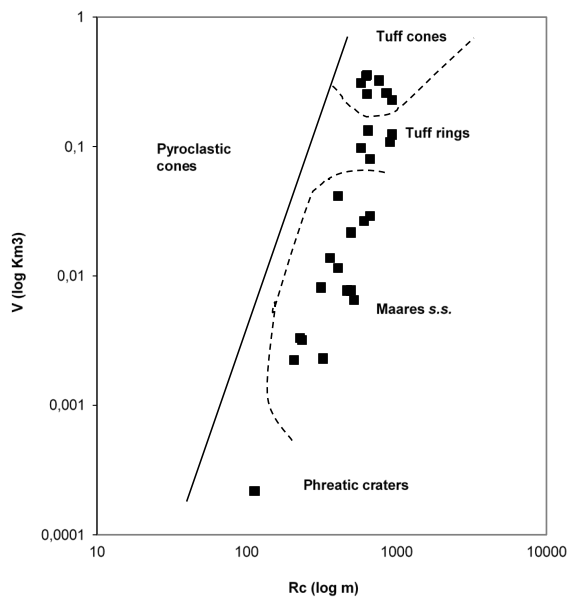


Fig. 3 – Logarithmic diagram radius (Rc) / volume (V) of maars lakes analyzed from CVF. Source: Head et al., 1981.

	Dc	dc	Dm_c	Ec	Df	Df	Dm_f	Ecf	P	A	V
Average	1,078.2	872.7	975.5	1.28	703.6	498.4	601	1.44	37.04	1.01	0.1
Median	1,152	882	1,053	1.29	666	450	540	1.38	13	0.8	0.03
Mode	990	558	1,089	1.25	990	324	774	-	7	0.8	-
Standard deviation	450.49	420.48	432.3	0.16	323.06	227.7	270.7	0.29	46.16	0.78	0.13
Varianza	202,942.6	176,804.6	186,926	0.03	104,366	51,866.2	73,282.2	0.08	2,130.8	0.61	0.02
Kurtosis	-0.61	-0.21	-0.44	2.57	-0.52	-0.09	-0.29	0.1	2.22	-0.1	-0.55
Asymmetry	0.04	0.51	0.26	1.17	0.55	0.63	0.59	0.91	1.74	0.96	1
Minimun value	225	144	184.5	1.06	225	144	184.5	1.09	2	0.05	0.0002
Maximun value	1,863	1,710	1,786.5	1.77	1,404	1,026	1,215	2.17	165	2.8	0.36
Total amplitude	1,638	1,566	1,602	0.72	1,179	882	1,030.5	1.07	163	2.75	0.36

Tab. 1 – Descriptive statistics of the morphometric parameters of maars lakes of CVF (N = 27). (Dc= Larger diameter of crater; dc = Minor diameter of crater; Dm_c = Average diameter of crater; Ec = Elongation of crater; Df = Larger diameter of bottom of crater; df = smaller diameter of the bottom of crater; Dm_f = Average diameter of the bottom of crater; Ecf = Elongation of the bottom of crater P = Maximum depth; A = Area of crater and V = Volume of maar).

Spatial and morphometric analyses of Anaun monogenetic volcanic field (Sredinny Range, Kamchatka)

Dmitry Melnikov, Anna Volynets

Institute of volcanology and seismology FEB RAS, Petropavlovsk-Kamchatsky 683006, Russia. dvm@kscnet.ru

Keywords: Kamchatka, morphometric analyses, spatial distribution

Monogenetic volcanic fields are frequently located in the faulted area and in clusters which are associated with the particular geometry of the magmatic chambers and structures of the magma plumbing system in the crust. The method of cluster analyses of the spatial distribution and morphometric characteristics of the cinder cones was used in our research of the conditions of origin and evolution of one of the largest monogenetic fields in Kamchatka back-arc – the Anaunsky Dol, or Anaun MVF. Kamchatka subduction system is located at the north-western part of the Pacific at the convergent boundary of the Okhotsk and Pacific plates. Today, Sredinny Range represents its back-arc part and is characterized by the wide distribution of the monogenetic volcanic fields: it has more than 1000 cinder cones, which deposits cover the area of about 8500 km² (Laverov, 2005; Ogorodov et al., 1972) (Fig. 1). Sredinny Range has a complex structure with several volcanic provinces with different geological history and variable composition of products. Anaun monogenetic volcanic field occupies one of the lowest sections of the whole Sredinny Range. The youngest volcanism in this area (according to the geological map, it was formed in Quaternary times, although our geochemical research and isotopic dating shows its earlier age) is confined to the lowered block of basement rocks. Shield volcanoes, volcanic ridges, cinder and lava cones are located on a low-lying volcanic dale. We made an attempt to make a spatial analysis of distribution of the volcanic edifices and to quantitatively estimate the structural control of the magma plumbing channels. Based on a digital relief model (DEM SRTM, spatial resolution 30 m) we distinguished more than 100 morphometrically expressed cinder cones. For them, using semi-automatic mode, we estimated the morphometric characteristics: height, diameter of the basement, height/basement ratio, angle of the slope, volume of the edifice. With time, cinder cones change their shape due to the erosion processes. Therefore, finally the edifice height is decreased while the basement diameter increased. Determination of the morphometric parameters allowed us to compose a relative age scale for the cinder cones located in Anaun monogenetic volcanic field.

Spatial analysis has shown that cones tend to form series of clusters, which are associated with the systems of lineaments. Statistically significant patterns in the cinder cones distribution were then compared with the strike of lineaments to estimate possible location of the magma feeding channels.

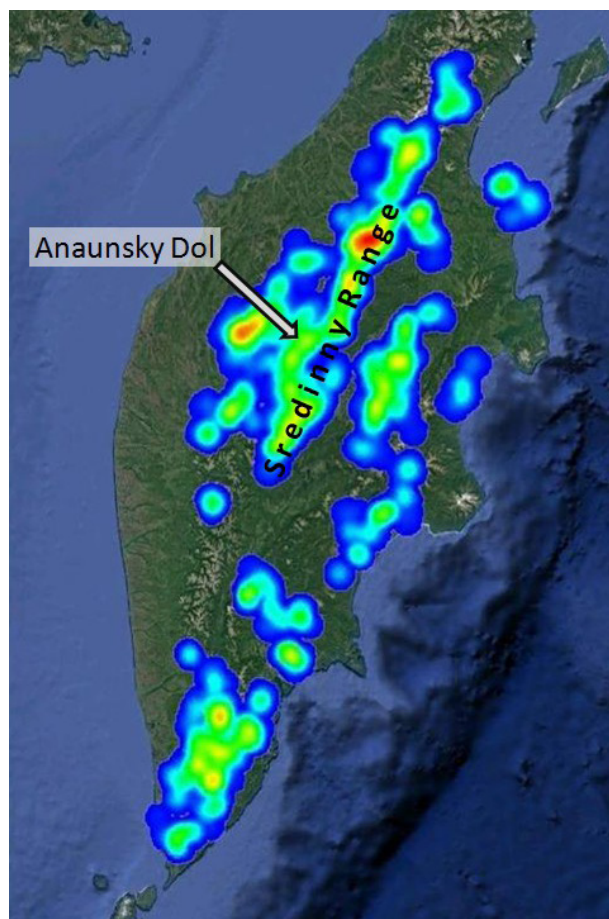


Fig. 1 – Scheme of the spatial distribution of the cinder cones in Kamchatka (HEAT-map), on a base of data from the database “Holocene volcanism of Kamchatka” (geoportal.kscnet.ru/volcanoes/geoservices/hvolc.php)

Acknowledgements

Financial support by RFBR grant #17-05-00112

References

- Laverov, N.P. (ed.) 2005. Newest and contemporary volcanism in Russia. Moscow: Nauka: 604 p. In Russian.
 Ogorodov, N.V., Kozhemiaka, N.N., Vazheevskaya, A.A., Ogorodova A.S. 1972. Volcanoes and quaternary volcanism of the Sredinny Range of Kamchatka. Moscow: Nauka. In Russian.

Geomorphology of the Cuelgaperros maar: interferences between its hydromagmatic activity and the fluvial dynamics of the Jabalon river (Campo de Calatrava Volcanic Field, Spain)

Miguel Ángel Poblete, Salvador Beato and José Luis Marino

*Oviedo University, Humanities Faculty, Geography Department. Campus de El Milan, 33011 Oviedo, Asturias, Spain.
mpoblete@uniovi.es*

Keywords: Maar, Geomorphology, Spain.

The Campo de Calatrava Volcanic Field (CCVF), located in the center of the Iberian Peninsula midway between Montes de Toledo and Sierra Morena in the province of Ciudad Real, has more than 200 eruptive centers dispersed over an area of 3,000 km². The CCVF is one of the Spanish quaternary volcanic regions belonging to the European Cenozoic Rift System. The Campo de Calatrava monogenetic volcano field consists of, according to Poblete (1994) and Poblete et al. (2016), four types of volcanoes (maars, cinder cones, lava domes and small shield volcanoes) and range in age from Upper Miocene (8.6-6.5 Ma) (Ancochea, 1983) to Upper Pleistocene-Holocene (Poblete and Ruiz, 2007; González et al. 2010; Poblete et al. 2014).

Cuelgaperros maar (38°53'N / 3°54'W) is situated in the center of CCVF specifically 2 km to the WNW of La Puebla, between the exogenous domes of El Cominal and Las Moreras. It's one of the greatest maars, along with El Pardillo, from the lower basin of the Jabalon River. It consists of a semi-elliptical crater, open to the west, of great proportions, with 1.68 km of major axis and a depth of 50 m. It has been excavated on pliocene sedimentary materials of the subbasin of Ciudad Real through several hydromagmatic explosions. It has been the subject of several previous studies (Ancochea, 1983; Poblete, 1994), so the purpose of this research is to review the evolution and chronology of hydromagmatic activity and its interference with fluvial dynamics of the Jabalon River.

The methodology consisted of the fieldwork, specifically in the elaboration of morphoeruptive and volcanostratigraphic analyzes fundamentals to know the evolution of the eruptive activity and the relations between the hydromagmatic deposits of Cuelgaperros and the fluvial ones of Jabalon River. Optically stimulated luminescence (OSL) dating has also been performed to ascertain the age of the fluvial deposits. In particular, two samples fossilized by dilute PDC deposits corresponding to the level of fluvial terrace +15-20 m have been dated. The first of them (M1) carried out in a small quarry 4 m deep and the second (M2) was made below the tephra ring, 2 m from the ground surface. In both cases, fine sand levels were intercalated between packages of quartz gravels. In the sampling, precaution was taken to avoid areas with signs of water circulation

and exposure to light. The sediments were measured in the Dating and Radiochemistry Laboratory of the Universidad Autonoma de Madrid (Table 1).

Sample	Deposit	Dating	Age
M-1. Mad-6221 Bin	T+15-20 m	OSL	34427±2229 years BP
M-2. Mad-6364 Bin	T+15-20 m	OSL	35048±2849 years BP

Table 1. Optically stimulated luminescence (OSL) dating of fluvial terrace +15-20 m of the Jabalon River.

The fundamental keys to find out in which conditions and when the eruptive activity took place in Cuelgaperros maar reside in the southern edge, where a calcrete of 1.8 m thick is located. In this deposit are distinguished two levels: one lower of 1.3 m and another upper of 50 cm. The lower contains lapillis, ashes and quartzites and slates of small size inserted in microcrystalline cement affected by bioturbation processes. So, it seems logical to deduce that it has formed in a shallow lake, where explosive volcanic materials fell. In the upper level, the carbonated cement has a micropisolytic structure and includes a large number of explosive breccias (quartzites, slates) and even volcanic bombs, showing that they are lacustrine materials subsequently edaphized in subaerial conditions. Above this calcrete rests a fluvial deposit +15-20 m of the Jabalon River, fossilized in turn by the tephra ring of the Cuelgaperros maar (Fig. 1).

Therefore, the Cuelgaperros maar has been formed from two hydromagmatic explosive phases. The first phase of small magnitude was synchronous to the formation of the calcrete with a minimum age of 34.7±2.5 ka BP. Thereafter, a period of rest takes place during which the deposition of

the fluvial terrace + 15-20 m of the Jabalon River occurs, that lies above the mentioned calcrete, located in the southern edge of the maar. Later, the volcanic activity of Cuelgaperros resumes giving rise to the second hydromagmatic phase of greater virulence and morphological capacity, which partially destroys the calcrete and part of the fluvial terrace. It behaves like a lateral blast that originates a fan cloud directed to the east, depositing the tephra ring that fossilizes the fluvial terrace +15-20 m. Therefore, this second hydromagmatic explosion has a maximum age of 34.7 ± 2.5 ka BP. Finally, dilute PDC deposits expelled from Cuelgaperros and located between 2 and 5 km NE of the maar are fossilized by other calcrete, whose age attributed to the Pliocuatnario has to be advanced, at least, to the Upper Pleistocene or the Holocene.

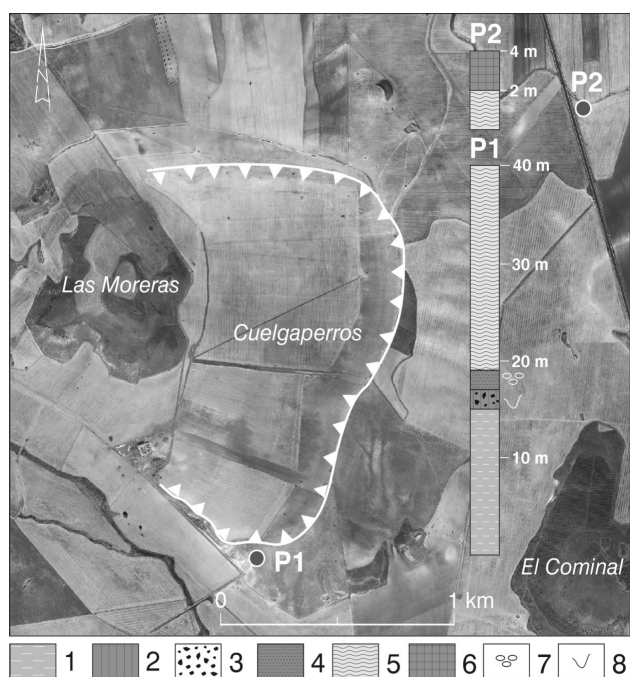


Fig. 1 – Volcanostratigraphic profiles in the Cuelgaperros maar. 1. Pliocene marls. 2. Calcrete. 3. Volcanic bombs and explosive breccias. 4. Fluvial terrace +15-20 m. 5. Dilute PDC deposits. 6. Holocene calcrete. 7. Ostracods. 8. Fragments of ostracods.

Acknowledgements

We are grateful for the helps of the Westminster Foundation and Mancomunidad del Campo de Calatrava. This research was also supported by the FPU program of Ministerio de Educacion, Cultura y Deportes through doctoral fellowship of Salvador Beato Bergua (grant number MECD-FPU14/03409).

References

Ancochea, E. 1983. Evolución espacial y temporal del volcanismo reciente de España Central. Madrid, Universidad Complutense de Madrid.

González, E., Gosálvez, R.U., Becerra, R., Escobar, E. 2010. Evidencias de actividad hidromagmática holocena en el volcán Columba, in González, E., Escobar E., Becerra, R., Ubaldo, R., and Dóniz, J., eds., Aportaciones recientes en Volcanología, 2005- 2008, Almagro, 67-74.

Poblete, M.A., 1994. El relieve volcánico del Campo de Calatrava (Ciudad Real). Gijón. Junta de Comunidades de Castilla-La Mancha and Departamento de Geografía de la Universidad de Oviedo. Poblete, M.A., Ruiz, J. 2007. Revisión de la edad del volcanismo en la Región Volcánica Central de España: evidencias geomorfológicas de actividad volcánica cuaternaria. Actas de la XII Reunión Nacional de Cuaternario, Avila, 163-164.

Poblete, M.A., Ruiz, J., Beato, S., Marino, J.L., García, C. y Gallinar, D. 2014. Cronología y evolución morfoeruptiva de los volcanes Columba y de las Cuevas: revisión y nuevas aportaciones (Sector oriental del Campo de Calatrava, C. Real), in Schnabel, S., and Gómez, A., eds. Avances de la Geomorfología en España 2012-2014. Cáceres, Sociedad Española de Geomorfología, 409-412.

Poblete, M.A., Beato, S., Marino, J.L., 2016. "Landforms in the Campo de Calatrava Volcanic Field", Journal of Maps 12: 271-279. DOI: 10.1080/17445647.2016-1195302.

A proposal for a classification of types of hydrovolcanoes based on geomorphic criteria

Miguel Ángel Poblete, Salvador Beato and José Luis Marino

*Oviedo University. Humanities Faculty, Geography Department. Campus de El Milan, 33011 Oviedo, Asturias, Spain.
mpoblete@uniovi.es*

Keywords: Geomorphology, classification, hydrovolcanoes.

Based on classical classifications of volcanic landforms (Cotton 1944, Ollier, 1970) and the contributions on monogenetic volcanoes (Lorenz, 2003; Kereszturi and Németh, 2012), we have elaborated an essay of classification of hydrovolcanoes from morphoeruptive criteria, which allow to distinguish 7 hydrovolcanic structures, 14 types and 7 subtypes.

1. Maars. They are volcanic forms that consist of a crateric depression excavated below the pre-eruptive topographic surface, resulting from deep phreatic or phreatomagmatic explosions. The following types and subtypes are differentiated:

1.1. Single and isolated maars. The shapes and dimensions of such depressions are very diverse, that is, of circular, semicircular, elliptical and horseshoe plant, with flat or funnel bottom, from tens to several kilometers in diameter and from tens to several hundred meters deep. Within the single maars we can distinguish two subtypes:

-Embedded maars with vertical slopes. Such maars lack tephra ring and are cut into crystalline rocks of Precambrian and Paleozoic massifs, presenting vertical slopes. The maars of Mahiga, Kitigata, Murumuli and Butachinga in the Ruwenzori Massif (Uganda) correspond to this modality, as well as those of La Posadilla, Acebuche and Cervera in the Campo de Calatrava Massif (Spain).

-Carved maars with gentle slopes. Such maars are modeled on soft rocks, that is, in tertiary and quaternary sediments. They are morphologically characterized by having a tephra ring with gentle slopes less than 10°. Worthy of mention are those of the basin of Fort Rock (USA): Hole-in-the-Ground and Big Hole and those of the Orway basin (Australia): Keilambete and Perrumbete.

1.2. Cluster maars. These are groups of single maars very numerous and close to each other to the point of sharing the tephra rings. The maars of Red Rock and Mt. Gambier (Australia) stand out.

1.3. Compound or overlapping maars. These maars configure wide crateric depressions of irregular plant, with diameters that reach between 3 and 5 km. Its polylobulated contours indicate that they have originated from several explosions coming from nearby vents, which intersect

their crateric rims. Examples include the maars of Schalkenmehrener (bicrateric, Germany), La Preciosa (tricrateric, Mexico), Kanyamiombe (tetracrateric) and Rwengaga (pentacrateric) in the Ruwenzori Massif (Katwe, Uganda).

1.4. Nest-type maars. These maars contain, at the bottom of the depression, other volcanoes formed after changing the eruptive style from phreatomagmatic to strombolian, effusive or extrusive. We have the following varieties:

-Maars with nested cones. They house inside cinder cones of different sizes that nest in the center or in eccentric position. As a sample it is worth highlighting the maars of Clossa de San Dalmai (Girona), Beaunit (France), Tower Hill (Australia), Zuni Salt Lake and Red Hill Maar (USA).

-Maars with lava lacs or nested lava flows. The lava flows emitted at the end of the eruption are retained in the form of lakes or sometimes break the tephra rings. To this category belong Potrillo (USA), Tecuítlapa (Mexico), Reboulet-Panouval (France).

-Maars with tholoids. A change in eruption style from explosive to extrusive led to the emplacement of plug domes or pitons and cumulo-domes. The trachytic protrusions of Puy Chopine, Puy Vasset and Grand Sarcouy (France) illustrate this type of nested structure.

1.5. Subsided crater rim maars. They lack tephra rings and the crater rims are formed by calcareous remnant (whose central part have been destroyed by phreatomagmatic explosion) inclined between 20 and 40° and with periclinal tips toward the center of the depression. Such tiltings are due to the volcano-tectonic subsidence experienced by the rim of crater and diatreme after the posteruptive distension, as a consequence of the opening of ring fractures and diagenesis of breccias that fill the volcanic conduct. It is worth mentioning the maars of Las Higuieruelas (Spain), Randeck (Germany) and Rongheat (La Comté, France).

2. Tuff rings. They are composed of craters that lie well at ground level or above the pre-eruptive surface, since the ascending magma contacts with water near the ground surface. These volcanic landforms originate in lacustrine or shallow coastal areas, building tephra rings of greater height, between 100 and 200 m, with external slopes between 10 and 20°. The following types can be distinguished:

2.1. Single and isolated tuff rings. Circular, elliptical or horseshoe shapes predominate. Prototypes include Fort Rock (USA), Diamond Head and Ulupau Head (Hawaii, USA) and Hverfjall, Ludent and Hrossaborg (Iceland).

2.2. Cluster tuff rings. The cluster of tuff rings from the Bishoftu area (Ethiopia) integrated by Haro Maja, Kilotes, Hora and Biete Mengest stand out.

2.3. Compound or overlapping tuff rings. They give place to the tuff rings of greater amplitude and irregular plant with polylobulades forms, being resultant of explosions coming from several nearby vents. The tuff rings of Salt Lake Crater, Aliamanu Crater, Makalapa Crater and Aliamanu School Crater (Oahu, Hawaii, USA) stand out as examples.

2.4. Nest tuff rings. They house small cinder cones, tholoids and lacs of lava.

-Tuff rings with nested cinder cones, lacs and lava flows. They consist of small cinder cones such as Malpais (USA) and lavic flows retained as Riley and Split Butter in USA.

-Tuff rings with nested cumulo-domes (tholoids). If the hydrovolcanic eruption occurs in acidic magmas, at the end of the explosion they can extrude cumulo-domes. This typology includes Panum Crater, Obsidian Dome and the Coso complex in the USA.

3. Tuff cones. They are very similar to cinder cones, however, they originate in lacustrine and marine environments as a result of water-magma contact on the pre-eruptive surface. They build breached cones that rise about 200-400 m above the surface and have steep slopes between 20 and 40° and horseshoe shaped crater. Examples include El Golfo (Lanzarote, Spain), Capelinhos (Portugal), Koko Crater (Oahu, Hawaii) and Lehua (Hawaii).

3.1. Tuff cones with nested lava flows. It is also frequent the subsequent emission of lava that can be retained as lava lakes (Table Rock, USA) or suffer frequent overflows as in Surtur I and II (Iceland).

4. Diatreme necks or plugs. Diatremes are exposed after a prolonged and intense denudation in which the maars are destroyed partially or completely, showing the volcanic conduit. There are two types:

4.1. Exhumed diatremes. They stand out for their pyramidal shape and steep slopes that rise well above the surrounding relief. To this typology of deeply eroded diatremes belong Ship Rock (USA), Gorro Frigio (Argentina), Rocher Ceysac and Rocher Saint-Michel d'Aiguilhe (Velay, France).

4.2. Emerging diatremes. A weak and superficial erosion hardly affects the roof of volcanic chimneys, forming structures of flattened forms; such is the case of Rocher d'Esplay and Plot de Cèreix (Velay, France).

5. Subglacial volcanoes. They originate from the heat of magma that causes melting of ice sheet and the succession of effusive aquatic, explosive and mixed subaerial phases. The morphological results are tuyas and tindas.

5.1. Tuyas. They are circular table mountains that rise between 1,000 and 1,500 m a.s.l. above the surrounding relief. They are characterized by its flat-topped or gently convex backs defined by very thick lava flows overlapping on the hyaloclastites and pillows-lavas, in which very pronounced rectilinear slopes are modeled. They are located mainly in British Columbia, highlighting among others Tuya Butte, Hoodoo and Ash Mountain. In Iceland, the ones by Bláfell, Bláfjall and Herdubreid stand out.

5.2. Tindas. They originate from subglacial eruptions of a fissural nature. They are characterized by steep-sided ridges of walled and serrated form, from several hundred to thousands of meters high, which extend tens of kilometers in length. They emphasize Armannsfell, Tindaskagi, Kalfsrindar, Lágafell and Midfell (Iceland).

6. Pseudocraters and littoral cones. They are features of small size formed from the burst of lava flows that reach lacustrine or marine areas, by the sudden expansion of water vapor trapped inside. The first ones proliferate in lacustrine areas, while the second ones are concentrated in the coast. The pseudocraters of Skutustadir and Adaldalshraun in Iceland and the pseudocones of Hoyberg (Jan Mayen) and Puu Hou in Hawaii stand out.

7. Hydrothermal craters. They are shallow but very wide craters, because their diameter can reach up to 2,500 m. They are formed from small explosions at shallow depth, without the intervention of magma, as a result of the sudden transformation of superheated water into steam. They are very abundant in Yellowstone (USA) and Kaweru (New Zealand).

References

Cotton, C.A. 1944. Volcanoes as landscape forms. Withcombe and Tombs Publ., Christchurch, 416 pp.

Ollier, C., 1970. Volcanoes. An introduction to systematic geomorphology. Mit Press, Cambridge, 370 pp.

Kereszturi, G., Németh, K. 2012. Monogenetic basaltic volcanoes: genetic classification, growth, geomorphology and degradation, in Németh, K. ed., Updates in Volcanology – New Advances in Understanding Volcanic Systems, 3-88. DOI: 10.5772/51387.

Lorenz, V. 2003. Maar-diatreme volcanoes, their formation, and their setting in hard-rock or soft-rock environments. Geolines 15: 72-83.

A preliminary UAV application on Kula Monogenetic Field (western Anatolia, Turkey)

Göksu Uslular¹, Çağdaş Sağır¹, Gonca Gençalioglu-Kuşcu¹, Bedri Kurtuluş¹

¹ Department of Geological Engineering, Muğla Sıtkı Koçman University, Kötekli Campus, 48000 Muğla, Turkey. goksu.uslular@gmail.com

Keywords: UAV, scoria cone, Kula.

Monogenetic basaltic volcanoes are spectacular volcanic edifices formed in all tectonic settings, but especially common in within-plate settings. Of these, scoria (or cinder) cones and maars are the most abundant monogenetic landforms on Earth. They are mutually exclusive volcanoes in terms of eruptive mechanism, as scoria cones are formed by magmatic (Hawaiian, Strombolian, and violent Strombolian) eruptions while maars are formed by phreatomagmatic eruptions.

Morphometric parameters of scoria cones have been widely used for different purposes (e.g. characterization of cone degradation and tectonic setting, and estimation of relative ages). Calculation of Dense Rock Equivalent (DRE) volume in monogenetic fields by using morphometric parameters of not only scoria cones but also other monogenetic edifices (e.g. maar, lava dome) and related lava flows may contribute the understanding of evolutionary processes. In addition, the size of an eruption (namely Volcanic Explosivity Index-VEI) in the monogenetic fields can be envisaged. Last but not the least, spatiotemporal and size distribution (i.e. power-law relation) of scoria cones are also important considerations for the future eruptions.

The traditional methods (e.g. topographic maps, stereoscopic air photos) used for the measurement of morphological parameters of monogenetic volcanoes has been expired due to the increasing amount of Digital Elevation Models (DEMs). There are numerous sources for DEMs, and each has own characteristics (Grosse et al. 2012). Therefore, the quality of measured morphologic parameters is directly related to resolution of DEMs. A recent but very expensive method used for the extraction of high resolution DEMs, airborne Light Detection and Ranging (LiDAR), has been particularly applied on small edifices such as scoria cones (Favalli et al. 2009). Alternatively, comparably low-cost method called Unmanned Air Vehicle (UAV) has been recently used for creating high resolution DEMs of small-scale monogenetic fields (e.g. Harvey et al., 2016).

Kula Monogenetic Field (KMF) in the western Anatolia ("Katakakeumene-burned lands" of Strabo) is the youngest monogenetic field with numerous scoria cones and related widespread lava flows, and a few maars (Fig. 1) (Hamilton and Strickland, 1841; Erinc, 1970; Richardson-Bunbury, 1996; Şen et al. 2014).

Three distinct stages have been proposed for the evolution of KMF based on the geomorphological observations (Hamilton and Strickland, 1841; Erinc, 1970; Şen et al. 2014) and the available age data (e.g. Richardson-Bunbury, 1996; Westaway et al. 2006; Heineke et al. 2016). The first stage (~1.94-0.99 Ma) is mainly represented by plateau-type ba-

saltic lava flows while the later stages (~240-4 ka) are characterized by numerous scoria cones (~64), fissure-related small cones (~16), spatter cones (~8), tumuli (~6), and maars (~5) (Richardson-Bunbury, 1996; Westaway et al. 2006; Şen et al. 2014). Third stage scoria cones and related a'a type lava flows are especially spectacular landforms with the pristine outcrops and the steep cone morphology (slope ≥ 30) (Fig. 2). In addition, human footprints had been found on the fallout deposits of one of the third stage scoria cone, and recently dated as ~11ka (Heineke et al. 2016). The KMF was also designated as a geopark in 2013 by UNESCO, but the area has been recently under the risk of scoria quarrying and environmental pollution due to use of scoria cones as a damp site (Şengör and Lom, 2017).

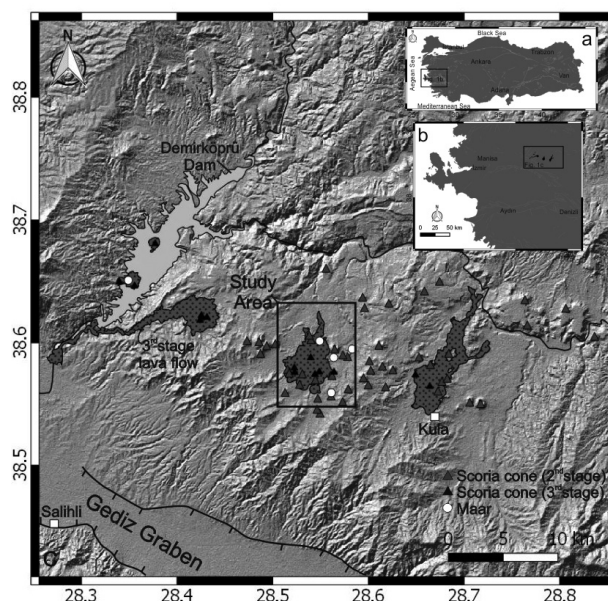


Fig. 1 – Shaded relief of ASTER GDEM (30x30m resolution) displaying scoria cones and maars (Şen et al. 2014) with related lava flows (only 3rd stage lava flows are shown; Erinc, 1970).

Şen et al. (2014) revealed detailed morphological parameters of the scoria cones and maars within the KMF by using the field observations and also the topographic maps and the aerial photos. They calculated the volume and the DRE of the scoria cones and related deposits as 1.06 km³ and 3.25 km³, respectively. The total DRE content of the pyroclastics in the KMF with the consideration of maar deposits (0.34 km³) was calculated approximately as 3.6 km³ (Şen et al. 2014).

In this study, we aim to recalculate the morphometric parameters of scoria cones and maars in the middle part of the KMF as a preliminary study using high resolution (<1 m) Digital Surface Models (DSMs) created by UAV images (Fig. 2). Not only technology in producing the high resolution DEMs, but also nomenclature and technique in the determination of both morphological and depositional characteristics of the monogenetic volcanoes progress (e.g. Kereszturi et al. 2013; Bemis and Ferencz, 2017). Therefore, recalculation of the volume and DRE content of the volcanics in the KMF using high resolution DEMs and consideration of the recent development in the volcanology literature will probably provide new insight into the evolution of the KMF. This study will further enable the volcanology community to attain a better understanding of the advantages and the limitations of the UAV application on monogenetic fields.

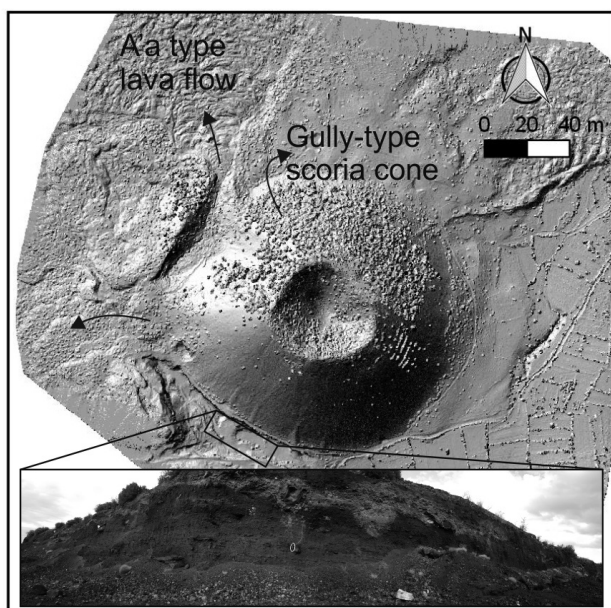


Fig. 2 – DSM of a scoria cone within the KMF created by UAV (DJI Phantom 3 Professional) images performed on Pix4d. Inset photo shows inner structure of the scoria cone. Circled hammer is as a scale.

Acknowledgements

GU would like to thank Rana Salihoğlu, Günseli Erdem and Ersin Ateş for the help during the fieldwork.

References

- Bemis, K., Ferencz, M., 2017. Morphometric analysis of scoria cones: the potential for inferring process from shape, in Nemeth, K., Carrasco-Nunez, G., Aranda-Gomez, J.J., Smith, I.E.M., eds., *Monogenetic Volcanism Geological Society London Special Publications* 446:61-100.
- Erinç, S., 1970. The young volcanic topography of the Kula-Adala area. *Istanbul Üniversitesi Coğrafya Enstitüsü Dergisi* 17: 7-33 (in Turkish).
- Favalli, M., Karátson, D., Mazzarini, F., Pareschi, M. T., Boschi, E., 2009. Morphometry of scoria cones located on a volcano flank: a case study from Mt. Etna (Italy), based on high-resolution LiDAR data. *Journal of Volcanology and Geothermal Research* 186(3): 320-330.
- Grosse, P., de Vries, B. V. W., Euillades, P. A., Kervyn, M., Petrinovic, I. A., 2012. Systematic morphometric characterization of volcanic edifices using digital elevation models. *Geomorphology* 136:114-131.
- Hamilton, W. J., Strickland, H. E., 1841. On the geology of the western part of Asia Minor. *Transactions of the Geological Society of London* 6:1-39.
- Harvey, M. C., Rowland, J. V., Luketina, K. M., 2016. Drone with thermal infrared camera provides high resolution georeferenced imagery of the Waikite geothermal area, New Zealand. *Journal of Volcanology and Geothermal Research* 325:61-69.
- Heineke, C., Niedermann, Hetzel, R., Akal, C., 2016. Surface exposure dating of Holocene basalt flows and cinder cones in the Kula volcanic field (western Turkey) using cosmogenic ³He and ¹⁰Be. *Quaternary Geochronology* 34:81-91.
- Kereszturi, G., Németh, K., Cronin, S. J., Agustin-Flores, J., Smith, I. E. M., Lindsay, J., 2013. A model for calculating eruptive volumes for monogenetic volcanoes- implication for the Quaternary Auckland Volcanic Field, New Zealand. *Journal of Volcanology and Geothermal Research* 266:16-33.
- Richardson-Bunbury, J. M., 1996. The Kula volcanic field, western Turkey: the development of a Holocene alkali basalt province and the adjacent normal-faulting graben. *Geological Magazine* 133(3): 275-283.
- Şen, E., Aydar, E., Bayhan, H., Gourgaud, A., 2014. Volcanological characteristics of alkaline basalt and pyroclastic deposits, Kula volcanoes, Western Anatolia. *Bulletin of the Earth Sciences Application and Research Centre of Hacettepe University* 35:219-252 (in Turkish with English abstract).
- Şengör, A. M. C., Lom, N., 2017. Stop ruining Turkey's geological heritage. *Nature* 547:32.
- Westaway, R., Guillou, H., Yurtmen, S., Beck, A., Bridgland, D., Demir, T., Scaillet, S., Rowbotham, G., 2006. Late Cenozoic uplift of western Turkey: improved dating of the Kula Quaternary volcanic field and numerical modelling of the Gediz River terrace staircase. *Global and Planetary Change* 51:131-171.

Maar structures in Southern Peru and their application on geothermal resources explorations

Guillermo Diaz H¹

¹ Universidad Nacional Mayor de San Marcos & Universidad Peruana Científica Lima Perú. guillermo_1052@yahoo.es

Keywords: maar, explosion crater, phreatomagmatic

The South of Peru features large deposits of volcanic rocks including the explosive-origin type in the shape of widespread pyroclastic deposits and the effusive-origin ones corresponding to lavas, where one highland named Cordillera Volcánica del Barroso (CVB) stands out for the formation of a series of stratovolcanoes, monogenetic volcanoes and volcanic domes from the Neogene Period until now as well as the presence of thermal waters of high temperature (80° - 100°C) which led the Peruvian State to start Geothermal Explorations through its respective Institutes and corporations.

Satellite Imagery Analysis has revealed the presence of circular structures: while some of them correspond to calderas formed by volcanic collapse the other ones which are associated to volcanoes have a smaller diameter. Furthermore, the presence of other shallow and minor structures with circular or oval shape have been determined which are mainly composed by pyroclasts (volcanic ash rocks or tuff), rhyolitic lavas and the presence of breccia. In some cases, these depressions are water-filled (or not) forming lakes which correspond to the maar volcanic structure being very important in regard to Heat Sources (Magma chamber) and a key condition in the formation of a Geothermal Deposit.

Local Geological Context

In South Peru, the Western Cordillera of the Andes stands out for the broad volcanism from the Pleistocene and Quaternary period (Fig. 1) resulting from the activity of a Calc-Alkaline Volcanic Arc (de Silva y Francis, 1991) which is located to the west of the Cordillera.

The Calc-Alkaline Volcanism results from the subduction of the Nazca Plate in connection with the Continental Plate. The plate convergence direction is N79°E with an average velocity of 5 – 6 cm/yr (Norabuena et 1999).

Another example of thin and discontinuous Volcanic Arc is Shoshonitic and can be found to the East of the Cordillera. In accordance with the Local Southamerican Context, South Peru volcanism is part of the Central Volcanic Area (ZVC) which comprises territories of Peru and Chile. The application of the photo-interpretation by satellite images in order to search geothermal deposits has been executed by interpreting and locating what is traditional, meaning evidences on the Surface such as: points of high temperature thermal water upwelling, volcanic domes, volcanic calderas, travertine rocks, which are employed

in order to identify potential geothermic areas presently considered at the stage of Pre-feasibility study.

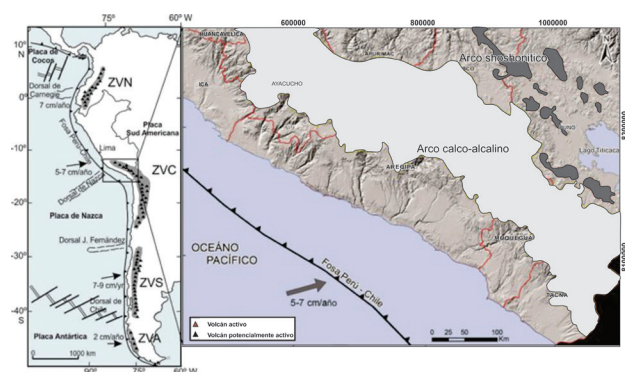


Fig. 1 The image on the right shows the Mio-Pleistocene calc-alkaline volcanic arc (area in light gray color) and the shoshonitic volcanic arc (área in dark gray) as well as the distribution of active and potentially active volcanoes in the south of Peru; whereas the image on the left shows the existing volcanic areas in the Southamerican Andes: ZVN, Northern Volcanic Area; ZVC, Central Volcanic Area; ZVS, Southern Volcanic Area and ZVA, Austral Volcanic Area.

Due to photo-interpretation it has been found other circular structures not as spectacular as the Collapse Volcanic Calderas but which show a circular structure with low rims and a depression in the center corresponding to Maar Volcanic Structures like Pallca which would be associated with the presence of magma chamber located underground which will be described hereafter.

Pallca's Maar Volcanic Structure.

An analysis of the satellite image has identified to the North of the Chachanini Volcanic Complex a series of volcanic structures with N-S direction which are part of the Cordillera Volcánica Barroso (CVB) where there are stratovolcano domes and where circular structures (Fig. 2) with not so high walls can be appreciated as well as a depression in the center corresponding to a maar volcanic structure which has been named Palca's Maar Volcanic Structure (Fig. 2).

As it is well-known a maar structure results from the deep underground interaction between water and heat coming from an active magma chamber where the saturation of high temperature and pressures originate a phreatomagmatic explosion originating a depression. Therefore, the location of this kind of structures will determine other potential places for Geothermal Deposits.

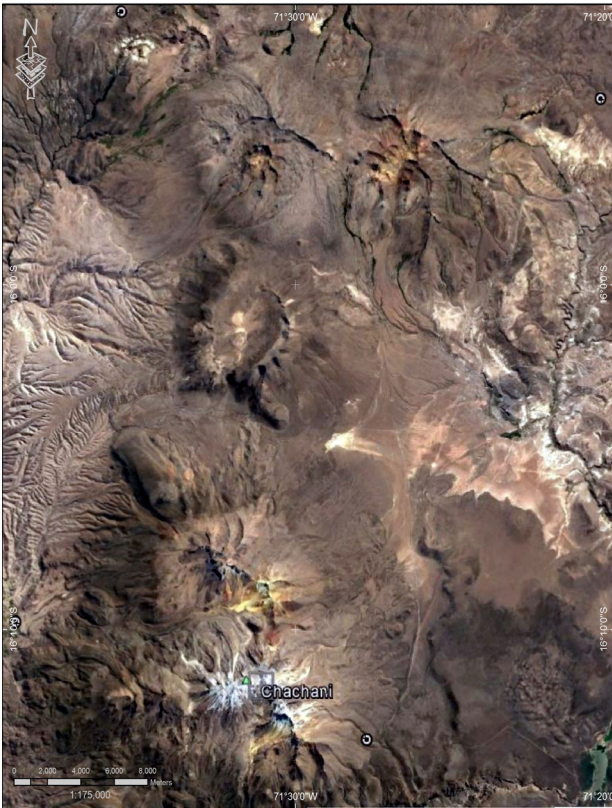


Fig. 2 Palca's Maar Volcanic Structure location

Conclusions

- South Peru shows calc-alkaline volcanism mainly generated by the partial fusion of the mantle wedge due to dehydration of the subducted oceanic crust.
- The Cordillera Volcánica Barroso (CVB) is a part of the Western Cordillera which has numerous stratovolcanoes where maar-based structures stand out.
- One of the criteria that can be employed for Geothermal Explorations in order to locate potential areas of geothermal activity is the presence of maars which are generally associated to heat sources (deep magma chamber)

Acknowledgements

I would like to thank the Organizing Committee of the 7th International Maar Conference for giving me the opportunity to present this abstract.

References

De Silva, S.L., Francis, P.W. -Volcanoes of the Central ANDES. Berlin: Springer – 216 p.

Dostal, J., Dupuy, C. & Lefevre, C. (1977) - Rare earth element distribution in Plio – Quaternary volcanic rock from southern Peru; *Lithos* 10;173 -183.

Gerbe, M.-C. & Thouret, J.-C. (2004) – Role of Magma mixing in the Petrogenesis of lavas erupted during the 1990–98 explosive activity of Nevado Sabancaya, southern . *Bulletin of volcanology* , 66(6):541-561

Harpel, C. J., de Silva, S., & Salas, G. (2011) – The 2 eruption of Misti volcano, southern Peru - The most recent plinian eruption of Arequipa's iconic volcano, *Geological Society of America, Special Paper 484*, 1-72.

INGEMMET-ELECTROPERU,(1994) – Estudio geovolcánico e Inventario sistemático de manifestaciones geotermiales del Lote de Tutupaca (Informe Interno, Tomos; I,II,III)

Lefevre, C(1979) – Un exemple de volcanisme de marge active dans les Andes du Perou (sud) Miocene a l' actuel (zonation et C).

Contained sub-surface Kimberlite explosions in Snap Lake Dyke and CL186, NWT, Canada

Stephan Kurszlauskis¹ and Alexandrina Fulop¹

¹ De Beers Canada Inc., 1601 Airport Road NE, Suite 300, Calgary, AB, Canada. stephan.kurszlauskis@debeersgroup.com

Keywords: kimberlite, breccia, explosion

The Snap Lake kimberlite dyke system dated at 523 +/- 6.9 Ma is located in the south-central Slave Craton of northern Canada and intrudes Archean granitoids, leucogabbro, and basic amphibolite-bearing meta-volcanic rocks. The dyke system dips at ~15° to the north-east and the main dyke has an average thickness of 2.8m. It extends over a known distance of 3.5 km in north-south direction and 2.4 km in east-west direction. The dyke thickness decreases outward from a central axis trending roughly NE-SW. About 3 km East of the thickest dyke zone, the dyke system can still be traced by drilling; this part of the resource is called "East Dyke". A negative geomagnetic anomaly, CL186, located on East dyke was drilled with several drill cores, three of which intersected an intact granite roof close to surface with a granite breccia under-neath and less diluted volcanoclastic kimberlite at the bottom of the sequence. Snap Lake dyke itself also shows the presence of localized breccias in which both the country rock and the kimberlite is fragmented. These breccias show a convincing relationship with older faults, joint sets and Proterozoic diabase dykes that are crosscut by the kimberlite dyke.

The most prevalent faults on the Slave craton include a conjugate system of northeast-striking dextral and northwest-striking sinistral strike-slip faults, and penecontemporaneous northerly trending oblique-sinistral faults (e.g. Stubbley, 1998) which have been active about 1.84 – 1.74 Ga ago. Cratonization of the Slave Province was completed by the intrusion of diabase dykes since there are no lateral displacements evident along these dykes (e.g. Hoffman, 1988; Pehrsson et al., 1993). The predominant fault system in the Snap Lake area is the east-west striking Snap-Crackle fault zone that controls the disposition and development of many structural features in the vicinity. The fault zone is comprised of two principal faults, Snap and Crackle, and several subsequent anastomosing faults which show significant displacement (several 100m) of older diabase dykes (Stubbley, 1998). The erosion rate since emplacement is difficult to estimate, but may be in the order of 900m (Zhang et al., 2012) or 750-1500m (Ault et al., 2009).

Geometry of CL186 and Snap Lake breccias

CL186 was targeted by several drill holes, three of which intersected a country rock breccia with increasing proportions of fragmental kimberlite towards depth. The base of the sequence is comprised of relatively dilution-poor kimberlite, which itself has a sharp base to the underlying unbrecciated country rocks. The lateral and vertical extend of the breccia is relatively well controlled by additional 10

drill holes. The base of the breccia correlates well with the position and dip of East Dyke (Fig. 1).

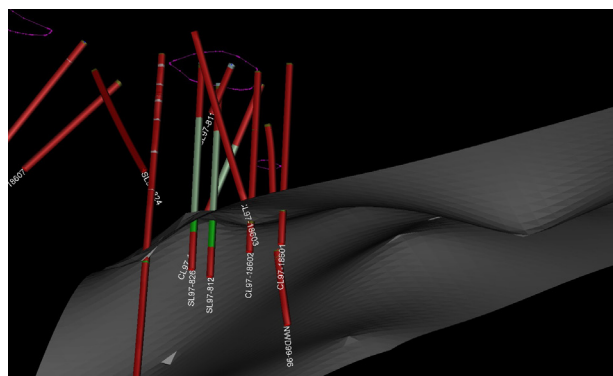


Fig. 1 – Drill hole locations controlling the geology of CL186. The surface of East Dyke is shown as grey sheet, kimberlite in green and breccias in light green.

The vertical depth of the breccia intersected in drill core SL97-812 is about 115m and in SL97-826 it is 123m. In the inclined drill core CL97-18604 it is almost 70m. Its lateral extent (in W-E direction, assuming that the breccia intersects in SL97-826, SL97-812 and CL97-18604 are connected) is about 120m. This size of the breccia is significant and comparable with the size of root zones underlying large South African kimberlite pipes (Lorenz and Kurszlauskis, 2007). However, it should be noted that most of this breccia zone is occupied by country rock debris. Kimberlite is most abundant (=least diluted) towards the bottom of the vertical drill core intersects (34.4m in SL97-812 and 23.6m in SL97-826). The breccia zones appear to have a sharp bottom contact with underlying granite and both drill cores were drilled for a significant distance (36.5m in SL97-812 and 46.8m in SL97-826) into unfractured granite after exiting the kimberlite. This, and the general alignment of the Kimberlite/granite bottom intersect with the dip and strike of East Dyke, suggests that the breccia zone was sourced from the NNE dipping East Dyke.

The breccias intersected in Snap Lake Dyke (in the area of the underground mine) are smaller in extent. They measure mostly less than 20m in width, but can extend to several 100m in length along faults. Due to extensive underground mapping, a correlation between the breccias and pre-existing faults could be established.

Geology of the breccias

The geology of the breccias in Snap Lake and East Dyke

(CL186) appears similar, although on a different scale. In both locations the breccias emerge from the north-east dipping dykes and most if not all of the brecciation occurs above the dyke and not below it.

In CL186, the kimberlite at the base is least diluted (25-30% local basement clasts) and, at the time of our study, was already extensively sampled. The remaining kimberlite is so highly altered that it is difficult to say whether the kimberlite at the very base is coherent or fragmental. The breccia occurring between the kimberlite base and the non-fragmental granite roof can be separated in 4 zones:

A) A breccia that has less than 50% granite xenoliths and fragmental kimberlite in the matrix. These breccias are very similar to breccias occurring in kimberlite diatremes. The medium to coarse breccia is poorly sorted and consists of clasts which are either angular with sharp tips or may be subangular to subround in more matrix-supported sections. There is mixing of local basement lithologies where granitic clasts occur next to aplitic and pegmatitic fragments. Some clasts show a higher degree of alteration towards the margins while others are fresh. Fine fragmentation of granite is abundant and forms part of the matrix.

B) A granite dominated breccia that shows little obvious evidence for the presence of kimberlite. However, serpentine and the presence of micro-diamonds indicate that even this distal breccia was originally injected with kimberlite, which is also supported by the presence of accretionary pyroclasts. Especially the breccia in this zone shows a very high abundance of granitic fine fragmentation, which reaches the fine sand and even silt fraction and which forms the matrix of the breccia. In their interstitial spaces, some samples show evidence for horizontal to inclined fine bedding to lamination of the matrix and also of soft sediment deformation, giving clear evidence for the presence of water during the formation of the breccia.

C) The breccia clasts are very angular and show jigsaw fit textures with evidence for water-lain open framework sedimentation of finely granulated local basement material. No juvenile material is present. A secondary carbonate cement fills the remainder of the interstitial spaces that is not filled by finely comminuted granite material.

D) In this zone unbrecciated granite interchanges several times with angular, jigsaw-fit brecciated granite over several meters. Close to surface the granite is undisturbed and shows no sign of brecciation at all.

Relevance of breccias for kimberlite emplacement processes

The close relationship of breccias with pre-existing fractures in the country rocks, the high degree of fine fragmentation, the waterlain nature of some interclast sediments and the presence of accretionary pyroclasts all give evidence that the kimberlite reacted explosively with groundwater locally available along faults. The unbrecciated roof of the breccia zone also gives evidence that the explosions were contained in their subsurface

location and did not reach the surface. These contained explosion breccias are equivalent to contact breccias surrounding the root and lower diatreme zones in kimberlite pipes (Lorenz and Kurszlaukis, 2007). Our observations are in alignment with the pre-conditioning of country rocks by contained explosions prior to diatreme formation, as suggested by Valentine et al. (2014).

Acknowledgements

De Beers Canada is thanked for permission to publish these data.

References

- Ault, A.K., Flowers, R., Bowring, S., 2009. Phanerozoic burial and unroofing history of the western Slave craton and Wopmay orogen from apatite (U-Th)/He thermochronometry. *Earth and Planetary Science Letters* 284: 1-11.
- Hoffman, P.F., 1988. Geology and tectonics: East Arm of Great Slave Lake, Northwest Territories; Geological Survey of Canada, Map 1628A, scale 1:250,000.
- Lorenz, V., Kurszlaukis, S., 2007. Root zone processes in the phreatomagmatic pipe emplacement model and consequences for the evolution of maar-diatreme volcanoes. *Journal of Volcanology and Geothermal Research Special Volume* 150: 4-32.
- Pehrsson, S.J., van Breemen, O., Hanmer, S., 1993. Ages of diabase dyke intrusions, Great Slave Lake shear zone, Northwest Territories; in *Radiogenic Age and Isotopic Studies: Report 7*; Geological Survey of Canada Paper 93-2: 23-28.
- Stubley, M.P., 1998. Bedrock geology of the Snap Lake area. A report to accompany a 1:10,000 scale geological map. Stubley Geoscience. 31pp.
- Valentine, G.A., Graettinger, A.E., Sonder, I., 2014. Explosion depths for phreatomagmatic eruptions. *Geophysical Research Letters* 41: 3045-3051
- Zhang, N., Zhong, S., Flowers, R. 2012. Predicting and testing continental vertical motion histories since the Paleozoic. *Earth and Planetary Science Letters* 317-318: 426-435.

Monogenetic volcanism at El Hierro Island: the Ventejís–Pico de los moles eruption

Laura Becerril¹, Dario Pedrazzi¹, Domenico Doronzo¹, Adelina Geyer¹, Joan Martí¹

¹ Institute of Earth Sciences Jaume Almera, ICTJA, CSIC, Group of Volcanology, SIMGEO UB-CSIC, Lluís Sole i Sabaris s/n, 08028 Barcelona, Spain. laurabcar@gmail.com

Keywords: hydromagmatism, Canary Islands

Monogenetic volcanism produces small-volume volcanoes with a wide range of eruptive styles, lithological features and geomorphic architectures (Németh and Kereszturi 2015). Hydromagmatic eruptions represent a particular hazardous volcanic scenario in any volcanological context depending on the way water interacts with the rising or erupting magma; even small-volume eruptions can be highly explosive. Hydrovolcanic eruptions are common in coastal environments, where erupting magma is prone to interact with seawater in either shallow subaqueous or subaerial settings (Sheridan and Wohletz 1983).

The Canary Archipelago (Spain), a set of seven major volcanic oceanic islands, has hosted during its whole geological evolution numerous eruptions where magma has interacted with external and internal water sources. In these cases coastal hydrovolcanic edifices and phreatomagmatic craters were created giving in large part tuff rings, maars and rhythmic laminated sequences interbedded with magmatic sequences. Spatial and temporal distribution of recent volcanism at the Canary Islands Archipelago demonstrates that the archipelago is a highly active volcanic zone and that future eruptions may occur at many different vent sites in any of the islands (Carracedo 1994). The youngest and southwestern most island of the Canary Islands, El Hierro (Figure 1), is characterized by a monogenetic volcanic field, where 205 cinder cones, 1 tuff ring and 3 explosion craters associated with phreatomagmatic activity and 168 submarine cones have been recognised (Becerril 2014). Hydromagmatic eruptions include the interaction of magmas both with phreatic and sea water. Hydromagmatic episodes have been described for Ventejís, La Caldereta and Hoya de Fileba (Figure 1) with rhythmic laminated sequences of coarse juvenile ash and lapilli scoriae rich beds with accidental lithic fragments, also occurred at the interior of the island but in less frequency than those above mentioned (IGME 2010). In addition, some hydromagmatic eruptions occurred along the coast producing tuff ring deposits (Anillo tobas del Verodal-Figure 1) at the western part of the Island (Carracedo et al 2001; IGME 2010).

The Ventejís-Pico de los Moles eruptions belongs to the last stages inside Tiñor cycle, that is the first volcanic edifice of the island (1.12-0.88 Ma; Guillou et al., 1996). They have been dated in 1.04 ± 0.02 Ma by Guillou et al. (1996). Only succinct descriptions about the main products of these eruptions are given in the geological map docu-

ments (IGME 2010). The Ventejís-Pico de los moles eruption is described as a large emission of explosive products in which also appear pyroxene xenoliths.

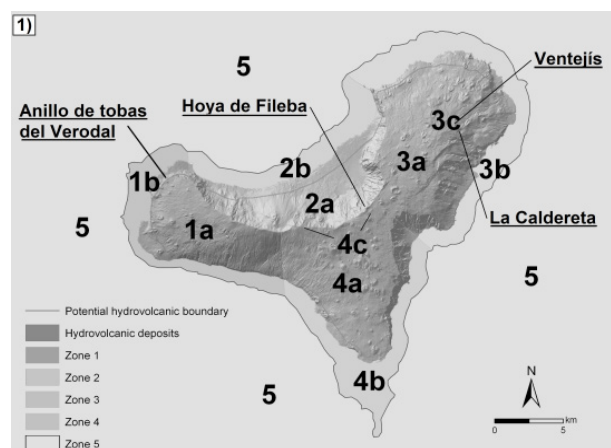


Fig. 1 – Sectors and subsectors defined on El Hierro. Sectors 1–4 show onshore division while sector 5 represents the offshore area. The division is based on differences in structural patterns, spatial probability of hosting new vents and expected hazards. Subsectors a–c take into account the potential occurrence of hydrovolcanic Episode (From Becerril et al. 2014)

Due to the lack of a comprehensive study of these eruptions, a preliminar geomorphometric study and a first field recognition of the products was carried out. Geomorphological characteristics, tectonic features and phreatomagmatic deposits point out that Ventejís edifice may be considered as a maar-crater. This monogenetic volcano shows a crater 1 km long with a diameter of approximately 2.5 km (V-Figure 2). Deposits related to this eruption are more abundant than initially thought, reaching almost 4 km from the vent up to the east coast near La Caleta. Volcano-structural features in the area indicate that exist a fault system that conforms a graben (Becerril et al. 2015) and that could have affected the area, thus producing a larger eruption, since the main aquifer of the island is located in this sector. Also, there is a phreatomagmatic crater (LC-Figure 2) that nowadays serves as a pool for the hydro-electric central of the island.

We propose a systematic and comprehensive study in this area in order to reconstruct the volcanic evolution of the hydromagmatic craters with special references to Ventejís-Pico de los Moles edifices. Volcanic hazard assessment

must necessarily be based on good knowledge of the past eruptive history of the volcanic area.

Monogenetic eruptions are the most common eruption type to have occurred in El Hierro's recent geological past, especially over the last 158 ka. In addition, due to the oceanic nature of the island, hydrovolcanic eruptions (submarine, litoral eruptions affecting coastal areas or phreatomagmatic explosions) are also expected in the future in other areas at El Hierro Island

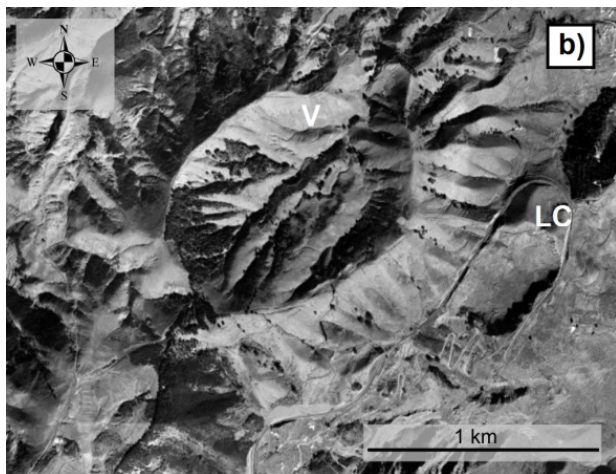


Fig. 2 – Ventejís (V) and La Caldereta (LC). Image from Google Earth 2000.

Acknowledgements

We would like to thank the Cabildo de El Hierro for the logistic support.

References

Becerril, L., 2014. Volcano-structural study and long-term volcanic hazard assessment on El Hierro Island (Canary Islands) (Doctoral dissertation, PhD Thesis document, University of Zaragoza, Spain ISBN: 978-84-617-3444-3.

Becerril, L., Bartolini, S., Sobrado, R., Martí, J., Morales, J. M., Galindo, I., 2014. Long-term volcanic hazard assessment on El Hierro (Canary Islands). *Natural Hazards and Earth System Sciences*, 14(7): 1853-1870.

Becerril, L., Galindo, I., Martí, J., Gudmundsson, A., 2015. Three-armed rifts or masked radial pattern of eruptive fissures? The intriguing case of El Hierro volcano (Canary Islands). *Tectonophysics* 647: 33-47.

Carracedo, J. C., 1994. The Canary Islands: an example of structural control on the growth of large oceanic-island volcanoes. *Journal of Volcanology and Geothermal Research* 60(3-4): 225-241.

Carracedo, J. C., Rodríguez Badiola, E., Guillou, H., Nuez Pestana, J. D. L., Perez-Torrado, F. J., 2001. Geology and volcanology of La Palma and El Hierro, Western Canaries.

Guillou, H., Carracedo, J. C., Torrado, F. P., Badiola, E. R., 1996. K-Ar ages and magnetic stratigraphy of a hotspot-induced, fast grown oceanic island: El Hierro, Canary Islands. *Journal of Volcanology and Geothermal Research* 73(1): 141-155.

IGME, 2010. Mapa Geológico de España, Escala 1:25.000. Isla de El Hierro, Hoja 1105 II Valverde: 96 pp

Németh, K., Kereszturi, G., 2015. Monogenetic volcanism: personal views and discussion. *International Journal of Earth Sciences*, 104(8): 2131-2146

Sheridan, M. F., Wohletz, K. H., 1983. Hydrovolcanism: basic considerations and review. *Journal of Volcanology and Geothermal Research* 17(1-4): 1-29.

Maars in the Calatrava Massif. (Campo de Calatrava, Spain)

M^a Elena González^{1,2}, Rafael Becerra^{1,2}, Rafael Ubaldo Gosálvez^{1,2}, Estela Escobar^{1,2} and Javier Dóniz^{2,3}

¹ *Geography and Land Planning, UCLM, Camilo José Cela s/n, 13071, Ciudad Real, Spain. elena.gonzalez@uclm.es*

² *Canary Islands Volcanology Institute -INVOLCAN Carretera de Taoro s/n, 38400 Puerto de La Cruz, Spain.*

³ *Departamento de Geografía e Historia, Universidad de La Laguna, Campus de Guajara s/n, 38071, La Laguna, Spain*

Keywords: Maars, Campo de Calatrava, volcanism

The Campo de Calatrava is a Volcanic Region located in the south of the Spanish Central Plateau. It is integrated into European Intracontinental Volcanism, Cebriá and López-Ruiz (2010) and it has developed over eruptive cycles with a temporality comprised between 8.6 million years and 3.500 years B.P. It has developed more than 300 volcanoes of which approximately half have a phreatomagmatic character with the development of maars of different types and the emission of unidirectional density currents, embedded in the pre-existing fluvio-torrential network, each of them presents a complete tuff ring at different degree of conservation.

The phreatic and phreatomagmatic eruptions, have played a first-rate role at Campo de Calatrava volcanism. They have taken place throughout all the region eruptive stages and given rise to some landscape distinguished by the presence of big explosive depressions, opened both in mountainous territories like in Cenozoic sedimentary basins.

The Calatrava Massif, García (1995) is located in the SE of the volcanic region. It constitutes the mountainous link between the long eroded anticlines that give rise to the development of the Argamasilla-Abenójar and Almagro basins. Fig. 1.

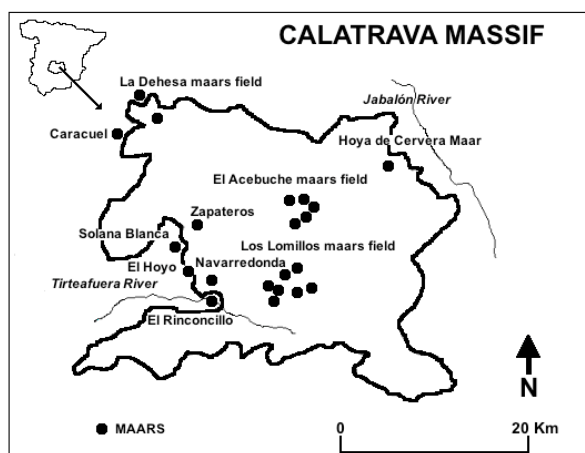


Fig. 1 – Distribution of the main maars in Calatrava Massif.

This mountainous massif, of hercynian age, presents one of the more dense concentrations of volcanoes in the

whole Campo de Calatrava because in it converge the two main eruptive axes of the volcanic region and because it develops a dense network of fractures showing a predominant direction NE-SW, NW-SE and WE.

The eruptive patterns allow the individualization of two zones: central and southern in which the phreatomagmatic dynamics are predominant, while to the north and east the activity is fundamentally magmatic. In the limits of the massif, marked by tectonic pits, we find an area of new hydrovolcanic activity.

Largest maars are located in these areas. In the central space are included: El Acebuche, Las Setecientas, Hoya del Cura, Hoya de Navalacierva; while in the south, we can find: Las Carboneras, Los Cuartos, Los Lomillos and the alignment of La Encina that coexist with others of smaller size, González, (2002).

At the West are located the next phreatomagmatic craters: La Dehesa, Pozo de Vilchez, Caracuel, Solana Blanca, El Hoyo, La Covezuela, Navarredonda and El Rinconcillo. On the eastern edge it is only located the maar of Hoya de Cervera.

In these eruptions have been emitted large volumes of deposits of pyroclastic flows, intensely lithified with thicknesses that, punctually, can reach 60 meters, Fig. 2. These deposits are affected by hydrothermal alteration and post-depositional carbonations, as well as settlement breakages and cooling cracks.

In these quartzite territories there is a scarce presence of superficial water and its storage takes place at different depths, depending on the fracturing, cracking and porosity of the rocks. Magma-water contact is produced at a certain depth which manifests itself in continued explosions caused by the maintenance of the hydric conditions of the environment White and Houghton (2000).

The continuously sustained activity generates craters embedded, juxtaposed and tangent, with a total or partial destruction of previous land forms and the creation of new ones. The disparity in the size and geometry of the craters resulting from hydromagmatic activity indicates that the water-magma contacts take place at different depths. The direction and location of the density currents are controlled by the topography prior to the eruption and by



Fig. 2 – Eroded remains of the tuff ring of La Encina maar.

the immediately resulting from the explosive events.. In the maars of the Calatrava Massif we find: marked horizontality in the bottoms of the maars filled by materials coming from the collapse of the eruptive columns developed during the hydromagmatic eruption with abundant presence of accretionary lapilli, discrete subsidence processes, strong asymmetries in the size of the rock walls that border the maar due to different resistance of the materials. Under certain conditions the density currents behaves in an unidirectional mode and generates deposits controlled by the topography that modifies these profiles of the valleys in which they are fitted by filling or they are arranged in a fan shape on the piedmont, developing lobed or convex fronts. The degree of erosion of the deposits is accentuated according to the position they occupy. When they are in depressed areas they present in general a good state of conservation. Those located on rocky hills and in a shady position, could be intensely eroded.

In rainy season, the impermeability of depression bottoms and the sealing provided by the tuff rings and the rock walls, allows the storage of sheets of water that give rise to an extensive and rich wetland, unique in Europe, Gosálvez et al., (2010).

Some of these maars are cataloged as a natural monument being subject of didactic and tourist activity.

In the maars of the Calatrava Massif we find: marked horizontality in the bottoms of the maars filled by materials coming from the collapse of the eruptive columns developed during the hydromagmatic eruption with abundant presence of accretionary lapilli, discrete subsidence processes, strong asymmetries in the size of the rock walls that border the maar due to different resistance of the materials. Under certain conditions the density currents behaves in an unidirectional mode and generates deposits controlled by the topography that modifies these profiles of the valleys in which they are fitted by filling or they are arranged in a fan shape on the piedmont, developing lobed or convex fronts. The degree of erosion of the deposits is accentuated according to the position they oc-

cupy. When they are in depressed areas they present in general a good state of conservation. Those located on rocky hills and in a shady position, could be intensely eroded.

In rainy season, the impermeability of depression bottoms and the sealing provided by the tuff rings and the rock walls, allows the storage of sheets of water that give rise to an extensive and rich wetland, unique in Europe, Gosálvez et al., (2010).

Some of these maars are cataloged as a natural monument being subject of didactic and tourist activity.

References

- Cebriá, J.M., López-Ruiz, J., 2010. Modelos petrogenéticos y geodinámicos para el Campo de Calatrava. In: González, E.; Escobar, E.; Becerra, R.; Gosálvez, R.; Dóniz, F.J. Aportaciones recientes en Volcanología 2005-2008. MCT, UCLM, 45-49
- García, J.L. 1995. Los paisajes naturales de la comarca de Los Montes-Campo de Calatrava. BAM
- González, M.E. 2002. Depósitos de oleadas basales Y su papel en el relieve volcánico del Campo de Calatrava. In. Estudios recientes en Geomorfología: Patrimonio, Montaña y Dinámica territorial. SEG, U. Valladolid, 455-465
- Gosálvez, R.U.; González, E.; Escobar, E.; Becerra, R. 2010. Análisis biogeográfico de las lagunas volcánicas de la Península Ibérica. In. Geografía, Territorio y Paisaje. Actas del XXI Congreso de Geógrafos Españoles. UCLM-AGE, 147-149
- White, J.; Houghton, B. 2000. Surtseyann and Related Phreatomagmatic Eruption. In. Encyclopedia of Volcanoes (H. Sigurdsson, ed.) Academic Press San Diego, 495-512

The role of phreatomagmatism on scoria cone forming eruptions in the Quaternary Auckland Volcanic Field (New Zealand)

Gabor Kereszturi¹ and Károly Németh¹

¹ Geosciences, School of Agriculture and Environment, Massey University, Private Bag 11 222, Palmerston North, New Zealand, g.kereszturi@massey.ac.nz

Keywords: cinder cone, basalt, phreatomagmatism

Scoria cones are small-volume (10–1–10⁵ km³) volcanic landforms that are characterized by conical geometry with a crater on top. They are dominantly composed of scoriaceous coarse ash to lapilli with blocks/bombs from mafic to intermediate magma compositions (Wood, 1980, Kereszturi and Németh, 2012). The limited magma supply during the eruption results in generally simple facies architecture of the volcanic edifice that is built by relatively ‘homogenous’ pyroclastic units of dominantly fall and ballistic origin (Wood, 1980, Kereszturi and Németh, 2012). Occasional low energy explosive eruptions however can produce weak pyroclastic density currents, which may deposit dune-bedded, stratified unsorted fine ash within the otherwise scoria ash and lapilli dominated cone-forming successions. Eruption that fed from small-volume magma batch or several magma batches may go through a variety of eruptive styles, including magma-water interactions related phreatomagmatic explosive ones (e.g. Agustín-Flores et al., 2014). In such case, a typical eruptive sequence starts with a fine ash and lapilli dominated stratified to dune-bedded single layers to more pronounced tephra rings that later on completely covered by the growing scoria cone when external water used up in the course of the eruption preventing phreatomagmatic magma-water interactions. While this is the most common eruptive sequence in such complex cones, phreatomagmatism can occur any time during the cone growth if external water is available or the conduit conditions allow it to access to the hot melt.

The application of scoria cones as a reliable proxy for unrevealing patterns and evolution of low-magma output magmatic systems (<1 km³/ky) requires a good understanding of the conditions that influences scoria cone emplacement processes. Many recent studies on scoria cones, such as works on Tolbachik, Russia (Doubik and Hill, 1999), Lathrop Wells, Nevada (Valentine et al., 2007), Pelagatos, Mexico (Guilbaud et al., 2009), Sunset crater, Arizona (Ort et al., 2008), Irao, Japan (Kiyosugi et al., 2013), Cerro Negro, Nicaragua (Courtland et al., 2013), Los Morados, Argentina (Németh et al., 2011) and El Croscat, Spain (Di Traglia et al., 2009) found that these small-volume volcanoes composed of eruptive sequences reflecting great variety of eruption styles responsible for their formation ranging from pure dry explosive phases to more external water-influenced explosive phases. In addition, the order

of volcanic units reflecting various eruption styles seems to be very diverse from units associated with eruptions driven by wet to dry, dry to wet or completely random eruption style patterns. These studies also provided evidence of departures from simple facies architecture towards more complex eruptive mechanism forming scoria cones, involving base surges, convective plumes, and/or lava-fountaining that is not consistent with the classical Strombolian eruptive regime (c.f. McGetchin et al., 1974). Complementing previous studies, this paper provides a reconstruction of eruptive and pyroclastic transport mechanism involved in the formation of eight scoria cones of the Auckland Volcanic Field (AVF), based on their pyroclastic successions’ sedimentary record characterized by their grain size, density, vesicularity, 2D fragment morphology, eruptive sequences. Three scoria cones, such as Otuaatua, Browns Island and Rangitoto showed different pyroclasts textures in comparison to the other five studied sites in respect of their grain morphologies, grain size and degree of welding/agglutination.

The scoria cone outcrops in the AVF are various in qualities due to vegetation cover and urban development. This limits the ability to compare directly samples’ and outcrops’ features on a cone-by-cone basis. To overcome this limitation of the sedimentological data a simple and generalized facies model was constructed based on the studied scoria cones from the AVF. In this model, there are three facies identified from proximal to distal positions: crater/vent, flank and distal tephra (Fig. 1).

The eight scoria cone investigated in this study show distinct differences in terms of grain size distributions, densities and grain morphologies. These physical characteristics coupled with bedding, and stratigraphic information might be used to discriminate subtle difference in eruptive mechanism of scoria cones. The Otuaatua end-member in the AVF is characterized by grain size, density and vesicularity data that is consistent with lava fountaining eruption activity with intermitted Strombolian explosions. The other two end-members, such as Browns Island and Rangitoto, show features that are characteristics of more energetic eruption styles, such as Strombolian and violent Strombolian activities.

The most important effect of phreatomagmatism on scoria cone forming processes in the AVF is due to the small-eruptive volumes. The magma supply for this type

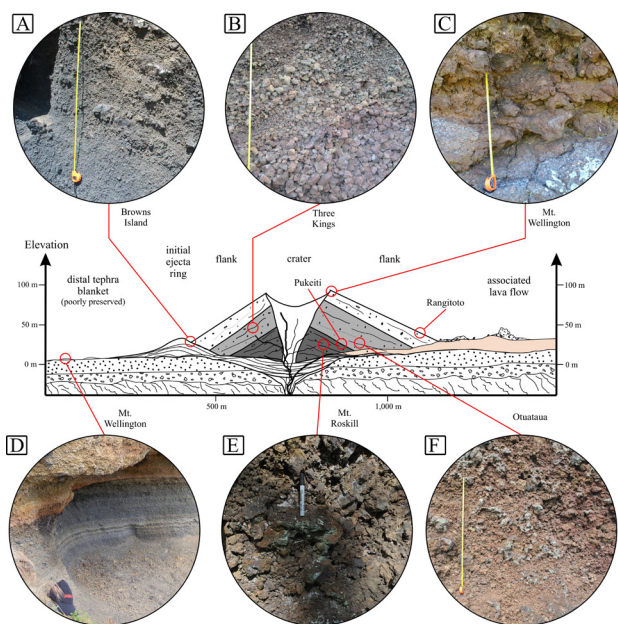


Fig. 1 – Facies interpretation of sampling locations of the eight studied scoria cones in the AVF

of eruptions is usually limited to 50×10^6 m³ (Kereszturi et al., 2013). If phreatomagmatic eruptions occur, it can reduce the magma that is potentially available to form a sensu stricto scoria cone. Therefore, intra-crater scoria cones can be ‘supply-limited’, such as Browns Island. Based on the sedimentary record, the AVF’s scoria cones are rather formed under such ‘supply-limited’ conditions with minimal (e.g. Mt. Roskill) to extensive phreatomagmatic eruptions (e.g. Browns Island) mostly in the early stage of the eruption. This highlights that the eruption sequences and broader environmental influences, such as groundwater availability, might have an indirect feedback to otherwise “dry”, magmatic cone building processes.

Acknowledgements

This research was partially funded through GK’s MU Early Career Research Grant of “Building spectral libraries for volcanic rocks of New Zealand”.

References

- Agustín-Flores, J., Németh, K., Cronin, S.J., Lindsay, J.M., Kereszturi, G., Brand, B.D. and Smith, I.E.M., 2014. Phreatomagmatic eruptions through unconsolidated coastal plain sequences, Maungataketake, Auckland Volcanic Field (New Zealand). *J. Volcanol. Geotherm. Res.*, 276: 46-63.
- Courtland, L., Kruse, S. and Connor, C., 2013. Violent Strombolian or not? Using ground-penetrating radar to distinguish deposits of low- and high-energy scoria cone eruptions. *Bull. Volcanol.*, 75(12): 1-13.
- Di Traglia, F., Cimarelli, C., de Rita, D. and Gimeno Torrente, D., 2009. Changing eruptive styles in basaltic explosive volcanism: Examples from Croscat complex scoria cone, Garrotxa Volcanic Field (NE Iberian Peninsula). *J. Volcanol. Geotherm. Res.*, 180(2-4): 89-109.
- Doubik, P. and Hill, B.E., 1999. Magmatic and hydromagmatic conduit development during the 1975 Tolbachik Eruption, Kamchatka, with implications for hazards assessment at Yucca Mountain, NV. *J. Volcanol. Geotherm. Res.*, 91(1): 43-64.
- Guilbaud, M.-N., Siebe, C. and Agustín-Flores, J., 2009. Eruptive style of the young high-Mg basaltic-andesite Pelagatos scoria cone, southeast of México City. *Bull. Volcanol.*, 71(8): 859-880.
- Kereszturi, G. and Németh, K., 2012. Monogenetic basaltic volcanoes: genetic classification, growth, geomorphology and degradation. In: K. Németh (Editor), *Updates in Volcanology - New Advances in Understanding Volcanic Systems*, InTech, pp. 3-88.
- Kereszturi, G., Németh, K., Cronin, S.J., Agustín-Flores, J., Smith, I.E.M. and Lindsay, J., 2013b. A model for calculating eruptive volumes for monogenetic volcanoes — Implication for the Quaternary Auckland Volcanic Field, New Zealand. *J. Volcanol. Geotherm. Res.*, 266: 16-33.
- Kiyosugi, K., Horikawa, Y., Nagao, T., Itaya, T., Connor, C. and Tanaka, K., 2013. Scoria cone formation through a violent Strombolian eruption: Irao Volcano, SW Japan. *Bull. Volcanol.*, 76(1): 1-14.
- Németh, K., Risso, C., Nullo, F. and Kereszturi, G., 2011. The role of collapsing and cone rafting on eruption style changes and final cone morphology: Los Morados scoria cone, Mendoza, Argentina. *Cent Eur J Geosci*, 3(2): 102-118.
- Ort, M.H., Elson, M.D., Anderson, K.C., Duffield, W.A., Hooten, J.A., Champion, D.E. and Waring, G., 2008. Effects of scoria-cone eruptions upon nearby human communities. *Geol Soc Am Bull*, 120(3-4): 476-486.
- Valentine, G.A., Krier, D.J., Perry, F.V. and Heiken, G., 2007. Eruptive and geomorphic processes at the Lathrop Wells scoria cone volcano. *J. Volcanol. Geotherm. Res.*, 161(1-2): 57-80.
- Wood, C.A., 1980. Morphometric evolution of cinder cones. *J. Volcanol. Geotherm. Res.*, 7(3-4): 387-413.

Lava lakes filling phreatomagmatic craters at Twin Peaks, Hopi Buttes volcanic field, Navajo Nation, Arizona

Benjamin Latutrie¹, Pierre-Simon Ross¹

¹ Institut National de la Recherche Scientifique, Centre Eau Terre Environnement, 490 Rue de la Couronne, Québec (QC), G1K 9A9, Canada: Benjamin.Latutrie@ete.inrs.ca

Keywords: diatreme, crater, eruptive regimes.

The Hopi Buttes volcanic field (HBVF) is located on the Colorado Plateau in Arizona (USA). This Miocene volcanic field provides excellent exposures of maar-diatreme volcanoes (White and Ross, 2011). In the HBVF, the variable erosion level allows the study of maar-diatremes from top to bottom. Williams (1936) defined the typical HBVF volcanic necks as “plug”-dominated (i.e. mostly filled by coherent rocks) and those of the older Navajo volcanic field (NVF) further north as a tuff-breccia “shafts” (i.e. mostly pyroclastic). Yet the plug-dominated necks of the HBVF have received little scientific attention so far, with almost all recent studies addressing diatremes filled by pyroclastic rocks.

Twin Peaks is a complex of two adjacent “plug”-dominated necks in the eastern HBVF, called informally the north peak and south peak. Our overall interpretation is that each peak represents a maar-diatreme volcano which evolved into a lava lake filling the crater, possibly all the way to the pre-eruptive surface. The base of the lava lakes lie about 60 m below the current summits and corresponds to the bottom of the craters at the end of the explosive phase of the eruptions. This elevation is also inferred to correspond approximately to the contact between the Jurassic Moenave Fm and the Miocene Bidahochi Fm (Billingsley et al., 2013).

One month of field work was carried out at Twin Peaks. We mapped four main volcanic units, the first three being pyroclastic and the final one coherent. Those units occur in stratigraphic order from bottom to top; for simplicity in this abstract we give them numbers (Fig. 1) and a description of each unit is presented below. Unit 1 is only visible in the north peak but the others occur on both peaks. We described and sampled all these units and then did componentry measurements using the line count method proposed by Lefebvre (2013).

Unit 1 is brown and typically bedded, with layers tens of centimeters to several meters thick. Some layers are lensoid in appearance and cross-bedding occurs locally. The rocks range from fine lapilli tuff to tuff breccia and are poorly sorted, with particles from ash to block in size. Beds are relatively juvenile-rich in composition (65-80%). Juvenile clasts are light grey to black and often brown (10-75%) due to palagonite alteration. They are dense to vesicular (10 to 60% vesicles) and blocky to amoeboid in shape. The lithics are mainly from the Bidahochi and

Moenave Fms but some are from the Chinle Fm and the Moenkopi Fm, 200-400 m below their current location. We think that this unit is phreatomagmatic in origin.

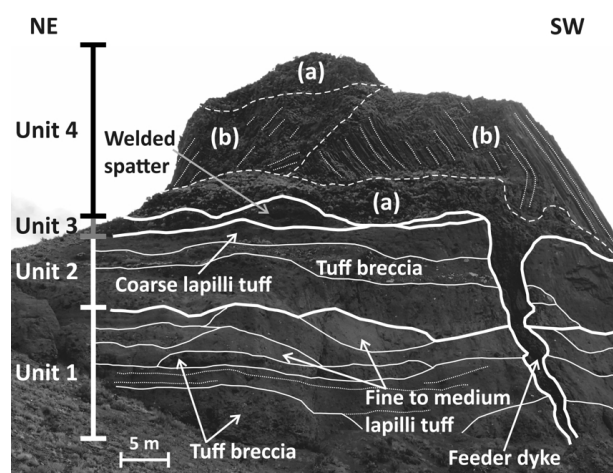


Fig. 1 – The four main units present on the northwest cliff of the north peak at Twin Peaks.

The overlying **unit 2** is darker brown and composed of three beds several meters in thickness. The beds are poorly sorted with a high proportion of ash matrix (up to 30%) and range from medium lapilli tuff to tuff breccia. Juvenile fragments constitute 70-80% of the rock and are mainly sub-round to amoeboid and sometime flat like spatter, with a vesicularity ranging from 10 to 70%. Dense clasts and spindle bombs are present in this unit but they are rare. The lithics are mainly white in color (Bidahochi Fm, or cooked Moenave Fm clasts, or greyish Moenkopi Fm). We interpret the eruptive style as phreato-strombolian.

The ~3-10 m-thick **unit 3** consists of black coarse lapilli tuff to tuff breccia. These rocks are extremely spatter-rich with just a few randomly scattered lithics. At the bottom of this unit the spatter clasts are non-welded in a matrix of fine lapilli to ash and at the top the spatter is tack-welded to strongly welded, grading locally into small lenses of clastogenic lava. Spatter fragments are generally flat and extremely vesicular (up to 80%) with bigger vesicles in the middle. This unit corresponds to a hawaiian explosive phase.

Finally **unit 4** forms the lava lakes. The coherent samples from this unit are porphyritic with about 15% olivine, 7% euhedral clinopyroxene and 0-1% vesicles. On the south

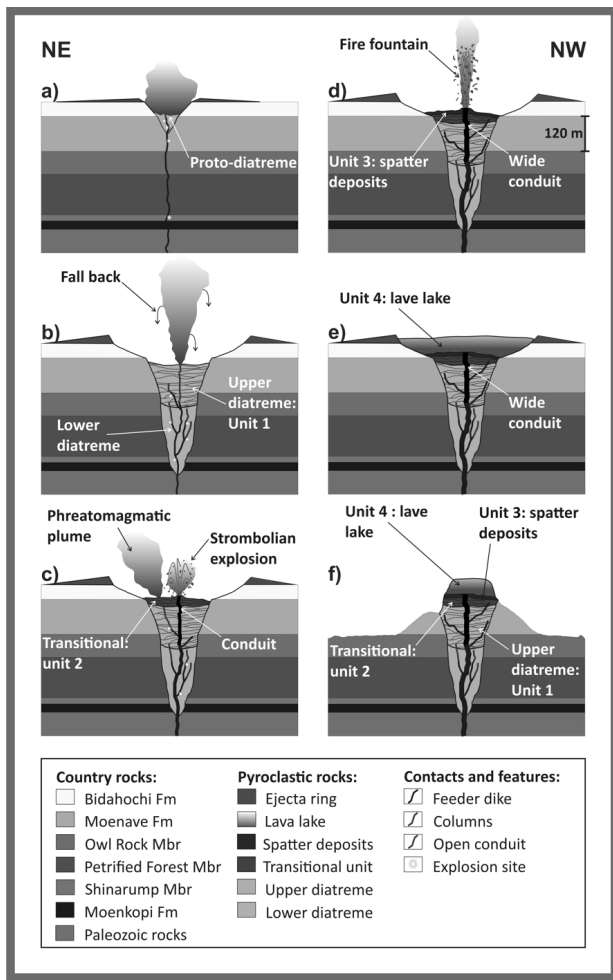


Fig. 2 – Preliminary model representing the steps leading to the current outcrop at Twin Peaks, for one of the peaks only.

peak the lava lake is entirely jointed but in the north peak a portion of the unit lacks well-developed columnar joints (zones “a” versus “b” on Fig. 1).

Our preliminary model for Twin Peaks has six steps and it can be applied to the two peaks (Fig. 2).

(g) Onset of the activity at Twin Peaks when a dyke rises and generates phreatomagmatic explosions by interaction with a wet substrate.

(h) Ongoing phreatomagmatic activity until a well-developed maar-diatreme is formed. The lower part of the diatreme is composed of massive deposits (not exposed) while the upper part is composed of the bedded phreatomagmatic facies (unit 1) that crops out in the north peak. At this stage the craters may have been 400-500 m in diameter and 60 m deep.

(i) The eruptive regime switches to a transitional phreato-strombolian style (unit 2). This can be due to the formation of a better-sealed conduit linked to the increase in the magmatic flux in the dyke (Valentine and White, 2012) or perhaps to external water becoming depleted, or to simultaneously active strombolian and phreatomagmatic vents (e.g., Ukinrek 1977).

(j) The magmatic flux increases again, or water runs out completely. A large dike/conduit is now able to transport relatively large quantities of magma up to the surface. Fire fountains form spatters deposits of unit 3.

(k) This evolves into a lava lake (unit 4), which mostly or complete fills the crater and may have fed a lava flow beyond the crater (not shown).

(l) Erosion leads to the current outcrop at Twin Peaks.

Acknowledgements

Twin Peaks was first visited by PSR during a field trip with James White, Greg Valentine, and Nathalie Lefebvre. These researchers have influenced our ideas through discussions and their papers. Romain Jattiot helped us during the field work in the steep slopes. We thank the Morris family for allowing us to work at Twin Peaks. Any persons wishing to conduct geological investigations on the Navajo Nation must first apply for, and receive, a permit from the Navajo Nation Minerals Department, P.O. Box 1910, Window Rock, Arizona 86515, USA, telephone 1-928-871-6587.

References

- Billingsley, G.H., Block, D., Hiza-Redsteer, M., 2013. Geologic map of the Winslow 30' x 60' quadrangle, Coconino and Navajo Counties, northern Arizona. US Geological Survey Scientific Investigations, Map 3247, Scale 1:50000.
- Lefebvre, N.S., 2013. Volcanology of maar-diatreme volcanic vent complexes, Hopi Buttes Volcanic Field, Navajo Nation, Arizona, USA. PhD thesis, University of Otago, 282 p.
- Valentine, G.A., White, J.D., 2012. Revised conceptual model for maar-diatremes: Subsurface processes, energetics, and eruptive products. *Geology* 40(12): 1111-1114
- White, J.D., Ross, P-S., 2011. Maar-diatreme volcanoes: a review. *Journal of Volcanology and Geothermal Research* 201: 1-29.
- Williams, H., 1936. Pliocene volcanoes of the Navajo-Hopi country. *Geological Society of America Bulletin* 47(1): 111-172.

Magma ascent dynamics and eruptive mechanisms at monogenetic volcanoes: Wiri Mountain, Auckland Volcanic Field, New Zealand.

April Foote¹, **Károly Németh**², Heather Handley¹ and Jan Lindsay³

¹ Department of Earth and Planetary Sciences, Macquarie University, Sydney, Australia. april.foote@hdr.mq.edu.au

² Institute of Agriculture and Environment, Massey University, Palmerston North, New Zealand.

³ School of Environment, University of Auckland, Auckland, New Zealand.

Keywords: phreatomagmatic, tuff ring, scoria

The Auckland Volcanic Field (AVF) of New Zealand is a Quaternary monogenetic basaltic field that has produced 53 eruptive centres over c. 200 ka (eg. Hopkins, et al., 2017). The AVF represents the youngest addition in the progressive northwards development of intraplate volcanic fields in the North Island, predated by Okete, Ngatutura and South Auckland volcanic fields respectively (Briggs, et al., 1994). The city of Auckland is the largest in New Zealand with a current population of 1.5 million people, many living within close proximity of past eruptive centres.

Almost all volcanic centres in the AVF began with phreatomagmatic eruptions, the style and size of which were determined by the degree of magma-water interactions, followed by either Strombolian style explosive eruptions, effusive activity or both (Kereszturi, et al., 2014).

Wiri Mountain is one of the southernmost volcanic centres in the AVF and is estimated to be 32-34 ka old (Lindsay, et al., 2011). It once consisted of an initial tuff ring filled in with a 90 m high scoria cone deposited by pyroclastic fall beds from multiple vents, both covered by interbedded lava flows, agglutinate and lava spatter (Searle, 1961; Rout, et al., 1993).

Quarrying activities since the late 1950's have removed most of the volcanic deposits and features of Wiri Mountain, with the exception of a well-preserved lava tunnel that has been protected as a scientific reserve. There has been little prior study of the volcanic stratigraphy, magma ascent and eruption dynamics of Wiri Mountain. The volcanic centre was included in a study of source melting processes in the AVF (McGee, et al., 2013), suggesting Wiri was supplied by melting of a fertile, deep garnet-bearing source and the associated melting and incorporation of 2% lithospheric mantle.

A spectacular 200 m-long outcrop has been exposed by quarrying, and features a section through the initial tuff ring, comprised of alternating ash and accidental lithic-rich beds rich in accretionary lapilli (Fig. 1). These beds transition upwards into juvenile-rich beds corresponding to a gradual shift in eruption style from phreatomagmatic to magmatic. This likely occurred as the result of the exhaustion of external water available to fuel magma-water

interactions, suggesting increasing stability of the vent, or an increase in magma flux, or both. An increase in pyroclastic density current-dominated, finer-grained tuff layers, becoming more sorted upwards through the section, suggests that the explosion depth and energy involved remained the same during the eruption and build up of the initial tuff ring (Graettinger, et al., 2015).

Once magma-water interaction had ceased, magma flux reduced and may have even stopped. Activity then resumed along with magma flux. An angular unconformity separates the two phases of activity (Fig. 2), which is overlain by deposits rich in angular accidental lithics that gradually grade upwards to more juvenile-rich deposits that represent a change to explosive magmatic activity along a fissure within the crater, producing scoria fall beds up to 2 m thick. These beds have a lava spatter dominated base that grade upwards to become scoriaceous and finer grained (Fig. 3), from initial lava fountaining shifting to more regular Strombolian style eruptions, likely due to the eventual establishment of a stable conduit. These were later covered, along with the underlying tuff ring, by alternating lava spatter and rubbly pahoehoe to a'a lava flows.



Fig. 1 - Accretionary lapilli-rich, fine-grained tuff beds from the initial tuff ring at Wiri Mountain

The aims of this case study are: 1) determine the eruption history using stratigraphy and facies analysis, and

document variations in eruptive styles and fragmentation depth as well as vent and conduit morphology and stability, 2) analyse the petrography and petrology of all units, as well as magmatic processes involved and the geochemical evolution over time, 3) provide further understanding of magma ascent dynamics in relation to monogenetic eruptive processes. The deposits exposed at Wiri reveal a very complex volcanic history that will contribute greatly to the understanding of fine scale volcanic and plumbing system evolution of small volume monogenetic basaltic systems.



Fig. 2 – Angular unconformity separating early tuff ring deposits from a later change towards more explosive magmatic and later effusive activity.



Fig. 3 – Section through intra-crater scoria beds representing initial lava fountaining transitioning to Strombolian style eruptions, followed by later alternating lava spatter and pahoehoe to a'a lava flows.

References

- Briggs, R. M., Okada, T., Itaya, T., Shibuya, H., & Smith, I. E. (1994). K-Ar ages, paleomagnetism, and geochemistry of the South Auckland volcanic field, North Island, New Zealand. *New Zealand Journal of Geology and Geophysics* 37/2: 143-153.
- Graettinger, A. H., Valentine, G. A., Sonder, I., Ross, P. -S., & White, J. D. L. (2015). Facies distribution of ejecta in analog tephra rings from experiments with single and multiple subsurface explosions. *Bulletin of Volcanology* 77:66.
- Hopkins, J. L., Wilson, C. J., Milled, M., Leonard, G. S., Timm, C., McGee, L. E., Smith, I. E. M., & Smith, E. G. (2017). Multi-criteria correlation of tephra deposits to source centres applied in the Auckland Volcanic Field, New Zealand. *Bulletin of Volcanology* 79/55: 0-35.
- Kereszturi, G., Németh, K., Cronin, S. J., Procter, J., & Agustin-Flores, J. (2014). Influences on the variability of eruption sequences and style transitions in the Auckland Volcanic Field, New Zealand. *Journal of Volcanology and Geothermal Research* 286: 101-115.
- Lindsay, J. M., Leonard, G. S., Smid, E. R., & Hayward, B. W. (2011). Age of the Auckland Volcanic Field: a review of existing data. *New Zealand Journal of Geology and Geophysics* 54/4: 379-401.
- McGee, L. E., Smith, I. E., Millet, M., Handley, H. K., & Lindsay, J. M. (2013). Asthenospheric Control of Melting Processes in a Monogenetic Basaltic System: a Case Study of the Auckland Volcanic Field, New Zealand. *Journal of Petrology* 54/10: 2125-2153.
- Rout, D. J., Cassidy, J., Locke, C. A., & Smith, I. E. (1993). Geophysical evidence for temporal and structural relationships within the monogenetic basalt volcanoes of the Auckland volcanic field, northern New Zealand. *Journal of Volcanology and Geothermal Research* 57: 71-83.
- Searle, E. J. (1961). Volcanoes of the Otahuhu-Manurewa district, Auckland. *New Zealand Journal of Geology and Geophysics* 4/3: 239-255.

Maars of the Arxan-Chaihe Volcanic Field, Inner Mongolia, China

Bo-Xin Li¹, **Károly Németh**¹

¹ Institute of Agriculture and Environment, Massey University, Palmerston North, New Zealand

Keywords: monogenetic, phreatomagmatic, crater lake

The Arxan-Chaihe Volcanic Field (Fig. 1) represents a manifestation of intracontinental monogenetic volcanism occurred during the late Cenozoic (Németh et al., 2017). The base of the volcanic field composed of eroded Mesozoic crystalline and metamorphic rocks, which are raised up to about 1500 m. The volcanic field shows strong structural control as the vent distribution of 27 identified vents follows main structural elements of the basement in this region (Fig. 1).

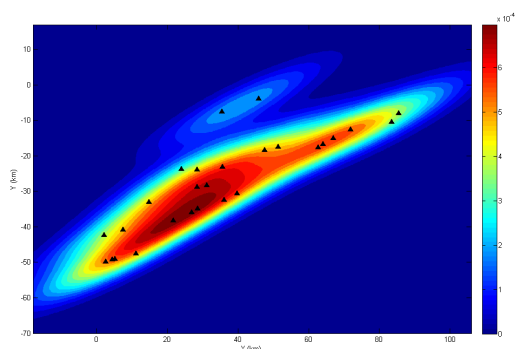


Fig. 1 – Kernel-density map of the ACVF. The youngest volcanoes are located in the highest vent density regions of the field. Two large maars of this study are located in the NE and SW edge of the field.

Tongxin volcano is located on the eastern side of the Arxan-Chaihe Volcanic Field (Fig. 2). The ~2 km wide depression represents the preserved crater of one of the largest phreatomagmatic volcano of the ACVF (Fig. 3). Chaihe Town is sitting on the phreatomagmatic tephra preserved in the eastern side of the crater. In the southern side of the crater of the Tongxin volcano (which is marked as a yellow eclipse dot on Fig. 2) at least 10 m thick lapilli tuff and tuff successions are exposed. The pyroclastic deposits composed of the base surge and minor phreatomagmatic fall tephra (Fig. 4). The deposits are rich in accidental lithic fragments ranging from fine ash to bomb and block size. Transportation indicators show good agreements to locate the source of explosions in the present day depression of the Tongxin basin. The pyroclastic deposit also contains abundant loaded or cored bombs and lapilli indicating some pre-mixing of rising basaltic magma and host country rocks. Magma likely invaded fractured granitoid rocks and/or captured already fragmented crystalline rocks (eg. gravels) that then were picked up and thrown out from the growing crater as loaded/cored bombs and lapilli.

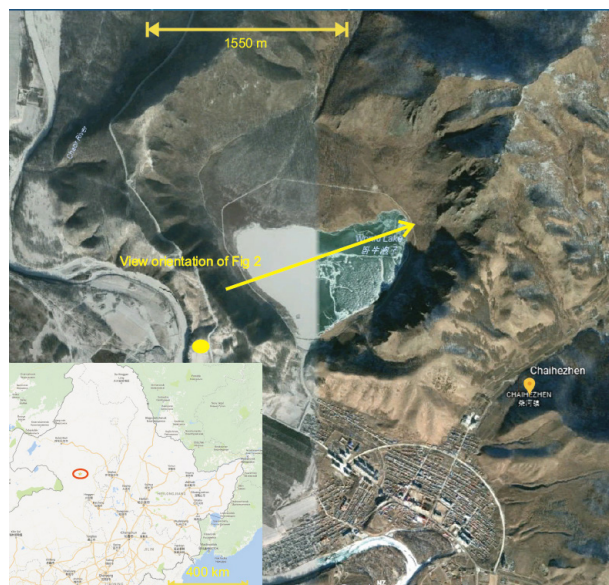


Fig. 2 – The Tongxin volcano area is observed from the satellite view. The red eclipse marks the area on the inset map.

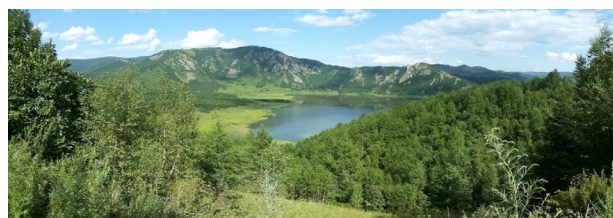


Fig. 3 – The field view of the Tongxin Lake. The orientation of the sight is marked in the Fig 2 with the yellow arrow.

A long suspected maar, a lake-filled basin in the SW edge of the field is the location of the Wusulangzi volcano (Fig. 5). In this location a newly find section shows typical base surge dominated medial succession of a maar that is linked to the Wusulangzi basin (Fig. 6).

By utilizing the X-ray Fluorescence for the major elements evaluations a range of Harker Diagrams has been plotted. Figure 7 depicts measured major oxide versus MgO. The fractional crystallization can be determined. All the studied rocks are basalts to trachybasalts and belong to the alkaline series.

The magma type represented by XRF experiments and TAS diagram suggests a deeper source and small degrees of partial melting with the rapid magmatic ascent.

It seems that the chemical composition of the magmas erupted from Tongxin and Wusulangzi volcanoes are distinct from other volcanoes of the ACVF, hence potentially could be used to identify tephra preserved in the crater and maar lake elsewhere in the ACVF (Sun et al., 2014). Observing and evaluating the shapes and vesicularity of the juvenile pyroclast samples, we can infer that the Tongxin and Wusulangzi volcanoes must have undergone a series of phreatomagmatic eruption phases. The Tongxin maar crater in addition is inferred to be formed in an already existed intra-mountain basin.

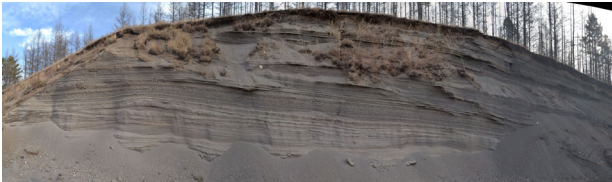


Fig. 4 – The pyroclastic successions of Tongxin volcano present a series of accidental lithic-rich and dune bedded pyroclastic beds indicative of base surges-dominated phreatomagmatic eruptions responsible for the formation of the volcano.



Fig. 5 – Wusulangzi is a suspected maar.



Fig. 6 – The accidental lithic clast dominated pyroclastic density current deposits crop out along the Halaha River are inferred to be sourced from Wusulangzi volcano.



Fig. 7 – The Harker-diagrams clearly demonstrate fractional crystallisation occurred during the eruption process. Comparing with the monogenetic volcanoes around the world, it appears the Wusulangzi and Tongxin volcanoes have similar petrogenetic signature to Auckland Volcanic Field (McGee et al., 2013) (blue circles) and some Saudi Arabian fields (Duncan et al., 2016) (red circles). Whereas it is distinctly different from the adjacent volcanic fields in China (Zhao et al. 2014) (purple circles).

References

Duncan, R.A., Kent, A.J., Thornber, C.R., Schlieder, T.D., & Al-Amri, A.M. (2016). Timing and composition of continental volcanism at Harrat Hutaymah, western Saudi Arabia. *Journal of Volcanology and Geothermal Research*, 313, 1-14.

McGee, L.E., Smith, I.E., Millet, M.A., Handley, H.K., & Lindsay, J.M. (2013). Asthenospheric control of melting processes in a monogenetic basaltic system: a case study of the Auckland Volcanic Field, New Zealand. *Journal of Petrology*, 54(10), 2125-2153.

Németh, K., Wu, J., Sun, C., & Liu, J. (2017). Update on the Volcanic Geoheritage Values of the Pliocene to Quaternary Arxan-Chaihe Volcanic Field, Inner Mongolia, China. *Geoheritage*, 1-19.

Sun, C., Liu, Q., Wu, J., Németh, K., Wang, L., Zhao, Y., & Liu, J. (2017). The first tephra evidence for a late glacial explosive volcanic eruption in the Arxan-Chaihe volcanic field (ACVF), north-east China. *Quaternary Geochronology*, 40, 109-119.

Zhao, Y. W., Fan, Q. C., Zou, H., & Li, N. (2014). Geochemistry of Quaternary basaltic lavas from the Nuomin volcanic field, Inner Mongolia: Implications for the origin of potassic volcanic rocks in Northeastern China. *Lithos*, 196, 169-180

Structural control on intraplate volcanism in the volcanic fields of Los Encinos and Santo Domingo, San Luis Potosí, México

Claudia Peredo Mancilla¹, Vsevolod Yutsis¹, Xavier Bolós²

¹ Instituto Potosino de Investigación Científica y Tecnológica A. C., División de Geociencias Aplicadas, 78216, S. L. P., San Luis Potosí, México. claudia.peredo@ipicyt.edu.mx

² Institute of Geophysics, UNAM, Campus Morelia, 58190 Morelia, Michoacán, Mexico

Keywords: Intraplate volcanism, basement fault, geophysical analysis.

The complexity of studying intraplate magmatism lies in characterizing both the magmatic processes and their relation to the geodynamics of the Earth's mantle and processes associated with tectonism. Although in most cases the volcanism associated with intraplate zones is related to hot spots activity or the rise of the asthenosphere, some of these may have more uncertain relationship with the tectonic environment (Shabanian et al., 2012). The presence of preexistent lithospheric structures plays an important role to control magma rise to the surface.

An important period of intraplate volcanism is presented in Mexico from Late Oligocene to Quaternary, consistent in time with a change in the tectonic regime from east-northeast compression, associated to subduction on the east of Farallon plate, to east-northeast extension. This regime has predominated since the instauration of Basin and Range Province on Early Oligocene (Luhr et al., 2001). Although there is a temporal and spatial correspondence between both geological events, the relationship between magmatism and extensional faulting is still under discussion. In the case of Mexico, there are volcanic fields in which stratigraphic evidence exhibit that volcanism and cortical extension were partially synchronous (e. g. volcanic fields of Moctezuma, Sonora; Camargo, Chihuahua and Metates, Durango (Aranda-Gómez et al., 2005)). However, in most cases the relationship between magmatism and extension is diffuse. The indirect manifestations of this relation, are represented by the alignment of cones and volcanic deposits that in some cases are situated along or close to normal faults, while in others they are located in old basement faults that delimit important tectonic domains. In these sense, there are sites where the presence of important structural discontinuities suggest the presence of basement faults, nevertheless, their existence is only implied by the physiographic features and no clear evidences of its presence and extension has been documented. This work focuses on the last category seeking to determine the possible connection between preexisting basement discontinuities and the presence of two intraplate volcanic fields.

The study area corresponds to the volcanic fields of Los Encinos (CVLE) and Santo Domingo (CVSD) located in San Luis Potosí, Mexico. This region is located on the bound-

ary between the physiographic provinces of Mesa Central (west) and Sierra Madre Oriental (east). The trace is also consistent with the border of the Valles-San Luis Potosí Platform and the Mesozoic Basin of Central Mexico respectively, two paleogeographic elements formed during the opening of the Gulf of Mexico. The volcanic fields are located on the trace of an apparent regional lineament with N50°W orientation whose distribution seems to extend more than 200 km from the northeast of Zacatecas to the central part of San Luis Potosí. This lineament has been interpreted as a probable basement structure (Luhr and Aranda-Gómez, 1997), which trace is consistent with the San Tiburcio regional lineament (Mitre-Salazar, 1989) interpreted as a fault splay of the Mojave-Sonora megashear (Sedlock et al., 1993). Both fields are constituted by intraplate mafic rocks with alkaline affinity. Nevertheless, in the case of the Santo Domingo volcanic field are present more recent products with ages of Middle Pleistocene (0.35 to 0.45 Ma.) composing at least four quaternary maars, two cinder cones and lava flows. In the case of Los Encinos volcanic field has ages of Middle to Upper Miocene (13.6 to 10.6 Ma.). Moreover, in this area there are a series of volcanic necks with prominent columnar joints and lava flows covering small plateaus. The possible presence of a regional basement structure seems to be evidenced by its influence on the physiography of the region. In the area near Santo Domingo volcanic field, there is a notable change in the orientation of the mountain ranges formed by Laramidic folds. At the north of the trace of this inferred structure, the folds present orientations N to NNE while to the south, they are projected with approximate orientations of N45°W. This configuration suggests the possibility that this tectonic structure could have been active during the Laramide deformation, making evident its behavior as a long-lived lithospheric fault.

Accomplish to document evidence of the presence of a deep structure in the lithosphere that could have channeled magmatism in the fields is not a simple work. Geological structures are hidden under the sedimentary infill and/or recent volcanic sequences, and thus identification using only direct methods is limited.

For this reason, we apply a combination of geophysical studies, such as: gravity and magnetic geophysical meth-

ods, as well as, fieldwork and remote sensing in order to perform an integral geological-geophysical model. This schematic model allows us to compare both volcanic fields with different ages identifying if the intraplate magmatism was promoted by the presence of regional lithospheric structures.

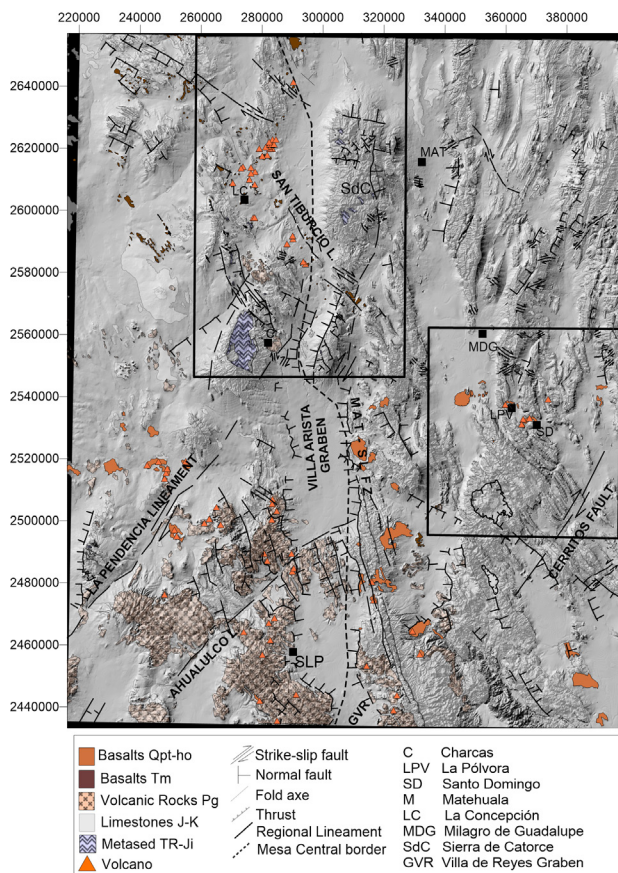


Fig. 1 – Regional geological map and study area. Top rectangle corresponds to CVLE and bottom to CVSD.

The digital elevation model (ASTER GDEM), the aeromagnetic analysis (SGM), and the satellital gravimetric anomalies (IGB) suggest an important regional discontinuity in the area. Moreover, the analysis of lineaments, show a good correlation between the trace of the proposed San Tiburcio lineament and its probable south-east extension over the area of the volcanic fields. The location of this regional geomorphological and geophysical lineaments is coinciding as well with a series of lateral and normal faults that cut the Sierra de Charcas and the Sierra de Catorce Ranges, extending to the north of the CVSD in the region of Milagro de Guadalupe.

It is important to mention the presence of a NNE orientation system that apparently also controlled the location of the volcanic structures at least in the CVLE. The arrangement of both NW and NNE orientations in this volcanic field is consistent with deformational patterns reported for the Mesa Central extensional events (Nieto-Samaniego et al., 1997). This structural pattern is also visible in the geophysical anomalies, particularly in the 2nd vertical derivative map of the Residual Magnetic Field were an

important regional magnetic alignment orientated NNE show a good correlation with the presence of intrusive bodies from the Tertiary (?).

Furthermore, in the western limit of the Sierra de Catorce, located on a tectonic pillar with N to NNE orientation, active normal faulting has been identified through the presence of alluvial fans. As a result the burial of nearby volcanic necks of the CVLE is in process. According to Aranda-Gómez et al. (2005) this processes may suggest a possible event of Quaternary reactivation.

References

- Aranda-Gómez, J. J., Luhr J. F., Housh T., Valdez-Moreno G., Chávez-Cabello G., 2005. El volcanismo tipo intraplaca del Cenozoico tardío en el centro y norte de México: una revisión. *Boletín de la Sociedad Geológica Mexicana* 3: 187-225.
- Luhr, J. F., Aranda-Gómez, J. J., 1997. Mexican peridotite xenoliths and tectonic Terranes: correlations among vent location, texture, temperature, pressure, and oxygen fugacity. *Journal of Petrology* 38, 8: 1075-1112.
- Luhr, J.F., Henry, C.D., Housh, T.B., Aranda-Gómez, J.J., McIntosh, W.C., Luhr, J.F., Henry, C.D., Housh, T.B., Aranda-Gómez, J.J., McIntosh, W.C., 2001. Early extension and associated mafic alkalic volcanism from the southern Basin and Range province: Geology and petrology of the Rodeo and Nazas volcanic fields, Durango (Mexico). *Geological Society of America Bulletin* 113: 760-773.
- Mitre-Salazar, L. M., 1989. La megafalla Laramídica de San Tiburcio, Estado de Zacatecas. *Revista del Instituto de Geología, Universidad Nacional Autónoma de México*, 8: 47-51.
- Nieto-Samaniego, A. F., Alaniz-Alvarez, S. A. Labarthe-Hernández, G., 1997. La deformación Cenozoica poslaramídica en la parte meridional de la Mesa Central, México. *Revista Mexicana de Ciencias Geológicas*, 14: 13-25.
- Sedlock, R. L., Ortega-Gutiérrez, F., Speed, R. C., 1993. Tectonostratigraphic terranes and tectonic evolution of Mexico: Boulder, Colorado. *Geological Society of America, Special Paper*, 278, 153 p.
- Shabanian E., Acocella V., Gioncada A., Ghasemi H, Bellier O., 2012. Structural control on volcanism in intraplate post collisional settings: Late Cenozoic to Quaternary examples of Iran and Eastern. *Tectonics* 31.

Evaluation of the presence of extrusive carbonatites in the Cabezo Segura volcano (Calatrava Volcanic Field, Spain)

Fernando Sarrionandia¹, Manuel Carracedo-Sánchez², Eneko Iriarte³, Jon Errandonea-Martin² and José Ignacio Gil-Ibarguchi²

¹ University of the Basque Country UPV/EHU, Faculty of Pharmacy, Geodynamics Department, Campus de Álava, 01006 Vitoria-Gasteiz, Spain. fernando.sarrionandia@ehu.eus

² University of the Basque Country UPV/EHU, Faculty of Science and Technology, Mineralogy and Petrology Department, Campus de Bizkaia, 48940 Leioa, Spain.

³ University of Burgos, Laboratorio de Evolución Humana, Plaza Misael Bañuelos s/n, 09001, Burgos, Spain.

Keywords: carbonatite, Cabezo Segura, Calatrava Volcanic Field.

The Calatrava Volcanic Field (CVF; Ciudad Real province, Spain) constitutes an alkaline, continental intraplate volcanic region formed by ~200 volcanoes dispersed over an area of 5000 km². The volcanic activity comprised the emission of leucitites, alkali basalts, basanites, nephelinites and melilitites in two distinct magmatic events: (1) at 8.07-6.3 Ma, and (2) at 5.0-0.7 Ma (López Ruiz et al., 2002; Ancochea, 2004). Such types of rocks are usually associated elsewhere in time and space with carbonatitic melts. Alleged first evidence of the possible existence of extrusive carbonatites in the CVF was reported by Bailey et al. (2005) who interpreted as extrusive carbonatites the carbonates within tephra of the Nava maar and Pico de la Zarza volcano. Subsequently, Stoppa et al. (2011) mentioned the existence of similar 'extrusive' carbonatites in the Cabezo Segura volcano. Yet, Carracedo Sánchez et al. (2016) demonstrated the existence of igneous calcite crystals in microscopic ocelli within a dyke of this volcano but discarded the existence of carbonatites stricto sensu (rocks with >50 vol. % of igneous carbonate).

Furthermore, Humphreys et al. (2010) interpreted the Ca-carbonate inclusions in olivine of lava flows from the Morrón de Villamayor volcano as mantle carbonates stabilized at a depth of about 100–150 km. Nevertheless, Lustrino et al. (2016), on the basis of mineral compositions and O and C isotope ratios, concluded that those carbonate inclusions were sedimentary carbonates incorporated in the crystallizing magma chamber.

It appears therefore that the origin of either interbedded or mixed carbonates related to pyroclastic deposits of the CVF is poorly demonstrated to say the least. This has motivated a detail study of the textural and compositional characteristics of the carbonate-rich layers within cone deposits of the Cabezo Segura volcano. The preliminary results of the study are presented in this contribution.

The Cabezo Segura volcano was built up onto lacustrine-pallustrine biomicritic limestones, rich in macroscopic fossils (characean algae, gasteropods, bivalves and vegetation remains moulds) that could represent shore sediments of a shallow lake. This volcano emitted lavas with compositions that comprise picrobasalts, ba-

sanites, and olivine nephelinites. In view of the preserved deposits, the eruptive styles were also varied and include Hawaiian-, Strombolian-, violent Strombolian-, and Phreatomagmatic-phases (Carracedo et al., 2009).

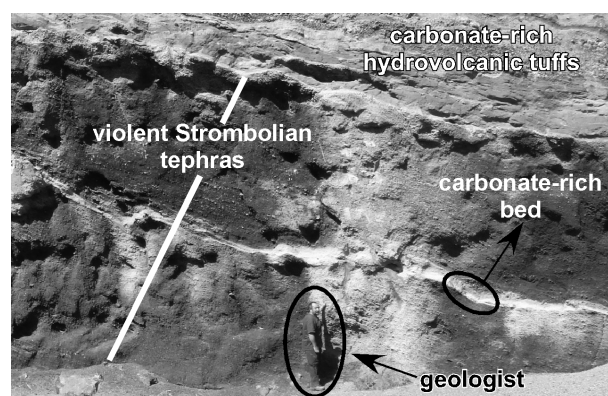


Fig. 1 – Overview of the carbonate-rich hydrovolcanic deposits underlain by violent Strombolian tephra, where stands out a whitish, carbonate-rich bed (Cabezo Segura volcano; Calatrava Volcanic Field).

Carbonates in the Cabezo Segura volcano generally appear as coatings/infills of ultramafic pyroclasts, acting as a cement that consolidated the original volcanic tephra. Carbonates appear irregularly distributed in the cone deposits (Fig. 1) and generally exhibit a massive structure, with a crystalline texture (e.g., pendant-type growths). In some places, they also appear as ooidal aggregates and also defining discrete beds (up to 20 cm thick), very continuous (> 15 m), with variable dips and trends (Fig. 1). The carbonates of these beds appear as aggregates of powdered aspect and poorly consolidated enclosing variable amounts of pyroclasts (Fig. 2).

Under the microscope, the carbonates constitute a groundmass of micrite and microsparite, which may preserve biogenic microstructures (algae lamination, bioclastic fragments) and ooids. Irregular voids, up to 1 mm in size, filled with equant calcite crystals are common. Neither Sr, Ba, REE, Zr-rich phases (e.g., garnet, apatite, perovskite) or xenocrystic olivine, phlogopite and diopside, distinctive of extrusive carbonatites (Stoppa and Schiazza, 2013), have been identified.

Microprobe and LA-ICPMS determinations on the largest crystals indicate that they correspond essentially to Ca carbonate (calcite or aragonite, both phases have been identified by XRD, with MgO up to 3.61 wt. %), being poor in Sr (≤ 0.35 ppm), Ba (≤ 0.06 ppm), MnO (≤ 0.04 wt %), Zr (≤ 0.05 ppm) and Nb (≤ 0.02 ppm), compared with those of mantle-derived carbonatites (e.g., Stoppa and Schiazza, 2013). Dolomite is also found although in minor amounts. Oxygen and carbon isotope values attest to light carbon ($\delta^{13}\text{CPDB} < -7.92$ ‰) and relatively heavy oxygen isotopic compositions ($\delta^{18}\text{OSMOW} > +25.38$ ‰). These values are far from those of primary carbonatites (e.g., Taylor et al., 1967) and close to those of carbonates in equilibrium with meteoric water (e.g., Hay and O'Neil, 1983; Fig. 3).

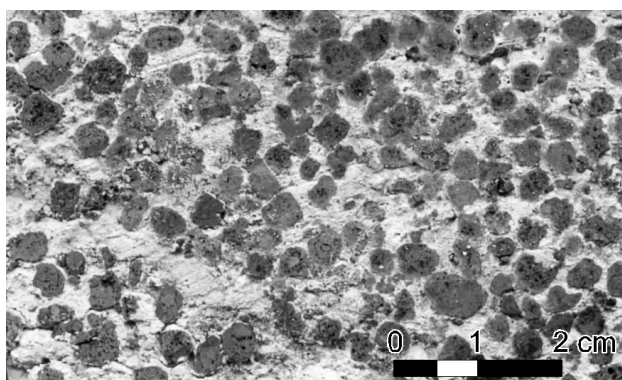


Fig. 2 – Detail of carbonate coating/infill (whitish area) in a lapilli-tuff of the Cabezo Segura volcano.

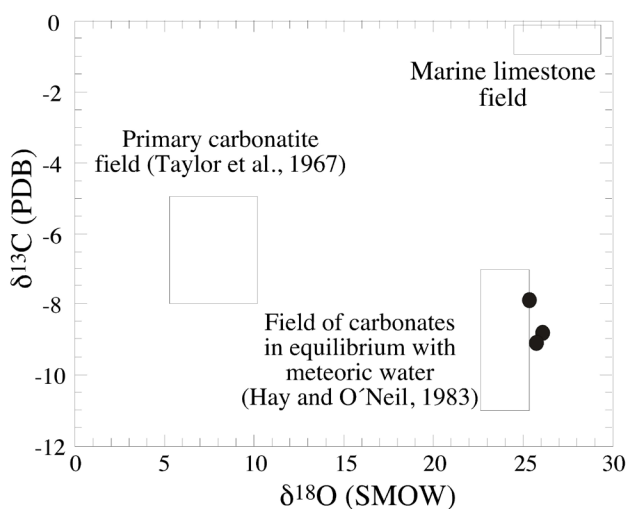


Fig. 3 – $\delta^{13}\text{C}$ – $\delta^{18}\text{O}$ diagram for carbonates of carbonate-rich beds and coating/infill material.

According to their petrography, mineral chemistry and O-C isotope ratios, we conclude that the massive carbonates of the Cabezo Segura volcano are sedimentary in origin and might have been precipitated from meteoric water.

Acknowledgements

Financial support by the Spanish Ministerio de Ciencia e Innovación (grant CGL2015-63530-P) is acknowledged.

References

- Ancochea, E., 2004. La región volcánica del Campo de Calatrava. In: *Geología d España* (J.A. Vera Ed.), SGE-IGME, Madrid, 676-677.
- Bailey, K., Garson, M., Kearns, S., Velasco, A.P. 2005. Carbonate volcanism in Calatrava, central Spain: a report on the initial findings. *Mineralogical Magazine* 69 (6): 907-915.
- Carracedo, M., Sarrionandia, F., Arostegui, J., Larrondo, E., Gil-Ibarguchi, J.I. 2009. Development of spheroidal composite bombs by welding of juvenile spinning and isotropic droplets inside a mafic eruption column. *Journal of Volcanology and Geothermal Research* 186: 265-275
- Carracedo Sánchez, M., Sarrionandia, F., García de Madinabeitia, S., Gil Ibarguchi, J.I. (2016). Sobre la presencia o ausencia de carbonatitas en la región volcánica de Campo de Calatrava. Nuevas evidencias a partir del microanálisis elemental e isotópico de (Sr) de carbonatos. *Geotemas*, 16(1): 451-454.
- López Ruiz, J., Cebriá, J.M., Doblas, M. 2002. Cenozoic Volcanism: The Iberian Peninsula. In: *The geology of Spain* (W. Gibbons and T. Moreno, Eds). Geol. Soc (London), 417-438.
- Hay, R.L., O'Neil, J.R. 1983. Carbonatite tuffs in the Laetoli Beds of Tanzania and the Kaiserstuhl in Germany. *Contributions to Mineralogy and Petrology* 82: 403-406.
- Humphreys, E.R., Bailey, K., Hawkesworth, C.J., Wall, F., Najorka, J., Rankin, A.H. 2010. Aragonite in olivine from Calatrava, Spain-Evidence for mantle carbonatite melts from >100 km depth. *Geology* 38: 911-914.
- Lustrino, M., Prelević, D., Agostini, S., Gaeta, M., Di Rocco, T., Stagno, V., Capizzi, L.S. 2016. Ca-rich carbonates associated with ultrabasic-ultramafic melts: Carbonatite or limestone xenoliths?. A case study from the late Miocene Morrón de Villamayor volcano (Calatrava Volcanic Field, central Spain). *Geochimica et Cosmochimica Acta* DOI: 10.1016/j.gca.2016.02.026.
- Stoppa, F., Schiazza, M. 2013. An overview of monogenetic carbonatitic magmatism from Uganda, Italy, China and Spain: Volcanologic and geochemical features. *Journal of South American Earth Sciences* 41: 140-159.
- Taylor, H.P., Jr., Frechen, J., Degens, E.T. 1967. Oxygen and carbon isotope studies of carbonatites from the Laacher See district, West Germany and the Alno district, Sweden. *Geochimica et Cosmochimica Acta* 31: 407-430. doi: 10.1016/0016-7037(67)90051-8.

Early phreatomagmatic tuffs in the Columbia River flood basalts

David W. Unruh¹, John A. Wolff¹, and Klarissa N. Davis¹

¹ Washington State University, School of the Environment, Pullman, WA, USA. david.unruh@wsu.edu

Keywords: maar, flood basalt, degassing

Products of explosive basaltic volcanism have been recorded from several large igneous provinces (Ross et al. 2005). The common occurrence of phreatomagmatic tuffs and other types of volcanoclastic deposits, especially in the basal portions of continental flood basalt sequences, has been ascribed to (i) tectonic settings controlling the availability of surface water, (ii) eruption through volatile-rich subsurface rock formations, or (iii) very high intrinsic magmatic volatile contents. In the Columbia River flood basalt province, early volcanoclastic rocks appear to be uncommon and have not previously been documented in detail. Here, we describe a sequence of phreatomagmatic basaltic tuffs near the base of the Imnaha Basalt, at

Lookout Mountain in northeast Oregon. The tuffs contain fresh glassy lapilli; chemical analysis demonstrates affinities with the American Bar chemical lava type, consistent with the stratigraphic position of the tuffs (Hooper et al. 1984). The Lookout Mountain sequence consists of two distinct tuffs with different textural and lithological characteristics interstratified with basalt flows. The lower tuff (Tbt₁) is 5 m thick and consists of non welded, largely devitrified ash and scoriaceous lapilli. Consistently horizontally oriented spatter clasts are common in this unit. The character of this unit suggests a proximal location to a shallow vent due to the lack of basement lithics and presence of spatter clasts. It is interpreted as phreatomag-

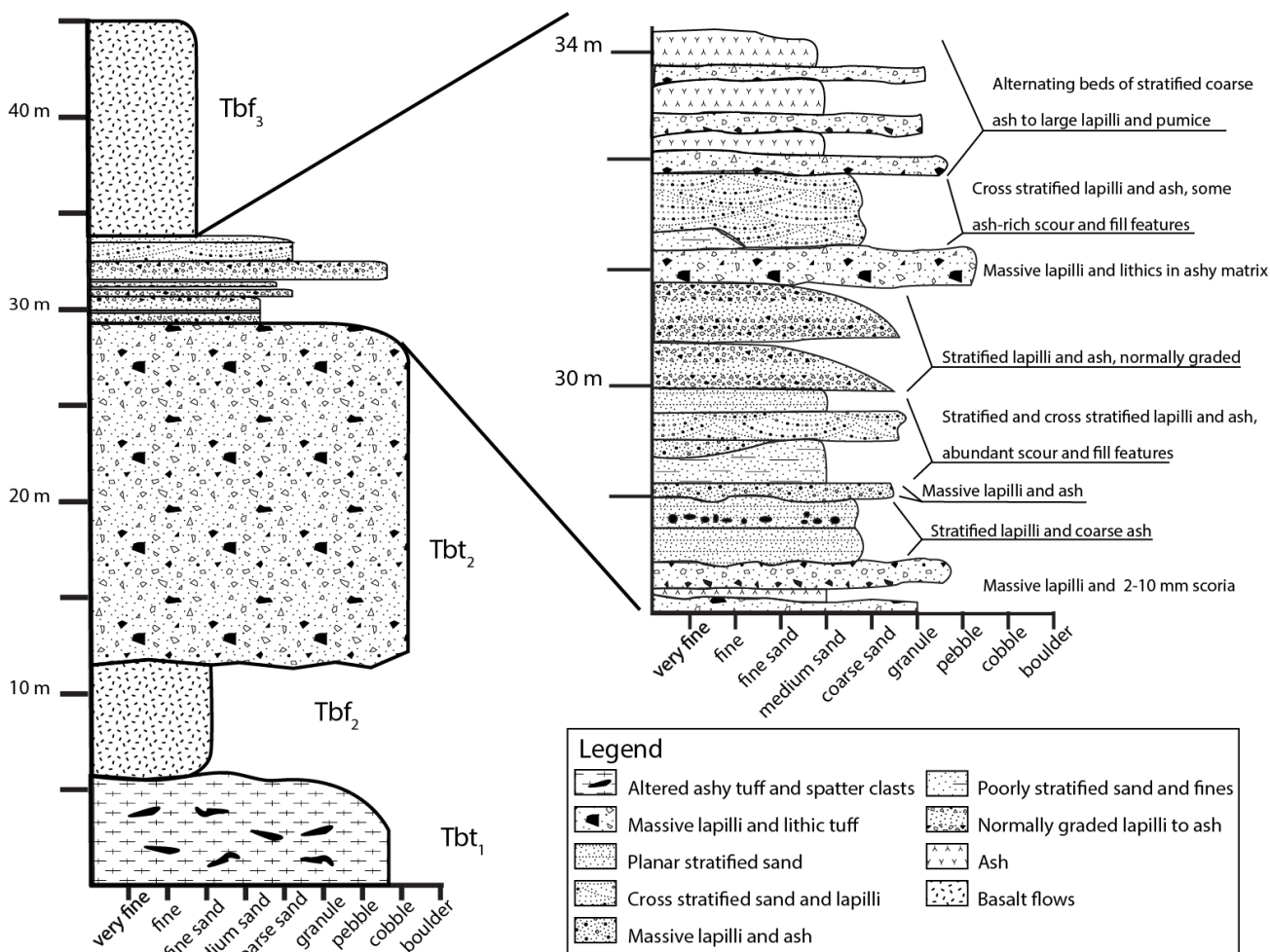


Figure 1- Representative stratigraphic section taken through the Lookout Mountain exposure. Reworked strata are expanded on the right for clarity.

matic in origin due to the blocky texture of juvenile lapilli and palagonitized ash matrix. This stratum is overlain by a vesicular and highly palagonitized basalt flow (Tbf2). The flow contains abundant plagioclase phenocrysts, typical of Imnaha basalts.

The upper tuff (Tbf2) consists of 26 m of massive basaltic tuff with abundant 1-4 mm glassy lapilli, basement lithic fragments up to 1 m in diameter, and vegetation casts. No internal structure is visible in this unit. The clast assemblage in this stratum consists of juvenile basalt (~50%), phyllite (~35%), and granodiorite (~15%) clasts. The proportion of these clasts remains relatively constant over the exposure. The tuff is overlain by a 4 m thick sequence of pyroclastic density current and ashfall deposits, interbedded with fluvially reworked ash and lapilli. This upper, dominantly reworked section of Tbt2 is extremely laterally variable across the deposit. Scour and fill features up to .5 m deep, cross-stratification, and soft sediment deformation features are common in reworked strata (Fig. 1). Primary pyroclastic surge and flow deposits are interbedded with the reworked strata and are also generally laterally discontinuous. Two sets of normally graded lapilli and ash strata are traceable across the entirety of the deposit (Fig. 1). A poorly bedded lapilli sandstone marks the top of the reworked section. The tuff units are capped with a nearly aphyric basalt flow (Tbf3).

The overall character of the upper unit is 'wetter' than the lower tuff. In the upper unit, abundant rock fragments with lithologies identical to locally exposed basement indicate significant excavation of bedrock during a maar-type eruption. In neither case is the vent or a feeder dike exposed.

Microanalysis of lapilli melt inclusions and host glasses was completed on the Washington State University GeoAnalytical Lab JEOL-8500 microprobe. Mineral phases present in the lower tuff include plagioclase, pyroxene, olivine, and rare Fe-Ti oxides. The upper tuff is dominated by plagioclase and pyroxene phenocrysts. The basalt flows are phaneritic, and contain similar mineral phases. Lapilli host glasses and melt inclusions were analyzed for major element concentrations as well as S and Cl abundances. WDS analysis of major element concentrations was completed with typical count times and beam conditions (15 kV, 10 nA) and was followed by a second pass on the same points with a higher current beam (30 nA) and longer count times to analyze for S and Cl abundances. Using this technique, detection limits in the tens of ppm were possible for S and Cl.

Results of microprobe analysis support field observations. Tbt2 lapilli glasses and inclusions are generally less degassed than Tbt1 samples, consistent with the wetter character of the deposits (Fig. 2).

Both units have the overall characteristics of phreatomagmatic deposits that are common products of smaller-scale volcanism, consistent with fortuitous interaction of rising magma with surface water or a shallow aquifer. This contrasts with most of the Imnaha Basalt, which was

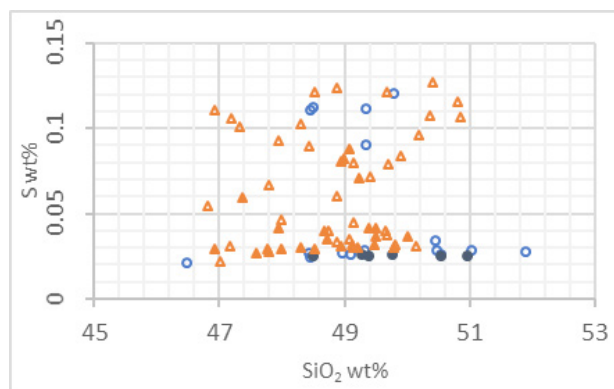


Figure 2- Sulfur content versus SiO₂ plotted for lapilli from Lookout Mountain tuffs. Tbt1 lapilli host glass data are noted by closed circles, melt inclusions by open circles. Tbt2 host glass data are noted by closed triangles, melt inclusions by open triangles.

emplaced in a dominantly dry continental environment (Hooper et al. 1984). Examination of this deposit is consistent with the observations made by Ross et al. (2005) about the importance of ground and surface water interactions driving fragmentation of volcaniclastic deposits in Large Igneous Provinces rather than high volatile budgets.

Acknowledgements

We thank the Washington State University Geoanalytical Lab, Joe Boro, Scott Boroughs, Owen Neill, and Laura Pianowski for their assistance gathering and processing samples for this research.

References

- Hooper, P.R., Kleck, W. D., Knowles, C.R., Reidel, S.P., and Theissen, R. L., 1984. Imnaha Basalt, Columbia River Basalt Group: *Journal of Petrology* v. 25, p. 473-500.
- Ross, P.-S., Ukstins Peate, I., McClintock, Y.G., Xu, P.G., Skilling, I.P., White, J.D.L., and Houghton, B.F., 2005. Mafic volcaniclastic deposits in flood basalt provinces: A review: *Journal of Volcanology and Geothermal Research*, v. 145, p. 281-314

Analog Experiment for Rootless Eruption

Rina Noguchi¹, Ai Hamada², Ayako Suzuki³ and Kei Kurita⁴

¹ Volcanic Fluid Research Center, Tokyo Institute of Technology, Japan. r-noguchi@ksvo.titech.ac.jp

² Central Research Inst. of Electrical Power Industry, Japan.

³ Institute of Space and Astronautical Science, Japan Aerospace Exploration Agency, Japan.

⁴ Earthquake Research Institute, The University of Tokyo, Japan.

Keywords: rootless eruption, analog experiment, rheological control.

Introduction:

Rootless cone is one of peculiar types of pyroclastic cones, which is formed by magma-water interaction when hot lava flows in water-logged regions (Fagents et al., 2002; Fagents and Thordarson, 2007). Though the occurrence on the Earth is quite limited, large numbers of small cones on Mars are suspected to be rootless cones. Why they are so much abundant on Mars is our stating point. Comparing to other types of magma-water interaction such as phreatic/phreatomagmatic eruptions, rootless cone eruption seems rather steady in somehow ordered fashion. This can be inferred from morphological comparison of the cones (Noguchi et al., 2016). Phreatic/phreatomagmatic eruptions are usually violently explosive and transient while rootless cone eruption continues steadily for a certain time period to form a regular cone. To explore this different formation process, we conducted a simple analog experiment. Identification of rootless cone is crucially important in the characterization of terrain origin.

Analog Experiment:

The basic experimental setup to simulate the rootless eruption utilizes the reaction of thermal decomposition of sodium bicarbonate solution to induce CO₂ gas emanation. To promote this we pour high temperature viscous fluid on the solution, which is an analog of hot lava. The experimental procedure is as follows; we put a mixture of sodium bicarbonate powder and sugar syrup in a container at room temperature. The mass fraction of the sodium bicarbonate is varied from 0 % to 100 %. The viscosity of the mixture layer depends on the mass fraction. Heated condensed sugar syrup (T - 130°C) is poured at the top of the mixture layer. When the heated sugar syrup gradually sinks as Rayleigh-Taylor Instability the mixture layer is gradually heated and decomposes to emit CO₂ gas, which forms vesiculated structure until the temperature cools down to be solidified. We measured the mass loss associated with the thermal decomposition, which amounts to the emanation of CO₂ gas.

Vesiculation Process:

Figure 1 shows images after the experiment. Contrasting degree of vesiculation is evident. Interesting point is severe vesiculation for the sample of less amount of sodium bicarbonate, which is the source material of CO₂. Figure 2 shows the total amount of mass loss as a function of the amount of sodium bicarbonate. As is clearly shown

the maximum vesiculation/CO₂ emanation occurs at the intermediate amount, 15 g. The mass loss corresponds to the amount of reaction of the thermal decomposition. The shape of the graph (Figure 3) reminds us the Wohletz diagram, which represents the magnitude of water-magma interaction (Wohletz et al., 2013).

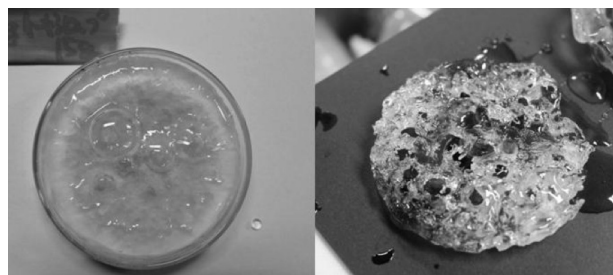


Fig. 1 – The contrasting vesiculations. Left figure is for sodium bicarbonate: 35 g and syrup: 15 g. Right figure is for sodium bicarbonate: 13 g and syrup: 37 g.

Importance of Rheology to Control the Eruption Process:

Figure 4 shows viscosity of the mixture as a function of mass of sodium bicarbonate. The viscosity values were measured at room temperature by a cone-plate type rheometer. The viscosity increases with the amount of sodium bicarbonate and above 35 g the mixture behaves as a solid.

Combining the results of mass loss and rheology, control of the rheology in vesiculation is remarkable. The large amount of mass loss at relatively low concentration of sodium bicarbonate (source material) shows low viscosity of the mixture can enhance the thermal decomposition. In low viscosity medium, high temperature syrup can sink deeply within a limited time to cool having small scale heterogeneities at the interface. This can cause efficient mixing and heat transfer to the medium, which promotes the reaction of thermal decomposition. In rootless eruptions, a similar rheological control should be important; the rheological properties of water-logged region which is covered by hot lava flows determines efficiency of mixing/contact area. The abundant occurrence of rootless cone on the martian surface may indicate unique properties of sub-surface material rather than the terrestrial environments.

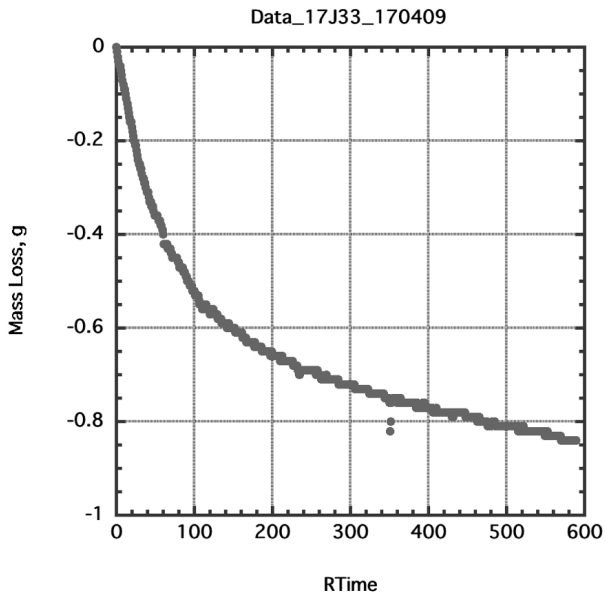


Fig. 2 – Mass loss during the experiment for the sample sodium bicarbonate:17 g and syrup: 33 g.

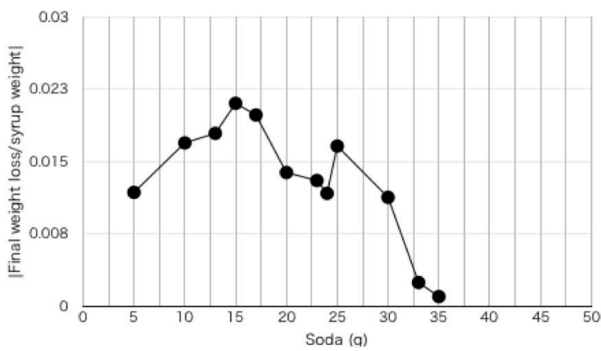


Fig.3 – Total amount of mass loss as a function of the amount of sodium bicarbonate.

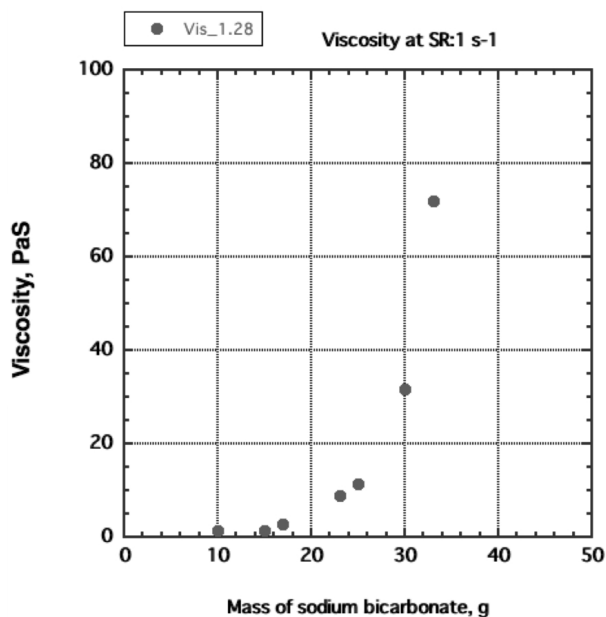


Fig.4 – Viscosity of the mixture of sodium bicarbonate and syrup.

References

Fagents, S. and Thordarson, T., Rootless volcanic cones in Iceland and on Mars. In *Geology of Mars*, Cambridge Univ.Press p151-1777, 2007.

Fagents, S., Lanagan, P. and Greeley, R., Rootless cones on Mars, *Geol. Soc. London*, SP202, 295-317, 2002.

Noguchi, R., Hoskuldsson, A. and Kurita, K., Detailed topographical, distributional and material analyses of rootless cones in Myvatn, Iceland, *J. Volcan. Geotherm. Res.*, 318 89-102, 2016.

Wohletz, K., Zimanowski, B., and Buttner, R., Magma- water interactions, In *Modeling Volcanic Processes*, Cambridge Uni. Press, 230-257, 2013.

Fragmentation studies: towards a uniform 'recipe' for characterization of juvenile pyroclasts

Pierre-Simon Ross¹, Nathalie Lefebvre², Tobias Dürig³, Pier Paolo Comida¹, Juanita Rausch⁴, Daniela Mele⁵, Bernd Zimanowski⁶, Ralph Büttner⁶, James White³

¹ Institut national de la recherche scientifique, 490 de la Couronne, Québec (Qc), G1K 9A9, Canada, rossps@ete.inrs.ca.

² ETH Zurich, Institute of Geochemistry and Petrology, Clausiusstrasse 25, 8092 Zurich, Switzerland

³ Department of Geology, University of Otago, 360 Leith Street, Dunedin 9016, New Zealand

⁴ Particle Vision GmbH, c/o Fri Up, Annex 2, passage du Cardinal 11, 1700, Fribourg, Switzerland

⁵ Dipartimento di Scienze della Terra e Geoambientali, Università degli studi di Bari Aldo Moro, Via Orabona, Bari, Italy

⁶ Physikalisch Vulkanologisches Labor, Universitaet Wuerzburg, Pleicherwall 1, D-97070 Würzburg, Germany

Keywords: fragmentation, juvenile pyroclasts, uniform methodology

For unwitnessed explosive eruptions, volcanologists rely on pyroclastic deposits to reconstruct eruptive style, modes of transport, dispersal and fragmentation processes. Interpretation of magma fragmentation processes is based largely on the morphological, surface and textural characteristics of juvenile pyroclasts, especially ash particles. Such characteristics have been studied for several decades, but with quite variable methodologies and often for deposits where the eruption styles are inferred (e.g., Dellino and La Volpe 1995; Ross and White 2012; Jordan et al. 2014; Bagheri et al. 2015; Leibrandt and Le Pennec 2015; Liu et al. 2015; Dioguardi et al. 2017). Thus, it is not yet entirely clear how to specifically link juvenile ash characteristics (particle size, shape, internal features such as crystals and vesicles, surface features, chemical composition) with specific eruptive styles or fragmentation processes.

In order to build on our understanding of fragmentation processes, it is essential to be able to directly compare juvenile pyroclasts from different volcanoes, starting with those with fresh deposits where the eruption was observed, and artificial pyroclasts resulting from experiments where eruption parameters are well constrained. To achieve this goal, the volcanological community needs to agree on a unified methodology, i.e. a standard 'recipe'. Here we summarize a preliminary proposal, to be later submitted as a journal article by the authors of this abstract and several others. The recipe has mandatory, recommended and optional steps to allow for systematic data comparison and also for freedom of additional desired techniques enabling to address very specific questions. Due to space constraints, we present only the mandatory parts here.

The recipe prescribes steps within the stages of sample selection and preparation, and then data acquisition and analysis (Fig. 1). Bulk pyroclastic samples are taken from representative units of a well-established geological framework. Each bulk pyroclastic sample is hand sieved, ideally one sieve at a time to minimize particle breakage. Two size fractions are extracted: a fine one (4 phi), and a medium one (1 phi). The 4 phi size fraction is selected because it should be small enough to directly record the

magma fragmentation mechanism since these particles cool extremely quickly (e.g., Heiken and Wohletz 1985; Dellino et al. 2012), and is considered by many workers as the most appropriate to identify certain surface features diagnostic of explosive magma-water interaction (e.g., Dellino et al. 2012; Murtagh and White 2013; Zimanowski et al. 2015; Valentine and White 2017).

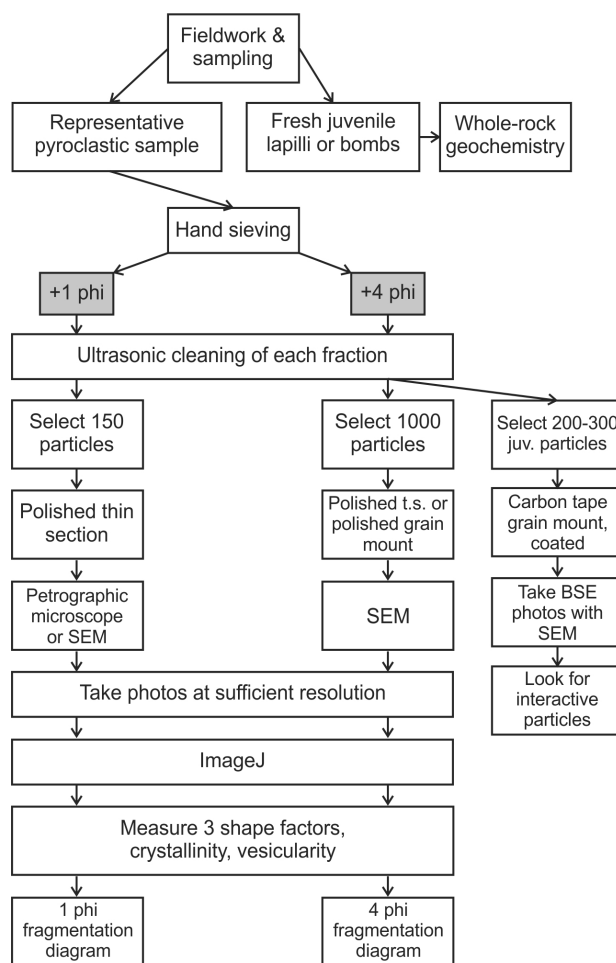


Fig. 1 – Proposed workflow, showing the mandatory steps only.

However, as the 4 phi is too small to be representative of the magma vesicularity and crystallinity at fragmentation, the 1 phi must also be studied. This size fraction should be representative for the majority of vesicles and crystals but fine enough to likely not have experienced post-fragmentation effects. Each selected size fraction is cleaned in an ultrasonic bath with distilled water.

The next step is juvenile particle selection and preparation. For the 1 phi fraction, 150 representative juvenile particles are selected under a binocular microscope to make a polished thin section. For the 4 phi fraction, about 1200-1300 juvenile particles are randomly selected under binocular microscope: ~200-300 particles for a carbon tape grain mount and ~1000 for a polished epoxy grain mount or a polished thin section.

Subsequently, 2D cross-sectional area image analysis (Liu et al. 2015) is performed on both the 1 phi and the 4 phi polished grain mounts or thin sections using the Scanning Electron Microscope (SEM) in Backscatter Electron mode (BSE). From the images, 2-D shapes, vesicularity and crystallinity are quantified using the ImageJ software. Three independent shape parameters that capture the particle form (axial ratio), morphological roughness (solidity) and textural roughness (convexity) are calculated after Liu et al. (2015). These parameters capture different aspects of shape, are largely independent of particle orientation, and are easily measured with freeware. The three shape factors, crystallinity and vesicularity are the variables from which two fragmentation diagrams will be constructed for the 1 and 4 phi size fractions.

Interactive particles are identified using the carbon tape grain mount (4 phi) and an SEM. These interactive particles have 'seen' external water and have been fragmented at very high stress rates (Zimanowski et al. 2015).

By applying multivariate statistical tools to the data, such as cluster analyses, t-tests and equivalent tests (Dürig et al. 2012), the analyzed particles can be classified and compared. In addition, potential subgroups in the particle population can be identified, which can facilitate the identification of underlying generation mechanisms.

It is anticipated that by applying the recipe to obtain uniform juvenile particle data, we can eventually develop new "fragmentation diagrams" which would allow different styles of phreatomagmatic and magmatic explosive eruptions to be distinguished based on their products, including variable magma compositions, crystallinities and vesicularities.

Acknowledgements

PSR is supported by a Discovery Grant from NSERC. NL was supported by the Swiss National Science Foundation Marie Heim-Voegtlin post-doctoral research grant.

References

- Bagheri, G.H., Bonadonna, C., Manzella, I. and Vonlanthen, P., 2015. On the characterization of size and shape of irregular particles. *Powder Tech.*, 270: 141-153.
- Dellino, P. and La Volpe, L., 1995. Fragmentation versus transportation mechanisms in the pyroclastic sequence of Monte Pilato-Rocche Rosse (Lipari, Italy). *J. Volcanol. Geotherm. Res.*, 64: 211-231.
- Dellino, P., Gudmundsson, M.T., Larsen, G., Mele, D., Stevenson, J.A., Thordarson, T. and Zimanowski, B., 2012. Ash from the Eyjafjallajökull eruption (Iceland): Fragmentation processes and aerodynamic behavior. *J. Geophys. Res.*, 117, DOI 10.1029/2011JB008726.
- Dioguardi, F., Mele, D., Dellino, P. and Dürig, T., 2017. The terminal velocity of volcanic particles with shape obtained from 3D X-ray microtomography. *J. Volcanol. Geotherm. Res.*, 329: 41-53.
- Dürig, T., Mele, D., Dellino, P. and Zimanowski, B., 2012. Comparative analyses of glass fragments from brittle fracture experiments and volcanic ash particles. *Bull. Volc.*, 74: 691-704.
- Heiken, G. and Wohletz, K., 1985. *Volcanic ash*. University of California Press, Berkeley, California, 246 p.
- Jordan, S.C., Dürig, T., Cas, R.A.F. and Zimanowski, B., 2014. Processes controlling the shape of ash particles: Results of statistical IPA. *J. Volcanol. Geotherm. Res.*, 288: 19-27.
- Leibrandt, S. and Le Pennec, J.-L., 2015. Towards fast and routine analyses of volcanic ash morphometry for eruption surveillance applications. *J. Volcanol. Geotherm. Res.*, 297: 11-27.
- Liu, E.J., Cashman, K.V. and Rust, A.C., 2015. Optimising shape analysis to quantify volcanic ash morphology. *GeoResJ*, 8: 14-30.
- Murtagh, R.M. and White, J.D.L., 2013. Pyroclast characteristics of a subaqueous to emergent Surtseyan eruption, Black Point volcano, California. *J. Volcanol. Geotherm. Res.*, 267: 75-91.
- Ross, P.-S. and White, J.D.L., 2012. Quantification of vesicle characteristics in some diatreme-filling deposits, and the explosivity levels of magma-water interactions within diatremes. *J. Volcanol. Geotherm. Res.*, 245-246: 55-67.
- Valentine, G.A., White, J.D.L., Ross, P.-S., Graettinger, A.H. and Sonder, I., 2017. Updates to concepts on phreatomagmatic maar-diatremes and their pyroclastic deposits. *Frontiers in Earth Science*, 5(68).
- Zimanowski, B., Büttner, R., Dellino, P., White, J.D.L. and Wohletz, K., 2015. Magma-water interaction and phreatomagmatic fragmentation. In: H. Sigurdsson, B. Houghton, S.R. McNutt, H. Rymer and J. Stix (Editors), *Encyclopedia of Volcanoes*, Second edition. Academic Press, London, pp. 473-484.

A new analogue for Maar-diatremes?: Fluidized bed chemical reactors

Bob Tarff¹ and Simon Day²

¹ Department of Earth and Planetary Sciences, Birkbeck, University of London, Malet Street, London WC1E 7HX: bobanddonna@talktalk.net

² Institute for Risk and Disaster Reduction, Department of Earth Sciences, University College London

Keywords: fluidized-bed, diatreme, fluidization.

Various analogue systems for maar-diatremes have been proposed. Here, we consider features of the Cova de Paul maar-diatreme (near the summit of the Cova de Paul volcano, Santo Antao, Cape Verde Islands) that may be explained by an analogy with fluidized-bed chemical reactors.

A fluidized-bed reactor (FBR) is a device that is used for industrial multiphase chemical reactions (Duduković, Larachi et al. 2002), typically involving two fluids whose reaction is catalyzed by a solid. These fluids (gas or liquid) are passed through a granular bed of the solid at velocities high enough to fluidize the granular bed: benefits of this include maintenance of a homogenous permeability and continuous abrasion of the solid particles to maintain fresh reaction surfaces. Where reactions are exothermic large gas bubbles can develop within the bed. These can readily escape to the surface if there are no barriers to prevent their flow, but if the permeability of the fluidized solid is insufficient to allow free flow of the fluid then dangerous instabilities can develop in the reactor.

In our analogy, the exothermic reaction is analogous to the heat contained in the hot magma intruded into a diatreme, which is transferred to the pyroclastic fill of the diatreme and generates gas by vaporization of the pore water. Whether this can escape depends critically on the permeability structure of the diatreme fill: if its permeability is insufficient, the fill may first fluidize and then form explosively expanding bubbles.

The internal structure of diatremes, revealed by erosion or by mining, shows some evidence for this analogy in the form of the widely recognized vertical variation from bedded upper diatreme units downwards into lower units intruded by dikes (Fig. 1).

Upper diatreme sequences are composed of alternating thin and thick bedded tephra, which are produced by the sedimentation of erupted airfall material that has fallen back into the crater and the reworked rock from the subsidence of the diatreme wall and maar rim (White and Ross 2011) (Fig. 1). These deposits present a barrier for magma rising to the surface.

The lower diatreme deposits are characterized by an absence of bedding, and the fill is described as homogenized or well mixed (White and Ross 2011). The deposits are massive and poorly sorted, with regions of differing

particle populations that are separated by gradual to sharp contacts (Fig. 1). This difference may indicate that the particles are moving as fluids within the fill prior to mixing. However, the temporal relationship between the fluidization of the lower diatreme fill and the development of violent explosions are unclear in diatremes, since the exposed rocks represent the end products of complex eruptions. To understand this temporal relationship, therefore, it is necessary to examine clast populations in proximal erupted sequences on the rims of maar-diatreme craters.

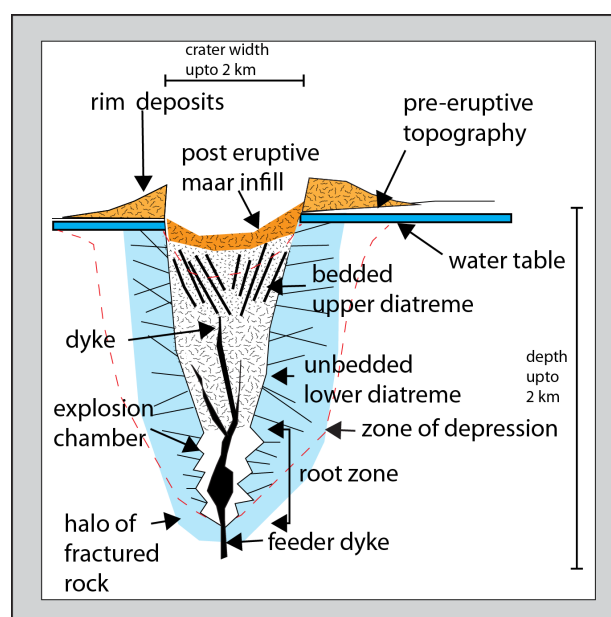


Fig. 1: Schematic of a typical maar-diatreme crater and pipe, not drawn to scale (adapted from Lorenz and Kurszlauskis (2007) and White and Ross (2011).

The lower diatreme deposits are characterized by an absence of bedding, and the fill is described as homogenized or well mixed (White and Ross 2011). The deposits are massive and poorly sorted, with regions of differing particle populations that are separated by gradual to sharp contacts (Fig. 1). This difference may indicate that the particles are moving as fluids within the fill prior to mixing. However, the temporal relationship between the fluidization of the lower diatreme fill and the development of violent explosions are unclear in diatremes, since the exposed rocks represent the end products of complex eruptions. To understand this temporal rela-

tionship, therefore, it is necessary to examine clast populations in proximal erupted sequences on the rims of maar-diatreme craters.

The phreatomagmatic phase of the eruption of the Cova de Paul maar/diatreme system contained two distinct cycles that each culminated in a violent explosive event. These explosive events generated dense, valley-filling pyroclastic density currents (PDCs), and we suggest they were initiated by transient explosion chambers formed within the diatreme infill. The PDC deposits are coarse, poorly sorted and well-indurated, matrix-rich breccias, which were formed by dense, ground-hugging PDCs that flowed into valleys incised into the flanks of the Cova de Paul volcano. Whilst the matrix is dominantly coarse ash, the larger clasts range up to boulder size. They were accompanied, especially in the latter part of the violent explosive events, by cross-bedded units formed from dilute, high velocity PDCs. A characteristic of the finest ash component of these deposits is that it contains abundant lithic fragments, indicating formation by progressive mechanical fragmentation of larger grains within the diatreme fill as much as by intense fragmentation of juvenile magma.

A common factor of all juvenile grains from the phreatomagmatic phase of the maar/diatreme eruption of the Cova de Paul Crater is they contain entrained lithic grains from the diatreme fill. One particularly large and irregular clast with many included lithic grains was also found to have a chilled crust containing abundant embedded lithic grains (Fig. 2). It was found as a single, sheet-like clast but was broken up for production of thin-sections from parts c, d and f (Fig. 2).

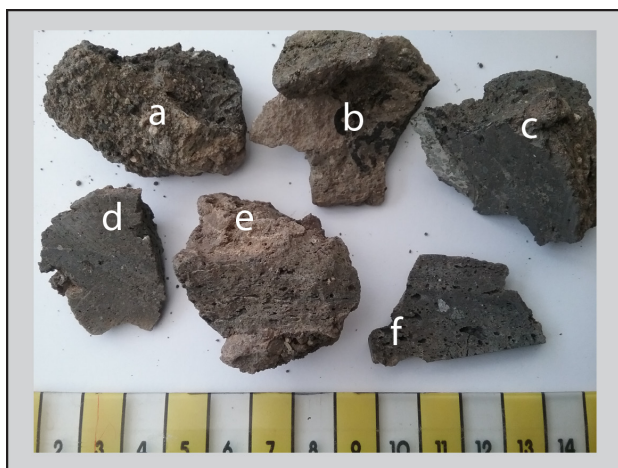


Fig. 2: Fragments of a juvenile clast SA10RT089 from the top of unit 5. This clast has a knobby, lobate outer surface embedded with phonolite fragments and ash (a and b); (e) shows an outer rind and a core with elongated vesicles parallel to the outer rind that appears to indicate flow within the core of the clast; (c, d and f) have phonolite inclusions and (f) shows flow.

We interpret this fragment as part of a magma feeder tube for transient explosion chambers within the diatreme fill, which is located in a part of the fill with lithic clasts dominantly in the medium ash to fine lapilli size range. This

feeder tube would not have been stable as it was formed in the loosely packed rubble of the diatreme infill, whilst on a smaller scale the abundance of grains entrained into the juvenile clast indicates that the cohesion of the fill was low. Although the evidence is not conclusive, we suggest that the fill was at least partly fluidized at the time that the magma feeder tube, of which SA10RT89 is a part, was emplaced into it.

Previous evidence of some fluidization within diatremes is provided by the tephra pipes found in some kimberlite diatremes. Lorenz and Kurszlaukis (2007) suggest these are formed by a fluidized mass of ash and liquid that originates in the root-zone and travels as a stream to the surface. We suggest that, if magma is reaching shallower levels within the diatreme, localized fluidization is also occurring and forming similar pipes to the surface.

Valentine et al (2014) suggest mixing is occurring within the lower diatreme as more shallow explosions churn deep-sourced wall-rock into the upper levels of the lower diatreme from where they are erupted. We suggest that mixing is also occurring by at least partial fluidization of the fill in a similar way to an industrial fluidized-bed reactor, and that this fluidization becomes more intense as fragmentation of the existing material in the diatreme reduces the permeability of the diatreme fill. We propose a positive feedback loop, in which this permeability reduction raises pore pressures in the fill and further intensifies fluidization of the deeper levels of the diatreme until a violent explosion develops. The cyclicity in the Cova de Paul Crater eruption sequence may, therefore, have been driven by fragmentation in the fluidized regions of the diatreme fill.

References

- Duduković, M. P., F. Larachi, et al. (2002). "Multiphase catalytic reactors: a perspective on current knowledge and future trends." *Catalysis reviews* 44(1): 123-246.
- Lorenz, V. and S. Kurszlaukis (2007). "Root zone processes in the phreatomagmatic pipe emplacement model and consequences for the evolution of maar-diatreme volcanoes." *Journal of Volcanology and Geothermal Research* 159(1): 4-32.
- Valentine, G., Valentine, A., Graettinger, I. and Sonder (2014). "Explosion depths for phreatomagmatic eruptions." *Geophysical Research Letters* 41(9): 3045-3051.
- White, J. D. and Ross, P.-S. (2011). "Maar-diatreme volcanoes: a review." *Journal of Volcanology and Geothermal Research* 201(1): 1-29.

Geophysical and geochemical survey across El Hierro (Canary Islands) during the 2011–2012 monogenetic eruption

Stéphanie Barde-Cabusson¹, Xavier Bolós², Víctor Villasante Marcos³, Helena Albert⁴, Ilazkiñe Iribarren Rodríguez⁵, Natividad Luengo-Oroz⁵, Dario Pedrazzi¹, Llorenç Planagumà⁶, and Joan Martí¹

¹ Institute of Earth Sciences Jaume Almera, ICTJA, CSIC, Group of Volcanology, SIMGEO UB-CSIC, Lluís Sole i Sabaris s/n, 08028 Barcelona, Spain. s.barde.cabusson@gmail.com

² Institute of Geophysics, UNAM, Campus Morelia, 58190 Morelia, Michoacán, Mexico

³ Observatorio Geofísico Central, Instituto Geográfico Nacional, Madrid, Spain.

⁴ Earth Observatory of Singapore, Nanyang Technological University, 639798, Singapore, Singapore..

⁵ Centro Geofísico de Canarias, Instituto Geográfico Nacional, Santa Cruz de Tenerife, Spain.

⁶ Tosca, Environment Services of Education. Casal dels Volcans, Av. Santa Coloma, 17800 Olot, Spain.

Keywords: monogenetic eruption, self-potential, soil CO₂ flux.

Enhancing volcanic risk assessment and developing new methodologies for volcanic activity are among the main challenges in Geosciences. In the field of Volcanology, it depends directly on our understanding of when, where, and which type of volcanic eruptions will take place. In the case of polygenetic volcanoes the emphasis is usually on “when will the eruption take place? In the case of the monogenetic volcanism, while a certain monotony exists in the composition of magmas from an eruption and another, we can observe a huge diversity in the eruptive dynamics inside a volcanic field and sometimes for a single edifice (e.g. Smith and Nemeth, 2017), switching from low-energy lava flows to violent hydromagmatic explosions. As a consequence, understanding which type of eruption we can expect is crucial. Contrary to polygenetic volcanoes, for which the eruptive activity is mostly centered on the edifice, the magma can reach the surface almost anywhere in a monogenetic field, depending on tectonics, local geology, etc. Knowing where the next eruption will take place becomes a big challenge as well. In any case, some major issues consist in (1) understanding the local features affecting the triggering of eruptions and the volcano dynamics, (2) understanding which of the measurable parameters are relevant for the observation of monogenetic activity, and (3) implementing observation methods adapted to monogenetic fields.

On another hand another challenge in Volcanology consists in finding new methods for the prevision of hazards related to “discreet eruptions”, which are eruptions with no classical precursors such as seismic activity and deformation. The phreatic eruption of Mount Ontake (Japan) in 2014 is one of the most recent and sadly famous example of this phenomenon (e.g. Kagoshima et al., 2016). When this type of eruption can occur in a monogenetic field the real struggle is to propose a strategy to reply simultaneously to the three questions “where, when, and which” eruption will take place? In the island of El Hierro (Canary Islands, Spain), monogenetic volcanism is common (Fig. 1).

A submarine monogenetic eruption started on the 10th of October 2011 and lasted until the 5th of March 2012. This eruption was not discreet as the local monitoring network registered almost 10000 earthquakes, deformation, and some geochemical and geomagnetic anomalies before the eruption (Lopez et al., 2012). However, knowing where the magma would reach the surface was a major concern as the earthquakes were migrating from the north to the south of El Hierro, until the eruption started 2 km south of La Restinga, the southern point of the island. The second concern was the about the possibility of a hydromagmatic eruption taking place near the inhabited coast of El Hierro.

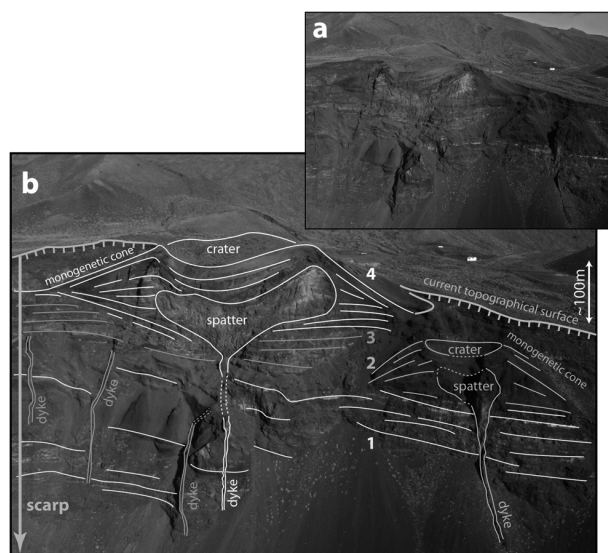


Fig. 1 - two monogenetic cones spotted at the western point of the island of El Hierro. The internal structure of the edifices was exposed by the erosion of the coast line (figure from Barde-Cabusson et al., 2013).

Putting all the pieces together, we feel that a double approach is necessary in order to better understand monogenetic volcanic systems and their dynamics (past and present), as an essential prerequisite to improving erup-

tion forecasting in time, space, and concerning the type of the eruptions:

- A structural approach consisting in using methods sensitive to fluid circulations: they allow to map rising hydrothermal fluids and infiltrating meteoric water, as well as the main structural features guiding them.

- A dynamic approach consisting in developing new monitoring methods measuring hydrothermal activity variations related to the magmatic activity.

Here we focus on the first approach, with the results of a geophysical and geochemical survey (self-potential and soil CO₂ flux) crossing the island of El Hierro, performed during the seismic crisis and eruption of 2011-2012.

Acknowledgements

We sincerely thank the authorities of El Hierro that provided support and all the necessary authorizations to our work. This research has been supported by IGN and CSIC, and funding by the European Commission (282759: "VUELCO") and the MINECO grant CGL2011-16144-E. S. Barde-Cabusson was funded by JAE-Doc Program (JAE-Doc_09_01319).

References

- Barde-Cabusson S., Bolós X., Pedrazzi D., Lovera R., Serra G., Martí J., Casas A., 2013. Electrical resistivity tomography revealing the internal structure of monogenetic volcanoes. *Geophys. Res. Lett.* 40: 2544-2549.
- Kagoshima T., Sano Y., Takahata N., Ishida A., Tomonaga Y., Roulleau E., Pinti D., Fischer T.P., Lan T., Nishio Y., Tsunogai U., Guo Z., 2016. Spatial and temporal variations of gas geochemistry at Mt. Ontake, Japan. *J. Volcanol. Geoth. Res.* 325: 179–188.
- López C., Blanco M. J., Abella R., Brenes B., Cabrera Rodríguez V. M., Casas B., Domínguez Cerdeña I., Felpeto A., Fernández de Villalta M., del Fresno C., García O., García-Arias M. J., García-Cañada L., Gomis Moreno A., González-Alonso E., Guzmán Pérez J., Iribarren I., López-Díaz R., Luengo-Oroz N., Meletlidis S., Moreno M., Moure D., Pereda de Pablo J., Rodero C., Romero E., Sainz-Maza S., Sentre Domingo M. A., Torres P. A., Trigo P., Villasante-Marcos V., 2012. Monitoring the volcanic unrest of El Hierro (Canary Islands) before the onset of the 2011–2012 submarine eruption. *Geophys. Res. Lett.* 39: L13303.
- Smith I.E.M., Németh K., 2017. Source to surface model of monogenetic volcanism: a critical review. In Németh K, Carrasco-Núñez G, Aranda-Gómez JJ, Smith IEM (eds) *Monogenetic volcanism*. *Geol. Soc. Lond. Spec. Publ.* 446:1–28.

Magnetometric survey of la Joya Honda Maar (México) and surroundings; volcanic implications.

Héctor López Loera, David Ernesto Torres Gaytan, José Jorge Aranda-Gómez

Instituto Potosino de Investigación Científica y Tecnológica, A.C., División de Geociencias Aplicadas, P.O.Box 3-74. San Luis Potosí, S.L.P., 78216, México. hector.lopez@ipicyt.edu.mx

Keywords: Joya Honda, Magnetometry, VOXI.

Joya Honda (JH) is a Quaternary maar (K-Ar, matrix 1.1 My) excavated in a sequence of folded Mesozoic limestone and limestone and shale units. It is located in central Mexico and belongs to the Ventura volcanic field (VVF), which is composed by cinder cones and maars made in-plate-type mafic alkalic rocks. Volcanoes in the región form ~N40W lineaments, roughly parallel to one of the two regional set of normal faults, but there is not obvious relation between these faults and vent distribution in the exposed geology around the maar. The volcanic rock volumen is small in the VVF, and most volcanoes and their products are scattered in a región where outcrops are dominated by limestones and alluvium (Aranda-Gómez and Labarthe-Hernández, 1985). JH has an elliptical shape, with 1,100 and 850 m long axes. Maximum relief from the floor of the cráter, to the highest point on the rim is nearly 300 m, and the walls are nearly vertical.

The study and 3D modeling of aerial and terrestrial magnetometry allowed us to identify and characterize the magnetic anomalies related to the JH maar, which are correlated with sources that are located at depths ranging from 230 m to 370 m. Aeromagnetic survey of la Joya Honda are part of a more extensive study and covers also all the VVF and all the state of San Luis Potosí.

The aeromagnetic data was captured by the COREMI (today Mexican Geologic Service) with flight lines every 1,000 m and average flight height of the ground of 300 m. The processing of the data was done using Geosoft Oasis montaje software.

The analysis of aeromagnetometry shows that there are several aeromagnetic domains in the region (Fig. 1). The visual comparison with the geological chart of the same area, it is concluded that the intensities and high frequencies are associated with areas where volcanic rocks abound. The second magnetic sector with low intensities and frequencies coincides with outcrops of Mesozoic rocks

The aeromagnetic anomaly associated to the JH has an irregular shape similar to a horseshoe, with a low in the central part. Towards the SE there is an inverted anomaly that is interpreted associated with a volcano buried below the products of JH and located immediately to the E of the mar.

Seven terrestrial magnetic sections were performed with total magnetic field reading stations every 25 to 50

m. With these sections a contour map was made in and around the JH (López-Loera et al., 2008), obtaining a terrestrial magnetic anomaly in the south central portion of the crater that was modeled in 3D with the software of Geosoft VOXI (Ellis et al., 2012), obtaining a vertical cylindrical body that resembles a diatreme (Fig. 2).

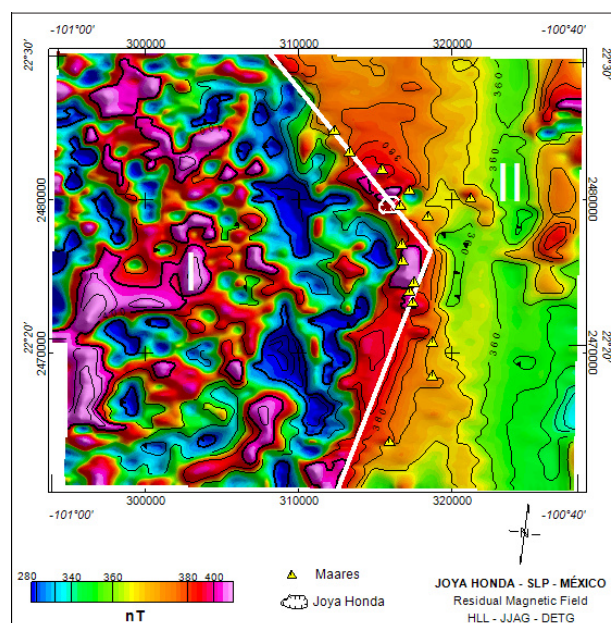
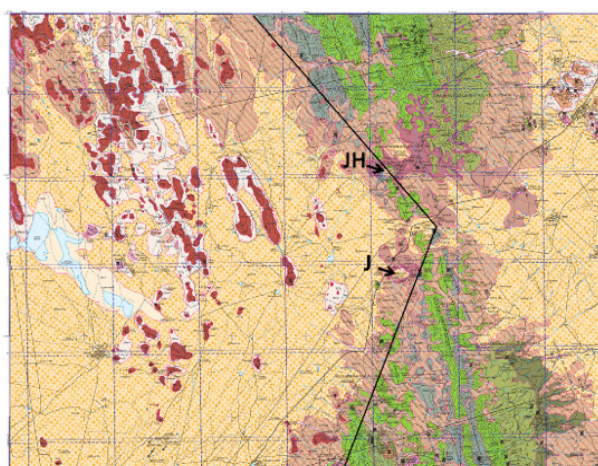


Figure 1. Geologic (A) and Aeromagnetic (B) maps.

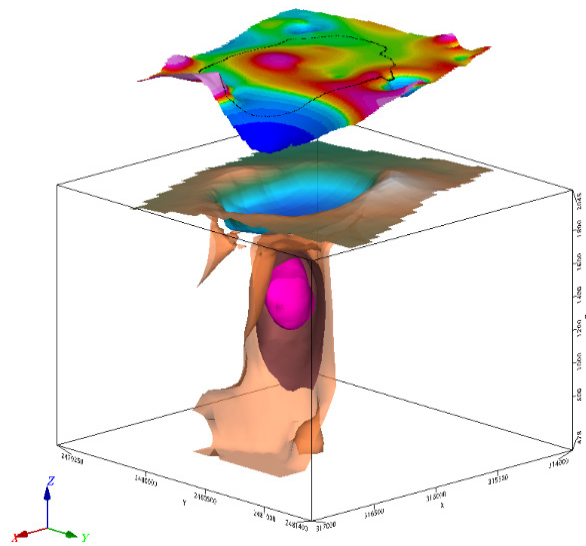
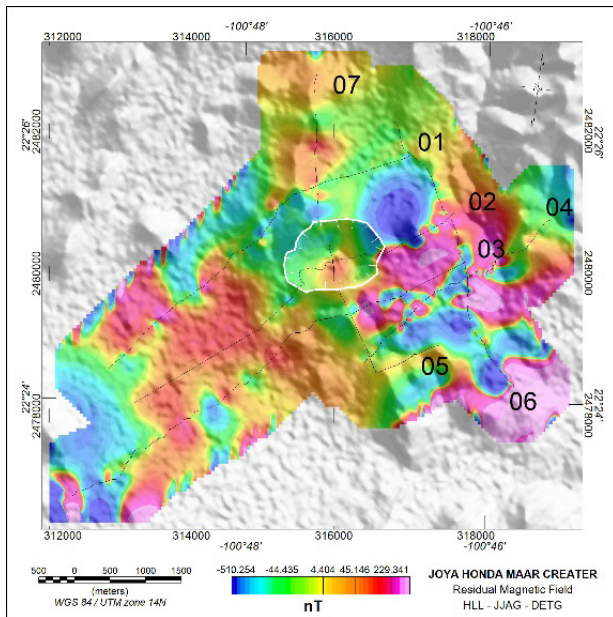


Figure 2. Magnetic terrestrial contour map of the residual magnetic field (A). 3D voxel model of the JH magnetic anomaly.

References

Aranda-Gómez, J.J., Labarthe-Hernández, G., 1975. Estudio Geológico de la Hoja Villa Hidalgo, S.L.P., Folleto Técnico, Inst. De Geología y Metalurgia (México), 53: 33-58.

Ellis, R. G., de Wet, B., MacLeod, I. N. 2012. Inversion of magnetic data for remanent and induced sources. ASEG Extended Abstracts 2012, 1-4

López-Loera, H., Aranda-Gómez, J.J., Arzate, J. A., Molina-Garza, R. S., 2008. Geophysical surveys of the Joya Honda maar (México) and surroundings; volcanic implications. Journal of Volcanology and Geothermal Research 170: 135-152.



Oral *Session 2*

Geochemistry and petrology of monogenetic volcanism related magmas


Conveners

Ian Smith (ie.smith@auckland.ac.nz)

Giovanni Sosa-Ceballos (giovanni@geofisica.unam.mx)

Claus Siebe (csiebe@geofisica.unam.mx)

Monogenetic volcanoes have been traditionally linked to direct magma transfer from the mantle to the surface. However, recent detailed petrological and geochemical studies of some monogenetic eruptions suggest that magmas coming from depth in dikes are not able to rise straight to the surface, but stall at some intermediate depth developing an environment in which processes such as magma mixing, crystal fractionation and/or crystal assimilation can occur. Understanding the processes and magma plumbing systems that lead to monogenetic eruptions is fundamental for better interpreting the monitoring data of the unrest episodes in monogenetic volcanic fields and thus improve the eruption forecasting in these regions. We invite contributions that include field observations, geochemical, isotopic and petrological data, analogue models of dike propagation and experimental petrology of magma ascents.



Felsic rocks within the Michoacán-Guanajuato monogenetic volcanic field; mafic magma-crust interaction?

Giovanni Sosa-Ceballos¹, Mario Emmanuel Boijsseaneau-López², Juan Daniel Pérez-Orozco¹

¹ Institute of Geophysics, UNAM, Campus Morelia, 58190 Morelia, Michoacán, Mexico. giovannis@igeofisica.unam.mx

² Graduate School in Earth Sciences, UNAM, Campus Morelia, 58190 Morelia, Michoacán, Mexico

Keywords: Michoacán, felsic rocks, Tzirate, mafic magmas

Felsic rocks have been greatly underestimated within the Michoacán-Guanajuato Volcanic Field (MGVF). The MGVF contains the largest concentration of monogenetic mafic-andesitic vents on Earth; more than 1,100 edifices comprising scoria cones (including the Parícutin volcano), semi-shield volcanoes, maars, tuff rings and spatters (Hasenaka and Carmichael, 1985).

In order to investigate the origin of felsic rocks at the MGVF, we analyzed a series of dacitic-mafic rocks from the Tzirate Volcanic Complex (TVC) and the classic MGVF mafic volcanism from the surroundings. The composition of rocks were discussed according to their deformation regime. In addition, we performed a series of hydrothermal experiments in order to constrain how much a mafic magma can change its composition with assimilation of local, felsic-basement rocks.

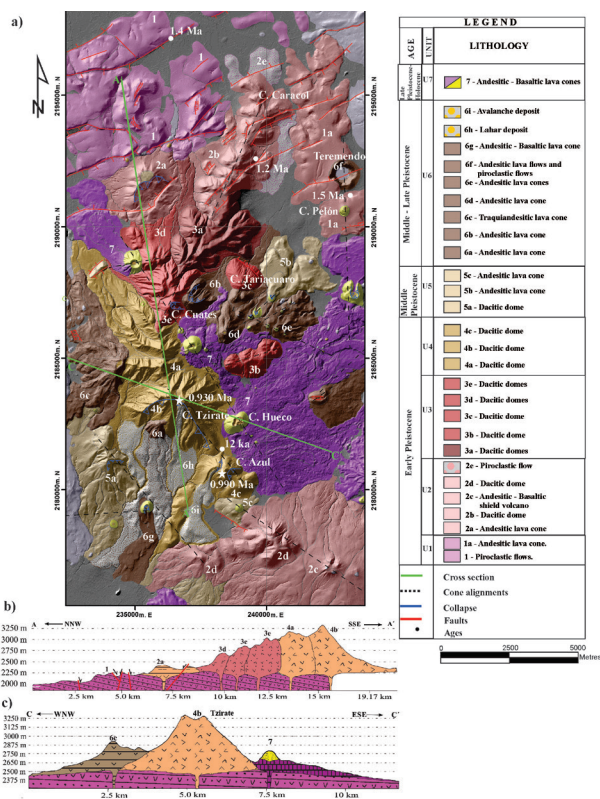


Fig. 1 – Geologic map (a) and cross sections (b,c) from the TVC. Units 2c and 6g represents the mafic magmatism that dominates the MGVF. All other units are felsic andesitic-dacitic domes.

Although the presence of felsic rocks (silica-rich andesites and dacites) are reported in the MGVF, e.g., Tancitaro and Patambán stratovolcanoes, (Ownby et al., 2006), their relative volume and occurrence has been minimized and overall poorly studied. Recent studies have shown the presence of numerous dacitic domes within the MGVF (e.g., La Muela, La Nieve, Quinceo, El Aguila, El Tzirate) and their origin is currently under investigation.

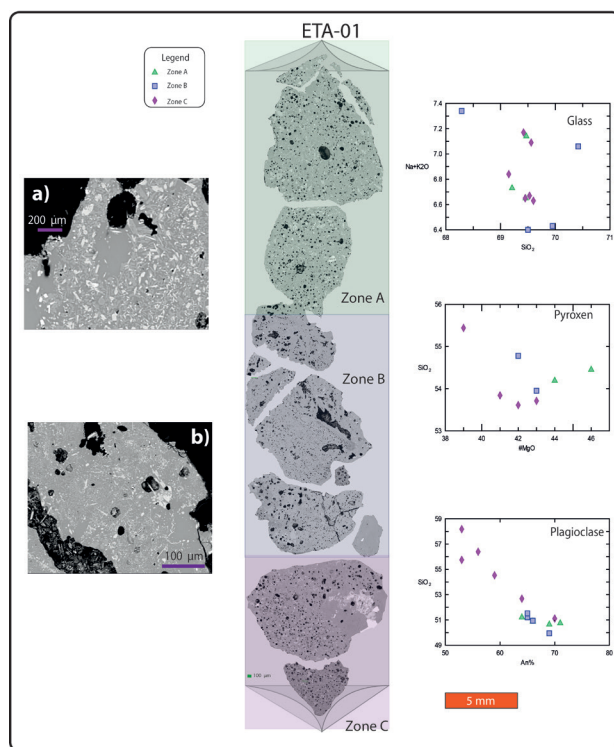


Fig. 2 – Experimental results. The mosaic (zones A, B and C) are quenched glasses recovered from a Ag-Pd capsule; Zone C is the bottom of the capsule and contain the remnants of the doped assimilant. The BSE images (a and b) show different degrees of crystallization in the experiment; note that the volcanic experimental charge was driven to its liquidus before being doped with assimilant. Glass, pyroxene and plagioclase result in variable composition depending on its proximity to the assimilant.

The TVC is located at the center of the MGVF, central Mexico. It is characterized by a series of andesitic-dacitic domes and by the active faulting of the Morelia-Acambay fault system. The dacitic volcanism of the TVC occurred during the Early Pleistocene with the eruption of lavas that formed a series of dacitic domes ($\text{SiO}_2 = 63 - 69 \text{ wt.}\%$) aligned in NNE-SSW and NW-SE directions. The area is covered by andesitic-basaltic cinder cones from the Early Pleistocene to the Late Pleistocene-Holocene produced by the typical monogenetic volcanism of the MGVF.

The structural analysis show that the principal stress was horizontally oriented, prevented the rise of dikes to the surface and favored the development of shallow magma chambers in the crust. Assimilation of the local basement was enhanced and probably contributed to the formation of felsic magmas. Subsequently, the local stress field became extensional, and the vertical principal stress developed normal or extensional faults that reached the magma chamber and served as the plumbing system for the rise of felsic lava.

The experimental results (Fig. 2) show that intrusive felsic rocks from the local basement can be partially digested by a basaltic-andesitic melt in 23 hours at 850°C and 150 MPa. The glass produced by the assimilation could be more silica-rich than the assimilant because of high crystallization of plagioclase and pyroxene. The peritectic crystals of plagioclase and pyroxene are more Na-rich and Fe-rich respectively.

We recognize that the origin of intermediate-felsic rocks worldwide is still under debate, at least not a single method can be claimed to be the universal petrogenetic process. Our structural-experimental evidences suggest that indeed, the occurrence of felsic rocks within the MGVF could be controlled by the deformation style, the rock type in the local basement and the time of magma entrapment in upper crust reservoirs. Although this model is a good approximation for the TVC, more fieldwork is needed to investigate the deformation style in other felsic rock centers within the MGVF.

References

- Hasenaka, T., Carmichael, I.S.E., 1985. A compilation of location, size, and geomorphological parameters of volcanoes of the Michoacan-Guanajuato volcanic field, central Mexico. *Geofis. Int.* 24, 577-607.
- Ownby, S., et al., 2007. Volcán Tancítaro, Michoacán, Mexico, $^{40}\text{Ar}/^{39}\text{Ar}$ constraints on its history of sector collapse. *J. Volcanol. Geotherm. Res.* 161, 1-14.

Small- scale basaltic systems and the behavior of the mantle

Ian E M Smith

School of Environment, University of Auckland PB 92019 Auckland Mail Center 1142, Auckland, New Zealand. ie.smith@auckland.ac.nz

Keywords: insert, three, keywords.

Small scale basaltic systems form fields of small monogenetic cones at the Earth's surface; they are found in all of the main plate tectonic settings and are the most widespread expression of volcanism on Earth. Monogenetic volcano fields are the low volume extreme of a spectrum of systems encompassing magmatic flux rates ranging from $<.005 \text{ km}^3$ to $\sim 1.0 \text{ km}^3/\text{year}$. Despite their small size they form over time periods comparable to or longer than those of larger systems.

A working paradigm for volcano fields is the eruption of a chemically discrete batch of magma which, within a defined, brief (weeks to decades), period produces a monogenetic cone. The question of how such magma batches are generated lies at the heart of the concept of monogenetic volcanism and of the development of fields of discrete volcanic cones.

Monogenetic volcano fields require melting conditions in the upper mantle on a very small scale that in some cases last for millions of years. Decompression melting of a rising mantle source satisfies many of the temporal and spatial aspects of these magmatic systems. This is an essentially passive model that contrasts with the dynamism of a mantle plume model. However, in detail it does not explain the surprising range of chemical compositions or the patterns in time and space exhibited by monogenetic volcano fields.

The volumes of individual magma batches are typically small, $<1 \text{ km}^3$ and commonly $<<0.1 \text{ km}^3$. With magma rise driven by density contrasts smaller volumes would be expected to stall within the crust and in fact this may be a limiting factor to the size of basaltic monogenetic volcanoes.

The chemical compositions of basaltic monogenetic volcanoes are the result of small-scale partial melting (+ 0.5%) of upper mantle sources and reflect the history of their mantle source, melting processes and to varying degrees the environments that rising magmas experience on their way to the Earth's surface. Their observed range of compositions reflects the petrographic heterogeneity of mantle sources and a range of melting proportions. Because these magmas rise rapidly from their sources their chemical compositions provide a window into the way the mantle behaves during melting events.

The following discussion of these ideas is based on recent work on the nature and origin of small-scale magmatism of the Auckland Volcanic Field in northern New Zealand (McGee et al., 2013 and references therein). The Auckland Volcanic Field is young ($< \sim 200 \text{ ka}$) and so rocks are fresh, because of its urban setting (Auckland City) detailed sampling is possible in artificial exposures (construction sites, road cuttings) and in drill cores as well as from natural exposures and because of the potential for future eruptive activity to cause hazards to Auckland City it has been intensively studied in recent times.

In spite of its small total volume ($<4 \text{ km}^3 \text{ DRE}$) Auckland's volcanoes show a surprising overall compositional range from nephelinite to tholeiite. Each individual volcano represents the eruption of a discrete batch of magma within this range or less commonly more than one compositionally and temporally distinct magma batch. Within the broad compositional spectrum there are well defined trends and correlations which provide clues to the origin of the magmatic system that gave rise to them. A fundamental observation is that there is a correlation between composition and volume; small volume volcanoes are lower in silica and have higher incompatible element content whereas larger volume volcanoes trend toward higher silica, lower incompatible element abundances and tholeiitic characteristics (McGee et al., 2012). A second characteristic is that there are consistent compositional trends correlated with stratigraphy within individual volcanoes; the initial eruptive products of any particular eruption sequence are more evolved, generally lower in silica and higher in alkalis and other incompatible elements relative to material erupted later in the eruption sequence. A third characteristic of Auckland's volcanoes is that each volcano has a distinctive compositional range within the compositional spectrum of the field as a whole. This supports the notion of individual magma batches arising from discrete events in the source and ascending along unique trajectories and is encapsulated in the concept of monogenetic volcanism.

Compositional variation within individual eruption sequences of the Auckland Volcanic Field is explained by near source fractionation (e.g. Smith et al., 2008), differential melting in their source (e.g. McGee et al 2013) and to mixing of discrete melt fractions during extraction.

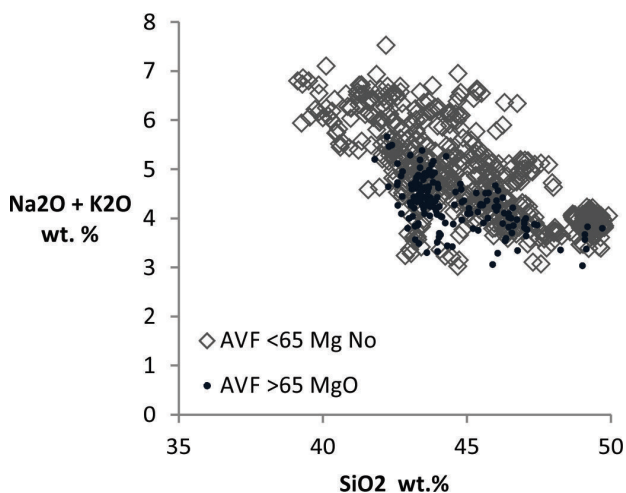


Fig. 1 – Alkali vs silica plot for Auckland Volcanic field samples.

Compositional differences between magma batches (eruptive centers) in the field as a whole arise from different degrees of melting of multicomponent sources together with mixing along trajectories defined by these sources.

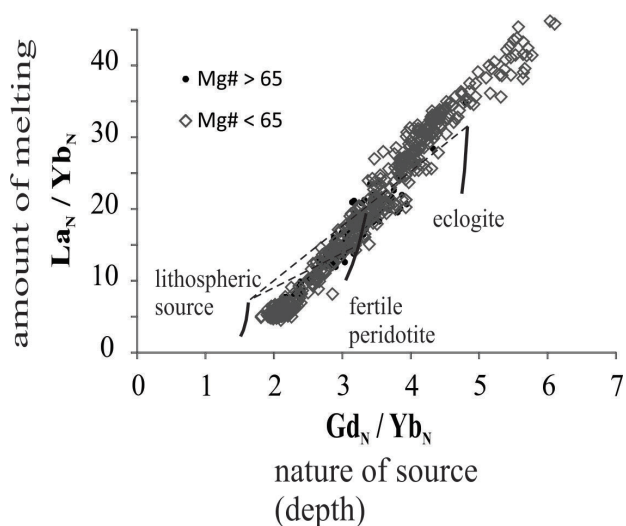


Fig. 2 – Normalised REE ratio plot for the Auckland Volcanic Field samples (after McGee et al. Calculated trajectories of low melting fractions of potential mantle sources are indicated by bold lines. Dotted lines indicate mixing trends.

Melts of differing compositions are formed by different degrees of melting of petrographically distinct sources including fertile peridotite, an enriched eclogitic or more alkalic component and a lithospheric component (Fig.2). These are envisaged to exist within a crystal/liquid mush formed within an upwardly convecting mantle. Such a mush would contain melts of varying composition in distinct domains which at low melt/solid ratios could co-exist for relatively long periods of time. The formation and subsequent generation of a magma batch is a segregation event and its composition is controlled by mixing of different proportions of melts and at various depths. A further factor is created by contrasts in the nature of magma rise. Flow within channels is relatively rapid and can lead to the emergence of relatively simple magma batches that

have been modified by near source side wall fractionation as described by Smith et al 2008. More complex scenarios occur when diffusive upwelling involves a wider range of melt compositions.

A mantle mush capable of yielding a range of compositions can exist in a quasi-stable state for relatively long time periods. Extraction events leading to the rise of a batch of magma may be the result of a tectonic event.

References

McGee, L. E.; Smith, I. E. M.; Millet, M-A., Handley, H. K., Lindsay, J.M. 2013. Asthenospheric Control of Melting Processes in a Monogenetic Basaltic System: a Case Study of the Auckland Volcanic Field, New Zealand. *Journal of Petrology* 54, 2125-2153

McGee, L. E., Millet, M. -A., Smith, I. E. M., Lindsay, J. M., Németh, K. 2012. The inception and progression of melting in a monogenetic eruption: Motukorea Volcano, the Auckland Volcanic Field, New Zealand. *Lithos*.

Smith, I.E.M. Blake, S., Wilson, C.J.N., Houghton B.F., 2008. Compositional zoning in a small volume monogenetic basaltic volcano in the Auckland volcanic field, New Zealand. *Contributions to Mineralogy and Petrology*, 155, 511-527.

Tolbachik group of volcanoes (Kamchatka): the areal type of volcanic activity

Anna Volynets¹, Yulia Kugaenko²

¹ Institute of volcanology and seismology FEB RAS, Petropavlovsk-Kamchatsky 683006, Russia. a.volynets@gmail.com

² Geophysical Survey of Russian Academy of Sciences, Kamchatka Branch, Petropavlovsk-Kamchatsky 683006, Russia

Keywords: magma plumbing system, monogenetic volcanic field, Tolbachik

Tolbachinsky Dol (TD) is a large (length ~70 km, area 875 km²) monogenetic volcanic field (MVF) situated in the Central Kamchatka Depression in Kamchatka. Kamchatka subduction system is located at the north-western part of the Pacific at the convergent boundary of the Okhotsk and Pacific plates. Quaternary volcanism in Kamchatka occurs in three zones, parallel to the trench: Eastern Volcanic Front, graben-like Central Kamchatka Depression (CKD) and Sredinny Range in the back-arc. According to Kozhurin and Zelenin (2017), CKD is extending with a rate of 17 ± 3 mm/yr over mid-late Quaternary time. TD adjoins two stratovolcanoes (Ostry and Plosky Tolbachik) and consists of two flanks, located at the SSW and NE slopes of Plosky Tolbachik edifice. Cinder cones, formed here during the last 10 Ka, are located along the SW-NE fissure and tend to cluster: 80% of the cones are concentrated in the narrow band 3-4 km wide (Churikova et al., 2015b). Tolbachinsky Dol is composed by the lavas of contrast composition: (1) high-Mg, medium-K basalts, (2) high-Al, high-K basalts and basaltic andesites, (3) the transitional varieties (intermediate and K-rich high-Mg basalts), and (4) trachybasaltic andesites with high titanium and alkali content, appeared at the surface during the last eruption in 2012-13 (Churikova et al., 2015a, b; Volynets et al., 2015). TD crosses a stratovolcano (Plosky Tolbachik) with the similar (high-Mg and high-Al) composition of its products (Churikova et al., 2015a). It was formed at the beginning of Holocene and to the time of fissure eruptions of 1975 and 2012 already lost its activity (Flerov et al., 2015). Due to the two big eruptions happened here during the last 50 years (Great Fissure Tolbachik Eruption in 1975-76 and Tolbachik fissure eruption in 2012-2013) this area is very well studied by a variety of methods; it is probably one of the best-studied MVFs in the world and thus it may serve as an etalon object for testing various hypotheses on the mechanisms and reasons of a contemporary volcanic activity and relationships of monogenetic and polygenetic volcanism.

According to the results of numerous studies, Tolbachik MVF has several distinctive features, which are not typical for individual monogenetic edifices or polygenetic volcanoes, but are in a good agreement with the new classification suggested by Nemeth and Keresturi (2015), which implies separation of MVFs from monogenetic type of activity *sensu stricto*. (1) Eruptive centers in TD are concentrated along the elongated zone of the deep fault (rift); monogenetic edifices tend to cluster. (2) Petrological investigations show polymagmatic origin of individual eruptive centers (expressed as eruptions of

the magmas with contrast composition and/or multiple sources involved in magma generation). High-Mg basalts are produced by fractionation of the primary mantle melts; high-K high-Al basalts and trachybasaltic andesites of 2012-2013 eruption are the result of the long-term evolution of this magmatic system, with fractionation of Mg basaltic magmas *in situ*, while basalts with intermediate composition are produced by mixing between high-Al and high-Mg magmas (Portnyagin et al., 2015). (3) Eruptive centers of different composition are unevenly distributed within the MVF both in space and time. (4) Tolbachik MVF is superimposed to Plosky Tolbachik stratovolcano. Most likely, at the end of Holocene Plosky Tolbachik already serves as one of the eruptive centers of this MVF. Geophysical data confirm its subordinate role with respect to the superimposed MVF. (5) New instrumental seismic data allow us to complement and detail the model of Tolbachinsky Dol magma plumbing system, on a base of quantitative estimates. The results of the microseismic sounding (2010-2015, Kugaenko et al., 2013) and detailed seismic tomography experiment (2014-2015, Koulakov et al., 2017) revealed parametric anomalies which can be interpreted as elements of the magma plumbing system (Fig. 1). Tolbachik MVF has a complicated magma plumbing system, which can be visualized as a superposition of subvertical and sublateral magma conduits. Our research reveals a system of independent magma conduits and magmatic reservoirs. Finally, there are no pronounced subvertical channels above the crystalline basement level. This conclusion contradicts the existing ideas of simple subvertical magma supplying channels, feeding the monogenetic centers. Petrological data confirm the existence of the complicated magmatic system with mantle feeding and open fractionation in the crustal reservoirs.

Therefore, characteristics of Tolbachik monogenetic volcanic field strongly support the separation of MVFs from monogenetic and polygenetic volcanoes in the classification suggested by Nemeth and Keresturi (2015). In Russian (mainly, but not exclusively) literature there is a special term for this type of volcanic activity – “areal volcanism”. Taking into account all the facts stated above, which come into conflict with the definition of the monogenetic volcanism *sensu stricto*, we believe it might be prudent to accept term “areal volcanism” or “areal volcanic fields” (AVF instead of MVF) as defining this special type of volcanic activity, because it allows eliminating confusion caused by genetic meaning of the used terms.

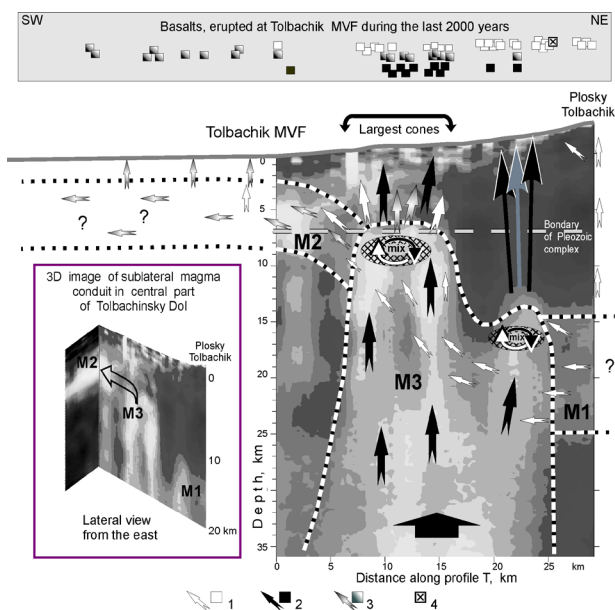


Fig. 1 – The conceptual scheme of magma plumbing of Tolbachik monogenetic field on a base of vertical cross section along the microseismic profile. Arrows indicate possible pathways for basaltic magmas of different composition according to the model of magma fractionation and mixing (Portnyagin et al., 2015). The scheme provides possible explanation for the uneven spatial distribution of the basalts of different composition in TD. Legend: 1-3 – basalts: 1 - High-Al, 2 – High-Mg, 3 – intermediate; 4 – trachybasaltic andesites. M1, M2, M3 – elements of magma plumbing system under central part of Tolbachik MVF according to MSM results (Kugaenko et al., 2013): M1 – sublateral magma conduit at 15-25 km depth, going under Plosky Tolbachik; M2 – sublateral magma conduit at 4-8 km depth, going along the rift from the central to the southern part of TD; M3 – trans-crustal area of magma conductivity (dyke complex) under the central part of TD, under the chain of the highest cinder cones.

Acknowledgements

The work is supported by IVS FEB RAS, Kamchatka Branch of GS RAS and RFBR grant #18-05-00271.

References

- Churikova, T.G., Gordeychik, B.N., Iwamori, H., et al. 2015a. Petrological and geochemical evolution of the Tolbachik volcanic massif, Kamchatka, Russia. *Journal of Volcanology and Geothermal Research* 307: 156–181.
- Churikova, T. G., Gordeychik, B. N., Edwards, B. R., et al. 2015b. The Tolbachik volcanic massif: A review of the petrology, volcanology and eruption history prior to the 2012–2013 eruption. *Journal of Volcanology and Geothermal Research* 307: 3–21.
- Flerov, G.B., Anan'ev, V.V., Ponomarev, G.P. 2015. The petrogenesis of rocks of the Ostriy and Ploskii volcanoes and the relationship between volcanic occurrences of basaltic and trachybasaltic magmas in the Tolbachik Dol area, Kamchatka. *Journal of Volcanology and Seismology* 9 (3): 162–181.
- Koulakov, I., Abkadyrov, I., Arifi, N., et al. 2017. Three different types of plumbing systems beneath the neighboring active volcanoes of Tolbachik, Bezymianny and Klyuchevskoy in Kamchatka. *Journal of Geophysical Research. Solid Earth*, 122 (5): 3852–3874.
- Kozhurin, A., Zelenin, E. 2017. An extending island arc: The case of Kamchatka. *Tectonophysics* 706-707: 91–102.
- Kugaenko, Yu.A., Saltykov, V.A., Gorbatikov, A.V., Stepanova, M.Yu. 2013. Deep structure of the North Vent area, Great Tolbachik Fissure Eruption of 1975–1976, Kamchatka: Evidence from low-frequency microseismic sounding. *Journal of Volcanology and Seismology* 7(5): 313–327.
- Nemeth, K., Kereszturi, G. 2015. Monogenetic volcanism: personal views and discussion. *International Journal of Earth Sciences*, 104: 2131–2146.
- Portnyagin M., Duggen S., Hauff F., et al. 2015. Geochemistry of the Late Holocene rocks from the Tolbachik volcanic field, Kamchatka: towards quantitative modeling of subduction-related open magmatic systems. *Journal of Volcanology and Geothermal Research* 307: 133–155.
- Volynets, A., Edwards, B., Melnikov, B., et al. 2015. Monitoring of the volcanic rock compositions during the 2012–2013 fissure eruption at Tolbachik Volcano, Kamchatka. *Journal of Volcanology and Geothermal Research* 307: 120–133.

Monogenetic volcanoes in the northernmost volcanic arc of the Colombian Andes

Hugo Murcia^{1,2}, Carlos Borrero² and Károly Németh³

¹ Geological Sciences Department, Universidad de Caldas, Manizales, Colombia. hugofmurcia@gmail.com

² Instituto de Investigaciones en Estratigrafía (IIES), Universidad de Caldas, Manizales, Colombia.

³ Institute of Agriculture and Environment, Massey University, Palmerston North, New Zealand.

Keywords: subduction volcanoes, calc-alkaline magmatism, monogenetic volcanic fields

Monogenetic volcanoes are commonly related to rifts and/or intraplate tectonic settings. However, they are also less commonly associated with subduction zones, including both front and back-arc volcanoes. To nourish this tectonic location, we show here that monogenetic volcanoes also appear at the northernmost part of the Andes Northern Volcanic Zone (NVZ) (2° S to $4^{\circ}30'$ N), and that they are associated with the main axis of the Quaternary active polygenetic volcanic chain. Presently, three monogenetic volcanic fields, with a typical calc-alkaline signature, have been identified on both sides of the San Diego – Cerro Machín Volcano Tectonic Province (~140 km long; SCVTP). From south to north, they are:

1) Pijaos Monogenetic Volcanic Field (PMVF) located ~25 km south of Cerro Machín volcano, the southernmost active volcano of the SCVTP. This field is evidenced by the occurrence of at least two eruptions with both effusive and explosive styles. Three cones and a maar are recognised. The volcanoes are basaltic and basaltic andesitic in composition, having the most mafic expression (MgO: 10-11 wt.%) in the whole SCVTP (cf. Galindo, 2012). Its source is related to the same, but less evolved magma that feeds the volcanoes in the SCVTP. Stratigraphic relationships show that the volcanoes are younger than the underlying alluvial and volcaniclastic Ibagué fan (<2.58 Ma). In addition, due to the well-preserved maar structure, this field it is not discarded as an active monogenetic field.

2) Villamaría – Tarmales Monogenetic Volcanic Field (VTMVF) located to the northwestern part (>5 km) of the SCVTP (Botero et al., 2017; Osorio et al., 2017). This field is made up of at least 14 volcanoes aligned with the active Villamaría – Tarmales fault system. The volcanism has been mainly effusive, represented by lava domes and some lava flows. The volcanoes are andesitic to dacitic in composition. It is inferred that the magmatic source is a shallow (20-30 km) magma reservoir underneath the SCVTP. Based on stratigraphic and field relationships, it is assumed that the last eruption occurred <38 ka (Botero et al., 2017).

3) Samaná Monogenetic Volcanic Field (SMVF) located ~50 km north of Romeral volcano (composite volcano), the northernmost active volcano from the SCVTP (cf. Borrero et al., 2017; Sánchez-Torres et al., 2017). This field comprises at least three volcanoes: A maar (~20 ka years old), a pyroclastic cone (~33 ka), and an older undefined

structure, which was destroyed by the ~33 ka eruption. The volcanic products exhibit dacitic composition. It is inferred that this field is fed from the same reservoir that feeds the magma chambers of the polygenetic volcanoes in the SCVTP.

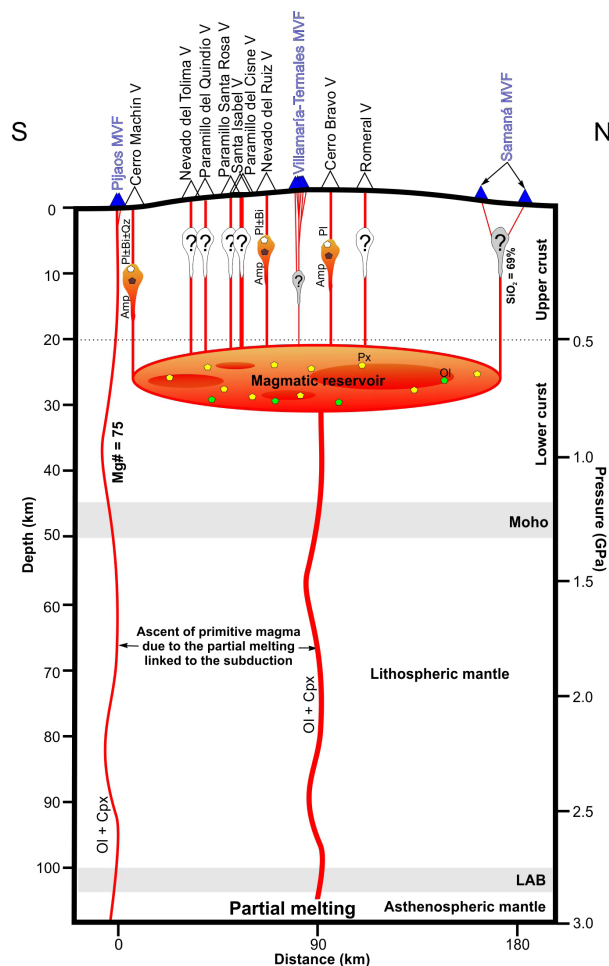


Fig. 1. Proposed magmatic plumbing system of the San Diego – Cerro Machín Volcano Tectonic Province (SCVTP; cf. Martínez et al., 2014). Cerro Machín magma chamber from Laeger et al. (2013); Nevado del Ruiz magma chamber from Londoño (2017); Cerro Bravo magma chamber from Pinzón et al. (2017); Magmatic reservoir from Londoño (2016); Lithosphere-Asthenosphere Boundary (LAB) from Blanco et al. (2017); Moho location from Idarraga-García et al. (2016). Mg# in PMVF from Galindo (2012). SiO₂ value in SMVF from Borrero et al. (2017).

Overall, it is evidenced here that monogenetic volcanoes are not atypical in the area. We thus envision an integrated SCVTP magmatic plumbing system feeding both the monogenetic and polygenetic volcanoes related to the subduction arc (Fig. 1). Finally, we open a discussion about the ambiguity related to the minimum number of “necessary” volcanoes for a proper definition of a volcanic field; even further, when it comes to fields closely integrated to polygenetic volcanism, as represented in the Fig. 1.

References

Blanco, J. F., Vargas, C. A., & Monsalve, G. (2017). Lithospheric thickness estimation beneath Northwestern South America from an S-wave receiver function analysis. *Geochemistry, Geophysics, Geosystems*, 18(4), 1376-1387.

Borrero, C., Murcia, H., Agustín-Flores, J., Arboleda, M. T., & Giraldo, A. M. (2017). Pyroclastic deposits of San Diego maar, central Colombia: an example of a silicic magma-related monogenetic eruption in a hard substrate. In: K. Németh, G. Carrasco-Núñez, J.J. Aranda-Gómez, I.E.M. Smith (Eds.) *Monogenetic volcanism*. Geological Society, London, Special Publications, 446(1), 361-374.

Botero, L., Osorio, P., Murcia, H. & Borrero, C. (2017). Análisis morfométrico y espacio-temporal de las estructuras que conforman el Campo Volcánico Monogenético Villamaría-Termale, Cordillera Central de Colombia. XVI Colombian Geological Congress. August 28 – September 01. Santa Marta, Colombia.

Galindo, D. A. (2012). Caracterización y modelo genético del Volcán Guacharacos. Bachelor thesis. Geology Program. Universidad de Caldas, Colombia. 63 p.

Idárraga - García, J., Kendall, J. M., & Vargas, C. A. (2016). Shear wave anisotropy in northwestern South America and its link to the Caribbean and Nazca subduction geodynamics. *Geochemistry, Geophysics, Geosystems*, 17(9), 3655-3673.

Laeger, K., Halama, R., Hansteen, T., Savov, I. P., Murcia, H. F., Cortés, G. P., & Garbe-Schönberg, D. (2013). Crystallization conditions and petrogenesis of the lava dome from the ~900 years BP eruption of Cerro Machín Volcano, Colombia. *Journal of South American Earth Sciences*, 48, 193-208.

Londoño, J. M. (2016). Evidence of recent deep magmatic activity at Cerro Bravo-Cerro Machín volcanic complex, central Colombia. Implications for future volcanic activity at Nevado del Ruiz, Cerro Machín and other volcanoes. *Journal of Volcanology and Geothermal Research*, 324, 156-168.

Londoño, J.M. (2017). Modelo conceptual del sistema magmático del volcán Nevado del Ruiz (Colombia) derivado de la reciente actividad eruptiva, 1985-2017. XVI Colombian Geological Congress. August 28 – September 01. Santa Marta, Colombia. Martínez, L., Valencia L., Ceballos, J., Narváez, B., Pulgarín, B., Correa, A., Navarro, S., Murcia, H., Zuluaga, I., Rueda, J. & Pardo, N. (2014). Geología y estratigrafía del Complejo Volcánico Nevado del Ruiz. Informe final, Bogotá – Manizales – Popayán. Servicio Geológico Colombiano. 853p.

Pinzón, C., Echeverri, F., Murcia, H. & Schonwalder, D. (2017). Petrogénesis y condiciones de cristalización del domo que

representa la última fase de la erupción más del volcán Cerro Bravo, Colombia. XVI Colombian Geological Congress. August 28 – September 01. Santa Marta, Colombia.

Osorio, P., Botero, A., Murcia, H., Borrero, C. & Grajales, J. (2017). Campo Volcánico Monogenético Villamaría-Termale: vulcanismo adakítico en el flanco occidental de la Cordillera Central de Colombia. XVI Colombian Geological Congress. August 28 – September 01. Santa Marta, Colombia.

Sánchez-Torres, L., Murcia, H., Borrero, C., Gómez-Arango, J. (2017). Volcán El Escondido (Samaná, Colombia): características composicionales y texturales de sus productos. XVI Colombian Geological Congress. August 28 – September 01. Santa Marta, Colombia.



Quaternary monogenetic volcanism in the Chyulu Hills volcanic field, Kenya: compositional variations in time and space

Elisabeth Widom¹, and Dave Kuentz¹

¹ Department of Geology and Environmental Earth Science, Miami University, Oxford, Ohio 45056, USA. widome@miamiOH.edu

Keywords: Kenya, EARS, geochemistry

The Chyulu Hills Volcanic Field is an active, mafic, monogenetic volcanic field in southern Kenya, situated approximately 100 km east of the Kenya Rift Valley. The volcanic field is interpreted as a manifestation of off-rift volcanism associated with the East African Rift System (EARS) (Spath et al., 2000). The volcanism initiated in the northern part of the volcanic field during the Pleistocene (1.4 Ma), and moved progressively southward through time (Spath et al., 2000). The more recent eruptions in the Holocene have occurred in the southern part of the volcanic field, some during historic times, including the Umani eruption in 1470 ± 200 AD, and the Chaitani and Chainu eruptions both in 1855 ± 5 AD (Smithsonian Institution, 2017).

The temporal and spatial migration of volcanism in the volcanic field has been well documented, as has the associated change in magma composition. The eruptive products become progressively more silica-saturated with time, ranging from highly silica under-saturated magmas (e.g. nephelinites and basanites) through alkali basalts and hawaiites, with the youngest volcanism characterized by silica-rich orthopyroxene-normative subalkaline basalts (Spath et al., 2000). The variations in magma composition with time are consistent with a progressive increase in degree of melting, and associated decrease in depth of melting, from north to south (Spath et al., 2000). Negative K anomalies, incompatible trace element enrichments, and enriched Sr-Nd-Pb isotope signatures have been interpreted to reflect partial melting of metasomatized mantle with residual amphibole, suggesting that melting occurs in the sub-continental lithospheric mantle (SCLM) (Spath et al., 2001). In support of the interpretations based on geochemistry, seismic data likewise indicate the possible presence of a partially molten zone in the SCLM beneath this region (Ritter and Casper, 1997).

We have analyzed a suite of eight Chyulu Hills samples representing the Pleistocene through the most recent Holocene volcanism, for major and trace elements and Sr, Nd, Hf, Os and high precision Pb isotopes, in order to further constrain the nature of the mantle sources and the petrogenetic processes leading to the observed geochemical variations in time and space. Our data demonstrate that all of the magmas are relatively primitive, all with Ni >200 ppm and most with Cr >500 ppm. As silica increases, incompatible trace element abundances and La/Nb ratios decrease, consistent with a decrease in degree of melting with time. Multi-element patterns show that all of the magmas are OIB-like in character, although signatures change from HIMU- to EMI-like with

time. The latter exhibit constant Rb, Ba and K concentrations despite variable concentrations of other highly incompatible elements, potentially reflecting partial melting of a hydrous metasomatized SCLM source with residual amphibole and phlogopite. Decreasing Ce/Pb and Nd-Hf-Pb isotope ratios, and increasing Sr isotope ratios, with increasing SiO₂ suggest melting of heterogeneous mantle sources with a temporal progression from a deeper, possibly sub-lithospheric, HIMU source to a shallower EM-type source residing in the SCLM. Os isotope systematics are all more radiogenic than primitive upper mantle; most fall within the range of OIB, although others are more radiogenic and similar to those of some highly metasomatized mantle xenoliths associated with the Tanzanian craton [4]. These data are consistent with magmatism in the Chyulu Hills volcanic field being generated by mixing between sublithospheric and metasomatized SCLM-derived melts, as has been proposed here and in other regions of the EARS (Spath et al., 2001; Nelson et al., 2012).

Acknowledgements

Thanks to John Morton for assistance with major and trace element analyses, to Kim Medley and John Maingi for introducing us to the Chyulu Hills and for supporting field work from NSF grant #1061407 awarded to KM and JM. Support for analytical work was provided by the Janet and Elliot Baines Professorship awarded to EW.

References

- Nelson, W.R., Furman, T., van Keken, P.E., Shirey, S.B., Hannan, B.B., 2012. Os-Hf isotopic insight into mantle plume dynamics beneath the East African Rift System. *Chemical Geology* 320-321: 66-79.
- Ritter, J.R.R., Kasper, T., 1997. A tomography study of the Chyulu Hills, Kenya. *Tectonophysics* 278: 1498-169.
- Smithsonian Institution 2017. National Museum of Natural History, Global Volcanism Program, volcano.si.edu/volcano.cfm?vn=222130.
- Spath, A., Le Roex, A.P., Opiyo-Akech, N., 2000. The petrology of the Chyulu Hills Volcanic Province, southern Kenya. *Journal of African Earth Science* 31: 337-358.
- Spath, A., Le Roex, A.P., Opiyo-Akech, N., 2001. Plume-lithosphere interaction and the origin of continental rift-related alkaline volcanism – the Chyulu Hills volcanic province, southern Kenya. *Journal of Petrology* 42: 765-787.

Melt compositions relationships between large polygenetic and adjacent monogenetic edifices: results of melt inclusions study in minerals of two large volcanic centers (Kamchatka)

Maria Tolstykh¹, Anna Volynets², Maria Pevzner³

¹ Vernadsky Institute of geochemistry and analytical chemistry RAS, Moscow, Russia, mashtol@mail.ru

² Institute of volcanology and seismology FEB RAS, Petropavlovsk-Kamchatsky, Russia.

³ Geological Institute RAS, Moscow, Russia

Keywords: Shiveluch, Ichinsky, melt inclusion, Kamchatka

One of the actual problems of the nature of monogenetic volcanism is a problem of its genetic relationship to the adjacent large polygenetic volcanoes. A comparison of the melt-forming environments using thermobarogeochemistry may serve as a possible way for the solution of this problem. We studied melt inclusions in minerals of lava and tephra of monogenetic cones and stratovolcanoes of the largest volcanic centers in Kamchatka – Shiveluch and Ichinsky volcanoes.

Shiveluch is located at the north-eastern part of Kamchatka at the triple junction between Kurile-Kamchatka and Aleutian island arcs. It is the biggest active andesitic volcanic center in Kamchatka. Its products are represented mainly by Mg Pl-Amf middle-K andesites ($\text{SiO}_2 \geq 55\%$). At the same time, in some Holocene soil-pyroclastic covers at the foot of this volcano a basic tephra horizons was identified, deposited during 4600-3100 years BP interval (Volynets et al., 1997; Ponomareva et al., 2007, 2015, Pevzner, Babansky, 2011). Judging by its deposition area and size distribution of basic ash and lapilli particles it was supposed that this tephra is a result of several eruptions of the hidden monogenetic center located in the SW part of Shiveluch massif. The composition of this tephra corresponds to high-Mg high-K Ol-Pl-Px basalt (SiO_2 51%), with small amounts of phlogopite.

Ichinsky volcanic massif is located in Sredinny Range of Kamchatka – the largest volcanic structure of the peninsula, composed by Cretaceous-Paleogene metamorphic massif and N-Q volcanic belt; Quaternary period of its evolution is described as post-subduction geodynamic environment. Ichinsky is the largest volcano in Sredinny Range. It is a complex polygenetic volcano of Somma-Vesuvius type. Holocene deposits of the volcano are represented mainly by tephra, sometimes by andesite-dacitic middle-K lava flows. It is surrounded by a large monogenetic volcanic field, which produced in Holocene at least one voluminous eruption, called Southern Cherpouk; lavas of this center (Ol-Pl basaltic) formed spatial lava field and are dated 6500 years BP (Pevzner, 2004, Volynets et al., this meeting).

We studied melt inclusions in different minerals of the rocks with contrast composition:

- 1) In Px and Pl of basic lapilli, 4600 years BP (Shiveluch massif)
- 2) In different minerals of andesitic tephra younger than 4000 years BP (Shiveluch)
- 3) In Ol of the initial and final stages of the monogenetic eruption at Ichinsky massif (South Cherpouk, 6500 years BP)
- 4) In different minerals of dacitic tephra of the summit crater of Ichinsky volcano (6500 and 4200 years BP)

Melt inclusions were studied according to (Sobolev, 1996) method. A large dataset on melt inclusions compositions of Shiveluch center is presented in (Tolstykh et al., 2015). Melts of monogenetic and polygenetic edifices have very different composition both in Ichinsky and Shiveluch massifs (both in SiO_2 and femic components, fig. 1, 2). Concentrations of major elements in Ichinsky massif melts form continuous trends which may be interpreted in terms of fractionation, while Shiveluch melts demonstrate clear genetic difference of the sources of melts (fig. 1d).

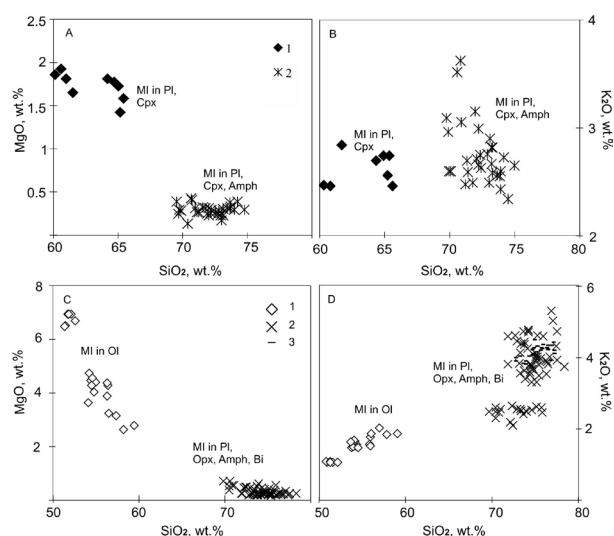


Fig. 1 – Harker diagrams for Shiveluch massif melts (a, b) and Ichinsky massif melts (c, d). Legend: 1 – melts of monogenetic centers; 2, 3 – melts of later and/or sub-synchronous eruptions of the polygenetic central volcano.

Trace elements distribution diagrams show melts characteristics even more clear (fig. 2). Basic melts in both cases are enriched by MREE and HREE. Monogenetic centers of Ichinsky massif are characterized by relative depletion by incoherent elements, while Shiveluch basalts have rather high LIL and fluid-mobile element concentrations. Such spectra can't be described in terms of fractional crystallization, which would be expressed by sub-parallel position of spidergrams with gradual enrichment from basic to acid varieties (as, for ex., is shown for Gorely volcano in (Tolstykh, 2012)). Genetic relationship between these melts is not reproducible using Petrolog or MELTs software.

Conclusions:

Monogenetic centers in Ichinsky and Shiveluch massifs serve as conduits for primitive mantle melts, whose characteristics reflect the composition of the primary mantle source.

Large magma chambers of Ichinsky and Shiveluch volcanoes are not produced by fractionation of the above mentioned primary mantle melts. There is no direct evidence of the participation of these basic primitive melts in magmatic mixing, which produces volcanic rocks of the polygenetic volcanic centers of Ichinsky and Shiveluch.

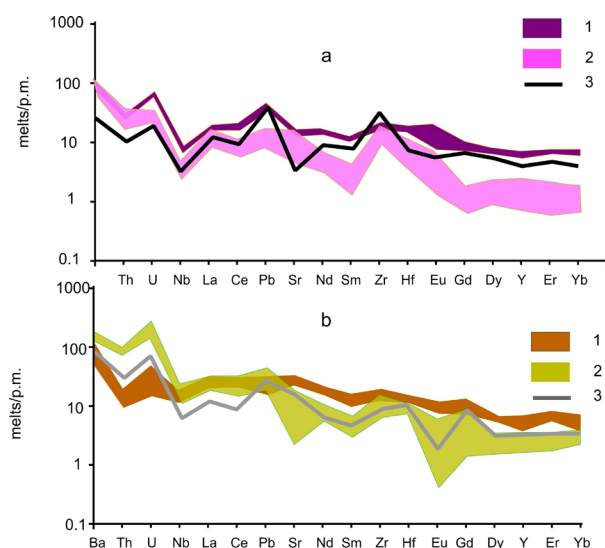


Fig. 2 – Primitive mantle-normalized diagrams of trace element distribution in volcanic rocks of Shiveluch (a) and Ichinsky massifs (b). Legend: 1 – melts of monogenetic centers; 2, 3 – melts of the polygenetic volcanoes. Composition of primitive mantle after Sun and McDonough (1989).

Acknowledgements

Financial support by RFBR grant # 17-05-00112.

References

- Pevzner M.M. The first geological data on the chronology of Holocene eruptive activity in the Ichinskii Volcano; Sredinnyi Ridge, Kamchatka. 2004. Doklady Earth Sciences 395: 335-337.
- Pevzner M.M., Babansky A.D. Episode 4600-3100 14C of basaltic activity in andezitic Shiveluch Volcano, Kamchatka. 2011. 7 th Biennial Workshop on Japan-Kamchatka-Alaska Subduction Processes: Mitigating Risk Through International Volcano, Earthquake, and Tsunami Scien: 262-263.
- Ponomareva, V., Portnyagin, M., Pevzner, M., Blaauw, M., Kyle, P., and Derkachev, A. Tephra from andesitic Shiveluch volcano, Kamchatka, NW Pacific: chronology of explosive eruptions and geochemical fingerprinting of volcanic glass. 2015. International Journal of Earth Sciences 104: 1459-1482.
- Sobolev A.V., 1996. Melt inclusions in minerals as a source of principle petrological information. Petrology 4: 209-220.
- Sun S.S., McDonough W.F. 1989. Chemical and isotopic systematics of oceanic basalts; implications for mantle composition and processes // Saunders, A.D., Norry, M.J. (eds) Magmatism in the ocean basins. Geological Society Special Publications 42: 313-345.
- Tolstykh M.L., Naumov V.B., Kononkova N.N., Gavrilenko M.G., Ozerov A.Y., 2012. Chemical composition, volatile components, and trace elements in the melts of the Gorely volcanic center, Southern Kamchatka: evidence from inclusions in minerals. Geochemistry International 50: 522-550.
- Tolstykh M.L., Naumov V.B., Kononkova N.N., Pevzner M.M., Babanskiy A.D., 2015. Types of parental melts of pyroclastic rocks of various structural-age complexes of the Shiveluch volcanic massif, Kamchatka: evidence from inclusions in minerals. Petrology 23: 480-517.
- Volynets A.O., Pevzner M.M., Tolstykh M.L., 2018. Triplex eruption at Ichinsky volcano (Kamchatka) 6500 14C years BP: a shift from monogenetic to polygenetic type of activity. 7th International Maar Conference.
- Volynets O.N., Ponomareva V.V., Babansky A.D., 1997. Magnesian basalts in Shiveluch andesitic volcano. Petrology 5: 206-211 (in Russian).

Implication of 2 Myr of volcanism at Kīlauea Pt., Kauaʻi for the Origin of Hawaiian Rejuvenated Volcanism

Michael O. Garcia¹, Thor Thordarson²

¹ Dept. of Geology-Geophysics, University of Hawaii, Honolulu, HI 96822, USA. mogarcia@hawaii.edu

² Faculty of Earth Sciences, University of Iceland, 101 Reykjavík, Iceland, torvth@hi.is

Keywords: Hawaii, monogenetic, rejuvenation

Rejuvenated stage, alkalic volcanism on Kauaʻi Island, the second oldest Hawaiian Islands, was long-lived and voluminous compared to other Hawaiian volcanoes (0.1-2.65 Ma; Garcia et al., 2010). The Kauai rejuvenated lavas and tephra rest unconformably on the shield-building tholeiitic lava (3.6-5.1 Ma), and are interbedded with sedimentary rocks. Vents for Kauaʻi rejuvenated volcanism (at least 41) are widely dispersed across the eastern two-thirds of the island. Most vents consist of scoria or lava cones that fed broad lava flow fields blanketing the island's lowlands. The northernmost vents near Kīlauea Point are unusual in including the only phreatomagmatic structure and rheomorphic flow on the island (Fig. 1). The central structure, Crater Hill, is a ~2 km wide tuff cone that is nearly twice the size of Diamond Head tuff cone, the famous Hawaiian landmark and classic example of rejuvenated volcanism. Kīlauea Point is unique among the Hawaiian islands in having experienced two pulses of rejuvenated volcanism ~1 Myr apart at the same location.

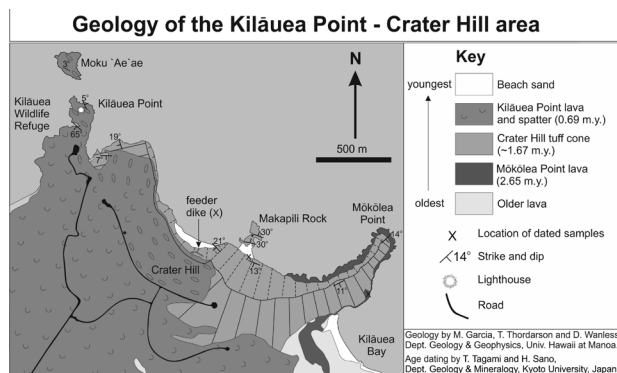


Fig. 1 – Geologic map of the Kīlauea Point area showing its three units of rejuvenated volcanism. Kīlauea Point is well known as a National Bird Refuge.

The Kīlauea Point rejuvenated sequence is superbly exposed along the northeast coast of Kauaʻi (Fig. 2). Tuff cone deposits overlie a basal melilite-phyric nephelinite subaerial lava (Mōkōlea flow) that yielded an unspiked K-Ar age of 2.65 ± 0.35 Ma (Fig. 1). This flow is overlain by the Crater Hill deposits, a ~90 m thick section of bedded phreatomagmatic tephra with decimeter to meters thick layers formed by interaction with seawater. Cross-bedded ash beds alternate with massive and poorly sorted lapilli tuff beds. The cross-bedded deposits were produced by dry and wet surges, whereas the poorly sorted beds repre-

sent fall deposits produced by sustained eruption column (i.e. continuous up-rush) or tephra jets (i.e., rooster-tail explosions). The juvenile clast population consists of olivine-phyric nephelinite. One of these clasts was dated by the K-Ar unspiked method at 1.67 ± 0.11 Ma. Lithic clasts in the tephra are fragments of underlying lava and reef limestone. The tephra sequence is cut by an ~1-m-thick, olivine-bearing basanitoid dike that produced fountain-fed spatter. The spatter welded near the vent forming an up to 100-m-thick rheomorphic lava (Kīlauea Point lava; Fig. 1) that overlies a 2-3 m thick horizon of highly oxidized tuff. The lava flow yielded unspiked K-Ar age of 0.69 ± 0.03 Ma.

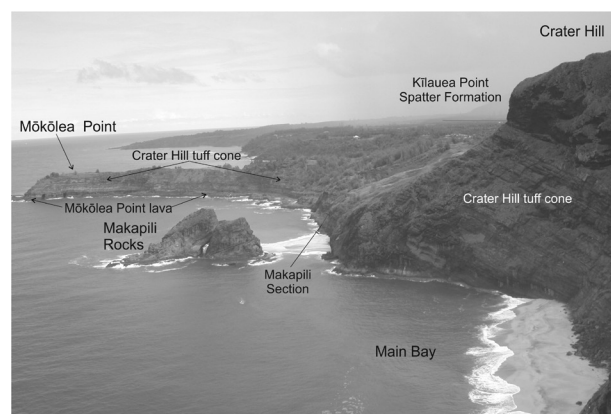


Fig. 2 – Photo looking east along the north coast of Kauaʻi Island showing the three main geologic units; Mōkōlea Point lava, Crater Hill tuff and the Kīlauea Point spatter unit.

The three rejuvenation-stage volcanic deposits at Kīlauea Point indicate that the island oscillated relative to sea level. Overall, the island has subsided several kilometers during and since its formation, probably at the rate of ~2-3 mm/yr (Bianco et al., 2005). The maximum extent of the shield stage shoreline extended at least 3 km offshore from Kīlauea Point during the rapid growth of the island until ~4 Ma. This shoreline is now ~1 km below sea level (Flinders et al., 2010). The Kīlauea Point was above sea level when the basal flow was deposited at ~2.65 Ma. The area sank below sea level before the tuff cone formed at ~1.7 Ma but then rose above sea level by 0.7 Ma with the Kīlauea Point lava was erupted. The island is now sinking due a combination of loading of the lithosphere by the rapid growth of the Kauai shield volcano and global sea level rise. The rising of the island after formation of the tuff

cone is ~1 Myr later than predicted by the passage of Kauai over the flexural arch that surrounds the rapidly forming new Hawaiian volcanoes (Fig. 3). However, the sinking period at does correspond to the increase in rejuvenated stage volcanism on Kauai (Fig. 3). Thus, rejuvenated volcanism may have been affected (perhaps initiated) by the uplift of the lithosphere under Kaua'i as it passed over the Hawaiian Arch (as predicted by some models). However, it was not the primary driving mechanism for the voluminous and prolonged period of rejuvenated stage volcanism on Kaua'i.

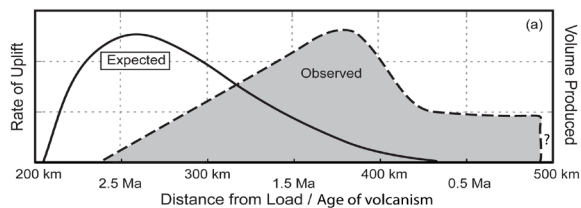


Fig. 3. – Qualitative representation of the temporal variation in predicted rate of flexural uplift (equivalent to magma flux rate) from the loading of the Pacific plate by new Hawaiian shield volcanism (from Bianco et al., 2005). The y-axis indicates relative intensity of predicted melt generation, which is plotted against observed eruption rate (based on 60 radiometric ages). Kaua'i is ~500 km from the load focus near Mauna Loa volcano. The Pacific plate is assumed to have moved NW at a rate of ~100 km/Myr (Garcia et al., 1987). Rejuvenated volcanism began ~0.3 Myr later than expected and continued for ~0.5 Myr longer than predicted (figure after Garcia et al., 2010).

Acknowledgements

The authors thank Taka Tagami and Hiroki Sano for unspiked K-Ar ages, J. M. Rhodes for XRF data and the Kilauea Pt. National Bird Refuge for access to this amazing geologic setting.

References

Bianco, T. Ito, G., Becker, J., Garcia, M.O., 2005. Secondary Hawaiian volcanism formed by flexural arch decompression. *Geochemistry, Geophysics, Geosystems* 6: Q08009, DOI: 10.1029/2005GC000945.

Flinders, A., Ito, I., Garcia, M.O., 2010. Gravity anomalies of the Northern Hawaiian Islands: implications on the shield evolution of Kauai and Niihau. *Journal of Geophysical Research* 115: B08412, DOI: 10.1029/2009JB006877.

Garcia, M.O., Swinnard, L., Weis, D., Greene, A.R., Tagami, T., Sano, H., and Gandy, C.E., 2010. Petrology, geochemistry and geochronology of Kaua'i lavas over 4.5 Ma: Implications for the origin of rejuvenated volcanism and the evolution of the Hawaiian plume. *Journal of Petrology* 51: 1507-1540, DOI: 10.1093/petrology/egq027.

Garcia, M.O., Grooms, D. and Naughton, J., 1987. Petrology and geochronology of volcanic rocks from seamounts along and near the Hawaiian Ridge. *Lithos* 20: 323-336.

Tephra laminae in the alginite succession of Pula maar recording large explosive eruptions of basaltic volcanoes of the Mio/Pliocene Bakony–Balaton Highland Volcanic Field (Hungary)

Ildikó Soós^{1,2}, Szabolcs Harangi^{1,2}, Károly Németh³, and Réka Lukács^{1,2}

¹ Department of Petrology and Geochemistry, Eötvös University H-1117 Budapest, Hungary, ildiko.soos14@gmail.com

² MTA-ELTE Volcanology Research Group, H-1117 Budapest, Pázmány Péter sétány 1/C, Budapest, Hungary.

³ Institute of Agriculture and Environment, Massey University, Palmerston North, New Zealand.

Keywords: volcanic glass shards, maar, tephrostratigraphy

In monogenetic basalt volcanic fields, most studies focus on proximal (edifice-building) deposits, since they are the best preserved products (Hawaiian, Strombolian and phreatomagmatic or effusive) of the volcanic eruptions. Distal ashes of larger eruptions, however, are rarely preserved, particularly in continental areas; therefore, there are much less attention these more violent volcanism, which could affect more severely the surrounding environment and therefore, they have to be considered in hazard and risk assessments. Large Strombolian and even sub-Plinian as well as large phreatomagmatic volcanic eruption could yield high eruption column and ash fall at extensive areas. However, for preservation of such rare, but important volcanic record requires a special depositional environment, such as long-lived lakes (10s+ ka).

There have been numerous volcanological reconstructions in the area of the Bakony-Balaton Highland Volcanic Field (BBHVF), but until now, none of them have taken into consideration the possibility of larger volcanic eruptions that may affected the entire territory of the volcanic field. The closed lacustrine sedimentary succession of the 4.25 Ma Pula maar (Németh et al., 2008) can offer, however, a good opportunity for investigate the potential of ash preservation. In the thick alginite suite, a 35 cm unit with at least 37 tephra laminae can be found. Németh et al. (2008) linked this to a wave-like turbidity current emplacement event in the maar lake, although they did not exclude the possibility that each of the volcanic ash layers could have been related to individual ash fall events. Below, we show arguments that these tephra laminae could be primary volcanic in origin and may record more major volcanic explosions in the BBHVF.

The Pula maar was formed by violent phreatomagmatic eruptions (Németh et al., 2008; Kereszturi et al. 2011) and following the volcanic activity, a closed lake occupied the wide crater, providing a calm deposition environment over at least 320 000 years. During the field observations and high-resolution study of collected hand specimens, 37 tephra laminae were separated, from which 24 were analyzed in detail. The origin of the tephra laminae

found in the alginite layer were investigated based on petrographic observations, geochemical analysis of the glass shards and we compared these results with volcanic glass shard data from other volcanic occurrences (Pula, Szigliget, Szentbékállá, Sitke) of the BBHVF and the nearby volcanic fields. We performed quantitative component analyses for each tephra lamina quantifying the different glass types and the ratio between the glass shards, solitary crystals and lithic clasts.



Fig. 1 – Tephra lamina-bearing unit within the alginite succession of the Pula maar. This section shows the upper part of the unit with both plane-parallel laminae overlain by deformed, convolute tephra beds.

Most of the tephra laminae show parallel deposition; their basal contacts are generally sharp while the upper ones are often diffuse. In many cases, poor normal gradation can be observed. Their thickness varies from a few tenths of a millimeter to 15–20 millimeters. In the lower and upper part of this tephra sedimentation unit, the tephra laminae are deformed, with a convolute appearance. This is interpreted as water escape channels. The glass shards found in tephra laminae are fresh, therefore suitable for determining the original geochemical composition. Preliminary measurements (Soós et al., 2014) supplemented with additional data confirm the presence of at least

three main geochemical groups (a trachybasalt and two phonotephrites). These geochemically different groups appear distinctly from each other in the tephra laminae. Above the basal deformed tephra units, undisturbed, parallel tephra laminae are composed of phonotephritic glass shards with low SiO₂ and high P₂O₅ and Al₂O₃ content. It is followed by trachybasaltic tephra laminae, overlain by a unit of tephra laminae with phonotephritic glass shards. This typically has higher SiO₂ and lower Al₂O₃ content than the lower phonotephrite unit. In the top, most tephra laminae contain glass shards with trachybasalt composition.

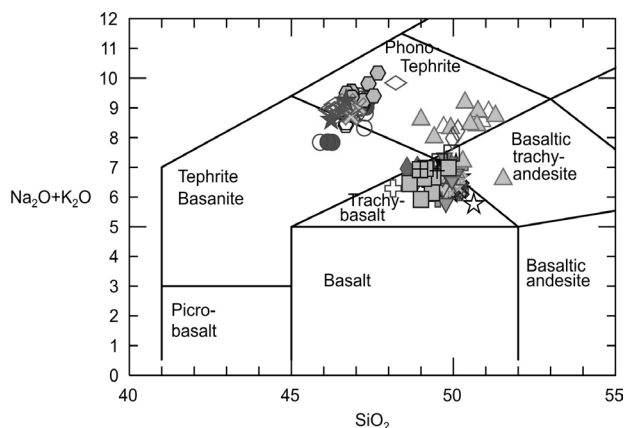


Fig. 2 – Compositional feature of the glass shards in the tephra laminae.

The glass shard composition in the primary volcanic layer of the Pula maar is similar to that of the lower phonotephritic group, however, a substantial difference is that glass shards from these tephra laminae do not contain olivine phenocrysts.

The quantitative componentry analysis is based on the textural diversity of the glass shards, on their vesicularity and their crystal content following the classification scheme of Liu et al. (2015). There are considerable differences between the tephra layers, however, the distinct characters follow the groups identified by major element composition of the glass shards. Glass shards are typically vesicular, in the fresh sideromelane glass there are plagioclase and clinopyroxene microlites. In the basal unit, quartz xenocrysts are typically found in glass shards. Here in some places the glass shards have a very thin wall (1-5 µm), with a fibrous, reticulate-like appearance, which differ from the glass shards found in other layers, where they tend to be blocky with less vesicles. In addition to the glass shards, quartz and muscovite (> 90% by weight) crystals can be found in the laminae, alone with much less (<10%) calcite and dolomite, sometimes clinopyroxenes and plagioclases. The textural types of glass shards suggest a poorly vesiculating magma, whereas the large number of quartz and muscovite crystals and the sideromelane glass shards suggest a phreatomagmatic fragmentation.

Based on the coherent and distinct glass chemical compositions and textural features, we suggest that the

tephra laminae could be primary in origin, i.e. they are distal accumulative deposits from remote large Strombolian (sub-Plinian?) and phreatomagmatic explosive volcanic eruptions. This is supported also by the lack of olivine phenocrysts, which could reflect transportation in ash cloud and density fractionation and deposition. If the glass shards originated from the Pula maar sequence, we would expect a heterogeneous and olivine-containing glass shard cargo in the studied tephra unit.

In summary, we infer that in a relatively short period of time, repetitive large explosive volcanic eruptions could have occurred in different basaltic volcanoes of the BBH-VF. Volcanic ash deposits disturbed the alginite sediment accumulation and formed tephra laminae in the maar lake. Based on the distinct geochemical composition change, explosive eruptions of at least 3 mafic magmas can be identified that might be related to three volcanoes. Based on the present knowledge on the glass composition of the BBHVF volcanoes, neither of the erupted volcanoes can be recognized, although such events could be readily missing in proximal deposits. However, these rare distal tephra layers could still document such events, which could largely affect the environment.

References

- Kereszturi, G., Németh, K., Csillag, G., Balogh, K., Kovács, J., 2011. The role of external environmental factors in changing eruption styles of monogenetic volcanoes in a Mio/Pleistocene continental volcanic field in western Hungary. *Journal of Volcanology and Geothermal Research* 201: 227-240.
- Liu, E.J., Oliva, M., Antoniadis, D., Giralt, S., Granados, I., Pla-Ribes, S., Toro, M., Geyer, A., 2015. Expanding the tephrostratigraphical framework for the South Shetland Islands, Antarctica, by combining compositional and textural tephra characterization. *Sedimentary Geology* 340: 49-61.
- Németh, K., Goth, K., Martin, U., Csillag, G., Suhr, P., 2008. Reconstructing paleoenvironment, eruption mechanism and paleomorphology of the Pliocene Pula maar, (Hungary). *Journal of Volcanology and Geothermal Research*, 177: 441-456.
- Soós, I., Harangi, Sz., Lukács, R., Németh, K., 2014: Tefra rétegek jellemzése a Pulai alginit rétegsorban. V. Közletani és geokémiai vándorgyűlés; Abstract vol. 78.

Optical and geochemical analysis of the tephra layers from the Hinkelsmaar (Eifel region, Western Germany)

Martina Vöggtli¹, Nikolaus J. Kuhn², Leander Franz³, Christian de Capitani⁴, and Martin Koziol⁵

¹ Department of Geography, University of Zurich, Winterthurerstr. 190, 8057 Zurich, Switzerland. martina.voegtli@uzh.ch

² Physical Geography and Environmental Change, University of Basel, Klingelbergstr. 27, 4056 Basel, Switzerland.

^{3,4} Mineralogisch-Petrographisches Institut, Bernoullistrasse 30, 4056 Basel, Switzerland.

⁵ Maarmuseum Manderscheid, Wittlicher Strasse 11, 54531 Manderscheid, Germany.

Keywords: Tephra layer, Laacher See eruption, geochemistry.

Sediments deposited in maar craters can often be used as environmental archives. To do so, dating the age of the maar and the sediment is critical. While methods such as isotope geochronology or thermoluminescence are widespread, their cost is often prohibitive, in particular within a small project and just a rough estimate is required. Identifying layers of sediment associated with a known event provides an inexpensive alternative, but also requires careful analysis.

The Hinkelsmaar is part of five cones and two maars of the Mosenberg-Meerfeld-group in the German West Eifel region. The maar was created through a phreatomagmatic explosion and is built inside upper devonian rocks and filled with lake sediments and peat. The Hinkelsmaar is a volcanic attraction: at the same place where the maar was formed a small cinder cone existed before. This can be proven by a slag wall inside the maar tephra wall. The accumulation of its sediments started approximately 28'400 a BP (Juvigné et al. 1988).

In the course of practical studies in environmental reconstruction, drill cores were taken in the central part of the Maar using a Swedish rock drill. Each core recovered 0.5 meters to a depth of 7 meters. Three tephra layers were discovered; namely T1, T2 and T3; in depths between 2.85-2.93 m (T1), 3.73-3.76 m (T2) and 5.32-5.35 m (T3). These three tephra layers offer the opportunity to date the sediments. The occurrence of three layers in the Hinkelsmaar has not been documented so far.

From the soft rock material of the three tephra layers, organics were removed by H₂O₂. Afterwards, the rock material was sieved and 25 grain mounts were prepared. The petrography of the grain mounts was investigated using a polarization microscope and Raman spectrometer while the chemical composition of volcanic glass shards was determined by electron microprobe analysis. For comparison, thin sections from tephra eruptions of nearby maar lakes (Pulvermaar and Holzmaar) were studied.

The grain mounts from the two upper tephra layers T1 and T2 are petrographically very similar with the dominant magmatic minerals aegirine-augite, Ti-hornblende and sanidine as well as accessory titanite.

Shards of both layers revealed a trachytic to phonolitic composition. The mineral ratios and the geochemistry of the shards are characteristic for the MLST and ULST tephra units of the Laacher See (see Fig. 1; cf. Bogaard & Schmincke 1985), which erupted 12'900 years ago in the East Eifel region.

The deepest tephra layer T3 showed a totally different petrography with plenty of olivine, Ti-augite and very few ultramafic (tephritic to foiditic) volcanic glass shards. Most probably, this layer belongs to the ultramafic tephra eruption of the Schalkenmehrener Maar in the West Eifel region, which erupted 20'000 – 25'000 a BP (Sirocko et al. 2012).

The results show that the Hinkelsmaar has more tephra layers than previously documented. Their mineralogic, petrographic and geochemical analysis offers the opportunity to contribute to a better understanding of the sequence of late Holocene volcanic eruptions in the Eifel. Especially the geochemistry of relatively instable phases like volcanic glass is well suitable for the identification of specific eruptions. These results are part of the bachelor thesis of the first author.

Acknowledgements

The authors are grateful to Struktur- and Genehmigungsdirektion Nord of Rheinland-Pfalz for the kind permission to access the nature reserve «Reihenkrater Mosenberg & Horngraben» and perform scientific investigations. We thank all people involved in the project regarding sample taking, laboratory work, grain mount preparation and critical review and the Maarmuseum Manderscheid/Vulkaneifel for the nice collaboration.

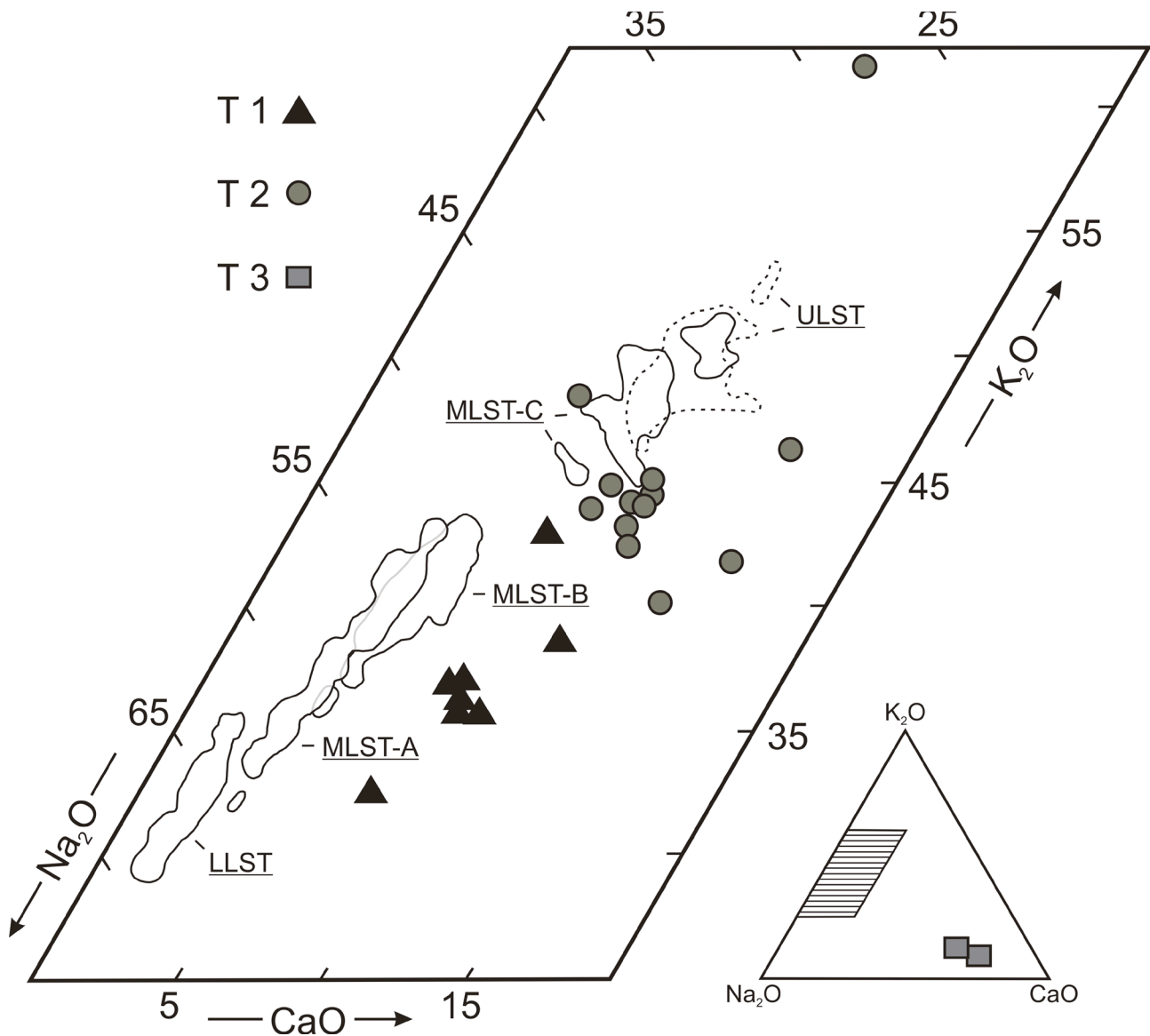


Figure 1: Microprobe analyses of glass shards from the three tephra layers of the Hinkelsmaar in the Na₂O-K₂O-CaO-plot. Distributive fields for glass shards from the LLST, MLST and ULST eruptions from the Laacher See are from Bogaard & Schmincke (1985).

References

Bogaard P., Schmincke H.-U. 1985. Laacher See Tephra: A wide-spread isochronous late Quaternary tephra layer in central and northern Europe. Geological Society of America Bulletin v.96: 1554-1569.

Juvigné E., Boenigk W., Brunacker K., Duchesne J.C., Windheuser H. 1988. Zur Schlotfüllung des Hinkelsmaar (Eifel, Deutschland): Alter und Genese. N Jb Geol Paläontol Mh 9: 544-562.

Sirocko F., Dietrich S., Veres D., Grootes P.M., Schaber-Mohr K., Seelos K., Nadeau M., Kromer B., Rothacker L., Röhner M., Krbeschek M., Appleby P., Hambach U., Rolf C., Sudo M., Grim S. 2012. Multi-proxy dating of Holocene maar lakes and Pleistocene dry maar sediments in the Eifel, Germany. Quaternary Science Review 62: 56-76.

Vögtli M. 2016: Lichtoptische und chemische Analyse der Tephra-schichten aus dem Hinkelsmaar. Bachelor Thesis, University of Basel. 42 pp.

Wagner H.W., Kremb-Wagner F., Koziol M., Negendank J.F.W. 2012. Trier und Umgebung. Geologie der Süd- und Westeifel, des Südwest-Hunsrück, der unteren Saar sowie Maarvulkanismus und die junge Umwelt- und Klimageschichte. Sammlung Geol. Führer 60, Bornträger, Stuttgart. 396 pp.

Crystal forensic studies to unravel the nature of pre-eruptive magmatic processes in basalt volcanic fields

Szabolcs Harangi^{1,2}, Éva M. Jankovics¹, Tamás Sági², and Theodoros Ntaflou³

¹ MTA-ELTE Volcanology Research Group, Pázmány sétány 1/C, 1117 Budapest, Hungary. szabolcs.harangi@geology.elte.hu

² Department of Petrology and Geochemistry, Eötvös Loránd University, Pázmány sétány 1/C, 1117 Budapest, Hungary.

³ Department of Lithospheric Research, University of Vienna, 1090 Vienna, Austria.

Keywords: crystal forensics, Pannonian basin, basaltpetrogenesis

High-resolution geochemical studies of crystal cargoes in volcanic rocks have revealed that most of the minerals represent crystallization in different stages, different time and often different magmas (Davidson et al., 2005). This implies that bulk-rock chemical composition data reflect mixture of minerals with various origin rather than a specific magma and thus, they have to be interpreted with caution. Although most of such studies focused on arc rocks with intermediate whole-rock chemistry, there are increasing evidences that many basaltic rocks have the same behavior (Kahl et al., 2011; 2015; Jankovics et al., 2012; 2013; 2015; Neave et al., 2013; 2017; Miller et al., 2017). This is particularly important since major and trace element data of basalts are often used for modelling of petrogenetic processes.

Texture, chemical composition and zoning patterns of crystals record sensitively the changing conditions during their growth. Reading the history of various crystals could help to reconstruct the magma evolution involving the pre-eruption processes in detail. Such crystal forensic sleuthing could help to understand the subvolcanic plumbing system that has significance also in the volcanic hazard assessments.

In basaltic systems, mineral phases such olivine, clinopyroxene and spinel have a particular importance since their chemical compositions closely reflect their host magma. Thus, they are important witnesses of the magmas, which played a role in the scene. Monogenetic basalt volcanic fields represent complex volcanoes, where eruptive centers are scattered both in space and in time. The individual volcanoes have a quite short lifespan and are considered to be fed by distinct magma batches rising either directly from the upper mantle source without significant compositional modification or representing various shallow-level differentiation processes (McGee and Smith, 2016; Smith and Németh, 2017). These two end-member processes have implications on the magma ascent velocity and thus, on the pre-eruption signs and time. In the first case, fast magma ascent, minor or no pre-eruption signals are expected and therefore the eruption could occur suddenly. In the second case, prolonged precursor activities indicate accumulation of magma

in the depth (e.g., Martí et al., 2013a; 2013b) although majority of these signals could be detected only by installed sensitive instruments.

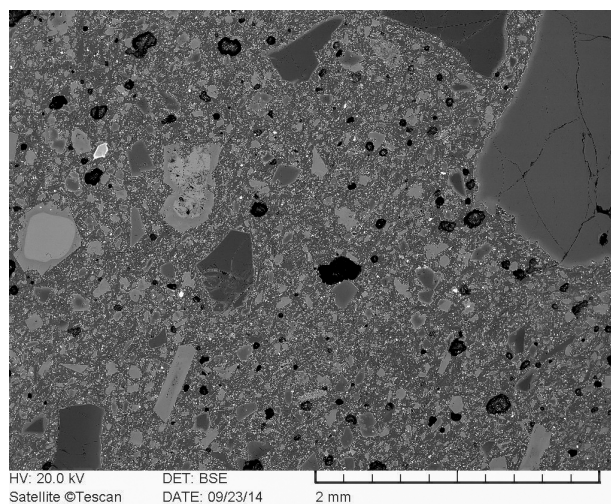


Fig. 1 – BSE image for a Mg-rich basalt (Bondoró) with diverse crystal cargo suggesting open-system magma evolution

Olivine and spinels are the usual liquidus minerals in alkaline mafic magmas accompanied occasionally by clinopyroxenes. Chromian spinels enclosed by olivine phenocrysts are a specific petrogenetic indicator, reflecting the primary characteristics of the basaltic melt and therefore providing important information about the mantle sources. Composition of the liquidus spinels is considered to be close to that of the spinels in the residual mantle source region, although other controlling factors such as magma differentiation, crystallization pressure, redox condition and the degree of partial melting also influence their composition. Spinel found in the alkaline basalts of this region show a wide compositional range suggesting heterogeneous mantle source region of the mafic magmas. Remarkably, spinels with distinct compositions can be found even in single samples and occasionally even in single olivine crystals indicating mixing of magmas coming from different mantle source regions (Jankovics et al., 2012; Harangi et al., 2013).

Olivine zoning pattern reflects also the deep magmatic processes at the crust-mantle boundary. Notably, prolonged and complex open-system magma evolution was detected for a basaltic volcano having very small volume of erupted volcanic material (around 0.01 km³; Kissomlyó; western Pannonian basin; Jankovics et al., 2015). Although the erupted basalts have homogeneous bulk rock chemical composition, five different olivine types were distinguished that represent distinct magma batches. A very complex magma evolution was detected also for the Fekete-hegy volcanic complex based on olivine and spinel compositional data (Jankovics et al., this volume). Among the basalt volcanic fields of the Pannonian basin, the most complex magmatic processes were recognized in the Nógrád-Gemer volcanic field, where in addition to olivine and spinel, clinopyroxene and amphibole played also a major role. Remobilization of the mafic crystal mush layers by fresh mafic magmas, mixing and further crystallization occurred mostly during the youngest volcanic activity at the center of the volcanic field, whereas the Putikóv basaltic magma, the youngest basalt in the entire Carpathian-Pannonian Region, could have undergone only limited modification and ascent rapidly.

Magma ascent rate was estimated based on Ca-diffusion in olivine xenocrysts embedded both in crystal-poor (Perşani) and crystal-rich (Bondoró) basaltic rocks and we obtained very similar results, i.e. the mafic magmas penetrated the continental crust within a couple of days. This ascent rate is comparable what was suggested for the El Hierro 2011-2012 eruption event.

References

Davidson, J.P., Hora, J.M., Garrison, J.M., Dungan, M.A. 2005. Crustal forensics in arc magmas. *Journal of Volcanology and Geothermal Research* 140: 157-170.

Harangi, Sz., Sági, T., Seghedi, I., Ntaflos, T. 2013. A combined whole-rock and mineral-scale investigation to reveal the origin of the basaltic magmas of the Perşani monogenetic volcanic field, Romania, eastern-central Europe. *Lithos* 180-181: 43-57.

Harangi, Sz., Jankovics, M.É., Sági, T., Kiss, B., Lukács, R., Soós, I. 2015. Origin and geodynamic relationships of the Late Miocene to Quaternary alkaline basalt volcanism in the Pannonian basin, eastern-central Europe. *International Journal of Earth Sciences* 104: 2007-2032.

Jankovics, M.É., Harangi, Sz., Ntaflos, T. 2009. A mineral-scale investigation of the origin of the 2.6 Ma Fűzes-tó basalt, Bakony-Balaton Highland Volcanic Field (Pannonian Basin, Hungary). *Central European Geology* 52: 97-124.

Jankovics, M.É., Harangi, Sz., Kiss, B., Ntaflos, T. 2012. Open-system evolution of the Fűzes-tó alkaline basaltic magma, western Pannonian Basin: Constraints from mineral textures and compositions. *Lithos* 140-141: 25-37.

Jankovics, M.É., Dobosi, G., Embey-Isztin, A., Kiss, B., Sági, T., Harangi, Sz., Ntaflos, T. 2013. Origin and ascent history of unusually crystal-rich alkaline basaltic magmas from the western Pannonian Basin. *Bulletin of Volcanology* 75:749.

Kahl, M., Chakraborty, S., Costa, F., Pompilio, M. 2011. Dynamic plumbing system beneath volcanoes revealed by kinetic modeling, and the connection to monitoring data: An example from Mt. Etna. *Earth and Planetary Science Letters* 308: 11-22.

Kahl, M., Chakraborty, S., Pompilio, M., Costa, F. 2015. Constraints on the Nature and Evolution of the Magma Plumbing System of Mt. Etna Volcano (1991–2008) from a Combined Thermodynamic and Kinetic Modelling of the Compositional Record of Minerals. *Journal of Petrology* 56: 2025-2068.

Martí, J., Pinel, V., Lopez, C., Geyer, A., Abella, R., Tarraga, M., Blanco, M.J., Castro, A., Rodríguez, C. 2013a. Causes and mechanisms of the 2011-2012 El Hierro (Canary Islands) submarine eruption. *Journal of Geophysical Research. Solid Earth*, 118: 823-839.

Martí, J., Castro, A., Rodríguez, C., Costa, F., Carrasquilla, S., Pedreira, R., Bolos, X. 2013b. Correlation of Magma Evolution and Geophysical Monitoring during the 2011–2012 El Hierro (Canary Islands) Submarine Eruption. *Journal of Petrology* 54:1349-1373.

McGee, L.E., Smith, I.E.M. 2016. Interpreting chemical compositions of small scale basaltic systems: A review. *Journal of Volcanology and Geothermal Research* 325: 45-60.

Miller, S.A., Myers, M., Fahnstock, M.F., Bryce, J.G., Blichert-Toft, J. 2017. Magma dynamics of ancient Mt. Etna inferred from clinopyroxene isotopic and trace element systematics. *Geochemical Perspectives Letters* 4: 47-52.

Neave, D.A., Passmore, E., Maclennan, J., Fitton, G., Thordarson, T. 2013. Crystal–Melt Relationships and the Record of Deep Mixing and Crystallization in the ad 1783 Laki Eruption, Iceland. *Journal of Petrology* 54: 1661-1690.

Neave, D.A., Buisman, I., Maclennan, J. 2017. Continuous mush disaggregation during the long-lasting Laki fissure eruption, Iceland. *American Mineralogist* 102: 2007-2021.

Smith, I.E.M., Németh, K. 2017. Source to surface model of monogenetic volcanism: a critical review. Geological Society, London, Special Publications 446: 1-28.

Application of Response Surface Methodology (RSM) to Instrumental Mass Fractionation (IMF) prediction in stable isotope SIMS analyses

Carles Fàbrega¹, David Parcerisa¹, Frances Deegan^{2,3}, Martin Whitehouse³, Valentin Troll², and Andrey Gurenko⁴

¹Departament d'Enginyeria Minera, Industrial i TIC, Escola Politècnica Superior d'Enginyeria de Manresa (UPC - Campus Manresa), Av. Bases de Manresa, 61-73, 08242, Manresa, Spain. E-mail: carlesfal@yahoo.es

²Department of Earth Sciences, Section for Mineralogy, Petrology and Tectonics, Uppsala University, SE-75236 Uppsala, Sweden

³Department of Geosciences, Swedish Museum of Natural History, SE-104 05, Stockholm, Sweden

⁴Centre de Recherches Pétrographiques et Géochimiques, UMR 7358, Université de Lorraine, 15 rue Notre-Dame des Pauvres, BP 20, 54501 Vandoeuvre-lès-Nancy, France.

Keywords: Response Surface Methodology, Instrumental Mass Fractionation, SIMS; Stable Isotopes.

Predicting and correcting for instrumental mass fractionation (IMF) is one of the key steps to obtain reliable results during in-situ stable isotope secondary ion mass spectrometry (SIMS) analysis. The IMF depends on multiple factors concerning the characteristics of each ion microprobe model, the specific instrumental working conditions used in the SIMS analyses and the major element composition of the analyzed minerals (Eiler et al., 1997; Kita et al., 2009).

During routine SIMS sessions, IMF is determined on reference minerals with demonstrated isotopic homogeneity at the analysis scale belonging to the same mineral group and with similar major element composition than the unknowns. IMF can be calculated as the average of two subsets of analyses (typically 5-10 analyses in each subset) of the reference minerals, bracketing subsets of analyses carried out on the unknowns, in the so-called "standard-bracketing method". In the case of solid-solution series, several standards are used to construct a regression of IMF for specific mineral compositions. Standardization of the session is usually complemented with regular sets of analyses on an independent standard to control possible time-related drifts of IMF. This methodology has proven to give satisfactory control on IMF during routine SIMS sessions.

In addition to the "standard-bracketing method", the IMF of stable isotope SIMS analyses can be predicted by the statistical approach of Response Surface Methodology (RSM). The method constructs a polynomial response surface model by eqn. (1):

$$y = \beta_0 + \sum_{i=1}^n \beta_i X_i + \sum_{j=2}^n \sum_{i < j} \beta_{ij} X_i X_j + \sum_{i=1}^n \beta_{ii} X_i^2 + \varepsilon \quad (1)$$

Where y is the predicted response, X_i , $i=1,2,\dots,n$, are the input variables, β_0 the constant term, β_i , β_{ij} , β_{ii} , $i,j=1,2,\dots,n$, the equation coefficients and ε the standard error of the prediction. The statistical significance of the model is evaluated by the ANOVA (analysis of the variance) test.

Usually, the level of significance (p-value) assumed for acceptance or rejection of the model and the model terms is a p-value ≤ 0.05 (i.e. 95% confidence level). The goodness of fit and the predictive capacity of the polynomial model are assessed by statistics including standard error of regression (S), r-square (R²), prediction r-square (pred-R²) and adjusted r-square (adj-R²). Extended mathematical and statistical aspects of RSM can be found in Myers et al. (2016).

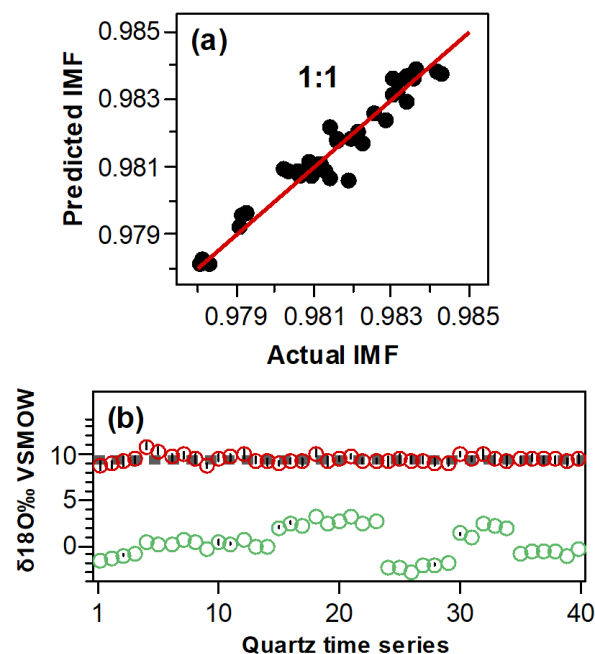


Fig. 1 –Graphs summarizing the predictive capability of the quartz model of Fàbrega et al. (2017). (a) The actual vs. predicted quartz IMF fall on a 1:1 slope, supporting the predictive capability of the quartz model. (b) Time series of the raw SIMS (green circles) and the RSM IMF-corrected (red circles) quartz $\delta^{18}\text{O}$ values. The IMF-corrected values satisfactorily match the $\delta^{18}\text{O}$ reference interval of quartz ($9.37 \pm 0.5\text{‰}$, 2σ) indicated by the horizontal dashed lines.

Thus, RSM has been successfully applied to IMF prediction of stable isotope SIMS analyses using input variables regarding instrumental setting and mineral composition. By RSM, a single IMF is predicted for each SIMS analysis. Using the statistical software Minitab 17 (Minitab Inc.), Fàbrega et al. (2017) fitted three satisfactory response surface models for IMF prediction of $\delta^{18}\text{O}$ SIMS analyses of plagioclase, K-feldspar and quartz. The input variables used in the models included the instrumental parameters X and Y stage position, primary beam intensity (PI), vacuum chamber pressure (CP) and electrostatic deflectors of the transfer part of the ion microprobe secondary column DefX and DefY. In addition, the models for plagioclase and K-feldspar included the compositional variables anorthite (An%) and orthoclase (Or%) and barium (BaO%), respectively. The models showed good predictive power (Fig. 1a), and the corrected values using the models' IMF predictions satisfactorily matched the $\delta^{18}\text{O}$ reference values of the plagioclase, K-feldspar and quartz standards (Fig. 1b).

To further test the same methodology, the IMF of SIMS $\delta^{18}\text{O}$ analyses of the pyroxene standards AG-1 (augite), EN-2 (enstatite) and JV-1 (diopside) published by Deegan et al. (2016) was fitted by RSM. The response surface model included the instrumental variables X and Y stage position, Field X and Field Y electrostatic deflectors and the compositional variable #Fe/(Fe+Mg) ratio. The developed model shows significant predictive capacity (Fig. 2a) and the corrected values were satisfactorily fitted to the reference values of the pyroxene (Fig. 2b).

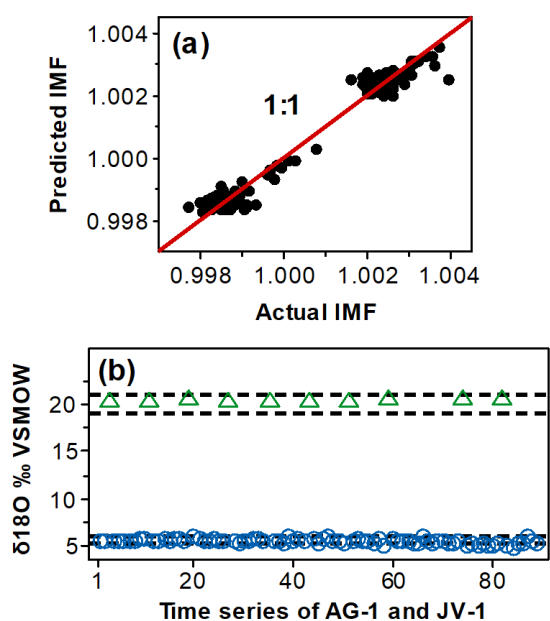


Fig. 2 – Graphs showing the predictive capability of the response surface model fitted using the $\delta^{18}\text{O}$ SIMS pyroxene data of Deegan et al. (2016). (a) Actual vs. predicted IMF fall on a 1:1 slope. (b) IMF-corrected values of the pyroxene standards AG-1 (blue circles) and JV-1 (green triangles) falling into the respective $\delta^{18}\text{O}$ reference intervals (horizontal dashed lines). AG-1: Augite; JV1: Diopside.

Concluding remarks:

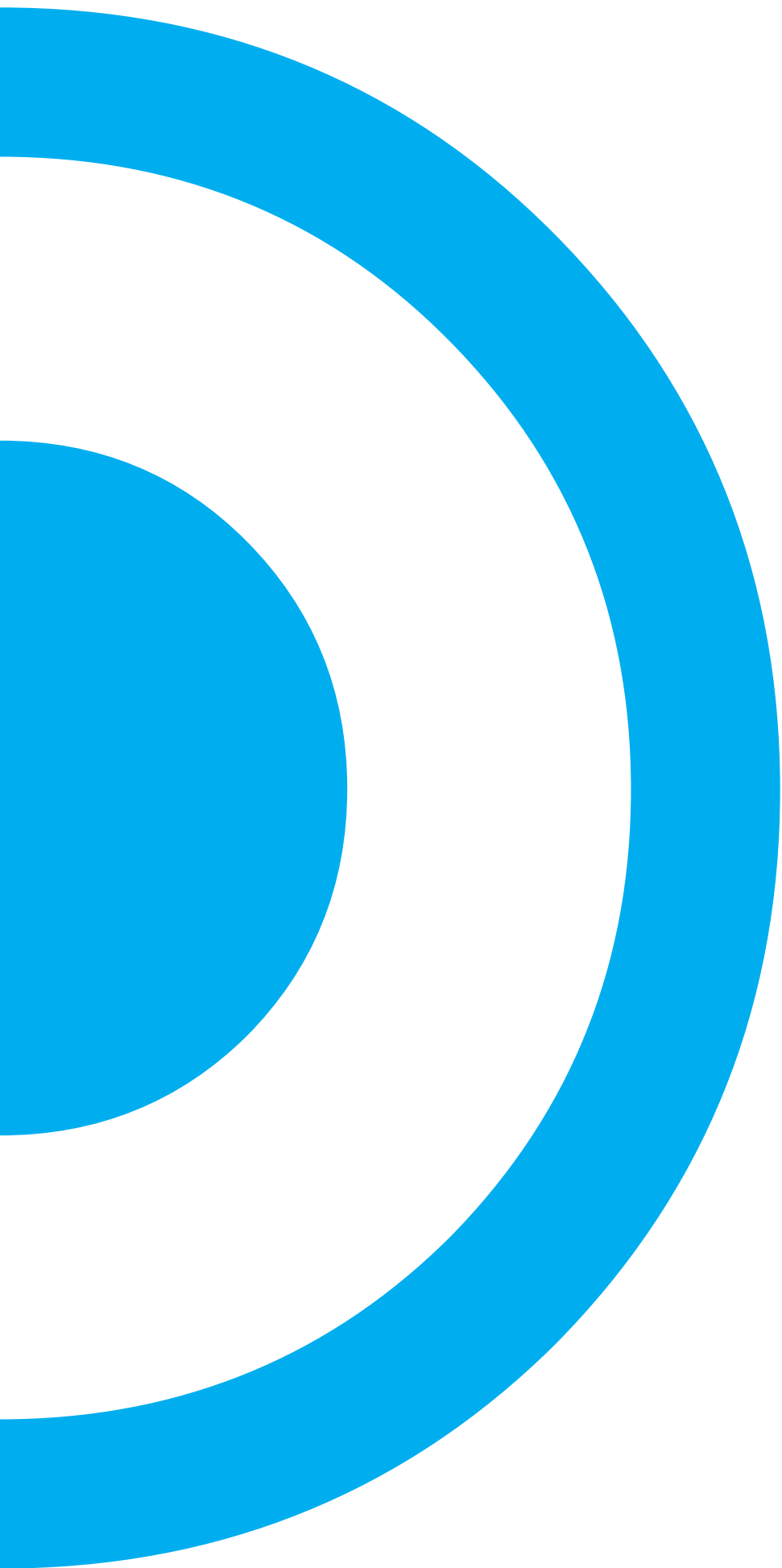
1. RSM can be confidently applied to IMF correction in routine stable isotope SIMS analyses.
2. The ranges of values of the compositional and instrumental variables obtained on the unknown samples must fit the ranges of values of the different standards, because RSM predicts by interpolation.
3. RSM has proven to be especially useful in the correction of IMF in solid solution series and in situations where the analyses on the standards and on the unknown samples have significant differences in the X-Y position and/or the electrostatic deflector values, making both sets of analyses susceptible to differing IMF.

Acknowledgements

Thanks to Dr. Joan Rosell, Escola Politècnica Superior d'Enginyeria de Manresa, Spain. Thanks to the members of the CRPG Ion Probe Group (Nancy, France). FD and VT acknowledge funding by the Swedish Research Council (VR, grant number 621-2013-5628). CF and DP acknowledge funding by the CGL2015-66335-C2-1-R of the Spanish Dirección General de Investigación Científica y Técnica and support of the Grup de Recerca Emergent en Minería Sostenible if the Generalitat de Catalunya.

References

- Deegan, F. M., Whitehouse, M. J., Troll, V. R., Budd, D. A., Harris, C., Geiger, H., & Hålenius, U. (2016). Pyroxene standards for SIMS oxygen isotope analysis and their application to Merapi volcano, Sunda arc, Indonesia. *Chemical Geology*, 447, 1-10.
- Eiler, J. M., Graham, C., & Valley, J. W. (1997). SIMS analysis of oxygen isotopes: matrix effects in complex minerals and glasses. *Chemical Geology*, 138(3), 221-244.
- Fàbrega, C., Parcerisa, D., Rosell, J. M., Gurenko, A., & Franke, C. (2017). Predicting instrumental mass fractionation (IMF) of stable isotope SIMS analyses by response surface methodology (RSM). *Journal of Analytical Atomic Spectrometry*, 32(4), 731-748.
- Kita, N. T., Ushikubo, T., Fu, B., & Valley, J. W. (2009). High precision SIMS oxygen isotope analysis and the effect of sample topography. *Chemical Geology*, 264(1), 43-57.
- Myers, R. H., Montgomery, D. C., & Anderson-Cook, C. M. (2016). *Response surface methodology: process and product optimization using designed experiments*. John Wiley & Sons.



Posters *Session 2*

Geochemistry and petrology of monogenetic volcanism related magmas

Conveners

Ian Smith (ie.smith@auckland.ac.nz)

Giovanni Sosa-Ceballos (giovanni@geofisica.unam.mx)

Claus Siebe (csiebe@geofisica.unam.mx)

Monogenetic volcanoes have been traditionally linked to direct magma transfer from the mantle to the surface. However, recent detailed petrological and geochemical studies of some monogenetic eruptions suggest that magmas coming from depth in dikes are not able to rise straight to the surface, but stall at some intermediate depth developing an environment in which processes such as magma mixing, crystal fractionation and/or crystal assimilation can occur. Understanding the processes and magma plumbing systems that lead to monogenetic eruptions is fundamental for better interpreting the monitoring data of the unrest episodes in monogenetic volcanic fields and thus improve the eruption forecasting in these regions. We invite contributions that include field observations, geochemical, isotopic and petrological data, analogue models of dike propagation and experimental petrology of magma ascents.

Magmatic evolution of the South Aegean volcanic arc: evidence from Milos, based on a hot zone model

Xiaolong Zhou, Pieter Vroon, Klaudia Kuiper, and Jan Wijbrans

Department of Geology and Geochemistry, VU University Amsterdam, De Boelelaan 1085, 1081HV Amsterdam, The Netherlands z.x.l.zhou@vu.nl

Keywords: Mediterranean, hot zone, Milos, $^{40}\text{Ar}/^{39}\text{Ar}$ dating, incubation time

Milos is a volcanic island in the central part of the South Aegean active volcanic arc (SAVA). This arc is composed of the volcanic centres Kos, Yali and Nisyros in the east, Santorini, Kolombo and Cristiania in the south, and Milos and volcanism in the gulf of Salamis in the west (Figure 1). Milos is one of the most prominent volcanic centres of the arc which was active for more than 3Ma. The SAVA volcanic centres are composed of mafic, andesitic, and felsic eruption products (Pe-Piper and Piper 2005).

Milos volcanic products are mainly composed of intermediate to felsic volcanic products erupting over a 3.05 Ma period. Although numerous studies have focused on the geochemical composition of the volcanics, it is not clear whether the volcanism of Milos was episodic or not. Previous geochronology using conventional K/Ar dating in the late 1970's (Fytikas, Giuliani et al. 1976, Fytikas, Innocenti et al. 1986) and SHRIMP U/Pb zircon dating is patchy, and while establishing an age range for the formation of the volcanic island, it is insufficient to address the research question that we set ourselves for the present study. Therefore, the main goal of our study is to establish if the occurrence of volcanism of Milos was in distinct time intervals or continuous, by systematically dating all volcanic centres on the island using the $^{40}\text{Ar}/^{39}\text{Ar}$ incremental heating method using the Amsterdam Argon Geochronology Laboratory's new Thermo Fisher Helix MC multi-collector noble gas mass spectrometer.

We produced 24 new $^{40}\text{Ar}/^{39}\text{Ar}$ age determinations on groundmass, biotite and amphibole samples (Figure 3), and did a detailed petrographic and geochemical study (see Figure 2). Group I volcanics are found in the SW and NE of the island and consist of (basaltic-)andesites; Group II volcanics are found in the centre of Milos and consist of andesites and dacites; Group III volcanics are found in the western and eastern parts of the island and consist of dacites and rhyolites; Group IV volcanics are found in the centre of the island and consist of rhyolites; Group V volcanics are found in the northern and southern parts of Milos and consist of rhyolites; Group VI volcanics are found southern part and also consist of rhyolites.

The youngest group is controlled by SE-NW faults, whereas the oldest group is only concentrated on the SW-NE part of Milos. These different age groups also display different geochemical characteristics, suggesting that the magma plumbing system of Milos varied over time.



Fig. 1 – Milos Location in South Aegean volcanic arc.

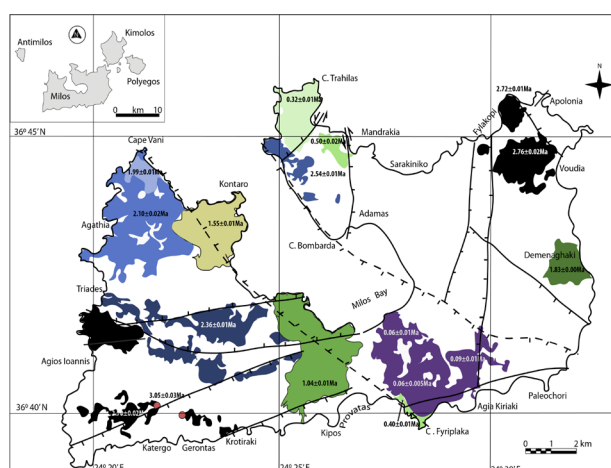


Fig. 2 – $^{40}\text{Ar}/^{39}\text{Ar}$ ages of volcanics from Milos.

The distribution of $^{40}\text{Ar}/^{39}\text{Ar}$ ages of Milos is related to the different fault systems on the island (see Figure 2 and 3). Most of the volcanic basement of the island was formed in a period between 3 and 2 Ma ago. The caldera formed prior to 1.55 ± 0.01 Ma ago. The youngest centre is in the south of the island with ages ranging between 90 – 60 ka.

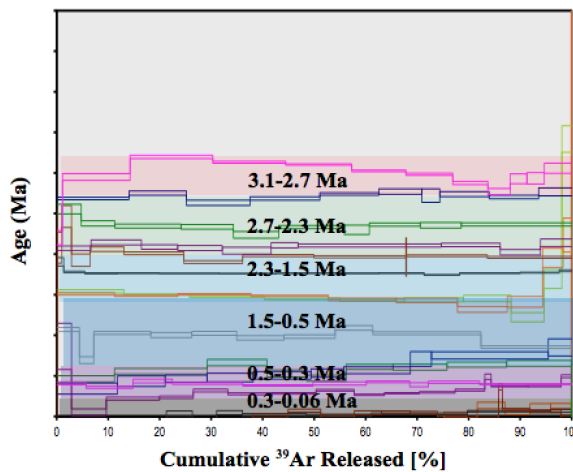


Fig. 3–Flat ages for samples from Milos divided by 6 groups

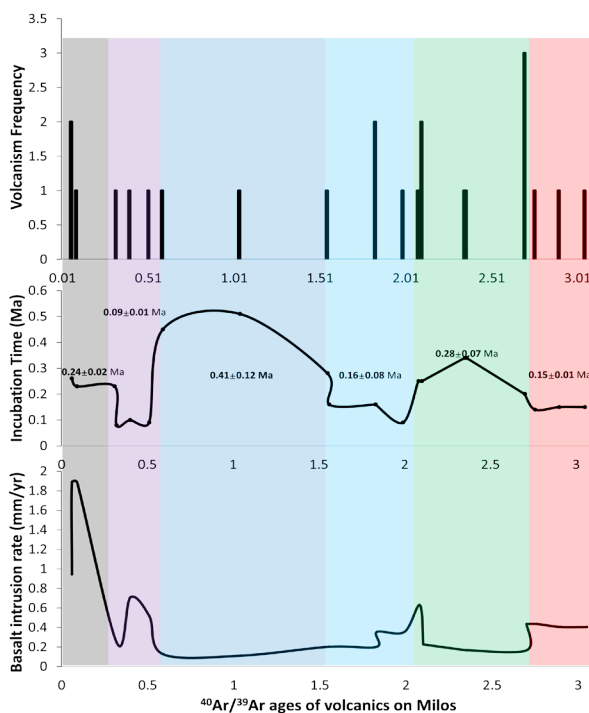


Fig. 4–Rate of basaltic intrusion varies as incubation time changes.

In addition, the age distribution can be modelled by the “hot-zone” model (Annen and Sparks 2002, Annen, Blundy et al. 2006). In this model, the supply rate of wet basaltic magma from deep, which is calculated by: basaltic intrusion rate (Annen, Blundy et al. 2015), and the rate of fractionation of amphibole, determine at which intervals felsic magma’s can rise to the surface. In the case of Milos, this results in incubation times which vary from approximately 0.1 to 0.5Ma.

Volcanism of Milos older than 2.7Ma is related to SW-NE fault systems, whereas the younger volcanism (<0.5Ma) is found close to SE-NW faults.

Milos volcanoes were active over a period of 3.05Ma. There are clear periods of volcanic activity, and periods

of 0.1-0.5Ma quiescence, corresponding to the rate of basaltic intrusion. The age distribution of volcanism of Milos can be explained by the hot-zone model from Annen et al. (2002,2006,2015).

Acknowledgements

$^{40}\text{Ar}/^{39}\text{Ar}$ ages measurement is supported by Amsterdam Argon Geochronology Laboratory. The mineral separation assistance of Roel van Elsas is greatly appreciated. The guidance and supervision of Jan Wijbrans, Pieper Vroon and Klaudia Kuiper on data analysis are really helpful and grateful.

References

- Annen, C., J. D. Blundy, J. Leuthold and R. S. J. Sparks (2015). “Construction and evolution of igneous bodies: Towards an integrated perspective of crustal magmatism.” *Lithos* 230: 206-221.
- Annen, C., J. D. Blundy and R. S. J. Sparks (2006). “The Genesis of Intermediate and Silicic Magmas in Deep Crustal Hot Zones.” *Journal of Petrology* 47(3): 505-539.
- Annen, C. and R. S. J. Sparks (2002). “Effects of repetitive emplacement of basaltic intrusions on thermal evolution and melt generation in the crust.” *Earth and Planetary Science Letters* 203(3-4): 937-955.
- Fytikas, M., O. Giuliani, F. Innocenti, G. Marinelli and R. Mazzuoli (1976). “Geochronological Data on Recent Magmatism of Aegean Sea.” *Tectonophysics* 31(1-2): T29-T34.
- Fytikas, M., F. Innocenti, N. Kolios, P. Manetti, R. Mazzuoli, G. Poli, F. Rita and L. Villari (1986). “Volcanology and Petrology of Volcanic Products from the Island of Milos and Neighboring Islets.” *Journal of Volcanology and Geothermal Research* 28(3-4): 297-317.
- Pe-Piper, G. and D. J. W. Piper (2005). “The South Aegean active volcanic arc: relationships between magmatism and tectonics.” *Developments in Volcanology* 7: 113-133.

Triplex eruption at Ichinsky volcano (Kamchatka) 6500 ¹⁴C years BP: a shift from monogenetic to polygenetic type of activity

Anna Volynets¹, Maria Pevzner², Maria Tolstykh³

¹Institute of volcanology and seismology FEB RAS, Petropavlovsk-Kamchatsky 683006, Russia. a.volynets@gmail.com

²Geological Institute RAS, Moscow, Russia

³Vernadsky Institute of geochemistry and analytical chemistry RAS, Moscow

Keywords: Kamchatka, back-arc, Sredinny Range

Kamchatka subduction system is located at the north-western part of the Pacific at the convergent boundary of the Okhotsk and Pacific plates. The latter is presently subducting under Kamchatka at the rate of 8-9 cm/year (Scholl, 2007, etc.). Quaternary volcanism in Kamchatka occurs in three zones, parallel to the trench: Eastern Volcanic Front, graben-like Central Kamchatka Depression and Sredinny Range (SR) in the back-arc. Today, SR is about 400 km away from the contemporary trench. Benioff zone is located at 350-400 km depth in the southern part of the Range, up to Khangar volcano latitude (Gorbatov et al., 1997), and is not traced further to the north (Davaille, Lees, 2004; Gorbatov et al., 2000). Ichinsky volcano, the largest volcanic edifice in SR, is located in its southern part. It is a complex stratovolcano of Somma-Vesuvius type. Numerous monogenetic centers occur in its vicinity. Until recent time, Ichinsky was considered as the only active volcano in SR due to its fumarolic activity and fresh geomorphologic surfaces of lava flows. A tephrochronological and radiocarbon dating accomplished during the last decades allowed to identify Holocene age of 14 summit eruptions of Ichinsky volcano and of two large eruptions at the monogenetic field to the south from the stratovolcano, which are called Southern Cherpouk and Northern Cherpouk (Pevzner, 2015).

A subject of this study, the triple eruption Southern Cherpouk (SCh) – Northern Cherpouk (NCh) – Ichinsky volcano (ICH) happened 6500 ¹⁴C years BP. Southern Cherpouk is a large cinder cone with a 22 km-long lava flow, covering the area of at least 56 km². The total volume of this eruption is estimated by Pevzner (2015) as ~2.5 – 2.65 km³. Products are represented by basaltic andesites. Northern Cherpouk is cinder cone built on one of the thick older lava flows of Ichinsky volcano. It has a huge 18 km – long lava flow produced by a large bokka located 0.7 km to the SW from the main cone. It covers the area of 31 km² and the total volume of the erupted products is estimated by Pevzner (2015) as ~2 km³. Remarkably for such a voluminous eruption in a monogenetic zone, lava and cinder are predominantly andesitic to dacitic in composition. Most voluminous eruption of Ichinsky stratovolcano in Holocene (ICH) happened right after NCh, with a center at the SW slope of somma. It is represented by block-and-ash flow, pyroclastic waves and several small dacitic lava flows. The total volume of this eruption is ~3.5 km³. Ash and cinder of the NCh

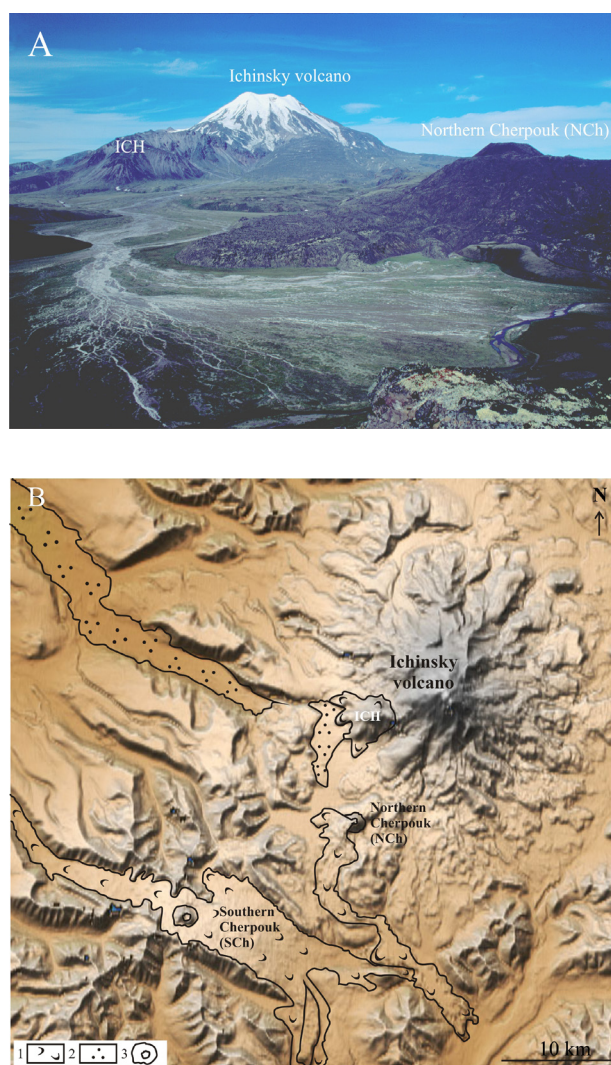


Fig. 1 – Ichinsky volcano. A) view from the SW (photo courtesy A. Kirilenko and N. Smelov). To the right from volcano – Northern Cherpouk cinder cone and lava flow, to the left – deposits of ICH (the 6500 ¹⁴C y. BP eruption of Ichinsky volcano); B) schematic map of Ichinsky volcano and adjacent monogenetic zone. Contours of 6500 ¹⁴C deposits are underlined. Legend: 1 – direction of lava flows movement; 2 – block-and-ash deposits; 3 – SCh and NCh cinder cones

eruption lay without interruption on the SCh deposits and are covered by the ash of ICH eruption; therefore, Pevzner (2015) proposed a sub-synchronous triplex eruption within Ichinsky massif 6500 ± 1400 years BP. At the same time, both SCh and NCh eruptions were usually considered as eruptions of the monogenetic zone which probably triggered the activity of the stratovolcano.

Here we discuss the geochemical compositions of rocks of this triplex event. Lava compositions form three distinct groups on Harker diagrams with a gap in SiO₂ between SCh and NCh and almost continuous trend from NCh to ICH compositions. At the same time, the youngest portions of NCh lava as well as earliest ejected lapilli are close in composition to SCh. Trace element distribution patterns provide us with further evidence of the genetic relationships between the three eruptions. SCh lava has elevated HFSE content and lower U/Nb, Th/Tb, Th/Ta, Ba/Nb ratios at higher La/Sm than NCh and ICH lavas, which are, in turn, rather close to each other in composition, with higher Cs, Rb, Th, U, Pb and lower REE. Trace element patterns of SCh are similar to those of the basaltic monogenetic zone volcanic rocks with various degree of enrichment by OIB-like mantle source (Churikova et al., 2001). NCh and ICH lavas have very similar trace element distribution patterns, almost identical in LILE part but crossing each other at HREE part of the spidergram. Most basic product of this triple event – SCh lava – have highest REE concentrations and therefore can't serve as a parent melt for more acid varieties of NCh and ICH eruptions. Relationship between NCh and ICH can hardly be explained by fractional crystallization only because of the HREE behavior, but the similarity of their major and LIL element concentrations suggests some kind of the genetic link between these two magmas. Moreover, composition of products of the youngest eruptions of Ichinsky stratovolcano in some cases is even closer to NCh than to ICH. These observations lead us to a conclusion that NCh is not a monogenetic edifice, but rather a side eruption of the stratovolcano, produced by the same magma chamber that is feeding the summit activity of Ichinsky. We propose that the eruption of the Southern Cherpouk cinder cone, which is beyond any doubt an example of monogenetic volcanic field activity, has served as a trigger for the further activity of Ichinsky stratovolcano. Geochemical affinities of the volcanic rocks of the triple eruption can be explained by the admixture of basic SCh magma to the andesitic-dacitic long-lived magma chamber under the stratovolcano, which is confirmed by the pyroclastic deposits compositions and existence of banded pumices and cinder in NCh deposits. This conclusion is a vivid example of the coexistence of the large stratovolcano with a complicated and long-lived magma plumbing system (Dobretsov et al., 2016) with the spacious monogenetic volcanic field with the deeper roots and contrast composition of magmas. Ichinsky volcano therefore can be opposed to Tolbachik volcanic massif, where the monogenetic volcanic field captured the extinct stratovolcano edifice and uses its magmatic system as one of the evacuation channels for magma supply to the surface (Volynets, Kugaenko, this meeting; Kugaenko, Volynets, submitted to JVGR).

Acknowledgements

Financial support by RFBR grant # 17-05-0012.

References

- Churikova, T., Dorendorf, F., Wörner, G. 2001. Sources and fluids in the mantle wedge below Kamchatka, evidence from across-arc geochemical variation. *Journal of Petrology*, 42 (8): 1567 – 1593.
- Davaille, A., Lees, J.M. 2004. Thermal modeling of subducted plates: tear and hotspot at the Kamchatka corner. *Earth and Planetary Science Letters* 266: 293 – 304.
- Dobretsov, N. L., Simonov, V. A., Kotlyarov, A. V., Kulakov, R. Y., Karmanov, N. S. 2016. Physicochemical parameters of crystallization of melts in intermediate suprasubduction chambers (by the example of Tolbachik and Ichinskii Volcanoes, Kamchatka Peninsula). *Russian Geology and Geophysics*, 57(7): 993-1015.
- Gorbatov, A., Kostoglodov, V., Suarez, G., Gordeev, E. 1997. Seismicity and structure of the Kamchatka subduction zone. *Journal of Geophysical Research*, 102 (B8): 17883 – 17898.
- Gorbatov, A., Widiyantoro, S., Fukao, Y., Gordeev, E. 2000. Signature of remnant slabs in the North Pacific from P-wave tomography. *Geophysical Journal International* 142: 27 – 36.
- Kugaenko, Yu., Volynets, A. Magmatic plumbing systems of the monogenetic volcanic fields: a case study of Tolbachinsky Dol, Kamchatka. Submitted to *Journal of Volcanology and Geothermal Research*.
- Pevzner, M.M. 2015. Holocene volcanism of Sredinny Range of Kamchatka (in Russian). *Transactions of the Geological Institute*, vol. 608. Resp.ed. Fedonkin, M.A. Moscow: GEOS. 252 p.
- Scholl, D.W. 2007. Viewing the tectonic evolution of the Kamchatka–Aleutian (KAT) connection with an Alaska crustal extrusion perspective, in Eichelberger, J., Gordeyev, Y., Izbekov, P., Kasahara, M., Lees, J.M., Eds., *Volcanism and Subduction: the Kamchatka Region*. AGU Geophys. Monogr. 172: 3–35.
- Sun, S.S., McDonough W.F. 1989. Chemical and isotopic systematics of oceanic basalts; implications for mantle composition and processes. *Geological Society of London Special Publications* 42: 313–345.

Cerro Tujle maar, southeast of the Salar de Atacama Basin, Chile: Morphological, petrographic and geochemical analysis

Gabriel Ureta¹, Felipe Aguilera^{2,3}, Karoly Németh⁴, and Andrew Menzies³

¹ Programa de Doctorado en Ciencias Mención Geología, Universidad Católica del Norte, Av. Angamos 0610, Antofagasta Chile. gabriel.ureta@ucn.cl

² Centro Nacional de Investigación para la Gestión Integrada de Desastres (CIGIDEN), Chile.

³ Departamento en Ciencias Geológicas, Universidad Católica del Norte, Av. Angamos 0610, Antofagasta, Chile.

⁴ Institute of Agriculture and Environment, Massey University, Palmerston North, New Zealand.

Keywords: maar, phreatomagmatism, compressional tectonism.

Cerro Tujle maar is one of the three maars located to east of the Salar de Atacama Basin in Antofagasta, Chile; together with Cerro Overo and Puntas Negras. Cerro Tujle maar is located 21 km to southeastern of the Salar de Atacama Basin (Fig. 1)

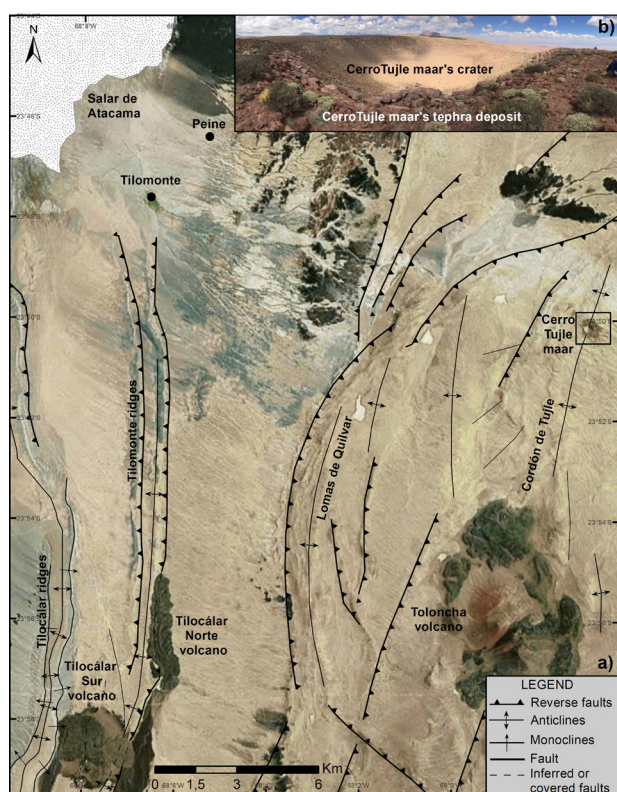


Fig. 1 - a) Location map of Cerro Tujle maar, northern Chile, based on a satellite image. Outlined box show the position of figure 1b. b) Zoom at Cerro Tujle maar showing its crater and tephra deposit.

This area is characterized by a thin-skinned deformation dominated by a series of eastvergent subparallel fault propagation folds and fault bend folds (Kuhn, 2002; Aron, 2008; González et al., 2009). Tucúcaro - Patao ignimbrites (3.2 - 3.1 Ma) covers the area and features one ridge called Cordón de Tujle, Toloncha or Toloncha-Socaire ridge

(Kuhn, 2002; Aron, 2008; González et al., 2009). Cordón de Tujle is an east-vergent asymmetric anticline with northward-dipping, which presents a fault propagation fold of a west dipping blind reverse fault (Aron, 2008; González et al., 2009). The ridge comprises ramp folds and fault bounded elongated pressure ridge associated with fault flank depressions (Kuhn, 2002; González et al., 2009). Cerro Tujle maar is situated at 3,554 m a.s.l. at the top of the northern termination of the easternmost anticline in the mapping region (Fig. 1b). This maar has an elliptical crater of 333 m across east-west and 279 m across north-south diameter with a surface area of 0.064 km². The crater has a depth of 73 m, which was estimated from the crater rim highest point to the deepest point of it. The crater's cavity presents a volume of the right circular cone of 0.002 km³ estimated on the basis of DEM (12.5 m). On the other hand, the tephra deposit inferred to erupted from the same volcano surround the crater present an extend of 390 m to north, 510 m to south, 540 m to east and 250 m to west from the center of the crater with an estimated erupted bulk volume of 0.024 km³ based on DEM (12.5 m) analysis

The material erupted by this maar correspond to at least two types of petrographically different lavas, which are covering the rhyolitic Tucúcaro - Patao ignimbrite. The first type of lava is an andesite characterized by a brown color with aphyric texture and 5 % vesicularity. It is possible to identify 5% of elongated and fractured fragments, which are aligned and correspond to dacitic fragments (0.5 mm - 10.2 cm) (Fig. 2a), euhedral to subhedral K-feldspar crystals and opaque minerals. In addition the lavas present magnetic susceptibility. The second type of lava, which lies over the brown andesite, corresponds to an andesite of black color. This lava is characterized by aphyric texture, however, it is possible to identify different crystal and rock fragments like plagioclase (2% of euhedral-subhedral crystalline crystals between 0.5-2.5 mm), olivine (1% anhedral cumulus of 2 mm), K-feldspar (1% subhedral of 0.5 mm) and dacitic fragments (1-2 mm) (Fig. 2b). Furthermore, these lavas present amygdales filled with epidote (2%), vesicles of 0.5 mm (5%) and magnetic susceptibility.

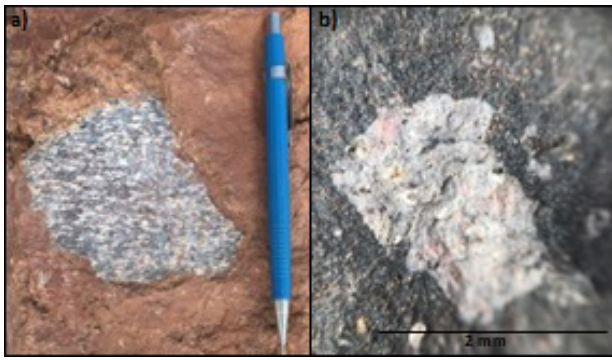


Fig. 2 – Lithic xenoliths in the Cerro Tujle´s lavas. a) Dacite of 10.2 cm in brown andesite. b) Dacite of 2 mm in black andesite.

Samples of the Cerro Tujle maar and Tucúcaro-Patao ignimbrite have been analyzed geochemically by x-ray fluorescence (XRF). Additionally published geochemical data were included (Ortega, 2008; Hoffmann, 2011) from the Tilocálar Norte and Tilocálar Sur monogenetic volcanoes to see major trends in chemical variations. These volcanoes are located along of the hinge zone of the Tilomonte ridge anticline (González et al., 2009) at 20 km and 24 km towards southwest from Cerro Tujle maar, respectively. The Cerro Tujle's lavas present a range of 56.68 – 58.41 wt % SiO₂; therefore, they can be classified as basaltic andesite, andesite and trachy-andesite. These rocks correspond to calc-alkaline series of metaluminous High-K (2.3 – 2.66 wt % MgO; 2.02 – 2.11 wt % K₂O). Cerro Tujle display the most elevated Fe₂O₃ (7.19 – 7.75 wt %) and TiO₂ (1.23 – 1.31 wt %) content relative to the other two monogenetic centers. The concentrations of Al₂O₃, K₂O, P₂O₅, Y, Nb, Rb have a tendency of positive distribution, that is to say, its concentration increases with the differentiation (incompatible components). The lavas of Cerro Tujle, Tilocálar Norte and Tilocálar Sur, which correspond to mafic component, present high Sr/Y (23.31 – 105.07) reasons, associated at high concentration of Sr (492 – 1,367 ppm) and low concentration of Y (7 – 22 ppm). On the other hand, Tucúcaro – Patao Ignimbrite, which correspond at felsic component, present low concentration of Sr/Y (5.34 – 8.23), associated at low concentration of Sr (141 – 196 ppm) and high concentration of Y (23.8 – 29 ppm). The Cerro Tujle lies directly on the hinge zone of the Cordón de Tujle ridge. The local changes of stresses have produced that through compressional structures interconnected by ramp structures or in fold core regions, the magma can be storage in magma reservoirs. These magma reservoirs are probably located in either the flat portions of reverse faults, which provided magma pathways from fault plane to surface. The magmatic evolution of the Cerro Tujle is controlled in part, by fractional crystallization process of plagioclase (compatible behavior of CaO and Sr), pyroxene (compatible behavior of CaO, MgO, Fe₂O₃ and Cr), titanomagnetite (compatible behavior of TiO₂ and V) and zircon (slight decrease of Zr). The high values of Sr/Y, the low concentrations of Y and the enrichments of incompatible components suggest that the magma has fractionated garnet ± amphibole in its origin. On the base of the structural evolution, the presence of accidental lithics in tephra deposits and geochemical char-

acteristics we can infer that the formation of Cerro Tujle was strongly controlled by phreatomagmatism (recorded by the stepwise vertical mixing of lithic xenoliths and juvenile material by upward-directed debris jets), where the magma sourced from partial melting of the mafic continental lower crust (depths > 70 km), suffered stalling and formation of upper crustal melt packets to form, then migrated toward the surface along reverse faults where it also interacted by ground water tables near surface.

Acknowledgements

We thank to Comisión Nacional de Investigación Científica y Tecnología (CONICYT) for the GU Doctoral Grant “Becas de Doctorado Nacional CONICYT - PCHA / Doctorado Nacional / 2016-21161286”, which allows funding this research. We also thank to Cristóbal González and Diego James for their support during fieldworks.

References

- Aron, F., 2008. Arquitectura y estilo de la deformación compresiva neógena del borde sur-oriental del Salar de Atacama, Norte de Chile (23° 30'S): su relación con el volcanismo Plio-Cuaternario de los Andes Centrales. Undergraduate Thesis, Universidad Católica del Norte.
- Gardeweg, M., Ramírez, C. F., 1982. Geología de los volcanes del Callejón de Tilocalar, Cordillera de los Andes-Antofagasta. In: III Congreso Geológico Chileno, A111–A123.
- González, G., Cembrano, J., Aron, F., Veloso, E. E., Shyu, J. B. H., 2009. Coeval compressional deformation and volcanism in the central Andes, case studies from northern Chile (23°S–24°S). *Tectonics* 28, TC6003.
- Hoffmann, C., 2011. Petrografía y geoquímica de los conos del campo de lavas Negros de Aras (23°57'–24°26' Lat. S. y 67°57'–68°42' Long. O.) al norte del volcán Socompa, Il región de Antofagasta, Chile. Undergraduate Thesis, Universidad de Concepción.
- Kuhn, D., 2002. Fold and thrust belt structures and strike-slip faulting at the SE margin of the Salar de Atacama basin, Chilean Andes. *Tectonics* 21, TC901042.
- Ortega, V., 2008. Estudio petrográfico y petrológico de las rocas de los volcanes Láscar, Tilocalar Norte y Tilocalar Sur. Undergraduate Thesis, Universidad Católica del Norte.

Tephra evidence for the most recent eruption of Laoheishan volcano, Wudalianchi volcanic field, northeast China

Chunqing Sun¹, Károly Németh², Tao Zhan³, Haitao You⁴, Guoqiang Chu¹, Jiaqi Liu¹

¹Key Laboratory of Cenozoic Geology and Environment, Institute of Geology and Geophysics, Chinese Academy of Sciences, Beijing 100029, China. suncq@mail.iggcas.ac.cn

²Institute of Agriculture and Environment, Massey University, Palmerston North, New Zealand

³The Second Hydrogeology and Engineering Geology Prospecting Institute of Heilongjiang Province, Haerbin, 150030, China

⁴Key Laboratory of Computational Geodynamics, College of Earth Science, University of Chinese Academy of Sciences, Beijing 100049, China

Keywords: Wudalianchi, Tephrochronology, Laoheishan

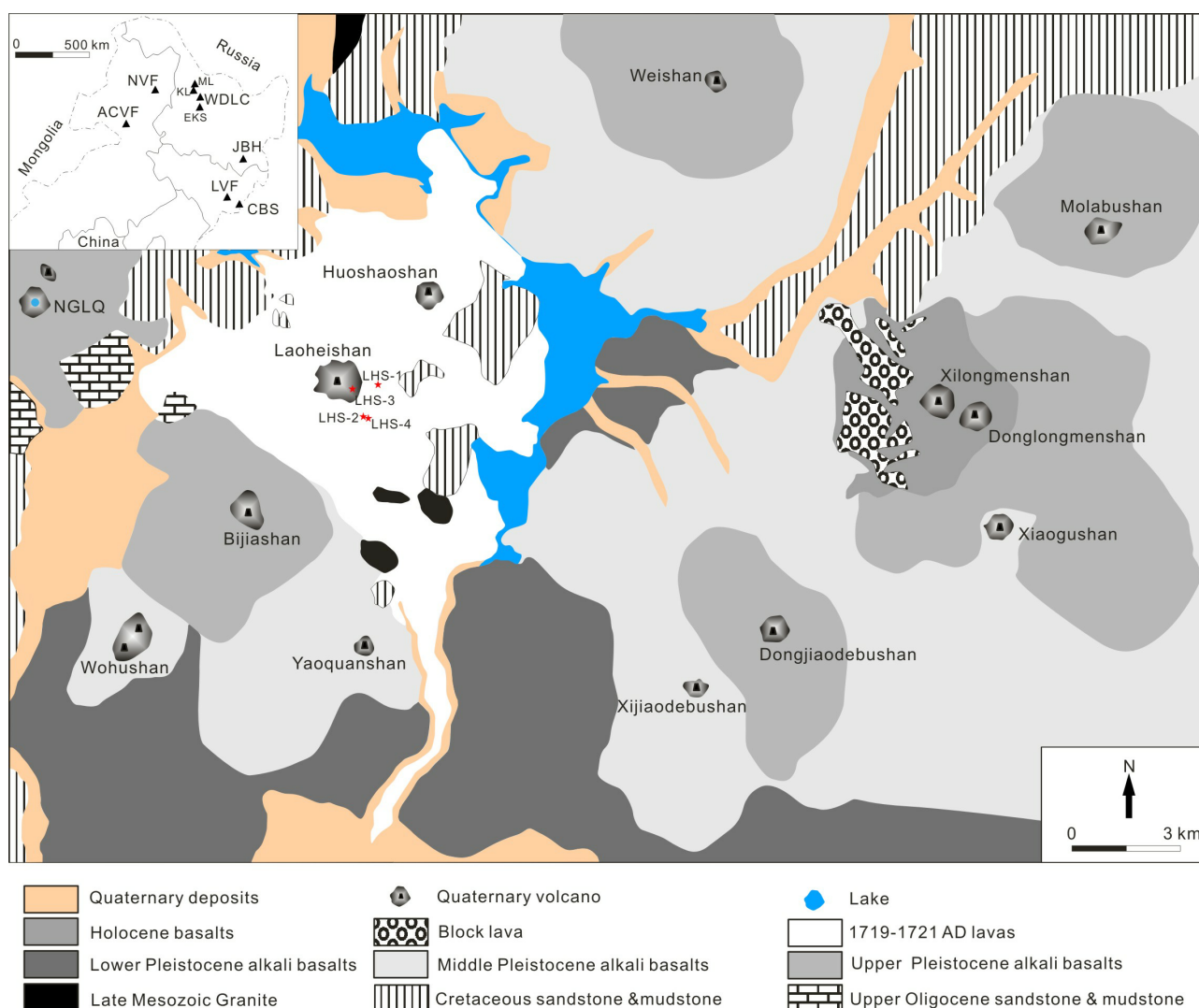


Fig. 1. Geological map of the Wudalianchi volcanic field (WDL) showing its position and other related volcanic fields (CBS: Changbaishan, LVF: Longgang, JBH: Jingbohu, ACVF: Arxan-Chaihe, NVF: Nuominhe, EKS: Erkeshan, KL: Keluo, ML: Menlu river) in northeast China (Modified from Xiao and Wang (2009)). The major Quaternary eruption centers including Laoheishan and Huoshaoshan, the lake of Nangelaqjushan (NGLQ), and proximal sampling sites around Laoheishan were marked in the map.

Abstract: Wudalianchi volcanic field (WDLC) is one of the major monogenetic volcanic regions in China (Fig. 1), and the AD 1719-1721 Laoheishan-Huoshashan eruption, and AD 1776 Laoheishan eruption are the latest eruptions in WDLC on basis of the local historical records. However, most of the recent explosive eruptive products around WDLC are attributed to the AD 1719-1721 Laoheishan-Huoshashan eruption while less attentions were paid on the AD 1776 Laoheishan eruption. There are two kinds of scoria fall deposits around Laoheishan volcano, i.e. the upper light grey high vesicular scoria deposit (US) and below dark low vesicular scoria deposit (BS). Broadly, all of these eruptive products from WDLC have extreme high potassium (usually >5%) geochemical characteristics with trachyandesitic to tephriphonolitic in composition that can be clearly distinguished from those from other near volcanic regions, such as Nuomin (~150 km to NGLQ), Arxan-Chaihe (~450 km to NGLQ), Longgang (~700 km to NGLQ) and Jingbohu (~550 km to NGLQ). However, there is still some difference between these two kinds of deposits, for example, most of the glass shards from US exhibit >4% N₂O while BS show <4% N₂O. In addition, US presents two different glass composition clusters, indicating complex eruptive phases during this eruption. A cryptotephra layer is clearly revealed as a distinct peak in magnetic susceptibility measurements from Nangelaqiushan Lake (NGLQ) ~ 8 km northwest to Laoheishan volcano. Glass composition of the cryptotephra layer recorded in NGLQ is similar to the proximal US around Laoheishan volcano. On basis of historical records and field outcrops, we ascribed US to the AD 1776 Laoheishan eruption and BS to the AD 1719-1721 Laoheishan-Huoshashan eruption. Consequently, historical records assigned a precise age (AD 1776) for the tephra recorded in NGLQ, and thus can be used to refine the age model of these lacustrine sediments.

Radiometric dating of Quaternary volcanoes in the western Zacapu lacustrine basin (Michoacán, México) reveals monogenetic clusters

Nanci Reyes-Guzmán¹, Claus Siebe¹, Oryaëlle Chevrel², Marie-Noëlle Guilbaud¹, Sergio Salinas¹, and Paul Layer³

¹Departamento de Vulcanología, Instituto de Geofísica, UNAM, Coyoacán, 04510 Ciudad de México, nanreyguz@gmail.com

²Université Clermont Auvergne, CNRS, IRDM OPGC, Laboratoire Magmas et Volcans, 6300 Clermont-Ferrand, France

³Department of Geology and Geophysics, University of Alaska, Fairbanks, AK, USA

Keywords: malpais, monogenetic cluster, Zacapu basin.

The Zacapu lacustrine basin (1980 m asl) is located in the northern-central part of the Michoacán-Guanajuato Volcanic Field (MGVF), which constitutes the western-central segment of the Trans-Mexican Volcanic Belt.

Geological mapping of a 395 km² quadrangle encompassing the western margin of the basin (Fig. 1), ⁴⁰Ar/³⁹Ar and ¹⁴C radiometric dating, whole-rock chemical and petrographic analyses of volcanic products provide infor-

mation on the stratigraphy, erupted volumes, and compositions of the volcanoes (Reyes-Guzmán et al., in press). A total of 47 monogenetic volcanoes were identified and include 19 viscous lava flows, 17 scoria cones with associated lava flows, 7 lava shields, 3 domes, and one maar. Eruptive centers are commonly aligned ENE-WSW following the direction of the regional seismically active Cuitzeo Fault System.

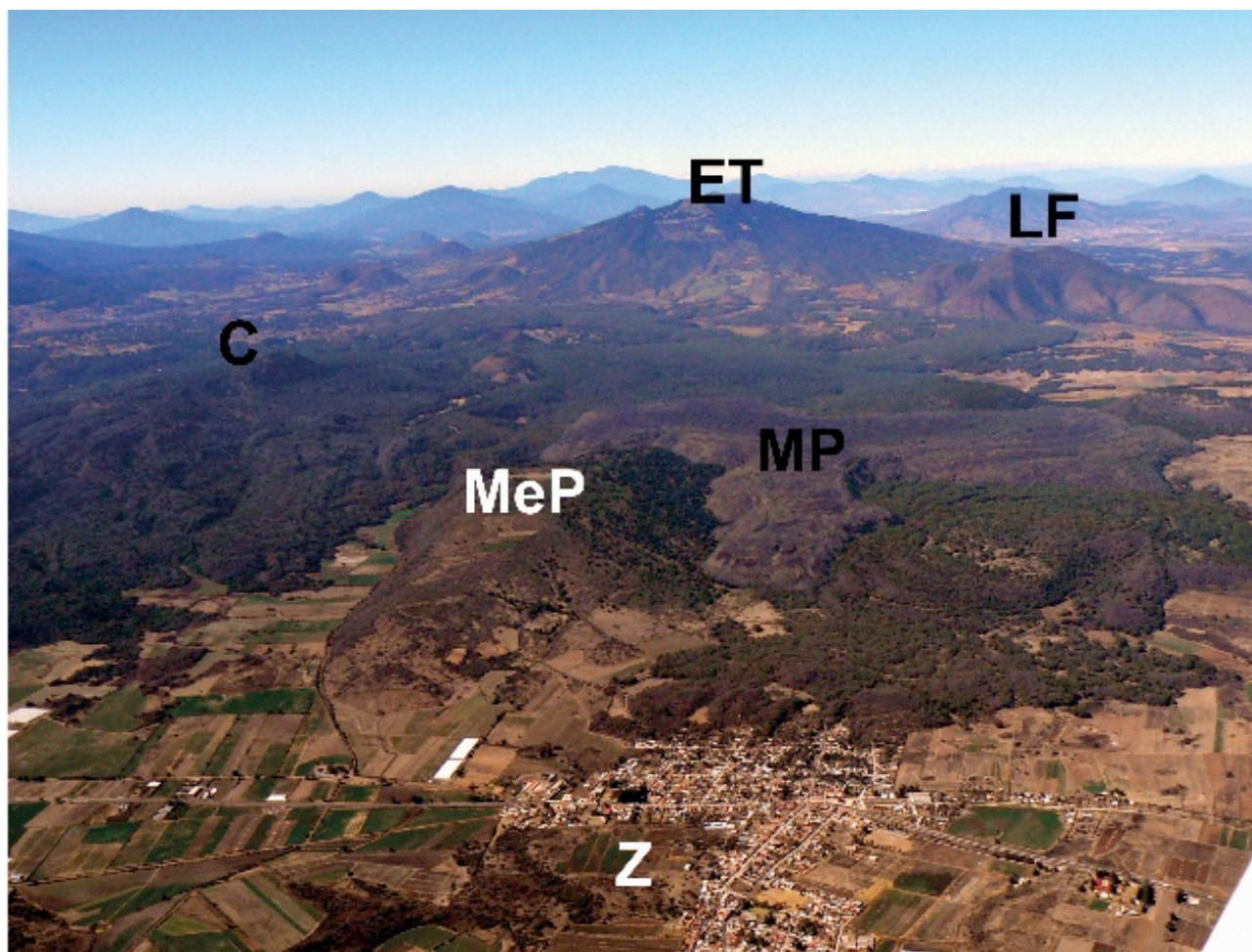


Figure 1. View of the study area to the W. In the foreground is the Zacapu lacustrine plain (Z), in the middle are the Holocene El Capaxtiro (C) and Malpais Prieto (MP) lava flows and Mesa El Pinal (MeP), and in the background El Tule shield (ET) and Las Flores dacite dome complex (LF).

Erupted products are mostly effusive and dominantly andesitic in composition with 42 km³ (~86 vol.%) followed by 4 km³ of dacite (~8 vol.%), 1.4 km³ of basaltic trachy-andesite (~3 vol.%), 1 km³ of basaltic andesite (~2 vol.%), and 0.14 km³ of rhyolite (~0.3 vol.%), while basalts are notably absent.

Radiometric dating reveals that the large majority of volcanic rocks is younger than ~2.1 Ma and that activity migrated with time towards the SE. Estimated minimum eruption rates (in km³/ka) for the different time periods are 0.007 for the Early Pleistocene, 0.03 for the Mid-Pleistocene, 0.13 for the Late Pleistocene, and 0.44 for the Holocene. Of these, the rate for the Holocene is relatively high and comparable in magnitude to the rate reported for the Tacámbaro-Puruarán area in the southern part of the MGVF (Guilbaud et al., 2012).

In the past 30,000 years eruptions occurred along a narrow 2-km-wide and 25-km-long, ENE-WSW oriented stripe, and were clustered during two main time periods. The first cluster (27,000-21,300 BC) includes four volcanoes (Alberca de los Espinos ~27,000 BC, Las Cabras ~25,750 BC, El Pueblito ~24,000 BC, and Las Pomas ~21,330 BC). After a period of almost 20,000 years with only one eruption (El Molcayete de Eréndira, ~16,000 BC), the second cluster (~1500 BC and ~AD 900) of five eruptions initiated with the eruption of Las Vigas basaltic andesite scoria cone that fed the El Infiernillo lava flow and ended with the eruption of the high-silica andesitic Malpaís Prieto lava flow (Fig. 2) at ~AD 900 (Mahgoub et al., in press). This second cluster is more restricted in space than the first one: most vents are <3 km apart from each other and fed thick viscous 'a'a to blocky flows emplaced on the margin of the lacustrine flats. For still poorly understood reasons, these apparently inhospitable lava flows were attractive to human settlement and eventually became one of the most densely populated heartlands of the pre-Hispanic Tarascan civilization (Michelet, 1992; Michelet et al., 1989). With an average eruption recurrence interval of ~900 years during the Late Holocene the western Zacapu lacustrine basin is one of the most active areas in the MGVF and should hence be of focal interest for regional volcanic risk evaluations.

Acknowledgements

Archaeologists G. Pereira and O. Quezada kindly provided archaeological information and showed us their excavation sites in the Zacapu area. Field and laboratory costs were defrayed from projects funded by Consejo Nacional de Ciencia y Tecnología (CONACyT-167231) and the Dirección General de Asuntos del Personal Académico (DGAPA-UNAM-IN103618, IN113517) granted to C. Siebe and M.N. Guilbaud.

References

- Guilbaud, M.N., Siebe, C., Layer, P., Salinas, S., 2012. Reconstruction of the volcanic history of the Tacámbaro-Puruarán area (Michoacán, México) reveals high frequency of Holocene monogenetic eruptions. *Bulletin of Volcanology* 74: 1187-1211.
- Mahgoub, A.N., Reyes-Guzmán, N., Böhnell, H., Siebe, C., Pereira, G., Dorison, A. (in press). Paleomagnetic constraints on the ages of the Holocene Malpaís de Zacapu lava flow eruptions, Michoacán (México): Implications for archaeology and volcanic hazards. *The Holocene*.
- Michelet, D., 1992. El Centro-Norte de Michoacán: características generales de su estudio regional. In *El Proyecto Michoacán 1983-1987. Medio ambiente e introducción a los trabajos arqueológicos*, pp. 9-52. CEMCA, Mexico.
- Michelet, D., Arnauld, M.C., Fauvet-Berthelot, M.F., 1989. El Proyecto del CEMCA en Michoacán. *Etapa 1: un balance*. *TRACE* 16: 70-87.
- Reyes-Guzmán, N., Siebe, C., Chevrel, M.O., Guilbaud, M.N., Salinas, S., Layer, P. (in press). Geology and radiometric dating of Quaternary monogenetic volcanism in the western Zacapu lacustrine basin (Michoacán, México): Implications for archaeology and future hazard evaluations. *Bulletin of Volcanology*.



Oral *Session 3*

Lakes in maar volcanoes: the sedimentary record of paleontology, climate change and hydrochemistry

Conveners

Oriol Oms (joseporiol.oms@uab.cat)

Dmitri Rowet (dmitrirowet@gmail.com)

The geometry of Maar-diatreme craters usually leads to develop hydrologically closed lakes that contain anoxic bottom conditions. Such settings are ideal for the preservation of complete and detailed sedimentary records of past environmental changes. These records include climate evolution, ecological reconstructions, hydrochemistry and human impact in natural systems. Exceptionally preserved fossils in such meromictic lakes are also an important source to study the history of life and its evolution.

This session wants to create synergies between volcanologists and other researchers dealing with limnology, hydrochemistry, mineralogy, paleontology, and climate proxies, among many others.



Volcanic lakes in Europe: the role of maar lakes in volcanic hazard assessment

Dmitri Rouwet

Istituto Nazionale di Geofisica e Vulcanologia, Sezione di Bologna, Via Donato Creti 12, 40128 Bologna, Italy. dmitri.rouwet@ingv.it

Keywords: volcanic lakes, Europe, maar .

Europe hosts approximately 105 volcanic lakes: 35 in the Azores Archipelago, 5 in the Auvergne-Puy de Dome volcanic field in France, 8 in the Eifel volcanic field in Germany, 2 in the Bakony-Balaton field in Hungary, 10 in Iceland, 12 in Italy, 1 in Romania, 26 in Spain, mainly in the Calatrava field, and 6 in Turkey. This compilation was presented in the data base VOLADA (Rouwet et al., 2014), and has been continuously fine-tuned afterwards. Volcanic lakes are pin-pointed on Google Earth Pro, and made open-access available as .kmz files.

The volcanic lakes are classified following the classification systems by (1) Pasternack and Varekamp (1997) for their physical properties and state of activity, (2) Varekamp et al. (2000) for the chemical properties of the lake water, and, recently, following (3) Christenson et al. (2015) for the genetic origin of the lake basins (with an alphanumeric code). The latter classification system enables to distinguish maar lakes, the focus of 7IMC, from volcanic lakes with another genetic origin. Maar lakes can be recognized for filling a basin without significant topographic highs, and hence with the water table of the lake near, or even below, topographic level (Németh and Kereszturi, 2015). As such, 66 out of 105 volcanic lakes in Europe are classified as maar lakes, 12 as crater lakes, 14 as lakes dammed by volcanic deposits, 12 caldera lakes and 1 hardly classifiable volcanic lake (Specchio di Venere on Pantelleria Island, Italy).

The 5 lakes in the Auvergne-Puy de Dome volcanic field in France, 8 in the Eifel volcanic field in Germany, and 25 (often ephemeral) lakes in the Calatrava volcanic field in Spain are all maar lakes. The Azores house a large variety of volcanic lake types with maars (12), caldera lakes (7), crater lakes (7) and some lakes dammed by volcanic deposits (9). Volcanic lakes in Italy are generally found in the less or non-active volcanic areas. Lago Bolsena, Bracciano and Vico are caldera lakes in the Roman-Tuscany Magmatic Province, with nearby maar lakes Martignano, Mezzano and Monterosi. Lago Averno, in the restless Campi Flegrei caldera is arguably a maar lake, whereas Lago Albano fills a 168 m deep 3.3 km x 2.1 km large basin of two nested craters. Together with Lago Nemi they are the two crater lakes of Colli Albani volcano, 10 km east of Rome. The two Monticchio lakes (Piccolo and Grande) are maar lakes inside the caldera of Vulture volcano (Fig. 1). Lake Nemrut is Turkey's caldera lake,

next to the alkaline 3,600 km² large Lake Van. Peculiarly, in Iceland there are many volcanic lakes, often related to the extensional tectonic regime, and hence classified as "lakes dammed by volcanic deposits". The Askja Caldera and neighboring Viti crater lake are renowned exceptions. The number of volcanic lakes in Iceland is presumably a lot higher than cataloged here, due to the complex relation with rifting and lava flow dynamics in this extensional regime.

This overview also sheds light on the level of study of the various volcanic lakes in Europe, from a volcanological point of view. A numerical code is assigned to each lake based on the level of study. The low number of well studied volcanic lakes (approx. 5% of total) in Europe stresses the need to better understand lake behavior, especially for those located in volcanically active areas (e.g. Azores, Iceland).



Fig. 1- Monticchio Piccolo (green) and Monticchio Grande lakes of Vulture volcano, Basilicata, Italy. Piccolo turned over during the winters of 2016-2017 and 2017-2018, leading to the green coloration (pic by D. Sabbatini).

Erupting and peak-activity lakes are not present in Europe. The most active volcanoes do not meet the necessary physical constraints to form and sustain a crater lake, due to insufficient meteoric water contribution (e.g. Teide, Vulcano), or a too high heat input (e.g. Etna, Stromboli) and/or not well enough developed hydrothermal system (e.g. Vesuvius). The most acidic crater lake in Europe is Viti (pH 2.5-2.7; Hasselle et al., in prep.), whereas the most alkaline lake is Specchio di Venere (pH up to 9.3; Pecoraino et al., 2015).

In terms of hazard assessment, on the one hand, some lakes are potentially “Nyos-type” lakes (Kusakabe, 2015): Lac Pavin, Laacher See, Lago Albano, and the Monticchio lakes. Nyos-type lakes have the capacity to store CO₂ from regional or magmatic degassing in the lake’s hypolimnion (i.e. the deepest water layer) as HCO₃⁻ and dissolved CO₂, and to periodically turn over leading to sudden CO₂ release. If accumulation times are sufficiently long to reach CO₂ super-critical pressures a CO₂ burst can become lethal, as was the case at Lake Nyos (Cameroon) in August 1986. Nevertheless, with the temperate climate conditions in Europe, many of the potential Nyos-type lakes “turn over” entirely or partially during the winter (Fig. 1).

Acknowledgements

DR wishes to thank G. Tamburello for help in the Google Earth Pro location; V. Chiarini for her help in the compilation of VOLADA.

References

Christenson, B., Németh, K., Rouwet, D., Tassi, F., Vandemeulebrouck, J., Varekamp, J.C., 2015. Volcanic Lakes. In: Volcanic Lakes. Springer-Advances in Volcanology (eds. Rouwet, D., Christenson, B., Tassi, B., Vandemeulebrouck, J.): 1-20.

Kusakabe, M., 2015. Evolution of CO₂ content in Lakes Nyos and Monoun, and sub-lacustrine CO₂-recharge system at Lake Nyos as envisaged from CO₂/3He ratios and noble gas signatures. In: Volcanic Lakes. Springer-Advances in Volcanology (eds. Rouwet, D., Christenson, B., Tassi, B., Vandemeulebrouck, J.): 427-450.

Németh, K., Kereszturi, G., 2010. Monogenetic volcanism: personal views and discussion. *International Journal of Earth Sciences* 104: 2131-2146.

Pasternack, G.B., Varekamp, J.C., 1997. Volcanic lake systematics I. Physical constraints. *Bulletin of Volcanology* 58: 528–538.

Pecoraino, G., D’Alessandro, W., Inguaggiato, S., 2015. The other side of the coin: geochemistry of alkaline lakes in volcanic areas. In: Volcanic Lakes. Springer-Advances in Volcanology (eds. Rouwet, D., Christenson, B., Tassi, B., Vandemeulebrouck, J.): 219-238.

Rouwet, D., Tassi, F., Mora-Amador, R., Sandri, L., Chiarini, V., 2014. Past, present and future of volcanic lake monitoring. *Journal of Volcanology and Geothermal Research* 272: 78–97. doi:10.1016/j.jvolgeores.2013.12.009.

Varekamp, J.C., Pasternack, G.B., Rowe Jr., G.L., 2000. Volcanic lake systematics II. Chemical constraints. *Journal of Volcanology and Geothermal Research* 97: 161–179.

Geological and paleontological Pliocene record: introducing the Camp dels Ninots maar (Catalan Coastal Ranges, Spain)

Oriol Oms¹, Xavier Bolós², Joan Martí³, Bruno Gómez de Soler^{4,5}, Gerard Campeny^{4,5}, Jordi Agustí^{4,5,6}

¹ *Universitat Autònoma de Barcelona, Facultat de Ciències, Departament de Geologia. Campus Bellaterra, 08193, Spain. joseporiol.oms@uab.cat.*

² *Institute of Geophysics, UNAM, Campus Morelia, 58190 Morelia, Michoacán, Mexico. 35Institute of Earth Sciences Jaume Almera, CSIC, 08028 Barcelona, Spain.*

³ *Institut Català de Paleoecologia Humana i Evolució Social (IPHES). C/ Marcel·lí Domingo s/n, Edifici W3 Campus Sescelades URV, 43007 Tarragona, Spain.*

⁴ *Àrea de Prehistòria, Universitat Rovira i Virgili (URV), Tarragona, Spain*

⁵ *Universitat Rovira i Virgili (URV). Facultat de Lletres. Av. Catalunya 35, 43002 Tarragona, Spain.*

⁶ *Institució Catalana de Recerca i Estudis Avançats (ICREA). Pg. Lluís Companys 23, 08010. Barcelona, Spain*

Keywords: Maar lake, sedimentary record, paleontology

Integrated studies on maar volcanoes can lead to a strong interaction among distant research disciplines. This is the case of the studies carried out at Camp dels Ninots maar (Pliocene, Catalan Coastal Ranges, Spain) (Fig. 1), an eroded and exhumed maar crater.

Despite such volcano is in a very accessible area at the surroundings of Caldes de Malavella village, it was unnoticed since 1999 when it was generally described by Vehí and co-authors (see brief historical review by Gómez de Soler et al., this volume). At first sight, the lack of outcrops should restrict the interest of this volcano to the large vertebrates remains that are excavated close to the surface, but other topics of interest have emerged, such as volcanology, paleolimnology, paleoclimatology, paleoecology, diagenetic processes etc.

Four scientific drill cores exist from Camp dels Ninots. Relevant ones are Can Cateura (75 m, drilled in 2009), Can Pla 1 and Can Pla 2 (112.8 and 145 m, respectively, drilled in 2015). Can Pla wells contain borehole imaging and logging. Boreholes imaging combined with core logging have been successfully applied to volcanic deposits and sedimentary facies characterization. Moreover, we have achieved correlation between cores and borehole ultrasonic televiewer oriented images. Borehole imaging techniques and logging data could be used for subsurface volcanic and sedimentary facies characterization especially in sections of low or no core recovery. The study of these cores is part of the El Camp dels Ninots research, which is here summarized together with future research topics.

The early excavation at Camp dels ninots resulted from an archaeological survey carried out in 2003 by URV-IPHES. These works lead to discover the first large mammal bones in anatomical connection. Since then, a large number of complete skeletons of large bovids, tapirs and rhinoceros have been excavated (Gómez de Soler et al., 2012). Probably they are the larger complete skeletons found in a maar setting Bone preservation is excellent (see Garcia et al., this

volume) although an integrated taphonomic study is still under work. Among other fossil vertebrate, amphibians are particularly abundant (Blain et al., this volume), fish (Prikryl et al., 2016), as well as turtles (Claude et al., 2014).

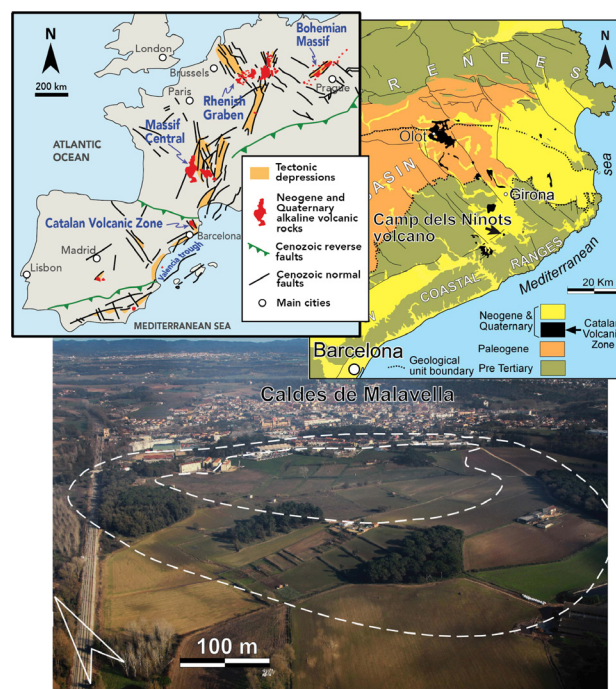


Fig. 1 – Geological settings of the Camp dels Ninots maar-diatreme. Location of the Catalan Volcanic Zone in the European Rift System (modified from Bolós et al., 2015). Situation in the Catalan Volcanic Zone. Aerial view of the studied area.

Flora is also a remarkable paleontological record. Macrofloral remains are abundant (Gómez de Soler et al (2012), Robles et al. (2013). Most relevant record is pollinic one by Jiménez-Moreno et al. (2013 and this volume), who studied the Can Cateura magnetostratigraphically dated core to determine the orbital forcing on pollen variations. Phyco-

logical studies (Oms et al., this volume) have revealed diatoms as a very good paleoecological indicator, that correlates with pollen variations and mineralogical proxies (see later).

Geological and volcanological research is based on geological mapping, outcrop description, core logging and shallow geophysics. This last (Oms et al., 2015) includes a gravimetric study and a grid of electrical resistivity tomography profiles. The acquisition and study of seismic lines is still missing at el Camp dels ninots. Volcanological research include maar-diatreme infill features recorded in borehole imaging (Bolós et al., 2016). The analysis of the boreholes reveals a progressive transition from the dike intrusion to vesiculated magma to welded pyroclasts and to country rock-rich breccia (the main section of the diatreme). Ongoing work includes the discussion about diatreme formation models from the information of the inner diatreme deposits that suggest several inter-diatreme explosions in different depth levels during the maar eruption. Future studies should focus on understanding the mechanisms and physical properties of this eruption types.

The diatreme infill also records the initial lacustrine sedimentation, which is distinctive in terms of laminites features, diatoms paleoecology and sulphide occurrence and stable isotopy and multy proxy correlation (Oms et al., this volume).

Camp dels ninots is also known for its abundant silicifications (menilite opal, among others). Such diagenetic process has also been studied in detail by Miró (2016a,b, this volume) both in outcrops and wells. The study of such processes in volcanic settings has been of interest by hydrocarbon industry as an analog for silicified rocks.

Although there is a significant work in progress in all the reviewed areas of knowledge, there is a main target to be explored: high resolution seismic profiles. Such data could be very helpful to create a 3D geological model of the maar diatreme and also to obtain a tectonostratigraphic picture of the lake sedimentation.

Acknowledgements

The Camp dels Ninots project is sponsored by projects 2014-100575, (Generalitat de Catalunya), SGR2014-901, SGR2017-1666 (AGAUR) and CGL2016-80000-P (MINECO).

References

Claude, J., Gómez de Soler, B., Campeny, G., Agustí, J., Oms, O. (2014). Presence of a chelydrid turtle in the late Pliocene Camp dels Ninots locality (Spain). *Bulletin de la Société Géologique de France*, t. 185, n° 4, pp. 253-256.

Bolós, X., Jurado, M.J., Oms, O., Martí, J., Crespo, J., Campeny, G., Gómez, B., Agustí, J. (2016). Maar-diatreme infill features recorded in borehole imaging. *Geotemas*

Gómez de Soler, B., Campeny, G., Van der Made, J., Oms, O., Agustí, J., Sala, R., Blain, H.A., Burjachs, F., Claude, J., García S.,

Riba, D., Rosillo, R. (2012). A new key locality for the Pliocene vertebrate record of Europe: the Camp dels Ninots maar (NE Spain). *Geologica Acta*, vol. 10, n°2: 1-17. DOI: 10.1344/105.000001702

Jiménez-Moreno, G., Burjachs, F., Expósito, I., Oms, O., Carrancho, Á., Villalaín, J.J., Agustí, J., Campeny, G., Gómez de Soler, B. & van der Made, J. (2013): Late Pliocene vegetation and orbital-scale climate changes from the western Mediterranean area. *Global Planet Change*, 108: 15–28.

Miró, J., Jurado, M.J., Crespo, J., Oms, O., Martín-Martín, J.D., Ibáñez, J., Anadón, P., Gómez de Soler, B., Campeny, G., Agustí, J. (2016a). Bore-hole image techniques applied to identification of chert and dolomite layers in lacustrine sediments. *Geotemas*, 16 (1).

Miró, J., Martín-Martín, J.D., Ibáñez, J., Anadón, P., Oms, O., Tritlla, J., Caja, M.A. (2016b). Opaline chert nodules in maar lake sediments from Camp dels Ninots (La Selva Basin, NE Spain). *Geotemas*, 16 (1): 387-390

Miró, J., Oms, O., Martín-Martín, J.D., Ibañez, J., Anadón, P., Tritlla, J., Gomez de Soler, B., Campeny, G. (2018, this volume). Origin and distribution of silica nodules in the Camp dels Ninots maar (La Selva Basin, NE Spain).

Oms, O., Bolós, X., Barde-Cabusson, S., Martí, J., Casas, A., Lovera, R., Himi, M., Gómez De Soler, B., Campeny Vall-Llosera, G., Pedrazzi, D., Agustí, J. (2015). Structure of the Pliocene Camp dels Ninots maar-diatreme (Catalan Volcanic Zone, NE Spain) *Bulletin of Volcanology*, 77 (11): 98.

Patrick, R. (1977). Ecology of freshwater diatoms and diatom communities. In D. Werner Ed. *The Biology of Diatoms*. Botanical Monographs (Chapter 10, volume 13).

Prikryl, T., Gómez de Soler, B., Campeny, G., Oms, O., Roubach, S., Blain, H.A., Agustí, J. (2016). Fish fauna of the Camp dels Ninots locality (Pliocene; Caldes de Malavella, province of Girona, Spain) – first results with notes on palaeoecology and taphonomy. *Historical Biology*, vol. 28, n°3, pp. 347-357. DOI: 10.1080/08912963.2014.934820.

Robles, S., Barrón, E., Cebolla Lozano, C. (2013). Estudio paleobotánico preliminar del afloramiento plioceno de Camp dels Ninots (Caldes de Malavella, Girona, España). *Macroflora del sector de Can Argilera*. *Boletín de la Real Sociedad Española de Historia Natural. Sección geológica*, 107(1): 75-89

Rodríguez-Salgado, P., Ibáñez, J., Anadón, P., Gómez de Soler, B., Campeny, G., Agustí, J. and Oms, O. (2018). Palaeoenvironmental reconstruction from the mineralogy of the Pliocene Camp dels Ninots maar lake sediments (Catalan Volcanic Zone, NE Iberia). This volume

Vehí, M., Pujadas, A., Roqué, C., Pallí, L. (1999). Un edifici volcànic inèdit a Caldes de Malavella (La Selva, Girona): el Volcà del Camp dels Ninots. *Quaderns de la Selva*, 11. Centre d'Estudis Selvatans, pp. 45-72.



High resolution pCO₂ variations in Lake Averno (Italy)

Nathalie Hasselle¹, Jacopo Cabassi², Franco Tassi^{2,3}, Dmitri Rouwet⁴, Rossella Di Napoli¹, and Alessandro Aiuppa^{1,5}

¹ Dipartimento DiSTeM, Università di Palermo, Palermo, Italy. nathalie.hasselle@unipa.it

² CNR-Istituto di Geoscienze e Georisorse, Via G. La Pira 4, 50121 Florence, Italy.

³ Dipartimento di Scienze della Terra, University of Florence, Via G. La Pira 4, 50121 Florence, Italy.

⁴ Istituto Nazionale di Geofisica e Vulcanologia, Sezione di Bologna, Italy.

⁵ Istituto Nazionale di Geofisica e Vulcanologia, Sezione di Palermo, Italy

Keywords: Lake Averno, pCO₂ variations, HydroC™ CO₂

Lake Averno (0.55 km²; Caliro and al., 2008) is situated in the northwestern part of the Phlegrean Fields caldera, an active volcano in the Naples area (Campania, Italy). The lake formed in the bottom of the homonymous maar soon after the 3,700 BP eruption (Rosi and Sbrana, 1987). The lake is located at the intersection of the dominant NE-SW, San Vito-Averno, and NW-SE, Pozzuoli bay, fault systems (Orsi et al., 1996).

Averno is a meromictic lake, since it shows a permanent vertical thermal and chemical stratification. A thermocline (between 5 to 15 m depth; Cabassi et al., 2013) separates the shallow aerobic epilimnion, affected by seasonal temperature changes, from the anaerobic hypolimnion. This stratification is occasionally broken by rollover events, especially occurring during the winter season, as recorded in 2002, 2003, 2005 and 2017 by fish killing events (Caliro et al., 2008). Fortunately, even if lake water hosts a CO₂- and CH₄-rich dissolved gas reservoir, the total amount of gas that can be released is not sufficient to cause a severe risk for the local population.

The lake is fed by rain and submerged springs and has an outlet towards the sea. A hydrothermal input was regarded as the main source of dissolved CO₂ at depth (Caliro et al., 2008), although CO₂ is also produced by bacterial processes occurring within the lake (Cabassi et al., 2013).

This study presents the first in-situ and continuous pCO₂ measurements carried out at Lake Averno in September 2016 and in July 2017 using a CONTROS HydroC™ CO₂ sensor (CONTROS System and Solutions GmbH, Kiel, Germany). Dissolved CO₂ concentrations are determined by a non-dispersive infrared (NDIR) detector after the gas diffuses through a membrane and equilibrates in the sensor gas stream. In order to increase the response time of the sensor (t₆₃ ~60 s at 25 °C), an external pump was used (SBE 5T, Sea-Bird Electronics) to continuously profiling at low speed (<0.3 m/s).

The HydroC™ CO₂ sensor was constructed to provide a small-sized instrument with a short response time allowing high time and spatial resolution for pCO₂ measurements in seawater. Here, we present the first application of this sensor in a lake. Due to its measurement range limitation (pCO₂ < 6000 μatm), this probe can only be used in waters which do not contain higher amounts of CO₂. However, in contrast to other methods (e.g. pCO₂ determination from punctual water samples), the probe allows detecting even

small pCO₂ values with a high accuracy.

pCO₂ values were measured along (i) vertical profiles at the center of the lake and (ii) patterns at fixed depth. Unfortunately, due to the limited pCO₂ measuring range of the sensor, we were not able to complete a vertical profile to the lake bottom (33 m depth). The CO₂ partial pressure in the epilimnion and in the thermocline was higher in July 2017 than in September 2016. In 2016, we measured ~2500 μatm of pCO₂ at 12.5 m depth. On the contrary in 2017, we measured similar partial pressures at 5 m depth. The higher CO₂ partial pressures in July 2017 only partially reflect incomplete dissolved CO₂ re-equilibration with the atmosphere, after the lake overturned in January 2017. It could also be explained by lower CO₂ consumption by photosynthesis in the early summer. The horizontal pCO₂ profiles were measured in the anoxic part of the lake, at 15 m (in 2016) and 5 m (in 2017) depth. The results show variations from 3300 to more than 4000 μatm in 2016 and from 2000 to more than 6000 μatm in 2017 and suggest depth variations of isoconcentration water layers. Smaller CO₂ peaks could also be attributed to a local higher organic production.

In addition to the high pCO₂ resolution, spatial investigations could be done easily in other lakes, in order to identify areas of higher CO₂ concentrations; to determine the shape of the surface of isoconcentration water layers or also to localize faults through which deep CO₂ enters at the bottom of the lake in poorly concentrated lakes.

References

- Cabassi, J., Tassi, F., Vaselli, O., Fiebig, J., Nocentini, M., Capecchiacci, F., ... & Biccocchi, G., 2013. Biogeochemical processes involving dissolved CO₂ and CH₄ at Albano, Averno, and Monticchio meromictic volcanic lakes (Central–Southern Italy). *Bulletin of volcanology* 75(683).
- Caliro, S., Chiadini, G., Izzo, G., Minopoli, C., Signorini, A., Avino, R., & Granieri, D., 2008. Geochemical and biochemical evidence of lake overturn and fish kill at Lake Averno, Italy. *Journal of Volcanology and Geothermal Research* 178(2): 305-316.
- Orsi, G., De Vita, S., & Di Vito, M., 1996. The restless, resurgent Campi Flegrei nested caldera (Italy): constraints on its evolution and configuration. *Journal of Volcanology and Geothermal Research* 74(3-4): 179-214.
- Rosi M., Sbrana A. Eds., 1987. Phlegrean Fields. CNR Quaderni Ricerca Scientifica 114, Roma, 167 p.

Event Sedimentation in Maar Lakes – the Change in Monotony

Peter Suhr

Senckenberg Naturhistorische Sammlungen Dresden, Königsbrücker Landstraße 159; 01109 Dresden, Germany Peter.Suhr@senckenberg.de

Keywords: event sedimentation, lake phases, mass flows

Maar lake sediments usually develop under meromictic conditions, thus preserving the typical seasonally controlled fine lamination. These so-called “normal” sediments mostly consist of autogenic remains of different types of algae and fine dust from the surroundings of the maar lake. The prevailing stable depositional environment characterizing maar lake deposits is superbly mirrored by the uniformity of their sedimentary record. Episodically intercalated event sediments, transported by different processes from the lake margin to its center, might represent the only variation within this monotony.

Each phase of lake development is indicated by its own type of event sediment. Pirrung et al. (2003) gave a subdivision of maar lake sediments into lithozones.

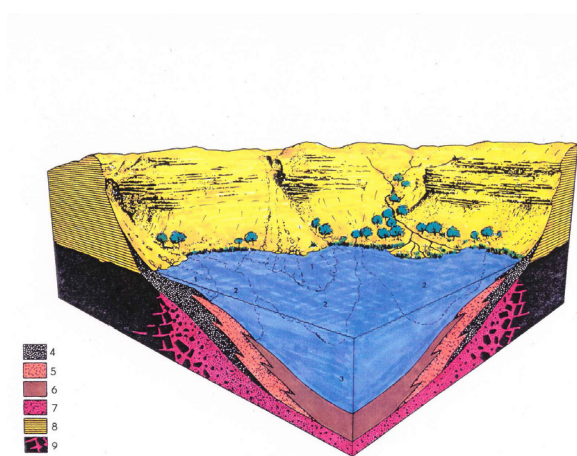


Fig. 1 - Maar lake with sediment types after Smith (1986). 4. debris flow deposits; 5. turbidites; 6. normal sediment; 7. collapse breccia; 8. ring wall; 9. country rock

The initial lake phase consists of the lithozones B, C and D1 (following Pirrung et al. 2003) showing a duration of some decades to hundreds of years. Event sediments of this interval are collapse breccias, grain flow deposits and minerogenic turbidites. Collapse breccias occur in maar structures, which formed in solid rocks like granite, sandstone etc. In contrast, the maar craters, which developed in soft sediments, e.g. sand, have typical champagne glass-like forms and no collapse breccias can be recognized. Grain flows result from air fall lapilli and their following redeposition into the lake.

The minerogenic turbidites characteristically represent the time-span, when no biogenic production occurs in the lake. During the initial lake phase, the crater wall is very steep and not vegetated, so rainwater can wash the ring wall deposits direct into the lake. Debris fans are formed subaerial and in the littoral zone. Parts of their unstable steep slopes episodically slip down into deeper water generating debris flows and turbidity currents. These mass flows can reach also the center of the lake.

Autochthonous biogenic production starts with the stable lake phase comprising lithozones D2 and D3. Within this stage, the remains of the ring wall already are covered by vegetation. Therefore, strong erosion can only be caused by heavy rainfall or by cutting the wall in consequence of headwater erosion. Due to continuous subsidence of the lake bottom resulting from compaction of the diatreme fill (Suhr et al. 2006), the marginal parts of the lake bottom overstep and further cause debris flows as well as turbidity currents. The latter only can reach as far as the central area of the lake. Turbidites of this interval always consist of minerogenic particles from the remains of the ring wall and of greater portions of redeposited organic lake sediments. This organic material could be dispersed in suspension or transported in clods.

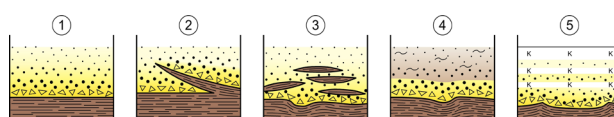


Fig. 2 - Different types of lake turbidites. 1. normal graded minerogenic turbidite; 2. rip up structures of consolidated lake sediments; 3. turbidite with clods of consolidated lake sediments; 4. turbidite with resuspended lake sediments in the upper part; 5. Multiple turbidites. K – bright kaolinitic layers.

Some bigger events can have enough energy to trigger turbidity currents, which run up the opposite slope and return forming multiple turbidites. During the stable lake phase, also different types of slumps and slides appear. These types of event sedimentation originate from redeposition due to gravitational instability along shear planes.

The content of the normal sedimentation gradually increases and the event sediments only make an exception. They could be found within the fine-grained and laminat-

ed normal sediments representing dewatering structures (e.g. loops, sedimentary dikes) caused by compaction processes. Rarely, little sand volcanoes have been observed on the bedding planes.

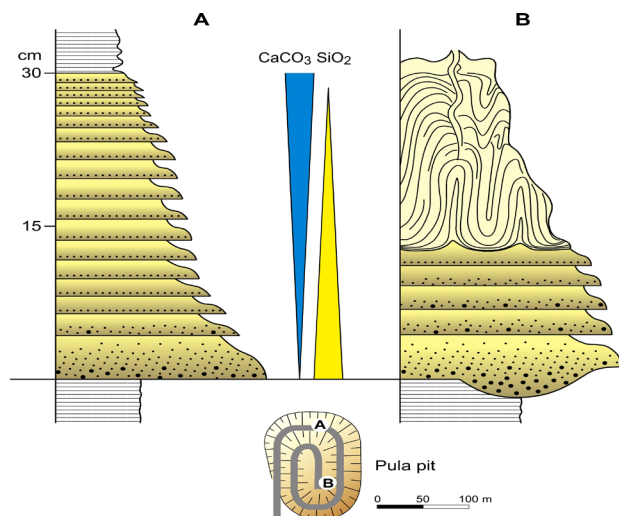


Fig. 3 - Multiple turbidite in the Pula maar (A) with dewatering structures and sand volcanoes (B) in the central part of the maar lake. After Nemeth et al. (2008)

Acknowledgements

Herbert Lutz (Mainz) is acknowledged for discussion and information about the event sediments in the Eckfeld maar lake (Eifel Mt.). Nadine Janetschke (Dresden) is kindly thanked for linguistic correction of the text.

References

Pirrung, M., Fischer, C., Büchel, G., Lutz, H. & Neuffer, F.-O. 2003: Lithofacies succession of maar crater deposits in the Eifel area (Germany). *Terra Nova* 15: 125–132.

Smith, R.M.H. 1986: Sedimentation and palaeoenvironment of the late Cretaceous crater-lake deposits in Bushmanland, South Africa. *Sedimentology* 33: 369–386.

Suhr, P., Goth, K., Lorenz, V. & Suhr, S. 2006: Long lasting subsidence and the deformation in and above maar - diatreme volcanoes – a never ending story. *Zeitschrift der Deutschen Gesellschaft für Geowissenschaften* 157: 491–511.

Németh, K., Goth, K., Martin, U., Csillag, G. & Suhr, P. 2008: Reconstructing paleoenvironment, eruption mechanism and paleomorphology of the Pliocene Pula maar, (Hungary). *Journal of Volcanology and Geothermal Research* 177: 441–456.

Enhanced contribution of ENSO to the East Asian Winter Monsoon in Northeast China since the Mid-Holocene

Jing Wu^{1,2}, Qiang Liu^{1,2}, Qiaoyu Cui³, Deke Xu^{1,2}, Guoqiang Chu^{1,2}, and Jiaqi Liu^{1,2}

¹ Key Laboratory of Cenozoic Geology and Environment, Institute of Geology and Geophysics, Chinese Academy of Sciences, Beijing, China. wujing@mail.iggcas.ac.cn

² Institutions of Earth Science, Chinese Academy of Sciences, Beijing, China.

³ Key Laboratory of Land Surface Pattern and Simulation, Institute of Geographical Sciences and Natural Resources Research, Chinese Academy of Sciences, Beijing, China.

Keywords: El Niño, palynology, volcanic lakes

The East Asian winter monsoon (EAWM) is the most active and powerful atmospheric circulation system during the Northern Hemisphere winter. The EAWM may have a global impact through its effects on the Walker circulation. Previous studies have indicated that the EAWM and the El Niño-Southern Oscillation (ENSO) are tightly coupled (An et al., 2017; Zhou et al., 2007). Generally, an El Niño event weakens the EAWM leading to a positive surface temperature anomaly across most parts of China through changes in anticyclonic circulation over the northwestern Pacific during the boreal winter, which is reversed in La Niña years (Cheung et al., 2012). On the other hand, a stronger (weaker) EAWM promotes the occurrence and development of El Niño (La Niña) events (Zhou et al., 2007).

On the interdecadal to decadal timescale, meteorological observations indicate a significant correlation between ENSO and EAWM (He and Wang, 2013; Kim et al., 2016; Wang et al., 2012a). Much effort has been made to understand the long-term variability of the EAWM using records from loess-paleosol sequences, lacustrine sediments, stalagmites and marine sediments. On longer time scales, however, only a few studies have examined possible links between ENSO and the EAWM based on climate model simulations and sediment records from low latitude regions (Zheng et al., 2014). In addition, there is a distinct lack of records from the most active region of the EAWM such as the mid-high latitudes of continental Asia.

The distribution of modern vegetation in Northeast China is significantly influenced by winter temperatures; for example, the boundary between the boreal forest and temperate deciduous forest, such as on the eastern margin of the Great Khingan Mountain Range, is largely determined by winter temperature. Here, we present a winter-temperature-sensitive pollen record from a Holocene lake sediment core from a volcanic lake, Northeast China to reconstruct the evolution of the EAWM in the Holocene, and to investigate the teleconnection between the EAWM and the ENSO on centennial/millennial timescales.

Lake Moon (47°30.36'N, 120°51.99'E, 1190 m above sea level) is in the Arxan-Chaihe volcanic field in the central part of the Great Khingan Mountain Range (Fig. 1). The surface area is ~0.03 km², the maximum water depth is 6.5 m, and there is no inflow or outflow. The vegetation surrounding Lake Moon is boreal deciduous broadleaf-conifer mixed forest, dominated by *Larix gmelinii* (Dahurian larch), *Betula platyphylla* (Siberian silver birch) and *B. dahurica* (Asian black birch), which can resist the long cold winter.

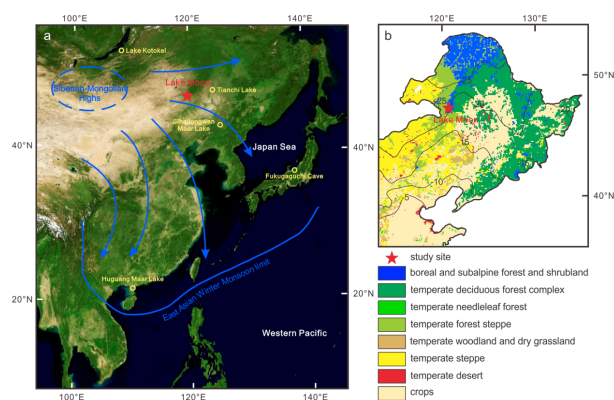


Fig. 1 – a. Location of the study site and other palaeoclimatic records mentioned in the text. The trajectory of the EAWM is indicated by blue arrows. b. Distribution of vegetation within the study region (Wang et al., 2013); winter temperature contours are in degrees C.

272 pollen samples from Lake Moon were analyzed for palynology, spanning the last 10.8 cal ka BP, with an average time resolution was 40 a. A simplified pollen diagram for Lake Moon is presented in Figure 2. The most prominent of which is the significantly higher frequencies of *Pinus* and *Quercus* since ca. 6.0 ka cal BP compared to their extremely low representation in the early Holocene. The temperate forest trees such as *Pinus* and *Quercus*, which are only sporadically present in the Great Khingan Mountain Range at

the present day, are damaged by spontaneous ice nucleation below -40°C ; thus, the winter temperature is a crucial limiting factor for their survival in mid-high latitude regions. Therefore, the immigration of *Pinus* and *Quercus* into the cold temperate boreal forest represents an increase in the winter temperature, and is linked to the weakening of the EAWM.

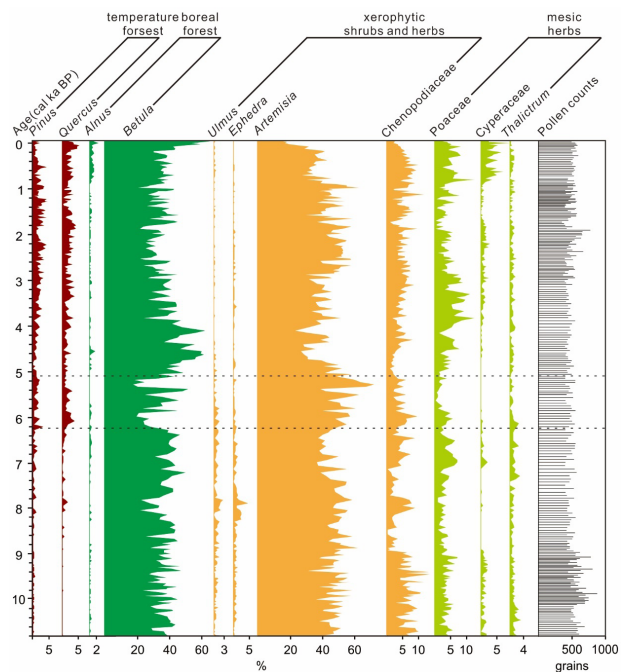


Fig. 2 – Simplified pollen percentage diagram for Lake Moon.

The increasing percentages of *Pinus* and *Quercus* at Lake Moon clearly demonstrate the weakening of the EAWM since ~ 6.0 ka cal BP. This trend is consistent with that of increasing winter (December-January-February) insolation at the latitude of study site throughout the entire Holocene (Fig. 3 f), which provides a partial explanation for the warmer winter temperatures in Northeast China after ~ 6.0 ka cal BP.

Secondly, the sea surface temperature (SST) of the western tropical Pacific Ocean could also affect the intensity of the EAWM. The SST in the western tropical Pacific Ocean has dropped $\sim 0.5^{\circ}\text{C}$ over the past 10.0 ka BP (Fig. 3 e). The cooling SST would reduce the land-sea thermal contrast between Pacific and Siberian air masses in winter, which weaken the strength of the EAWM under the assumption of constant Siberian high.

However, the relatively gradual changes in winter insolation and the SST of the western tropical Pacific Ocean cannot entirely explain the relatively abrupt weakening of the EAWM at 6-5 ka cal BP. Thus, other potential factors, like ENSO variability on centennial/millennial timescales need to be considered (Fig. 3 c, d; Cobb and Charles, 2013; Moy et al., 2002). Highly significant relationships between percentages of *Pinus*, *Quercus* and frequencies of El Niño events reveal a relatively strong relationship between the EAWM and ENSO events on centennial/millennial timescales.

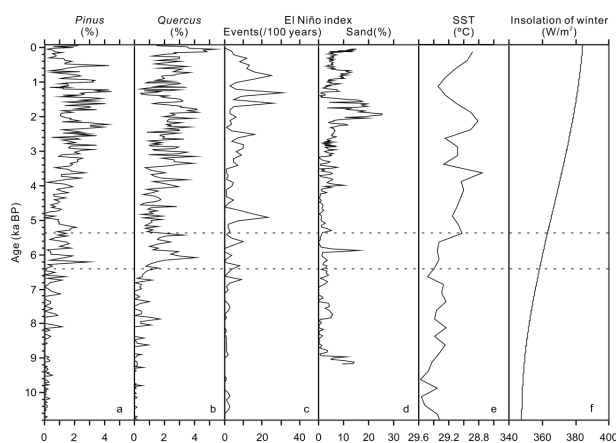


Fig. 3 – Comparison between the records of *Pinus* (a) and *Quercus* (b) from Lake Moon with two ENSO indices (c, d; revised from Cobb and Charles, 2013; Moy et al., 2002), SST record from the western tropical Pacific (e; revised from Stott et al., 2004) and winter insolation at 45°N (f; revised from Berger and Loutre, 1991).

A continuous high-resolution record of winter temperature since 10.8 ka BP was obtained on the changes in the frequencies of *Pinus* and *Quercus* pollen in the sediments of Lake Moon, in Northeast China. The data provide a robust record of changes in EAWM intensity in the mid-high latitude region of the EAM and it extends the timescale of a teleconnection between El Niño events and the EAWM from interannual/interdecadal to centennial/millennial.

Acknowledgements

This research was supported by the National Natural Science Foundation of China (41572353; 41202259; 41272392; 40872206; 41320104006 and 41561144010).

References

- An, S.-I., Kim, H.-J., Park, W., Schneider, B., 2017. Impact of ENSO on East Asian winter monsoon during interglacial periods: effect of orbital forcing. *Climate Dynamics*: 1-11.
- Cobb, K.M., Charles, C.D., 2013. Highly variable El Niño-Southern Oscillation throughout the Holocene. *Science* 339: 67-70.
- Moy, C.M., Seltzer, G.O., Rodbell, D.T., Anderson, D.M., 2002. Variability of El Niño/Southern Oscillation activity at millennial timescales during the Holocene epoch. *Nature* 420, 162-165.
- Zheng, X., Li, A., Wan, S., Jiang, F., Kao, S.J., Johnson, C., 2014. ITCZ and ENSO pacing on East Asian winter monsoon variation during the Holocene: Sedimentological evidence from the Okinawa Trough. *Journal of Geophysical Research Oceans* 119: 4410-4429.
- Zhou, W., Wang, X., Zhou, T.J., Li, C., Chan, J.C.L., 2007. Interdecadal variability of the relationship between the East Asian winter monsoon and ENSO. *Meteorology and Atmospheric Physics* 98: 283-293.



Palaeo-environmental impact of last volcanic eruptions in the Iberian Peninsula: preliminary multi-proxy analysis results from Pla de les Preses palaeolake (Vall d'en Bas, La Garrotxa, NE Iberia)

Jordi Revelles¹, Eneko Iriarte², Walter Finsinger³, Francesc Burjachs^{4,5,6}, Gabriel Alcalde⁷, and Maria Saña¹

¹ *Departament de Prehistòria, Universitat Autònoma de Barcelona, Fac. de Filosofia i Lletres, Edifici B, 08193 Bellaterra, Barcelona, Spain. jordi.revelles@uab.cat*

² *Laboratorio de Evolución Humana, Departamento Ciencias Históricas y Geografía, Universidad de Burgos, Plaza Misael Bañuelos, Edificio I+D+i, 09001 Burgos, Spain*

³ *Palaeoecology, ISEM (UMR 5554 CNRS/UM/EPHE/IRD), Montpellier, France*

⁴ *Institut Català de Recerca i Estudis Avançats (ICREA), Passeig Lluís Companys 23, 08010 Barcelona, Spain*

⁵ *Institut Català de Paleoecologia Humana i Evolució Social (IPHES), Zona Educacional 4 - Campus Sescelades URV (Edifici W3), 43007 Tarragona, Spain*

⁶ *Universitat Rovira i Virgili, Carrer de l'Escorxador, s/n, 43003 Tarragona, Spain*

⁷ *Departament Història i Història de l'Art, Universitat de Girona, 17071 Girona, Spain*

Keywords: palaeolake, volcanic eruptions, La Garrotxa.

Successive obstructions of Fluvià river by lava flows lead to the configuration of a lake in the deepest part of the valley in Vall d'en Bas (La Garrotxa, NE Iberia). Last obstruction would be associated with the most recent eruptions known to date, Croscat in 15710-13160 cal BP (Puiguirguer et al., 2012) and Puig Jordà, 17000 BP (Bolós et al., 2014). Nevertheless, recent studies in a core extracted from Vall d'en Bas provided younger evidence about the last eruption in the volcanic area of La Garrotxa, dated in the Late Glacial-Holocene transition.

In this work we present the preliminary results of a 15 m length core (PdP- Pla de les Preses core, Vall d'en Bas, Girona) covering the Late Pleistocene-Holocene transition. Multi-proxy analyses (chronostratigraphy, sedimentology, XRF geochemistry, sedimentary charcoal and macrofossils) enabled the reconstruction of palaeo-environmental evolution during the Late Pleistocene-Holocene transition and allowed the identification of volcanic eruptions in La Garrotxa volcanic region (Girona, NE Iberia). One of the main aims of this study is the evaluation of human-environment interactions during Mesolithic and probable environmental constraints for the development of last hunter-gatherers communities in NE Iberia. Interdisciplinary data enabled the reconstruction of local-scale environmental impact by rapid climate change episodes and by volcanic eruptions, in terms of sedimentary changes and the occurrence of fire episodes. Pla de les Preses core represents an outstanding record that in the near future will provide essential data to understand palaeo-environmental dynamics and ecological changes in the period of last volcanic eruptions in the area of La Garrotxa, as well as can furnish an explanation for the gap of population during the Late Mesolithic in this region.

References

Bolós, X.; Planagumà, LL. and Martí, J. 2014. Volcanic stratigraphy of the Quaternary La Garrotxa Volcanic Field (NE Iberian Peninsula). *Journal of Quaternary Science*, 29 (6), 547-560.

Puiguirguer, M.; Alcalde, G.; Bassols, E.; BURJACHS, F.; Expósito, I.; Planagumà, LL.; Saña, M. & Yll, E. 2012. 14C dating of the last Croscat volcano eruption (Garrotxa Region, NE Iberian Peninsula), *Geologica Acta*, 19 (1), 43-47.

Millennial and centennial-scale climatic variability recorded in the sediments of Laguna Azul (southern Patagonia, Argentina)

Bernd Zolitschka¹, Stephanie Janssen², Nora I. Maidana³, Christoph Mayr^{4,5}, Torsten Haberzettl⁶, Hugo Corbella⁷, Andreas Lücke⁸, Christian Ohlendorf¹, Frank Schäbitz²

¹ Universität Bremen, Institut für Geographie, GEOPOLAR, Celsiusstr. 2, 28359 Bremen, Germany. zoli@uni-bremen.de

² Universität zu Köln, Institut für Geographiedidaktik, Gronewaldstr. 2, 50931 Köln, Germany.

³ Universidad Nacional de Buenos Aires - CONICET-UBA, Ciudad Universitaria, Buenos Aires, Argentina.

⁴ Ludwig-Maximilians-Universität, GeoBio-CenterLMU und Department für Geo- und Umweltwiss., 80333 München, Germany.

⁵ Friedrich-Alexander-Universität Erlangen-Nürnberg, Institut für Geographie, Wetterkreuz 15, 91058 Erlangen, Germany.

⁶ Friedrich-Schiller-Universität Jena, Institut für Geographie, Physische Geographie, Löbdergraben 32, 07743 Jena, Germany.

⁷ Museo Argentino de Ciencias Naturales Bernardino Rivadavia, Av. Angel Gallardo 470, C1405DJR, Buenos Aires, Argentina.

⁸ Forschungszentrum Jülich, Institut für Bio- und Geowissenschaften, IBG-3: Agrosphäre, 52425 Jülich, Germany

Keywords: Southern Hemispheric Westerlies, crater lake, lake-level fluctuations, ectogenic meromixis, Pali Aike Volcanic Field.

Laguna Azul is one of two permanent lakes in extra-Andean southeastern Patagonia (52°05' S, 69°35' W, 100 m asl) and located 25 km N of the Strait of Magellan (Zolitschka et al., 2006). This crater lake is part of the Pliocene to Late Quaternary Pali Aike Volcanic Field (PAVF). Alkali basaltic and basaltic magmas deposited on molasse-type sediments of the Late-Miocene Santa Cruz Formation and on Plio-/Pleistocene glaciofluvial sediments characterize the volcanism of the PAVF (Ross et al., 2011; Coronato et al., 2013).

The volcanic edifice of Laguna Azul is located at the northern end of a 5 km long NW-SE trending fault zone. The main crater exhibits a complex history of explosive and effusive volcanism. Spatter, scoria and lapilli erupted and formed a pyroclastic ring wall 850 m in diameter, which rises ca. 10-20 m above the surrounding terrain. The central depression of the crater formed by gravitational collapse after phreatomagmatic explosions during an early maar stage. With a second Strombolian eruption, agglutinated spatter was produced followed by more effusive activity that formed a lava lake in the depression. High magma production caused lava overspill through a channel to the N creating a lava flow (Corbella et al., 2009). At the end of this eruptive phase, lava drained back into the vent. The morphometry of the depression exhibits several overlapping sub-basins located mainly along the NW-SE oriented alignment. The rugged morphology of the crater in which Laguna Azul is situated and the well-preserved pyroclastic ring wall point to a rather young monogenetic volcanic system (Németh & Kereszturi, 2015). This is supported by the ⁴⁰Ar/³⁹Ar age of the basaltic lava flow dated to 0.01 ± 0.02 Ma (Corbella, 2002).

After volcanic activities have ceased, a crater lake established in the depression. Today, the lake is elliptical in shape with a length of 560 m, a width of 240 m and a maximum water depth of 56 m. Located 50-60 m below the crater rim, the lake surface is sheltered from the west-

erly winds. The catchment area (0.24 km²) is restricted to the inner crater walls and small in relation to the lake's surface (0.15 km²). Laguna Azul is dimictic and holomictic and neither has a tributary nor an outlet – it is a ground-water-fed terminal lacustrine system.

Continuous logging of limnological parameters from March 2002 to February 2005 document a stratified water body with a well-developed metalimnion during southern summer (Mayr et al., 2005; Zolitschka et al., 2006; Messyasz et al., 2007). Epilimnic pH values during summer range between 8.5 and 9.0, electric conductivity averages 443 µS cm⁻¹ and salinity is 0.3 ‰. These values are comparable to measurements in nearby wells (Zolitschka et al., 2006). Based on limnological parameters the modern lake classifies as mesotrophic to eutrophic (Messyasz et al., 2007).

Laguna Azul is situated in the dry Magellanic grass steppe. The nearest subantarctic deciduous forests dominated by southern beech (*Nothofagus*) occur at the foothills of the Andes about 160 km to the W. Prevalence of Southern Hemispheric Westerly (SHW) winds distinguishes the climate of extra Andean southeastern Patagonia and causes the rain-shadow effect of the Andes. This setting results in a cool-temperate (6-7 °C mean annual temperature) and semiarid (200-300 mm of annual rainfall) semi-desert with extremely windy and highly evaporative conditions (Garreaud et al., 2013).

According to the radiocarbon-based age-depth model, the oldest lacustrine sediments recovered by piston coring date to 11,790 +390/-720 cal. BP and provide a minimum age for the termination of volcanic activity. Pollen-stratigraphy narrows down this timing by elaborating a Lateglacial pollen assemblage, i.e. a maximum age of ca. 15,000 cal. BP. Additionally, high-resolution multiproxy investigations (physical properties, sedimentology, mineralogy, geochemistry, stable isotopes, pollen, diatoms)

of the lacustrine sediment infill from Laguna Azul were carried out for climatic and environmental interpretation.

We interpret long-distant pollen transport of *Nothofagus* (after reestablishment of southern beech forest during the Lateglacial in the foothills of the Andes) as a direct signal of intensity and position of the SHW. This dominating climatic feature is of regional importance, but also controls global temperatures by influencing the air-to-sea CO₂ flux in the Southern Ocean (Mayr et al., 2013). The *Nothofagus* pollen record of Laguna Azul shows a millennial-scale variability. More intense SHW occurred between 10,100-8300 and since 3000 cal. BP. Weaker SHW under less arid conditions with development of a deep freshwater lake dominated between 8300 and 3000 cal. BP. Especially during the Early Holocene, SHW intensification was very pronounced and accompanied by strong anoxia (ectogenic meromixis) in the hypolimnion of Laguna Azul.

Centennial-scale climate variability overprinted this low-frequency signal since ca. 4000 cal. BP, i.e. with the onset of Neoglaciation. Simultaneously, a regional drop in mean annual (chironomid-based) temperature occurred from 12.2 °C during the Middle Holocene to 10.5 °C for the Late Holocene (Massaferro & Larocque-Tobler, 2013). This Late Holocene centennial variability, recorded by calcite maxima, is indicative for periods with low lake levels. Dry spells and/or windy periods are centered around 3700, 2200 and 1000 cal. BP as well as in the 20th century. Furthermore, we recognized the Little Ice Age (LIA) by increased precipitation as inferred by pollen-based reconstruction of rainfall, maximum expansion of local vegetation (high amounts of Poaceae pollen) and a decrease in minerogenic deposition.

In conclusion, we detected a superior climatic control on Holocene hydroclimatic conditions dominated by position and strength of the SHW. They overprinted the lake's ontogeny with impacts on the stratification type of the water column as well as on lake-level fluctuations with feedbacks on lakeshore erosion, algal communities, trophic conditions and authigenic mineral formation. Most likely, this variability is following an astronomical forcing, i.e. solar insolation. Superimposed on these millennial SHW fluctuations, Laguna Azul recorded a centennial variability for the Late Holocene. Although less arid periods are evident between these dry spells, the only distinctly moister period is representative for the LIA. Different from variations of the SHW, these centennial fluctuations are regionally synchronous for southern South America and the Northern Hemisphere. Changes in solar activity, large volcanic eruptions and/or modulations of ocean circulation are potential triggers.

Acknowledgements

This is a contribution to the "South Argentinean Lake Sediment Archives and modeling" (SALSA) project, funded in the framework of the German Climate Research Program (DEKLIM grants 01 LD 0034 and 0035) of the German Federal Ministry of Education and Research. The German Science Foundation (DFG) in the framework of the Priority Program 'ICDP' (grants ZO 102/5-1, 2, 3 and SCHA 472/12-1, 2) provided additional financial support.

References

- Corbella, H., 2002. El campo volcánico-tectónico de Pali Aike. In: Haller, M., ed., *Geología y Recursos Naturales de Santa Cruz*. Asociación Geológica Argentina, Buenos Aires, 285-302.
- Corbella, H., Ercolano, B., Tiberi, P., 2009. Laguna Azul: a unique volcanic lagoon in Pali Aike Holocene eruptive terrains, Patagonia Austral, Argentina. In: M.J. Haller, Massaferro, G.I., eds., *Third International Maar Conference*, 14-17 April 2009. Publicaciones Especiales, Resúmenes y Eventos. Asociación Geológica Argentina, Malargüe, Argentina, 17-18.
- Coronato, A. et al., 2013. Glacial, fluvial and volcanic landscape evolution in the Laguna Potrok Aike maar area, southernmost Patagonia, Argentina. *Quaternary Science Reviews* 71, 13-26.
- Garreaud, R. et al., 2013. Large-scale control on the Patagonian climate. *Journal of Climate* 26, 215-230.
- Mayr, C. et al., 2005. Palaeoenvironmental changes in southern Patagonia during the last millennium recorded in lake sediments from Laguna Azul (Argentina). *Palaeogeography, Palaeoclimatology, Palaeoecology* 228, 203-227.
- Mayr, C. et al., 2013. Intensified Southern Hemisphere Westerlies regulated atmospheric CO₂ during the last deglaciation. *Geology* 41, 831-834.
- Massaferro, J., Larocque-Tobler, I., 2013. Using a newly developed chironomid transfer function for reconstructing mean annual air temperature at Lake Potrok Aike, Patagonia, Argentina. *Ecological Indicators* 24, 201-210.
- Messyasz, B. et al., 2007. Summer phytoplankton and the hydrochemistry of the crater lake Laguna Azul (Santa Cruz, Argentina). *Oceanological and Hydrobiological Studies - International Journal of Oceanography and Hydrobiology XXXVI (Supplement 1)*, 95-105.
- Nemeth, K., Kereszturi, G., 2015. Monogenetic volcanism: personal views and discussion. *International Journal of Earth Sciences* 104, 2131-2146.
- Ross, P.-S. et al., 2011. Influence of the substrate on maar-diatreme volcanoes - an example of a mixed setting from the Pali Aike volcanic field, Argentina. *Journal of Volcanology and Geothermal Research* 201, 253-271.
- Zolitschka, B. et al., 2006. Crater lakes of the Pali Aike Volcanic Field as key sites for paleoclimatic and paleoecological reconstructions in southern Patagonia, Argentina. *Journal of South American Earth Sciences* 21, 294-309.

Joya de Yuriria maar (Guanajuato, Mexico): Geological, tectonic and paleo-hydrogeological environment

Pooja Kshirsagar¹, Norma Maritza Arriaga Hernández¹, Claus Siebe², Marie Noëlle Guilbaud² and Raúl Miranda-Avilés¹

¹Departamento de Ing. en Minas, Metalurgia, Geología y Ambiental, División de Ingenierías, Sede San Matías, Universidad de Guanajuato, Campus Guanajuato, México, pv.kshirsagar@ugto.mx

²Departamento de Vulcanología, Instituto de Geofísica, Universidad Nacional Autónoma de México, Ciudad Universitaria, Ciudad de México, México

Keywords: Maar volcano, paleo-hydrogeology, Michoacán-Guanajuato Volcanic Field, Quaternary

The Joya de Yuriria maar volcano, also known as Yuririapúndaro (Blood Lake in Purépecha, the language of the Tarascan people in central Mexico) probably derives its name from the red color produced by occasional algal blooms in its shallow crater lake. It is situated at the southern margin of the Yuriria inter-montane lake basin and is one of the 22 phreatomagmatic vents within the ~40,000 km² wide Plio-Quaternary Michoacán-Guanajuato Volcanic Field (MGVF), which includes >1000 scoria cones and associated lava flows, ~400 medium-sized shield volcanoes, and several dozen domes. This field also hosts the famous historical eruption (1943-52) of Parícutin volcano (Hasenaka and Carmichael, 1985; Guilbaud et al., 2011, 2012; Kshirsagar et al., 2015, 2016).

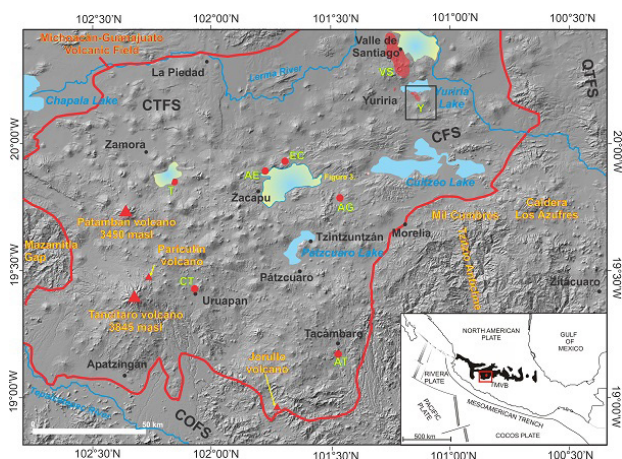


Figure 1. Location of the Joya de Yuriria and San Pedro maars at the margin of the lower slopes of El Capulín and Santiago shields.

The spatial and temporal occurrence of phreatomagmatic vents such as Joya de Yuriria depends on a balance between internal (magma composition, magmatic flux, ascent rate, viscosity, volatile content) and external (regional tectonics, topography, availability of surface and/or groundwater) factors, which in turn also influence the morphology and eruptive style of phreatomagmatic volcanoes such as tuff-cones, tuff-rings, and maars (Keresz-

turi and Németh, 2012). Here we first outline the geologic setting (tectonics, and volcanic stratigraphy) of the maar volcano and subsequently describe the sedimentological characteristics (sorting, grain-size distribution, compaction) of its deposits and the petrography and geochemistry of juvenile clasts, lava flows, xenoliths, and older volcanics occurring in its surroundings. All this information is then integrated to define the local paleo-hydrogeological environment that existed during the formation of this maar volcano.

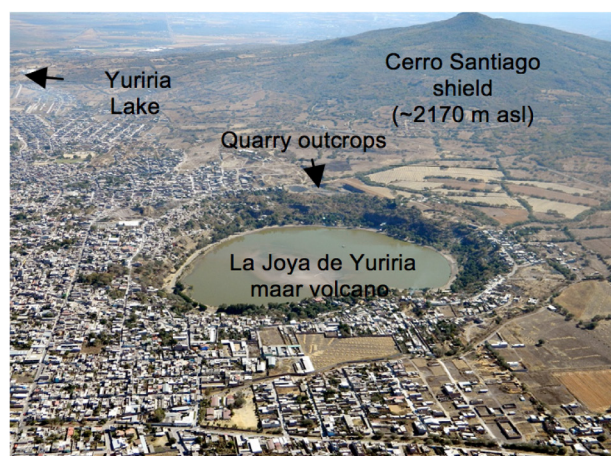


Figure 2. Aerial view of Joya de Yuriria maar lake from the west. Cerro Santiago shield volcano and key outcrops (arrows) are also shown.

The Joya de Yuriria maar crater is slightly elongated in a NW-SE direction with a rim-to-rim diameter of ~0.9 km and a crater height of ~60 m above the crater lake level (Fig. 2). It is located on the northern distal flanks of two older Pliocene/Early Quaternary (?) medium-sized El Capulín and Santiago shields (Figs. 1 and 2). Lavas of the Santiago shield are exposed as steep cliffs at the inner walls of the maar crater, where they are covered by a decameter-thick sequence of phreatomagmatic surge and fallout deposits (Fig. 3), which were studied in detail at two abandoned proximal quarries and at one distal location (Figs. 2 and 3). The tephra sequence consists of planar beds of clast-

supported, friable, lithic-rich, poorly sorted material with a poly-modal grain-size distribution ($Md\phi=0.35$ to -6.05 , $\sigma\phi=1.10$ to 3.28) with scarce juvenile clasts (<20 vol.%) of basaltic andesite ($SiO_2=54.4$ wt%, $Na_2O+K_2O=5.21$ wt%). The angular xenoliths range from 100 to few cm in diameter and are moderately vesicular to dense andesitic and basaltic andesite fragments of lava from the older underlying shield lava flows.



Figure 3. Quarry near crater rim exposing well-bedded, friable, coarse phreatomagmatic surge and fallout deposits dominated by angular accidental lithics from the underlying older shield lavas. Juvenile andesite clasts (cauliflower-type bombs) are occasionally present.

Geochemical and textural data confirm that the lava flows exposed at the inner crater wall belong to the Santiago shield volcano (also andesitic in composition: $SiO_2=57.4$ - 60 wt%, $Na_2O+K_2O=5.8$ - 6.0 wt%). These lava flows must have served as shallow aquifers that provided sufficient groundwater toward the vent (ascending dike) to allow for continuous magma-water interactions (fuel-coolant ratio of ~ 0.2) to successfully maintain the phreatomagmatic explosive nature of the eruption throughout the entire period of activity.

Previous studies have indicated that an optimal magma/water ratio requires favorable supply conditions that are determined by the local and regional paleo-hydrogeological framework, including climate, topography, tectonic configuration, etc. as well as an optimal magma discharge rate (all of which can be deciphered to a certain degree by applying methods outlined in Kshirsagar et al. 2015, 2016). The nearby occurrence of the remnants of the older San Pedro maar, located only 2 km to the NW of Joya de Yuriria (Fig. 1), indicates that conditions at the lower slopes of the Capulin and Santiago shields must have been optimal during repeated time periods. The general scarcity of phreatomagmatic vents in the MGVF suggests that favorable conditions were rarely met during the Quaternary (characterized by rapid climate changes) and the present study is aimed at better understanding monogenetic volcanism and its diverse eruptive styles within the MGVF in the context of its complex relationship with changing environmental conditions (namely paleo-hydrogeology).

Acknowledgements

Field and laboratory costs were defrayed from projects funded by Programa para el Desarrollo Profesional Docente (PRODEP 2017- 511-6/17-8074 to P. Kshirsagar and UNAM-DGAPA-IN103618 to C. Siebe.

References

Guilbaud, M.-N., Siebe, C., Layer, P., Salinas, S., Castro-Govea, R., Garduño-Monroy, V. H., Corvec, N. L., 2011. Geology, geochronology, and tectonic setting of the Jorullo Volcano region, Michoacán, México. *Journal of Volcanology and Geothermal Research* 201, 97-112. doi:10.1016/j.jvolgeores.2010.09.005 670.

Guilbaud, M. N., Siebe, C., Layer, P., Salinas, S., 2012. Reconstruction of the volcanic history of the Tacámbaro-Puruarán area (Michoacán, México) reveals high frequency of Holocene monogenetic eruptions. *Bulletin of Volcanology* 74(5), 1187-1211. doi:10.1007/s00445-012-0594-0.

Hasenaka, T., Carmichael, I. S. E., 1985. The cinder cones of Michoacán-Guanajuato, central Mexico: their age, volume and distribution, and magma discharge rate. *Journal of Volcanology and Geothermal Research* 25, 105-124.

Kereszturi, G., Németh, K., 2012. Monogenetic basaltic volcanoes: genetic classification, growth, geomorphology and degradation. In K. Németh (Ed.), *Updates in volcanology-new advances in understanding volcanic systems* (pages 3-88). InTech.

Kshirsagar, P., Siebe, C., Guilbaud, M.-N., Salinas, S., Layer, P., 2015. Late Pleistocene ($\sim 21,000$ yr BP) Alberca de Guadalupe maar volcano (Zacapu basin, Michoacán): Stratigraphy, tectonic setting, and paleo-hydrogeological environment. *Journal of Volcanology and Geothermal Research* 304, 214-236. doi:10.1016/j.jvolgeores.2015.09.003.

Kshirsagar, P., Siebe, C., Guilbaud, M.-N., Salinas, S., 2016. Geological and environmental controls on the change of eruptive style (phreatomagmatic to Strombolian-effusive) of Late Pleistocene El Caracol tuff cone and its comparison with adjacent volcanoes around the Zacapu basin (Michoacán, México). *Journal of Volcanology and Geothermal Research* 318 (2016) 114-133.

The Late Quaternary sediment record from Maar Lake Sihailongwan (northeastern China): diatom-based inferences of limnological and climatic changes

Patrick Rioual¹, Guoqiang Chu¹, Jens Mingram², Martina Stebich³, Qiang Liu¹, Jingtai Han¹ and Jiaqi Liu¹

¹ Key Laboratory of Cenozoic Geology and Environment, Institute of Geology & Geophysics, Chinese Academy of Sciences, Beijing 100029, China. prioual@mail.iggcas.ac.cn

² Deutsches GeoForschungsZentrum, Dep.5.2, Climate Dynamics and Landscape Evolution, Potsdam, Germany.

³ Senckenberg Research Institute and Natural History Museum, Research Station for Quaternary Palaeontology, Weimar, Germany.

Keywords: diatom, Lateglacial, Holocene.

The characteristics of Lake Sihailongwan, a 50-m deep maar lake located in the Longgang Quaternary volcanic field (Jilin Province, northeast China), allowed for the late Quaternary accumulation of an annually laminated (= varved) sediment sequence that is generally rich in diatom remains (Chu et al. 2005). The chronology of the sequence is based on varve counting and was corrected by a constant correction factor derived from 50 calibrated AMS 14C dating of terrestrial plant remains (Schettler et al. 2006, Stebich et al. 2009). This record represents an outstanding archive for the high-resolution study of past variations in limnological conditions and in climate on the basis of diatom analysis.



Fig. 1 – Maar lake Sihailongwan, Jilin Province, NE China.

The main events revealed by diatom analysis can be summarized as follows. During the Pleniglacial (17.4 – 14.8 ka BP), low diatom concentration combined with high percentages of the winter form *Cyclotella comensis* morphotype minima and of the oligotrophic species *Discostella stelligeroides* indicate low supply of nutrients to the lake. This interval matches with the “Mystery Interval” that is characterized in the Chinese speleothem records by weak summer monsoon precipitation (Zhang et al. 2014). The Bølling – Allerød interstadial (14.8 – 12.8 ka BP) is characterized by high percentages of the early-spring-blooming species *Stephanodiscus minutulus*.

This indicates longer and stronger period of mixing of the water column during spring and an increase in the rate of nutrient supply. The Younger-Dryas event is only evident

between 12.0 and 11.5 ka BP characterized by a sharp decline in diatom concentration and very low proportions of planktonic species that indicate intensely cold conditions. The onset of the Holocene is marked by a sharp increase in diatom concentration and rapid shifts in dominance among planktonic species such as *Discostella stelligeroides*, *Stephanodiscus minutulus*, *Cyclotella comensis*, *Cyclostephanos delicatus*, *Achnanthisidium catenatum* and *Fragilaria* spp. This large increase in diversity of planktonic species suggests a longer growing season allowing a more complex seasonal succession.

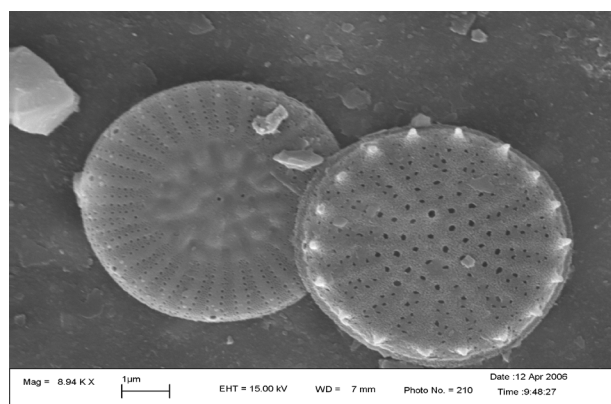


Fig. 2 – Scanning Electron Microscope (SEM) image of *Cyclotella comensis* (left) and *Stephanodiscus minutulus* (right), two species abundant during the early Holocene. Scale bar = 1 µm.

In the middle Holocene high abundance of *Stephanodiscus minutulus* indicate early and long spring season, conditions associated with mild climatic conditions in late winter and spring. After 6000 years BP, the sequence is marked by increased proportions of *Asterionella Formosa*, a species that fares better when spring mixing is delayed due to longer ice-cover, and *Fragilaria* species which prefer water with high silicon to phosphorus ratio (Si:P ratio). This shift may reflect a reduced intensity and/or the delay of mixing of the water column in spring and suggest cooler conditions. The last 3500 years of the sequence are dominated by *Lindavia balatonis* and *Discostella stelligeroides*.

This assemblage suggests a shift towards shorter spring (longer winter) and lower nutrient supply. This matches with a switch towards a colder and drier climate as inferred by the pollen records from the region (Stebich et al. 2015, Xu et al. 2014).

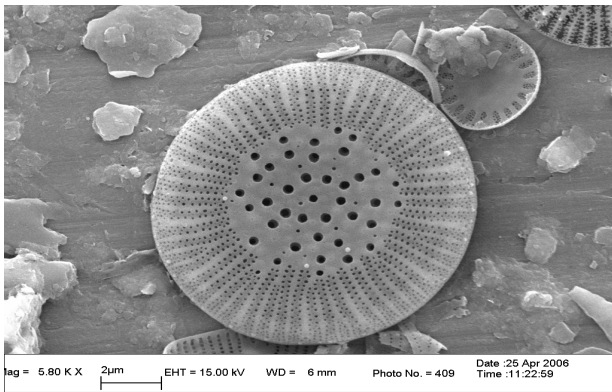


Fig. 3 – SEM image of *Lindavia balatonis* (large valve in the centre) and *Discostella stelligeroides* (small valve, top right), 2 species dominant during the Late Holocene. Scale bar = 2 μm.

This sequence illustrates the complexity of interpreting sifts in diatom assemblages as they may be caused by either the direct effects of seasonal climate on the limnology of the lake (in particular the duration and timing of ice cover, and length and strength of spring mixing) and/or catchment-mediated effects on the concentrations of nutrients such as P and Si.

Acknowledgements

This project was supported by the National Science Foundation of China (grant # 41320104006).

References

- Chu, G., Liu, J., Schettler, G., Li, J., Sun, Q., Gu, Z., Hu, H., Liu, T.S., 2005. Sediment fluxes and varve formation in Sihailongwan, a maar lake from northeastern China. *Journal of Paleolimnology* 34: 311-324.
- Schettler, G., Liu, Q., Mingram, J., Stebich, M., Dulski, P., 2006. East-Asian monsoon variability between 15000 and 2000 cal. Yr BP recorded in varved sediments of Lake Sihailongwan (northeastern China, Long Gang volcanic field). *The Holocene* 16: 1043-1057.
- Stebich, M., Mingram, J., Han, J., Liu, J., 2009. Late Pleistocene spread of (cool-) temperate forests in Northeast China and climate changes synchronous with the North Atlantic region. *Global and Planetary Change* 65: 56-70.
- Stebich, M., Rehfeld, K., Schlütz, F., Tarasov, P.E., Liu, J., Mingram, J., 2015. Holocene vegetation and climate dynamics of NE China based on the pollen record from Sihailongwan Maar Lake. *Quaternary Science Reviews* 124: 275-289.
- Xu, D., Lu, H., Chu, G., Wu, N., Shen, C., Wang, C., Mao, L., 2014. 500-year climate cycles stacking of recent centennial warming documented in an EaST Asian pollen record. *Scientific Reports* 4: 3611.
- Zhang, W., Wu, J., Wang, Y., Wang, Y., Cheng, H., Song, X., Duan, F., 2014. A detailed East Asian monsoon history surrounding the 'Mystery Interval' derived from three Chinese speleothem records. *Quaternary Research* 82: 154-163.

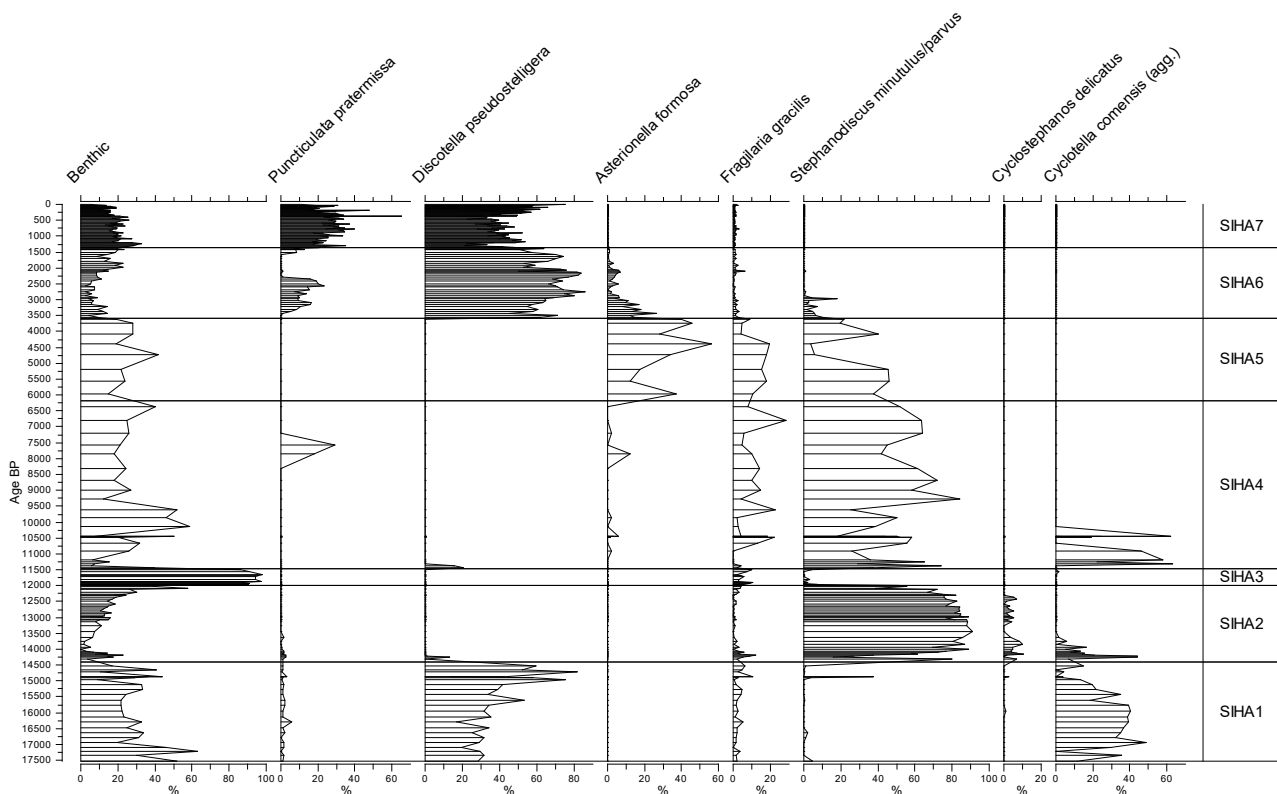


Fig. 4 – Summary diatom diagram for Lake Sihailongwan Late Quaternary sequence

Volcanic Closure of the Alf Valley During the Weichselian Pleniglacial – Witnesses of the Last Glaciation in the Quaternary Westeifel Volcanic Field (Germany)

Thomas Lange¹, Luise Eichhorn², Michael Pirrung¹, Thomas Jahr³, Karl-Heinz Köppen⁴ and Georg Büchel⁵

¹ Institute of Geosciences, FSU Jena, Department of Applied Geology, Burgweg 11, 07749 Jena. t.lange@uni-jena.de

² Landesverband Sachsen, DVL Pirna, Lange Straße 43, 01796 Pirna.

³ Institute of Geosciences, FSU Jena, Department of General Geophysics, Burgweg 11, 07749 Jena.

⁴ Engineering Office Boden und Wasser GmbH, Am Heidepark 6, 56154 Boppard.

⁵ Institute of Geosciences, FSU Jena, Burgweg 11, 07749 Jena.

Keywords: volcanic dam, lacustrine sediments, surface reconstruction

Volcanic elevations and depressions pervade the landscape of the Quaternary Westeifel Volcanic Field (WEVF) and characterize the regional surface (Büchel and Mertes 1982). Among other things, they influence the morphology of the typically narrow and deeply-cut valleys as well as the course of the river systems (Cipa 1956/1958, Wiencke 1979). Nowadays the progress of erosion by rivers and the processes of embossing during the Weichselian Glaciation until the beginning of the Holocene are difficult to understand.

However, in the Alf Valley near Gillenfeld and Strohn, these processes are readily traceable due to a unique arrangement of young volcanoes and the distribution of their ejected products. 17 of the 270 known eruption centers of the WEVF are situated in the vicinity of the Alf Valley (Lorenz and Zimanowski 2008), of which 3 are chained with each other, forming the Wartgesberg Volcano Complex (WVC). The WVC arose during the Weichselian Pleniglacial around 33 ka ago (Mertz et al. 2015, Eichhorn 2016 Schmidt et al. 2017) and was responsible for the complete closure of the Alf Valley. Due to its position and promoted agglutinates, lava and cinder, it led to the impoundment of the river and the leveling of the valley (Hemfler and Büchel 1991, Fig. 1). Depending on the local volume, geometry, inflow rate and its material composition (Capra 2007), the dam was able to persist for several thousand years (Eichhorn 2016). As a result, a high amount of lacustrine sediments was deposited within the so-called Paleolake Alf (Pirrung et al. 2007), halting the erosion and leading to a widening of the valley. Sedimentary records have been used to investigate past environmental changes since the formation of the WVC, Eichhorn 2016).

This study will present how volcanic activity influenced the morphological evolution of the Alf Valley and how analyses of high resolution digital terrain models (DTM) coupled with geophysical investigations can be used to reconstruct the paleo-surface, to detect the extent and size of glacial archives and to examine processes which took place during the Weichselian Pleniglacial (Fig. 2).

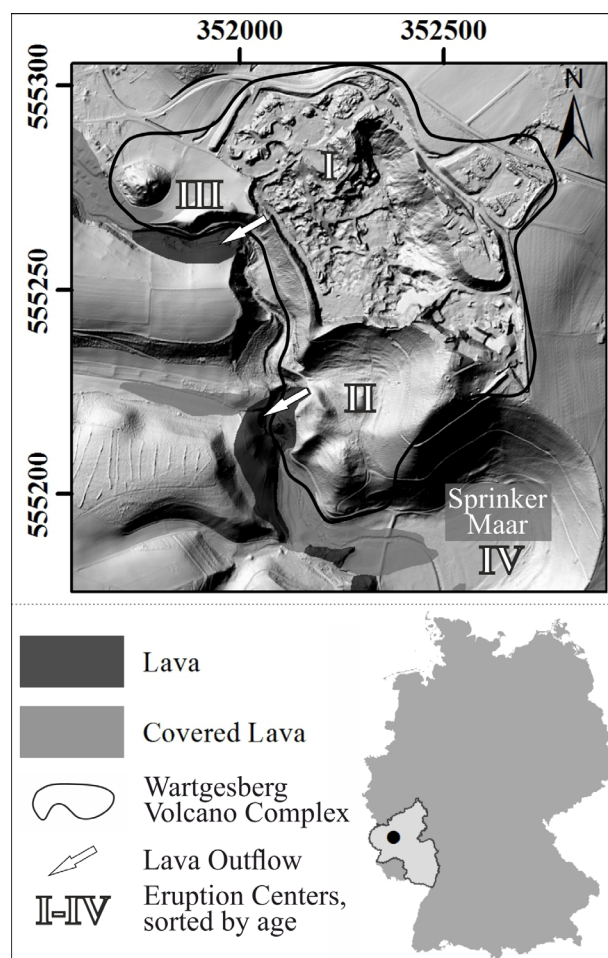


Fig. 1 – The Wartgesberg Volcano Complex and the distribution of its eruption centers. Between the eruption centers II and III, the natural dam, made out of cinder, agglutinates and lava, was situated. The two arrows are showing spots where lava was leaked. The flows followed the former valley course and preserved the paleo-valley surface; Source of DTM: State Office for Survey and Geobasis Information Rhineland-Palatinate.

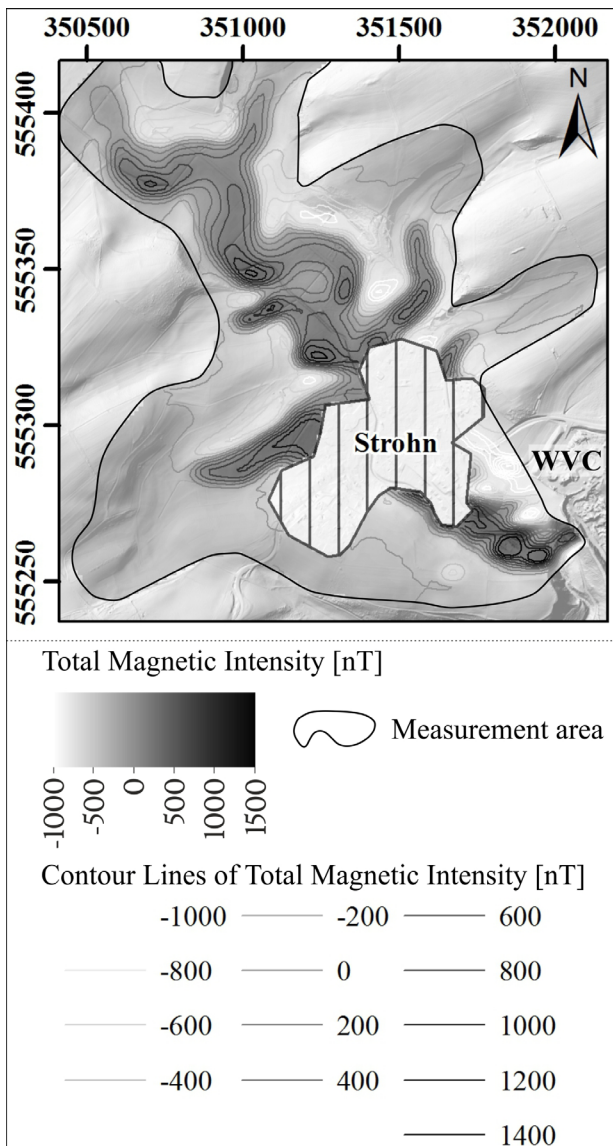


Fig. 2 – Anomaly map of the total magnetic field intensity (after Lange 2014, Lange and Büchel 2017). The data were collected with a GSM-19 proton magnetometer (GEM-Systems), where every 25 m (on average) a measurement took place. The anomaly is showing the covered lava flow of Strohn and provides clues about the paleo-valley morphology; Source of DTM: State Office for Survey and Geobasis Information Rhineland-Palatinate.

Acknowledgements

We express our gratitude to the working group of Applied Geology and General Geophysics of the Friedrich Schiller University Jena for many stimulating discussions.

References

Büchel, G. and Mertes, H. (1982): Die Eruptionszentren des West-eifeler Vulkanfeldes. – *Zeitschrift der Deutschen Geologischen Gesellschaft*, 133, 409-429.

Capra, L. (2007): Volcanic natural dams: identification, stability, and secondary effects. – *Natural Hazards*, 43, 45-61.

Cipa, W. (1956): Der Vulkanismus in der Umgebung des Pulvermaares. – *Decheniana*, 109, 53-75, Bonn.

Cipa, W. (1958): Erdmagnetische Vermessung einiger Lavaströme und Tuffschlote in der Vorder-Eifel. – *Geologisches Jahrbuch der BGR*, 75, 663-698.

Eichhorn, L. (2016): Reconstruction of environmental change and sedimentation processes during the Pleniglacial using fluvio-lacustrine sediments from volcanically-dammed Paleolake Alf, West Eifel Volcanic Field, Germany. – Jena, Friedrich-Schiller-University, Dissertation, 120 pp.

Hemfler, M. and Büchel, G. (1991): Influyente Verhältnisse als Folge der Trinkwassergewinnung im Alfbachtal bei Strohn (Westeifel). – *Pollichia Mitteilung*, 78, 35-83.

Lange, T. (2014): Paläotatlorekonstruktion des Alfbachtals im Zuge morphologischer Detailanalyse eines DGMs und geophysikalischer Geländeuntersuchung bei Gillenfeld und Strohn. – Jena, Friedrich-Schiller-University, Diploma Thesis, 170 pp.

Lange, T. and Büchel, G. (2017): Hochauflösende geo-magnetische Rasterkartierung des Strohner- und Sprinker Lavastroms im Alfbachtal – Quartäres Vulkanfeld der Westeifel. – *Mainzer geowissenschaftliche Mitteilungen*, 45, 177-202.

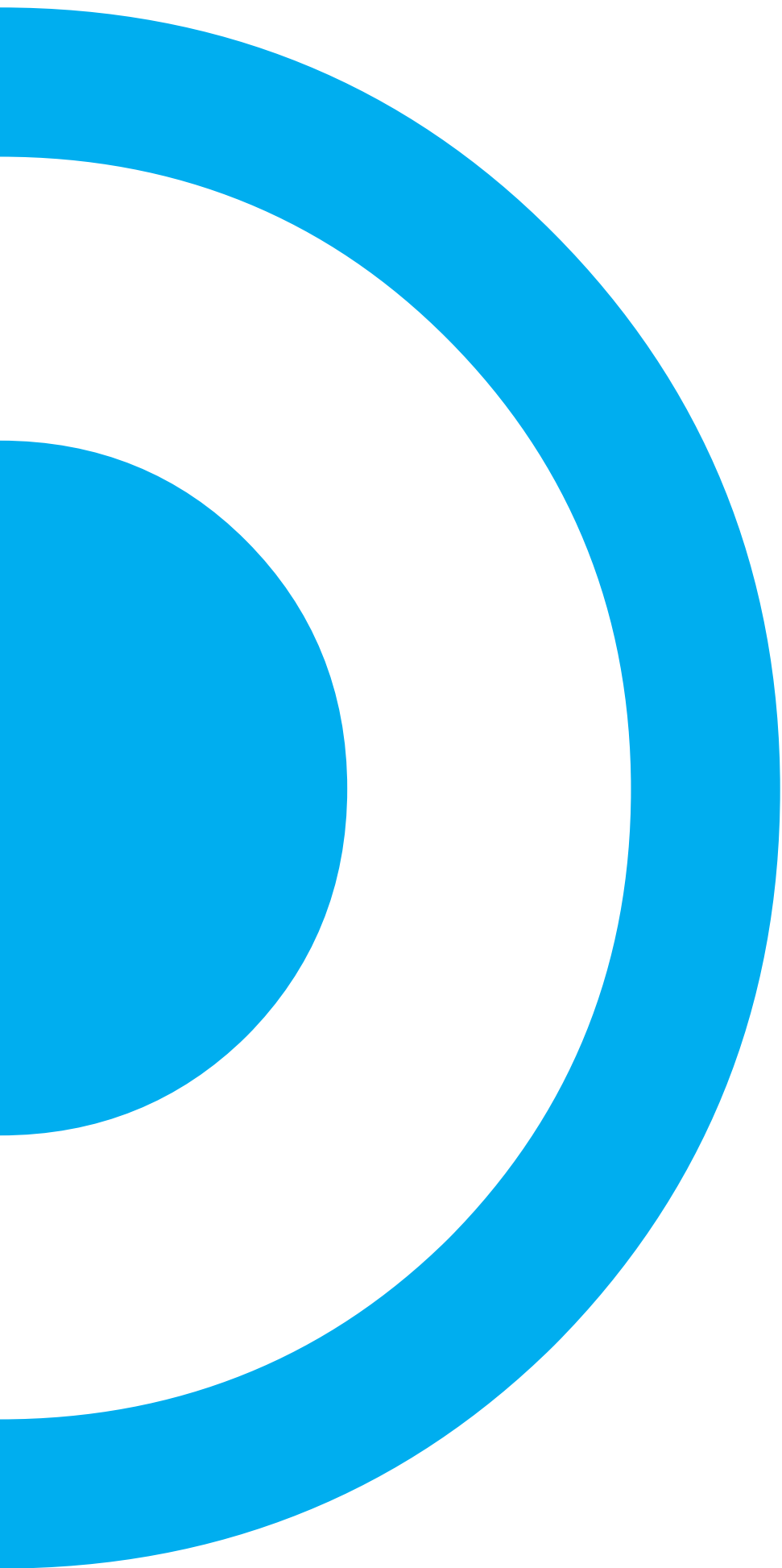
Lorenz, V. and Zimanowski, B. (2000): Vulkanologie der Maare der Westeifel (Volcanology of the West Eifel Maars). – In: Neuffer, F. O. und H. Lutz (eds.): *Exkursionsführer Internationale Maartagung, Daun / Vulkaneifel, 17.-27. August 2000*. – *Mainzer Naturwiss. Archiv*, 24, 5-51.

Mertz, D. F., Löhnertz, W., Nomade, S., Pereira, A., Prelevic, D., Renne, P. R. (2015): Temporal-spatial evolution of low-SiO₂ volcanism in the Pleistocene West Eifel Volcanic Field (West Germany) and relationship to upwelling asthenosphere. – *Journal of Geodynamics*, 88, 59-79.

Pirring, M., Büchel, G., Köppen, K.-H. (2007): Hoch-auflösende fluviolakustrine Sedimente des jüngeren Pleistozän aus dem Alfbachtal bei Gillenfeld (Westeifel)- erste Ergebnisse. – *Mainzer geowissenschaftliche Mitteilungen*, 35, 51-80.

Schmidt, C., Schaarschmidt, M., Kolb, T., Büchel, G., Richter, D., Zöller, L. (2017): Luminescence dating of Late Pleistocene eruptions in the Eifel Volcanic Field, Germany. – *Journal of Quaternary Science*, 32, 628-638.

Wienecke, K. (1979): Geologische und geophysikalische Untersuchungen im Vulkangebiet SE Gillenfeld (Westeifel). – Bonn, Friedrich Wilhelms University, Diploma Thesis, 108 pp.



Posters *Session 3*

Lakes in maar volcanoes: the sedimentary record of paleontology, climate change and hydrochemistry

Conveners

Oriol Oms (joseporiol.oms@uab.cat)

Dmitri Rowet (dmitrirowet@gmail.com)

The geometry of Maar-diatreme craters usually leads to develop hydrologically closed lakes that contain anoxic bottom conditions. Such settings are ideal for the preservation of complete and detailed sedimentary records of past environmental changes. These records include climate evolution, ecological reconstructions, hydrochemistry and human impact in natural systems. Exceptionally preserved fossils in such meromictic lakes are also an important source to study the history of life and its evolution.

This session wants to create synergies between volcanologists and other researchers dealing with limnology, hydrochemistry, mineralogy, paleontology, and climate proxies, among many others.

Orbital-scale environmental changes during the Late Pliocene in NE Spain: the Camp dels Ninots maar record

Gonzalo Jiménez-Moreno¹, Francesc Burjachs^{2,3,4}, Isabel Expósito^{3,4}, Oriol Oms⁵, Juan José Villalain⁶, Ángel Carrancho⁷, Jordi Agustí^{2,3,4}, Gerard Campeny^{3,4}, Bruno Gómez de Soler^{3,4} and Jan Van der Made⁸

¹Departamento de Estratigrafía y Paleontología, Universidad de Granada, Spain. gonzaloj@ugr.es

²ICREA, Barcelona, Spain

³IPHES, Tarragona, Spain

⁴Universitat Rovira i Virgili, Tarragona, Spain

⁵Universitat Autònoma de Barcelona, Spain

⁶Departamento de Física, Universidad de Burgos, Spain

⁷Departamento de Historia, Geografía y Comunicación. Universidad de Burgos, Spain.

⁸Museo Nacional de Ciencias Naturales, CSIC, Madrid, Spain

Keywords: pollen, climate, Late Pliocene.

The Late Pliocene is a very interesting period as climate deteriorated from a warm optimum at ca. 3.3–3.0 Ma to a progressive climate cooling. Simultaneously, the Mediterranean area witnessed the establishment of the Mediterranean-type seasonal precipitation rhythm (summer drought). These important climate changes produced significant vegetation changes, such as the extinction of several thermophilous and hygrophilous plant taxa from the European latitudes. Besides these long-term trends, climate was also characterized by cyclical variability (i.e., orbital changes) that forced vegetation changes (forested vs. open vegetation). In the Mediterranean area, cyclical changes in the vegetation were mostly forced by precession.

In this study high-resolution pollen analysis has been carried out on a sediment core taken from the Pliocene Camp del Ninots maar site, Girona, NE Spain (Jiménez-Moreno et al., 2013). Cyclical variations have been observed in the pollen record, with periods characterized by the abundance of *Abies*, *Larix*, *Cathaya*, *Tsuga*, *Engelhardia*, *Alnus* and *Botryococcus* algae, alternating with periods characterized by abundant *Poaceae*, *Cupressaceae*, *Ericaceae*, evergreen *Quercus* and *Oleaceae*, most-likely representing humid and dry conditions, respectively. The pollen variations seem to correlate fairly well with sedimentological changes depicted by the lithology and magnetic susceptibility (MS) records. Humid periods correspond to low MS and dark clays, which are probably related to higher lake level, productivity and organic sedimentation in the lake. On the other hand, arid periods seem to correspond to high MS and lighter clays, which were probably related with lower lake level, productivity and more detritic sedimentation in the lake. An increase in aridity is observed as well as cyclic variations throughout the studied sequence. Cyclicity was mostly forced by precession but also by obliquity and eccentricity. Precipitation seems to be the main factor controlling these cycles. These data allowed estimating a sedimentary rate of ca. 0.19 mm/yr and the time duration covered by the studied core, close to 200 ka. The combination of biostratigraphy, palaeomagnetism

and cyclostratigraphy allowed for a very precise dating of the sediments between ca. 3.3 and 3.1 Ma.

Acknowledgements

G.J.-M.- acknowledges funding from projects P11-RNM-7332 funded by Consejería de Economía, Innovación, Ciencia y Empleo de la Junta de Andalucía, the project CGL2013-47038-R funded by Ministerio de Economía y Competitividad of Spain and Fondo Europeo de Desarrollo Regional FEDER and the research group RNM0190 (Junta de Andalucía). The Camp dels Ninots project is sponsored by projects 2014-100575 (Generalitat de Catalunya), SGR2017-859 (AGAUR) and the Ministry of Economy and Competitiveness of Spain, under project CGL2016-80000-P (MINECO).

References

Jiménez-Moreno, G., Burjachs, F., Expósito, I., Oms, O., Carrancho, Á., Villalain, J.J., Agustí, J., Campeny, G., Gómez de Soler, B. & van der Made, J. (2013): Late Pliocene vegetation and orbital-scale climate changes from the western Mediterranean area. *Global and Planetary Change* 108: 15–28.

Water frogs (Anura, Ranidae) from the Pliocene Camp dels Ninots Konservat-Lagerstätte (Caldes de Malavella, NE Spain)

Hugues-Alexandre Blain^{1,2}, Iván Lozano-Fernández^{1,2}, Almudena Martínez-Monzón^{1,2}, Tomas Prikryl³, Oriol Oms⁴, Pèrre Anadón⁵, Pablo Rodríguez-Salgado⁶, Jordi Agustí^{7,1,2}, Gerard Campeny Vall-Ilosera^{1,2} and Bruno Gómez de Soler^{1,2}

¹ Institut Català de Paleoecologia Humana i Evolució Social (IPHES), Tarragona, Spain. hablain@iphes.cat

² Àrea de Prehistòria, Universitat Rovira i Virgili (URV), Tarragona, Spain.

³ Institute of Geology AS CR, v.v.i., Prague, Czech Republic.

⁴ Autonomous University of Barcelona. Science Faculty, Geology Department. Campus Bellaterra, 08193, Spain.

⁵ Institute of Earth Sciences Jaume Almera, ICTJA-CSIC, 08028 Barcelona, Spain.

⁶ Irish Centre for Research on Applied Geosciences (iCRAG), Belfield, Ireland.

⁷ ICREA, Institut Català de Recerca i Estudi Avançat (ICREA), Barcelona, Spain.

Keywords: Lissamphibia, Paleontology, Physical taphonomy.

Water frogs are one of the most common fossils in the European Cenozoic, and many taxa have been proposed for Miocene and Pliocene members of the group. Nevertheless, the rare reproductive phenomenon of hybridogenesis, as well as the absence of osteological studies on several living species within the group, makes it almost impossible either to distinguish fossil forms neither to distinguish between the various extant species (Sanchiz, 1998). Here we present the description of eleven articulated fossil water frogs (2 females, 3 males, 1 indeterminate sex and 5 metamorphs) and 353 isolated bones (corresponding to a total of 35 individuals including 4 females and 8 males) recovered from the 2005-2010 field campaigns at the Pliocene (ca. 3.2 Ma; MN15-16) Camp dels Ninots Konservat-Lagerstätte (NE Spain) (Fig. 1).

This locality corresponds to a lacustrine sedimentary sequence from maar infill which delivered complete articulated skeletons of large mammals (*Alephis tigresesi*, *Stephanorhinus jeanvireti* and *Tapirus arvernenis*), turtles (*Mauremys leprosa*) and small vertebrates (as rodents, frogs, newts and several fishes) (Gómez de Soler et al., 2012). Excellent preservation of the fossils was favored by the meromictic conditions of the lake.



Fig. 1 – Specimen of fossil water frog from the Pliocene of Camp dels Ninots (Girona, Spain) recovered during the 2005 excavation campaign (Photography G. Campeny – IPHES).

Frog's skeletons are all presented in dorsoventral aspect with snout-vent length ranging between 13 and 45 mm. Presence of diplasiocoelous vertebral column, with short and non-imbricate neural arch, sacrum unfused with the urostyle that bears cylindrical sacral apophysis, bicondylar sacro-urostyler articulation, absence of transverse processes of the urostyle and of ribs, firmisternous sternum with ossified omosternum, premaxilla and maxilla teeth bearing clearly refer to the family Ranidae.

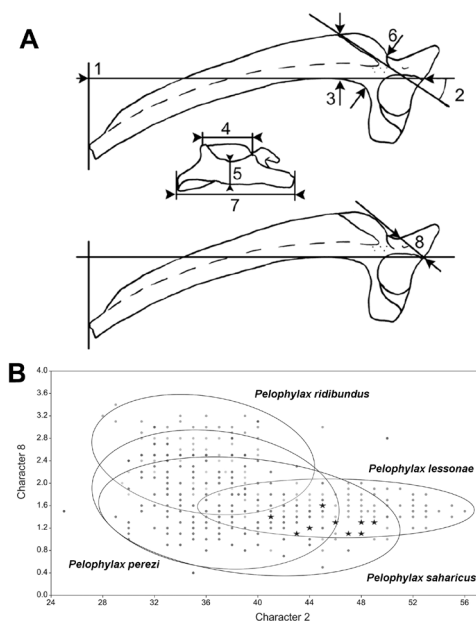


Fig. 2 – Morphometry. A) Measurements used on green frog's ilium (Blain et al., 2015). 1, length of ilium; 2, angle between tuber superior orientation and main iliac axis; 3, dorsal crest height; 4, acetabular diameter; 5, corpus thickness at the centre of the acetabulum; 6, 'iliac neck' (=smallest thickness of the crest on the corpus); 7, maximum width of the junctura ilioischiadica; 8, width of the pars ascendens. B) Projection of characters 2 and 8. Isolated ilia from the Pliocene Camp dels Ninots are represented by stars.

Attribution to water frogs (genus *Pelophylax*) relies on a higher dorsal crest on the ilial shaft and more open sacral apophysis (approximately 130°) than in genus *Rana*. Approximation to a more precise systematic attribution among extant European and North African water frogs has been done using morphometrical measurements on the ilium (Fig. 2A), using a comparative modern sample of 506 ilia (*P. ridibundus*: 116; *P. lessonae*: 168; *P. perezi*: 185; and *P. saharicus*: 37). Fossil ilia from Camp dels Ninots fall within the variability of extant *P. lessonae* (Fig. 2B), and thus would represent the earliest mention for this species. However attribution must be done carefully, as the status of the extinct species *Pelophylax pueyoi* from the late Miocene (MN9-10) Libros Konservat-Lagerstätte has still to be elucidated.

Preliminary description of their physical taphonomy is also done, taking into account their distribution, percentage completeness, percentage of articulation and limb position (Fig. 3), thus suggesting as possible cause of death: starvation during hibernation.

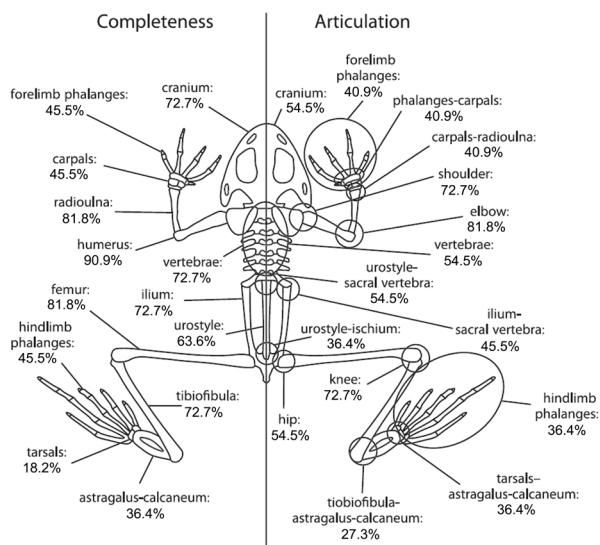


Fig. 3 – Outline drawing of a standard *Pelophylax* skeleton illustrating the major skeletal elements and joints. For each element and joint, the percentage of specimens in which that element is complete, or the joint articulated, is indicated. Individual elements of the cranium are not shown for clarity.

Acknowledgements

This study is part of the projects CGL2011-13293-E/BTE “Estudio paleontológico y preparación de los microvertebrados del Plioceno de Camp dels Ninots, Girona” (Spanish Ministry of Science and Innovation), CGL2016-80000-P (Spanish Ministry of Economy and Competitiveness), AGAUR 2014/100575 and SGR2017-859 (Generalitat de Catalunya), SYNTHESYS grant DE-TAF-3244 to HAB (EC funded project). We thank Dr. Marta Calvo Revuelta for allowing us to consult the anuran comparative collections of the Museo Nacional de Ciencias Naturales (Madrid, Spain) under her care.

References

Blain, H.-A., Lózano-Fernández, I., Böhme, G., 2015. Variation in the ilium of central European water frogs *Pelophylax* (Amphibia, Ranidae) and its implications for species-level identification of fragmentary anuran fossils. *Zoological Studies* 54: 5.

Gómez de Soler, B., Campeny Vall-Ilosera, G., van der Made, J., Oms, O., Agustí, J., Sala, R., Blain, H.-A., Burjachs, F., Claude, J., García Catalan, S., Riba, D., Rosillo, R., 2012. A new key locality for the Pliocene vertebrate record of Europe: the Camp dels Ninots maar (NE Spain). *Geologica Acta* 10(1): 1-17.

Sanchiz, B., 1998. *Salientia*. Handbuch der Paläoherpetologie Pars 4. Dr. Pfeil. Munich. 275 pp.

Macromammal taphonomy of the Camp dels Ninots maar site (Caldes de Malavella, NE Spain).

Francesc García^{1,2}, Isabel Cáceres^{2,1}, Bruno Gómez de Soler^{1,2}, Gerard Campeny^{1,2}, Oriol Oms³, Pablo Rodríguez-Salgado⁴, Jordi Agustí^{5,1,2}

¹ Institut Català de Paleoecologia Humana i Evolució Social (IPHES). C/ Marcel·lí Domingo s/n, Edifici W3 Campus Sescelades URV, 43007 Tarragona, Spain.

² Universitat Rovira i Virgili (URV). Facultat de Lletres. Av. Catalunya 35, 43002 Tarragona, Spain.

³ Universitat Autònoma de Barcelona, Facultat de Ciències, Departament de Geologia. Campus Bellaterra, 08193, Spain.

⁴ Irish Centre for Research on Applied Geosciences (iCRAG), University College Dublin, Belfield, Ireland.

⁵ Institució Catalana de Recerca i Estudis Avançats (ICREA). Barcelona, Spain.

Keywords: Fossil-Lagerstätten, Paleontology, Taphonomy.

The Camp dels Ninots maar site is located in the town of Caldes de Malavella, 20 km south of the city of Girona (UTM -ETRS89- 483202E and 46311454N and 93 m above the sea level). The site responds to a maar type volcano (Fig. 1) where a lake formed inside it during the Upper Pliocene (3.1 Ma). The sedimentary conditions of the lake had led to an exceptional preservation of complete skeletons of macromammals, icitiofauna, amphibians, as well as seeds and leaves, among others. This exceptional preservation makes it possible to include the Camp dels Ninots site in the category of fossil-Lagerstätte deposits (Gómez de Soler et al. 2012).



Fig. 1. Hypothetical reconstruction of the Camp dels Ninots maar site. (Mauricio Antón)

The first fossil finding occurred in 1985 (Vicente, 1985). More remains were found during the work of Vehí et al. (1999) to define the geomorphological structure as a maar-diatreme. In 2003, the "Institut Català de Paleoecologia Humana i Evolució Social" took charge of the first systematic excavation and multidisciplinary, paleontological, paleoenvironmental and geological studies.

From the first excavation campaign (2003) the fossil remains found have shown a very broad spectrum of fauna and flora that allow us to form a fairly accurate view of the climate and life during the Upper Pliocene in southern Europe (Jiménez-Moreno et al., 2013).

The macromammals are represented by tapirs (*Tapirus*

arvernensis), bovids (*Alephis tignerese*) and rhinos (*Stephanorhinus cf. jeanvireti*). In this work, we have focussed on the tapirs, and we are aimed to study the fossilization processes that take place under a volcanic environment. This will allow the creation of a protocol helping to recover future findings in the Camp dels Ninots site.



Fig. 2. Tapir recovered in 2011 campaign. Foto © IPHES.

We present the results of the study of three tapirs (*Tapirus arvernensis*), being the first taphonomic approximation to the group of macromammals of the Camp dels Ninots. These individuals were found in the southern area of the volcano crater in the sector known as Can Argilera during the campaigns of 2011 (Fig. 2), 2012 (Fig. 3) and 2016 (Fig. 4).

A descriptive methodology has been applied based on the study of surface and structural modifications of fossils. For this, a stereomicroscope (Euromex x60 magnification) and a digital microscope (Hirox KH-8700) were used. Chemical microanalysis (ESEM-FEI-QUANTA-600) and mineralogy (FTIR- Jasco FT / IR-600 Plus) has also been carried out. Also, it has been created a categorization of the taphonomic modifications observed during the process of studying fossil remains.

The skeletons were recovered completely and in anatomical connection, except some distal elements of the extremities (phalanges and metapodials). There are no mod-

ifications related to the action of predators. The superficial alterations identified are: cracks and fissures, pigmentation by oxides (Mn, Fe), chemical corrosion, as well as fractures, crushing and deformations related to sediment pressure. These modifications together with the absence of displacements suggest a rapid burial of the remains, which favored the good preservation of the skeletons.



Fig. 3. Tapir recovered 2012 campaign. Foto © IPHES.



Fig. 4. Tapir 2016 campaign. Foto © IPHES.

References

Gómez de Soler, B., Campeny, G., Van der Made, J., Oms, O., Agustí, J., Sala, R., Blain, H.A., Burjachs, F., Claude, J., García S., Riba, D., Rosillo, R. (2012). A new key locality for the Pliocene vertebrate record of Europe: the Camp dels Ninots maar (NE Spain). *Geologica Acta*, vol. 10, nº2: 1-17. DOI: 10.1344/105.000001702.

Jiménez-Moreno, G., Burjachs, F., Expósito, I., Oms, O., Carrancho, Á., Villalain, J.J., Agustí, J., Campeny, G., Gómez de Soler, B. & van der Made, J. (2013): Late Pliocene vegetation and orbital-scale climate changes from the western Mediterranean area. *Global Planet Change*, 108: 15–28.

Vehí, M., Pujadas, A., Roqué, C. & Pallí, L. (1999). Un edifici volcànic inèdit a Caldes de Malavella (La Selva, Girona): el Volcà del Camp dels Ninots. *Quaderns de la Selva*, 11. Centre d'Estudis Selvatans, pp. 45-72.

Vicente, J., 1985. Troballa d'un *Leptobos* a Caldes de Malavella (La Selva). *Societat d'Història Natural, Butlletí del Centre d'Estudis de la Natura del Barcelonès Nord*, 1(1), 86-88.

Research history and main discoveries of the fossil-Lagerstätte Camp dels Ninots maar (Caldes de Malavella, Girona, Spain).

Bruno Gómez de Soler^{1,2}, Gerard Campeny^{1,2}, Jordi Agustí^{3,1,2}, Pere Anadón⁴, Eduardo Barrón⁵, Xavier Bolós⁶, Hugues-Alexandre Blain^{1,2}, Francesc Burjachs^{3,1,2}, Isabel Cáceres^{2,1}, Àngel Carrancho⁷, Albert Casas⁸, Julien Claude⁹, Juan Diego Martín-Martín⁸, Isabel Expósito^{1,2}, Marta Fontanals^{2,1}, Francesc García^{1,2}, Mahjoub Himi⁸, Jordi Ibáñez⁴, Gonzalo Jiménez-Moreno¹⁰, María José Jurado⁴, Lucía López-Polín^{1,2}, Jan van der Made¹¹, Joan Martí⁴, Pablo Mateos^{1,2}, Jordi Miró⁸, Elena Moreno-Ribas^{1,2}, Oriol Oms¹², Tomas Prikryl^{13,14}, Pablo Rodríguez-Salgado¹⁵, Florent Rivals^{3,1,2}, Souhila Roubach^{1,2}, Oscar Sanisidro¹⁶ and Juan José Villalain¹⁷

¹ Institut Català de Paleoecologia Humana i Evolució Social (IPHES). C/ Marcel·lí Domingo s/n, Edifici W3 Campus Sescelades URV, 43007 Tarragona, Spain. E-mail: bgomez@iphes.cat

² Universitat Rovira i Virgili (URV). Facultat de Lletres. Av. Catalunya 35, 43002 Tarragona, Spain.

³ Institució Catalana de Recerca i Estudis Avançats (ICREA). Pg. Lluís Companys 23, 08010. Barcelona, Spain.

⁴ Institut de Ciències de la Terra Jaume Almera, CSIC, C/ Lluís Solé i Sabarís, s/n, 08028 Barcelona, Spain.

⁵ Museo Geominero. Instituto Geológico y Minero de España (IGME). Ríos Rosas, 23. 28003 Madrid. Spain.

⁶ Instituto de Geofísica, UNAM, Campus Morelia, 58190 Morelia, Michoacán, Mexico.

⁷ Área de Prehistoria, Departamento de CC. Históricas y Geografía, Universidad de Burgos (UBU). Pº Comendadores s/n, 09001 Burgos, Spain.

⁸ Universitat de Barcelona, Facultat de Ciències de la Terra. Martí i Franquès, s/n. 08028 Barcelona, Spain.

⁹ ISEM, Université de Montpellier 2. 2 Place Eugène Bataillon, 34095 Montpellier, cedex 5, France.

¹⁰ Departamento de Estratigrafía y Paleontología, Facultad de Ciencias, Universidad de Granada (UG). Av. Fuentenueva s/n, 18008 Granada, Spain.

¹¹ Museo Nacional de Ciencias Naturales, CSIC, C/ José Gutiérrez Abascal 2, 28006 Madrid, España.

¹² Universitat Autònoma de Barcelona, Facultat de Ciències, Departament de Geologia. Campus Bellaterra, 08193, Spain.

¹³ Institute of Geology, Academy of Sciences of the Czech Republic, v.v.i, Rozvojová 269, 16500 Prague 6, Czech Republic.

¹⁴ Faculty of Sciences, Institute of Geology and Paleontology, Charles University in Prague, Albertov 6, 12843 Prague 2, Czech Republic.

¹⁵ Irish Centre for Research on Applied Geosciences (iCRAG), University College Dublin, Belfield, Ireland.

¹⁶ Biodiversity Institute, University of Kansas. 1345 Jayhawk Boulevard - Dyche Hall 66045-7561 Lawrence, Kansas, USA.

¹⁷ Departamento de Física, Escuela Politécnica Superior, Universidad de Burgos (UBU). Avda. Cantabria s/n 09006, Burgos, Spain.

Keywords: Fossil-Lagerstätte, Paleontology, Paleoenvironment

The Camp dels Ninots is located in the western part of the town of Caldes de Malavella (Girona), at 20 km to the south of the city of Girona, with a 275.000 m² surface. Its UTM (ETRS89) coordinates are 483202E and 46311454N, and with a height of 93 m according to sea level (Fig. 1). The name Camp dels Ninots (field of puppets) is related to the presence of abundant diagenetic silica nodules with rounded shapes (menilites), which are mostly made of opal (SiO₂·nH₂O), that have been classically collected by locals.

The Camp dels Ninots site is a phreatomagmatic explosion volcano of Pliocene age (3.1 Ma) which subsequently formed a lake. The specific geological conditions, corresponding to lake sedimentation, make it ideal for the preservation of fossils. The appearance of complete skeletons mostly in anatomical connection makes the site to be considered, according to the German term, a Fossil-Lagerstätte.

Currently, the lands that make up the Camp dels Ninots are agricultural fields, mostly cereals, although, they are also remarkable for the many wells that, until a few years ago, were employed to extract water for industrial use.

The first studies were carried out by J.M Vidal (1882) who

considered the sediments as lacustrine Quaternary deposits. This interpretation was later followed by Bataller (1993), Llopis Lladó (1943) and Solé Sabarís (1946). The first fossil described from the Camp dels Ninots was a fragmentary bone, located during the excavation of a water well, which was assigned to the bovid *Leptobos* (Vicente, 1985). Several bones were found during the prospectings of Vehí et al. (1999), who first interpreted the basin as a maar. In 2003, the Institut Català de Paleoecologia Humana i Evolució Social (IPHES) initiated a multidisciplinary research project that includes the first systematic excavations and the study of the paleontological, paleobotanical and geological record of the Camp dels Ninots maar site.

The set of recovered fossils, plant and animal remains, provides direct data concerning the biological environment and climate of the northeast of the Iberian Peninsula during the Late Pliocene and allows comparing them to climate changes, which occurred in Europe during the last 3 million years.

The lake that formed inside the volcano offered optimal conditions for the establishment of ecological dynamics. The bodies of the animals that died near the maar were

deposited at the bottom of the lake. The characteristics of lake waters, sometimes mineral saturated, created the optimal conditions for an excellent conservation of the skeletons that we have discovered.

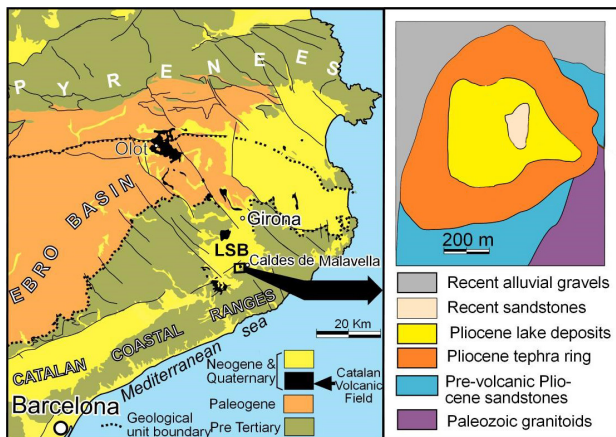


Fig.1. Left: Location of the Camp dels Ninots maar within the Northeast of the Iberian Peninsula. Right: Simply geological map of the Camp dels Ninots maar and its limits (modified from Oms et al., 2015).

The faunal remains consists in macrovertebrates, turtles, amphibians, fish and rodents. The macrovertebrates are represented by tapirs (*Tapirus arvernensi*), bovids (*Alephis tignerese*) and rhinoceros (*Stephanorhinus cf. jeanvireti*). Turtles are represented by the species *Mauremys leprosa* and *Chelydropsis cf. pontica*. The fossil assemblage is completed with amphibians like sharp-ribbed salamander (cf. *Pleurodeles sp.*), webbed newts (*Lissotriton aff. helveticus*) and green frogs (*Pelophylax sp.*), the freshwater fishes of the group of cyprinids (*Leuciscus sp.* and *Luciobarbus sp.*) and isolated remains from rodent *Apodemus atavus* (Gómez de Soler et al., 2012; Claude et al, 2014; Prikryl et al., 2016). All this fauna allows us to study the environment and the relationships between these different animal species.

The coexistence of *Stephanorhinus jeanvireti* and *Alephis tignerese*, and the paleomagnetic data obtained from all the stratigraphic sequence of the maar, give us a normal polarity (Gauss) for all the sequence with two inverse changes (Kaena and Mammoth), with a sedimentation rate that took place in 200 ka, situating the fossils layers in 3.1 Ma, near the MN15 and MN16 transition (Jiménez-Moreno et al., 2013).

The flora is abundant and is composed by vegetal macroremains as leaves imprints, fruits and trunks in the lacustrine clays and pollen remains captured in the sediment. These data corresponds to a subtropical climate and landscape, plenty of laurisilva Forest.

In conclusion, the large amount and variability of the recovered assemblage and its good preservation, enable us to consider the site as a Fossil-Lagerstätte. Its exceptionality offer a unique opportunity to study an ecosystem during the Pliocene, and provides paleoenvironmental data for understanding the dynamics of climate changes developed until today.

Acknowledgements

The Camp dels Ninots project is sponsored by projects 2014-100575 (Generalitat de Catalunya), SGR2017-859 (AGAUR) and the Ministry of Economy and Competitiveness of Spain, under project CGL2016-80000-P (MINECO).

References

- Bataller, J.R. (1933). Condiciones geológicas de las aguas minerales de Cataluña. Laboratorio de Geología del Seminario de Barcelona. Pub. Núm. 8, Barcelona, 84 p.
- Claude, J., Gómez de Soler, B., Campeny, G., Agustí, J., Oms, O. (2014). Presence of a chelydrid turtle in the late Pliocene Camp dels Ninots locality (Spain). *Bulletin de la Société Géologique de France*, t. 185, nº 4, pp. 253-256.
- Gómez de Soler, B., Campeny, G., Van der Made, J., Oms, O., Agustí, J., Sala, R., Blain, H.A., Burjachs, F., Claude, J., García S., Riba, D., Rosillo, R. (2012). A new key locality for the Pliocene vertebrate record of Europe: the Camp dels Ninots maar (NE Spain). *Geologica Acta*, vol. 10, nº2: 1-17. DOI: 10.1344/105.000001702
- Jiménez-Moreno, G., Burjachs, F., Expósito, I., Oms, O., Carrancho, Á., Villalain, J.J., Agustí, J., Campeny, G., Gómez de Soler, B. & van der Made, J. (2013): Late Pliocene vegetation and orbital-scale climate changes from the western Mediterranean area. *Global Planet Change*, 108: 15–28.
- Llopis Lladó, N. (1943). Estudio hidrogeológico de los alrededores de Caldas de Malavella (Gerona). *Speleon*, II. Oviedo, 1943, pp. 103-164.
- Prikryl, T., Gómez de Soler, B., Campeny, G., Oms, O., Roubach, S., Blain, H.A., Agustí, J. (2016). Fish fauna of the Camp dels Ninots locality (Pliocene; Caldes de Malavella, province of Girona, Spain) – first results with notes on palaeoecology and taphonomy. *Historical Biology*, vol. 28, nº3, pp. 347-357. DOI: 10.1080/08912963.2014.934820.
- Solé Sabarís, L. (1946). Características hidrogeológicas de los manantiales carbónicos de Gerona llamados Fonts Picants. *Anales del Instituto de Estudios Gerundenses*, 1, Girona, 1946, pp. 236-269.
- Vehí, M., Pujadas, A., Roqué, C. & Pallí, L. (1999). Un edifici volcànic inèdit a Caldes de Malavella (La Selva, Girona): el Volcà del Camp dels Ninots. *Quaderns de la Selva*, 11. Centre d'Estudis Selvatans, pp. 45-72.
- Vicente i Castells, J. (1985). Troballa d'un *Leptobos* a Caldes de Malavella (La Selva). *Butlletí del Centre d'Estudis de la Natura del Barcelonès Nord*, Barcelona, pp. 86-88.
- Vidal, L.I.M. (1882). Estudio geológico de la estación termal de Caldas de Malavella (Gerona). *Boletín de la Comisión del Mapa Geológico de España*, t. IX, Madrid, pp 65-91.

Multidisciplinary study of the Hindon Maar Fossil-Lagerstätte, Waipiata Volcanic Field, New Zealand

Uwe Kaulfuss¹, Daphne E. Lee¹, Andrew Gorman¹, Jennifer M. Bannister², Jon K. Lindqvist¹, John G. Conran³ and Dallas C. Mildenhall⁴

¹ Department of Geology, University of Otago, PO Box 56, Dunedin, New Zealand, uwe.kaulfuss@otago.ac.nz

² Department of Botany, University of Otago, PO Box 56, Dunedin, New Zealand

³ ACEBB, School of Earth & Environmental Sciences, Benham Bldg DX 650 312, University of Adelaide, Australia

⁴ GNS Science, PO Box 30368, Lower Hutt, New Zealand

Keywords: maar lake, palaeoecology, sedimentology

We summarize current knowledge on the geophysical structure, stratigraphy of crater sediments, age, and palaeoecology of the Hindon Maar Fossil-Lagerstätte, Waipiata Volcanic Field, southern New Zealand. Together with the nearby Foulden Maar Lagerstätte of early Miocene age, this is the second pre-Quaternary maar in the Southern Hemisphere that has been studied in some detail using a combined geological/geophysical/palaeo-ecological approach (Kaulfuss et al. *subm.*). Recent mapping and geophysical surveys have shown that the Fossil-Lagerstätte at Hindon is a maar-complex consisting of four sub-circular (at the surface) craters 500–1000 m in diameter. The four maars are partly eroded with their tephra rings and upper crater levels completely removed, they have limited surface outcrops of lacustrine crater sediment and in one case there is geophysical evidence of a deep-seated diatreme (Bowie 2015). Temporary excavations and drilling have encountered breccia and graded sandstone overlain by highly fossiliferous sediments in three of the maars (Kaulfuss and Moulds 2015). The fourth maar appears to be filled completely by reworked pyroclastics. The fine-grained lacustrine crater sediments comprise gyttja, spiculite and diatomite, with their laminated nature, high organic content and exceptional preservation of fossils indicating sedimentation on the lake floor under calm and anoxic conditions. Homogeneous or graded beds of mass-flow origin are interbedded with these laminated facies types. Underlying the lacustrine maar sediments are homogeneous and graded tuff and tuff breccia, which are interpreted as representing syn-eruptive lithologies of the upper diatreme.

In one of the maars, a basanite body occurring stratigraphically between diatreme fill and overlying lacustrine sediment is thought to have been emplaced on the maar floor under 'dry' conditions at the end of the maar-forming, phreatomagmatic eruptions. An ⁴⁰Ar/³⁹Ar age of 14.6 Ma obtained from this basanite is in agreement with a mid-Miocene age (Langhian; New Zealand local stage Lillburnian) derived from the palynomorph assemblages in the maar sediments.

Palaeontological investigations have established that the Hindon Maar Complex is a significant Cenozoic Fossil-La-

gerstätte with an exemplary record of terrestrial plants and animals, paralleled in the Southern Hemisphere only by the Foulden Maar (Lee et al. 2016). The diverse fossil biota preserved at the maar complex depicts a lake/forest ecosystem in southern New Zealand shortly after the mid-Miocene climatic optimum and at a time of increased land area following maximum marine transgression in the Oligocene.

Palynomorphs and plant macrofossils from at least 35 families and 43 genera of plants have been collected to date and indicate that the maar lakes were surrounded by Nothofagus/podocarp/mixed broadleaf forest growing under humid, warm temperate to subtropical conditions. The most common macrofossils are leaves of the southern beech Nothofagus, but the flora also includes conifers, cycads, monocots such as Ripogonum and palms, as well as Lauraceae, Myrtaceae and Araliaceae leaves and flowers. Many of the leaves are preserved with cuticle and flowers and conifer cones are found with in situ pollen, allowing the first certain assignment of previously known dispersed pollen types to their parent plants.

In terms of specimen numbers and diversity, the Hindon Maar Complex is now the second most important site for fossil insects from New Zealand after the Foulden Maar. Among c. 220 specimens collected to date are examples from at least 20 insect families, including the first fossil records of damselflies (Odonata: Zygoptera), jumping plant lice (Hemiptera: Psyllidae), shield bugs (Hemiptera: Pentatomidae), whiteflies (Hemiptera: Aleyrodidae) and springtails (Thysanoptera) from New Zealand. Other taxa from the orders Hemiptera, Coleoptera, Diptera, Hymenoptera and Trichoptera are also present, with beetles being the most common group. A diverse mid-Miocene insect fauna at the site is also evidenced by a high abundance of diverse insect damage types on leaves (Möller et al. 2017). The palaeontological value of the Hindon Maar Complex is further exemplified by the find of fish fossils with soft-tissue preservation (e.g., skin, eyes), including significant new records of fossil freshwater eels (*Anguilla* sp.) and the first finds of fossil bird feathers from New Zealand.

Acknowledgements

We thank the Neehoff family for kindly allowing access to the study site and acknowledge funding from the University of Otago and the Royal Society of New Zealand.

References

Bowie, E., 2015. The geophysical characterization of Hindon Maar. Unpublished MSc thesis, University of Otago, Dunedin, New Zealand. 149 p.

Kaulfuss, U., Moulds, M. 2015. A new genus and species of tettigarctid cicada from the early Miocene of New Zealand: *Paratettigarcta zealandica* (Hemiptera, Auchenorrhyncha, Tettigarctidae). *ZooKeys* 484: 83–94.

Kaulfuss, U., Lee, D.E., Wartho, J.-A., Bowie, E., Lindqvist, J.K., Conran, J.G., Bannister, J.M., Mildenhall, D.C., Kennedy, E.M., Gorman, A.R. submitted. Geology and Palaeontology of the Hindon Maar Complex: A Miocene terrestrial fossil Lagerstätte in southern New Zealand. *Palaeogeography, Palaeoclimatology, Palaeoecology*

Lee, D.E., Kaulfuss, U., Conran, J.G., Bannister, J.M., Lindqvist, J.K. 2016. Biodiversity and palaeoecology of Foulden Maar: an early Miocene Konservat-Lagerstätte deposit in southern New Zealand. *Alcheringa: An Australian Journal of Palaeontology* 40: 525–541.

Möller, A.L., Kaulfuss, U., Lee, D.E., Wappler, T. 2017. High richness of insect herbivory from the early Miocene Hindon Maar crater, Otago, New Zealand. *PeerJ* DOI: 10.7717/peerj.2985.

Origin and distribution of silica nodules in the Camp dels Ninots maar (La Selva Basin, NE Spain)

Jordi Miro¹, Oriol Oms², Juan Diego Martín-Martín¹, Jordi Ibañez³, Pere Anadon³, Jordi Tritlla⁴, Bruno Gomez de Soler⁵, Gerard Campeny⁵

¹ University of Barcelona, Department of Mineralogy, Petrology and Applied Geology, Barcelona, 08028, Spain. jmiropad@gmail.com

² Autonomous University of Barcelona. Department of Geology. Campus Bellaterra, 08193, Spain.

³ Institute of Earth Sciences Jaume Almera, CSIC, 08028 Barcelona, Spain.

⁴ Geological Specialist, Direction of Geology, Repsol Exploración. Madrid, 28045, Spain.

⁵ Institute of Human Paleocology and Social Evolution. Campus Sescelades URV. Tarragona, 40007, Spain.

Keywords: maar, silicification, silica, opal, hydrothermal system

The Camp dels Ninots Maar Diatreme (CNMD) is a Pliocene volcano located in La Selva Basin (NE Spain) (Gómez de Soler et al., 2012) (Fig.1). The CNMD was formed as a result of a phreatomagmatic eruption closely associated with the bounding faults of La Selva Basin (Oms et al. 2015 and references therein). The basement of the CNMD is composed by Late Carboniferous to Permian granites, schists, and pre-volcanic Pliocene alluvial sediments from the La Selva Basin. The lacustrine sediments filling the CNMD have been dated as 3.1 Ma (upper Pliocene; Oms et al. 2015 and references therein).

Silica nodules (i.e., menilitic opal) and silica crusts are common in the lacustrine sediments filling the CNMD. A recent drilling campaign (2015) allowed the study of the lacustrine succession as well as the silica manifestations. The aims of this study are (i) to characterize the mineralogy and texture of silica and associated host rocks; (ii) to address the source of the silica and its diagenetic evolution; and (iii) to build a conceptual model that explains the formation of the different silica occurrences. Host rock and silica samples were collected from recov-

ered cores and exploration trenches within the maar. The mineralogy of the samples was studied by using X-Ray powder diffraction (XRPD) and Raman spectroscopy. Petrography was accomplished by using polarization microscopy, cathodoluminescence and scanning electron microscopy (SEM). Furthermore, the silica $\delta^{18}O_{V-PDB}$ composition was analyzed in selected samples.

The lacustrine sediments filling the maar are made of: (i) laminated green-to-greyish mudstones; (ii) laminated dark mudstones, rich in organic matter; (iii) massive ochre dolomites with occasional intercalations of white, cm-thick beds rich in diatoms and opal-A microspheres. Core examination indicates that silica nodules appear through the complete succession, although they are more abundant within the dolostones, whereas silica crusts are observed exclusively in shallower depths and replacing dolostones (Fig.1C). Silica nodules are usually cm-sized, black to brown in colour with occasional zonation, and typically show irregular shapes and smoothed edges (Fig. 2A). The crusts, which are brown in colour and occasionally zoned, are cm-thick and have a lateral extent of several meters.

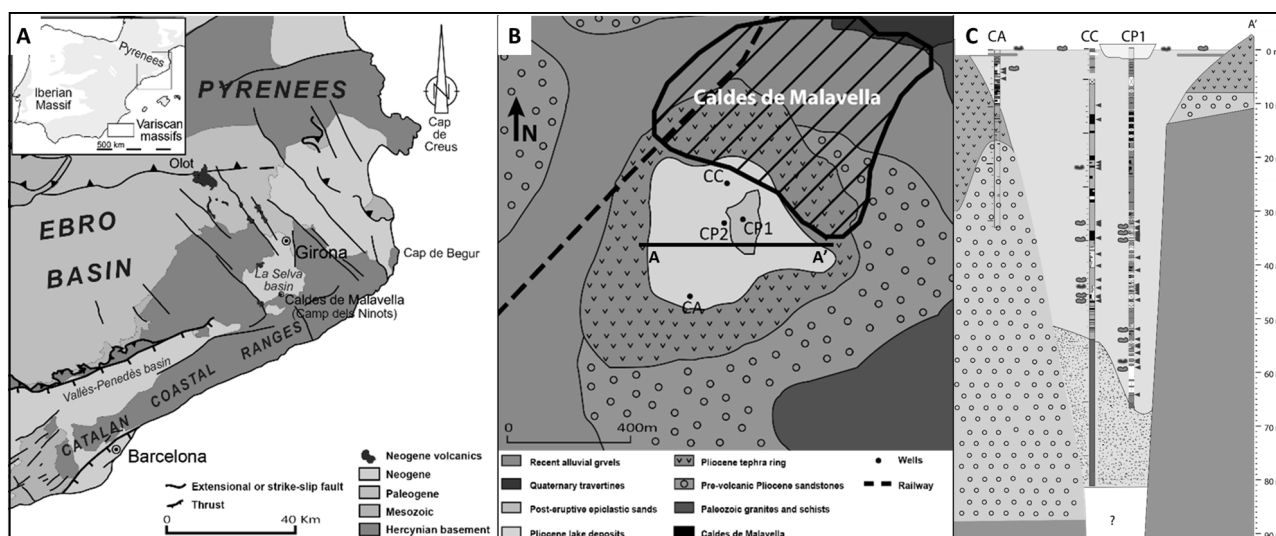


Fig. 1: A) Simplified geological map of NE Catalonia showing the Catalan Volcanic Field, fractures and the location of CNMD; B) Simplified geological map of the CNMD area with the location of the wells (CA, CC, CP1 and CP2); C) Synthetic cross section (A-A' in B) showing the structure of the CNMD and the location of the studied samples. The horizontal distribution is not scaled.

Mineralogical analyses indicate that silica nodules and crusts range in composition between opal-A and opal-CT. Petrographic observations reveal that perfectly preserved diatoms frustules coexist with opal-A microspheres in the white beds, suggesting that both formed from Si-rich lake waters and were deposited as part of the sediment. Opal-A rich nodules are composed by aggregates of ~2µm in diameter smoothed microspheres, and they frequently show diatom moulds (Fig.2 B-C). This, suggests that the dissolution of diatom frustules contributed to the formation of the nodules. Moreover, opal-A nodules replacing the dolostones typically engulf preserved dolomite crystals and contain dolomite moulds, evidencing a replacement process intimately associated with the growing of opal nodules (Fig. 2D). The opal-CT rich nodules are characterized by aggregates of ~8 µm in diameter microspheres, occasionally forming complex finger-like aggregates and bladed textures.

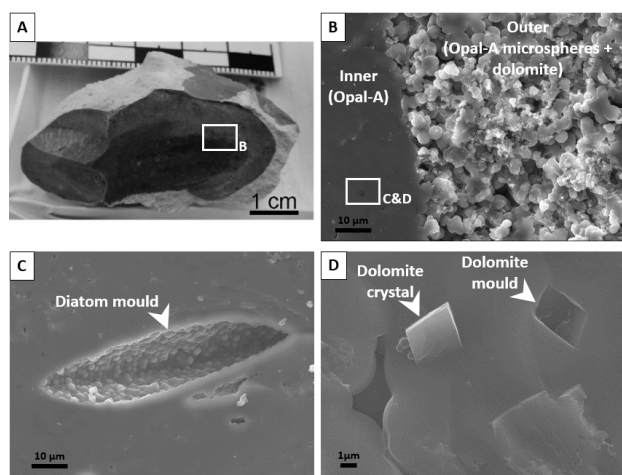


Fig. 2: A) Opal-A nodule showing zonation and the replaced host dolostone (ochre); B) SEM view of the edge of the nodule ; C) SEM view of a diatom mould within the opal-A mass; D) SEM view showing dolomite crystal and moulds within opal-A mass.

Diatom rich samples present silica $\delta^{18}\text{O}$ -PDB compositions ranging between +6.00 to +7.20‰. Opal-A rich nodules and crusts yielded $\delta^{18}\text{O}$ -PDB values varying from -0.34 to +6.82‰. Opal-A/CT show results of $\delta^{18}\text{O}$ -PDB between +3.43 to +5.95‰. Opal-CT rich nodules show $\delta^{18}\text{O}$ -PDB compositions ranging from +1.78 to +2.65‰. Opal veins cropping out in the surrounding of the CNMD present $\delta^{18}\text{O}$ -PDB composition tightly around -4‰, which is considered as representative of the isotopic signature of Si-rich hydrothermal fluids of the area.

Results indicate that the formation of silica nodules and crusts in the Camp dels Ninots maar resulted from a dissolution-recrystallization process involving the well-known opal-A to opal-CT transition. The process was most probably enhanced by the flow of Si-rich hydrothermal fluids that inflow the maar through the fracture system of the basin.

The initial stage of silica formation is associated with the dissolution of diatoms frustules and opal microspheres that form part of the lake sediment and subsequent re-

precipitation in the form of opal-A nodules and crusts. A further evolution to opal-A/CT and opal-CT mineralogy is associated with important textural changes and the progressive evolution to more depleted $\delta^{18}\text{O}$ -PDB values. The opal-A to opal-CT transition in the CNMD is not associated with progressive burial but with opal ageing (Herdianita et al., 2000), as the maar sediments present limited burial, temperature and time.

The growth of silica nodules and crusts was favored in more porous and permeable sediments like dolomite beds. Therefore, they are more abundant towards (i) the top of the sedimentary filling where dolomites are dominant, and (ii) the margin of the maar where the entrance of both meteoric and hydrothermal fluids was more probable.

The primary source of the silica is attributed to (i) the alteration of basement rocks during the circulation of hydrothermal fluids through it, and (ii) the weathering of the volcanic rocks both within the roots and the surrounding maar lake.

Acknowledgements

This research has been funded by Repsol Exploración through a collaborative project with the University of Barcelona. The well drilling, coring and the Camp dels Ninots project were sponsored by projects 2014-100575 (Generalitat de Catalunya), SGR2017-859 (AGAUR) and the Ministry of Economy and Competitiveness of Spain, under project CGL2016-80000-P (MINECO).

References

- Gómez de Soler, B., Campeny, G., Van der Made, J., Oms, O., Agustí, J., Sala, R., Blain, H-A., Burjachs, F., Claude, J., García S., Riba, D., Rosillo, R. (2012). A new key locality for the Pliocene vertebrate record of Europe: the Camp dels Ninots maar (NE Spain). *Geologica Acta*, 10(2):1-17.
- Herdianita, N. R., Browne, P. R. L., Rodgers, K. A., & Campbell, K. A. (2000): Mineralogical and textural changes accompanying ageing of silica sinter. *Mineralium deposita*, 35(1), 48-62.
- Oms, O., Bolós, X., Barde-Cabusson, S., Martí, J., Casas, A., Lovera, R., Himi, M., Gómez de soler, B., Campeny Vall-Llosera, G., Pedrazzi, d. & Agustí, J. (2015): Structure of the Pliocene Camp dels Ninots maar-diatreme (Catalan Volcanic Zone, NE Spain). *Bulletin of Volcanology*, 77(11): 1-13.

Early lake sedimentation in the Pliocene Camp dels Ninots maar (Catalan Coastal Ranges, Spain).

Oriol Oms¹, Alejandro Gil¹, Sergi Pla-Rabés², Pere Anadón³, Jordi Ibáñez³, Pablo Rodríguez-Salgado⁴, Esteve Cardellach¹, Bruno Gómez de Soler^{5,6}, Gerard Campeny^{5,6}, Jordi Agustí^{5,6,7}.

¹ Universitat Autònoma de Barcelona, Facultat de Ciències, Departament de Geologia. Campus Bellaterra, 08193, Spain. E-mail: joseporiol.oms@uab.cat.

² Centre de Recerca Ecològica i Aplicacions Forestals (CREAF). Campus Bellaterra UAB, 08193, Spain.

³ Institut de Ciències de la Terra Jaume Almera, CSIC, C/ Lluís Solé i Sabarís, s/n, 08028 Barcelona, Spain.

⁴ Irish Centre for Research on Applied Geosciences (iCRAG), University College Dublin, Belfield, Ireland.

⁵ Institut Català de Paleoecologia Humana i Evolució Social (IPHES). Campus Sescelades URV, 43007 Tarragona, Spain.

⁶ Universitat Rovira i Virgili (URV). Facultat de Lletres. Av. Catalunya 35, 43002 Tarragona, Spain.

⁷ Institució Catalana de Recerca i Estudis Avançats (ICREA). Pg. Lluís Companys 23, 08010. Barcelona, Spain.

Keywords: Maar lake, paleoecology, mineralogy

The Pliocene Camp dels Ninots maar-diatreme volcano is found in the Catalan Coastal Ranges (NE Spain, see figure 1 by Miró et al, this volume). The associated lake deposits contain a reference paleontological and stratigraphic record (Gómez de Soler et al., 2012, Jiménez-Moreno et al. 2013). Three relatively deep research cores have been drilled in order to understand the diatreme infill (Fig. 1): Can Cateura (75 m, drilled in 2009, Jiménez-Moreno et al., 2013), Can Pla 1 and Can Pla 2 (112.8 and 145 m, respectively, drilled in 2015, Miró et al., 2018 this volume).

All these drill cores display how the maar diatreme was first infilled by volcanic rocks (Bolós et al., 2016) and later by sedimentary rocks (Oms et al., 2015). The contact between these two kind of rocks is clearly identified (bottom of Fig. 1). The sedimentary infill consists on a succession of green mudstones, dark mudstones, whitish carbonates and silicifications (Miró et al., 2016). This note focuses on distinctive features that arise from the early sedimentation stage: (a) laminites features, (b) diatoms paleoecology, (c) sulphide occurrence and stable isotopy and (d) multy proxy correlation.

The succession in the studied wells is constituted by 4 main rock types. First, a dominant green-to-grayish laminated mudstones is found (basically clay minerals). Interestingly, in the early sedimentation of the studied cores, laminites appear disrupted by shaking during earthquakes. The second type consists of dark mudstones, with no evident lamination and larger amount of organic matter. The third type of rocks are whitish carbonates (mainly dolomite) that can be massive and indurated, or laminated. The fourth type are opaline chert nodules replacing diatomites and/or carbonate layers (Miró et al, 2016, this volume). The stratigraphic record of the Can Cateura well has been found to record climatic variations after palynological data (Jiménez-Moreno et al., 2013), which at the same time correlate with mineralogical data (Rodríguez-Salgado et al., 2018, this volume).

A preliminary paleoecological study based on diatoms was carried out in the basal part of Can Cateura core. Two main diatoms zones (Fig. 2) are observed: the

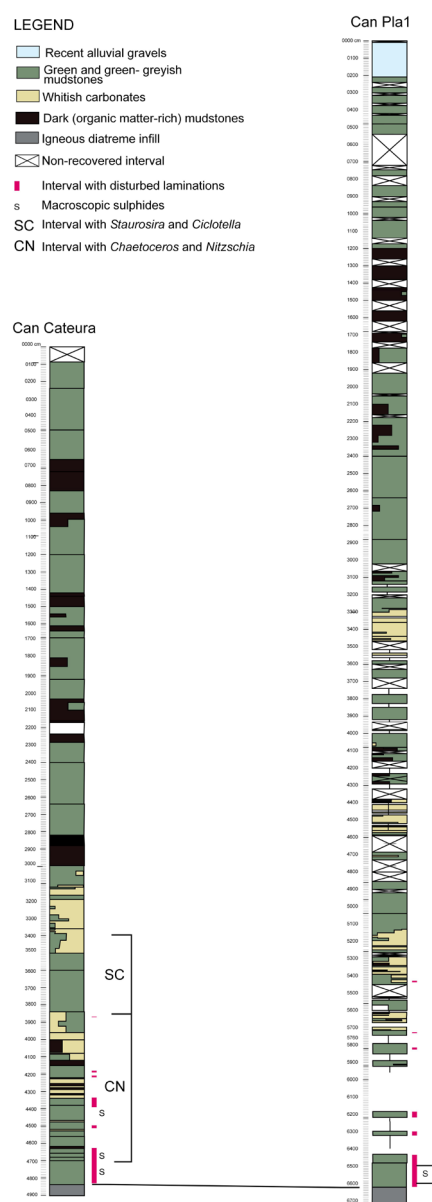


Fig.1. Can Cateura and Can Pla 1 wells, with location of the intervals where diatoms and isotopic data have been collected (Fig. 3). Thick intervals with disrupted laminations are also indicated.

lowermost 9 meters and the upper 7 ones. The basal nine meters are characterized by the occurrence of *Chaetoceros* and *Nitzschia* genus, together with the absence of *Staurosira* spp, *Cyclotella* spp, and other planktonic diatoms, which are dominant in the upper interval. Each taxonomic group correlates with characteristic hydrochemical conditions. *Nitzschia* spp. would indicate an increase in lake trophic state. On the other hand, *Chaetoceros* is typical from brackish waters having sulfates but not sulfides (Patrick, 1977). No nitrate or chlorides are found in the mineralogical data, so an original source of sulfates is deduced after diatoms occurrence and also geochemistry (see later). Regarding *Cyclotella* spp and *Staurosira* spp, they are typical from more diluted waters. Such variations also correlate with mineralogical changes, having *Nitzschia* -*Chaetoceros* interval, a direct correlation with dry climate periods (minimum in *Abies* pollen) and carbonate peaks (concentrated waters).

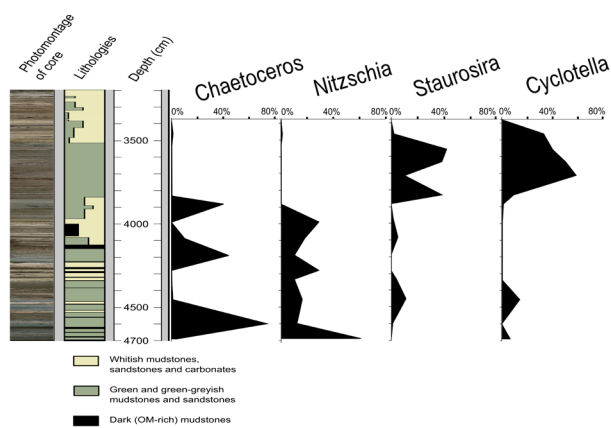


Fig. 2. Selected diatoms occurrence in the lower part of Can Cateura well (see Fig. 1 for location).

In the lower part of the two cores (Fig. 2), several sulphide-bearing layers (pyrite) were macroscopically detected. Pyrite occurs as framboidal aggregates, a texture usually associated to bacterial activity. As during drilling of Can Cateura core, pyrite rapidly oxidized to sulphates, when coring Can Pla-1, pyrite samples from depths between 65.05 and 66.10m were immediately analysed for their isotope composition. $\delta^{34}\text{S}$ values of pyrite range between +12.5 to +22.2‰ (n=6; mean of 20.02‰), suggesting a precipitation from an H_2S source related to a bacteriogenic reduction of dissolved sulfate (BSR). However, the origin of this dissolved sulfate is unclear. The low sulfate content of geothermal waters in the area (50 to 60 mg/l) precludes an evaporitic source (gypsum dissolution) (Piqué, 2008). A possible explanation could be related to disproportionation processes of oxidized sulfur species (SO_2) of magmatic origin, producing H_2S and sulfate, the latter having high $\delta^{34}\text{S}$ values. Whereas H_2S is diffused into the atmosphere the dissolved sulfate would be bacteriogenically reduced to H_2S in a closed system ($\delta^{34}\text{S}_{\text{H}_2\text{S}} \approx +14$ to +20‰), producing the heavy values obtained in pyrite. Interestingly, in the same hydrothermal system at Puig de les Moleres (1.5 km eastwards of el Camp dels Ninots, Piqué et al. 2005) describe $\delta^{34}\text{S}$ values in barite veins between +12 and +21‰, similar to those

of the pyrite obtained in this work, suggesting that hydrothermal waters with high $\delta^{34}\text{S}$ values of dissolved sulfate were active in the area. The fact that pyrite rich levels are only concentrated in the lower section of the cores is probably related to the availability of dissolved sulfate in the waters which in turn could be associated to the activation of fault systems (seismicity?) liberating gas-rich (CO_2 and SO_2) fluids from magmatic reservoirs at depth. In conclusion, the early limnological conditions for the maar lake infill at Camp dels Ninots are characterized by seismic activity and sulphate waters. Such hydrochemical characterization is deduced from both diatoms palaeoecology (abundant *Chaetoceros* occurrence) and $\delta^{34}\text{S}$ values. In sub-bottom interstitial waters, these sulphate waters underwent reduction processes as evidenced by pyrite precipitation.

Acknowledgements

Projects 2014-100575 (GENCAT), SGR2017-859 (AGAUR) CGL2016-80000-P (MINECO).

References

- Gómez de Soler, B., Campeny, G., Van der Made, J., Oms, O., et al. (2012). A new key locality for the Pliocene vertebrate record of Europe: the Camp dels Ninots maar (NE Spain). *Geologica Acta*, 10(2): 1-17.
- Jiménez-Moreno, G., Burjachs, F., Expósito, I., Oms, O., et al. (2013). Late Pliocene vegetation and orbital-scale climate changes from the western Mediterranean area. *Global Planet Change*, 108: 15-28.
- Oms, O., Bolós, X., Barde-Cabusson, S., Martí, J., Casas, A., et al. (2015). Structure of the Pliocene Camp dels Ninots maar-diatreme (Catalan Volcanic Zone, NE Spain) *Bulletin of Volcanology*, 77 (11): 98.
- Patrick, R. (1977). Ecology of freshwater diatoms and diatom communities. In D. Werner Ed. *The Biology of Diatoms*. Botanical Monographs, 13 (10).
- Piqué, À., Canals, À., Grandia, F., (2005). Geología y geoquímica del área geotérmica de Caldes de Malavella (Girona): hidrotermalismo del Neógeno a la actualidad. *Macla*, 3: 159-160. Proceedings XXV Meeting of the Spanish Mineralogical Society.
- Piqué, A. (2008). Insights into the geochemistry of F, Ba and Zn-(Pb) hydrothermal systems. PhD UB. 216p.

Palaeoenvironmental reconstruction from the mineralogy of the Pliocene Camp dels Ninots maar lake sediments (Catalan Volcanic Zone, NE Iberia)

Pablo Rodríguez-Salgado¹, Jordi Ibáñez², Pere Anadón², Bruno Gómez de Soler^{3,4}, Gerard Campeny^{3,4}, Jordi Agustí^{3,4,5} and Oriol Oms⁶

¹ Irish Centre for Research on Applied Geosciences (iCRAG), University College Dublin, Belfield, Ireland
pablo.rodriguez-salgado@icrag-centre.org

² Institut de Ciències de la Terra Jaume Almera (CSIC), C. Lluís Solé Sabarís sn, Barcelona, Spain.

³ Institut Català de Paleoecologia Humana i Evolució Social (IPHES). C/ Marcel·lí Domingo s/n, Edifici W3 Campus Sescelades URV, 43007 Tarragona, Spain.

⁴ Universitat Rovira i Virgili (URV). Facultat de Lletres. Av. Catalunya 35, 43002 Tarragona, Spain.

⁵ Institució Catalana de Recerca i Estudis Avançats (ICREA). Barcelona, Spain.

⁶ Universitat Autònoma de Barcelona. Departament de Geologia. 08193 Bellaterra, Spain.

Keywords: Mineralogy, Climate, XRD.

The Camp dels Ninots Maar Lake (Pliocene, La Selva basin) provides a remarkable climate record that allows one to compare external climatic proxies with mineralogical changes recorded in the lake. High resolution mineralogical analyses by means of powder X-ray diffraction (XRD) were conducted at the 75-m long Can Cateura well core. The core, obtained from a well drilled in the centre of el Camp dels Ninots maar-lake, was first studied by (Jiménez-Moreno et al., 2013), who performed a biostratigraphic and paleomagnetic analysis to study the late Pliocene climate in the western Mediterranean area.

The aim of the present work is to investigate how precisely long-term climate variations affect the mineralogy of a maar lake by comparing the compositional variation of different mineral assemblages with the palynological analyses (in particular abies pollen) provided by the work of Jiménez-Moreno et al. (2013).

The XRD scans reveal that the studied samples contain different amounts of feldspars (albite and microcline), quartz, dolomite and nontronite. Many weak reflections that appear in the XRD scans of some of the samples are assigned to minerals like calcite, aragonite, siderite, magnesite, pyrite, gypsum or illite. Amorphous material, which gives rise to a broad hump in the XRD scans, is abundant and is basically attributed to the presence of opal-A.

In order to assess the mineral assemblages, a correlation matrix, principal component analysis and a compositional diagram showing the vertical distribution of the main mineral species (Fig. 1) were prepared. The results show compositional variations in terms of detrital/authigenic mineral assemblages which, in turn, exhibit good correlation with external parameters such as pollen data. Principal component analysis from both the dominant mineral associations found in the XRD results and two palynological proxies (percentages of Abies and arid taxa) has allowed the identification of up to 11 different zones along the core (fig.1). The

identified zones can be classified in two different groups: zones 1a-f and zones 2a-f. These groups are described in terms of humid/arid taxa and are cyclically alternated along the core. Zones 1a-f are characterized by peaks of Abies pollen representing high altitude conifers (above 1800 m of altitude) that are typical of temperate and wet climates. On the other hand, zones 2a-f are characterized by dry taxa representing non-arboreous vegetation typical of cool and dry climates (Jiménez-Moreno et al., 2013)

It is concluded that enrichments in nontronite and other detrital minerals such as quartz and feldspars correlate with wet periods (Abies peaks and arid taxa lows). Conversely, intervals enriched in carbonates (mainly dolomite) correlate with dry periods (Abies lows and arid taxa peaks). This cyclical variation is attributed to humidity variations. In periods with relative high rainfall, clastic input would be enhanced (hydrologically open lake), while in periods of low rainfall ionic concentrations would substantially increase (hydrologically closed lake), giving rise to primary or early diagenetic dolomite as the main authigenic precipitate.

Acknowledgements

We would like to thank the land owners, for their permission to work in the area. The Town Council of Caldes de Malavella and the Departament de Cultura de la Generalitat de Catalunya for the economic funding of excavation. This study was partially funded by projects CGL2015-65387-C3-1-P and CGL2016-80000-P of the Spanish Government, the SGR2017-859 and the 2014-100575 of the Generalitat de Catalunya. XRD technical assistance was provided by Soledad Álvarez and Josep Elvira.

References

Jiménez-Moreno, G. et al., 2013, Late Pliocene vegetation and orbital-scale climate changes from the western Mediterranean area: Global and Planetary change, v. 108, p. 15-28.

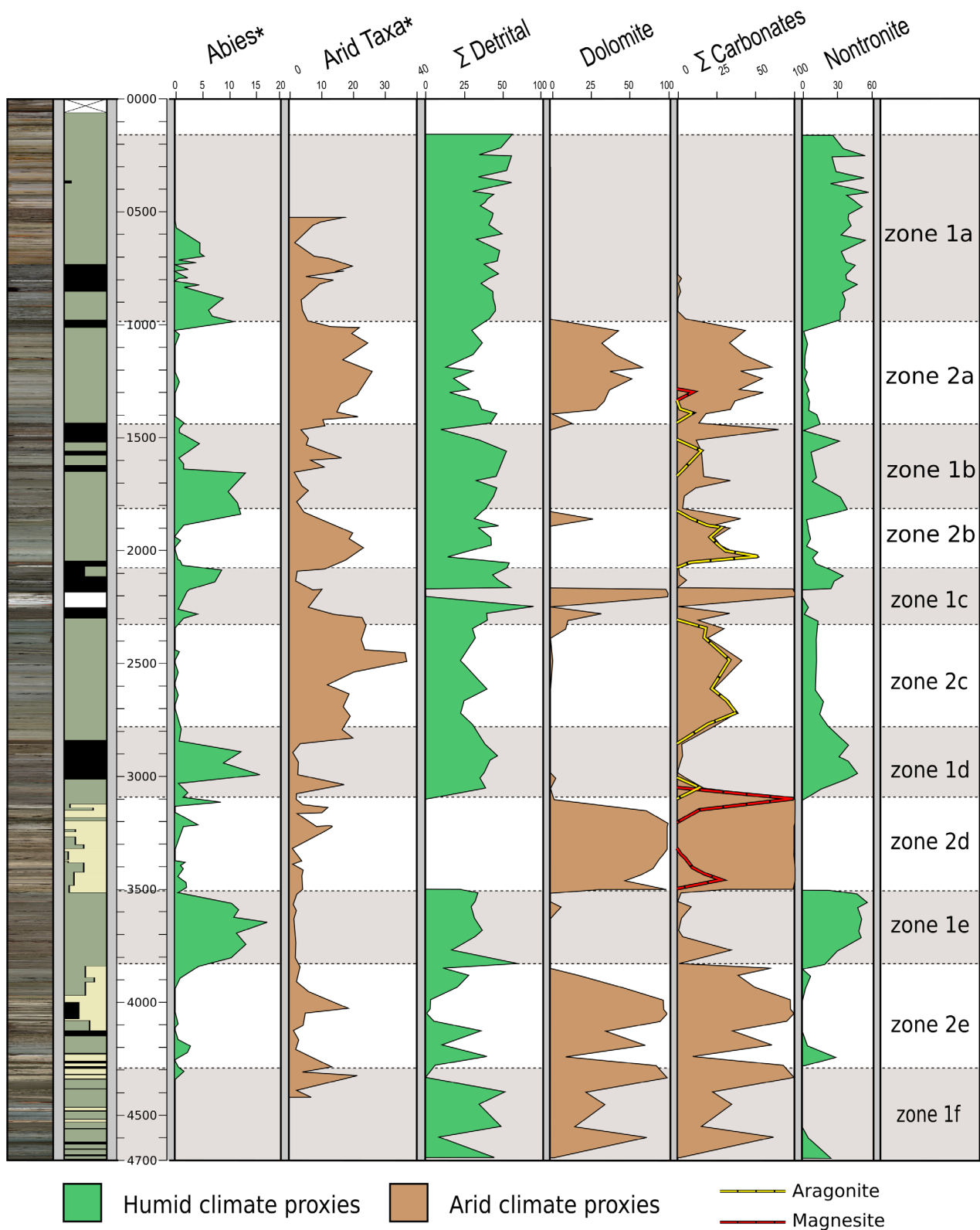


Figure 1. From left to right: Can Cateura section, selected pollen proxies from (Abies and arid taxa, by Jiménez Moreno et al 2013), and main mineralogical variations. Note the strong and independent correlation between pollen and mineralogical records

Maar sediment in central Vietnam Highland near Pleiku: An archive of regional monsoon intensity?

Arndt Schimmelmann¹, Hường Nguyễn-Văn², Dương Nguyễn-Thùy^{2a}, Jan P. Schimmelmann³, Antti E.K. Ojala⁴, Nguyệt Nguyễn-Ánh², Quốc Trọng Đỗ², Dương Thùy Nguyễn^{2b}, Phương Hòa Tạ², Vũ Huỳnh-Kim², Nhi Quỳnh Phạm-Nữ², Bernd Zolitschka³ and Ingmar Unkel⁵

¹ Department of Earth & Atmospheric Sciences, Indiana University, Bloomington, Indiana 47405, USA. aschimme@indiana.edu

² Faculty of Geology, aMineralogy, bPalynology, EOS Research Group, VNU University of Science, Hà Nội, Việt Nam.

³ University of Bremen, Institute of Geography, Celsiusstrasse 2, D-28359 Bremen, Germany.

⁴ Geological Survey of Finland, FI 02151, Espoo, Finland.

⁵ Institute for Ecosystem Research, Christian-Albrechts-Universität zu Kiel, D-24118 Kiel, Germany.

Keywords: flood layer, land use, monsoon.

Current global warming increases atmospheric humidity and will likely affect the East-Asian monsoon system across Vietnam. It is essential to understand the long-term regional climatic variability to properly evaluate present and potential future trends along global climate change. In the absence of a long written history and instrumental records in Vietnam, we must rely on geoarchives recording the paleoenvironmental history. Sediments from East-Asian maar lakes provide long-term records of monsoon variability, position and strength, for example in Cambodia, Myanmar and China (e.g., Sharma, 2014; Sun et al., 2016; Yang et al., 2016). Central Vietnam's Pleiku volcanic field features numerous maar lakes and dry maars which formed before 0.2 Ma ago (Nguyễn et al., 2013). Their natural sedimentary archives extend from the Holocene deep into the Pleistocene (Kitagawa et al., 2015; Nguyễn-Văn et al., 2017).

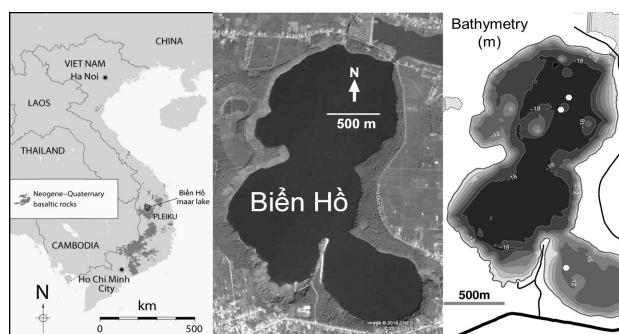


Fig. 1 - Central Vietnam's Highland features a cluster of maars near Pleiku. We cored the deepest and other parts of Biển Hồ maar lake (three white hexagons on bathymetric map) and some other maars in the area.

In three field campaigns between March 2016 and November 2017, we recovered numerous exploratory, up to 3.5 m deep gravity and piston cores from Biển Hồ maar lake near Pleiku (14° 03'03.5" N, 108° 00'00.2" E; Fig. 1) at water depths up to ~21 m (Fig. 2). A slightly cohesive microbial mat (Fig. 3B) has been observed to cover organic-rich, anoxic, sapropelic sediment below, except for occasional clay-rich flood layers following intense

precipitation, such as in the fall of 2016 (United Nations, Viet Nam Office, 2016).



Fig. 2 - Gravity and piston coring in November 2017 on an improvised platform on Biển Hồ maar lake from water depths up to ~21 m.

The most recent ~15 cm of sediment are visibly laminated, whereas deeper sediment is typically dark-olive with rare color boundaries, yet XRF and magnetic susceptibility data suggest mm-scale variance over depth. Deeper sediment recovered in November 2017 contained horizontally positioned, well-preserved leaves and grass fragments that are subject to AMS radiocarbon dating (Fig. 3A). A November 2017 hydrographic survey in Biển Hồ maar lake demonstrated thermal stratification and oxygen-depleted bottom water. By November 2017, iron (III)-containing reddish minerals in the topmost flood layer from 2016 (Fig. 3C) had been reduced to dark iron (II)-containing minerals and had been covered by a newly deposited bacterial mat on olive sediment.

Our preliminary observations suggest that Biển Hồ maar lake's suboxic bottom water protects modern laminated sediment from bioturbation (Fig. 4). Even if deeper, dark-olive sediment fails to be consistently laminated, careful documentation of its mineral content over depth may reveal a record of paleoflooding in terms of occasionally enhanced influx of weathering products from the maar's crater in response to potentially stronger monsoon activity or changes in landcover around the maar.

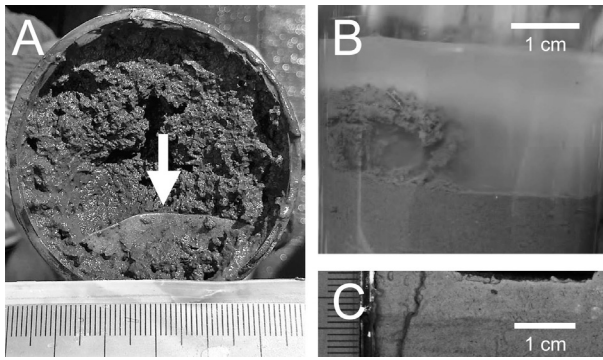


Fig. 3 – A: A well-preserved leaf was found in a core below the piston at a depth of 180 cm in Biển Hồ sediment. Other leaves, clusters of grass fragments, and wood bark were recovered in November 2017 from more than 12 horizons for radiocarbon dating. B: A curled-up microbial mat from the sediment/water interface after coring in March 2016. C: A reddish, freshly deposited 2016 flood layer was recovered in January 2017 above darker, olive sediment.

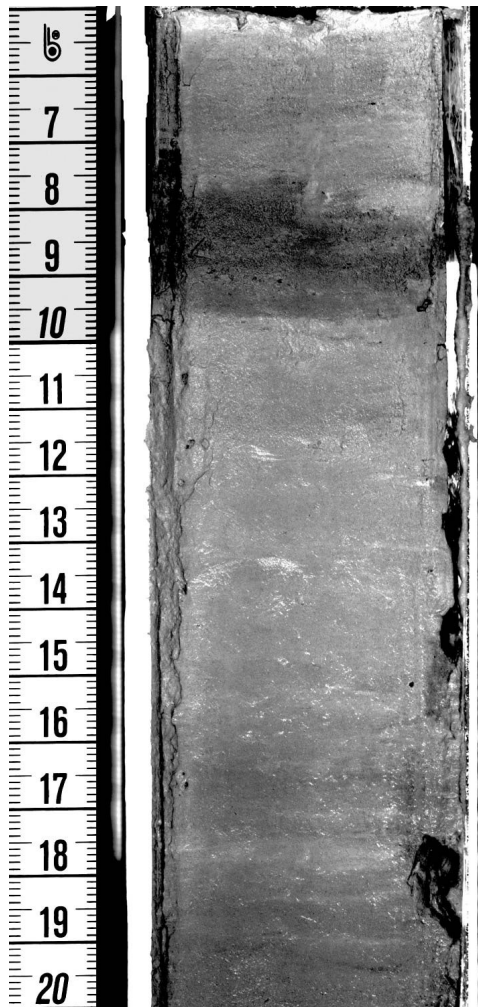


Fig. 4 – Photograph of a gravity core from Biển Hồ maar lake from March 2017 that was opened at LacCore in July 2017. Despite partial oxidation and disturbance at the top during transport from Pleiku to Hanoi, unrefrigerated storage in Hanoi, and transport to the USA, the core preserved evidence of lamination. The depth scale is in cm.

Acknowledgements

We are indebted to Thân Tạ-Văn from the Gia Lai Department of Natural Resources and Environment, Đỗ Văn Thạch, and Đỗ Ngọc Điệp for dedicated support during field work. We thank the staff of the National Lacustrine Core Facility (LacCore) at the University of Minnesota for invaluable training and analytical support.

References

- Kitagawa, H., Dang, X.P., Hayashida, A., Nakamura, T., 2015. Variations in South Asian Monsoon over the last 13 kyr inferred from biogeochemical properties of maar sediment in the central highland of Vietnam. AGU Chapman Conference, Hong Kong SAR, China, 14-18 June, 2015. <https://agu.confex.com/agu/monsoon/webprogram/Paper37349.html>
- Nguyễn, H., Flower, M.F.J., Cung, T.C., Phạm, T.X., Hoàng, V.Q., Trần, T.S., 2013. Collision-induced basalt eruptions at Pleiku and Buôn Mê Thuột, south-central Viet Nam. *Journal of Geodynamics* 69: 65-83. <https://doi.org/10.1016/j.jog.2012.03.012>
- Nguyễn-Văn, H., Nguyễn-Thùy, D., Schimmelmänn, J.P., Zolitschka, B., Tạ-Văn, T., Nguyễn-Ánh, N., Tạ Hòa, P., Đặng-Phương, T., Lê-Quyết, T., Nhi Phạm-Nữ, Q., Huỳnh-Kim, V., Schimmelmänn, A., 2017. Exploring the paleoenvironmental potential of laminated maar sediment in central Vietnam: An archive of regional paleo-flooding? PAGES Zaragoza 2017 5th Open Science Meeting, 9-13 May, 2017, Zaragoza, Spain. http://eosvnu.net/wp-content/uploads/2016/10/Poster_Spain.jpg
- Sharma, R.R., 2014. Precipitating Change. Holocene climatic change in the Asian monsoon based on sediment archives from tropical lakes. M.Sc. thesis, The University of Sydney, Australia, 170. https://www.google.com/url?sa=t&rct=j&q=&esrc=s&source=web&cd=10&ved=0ahUKewiKp6n0gvrXAhVLGpQKH-VuzBTsQFghVMAk&url=https%3A%2F%2Fses.library.usyd.edu.au%2Fbitstream%2F2123%2F12500%2F1%2F2015_Roshni_Sharma_thesis.pdf&usq=AOvWaw2KAcD_bpnLTPU8vrCbqIQ
- Sun, Q., Shan, Y., Sein, K., Su, Y., Zhu, Q., Wang, L., Sun, J., Gu, Z., Chu, G., 2016. A 530 year long record of the Indian Summer Monsoon from carbonate varves in Maar Lake Twintaung, Myanmar. *Journal of Geophysical Research: Atmospheres* 121 (10): 5620-5630. <https://dx.doi.org/10.1002/2015JD024435>
- United Nations, Viet Nam Office, 2016. Details for Viet Nam: Floods Central Viet Nam - Office of the Resident Coordinator Situation Report No. 1. http://un.org.vn/en/publications/doc_details/533-viet-nam-floods-central-viet-nam-office-of-the-resident-coordinator-situation-report-no-1.html
- Yang, Y., Zhang, H., Chang, F., Meng, H., Pan, A., Zheng, Z., Xiang, R., 2016. Vegetation and climate history inferred from a Qinghai Crater Lake pollen record from Tengchong, southwestern China. *Palaeogeography, Palaeoclimatology, Palaeoecology* 461: 1-11. <https://doi.org/10.1016/j.palaeo.2016.07.017>

Temperature records derived from glycerol dialkyl glycerol tetraethers (GDGTs) from 60 ka to 9 ka in Sihailongwan maar lake, northeastern China.

Zeyang Zhu^{1,2}, Jens Mingram³, Jiaqi Liu^{1,2}, Guoqiang Chu², Jing Wu² and Qiang Liu²

¹ University of Chinese Academy of Science, Beijing, China. zhuzeyang@mail.iggcas.ac.cn

² Key Laboratory of Cenozoic Geology and Environment, Institute of Geology and Geophysics, Chinese Academy of Sciences, Beijing, China.

³ GFZ German Research Centre for Geosciences, Section 5.2 - Climate Dynamics and Landscape Evolution, Telegrafenberg C109, 14473 Potsdam, Germany.

Keywords: : GDGTs, paleotemperature, maar lake

It was considered that climate change was forced by the solar radiation in high latitude, while some records from low latitude showed that climate change of low latitude probably be forced by the climatic processes of low latitude. For the sake of making certain of what and where forced the climate change, it is very necessary to gain absolute temperature records from the temperate latitude. However, the terrestrial absolute temperature records spanning the last glaciation in eastern Asia were scarce, which hampered our understanding of the mainly forcing factor in climate change from temperate latitude. Here, we present a biomarker climate records from Sihailongwan maar lake in the Longgang Volcanic Field (LGVF), Northeastern China.

Sihailongwan (42°17'N, 126°36'E) is a small maar lake with diameter 750 m situated in LGVF, northeastern China (Mingram et al., 2004). The lake is sensitive to climate change because of the characteristic morphology such as small catchment areas, limited inflows and outflows and big ratio of depth and diameter (Marchetto et al., 2015). The study site is located at eastern Asian monsoon area which climate is controlled by Siberia high pressure from northwest in winter and eastern Asian monsoon from south in summer (Fig. 1).

Sihailongwan is a dimictic lake and it freezes from November to next April, thus the bacteria producing GDGTs was limited in winter and boomed in warm seasons

especially in spring and autumn when the water volume was well mixed (Peterse et al., 2014; Shanahan et al., 2013). Therefore, the GDGTs-based temperature was weighted towards the warm seasons.

The GDGTs-based records showed that the mean warm season temperature in Sihailongwan ranged between 10.8 °C and 16.3 °C from 60 ka to 9 ka. The records revealed obvious temperature variations in the Younger Dryas (YD), the Bølling-Allerød (BA), the Oldest Dryas (OD) and the Heinrich events. Five Heinrich events could be showed obviously by the GDGT-based temperature sequence which were comprised markedly with $\delta^{18}\text{O}$ records in Greenland ice cores. The mean warm season temperature during the OD was 12.2 °C, followed by the BA event (13.3 °C) which began with a sharp rise and two-step drop to the YD. The BA event pattern of two-step drop in our records were associated with Greenland records and differed from the $\delta^{18}\text{O}$ records of stalagmite from Hulu Cave (Wang and Cheng, 2001). The YD event occurred with a mean temperature about 11.6 °C which only decreased 1.5-2 °C from BA event. Therefore, the amplitude of variation of the warm season temperature in Sihailongwan lake was smaller between the YD and BA than the winter temperature variation in Greenland and Huguangyan maar lake in tropic (Buizert et al., 2014; Chu et al., 2017) and supported previous hypothesis that abrupt climate change is mostly a winter phenomenon (Denton et al., 2005).

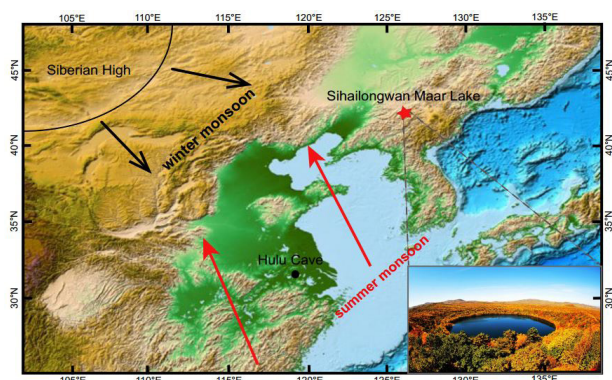


Fig. 1 – Location of Sihailongwan maar lake, paleoclimatic records site mentioned in the text and the Eastern Asian Monsoon system.

Acknowledgements

This study was supported by the National Natural Science Foundation of China (41320104006; 41561144010).

References

Buizert, C., Gkinis, V., Severinghaus, J.P., He, F., Lecavalier, B.S., Kindler, P., Leuenberger, M., Carlson, A.E., Vinther, B., Masson-Delmotte, V., White, J.W.C., Liu, Z., Otto-Bliesner, B., Brook, E.J., 2014. Greenland temperature response to climate forcing during the last deglaciation. *Science* 345: 1177-1180.

Chu, G., Sun, Q., Zhu, Q., Shan, Y., Shang, W., Ling, Y., Su, Y., Xie, M., Wang, X., Liu, J., 2017. The role of the Asian winter monsoon in the rapid propagation of abrupt climate changes during the last deglaciation. *Quaternary Science Reviews* 177: 120-129.

Denton, G.H., Alley, R.B., Comer, G.C., Broecker, W.S., 2005. The role of seasonality in abrupt climate change. *Quaternary Science Reviews* 24, 1159-1182.

Marchetto, A., Ariztegui, D., Brauer, A., Lami, A., Mercuri, A. M., Sadori, L., Vigliotii, L., Wulf, S., Guilizzoni, P. 2015. Volcanic lake sediments as sensitive archives of climate and environmental change. In Rouwet, D., Christenson, B., Tassi, F. & Vandemeulebrouck, J. (eds.): *Volcanic Lakes, Advances in Volcanology*, 379–399. Springer-Verlag, Berlin

Peterse, F., Vonk, J.E., Holmes, R.M., Giosan, L., Zimov, N., Eglington, T.I., 2014. Branched glycerol dialkyl glycerol tetraethers in Arctic lake sediments: Sources and implications for paleothermometry at high latitudes. *Journal of Geophysical Research: Biogeosciences* 119: 1738-1754.

Shanahan, T.M., Hughen, K.A., Van Mooy, B.A.S., 2013. Temperature sensitivity of branched and isoprenoid GDGTs in Arctic lakes. *Organic Geochemistry* 64, 119-128.

Wang, Y.J., Cheng, H., 2001. A High-Resolution Absolute-Dated Late Pleistocene Monsoon Record from Hulu Cave, China. *Science* 5550: 2345-2348.



Oral *Session 4*


Volcanic hazard and risk assessment in monogenetic volcanic fields

Conveners

Shane Cronin (s.cronin@auckland.ac.nz)

José Luis Macías (macias@geofisica.unam.mx)

Volcanic hazards threaten the economy, transport and natural environments within and surrounding volcanic fields. Alongside scoria cones and lava flows, many volcanic fields host maar-diatreme volcanoes and tuff-rings, which represent the second most common volcano type on land. These pose a specific suite of hazards, including violent lateral pyroclastic surges and efficient ash production, which often poses regional hazard. The locations of their future formation are also highly uncertain in most fields. Growth of population, increasingly complex infrastructure and changing technologies of our society, make assessment and mitigation of maar-related hazards important issues. We invite all contributions to this session in areas of evaluation of monogenetic volcanic hazard, including spatio-temporal forecasting methods, dynamic hazard and impact models and the characteristic hazards associated with maar-diatreme volcanism.



Using VOLCANBOX to conduct hazard assessment in monogenetic volcanic fields

Joan Martí, Laura Becerril and Stefania Bartolini.

Institute of Earth Sciences Jaume Almera, CSIC, c/ Lluís Sole Sabaris s/n, 08028 Barcelona, Spain. joan.marti@ictja.csic.es

Keywords: Volcanic hazard assessment, monogenetic fields. volcanbox

VOLCANBOX is a simple multiplatform method, capable of running on Windows, Mac OS X, and Linux, for assessing volcanic hazards and risks. It includes a series of e-tools that allow experts to evaluate the possible hazards that could affect a volcanic area and develop appropriate hazard and risk maps. VOLCANBOX allows experts to assess information and package it into a form that community planners need (Martí et al., 2017;

Currently, the VOLCANBOX platform includes five modules: spatial analysis, temporal analysis, simulation models, risk analysis, and communication protocols, plus a database design (using Volcanic Management Risk Database Design (VERDI) [Bartolini et al., 2014a], created to structure and store all data necessary to conduct hazard assessment.

Each of these modules includes different e-tools developed by the Group of Volcanology of Barcelona (www.gvb-csic.es): 1) Quantum Geographic Information Systems (GIS) for Volcanic Susceptibility (QVAST) [Bartolini et al., 2013], which provides quantitative assessments a new eruptive vent; 2) Hazard Assessment Event Tree (HASSET) [Sobradelo et al., 2014; Bartolini et al., 2016], an event tree structure that uses Bayesian inference to estimate the probability occurrence of a future volcanic scenario; 3) Volcanic Risk Information System (VORIS) [Felpeto et al., 2007], a GIS-based tool that allows users to simulate lava flows, and pyroclastic density current scenarios; 4) Volcanic Damage (VOLCANDAM) [Sciani et al., 2014], which generates maps that estimate the expected damage caused by eruptions; and 5) Bayesian Decision Model (BADEMO) [Sobradelo and Martí, 2015], which enables a previous analysis of the distribution of local susceptibility and vulnerability to eruptions to be combined with specific costs and potential losses.

VOLCABBOX is open to integrate other tools or models that have been developed by other authors. Also, it intends to offer experts different options based on the available data they may have and the accuracy they require.

VOLCANBOX is a resource to build the strategies required to successfully confront and minimize the impact of future volcanic eruptions in a homogeneous and systematic way. Experts select the tools in each module that they want to apply in a sequential workflow. The nature of this workflow can be adapted to a long- or short-term hazard assessment, and it takes the different tasks as-

sumed in the volcanic management cycle as a reference. For a long-term hazard assessment, for example, the user could obtain a susceptibility map (spatial analysis, e.g., QVAST) showing the probability of where a new vent form on a volcano, a temporal analysis of the occurrence of possible eruptive scenarios (e.g., HASSET), a simulation of possible volcanic and associated hazards and elaboration of qualitative and quantitative hazard maps (e.g., VORIS), vulnerability analysis (e.g., VOLCANDAM), and cost-benefit analysis to determine the most appropriate mitigation measures (e.g., BADEMO).

In the case of a short-term analysis (covering a single unrest episode), we would use the previous results and add monitoring information through the use of a specific (e.g., ST-HASSET) [Bartolini et al., 2016] to refine the spatial and temporal constraints of the most probable scenarios.

VeTOOLS also looks at how to make scientific information understandable for decision makers and community planners who manage risk in volcanic areas. Through instructions, scientists using VOLCANBOX show community planners how to identify the most probable eruptive scenarios and their potential effects, which helps officials triage emergency responses in the event of an eruption.

Moreover, the application of VOLCANBOX will help identify differences between the levels of hazard assessment in various volcanic areas and possible existing gaps in the basic information (e.g., census data, maps of key infrastructure) required to conduct volcanic risk management, regardless of local specific features. VOLCANBOX, if used at volcanoes across the globe, may help reveal such gaps.

Here, we present the results of the application of VOLCANBOX to different monogenetic volcanic fields located at different geodynamic environments that impose different local and regional stress conditions on these volcanic systems. The fact that in monogenetic volcanism each eruption has a different vent suggests that volcanic susceptibility has a high degree of randomness, so that accurate forecasting is subjected to a very high uncertainty. Recent studies on monogenetic volcanism reveal how sensitive magma migration may be to the existence of changes in the regional and/or local stress field produced by tectonics or lithological contrasts (i.e., intrusion of magma bodies), which may induce variations in the pattern of further movements of magma, thus

changing the location of future eruptions. This implies that a precise knowledge of the stress configuration and distribution of rheological and structural discontinuities in such regions is crucial to forecast monogenetic volcanism.

To illustrate these potential differences when conducting volcanic hazard assessment at monogenetic fields, we compute long term volcanic hazard for El Hierro and Lanzarote (intraplate ocean volcanic islands(Becerril et al., 2014; 2017) (La Garrotxa Volcanic Field (continental rifting), and Deception Island (back-arc basin) (Bartolini et al., 2014b), and compare the results obtained

Acknowledgements

This research have been partially funded by the European Commission grants EC ECHO SI2.695524: VeTOOLS and INFRADEV-3 EPOS-IP AMD-676564-42.

References

- Bartolini, S., A. Cappello, J. Martí, and C. Del Negro (2013), QVAST: A new Quantum GIS plugin for estimating volcanic susceptibility, *Nat. Hazards Earth Syst. Sci.*, 13(11), 3031–3042, doi:10.5194/nhess-13-3031-2013.
- Bartolini, S., L. Becerril, and J. Martí (2014a), A new Volcanic management Risk Database design (VERDI): Application to El Hierro Island (Canary Islands), *J. Volcanol. Geotherm. Res.*, 288,, 132–143, doi:10.1016/j.jvolgeores.2014.10.009.
- Bartolini, S., A. Geyer, J. Martí, D. Pedrazzi, and G. Aguirre-Díaz (2014b), Volcanic hazard on Deception Island (South Shetland Islands, Antarctica), *J. Volcanol. Geotherm. Res.*, 285, 168, doi:10.1016/j.jvolgeores.2014.08.009.
- Bartolini, S., R. Sobradelo, and J. Martí (2016), ST-HASSET for volcanic hazard assessment: A Python tool for evaluating the evolution of unrest indicators, *Comput. Geosci.*, 93, doi:10.1016/j.cageo.2016.05.002.
- Bartolini, S., Martí, J., Sobradelo, R., Becerril, . Probabilistic e-tools for hazard assessment and risk management. In In Bird, D., Jolly, G., Haynes, K., McGuire, B., Fearnley, C. : “Observing the volcano world. Volcanic Crisis Communication”. *Adv in Volcanology*, Springer, (2017) DOI: 10.1007/11157_2017_14. ISBN 978-3-319-44097-2. Series ISSN 2364-3277.
- Becerril, L., Bartolini, S., Sobradelo, R., Martí, J., Morales, J. M., and Galindo, I. (2014): Long-term volcanic hazard assessment on El Hierro (Canary Islands), *Nat. Hazards Earth Syst. Sci.*, 14, 1853–1870, <https://doi.org/10.5194/nhess-14-1853-2014>.
- Becerril, L., Martí, J., Bartolini, S., Geyer, A. (2017) Assessing qualitative long-term volcanic hazard at Lanzarote Island (Canary Islands) *Nat. Hazards Earth Syst. Sci.*, doi:10.5194/nhess-2017-2
- Felpeño, A., J. Martí, and R. Ortiz (2007), Automatic GIS-based system for volcanic hazard assessment, *J. Volcanol. Geotherm. Res.*, 166,, 106–116, doi:10.1016/j.jvolgeores.2007.07.008.
- Martí, J., Bartolini, S., Becerril, L. Enhancing safety in a volcano’s shadow, *Eos*, 97, doi:10.1029/2016EO054161. Published on 21 June 2016.
- Scaini, C., A. Felpeño, J. Martí, and R. Carniel (2014), A GIS-based methodology for the estimation of potential volcanic damage and its application to Tenerife Island, Spain, *J. Volcanol. Geotherm. Res.*, 278–279, 40–58, doi:10.1016/j.jvolgeores.2014.04.005.
- Sobradelo, R., S. Bartolini, and J. Martí (2014), HASSET: A probability event tree tool to evaluate future volcanic scenarios using Bayesian inference presented as a plugin for QGIS, *Bul. Volcanol.*, 76, 770, doi:10.1007/s00445-013-0770-x.

Deception Island, Antarctica: eruptive dynamics and volcanic hazards in a post-caldera monogenetic volcanic field

Dario Pedrazzi¹, Karoly Németh², Adelina Geyer¹, Antonio Álvarez-Valero³, Gerardo Aguirre-Díaz⁴ and Stefania Bartolini¹

¹ ICTJA, CSIC, Group of Volcanology, SIMGEO UB-CSIC, Institute of Earth Sciences Jaume Almera, Lluís Sole i Sabarís s/n, 08028 Barcelona, Spain. dpedrazzi@ictja.csic.es

² Volcanic Risk Solutions, CS-INR, Massey University, Private Bag 11 222, Palmerston North, New Zealand.

³ Departamento de Geología, Universidad de Salamanca, 37008 Salamanca, Spain.

⁴ Centro de Geociencias, Universidad Nacional Autónoma de México, Campus Juriquilla, Querétaro, Qro. 76230, Mexico.

Keywords: Crimson Hill, Kroner Lake, South Shetland Islands

Deception Island (DI) is an active Quaternary volcanic caldera of the South Shetlands Archipelago (Antarctica) (Fig. 1a, b).

Post-caldera volcanism includes over 30 eruptions during the Holocene (e.g. Orheim 1972) with more than 20 volcanic episodes registered over the past two centuries (Orheim 1972; Roobol 1982; Smellie et al. 2002) including the eruptions of 1967, 1969, and 1970 (Fig. 1c).

These eruptions, together with the 1992, 1999 (Ibáñez et al. 2003), and 2014–2015 (Almendros et al. 2015) unrest episodes, demonstrate that the volcanic system under DI is still very active and that the occurrence of a new eruption is likely.

Recent post-caldera volcanism is dominated by hydro-magmatic eruptions, with the water source being from Port Foster Bay seawater, from the underground aquifer and water from the glaciers (Baker et al. 1975; Smellie 2002; Pedrazzi et al. 2014). Even small-volume eruptions become highly explosive when located on waterlogged shorelines, or beneath ice caps (Baker et al. 1975; Smellie 2002; Pedrazzi et al. 2014). A detailed field revision of the historical (1829–1970) hydrovolcanic post-caldera volcanism at DI was carried out, with the aim of understanding how the location of a potential new eruptive vent can control magma-water interactions, and the related hazards to be expected during a new eruption on the island.

We focused on the Crimson Hill (dated between 1825 and 1829), Kroner Lake (dated between 1829 and 1912), 1967 and 1970 (Fig. 1c) eruptions as representatives of the entire spectrum of potential hydrovolcanic activity on the island. We also report the 1969 eruption because it exemplifies an important event in the eruptive record at DI due to magma-ice interaction with formation of a jökulhlaup (Smellie 2002). In addition to our own field observations, we incorporated the existing published data on the above-mentioned eruptions (Orheim 1971c; Roobol 1973, 1980, 1982; Baker and McReath 1975; González-Ferrán et al. 1971; Shultz 1972; Smellie 2002, Smellie et al. 2002). Volcanic activity during the Crimson Hill and Kroner Lake eruptions occurred in the shallow seawater of Whalers Bay. The Crimson Hill eruption shows a sequence dominated by turbulent dilute PDCs and subordinated

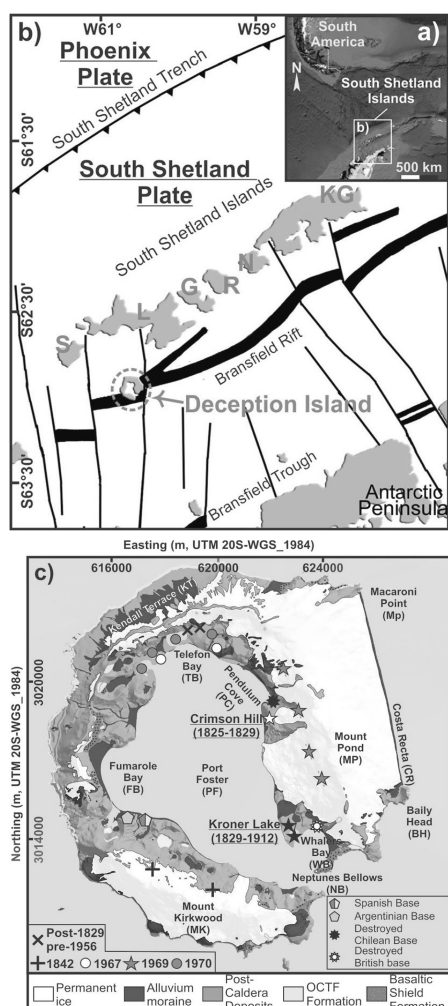


Fig. 1 – Location of the South Shetland Archipelago (Google Earth 2016-Image US Geological Survey). b South Shetland Islands Archipelago and location of Deception Island: S, Snow Island; L, Livingston Island; G, Greenwich Island; R, Robert Island; N, Nelson Island; KG, King George Island. C Simplified geological map of Deception Island with the location of the postcaldera explosive vents and recent volcanic activity modified from Pedrazzi et al. 2018).

fallout deposits. The Kroner Lake eruption is mostly characterised by fallout deposits with no significant shift from hydrovolcanic to magmatic styles. The 1967 and 1970 eruptions are characterised by clustered vents in shallow seawater or close to the coastline and are due to interaction with saturated or icy substrates. Field data from both eruptions suggest alternating volcanic and hydrovolcanic phases with fallout, ballistic blocks and bombs, and subordinate, dilute PDCs. Main hazard related to 1969 eruption was due to jökulhlaup. Styles and hazards posed by volcanism on the island are controlled by the location of the vents and the degree of magma interaction with the surrounding volcano-tectonic and water availability conditions.

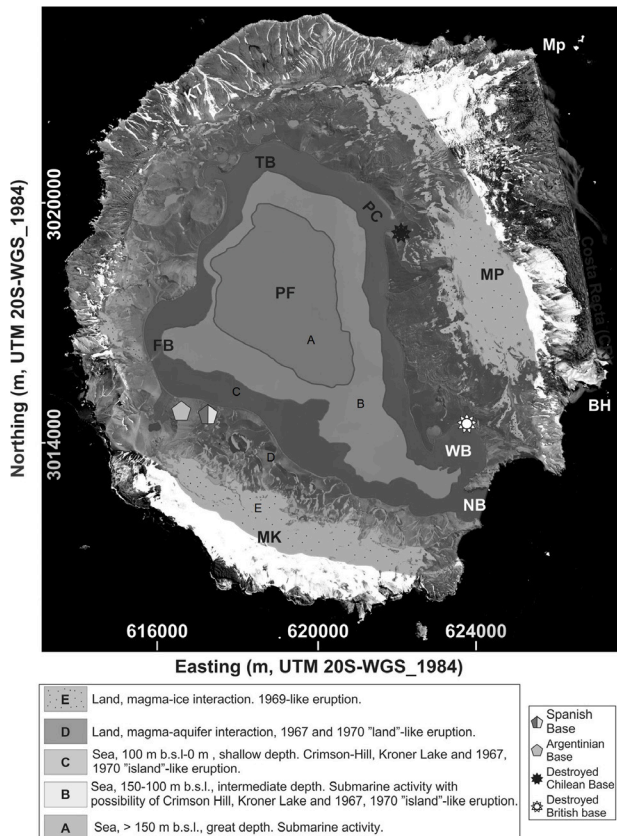


Fig. 2 – Map showing the type of volcanic activity depending on susceptibility inside the caldera at DI.

Based on the results obtained in this paper, we have tentatively mapped inside the DI caldera—according to the historical volcanism and following the structural limits proposed by Martí et al. (2013)—the possible type of hydrovolcanic activity to be expected during a future volcanic eruption at DI to depend on the outcoming vent location.

Acknowledgements

The project was partially funded by the POSVOLDEC project (CTM2016-79617 P)(AEI/FEDER-UE). D.P. is grateful for his Beatriu de Pinós contract (2016 BP 00086).

References

- Baker, P.E., McReath, I. 1971. Geological investigations on Deception Island. *Antarct J US* 6(4): 85–86
- Baker, P.E., McReath, I., Harvey, M.R., Roobol, M.J., Davies, T.G. 1975. The geology of the South Shetland Islands. V. Volcanic evolution of Deception Island. *British Antarctic Survey* 78: 81 PP
- González-Ferrán, O., Munizafam, F., Morenom, H. 1971. Síntesis de la evolución volcánica de Isla Decepción y la erupción de 1970. *Instituto Antártico Chileno Serie Científicas* 2: 1–14
- Ibáñez, J.M., Almendros, J., Carmona, E., Martí, C., Abril, M. 2003. The recent seismo-volcanic activity at Deception Island volcano. *Deep-Sea Res II Top Stud Oceanogr* 50(10): 1611–1629.
- Martí, J., Geyer, A., Aguirre-Díaz, G. 2013. Origin and evolution of the Deception Island caldera (South Shetland Islands, Antarctica). *Bull Volcanol* 75(6): 732.
- Orheim, O. 1971. Volcanic activity on Deception Island, South Shetland Islands. In: ADIE RJ (ed) *Antarctic geology and geophysics*. Universitetsforlaget, Oslo, pp 117–120
- Orheim, O. 1972. Volcanic activity on Deception Island, South Shetland Islands. *Ohio State University, Institute of Polar Studies*
- Pedraza, D., Aguirre-Díaz, G., Bartolini, S., Martí, J., Geyer, A. (2014) The 1970 eruption on Deception Island (Antarctica): eruptive dynamics and implications for volcanic hazards. *J Geol Soc* 171(6): 765–778
- Pedraza, D., Németh, K., Geyer, A., Álvarez-Valero, A. M., Aguirre-Díaz, G. and Bartolini, S. (2018). Historic hydrovolcanism at Deception Island (Antarctica): implications for eruption hazards. *Bulletin of Volcanology* 80(1): 11
- Roobol, M.J. 1973 Historic volcanic activity at Deception Island. *Brit Antarct Surv Bull* 32: 23–30
- Roobol, M.J. 1980 A model for the eruptive mechanism of Deception Island from 1820 to 1970. *Brit Antarct Surv Bull* 49: 137–156
- Roobol, M.J. 1982. The volcanic hazard at Deception Island, South Shetland Islands. *Brit Antarct Surv Bull* 51: 237-245
- Shultz, C.H. 1972. Eruption at Deception Island, Antarctica, August 1970. *GSA Bull* 83(9): 2837–2842
- Smellie, J.L. 2002. The 1969 subglacial eruption on Deception Island (Antarctica): events and processes during an eruption beneath a thin glacier and implications for volcanic hazards. *Geol Soc Lond, Spec Publ* 202(1): 59–7
- Smellie, J.L., López-Martínez, J., Headland, R.K., Hernández-Ci-fuentes, F., Maestro, A., Millar, I.L., Rey, J., Serrano, E., Somoza, L., Thomson, J.W. 2002. Geology and geomorphology of Deception Island. (BAS Geomap Series, Sheets 6A and 6B): 77 pp.

Significance of Holocene monogenetic clusters within the Michoacán–Guanajuato Volcanic Field (México)

Claus Siebe¹, Nanci Reyes¹, Ahmed Nasser Mahgoub², Sergio Salinas³, Harald Böhnel², Marie-Noelle Guilbaud¹, and Patricia Larrea¹

¹ Department of Volcanology, Instituto de Geofísica, Universidad Nacional Autónoma de México (UNAM), Coyoacán, 04510 México. csiebe@geofisica.unam.mx

² Centro de Geociencias, Universidad Nacional Autónoma de México (UNAM), Blvd. Juriquilla No. 3001, Querétaro, 76230 México.

³ División de Ingeniería en Ciencias de la Tierra, Facultad de Ingeniería, Universidad Nacional Autónoma de México (UNAM), Coyoacán, 04510 México.

Keywords: cluster, monogenetic volcano, Michoacán–Guanajuato Volcanic Field, México.

The Trans-Mexican Volcanic Belt (TMVB), one of the most complex and active subduction-related volcanic arcs worldwide, includes several volcanic fields dominated by monogenetic volcanoes. Among these, the Plio-Quaternary Michoacán–Guanajuato Volcanic Field (MGVF), situated in central Mexico (Fig. 1), is the largest monogenetic field in the world (Hasenaka and Carmichael, 1985). It includes >1100 scoria cones and associated lava flows, ~400 medium-sized volcanoes (Mexican shields, Chevrel et al., 2016), ~22 phreatomagmatic vents (maars and tuff cones:

e.g. Kshirsagar et al., 2015), as well as isolated domes and lava flows. The historical eruptions of Jorullo in 1759 (Guilbaud et al., 2011) and Parícutin in 1943 (Luhr and Simkin, 1993; Larrea et al., 2017) indicate that this area is still active and that more eruptions should be expected in the future.

Small monogenetic vents (scoria cones and isolated lava flows) are not distributed evenly throughout the MGVF. They occur either isolated or form small clusters, as re-

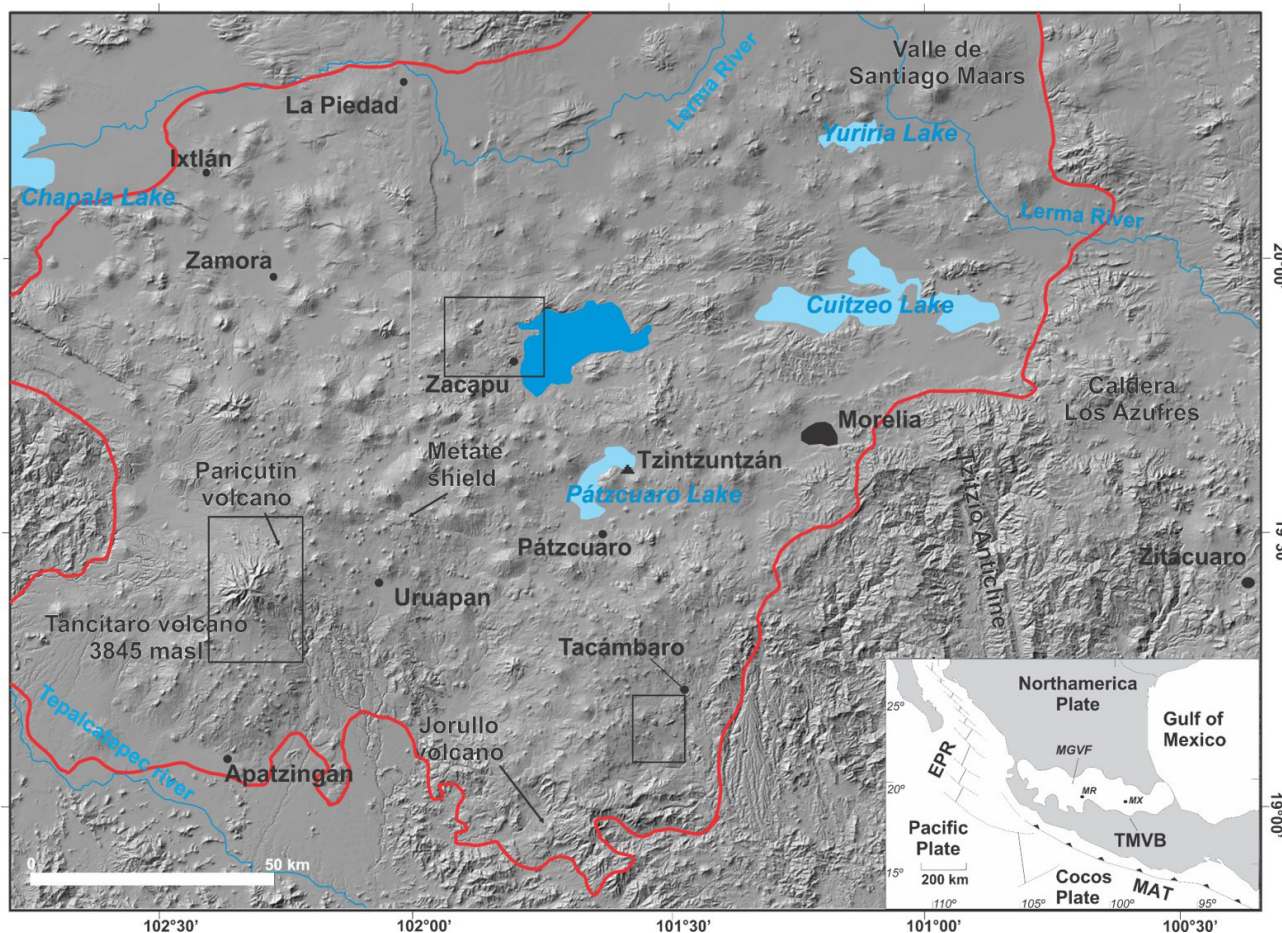


Fig. 1 – Location of the Tacámbaro, Zacapu, and Tancitaro volcanic clusters within the ~40,000 km² wide Michoacán–Guanajuato Volcanic Field, México (after Kshirsagar et al., 2015). Inset shows location of the MGVF within the Trans Mexican Volcanic Belt (TMVB) and associated tectonic framework.

cently documented near the cities of Tacámbaro (Guilbaud et al., 2012) and Zacapu (Reyes-Guzmán et al., in press). Both of these two clusters (Zacapu and Tacámbaro, Fig. 1) occur along important normal fault zones and each comprises four monogenetic vents that erupted in a sequence of geologically short time intervals (hundreds to few thousands of years) within a small area (few tens of km²). Erupted volumes and ages for each of the volcanoes comprising the clusters were determined (Mahgoub et al., 2017; 2018 in press) and compositional trends (from olivine-bearing basaltic andesite towards high silica hornblende-bearing andesite) could be recognized.

The recent identification of such small Holocene clusters in small areas within the MGVF opens several questions in regard to future volcanic hazard assessments in this region: Are the youngest (Holocene) clusters still “active” and is a new eruption likely to occur within their surroundings? How long are such clusters “active”? Will the next monogenetic eruption in the MGVF be a single short-lived isolated eruption, or will it be part of an already existing cluster, or the beginning of a new cluster? More specifically, is it possible that the historic basaltic andesite eruption of Jorullo represents the initiation of a cluster and should a new eruption in its proximity be expected in the future? In order to address these questions, a third case near the town of Tancitaro (not far from Paricutin, Fig. 1) is currently under study and preliminary results will be presented. Geologic mapping, geochemical analyses, radiometric dating, and paleomagnetic studies will help establish the sequence of eruption of the different vents, and shed more light on the conditions that allow several magma sources to be formed and then tapped in close temporal and spatial proximity to each other producing such small “flare-ups”.

Acknowledgements

Field and laboratory costs were defrayed from projects funded by Consejo Nacional de Ciencia y Tecnología (CONACYT-167231) and the Dirección General de Asuntos del Personal Académico (DGAPA-UNAM-IN103618) granted to C. Siebe.

References

- Chevrel, M.O., Siebe, C., Guilbaud, M.N., Salinas, S., 2016. The AD 1250 El Metate shield volcano (Michoacán): Mexico's most voluminous Holocene eruption and its significance for archaeology and hazards. *The Holocene* 26(3): 471-488.
- Guilbaud, M.-N., Siebe, C., Layer, P., Salinas, S., Castro-Govea, R., Garduño-Monroy, V. H., LeCorvec, N., 2011. Geology, geochronology, and tectonic setting of the Jorullo Volcano region, Michoacán, México. *Journal of Volcanology and Geothermal Research* 201, 97-112.
- Guilbaud, M.N., Siebe, C., Layer, P., Salinas, S., 2012. Reconstruction of the volcanic history of the Tacámbaro-Puruarán area (Michoacán, México) reveals high frequency of Holocene monogenetic eruptions. *Bulletin of Volcanology* 74: 1187-1211.
- Hasenaka, T., Carmichael, I. S. E., 1985. The cinder cones of Michoacán-Guanajuato, central Mexico: their age, volume and distribution, and magma discharge rate. *Journal of Volcanology and Geothermal Research* 25, 105-124.
- Kshirsagar, P., Siebe, C., Guilbaud, M.-N., Salinas, S., Layer, P., 2015. Late Pleistocene (~21,000 yr BP) Alberca de Guadalupe maar volcano (Zacapu basin, Michoacán): Stratigraphy, tectonic setting, and paleo-hydrogeological environment. *Journal of Volcanology and Geothermal Research* 304, 214-236.
- Larrea, P., Salinas, S., Widom, E., Siebe, C., Abbitt, R.J.F., 2017. Compositional and volumetric development of a monogenetic lava flow field: The historical case of Paricutin (Michoacán, México). *Journal of Volcanology and Geothermal Research* 348: 36-48.
- Luhr, J.F. and Simkin, T., 1993. Paricutin. The volcano born in a Mexican cornfield. Geoscience Press, Phoenix, Arizona, 427 pp.
- Mahgoub, A.N., Böhnell, H., Siebe, C., Salinas, S., Guilbaud, M.N., 2017. Paleomagnetically inferred ages of a cluster of Holocene monogenetic eruptions in the Tacámbaro-Puruarán area (Michoacán, México): Implications for volcanic hazards. *Journal of Volcanology and Geothermal Research* 347: 360-370.
- Mahgoub, A.N., Reyes-Guzmán, N., Böhnell, H., Siebe, C., Pereira, G., Dorison, A. (in press). Paleomagnetic constraints on the ages of the Holocene Malpaís de Zacapu lava flow eruptions, Michoacán (México): Implications for archaeology and volcanic hazards. *The Holocene*.
- Reyes-Guzmán, N., Siebe, C., Chevrel, M.O., Guilbaud, M.N., Salinas, S., Layer, P. (in press). Geology and radiometric dating of Quaternary monogenetic volcanism in the western Zacapu lacustrine basin (Michoacán, México): Implications for archaeology and future hazard evaluations. *Bulletin of Volcanology*.

Cyclic variation in intensity of explosivity during a maar–diatreme eruption on an ocean island volcano: implications for dynamic hazard models

Bob Tarff¹, Simon Day², Hilary Downes¹ and Ioan Seghedi³

¹ Department of Earth and Planetary Sciences, Birkbeck, University of London, Malet Street, London WC1E 7HX
 bobanddonna@talktalk.net

² Institute for Risk and Disaster Reduction, Department of Earth Sciences, University College London

³ Institute of Geodynamics, 19-21 Str. Jean-Luis Calderon, 020032, Bucharest, Romania

Keywords: phreatomagmatic, root-zone, diatreme

Phreatomagmatic explosive activity is a significant hazard that is difficult to predict, especially where a source of water is not apparent. The interaction of groundwater with magma rising rapidly to the surface through a conduit presents a physical problem with important implications for the management of volcanic hazards on Oceanic Island Volcanoes. In this study we seek to develop such a model through an investigation of the exceptionally well preserved and exposed near-vent deposits that formed in a prehistoric phreatomagmatic eruption at the Cova de Paul crater on the volcanic ocean island of Santo Antao, Cape Verde Islands.

The high altitude phreatomagmatic activity seen on Santo Antao can be unequivocally attributed to the interaction of groundwater with rising magma. The water for the phreatomagmatic eruption at the Cova de Paul volcano was supplied by high elevation aquifers within the volcano's summit region, and was entirely derived from orographic rainfall on the northern flanks of the volcano. This factor, together with the well-preserved exposures of phreatomagmatic deposits, makes Santo Antao an excellent field-work area for the study of groundwater/magma interactions.

From a series of stratigraphic logs of the eruptive deposits, it can be shown that the eruption began as a relatively benign Strombolian fire-fountain and formed a series of cinder cone deposits composed of plastic bombs, scoriae and spatter. The composition of the magma was phonotephrite, and no change in juvenile magma composition was detected in any of the eruption deposits. However, the eruption abruptly moved to a more explosive phase as a result of the ingress of water into the magma conduit, the start of which was indicated by the presence of a layer of sub-glassy blocks erupted just after the transition from the Strombolian phase. The physical structure of these blocks, e.g. internal folding and shearing, and low vesicularity, suggests that a plastic phase occurred prior to solidification, and that these blocks were not part of the fire-fountain eruption. It is therefore argued that these blocks are fragments of the chilled margin of the magma conduit and that the failure of the chilled margin precipitated the formation of the maar/diatreme system at the Cova de Paul crater (Tarff and Day 2013).

An investigation of the clasts derived from the diatreme provided insight into the changing explosive regimes within the infill. Two distinct cycles were identified, each of which culminated in a violent explosive event that generated dense, valley-filling pyroclastic density currents (PDCs). We suggest that transient explosion chambers formed within the diatreme infill to initiate these explosive events. The PDC deposits are coarse, poorly sorted and well indurated, matrix-rich breccias that were formed by dense, ground-hugging PDCs that flowed into valleys incised into the flanks of the Cova de Paul volcano. They were accompanied, especially in the latter part of the violent explosive events, by cross-bedded units formed from dilute, high velocity PDCs. The energetic blasts from the diatreme indicate that a steady-state model (Valentine et al. 2014) is not appropriate for this event.

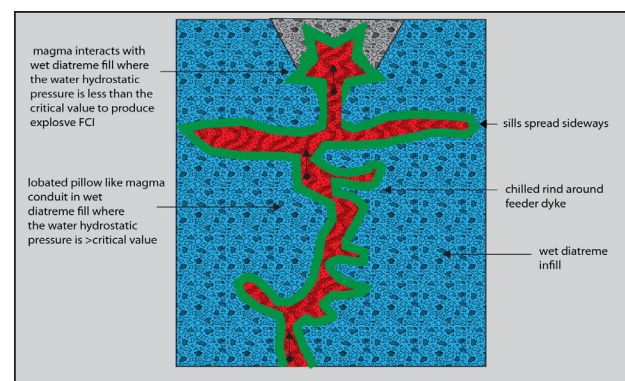


Fig.1: Schematic of a magma tube rising through wet diatreme infill that is being prevented from interacting with water until the hydrostatic water pressure drops below the critical value of 2-3 MPa (Zimanowski et al. 1997).

Figure 1 suggests that the cause of these cycles was magma bypassing the root-zone explosion chamber (Lorenz and Kurszlaukis 2007) and migrating to shallower depths, where the hydrostatic pressure was below the critical value for an explosive Fuel-Coolant Interaction (FCI) (Zimanowski et al. 1997). It is argued that the root-zone explosion chamber had ceased working, as it had excavated itself to a depth of some hundreds of metres where the water in the diatreme/brecciated halo was at a hydrostatic >2-3 MPa.

An exact value for the depth is uncertain as factors such as the density of the diatreme fill, its cohesion and permeability, and the extent to which pore fluid pressure and lithostatic pressure in the infill had equilibrated are generally unknown. When the confining pressure rises above the critical level, the pore fluid expansion during heating is restricted, with a corresponding low potential for the initiation of further explosive FCI.

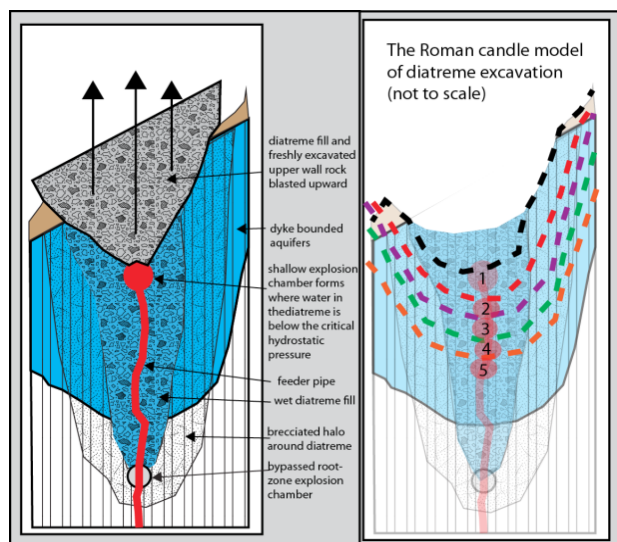


Fig. 2: Schematic cross-section of a magma tube rising through wet infill with 5 'Roman Candle' explosions in the sequence. Explosion chamber 1 removes infill and water (black dashed line). With the hydrostatic pressure lowered this allows explosion chamber 2 to remove more infill and water (red dashed line), and so on.

When the magma reached a height in the wet diatreme where the hydrostatic pressure was below the critical value, explosive FCIs would have occurred and possibly formed a temporary, shallow, explosion chamber that would have produced large phreatomagmatic blasts [FIG. 2]. Furthermore, the excavation of the diatreme fill above and around the temporary, shallow, explosion chamber would have decompressed the underlying diatreme fill. Thus, a new explosion chamber could have formed within the diatreme fill below the first one (Lorenz and Kurszlauskis 2007). In the manner of a Roman candle firework, it is envisaged that a series of phreatomagmatic blasts would have occurred, with each explosion being set off by the one above in a positive feedback chain reaction. In this way, the process would have been repeated with the temporary magma feeder tube feeding progressively deeper explosion chambers downwards into the infill as the expulsion of rubble and water reduced the hydrostatic pressure above the head of the feeder tube. Figure 2 represents the events at the end of the first cycle in which the presence of five distinct beds (two indurated lithic breccia beds and three massive breccia beds) in a unit on the rim of the crater suggests that there were at least five, separate, violent explosions from within the diatreme that emplaced the unit. The unit is completed by a set of alternating coarse ash cross-bedded and planar bedded horizons that lie over the five breccia beds. These beds indicate that the coarse material produced by any further

violent explosions was being contained within the now deeper and wider crater, with only dilute PDCs and ash clouds overtopping the rim.

This pattern of events was repeated during the final phase of the second cycle with coarse, well indurated material emplaced at the base of the unit capped by extensive, alternating coarse ash cross-bedded and planar bedded horizons at the top.

During fieldwork on the island evidence was discovered of several previously unknown similar eruptions in the geological record, and the hydrogeological and volcanic conditions for such activity still persist in wetter parts of the island. Therefore, it is probable that such an eruption will occur on Santo Antao in the future.

Acknowledgements

The funding for this research was provided by Birkbeck, University of London, the University of London Central Research Fund, the Open University Crowther Fund, the Mineralogical Society and the Geological Society (London).

References

- Lorenz, V. and S. Kurszlauskis (2007). "Root zone processes in the phreatomagmatic pipe emplacement model and consequences for the evolution of maar-diatreme volcanoes." *Journal of Volcanology and Geothermal Research* 159(1): 4-32.
- Tarff, R. W. and Day, S. J. (2013). "Chilled margin fragmentation as a trigger for transition from Strombolian to phreatomagmatic explosive activity at Cova de Paul Crater, Santo Antao, Cape Verde Islands." *Bulletin of Volcanology* 75(7): 1-14.
- Valentine, G., Valentine, A., Graettinger, I. and Sonder (2014). "Explosion depths for phreatomagmatic eruptions." *Geophysical Research Letters* 41(9): 3045-3051.
- Zimanowski, B., Büttner, R. and Lorenz, V. (1997). "Premixing of magma and water in MFCEI experiments." *Bulletin of Volcanology* 58(6): 491-495.



Oral *Session 5*

Natural resources and geotourism development in volcanic areas

Conveners

Károly Németh (K.Nemeth@massey.ac.nz)

Michael Ort (Michael.Ort@nau.edu)

Monogenetic volcanism provides the materials and landforms that scientists use to explore the volcanology and geochemistry of the Earth's interior. In addition to these scientific and, at times, theoretical studies, monogenetic volcanism also provides numerous economic benefits. Contributions are welcomed that focus on the diverse utilization of monogenetic volcanic fields, including use of mineral, rocks and water resources, landscape preservation (and degradation), geotourism and geoparks. We would like to emphasize this last point; volcanic geoparks and its complementary value, the environmental education and the sustainable entertainment related to volcanic landscapes to make a contribution to the sustainable development of the region. This session will highlight economic and social aspects of monogenetic volcanism and thus help bridge the gap between science and society.

Epithermal gold in felsic diatremes

Pierre-Simon Ross¹, Patrick Hayman², and Gerardo Carrasco Núñez³

¹ Institut national de la recherche scientifique, 490 de la Couronne, Québec (Qc), G1K 9A9, Canada, rossps@ete.inrs.ca

² Queensland University of Technology, 2 George Street, Brisbane 4000, Australia, patrick.hayman@qut.edu.au

³ Centro de Geociencias, UNAM, Boulevard Juriquilla 3001, 76230 Querétaro, Qro Mexico, gerardoc@dragon.geociencias.unam.mx

Keywords: pdiatreme, gold, felsic.

Felsic maar-diatreme volcanoes have not been well described in the volcanology literature, even though economic geologists have known about them for decades. Ross et al. (2017) presented a review of two Mexican maars and five gold mines sitting in diatremes, including new work at Mt Rawdon in Australia. They showed that felsic maar-diatremes have much in common with their ultramafic to mafic counterparts, in terms of their dimensions and the overall structure of the volcano; phreatomagmatism being the dominant eruptive style; and the textures, structures, componentry and depositional mechanisms of pyroclastic deposits (Fig. 1).

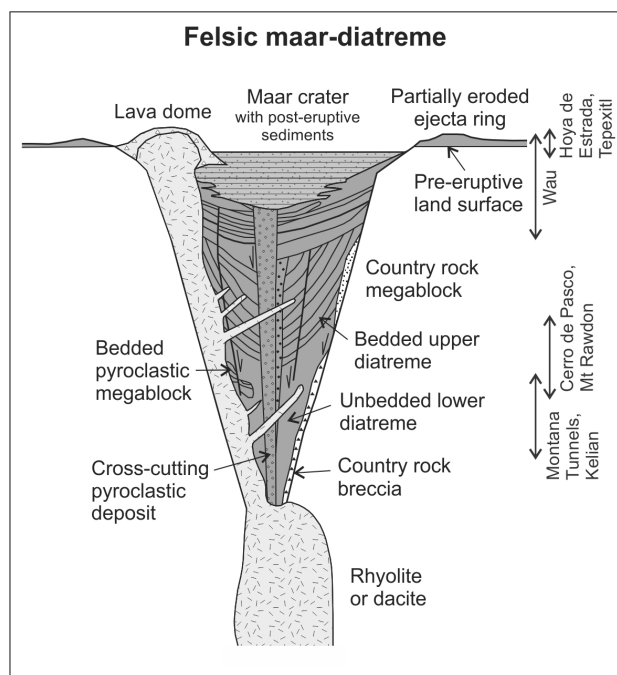


Fig. 1 – Schematic cross-section through a felsic maar-diatreme volcano, modified from Ross et al. (2017).

However, the processes of phreatomagmatic explosions involving felsic magmas may be different in detail (Austin-Erickson et al., 2008). In general, felsic maar-diatremes can be thought of as formed by dome-like eruptions strongly modified by phreatomagmatism. By analogy with domes, the eruption of the largest felsic maar-diatreme volcanoes may have lasted years to decades, compared to the days to months typically envisaged for their mafic to ultramafic cousins.

Felsic diatremes are excellent hosts for epithermal gold-silver ore deposits, for both low-sulfidation and high-sulfidation types. Three or four of the 14 largest circum-Pacific epithermal gold deposits occur in or near felsic diatremes according to Sillitoe (1997), making this the most common volcanic setting for that deposit type, along with flow-dome complexes. Here we present information on the diatreme-hosted epithermal gold deposits themselves, based on the sites reviewed by Ross et al. (2017) (including Kelian, Indonesia; Mt Rawdon, Australia, Montana Tunnels, USA; and Wau, Papua New Guinea) plus a literature survey which adds Acupan, Philippines (Cooke et al., 1996), Cripple Creek, USA (Thompson et al. 1985; Jensen, 2003), Martabe, Indonesia (Sutopo, 2013) and Roşia Montana, Romania (Wallier et al. 2006).

In diatreme-hosted epithermal gold deposits, tonnages tend to be high but grades relatively low, so open pit mining is the preferred method of production. The geometry of diatremes is also well suited for open pit mining. Mineralization occurs in veins, stockworks, hydrothermal breccias, and disseminations (Sillitoe, 1997). Ore can sit within the diatreme (Acupan, Cripple Creek, Martabe, Kelian, Montana Tunnels, Mt. Rawdon, Roşia Montana; Fig. 2), next to it in the country rocks or in extra-diatreme hydrothermal breccias (Acupan, Kelian, Martabe), and exceptionally, within the maar ejecta ring (Wau). Ore location depends on the permeability of the diatreme versus country rocks and on the style of mineralization.

Precious metals (Au, Ag) are commonly associated with pyrite (Kelian, Mt Rawdon, Montana Tunnels), but base metal associations are also known. Types of hydrothermal alteration present include sericitic (Acupan, Mt Rawdon, Montana Tunnels), advanced argillic (Martabe), adularia (Acupan, Roşia Montana), and propylitic (Acupan, Martabe). Siliceous and argillic alterations have also been reported.

Ross et al. (2017) propose that the eruptive rates and the type of magma degassing typical of domes also apply to felsic maar-diatremes. In both cases (maar-diatremes and domes), the setting is highly favorable for gold mineralization because there is a direct permeable connection between the magma chamber at depth and the newly emplaced volcanic features in the subsurface or surface (Sillitoe, 1997). This allows magmatic-hydrothermal fluids to rise quickly to sites suitable for ore deposition. In dia-

tremes, the permeability is represented by regional faults, the diatreme infill, and diatreme margin faults (Sillitoe, 1997). Also, in these settings (maar-diatremes and domes), the magma and fluids – and presumably, precious metals – are not catastrophically evacuated from the magma chamber directly into the atmosphere, as opposed to what occurs during large caldera-forming eruptions. Finally, diatremes intersect the water table and mineralization can form at shallow depths where many gold-ligand destabilizing mechanisms operate (e.g., depressurization, mixing with meteoric fluids or fluid-rock reactions).

Acknowledgements

P.-S.R. acknowledges Discovery Grant funding from NSERC. Evolution Mining Limited, in particular S. Wangi, is acknowledged for logistical support during field work at Mt. Rawdon. T. Watson showed the senior author some interesting core intervals at Mt Rawdon.

References

Austin-Erickson, A., Büttner, R., Dellino, P., Ort, M.H., Zimanowski, B., 2008. Phreatomagmatic explosions of rhyolitic magma: experimental and field evidence. *Journal of Geophysical Research* 113: paper B11201 doi:10.1029/2008jb005731.

Cooke, D.R., McPhail, D.C., Bloom, M.S., 1996. Epithermal gold mineralization, Acupan, Baguio District, Philippines; geology, mineralization, alteration, and the thermochemical environment of ore deposition. *Economic Geology* 91: 243-272.

Jensen, E.P., 2003. Magmatic and hydrothermal evolution of the Cripple Creek gold deposit, Colorado, and comparisons with regional and global magmatic-hydrothermal systems associated with alkaline magmatism. PhD thesis, University of Arizona, USA.

Ross, P.-S., Carrasco-Núñez, G., Hayman, P., 2017. Felsic maar-diatreme volcanoes: a review. *Bulletin of Volcanology* 79: Article 20.

Sillitoe, R.H., 1997. Characteristics and controls of the largest porphyry copper-gold and epithermal gold deposits in the circum-Pacific region. *Australian Journal of Earth Sciences* 44: 373-388.

Sillitoe, R.H., Graubeger, G.L., Elliott, J.E., 1985. A diatreme-hosted gold deposit at Montana Tunnels, Montana. *Economic Geology* 80: 1707-1721.

Sutopo, B., 2013. The Martabe Au-Ag high-sulfidation epithermal deposits, Sumatra, Indonesia: implications for ore genesis and exploration. PhD thesis, University of Tasmania, Australia.

Thompson, T.B., Trippel, A.D., Dwelley, P.C., 1985. Mineralized veins and breccias of the Cripple Creek District, Colorado. *Economic Geology* 80: 1669-1688.

Wallier, S., Rey, R., Kouzmanov, K., Pettke, T., Heinrich, C.A., Leary, S., O'Connor, G., Tămaş, C.G., Vennemann, T., Ullrich, T., 2006. Magmatic fluids in the breccia-hosted epithermal Au-Ag deposit of Roşia Montană, Romania. *Economic Geology* 101: 923-954.

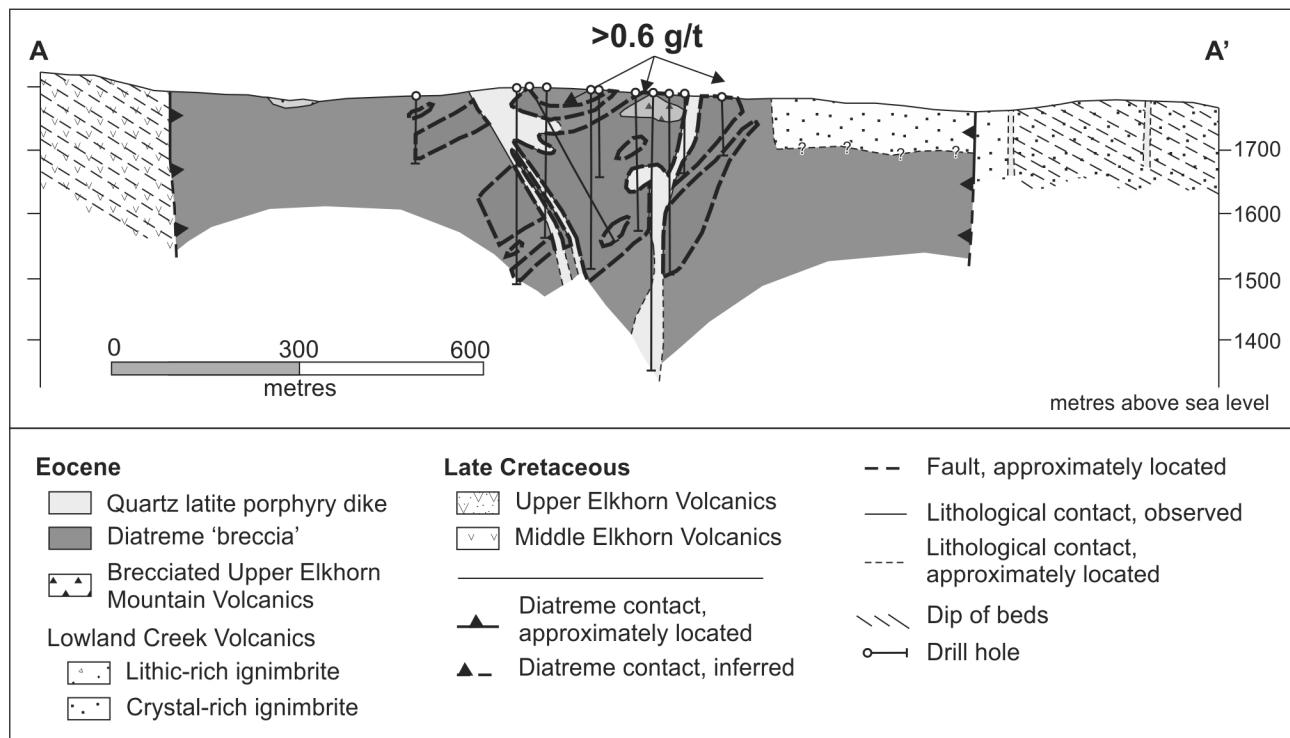


Fig. 2 – Cross-section through the Montana Tunnels diatreme, USA, simplified from Sillitoe et al. (1985). The gold mineralization (>0.6 g/t Au) is restricted to the middle portion of the diatreme.

We want you to “put in value the volcanism” in the “Styrian volcano land” (Austria)

Ingomar Fritz

Geology & Palaeontology, UMJ, Centre of Natural History, 8045 Graz, Austria. ingomar.fritz@museum-joanneum.at

Keywords: public relation, schools, diatremes.

The “Styrian volcano land” (“Steirisches Vulkanland”) comprises an economic region and trademark in eastern Styria, Austria. Up to now the main focus was a cooperation of communities to create a humanly – ecological – economical sustainability on their own authority. Based on this 20 years lasting successful economic development the authorities now want the geological, especially volcanic, history to be “put in value”. Geological “highlights” should be embedded in the available widespread trails network and connected with regional commercial enterprises. Main goal is to create different information platforms for the local population and tourists.



Fig. 1 – Landscape of the “Styrian volcano land” with the Castle of Riegersburg, placed on a diatreme.

Each conversation creates pictures in our head. Talking about volcanoes with “normal” people means, that they “see” a conical structure grown/growing on country surface. In the Styrian volcano land we mostly have the fossil remnants of maar volcanoes. Because some of our diatremes morphological look like “typical volcanoes” many things are to explain (e.g. regional geology, time, different genetic processes, weathering). Even if the local population know that they live in a region with former volcanism most of them (including tourism responsible) have little knowledge about these “upside-down volcanoes”.

For that reason a concept was developed and finally a LEADER-project submitted. The planned and partly implemented steps will be presented.

Based on a detailed mapping and description of (volcano-) geological features of the region a list of geological sites was compiled. Selected (volcano-) geological particularities were assigned to communities. Ten interested communities had to assure own commitment, own work and even financial support.

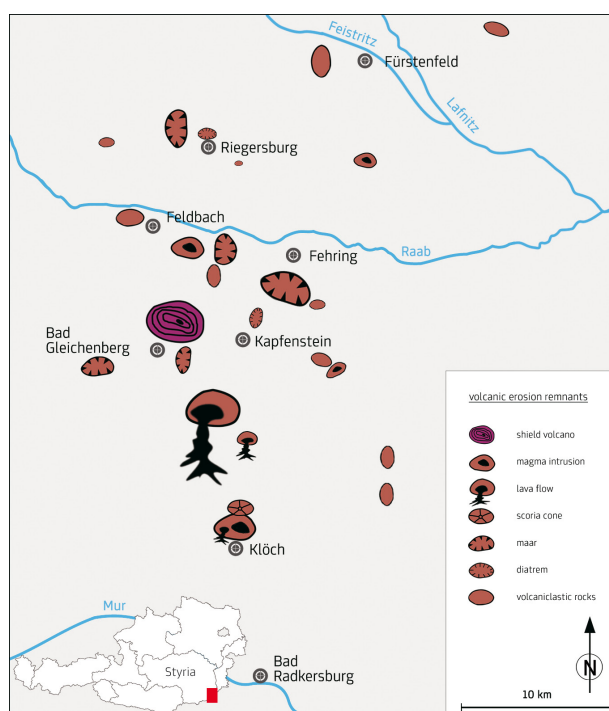


Fig. 2 – The “Styrian volcano land” – an economic region in the southeast of Austria with a dynamic earth history.

Many years of successful work with schools (about 40.000 pupils in 20 years guided to geological outcrops in Styria) have shown that earth sciences can be transported with well prepared pictures/ animations but especially when places of activity are offered. Besides explanation panels in the field and a popular science brochure especially outcrops where rocks can be collected or fossils can be searched are very essential to impart earth history.

By now earth science school subjects are not any more on the teaching curriculum in Austria. Offering interdisciplinary projects, for example preparing teaching materials with earth science background in and with schools is part of the mediation work. For example the production of rock suitcases with types of the regional lithology is part of this project. Each participating school develops one for the local community characteristic special rock type, e.g. sand. Besides collecting samples a description of the occurrence (outcrop) the composition (material description – grain size, components, fossils ...) and the (historic) usage are part of the work. The typical basaltic volcanic tuff, including different lithic clasts of the Neo-

gene (gravel, sand, silt, clay, or Limestone) reflects the 3-dimensional regional geology and is an example for networked cooperation of schools from different communities. Finally these independently developed information, collected rock samples augmented with maps, pictures and animations can be used in schools. The project's aim is to develop cross linked educational materials with schools not only for schools but as well for geotouristic initiatives.

References

Gross M., Fritz I., Piller W.E., Soliman A., Harzhauser M., Hubmann B., Moser B., Scholger R., Suttner T.J. & Bojar H.-P. 2007. The Neogene of the Styrian Basin – Guide to Excursions. *Joannea - Geologie und Paläontologie*, 9: 117-193.

Irazú's Southern Volcanic Field: A Place for Learning and Leisure.

E. Duarte

Volcanological and Seismological Observatory of Costa Rica (OVSI-CORI). Universidad Nacional. P. O. Box. P.O.Box 2346-3000 Heredia-Costa Rica; e-mail: eduarte@una.ac.cr

Keywords: Irazú, Costa Rica, Pasquí

Irazú's volcanic field (09° 56' 0164N, 83° 50' 5504W) is located some 15 kms NE of the former Capital of Costa Rica: Cartago, only few kms south of Irazú volcano. This field is composed of, at least, 6 volcanic cones (quaternary andesitic scoria cones and probable monogenetic vents) all seated in the small administrative district named Santa Rosa de Oreamuno. Effusive and explosive activity developed in some cases cones while in other produced craters whose fine materials were dispersed in the direction of the ejection and along the prevailing winds. Some well-defined deposits are easily recognized in the vicinity of our features of interest although in recent times top layers of tephra probably came from the neighboring Turrialba and Irazú volcanoes. (Fig. 1).



Fig. 1 – Irazú's Southern Volcanic Field; southernmost portion. Turrialba volcano in the foreground; to the east. Photo. G. Pucci.

Despite the vicinity to urban areas and to the well-known Irazú volcano these features are rarely mentioned or recognized, as volcanoes, by tourists or even settlers from the small, neighboring communities.

Some of the accepted names for the best known features are used by locals although they lack academic fixation due to poor research and study of such field. These structures appear now safely scattered in the landscape aligned in at least two main fissures; one trending N34°E while the other trends N26°W. Deeper studies on correlations between fractures and vent alignments are needed. From south to north (1 to 6) Cerro Santa Rosa (1) (2100 masl, Circular crater, used as pasture land), lies next to

the homonym town while (2) Pasquí (2600 masl, scoria cone partially exploited, mostly covered by pasture) lies just north of San Gerardo de Oreamuno: open to the south; towards the community. From here to San Juan de Chicú 4 features complete the system: 2 cones and 2 symmetrical craters.

A small cone called (3) Mendez (~2600 masl, half used to grow vegetables and half used for dairy purposes) with a nearby crater called (4) La Olla (~2600 masl, used for pasture this crater resembles a "cooking pan"; from there it gets its name).

Shortly to the east lies (5) Dussaint Hill (~2700 masl, a tall cone with not known crater in its summit this feature is used for pasture and cultivation although a good part of it is covered with a lush forest) and next to this last one lies (6) El Perol (~2800 masl which probably gets its name, "the pot", due to the shape of an inverted cooking pot). Beyond these six features and closer to Irazú volcano 2 more bigger volcanic features appear: Cerro Gurdán (~3066 masl, used mainly for growing potatoes although its summit is used as an strategic high point for radio, TV and microwave towers) and Cerro Nochebuena (~3200 masl, occupied with pasture, arable land and forest). (Fig. 2).

It is from the latter cones that one of the largest lava fields, in the Central American region, develops; an area composed of two lava flow fields occupying some 43 km² when added (Alvarado & Vega 2013). Such lava fields conform a singular economical and topographical feature in the region symbol of human adaptation and tenacity to tame a rugged environment. (Duarte & Fernández 2010). The almost forgotten Irazú volcanic field provides valuable areas, used for year-long production of vegetables and pasture land along with minor exploitations of quarry materials.

It is thanks to the fine and medium tephra size that the slopes are fertile and form part of an area known as the "barn of Costa Rica" due to the high production of vegetables, grains and dairy products.

Solid products from these structures and their lava flows are commonly extracted with commercial purposes although not in an industrialized or in a massive fashion. In fact one of the most notable features in the local land-

scape are the elongated rock walls gathered “manually” mainly from the arable areas. In the least of cases quarry material is used for residential construction and to improve their own road network (Thomas 1983).

In order to make use of this volcanic land; peasants have to mix rich volcanic soils with a thick tropical organic substratum developed there for hundreds of years. Not an easy task when dealing with a surface covered with scattered blocks, coarse tephra and random bigger blocks. Good soil conservation practices allow generations to exploit such asset in a year-round fashion.

This work will depict the various cones from different angles, including their economical current use. Illustrations of various agricultural activities on the cones and their surroundings will provide general ideas of the positive conditions for a regional socio-economic advancement in hand with conservation.

Given the natural beauty of these unusual volcanic features, their economic conditions and their educational potential such area should be better studied and proposed as a recreational loop for national and international tourists, educators and researchers.

Moreover, efforts at the political and economic levels should be made to ensure the betterment of roads and other secondary services for improving the actual visiting conditions.

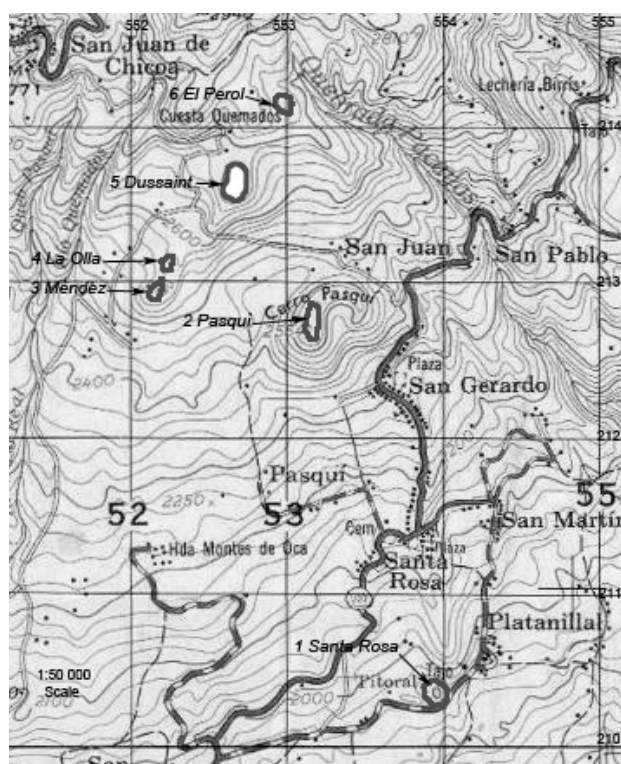


Fig. 2– From south to north (1 to 6) volcanic features described in this essay. Istarú topographical map.

Acknowledgements

To authorities from Universidad Nacional for supporting this work and my participation. To organizers for partial support.

References

Alvarado, G. & Vega, A. 2013. The Cervantes lava flow geomorphology, Riau Volcano (Costa Rica): Description of the Central America`s greater lava field. *Revista Geológica de América Central*. 48: 99-118.

Duarte, E, Fernández, E. 2010. La Colada de lava de Cervantes: Entre la Belleza, la Fertilidad y la Adaptación Humana. Technical report. www.ovsicori.una.ac.cr 4pages.

Thomas, K., 1983: An Investigation of the Cervantes Formation at Irazú Volcano, Costa Rica. - 29 pages. Dartmouth College, Hanover [Thesis BSc.].

Conservation of the macrovertebrates fossils from fossil-Lagerstätten Camp dels Ninots, as a principal element for disseminate heritage.

Souhila Roubach^{1,2}, Elena Moreno-Ribas^{1,2}, Bruno Gómez de Soler^{1,2}, Gerard Campeny^{1,2}

¹ Institut Català de Paleoecologia Humana i Evolució Social (IPHES). C/ Marcel·lí Domingo s/n, Edifici W3 Campus Sescelades URV, 43007 Tarragona, Spain. E-mail: souhilaroubach@hotmail.fr

² Universitat Rovira i Virgili (URV). Facultat de Lletres. Av. Catalunya 35, 43002 Tarragona, Spain.

Keywords: Conservation, Macrovertebrates fossils, Dissemination of heritage.

The good state of conservation of fossils is crucial for their manipulation for study and also for the exhibition in museums. Therefore, this work falls within the framework of conservation and restoration of the paleontological remains from the Pliocene site of Camp dels Ninots (Caldes de Malavella, Girona, Spain).

The Camp dels Ninots maar site is located in the western part of the town of Caldes de Malavella (Girona, Spain). It is a part of the Catalan Volcanic Complex which took place between 14 Ma and 10 Ka BP. in NE Spain. The site has been recently classified as a fossil-Lagerstätten (Gómez de Soler et al., 2012). A large range of fossils are recovered and most of them are complete and articulated (for more details, please see: Campeny & Gómez de Soler, 2010; Gómez de Soler et al., 2012; Jiménez-Moreno et al., 2013; Campeny et al., 2015, among others). The stratigraphy shows a lacustrine sedimentation in a maar which are ideal conditions for the preservation of fossils (Fig. 1).



Fig.1. Tapir skeletons from the Camp dels Ninots maar site (Caldes de Malavella, Girona, Spain).

However, the specimens recovered are highly fragile and the bones presented most of the time splits, cracks, and were friable in some parts. It is noteworthy that some parts of the fossils were flattened because of diagenetic processes.

Therefore, the interventions of conservation are necessary for the fossils to give them strength and shock resilience. In this work, the conservation treatments carried out on the macrovertebrates fossil, which are represented here by tapirs (*Tapirus arvernensis*) and bovids (*Alephis tigneris*), are described and documented both in situ and laboratory.

> In situ interventions: excavation, cleaning, consolidation, extraction of the fossil.

> Laboratory treatments: mini-excavation and cleaning, consolidation and restoration, adequate storage.

The excavation and cleaning of the fossils is handled first with small trowel and brush. Then, by using wooden and metallic instruments and for more detailed cleaning a mixture of water/alcohol is used. The consolidation of fragile bones is applied with Paraloid B72 at different concentration, with a syringe. The fossils, mostly, are extracted in situ in sediment block with a polyurethane support.

The interventions and choices made in situ are paramount for the rest of the treatments later in the laboratory. A good coordination between the two teams (in situ and laboratory) is necessary.

The purpose in the preservation of fossils besides the study is also to present them to the public as museum elements in order to disseminate heritage as an important part for the research project.

Acknowledgements

A lot of thank to the land owners for their permission to work in the area. We would like to thank also the Agencia Española de Cooperación Internacional y Desarrollo MAEC/AECID for the financial support of S. Roubach. Ph.D studies. The Camp dels Ninots project is sponsored by projects 2014-100575 (Generalitat de Catalunya), SGR2014-901 (AGAUR) and the Ministry of Economy and Competitiveness of Spain, under project CGL2016-80000-P (MINECO)

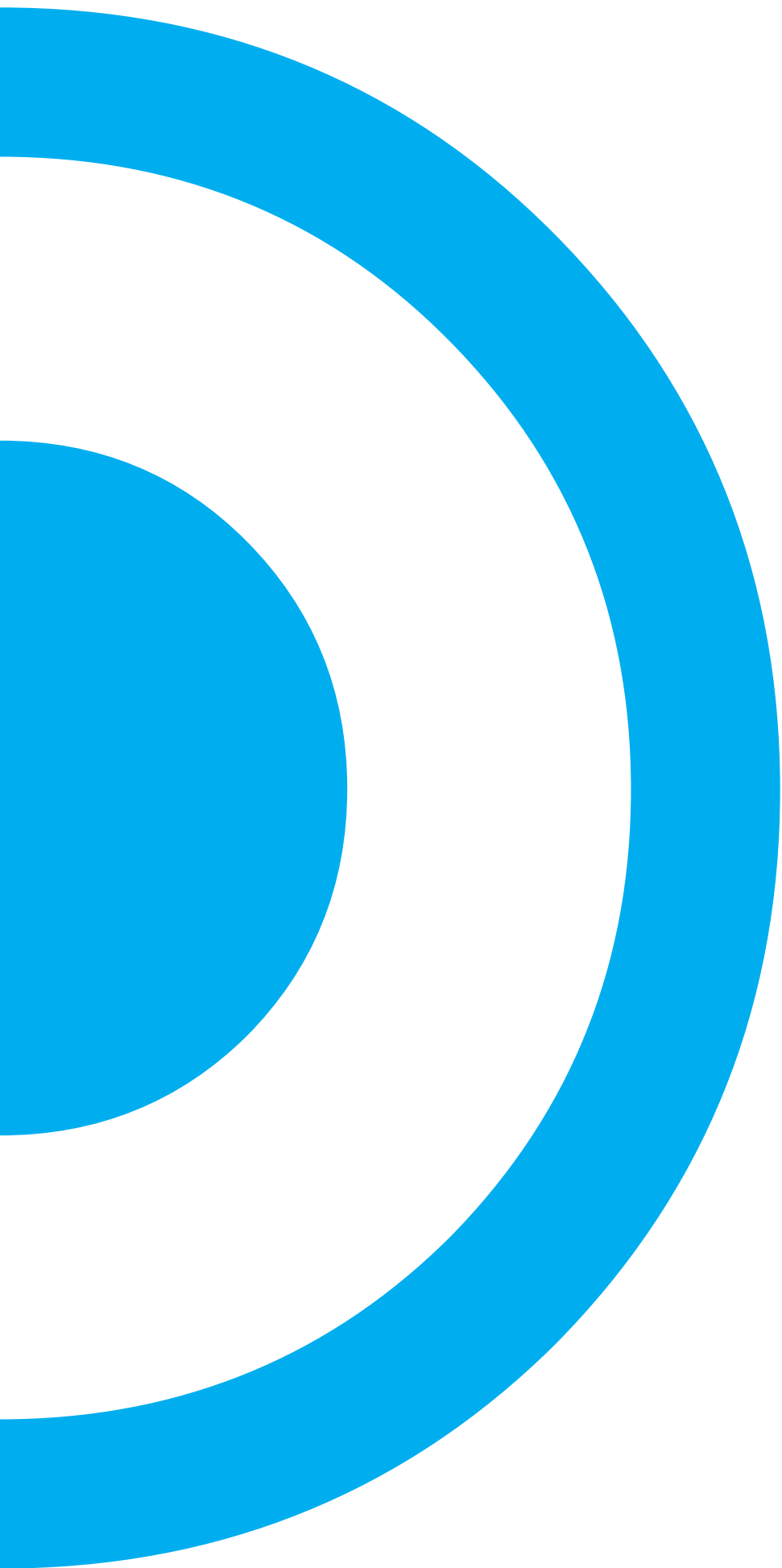
References

Campeny, G., Gómez de Soler, B., Agustí, J., Sala, R., Oms, O., Van der Made, J., Burjachs, F., Jiménez, G., Blain, H-A., Claude, J., Prikryl, T., Expósito, I., Villalaín, J.J., Carrancho, A., Barrón, E., Roubach, S., López-Polín, L., Bolós, X., Gómez Merino, G., Ibáñez, N., García, Ll., Mateos, P., Riba, D., Rosillo, R., Díaz, A. and, García Catalán, S. (2015). El Camp dels Ninots (Caldes de Malavella, la Selva): balanç de 10 anys d'intervencions arqueopaleontològiques. *Tribuna d'Arqueologia* 2012-2013: 141-163.

Campeny, G. & Gómez de Soler, B. (Eds.) (2010). *El Camp dels Ninots. Rastres de l'Evolució*. Edited by Ajuntament de Caldes de Malavella and IPHES. Caldes de Malavella, p. 200.

Gómez de Soler, B., Campeny, G., van der Made, J., Oms, O., Agustí, J., Sala, R., Blain, H.A., Burjachs, F., Claude, J., García Catalán, S., Riba, D. and, Rosillo, R. (2012). The Camp dels Ninots (NE Spain): a new key locality for the Middle Pliocene terrestrial faunas of Europe. *Geologica Acta* 10(2), 1-17.

Jiménez-Moreno, G., Burjachs, F., Expósito, I., Oms, O., Carrancho, A., Villalaín, J.J., Agustí, J., Campeny, G., Gómez de Soler, B. and, Van der Made, J. (2013). Late Pliocene vegetation and orbital-scale climate changes from the western Mediterranean area. *Global and Planetary Change* 108, 15-28.



Posters *Session 5*

Natural resources and geotourism development in volcanic areas

Conveners

Károly Németh (K.Nemeth@massey.ac.nz)

Michael Ort (Michael.Ort@nau.edu)

Monogenetic volcanism provides the materials and landforms that scientists use to explore the volcanology and geochemistry of the Earth's interior. In addition to these scientific and, at times, theoretical studies, monogenetic volcanism also provides numerous economic benefits. Contributions are welcomed that focus on the diverse utilization of monogenetic volcanic fields, including use of mineral, rocks and water resources, landscape preservation (and degradation), geotourism and geoparks. We would like to emphasize this last point; volcanic geoparks and its complementary value, the environmental education and the sustainable entertainment related to volcanic landscapes to make a contribution to the sustainable development of the region. This session will highlight economic and social aspects of monogenetic volcanism and thus help bridge the gap between science and society.

Public engagement with the history of life. A new fossil-Lagerstätten heritage site: the Camp dels Ninots maar

Gerard Campeny^{1,2}, Bruno Gómez de Soler^{1,2}, Marta Fontanals^{2,1}, Jordi Agustí^{3,1,2}, Oriol Oms⁴
and Robert Sala^{2,1}

¹ Institut Català de Paleoecologia Humana i Evolució Social (IPHES). C/ Marcel·lí Domingo s/n, Edifici W3 Campus Sescelades URV, 43007 Tarragona, Spain. E-mail: gcampeny@iphes.cat

² Universitat Rovira i Virgili (URV). Facultat de Lletres. Av. Catalunya 35, 43002 Tarragona, Spain.

³ Institució Catalana de Recerca i Estudis Avançats (ICREA). Pg. Lluís Companys 23, 08010. Barcelona, Spain.

⁴ Universitat Autònoma de Barcelona, Facultat de Ciències, Departament de Geologia. Campus Bellaterra, 08193, Spain.

Keywords: fossil-Lagerstätten, Paleontological heritage, Geotourism, Public engagement

The paleontological heritage sites with an exceptionally well-preserved fossils allow the structuration of integrated management models for research, conservation and dissemination, generating a high social impact for the knowledge of the history of life.

The research project that is being developed in the fossil-Lagerstätten of the Camp dels Ninots show the extraordinary significance for understanding the paleoecological and paleoenvironment evolution of the Late Pliocene of Europe. In 2015 was declared a National Cultural Interest site (BCIN) by the Catalan government. The scientific research with and legislative measures being implemented for its preservation, outreach and knowledge transfer activities are the third essential pillar of this research project. The site is located in the crater of a type maar volcano of Pliocene age (3.1 Ma) forming part of the Catalan volcanic field (Martí et al., 1992), which subsequently formed a lake. The special geological conditions of the area, lake sediments filling the crater, has allowed the preservation of an entire ecosystem (Gómez et al. 2012). The fossil record corresponds to species of macro and microvertebrates that are scarce represented in the European fossil record. This includes complete skeletons that can become as holotype material for each of its groups, as well as, in some cases, permitting the description of new species. Moreover, palynological studies of the lacustrine sequence, in addition to taxonomic studies of the plant imprints, reveal key data for understanding the climate and landscape evolution of the continental European record during the last 3 Ma. (Jiménez Moreno, et al. 2013).

In the last 15 years, the set of knowledge transfer actions related to the Camp dels Ninots has been remarkable. The joint commitment of the various public authorities, national and international research centers involved in the project, citizens, educational area and private companies, has forged a strategic planning program based on the criteria of heritage, identity and development.

In order to translate these evidences, an Enhancement of Heritage plan of the site has been developed, supported by a Municipal Tourism Development Plan, a Geocon-

servation Special Plan and associated to important investments mainly from the municipality and the Catalan government. It has started with the creation of a series of equipment and logistical resources oriented for a geotourism, educational and formative purposes. Of these actions, it is worth noting that the AQUAE space, a mixed center of interpretation, research and education. Its main objectives are to explain what has been the process by which the natural heritage of this territory, especially its thermal waters, has been the main engine for the configuration of an identity of its own, from the social, cultural and economic point of view.

The paleontological heritage of the fossil-Lagerstätten of Camp dels Ninots is becoming a relevant part of the socio-cultural identity of its region, and ultimately permit a deeper and better understanding of the life on Earth in the past.

Acknowledgements

The Camp dels Ninots project is sponsored by projects 2014-100575 (Generalitat de Catalunya), SGR2014-901 (AGAUR) and the Ministry of Economy and Competitiveness of Spain, under project CGL2016-80000-P (MINECO).

References

- Gómez de Soler, B., Campeny Vall-Ilosera G, Made J van Der, Oms O, Agustí J, Sala R, Blain H-A, Burjachs F, Claude J, García Catalán S, Riba D, Rosillo R (2012a) A new key locality for the Pliocene vertebrate record of Europe: the Camp dels Ninots maar (NE Spain). *Geol Acta*, 10 (1): 1–17
- Jiménez-Moreno G, Burjachs F, Expósito I, Oms O, Carrancho Á, Villalaín JJ, Agustí J, Campeny G, Gómez de Soler B, Made J van der (2013) Late Pliocene vegetation and orbital-scale climate changes from the western Mediterranean area. *Global Planet Change* 108:15–28.
- Martí J, Mitjavila J, Roca E, Aparicio A, (1992) Cenozoic magmatism of the Valencia trough (western Mediterranean): relationship between structural evolution and volcanism. *Tectonophysics* 203 (1–4), 145–165

Campo de Calatrava, the largest number of maar lakes in continental Europe

Rafael U. Gosálvez¹, Montse Morales¹, Máximo Florín² and Elena González¹

¹ GEOVOL Research Group, Departmente of Geography and Land Planning, UCLM, Campus Ciudad Real, 13071 Ciudad Real, Castilla-La Mancha, España. RafaelU.Gosalvez@uclm.es

² IHE Research Group-CREA, UCLM, Campus Ciudad Real, 13071 Ciudad Real, Castilla-La Mancha, España.

Keywords: maar, lake, Campo de Calatrava.

Lakes, shallow lakes and volcanic wetlands are one of the most spectacular geological elements of the planet (Christenson et al, 2015), being the result of the interaction between magma and water outside the volcanic system (hydromagmatism), generally associated with groundwater (phreatomagmatism). Water-magma interaction generates an explosion funnel (diatreme) that on the surface appears as a depression. This depression in geomorphology is known as maar.

The word maar comes from the Eifel region (Germany), a local place name that describes deep lakes that exist in this region. It is here where for the first time a relationship between lakes and a possible volcanic origin was established. In the European Cenozoic volcanism there have been hydromagmatic eruptions that have resulted in maars, although only a few of these maars currently accumulate water (lakes, shallow lake or wetlands).

The aim of this paper is to highlight the importance at European level of the set of maars with lake of Calatrava Volcanic Field. The method is based on a scientific literature review and field work.

When volcanologists refer to maars lakes in Europe, it is traditionally thought of two volcanic systems: Eifel Volcanic Field (Germany) and Auvergne Volcanic Field (France). In the first case, 9 maars lakes have been counted, while in the second case, 10 maars lakes have been counted. Other volcanic systems that present lakes in maars are those of continental Italy, also with 9 maars lakes, and the volcanic system of the Carpathians, with 3 maars lakes. Figure 1 shows distribution of the volcanic fields of continental Europe with maars lakes.

In front of the few maars with lakes in the volcanic fields of continental Europe, in the Calatrava volcanic field, located in the center of Spain, there have been counted up to 65 maars that accumulate water in its interior (Gosálvez, 2011), generally shallow lakes and wetlands (depth < 2 m). These convert Calatrava into the volcanic field with the largest number of maars lakes of continental Europe. Only the ignorance that exists internationally Calatrava volcanic field justifies that this fact is not known and that, for example, goes unnoticed even when an international conference of maars is held in Spain.

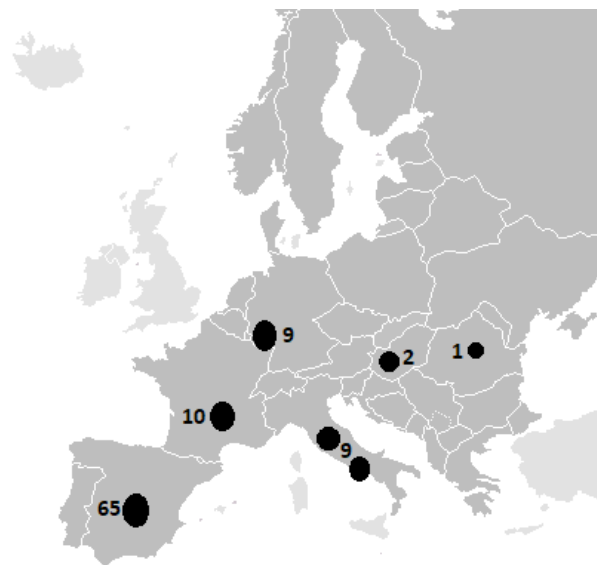


Fig. 1 – Location of volcanic fields with maars lakes of continental Europe. The number indicates maars with water.

Campo de Calatrava Volcanic Field is located in the centre of Spain where volcanic eruptions from the Miocene (8.6 Ma.) to the Quaternary (5500 BP). Landforms associated to the eruptions of Calatrava, are the typical of effusive eruptions, typical of Strombolian and of explosive events of marked hydrovolcanic nature. The investigations raise more than 300 volcanoes in the Calatrava volcanic field, half of them are maars.

Chemistry of the volcanic rocks of Calatrava guarantees the hypothesis of a rifting process in the origin of this volcanism and in the rest of the cenozoic volcanism of Europe (Ziegler, 1992).

Landforms derived from the hydrovolcanic activity are conditioned as by the water location which interacts with magma by the competition of the materials over the explosion is developed (González, 2002). Maars are the most widespread morphologies in Calatrava Volcanic Field, characterized by the presence of an explosive depression opened under the pre-eruptive topographic surface. Table 1 shows the main geological and hydro-

Volcanic Field	A (ha)	D (m)	d (m)	pH	Cond.
EIFEL (Ge)					
Average	11,7	439,6	29,2	7,8	13867
Standard deviation	10,5	197,7	22,3	0,2	12058
Minimum value	1,1	170	3	7,5	4600
Maximum value	34	770	70	8	27500
N	9	9	9	6	3
MCF (Fr)					
Average	33,6	599,7	45,7	6,4	49,2
Standard deviation	25,1	309,7	36,5	0,5	38,2
Minimum value	1,4	135	5	5,5	18
Maximum value	88,3	1212	109	7	131
N	10	10	10	10	10
ITALY					
Average	135,3	1254,7	46,0	8,2	657
Standard deviation	192,2	930,5	48,6	0,7	966
Minimum value	12	500	7	7,4	179
Maximum value	602	3300	170	9	2840
N	9	9	9	8	7
Sfanta Ana (Ro)	20	627	7	8,1	8
Külsö (Hu)	73	1083			
Belsö (Hu)	36	860			
CALATRAVA (Sp)					
Average	32,9	773	0,7	8,8	4700
Standard deviation	32,2	505	0,4	2,1	7440
Minimum value	1,8	175	0,3	6,44	100
Maximum value	122,9	2580	2	10,65	35200
N	27	27	27	123	140

Tab. 1 – Main morphometric and hydrological characteristics of the maars lakes of continental Europe. A: Area; D: Diameter; d: Depth; Cond: Conductivity ($\mu\text{S}/\text{cm}$). (Ge: Germany, Fr: France; MCF: Massif Central French; Ro: Romania; Hu: Hungary; Sp: Spain)

logical characteristics of the lake maars of continental Europe. From the data of the averages of each variable for each volcanic field contained in table 1, a cluster analysis has been carried out. The purpose of this analysis is to measure the similarity between the different volcanic fields of continental Europe in order to establish homogeneous groups internally and different from each other. Figure 2 shows the result of the cluster analysis. It is striking how the Eifel volcanic field is separated from the rest of the volcanic fields at the beginning of the analysis, leaving the rest of the volcanic fields grouped in the same group, although within this large group the Calatrava volcanic field is clearly separated from the volcanic fields of Eifel, Italy and Lake of Sfanta Ana (Romania). Small average size of the maar lakes and the high average conductivity determine the separation of Eifel from the rest of European volcanic fields. Calatrava is separated from the volcanic fields of Auvergne, Italy and maar lake Sfanta Ana because of the low average depth of the bodies of water and the high average conductivity of the water.

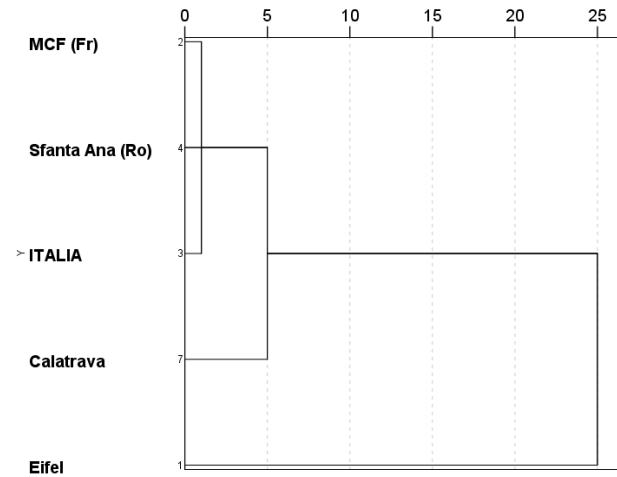


Fig. 2 – Dendrogram of classification of the volcanic fields of continental Europe according to their main morphometric and hydrological characteristics.

References

- Christenson, B., Németh, K., Rouwet, D., Tassi, F., Vandemeulebrouck, J., Varekamp, J.C. 2015. Volcanic lake, in Rouwet et al. (eds.), Volcanic Lakes, Advances in Volcanology, DOI 10.1007/978-3-642-36833-2_1
- González-Cárdenas, E. 2002. Depósitos de Oleadas Basales y su papel en el relieve volcánico del Campo de Calatrava (España), in VV.AA.: Estudios recientes (2000-2002) en Geomorfología, Patrimonio, Montaña y dinámica territorial. SEG, UVA, Valladolid; pp. 455-464.
- Gosálvez, R.U. 2011. Análisis biogeográfico de las lagunas volcánicas de la península Ibérica. Bases científicas para su gestión Tesis doctoral UCLM, Ciudad Real. 1040 p.
- Ziegler, P.A. 1992. European Cenozoic rift system. Tectonophysics 208:91-111.

From hydrogeological and geophysical investigations to the hydraulic structure of the Ulmener Maar, West Eifel Volcanic Field, Germany

Sven Philipp¹, Karl-Heinz Köppen², Thomas Lange³

¹ Engineering Office Wasser und Boden GmbH, Am Heidepark 6, D-56154 Boppard-Buchholz, philipp@wasserundboden.de

² Engineering Office Wasser und Boden GmbH, Am Heidepark 6, D-56154 Boppard-Buchholz, koeppe@wasserundboden.de

³ Institute of Geosciences, FSU Jena, Department of Applied Geology, Burgweg 11, D-07749, t.lange@uni-jena.de

Keywords: applied hydrogeology, maar lakes, local water supply

For the understanding of hydrogeological systems, it is crucial to achieve a comprehensive and integrated view of the basic geological structure, especially in such complex systems as maars. These phreatomagmatic volcanic edifices represent very sensitive and local groundwater resources, which can be used for drinking water supply under strict requirements and controls (Köppen et al., 2000). With regard to this, the aim of this study was to receive a basic geological model of the Ulmener Maar, which describes the groundwater behavior and flow and defines distinct hydrochemical zones.

The Ulmener Maar is situated in the western part of Germany, between Trier and Koblenz (Rhineland-Palatinate). Geologically, it belongs to the West Eifel Volcanic Field (WEVF). The age of the Ulmener Maar can be dated back to approx. 10,000 yr. BP by radiocarbon measurements and varve chronology (Zolitschka et al., 1995), making it the youngest maar structure in the WEVF. Geomagnetic measurements revealed a positive anomaly in the northern part of the Ulmener Maar with high values of +1,255 nT (Büchel, 1984). This magnetic anomaly can be correlated with a 2.4 m thick slag layer (Seyferth, 1995).

The Siegen main thrust southwest of the Ulmener Maar strikes in a SW-NE direction. Weisser (1965) describes two big anticlines in the area northeast of Ulmen, which dip to southwest, building up NNE-SSW striking flexure zones. External (Büchel, 1984; Seyferth, 1995) and own geological mapping shows that the eastern and southern steep edge of the Ulmener Maar is built up by Lower Devonian sandstones and schists.

The structure of the Ulmener Maar can be described as an oval stretched in the N-S direction. The northwestern and northeastern edges (forest and meadows) have higher altitudes compared to the southwestern part (city of Ulmen). A cemetery is located on the northwestern (higher) edge. Furthermore, the Ulmener Maar is connected to the elder Jungferweiher Maar in the north by a tunnel, the so called "Jungferweiher Stollen".

The local drinking water supply company operates eight groundwater extraction wells at the Ulmener Maar. With an average output of groundwater of 700,000 m³/a, the drinking water is distributed to around 8,000 inhabitants and additional water consumers (industry etc.).

The assignment from the local drinking water supply company was to redefine the water protection zones of the groundwater extraction wells north of the Ulmener Maar and to evaluate the possible hydrogeological influence of the cemetery southwest of the extraction wells. With regard to this applied question, hydrogeological and geophysical investigations were carried out in the year 2016. In particular, 11 boreholes were drilled and set up to groundwater measurement points (GWP). Two geomagnetic planimetries, one geoelectric profile and geological mapping were done. In addition, a 265 h pumping test from February 11th to 22nd 2016 with continuous groundwater level measurements and 17 hydrochemical analyses from GWPs and the "Jungferweiher Stollen" was done, too.

Own measurements of the Lower Devonian sandstones and schists at the western and southern edge reveal a SW-NE striking (average: 138°/42°, Clar's notation). Therefore, the Ulmener Maar is situated south of the striking axes of the above-mentioned, southern anticline. Maar tephra at the western shoreline east of the cemetery shows a SE NW striking (average: 059°/23°). The western maar tephra outcrop (wall) west of the cemetery shows a N-S striking (average: 278°/14°). At the eastern maar tephra outcrop (wall) inclination can be estimated with 105°/10° to the east.

In the "Jungferweiher Stollen" a straight profile can be observed: In the southern part of the tunnel the Devonian schists show a SW-NE striking with an average of 150°/55°. The unconformity between the schists/sandstones and the tephra at the southern entrance of the tunnel has a SW-NE striking with 136°/38° (inner facies). 100 m from the southern entrance of the tunnel the unconformity is flat-bottomed. In the middle part at around 50 m from the entrance, the unconformity shows an estimated dipping of 306°/30° (outer facies).

The results of the geophysical measurements confirm this assumption: a very sharp geomagnetic anomaly east of the cemetery from around 300 nT to 800-1400 nT occurs, and can be traced around the Ulmener Maar with radial breaches. Geoelectrical resistivity soundings (conducted by terratec geophysical services GmbH & Co. KG) reveal a difference of the specific electrical resistance in

the deeper underground east of the cemetery between 200-250 Ohm*m (possibly Devonian sandstones) and 10-50 Ohm*m (possibly Devonian schists).

The conducted long-term pumping test indicates a southward groundwater flow west of the cemetery and a water divide east of the cemetery, where water flows to the north (straight to the extraction wells) and to the south (in direction to the receiving water, probably joining the groundwater coming from the north). Groundwater level east of the cemetery is responding directly during the pumping test, whereas groundwater level west of the cemetery is stable (even showing a slightly increase of 0,1 m at one GWP). Groundwater contours before and during the pumping test show equal hydraulic conditions. In comparison, the groundwater level west of the cemetery is significantly higher than east of the cemetery, amounting to 5 m.

The waters from the Ulmener Maar can be described as (Na-)Mg-Ca-CO₃-Cl-waters in different ratios, where the groundwater from the GWP is more diverse than the groundwater from the extraction wells. In particular, the groundwater east of the cemetery shows higher pH-values and electrical conductivities (pH: 7.92-8.76, EC: 283 331 µS/cm) compared to the groundwater from west of the cemetery (pH: 7.19-7.85, EC: 535 1205 µS/cm). Groundwater from the GWP south of the highway A48 and in the center of the city of Ulmen show high sodium (41.7-119.0 mg/l) and chloride concentrations (76.0-238.0 mg/l), caused by de-icing salt for the highway traffic in winter seasons.

From these findings, the genesis and structure of the Ulmener Maar can be described as follows: It is oval-shaped with a steep western Devonian edge and a flattened eastern tephra layer. This can be traced back to a (deflected) maar explosion with the main hydrostatic pressure to the NW/W. The explosion root zone follows the main tectonic orientation with a dipping of the Devonian Schists of around 138/42 to SE. Consequently, the western edge of the Ulmener Maar was removed, whereas the eastern, stable Devonian edge still exists. Because of this, the eastern Pre-Ulmener Maar Devonian paleo-surface (around 450 m a.s.l.) is 30 m lower than the western Devonian paleo-surface (420 m a.s.l.).

Based on this geological structure of the Ulmener Maar, the hydrogeological model can be described as follows: The eastern edge (Devonian sandstones and schists) is hydraulically inactive, whereas the western (topographically lower) edge (maar tephra) is connected to the lake hydrology and inner maar hydrogeology. The western Devonian hump (palaeo-surface) acts as a hydraulic barrier, leading to a hydraulic activity at the GWP east of the hump and a hydraulic inactivity at the GWP west of the hump. Furthermore, this hydraulic barrier leads to different hydrochemical characteristics and groundwater flow. In consideration of this hydrogeological model, the cemetery is situated west of the Devonian hump, not connected to the water catchment area of the extraction wells. Groundwater flows from there to the south follow-

ing the Devonian paleo-surface to the receiving waters. Therefore, hydraulic influence of the cemetery to the extraction wells can be excluded.

Nevertheless, it is recommended to monitor and observe the groundwater level and hydrochemical parameters in future, on the one hand to understand the hydrogeological system of the Ulmener Maar better and on the other hand to provide precaution for drinking water protection.

Acknowledgements

These investigations at the Ulmener Maar were carried out on behalf of the "Kreiswasserwerk Cochem-Zell" for redefining the water protection zones and evaluation of the influence of the cemetery. Therefore, we want to thank the "Kreiswasserwerk Cochem-Zell" for the (financial) support.

References

- Zolitschka, B., Negendank, J. F. W., Lottermoser, B. G., 1995. Sedimentological proof and dating of the Early Holocene volcanic eruption of Ulmener Maar (Vulkaneifel, Germany). *Geol. Rundsch.* 84:213-219. DOI: 10.1007/BF00192252.
- Büchel, G., 1984. Die Maare im Vulkanfeld der Westeifel, ihr geophysikalischer Nachweis, ihr Alter und ihre Beziehung zur Tektonik der Erdkruste. Diss. Univ. Mainz, 1-385, Mainz. unpublished.
- Köppen, K.-H., Justen, A., Büchel, G., 2000. Hydrogeologie von Maaren - Wasserwirtschaftliche Bedeutung am Beispiel einiger Maare der Eifel. *Terra Nostra* 2000/6; International Maar Conference. 208-210. Daun/Vulkaneifel.
- Seyferth, M.H., 1995. Zur Geologie des Ulmener Maares (Westeifel) und seiner Umgebung. Diploma Thesis. 1-145. Würzburg. unpublished.
- Weisser, D., 1965. Tektonik und Barytgänge in der SE-Eifel. *Zeitschrift der Deutschen Geologischen Gesellschaft* 115/I: 33-68.

The evidence of Maar-diatreme system in the Madneuli Copper-gold-polymetallic deposit, Lesser Caucasus, Georgia

Nino Popkhadze¹, Robert Moritz²

¹ A.Janelidze Institute of Geology, I Javakhsivili Tbilisi State University, nino_popkhadze@yahoo.com

² Department of Earth Sciences, University of Geneva, Switzerland,

Keywords: host rock, pumice breccia, maar-diatreme

Bolnisi ore district in the Lesser Caucasus is known as a rich metallogenic region, where numerous ore deposits are distributed. Formation of these deposits are connecting with the upper Cretaceous explosive volcanism, associated in different stratigraphic levels. Still producing the Madneuli copper-gold polymetallic deposit is a major ore deposit in this region.

The Bolnisi district is a Northern part of the Somkhe-to-Karabakh island arc of the Lesser Caucasus, which is known in Georgia as an Artvin-bolnisi belt: Moritz et al. (2016). This extends towards the West in the Eastern Pontides, Turkey (Fig.1).



Fig.1 Location of the Bolnisi district in the Lesser Caucasus; GCS – Greater Caucasus Suture; T – Transcaucasus; AT – Southern Black Sea Coast-Achara-Trialeti Unit; AB – Artvin-Bolnisi Unit; BK – Bayburt-Karabakh Imbricated Unit; MALCS – North Anatolian-Lesser Caucasus Suture; AI-Anatolian-Iran Platform.

The Artvin-Bolnisi Unit is bordered to the North along the Southeastern Black Sea by the Adjara-Trialeti unit (interpreted as a Santonian-Campanian back-arc) and the Imbricated Baiburt-Karabakh unit to the South (interpreted as an Upper Cretaceous fore-arc) (Fig.1). It represents the northern part of the southern Transcaucasus and the central part of the Eastern Pontides, which formed the active margin of the Eurasian continent: Yilmaz et al. (2000).

Our study, based on physical volcanology and sedimentary basin analysis is the first detailed approach for the host rocks of the Madneuli deposit, which still need to be carried out in future investigations in similar environments along the Lesser Caucasus and the Eastern Pontides,

where the host rocks and the depositional environment of rock units is still very much debated or poorly constrained.

First time was interpreted the maar-diatreme system in this region on the Madneuli deposit; Popkhadze et al. (2017); Popkhadze et al. (2017). Detailed field based, facies oriented investigations allow us to interpret the following facies types on the Madneuli deposit: tuff ring, crater infill facies, lower diatreme (root zone?) with mineralization, phreatomagmatic breccia, lava dome and cross cutting rhyodacitic extrusive. The main volcanic and volcano-sedimentary facies units in the Madneuli deposit, associated with phreatomagmatic eruption and formation of the maar-diatreme system in the open pit.

The tuff ring is divided in two part: lower non-bedded and upper bedded unit, separated by an undulating contact. The best preserved section of the tuff ring is in the eastern part of the open pit. Lower non-bedded part, represented by massive, non-bedded pyroclastic rocks – ash rich, reversely graded pumice-fiamme breccias and is strongly silicified and mineralized. Vesiculated bedded tuff alternate with fine grained tuff, accretionary bearing and pumice tuff horizons in the upper bedded tuff ring. Accretionary bearing tuff is widespread in all flanks of the open pit and serve as a marker horizons during the interpretation and correlations of facies types to follow the stratigraphy on the open pit. The recognition of two type of hyaloclastite (lobe hyaloclastite), carapace breccia and internal coherent facies with lobe structure in the open pit, allow us to interpret a rhyodacite dome, located out of the tuff ring: Popkhadze et al. (2014), Popkhadze (2012).

The diversity of facies types is characteristic for the crater infill facies: bedded horizons with classical slide slump unit (Fig.2a), huge blocks of bedded rocks (Fig.2b), is alternated with altered pumice (fiamme) breccia (Fig.2c), which is deposited a below-wave-base subaqueous setting - ash from nearby subaerial probably phreatomagmatic eruptions being washed in and accumulating rapidly; and also with very thinly bedded tuffaceous mudstone (Fig.2d). Tuffaceous mudstone below the pumice breccia bed showing the soft-sediment deformation features which suggest that the deposit was waterlogged. These deposits are interpreted explosive eruption-fed products: Jutzeler et al. (2014).

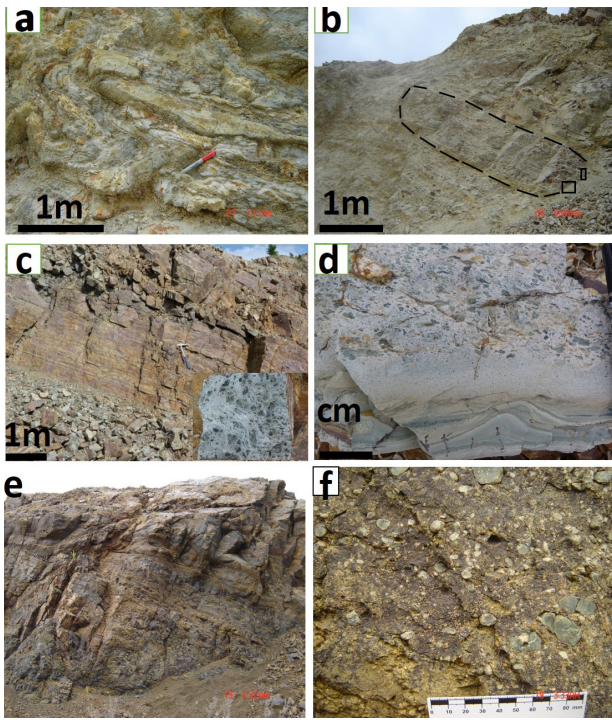


Fig.2 Diversity of facies types in the crater infill structure: a) slide slump units; b) huge block of bedded rocks; c) altered pumice (fiamme) breccia; d) tuffaceous mudstone; e) cross-bedding; f) rounded conglomerate unit.

The uppermost units are represented by bedded tuff with cross-bedding texture and tuff with well-rounded conglomerate unit.

Based on detailed host rock facies architecture and their stratigraphy in the Upper Cretaceous Madneuli polymetallic deposit, we define the felsic maar-diatreme volcano, associated with lava dome in shallow marine environment. The dome occurs here outside of the crater and its formation is contemporaneous with maar-diatreme volcanos.

There is evidence of a shallow marine environment, and no evidence for a lacustrine sedimentary environment. So, it still remains open to question in what setting the maar was formed (subaerial or shallow marine setting).

Acknowledgements

The research was supported by the Georgian National Science Grant and Swiss National Science Foundation research grants. SCOPES Joint Research Projects IB7620-118901 and IZ73Z0-128324. The author would like to thank the participants of the project and the staff of the “Madneuli Mine” for arranging access to the mine.

References

- Yilmaz, A., Adamia, Sh., Chabukiani, A, Chkhotua, T., Erdogan, K., Tuzcu, S., Karabilykoglu, M., 2000. Structural correlation of the southern Transcaucasus (Georgia)-Eastern Pontides (Turkey)-Tectonics and magmatism in Turkey and the surrounding area. Geological Society of London Special Publication 173:171-182
- Popkhadze, N., Moritz, R., Natsvlshvili, M., Bitsadze, N., 2017. First evidence of phreatomagmatic breccia at the Madneuli Polymetallic Deposit, Bolnisi district, Lesser Caucasus, Georgia. Mineral resources to discovery, 14th SGA Biennial Meeting, 20-23 August 2017, Quebec City, Canada, v.1:323-326
- Popkhadze, N., Moritz, R., Kekelia, S., 2017. Maar-diatreme volcano on the Madneuli polymetallic deposit: Lesser Caucasus, Georgia (implication for the host rock facies architecture). 4rd International Volcano Geology Workshop: Challenges of mapping in poorly-exposed volcanic areas. Eastern Transylvania, Romania, October 8-14.
- Popkhadze, N., Moritz, R., Gugushvili, V., 2014. Architecture of Upper Cretaceous rhyodacitic Hyaloclastite at the polymetallic Madneuli deposit, Lesser Caucasus, Georgia. Central European Journal of Geosciences. 6(3):308-329
- Popkhadze, N., 2012. First evidence of Hyaloclastites at Madneuli deposit, Bolnisi district, Georgia. Bulletin of the Georgia National academy of sciences v.6, no.3: 83-90
- Jutzeler, M., McPhie, J., Allen, S.R. 2014. Facies architecture of a continental, below-wave-base volcanoclastic basin: The Ohanapocosh Formation, Ancestral Cascades arc (Washington, USA). Geological Society of America Bulletin.126/3-4:352-376
- Moritz, R., Melkonyan, R., Selby, D., Popkhadze, N., Gugushvili, V., Tayan, R., Ramazanov, V. (2016) Metallogeny of the Lesser Caucasus: From Arc Construction to Postcollision Evolution. Society of Economic Geologists, Special Publication 19, pp.157-192

Perşani Mountains, a small monogenetic volcanic field (Southeastern Carpathians, Romania) with remarkable geodiversity and high geoheritage values

Ildikó Soós^{1,2}, Szabolcs Harangi^{1,2}, János Szepesi², and Károly Németh³

¹ Department of Petrology and Geochemistry, Eötvös University H-1117 Budapest, Hungary, ildiko.soos14@gmail.com

² MTA-ELTE Volcanology Research Group, H-1117 Budapest, Pázmány Péter sétány 1/C, Budapest, Hungary

³ Institute of Agriculture and Environment, Massey University, Palmerston North, New Zealand.

Keywords: volcanic geoheritage, geopark, geosite evaluation.

The Perşani Mountain is located in the inner part of the Carpathian Bend Area, at the north-western margin of the Braşov Basin. The >176 km² Perşani Volcanic Field (PVF) with 21 identified volcanic structures was developed during 1.2-0.6 Ma hence it represents the youngest manifestation of dispersed type of volcanism in the Carpathian-Pannonian Region (Harangi et al., 2015; Seghedi et al. 2016). It contains lava flows, maars and scoria cones. However, the PVF and the surroundings are more diverse than just that with a complex geological structure. Near the youngest volcanic rocks on the surface, ~550 Ma old gneiss is also exposed that formed during the Cadomian Orogeny. It is an important territory from palaeontological point of view as well, known especially for its Upper Jurassic-Lower Cretaceous ammonites and Upper Cretaceous inoceram faunas. In the PVF, the Racoş basalt col-

umns, the Hegheş Hill scoria quarry and the Brazi basalt quarry partially filled by the "Emerald Lake" are the most spectacular geosites of the area offering beautiful view point for the visitors. Both the volcanic and fossil sites represent great scientific and touristic values. The geodiversity is represented also by the Dopca Gorge and 3 caves with different protection levels. The Perşani Mountains territory protected biodiversity is composed of 5 Natura2000 sites and 1 bird and fauna nature reserve. Another attraction is the approximately 900 years old oak from Mercheaşa. The cultural heritage is also significant, being represented by many historical monuments (archaeological sites, medieval fortresses, castles and fortified churches) and contemporary folklore. To make this area better known and appreciated for its scientific and touristic values we need to make a prelim-

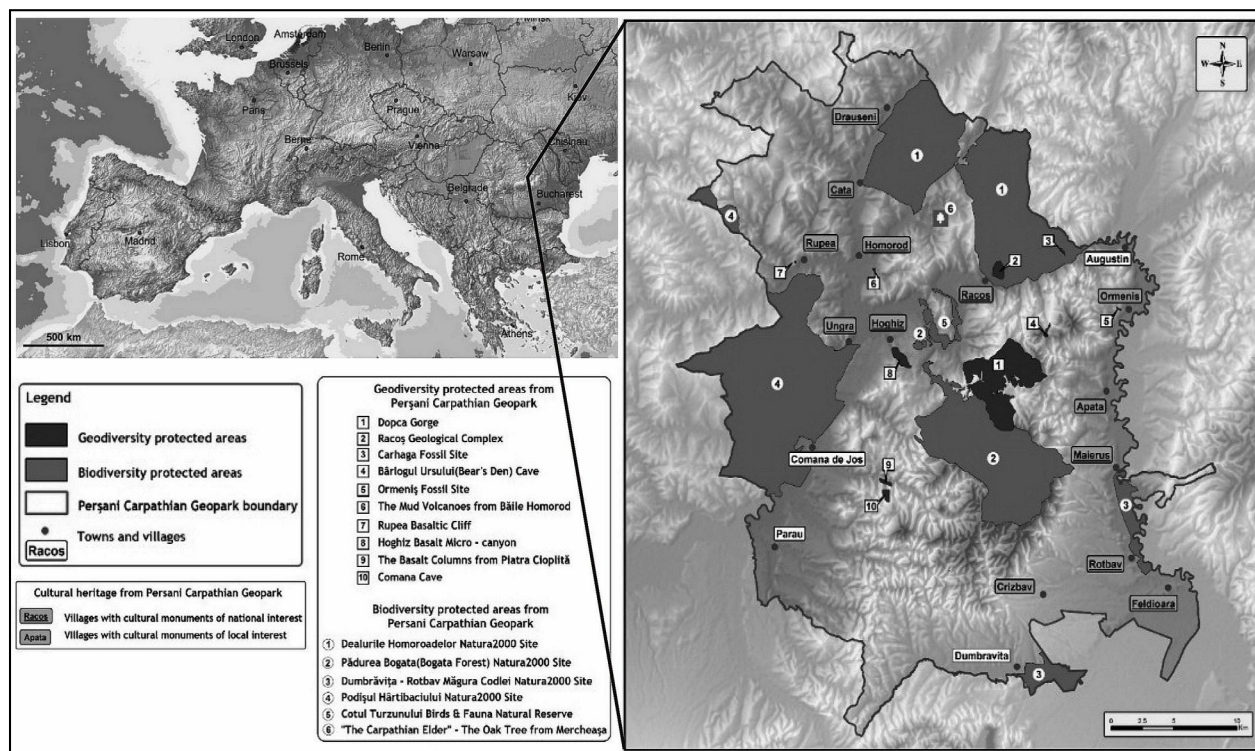


Fig. 1 – Location of the studied area and the boundaries of the future geopark with the main natural and cultural heritage sites.

inary geosite assessment. In the last three decades this topic has become an attractive and necessary research field due to its importance in geosite conservation, protection and introduction for the public by a new branch of tourism, termed geotourism. This provides also a great opportunity for sustainable development in regions with unique natural and cultural heritage in the benefit of the local communities. Good evidence is that this idea works in the presence of the 127 UNESCO Global Geopark and others in national and regional organizations.

After an attentive study of the specific literature for geosite assessment we decided to follow the stages of the work described by Reynard et al. (2016). A careful search of the scientific references of the Perşani Mountains area was made before the systematic field work. All the volcanic geotopes found in the literature, marked on the geological and topographic maps, were identified. After the field work a preliminary geotope list was set up. A few of these geosites were already evaluated by different methods found in the specific literature in order to see which one is the most competent for the studied area.

One of the preferred methods is the geosite assessment model (GAM) of Vujičić et al. (2011), used to define the main and additional values. We take into consideration the three indicators of the main values: scientific/educational, scenic/ aesthetical and protection. The additional values are indicated by the functional and touristic values. The matrix resulted from these indicators highlights the issues which should be strengthened in the studied area such as the promotion for tourism or the infrastructure of the region. At the end a geotourism potential map was made from the results given by these methods.

The model by Brilha (2016) has been applied in our preliminary study turned also to be very useful. He categorized the indicators in four main groups: scientific value, educational and touristic potential and also the degradation risk. Due to this model we had to decide the purpose of each geosite. In order to make the right assessment we have to know if a geosite has scientific value or touristic or maybe both of them. The vulnerability of the sites is also very important to evaluate near the values of each site however to do this subjectively is difficult.

The Perşani Mountains and its area has an exceptional natural (geodiversity & biodiversity) and an important cultural heritage with a high sustainable development potential, containing 15 natural protected sites, from which 10 are geological sites, comprising a total area of 1100.00 km² and a population of over 50000 inhabitants, living in 14 communities. With the complex geological structure provide an excellent educational material on the Carpathian Mountains formation and evolution as an episode of the Earth Natural History.

This work is the beginning of the detailed quantitative assessment using various, recently developed approaches to evaluate the volcanic geoheritage of this area that could help to transfer these values to touristic attention. The results of this study could contribute also to the de-

velopment of a future geopark, which would promote the local tourism and economy.

In the Carpathian - Pannonian region we can find a huge variety of volcanic geoheritage sites, particularly those represent volcanism in the Miocene to Pliocene time slice. In many places we can take a look "inside" the volcanos which offers a strong interest for scientists and for tourists as well. Some of these sites have been already inventoried by Szepesi et al. (2017) and the idea to connect these volcanological sites by a 900 km long volcano route was also presented recently (Harangi et al. 2015). Making the inventory of the Perşani Mountains could help also to connect the region with the planned volcano route which one day could be part of the European Volcano Route.

References

- Brilha, J. 2016. Inventory and quantitative assessment of geosites and geodiversity sites: a review. *Geoheritage* 8:116. DOI: 10.1007/s12371-014-0139-3
- Harangi, Sz., Németh, K., Korbély, B., Szepesi, J., Szarvas, I., Lukács, R. Soós, I. 2015. The Pannonian Volcano Route: a plan to connect volcanic heritage sites across Hungary. 2nd Volcanopark Conference, Lanzarote Abstract Book 40-4.
- Harangi, Sz., Jankovics, M.E., Sági, T., Kiss, B., Lukács, R., Soós, I. 2015. Origin and geodynamic relationships of the Late Miocene to Quaternary alkaline basalt volcanism in the Pannonian basin, eastern-central Europe. *Int J Earth Sci* 104(8):2007-2032
- Reynard, E., Perret, A., Bussard, J., Grangier, L., Martin, S. 2016. Integrated Approach for the Inventory and Management of Geomorphological Heritage at the Regional Scale. *Geoheritage*, 8(1): 43–60.
- Seghedi, I., Popa, R-G., Panaiotu, C. G., Szakacs, A., Pecsikai, Z. 2016. Short-lived eruptive episodes during the construction of a Na-alkalic basaltic field (Perşani Mountains, SE Transylvania, Romania). *Bull Volc* 78:69
- Szepesi, J., Harangi, Sz., Ésik, Zs., Novák, T., Lukács R., Soós, I. 2017. Volcanic Geoheritage and Geotourism Perspectives in Hungary: a Case of an UNESCO World Heritage Site, Tokaj Wine Region Historic Cultural Landscape, Hungary. *Geoheritage* 8/27: 1–21.
- Vujičić, M. D., Vasiljević, D. A., Marković, S. B., Hose, T. A., Lukić, T., Hadzic, O., & Janicević, S. 2011. Preliminary geosite assessment model (GAM) and its application on Fruska Gora Mountain, potential geotourism destination of Serbia. *Acta Geogr Slovenica*, 51(2): 361–37.

Assessment of hydromagmatic geomorphosites in the Campo de Calatrava Volcanic Field (Ciudad Real, Spain)

Salvador Beato, Miguel Ángel Poblete and José Luis Marino

Oviedo University. Humanities Faculty, Geography Department. Campus de El Milan, 33011 Oviedo, Asturias, Spain.
beatosalvador@uniovi.es.

Keywords: Geomorphosites, assessment, hydromagmatic geoheritage

Recently, numerous works on volcanic geoheritage (Henriques and Neto, 2015; Martí and Planagumà, 2016) specifically geosites (Reolid et al. 2013) as well as geomorphosites (Joyce, 2009; Costa, 2011; Dóniz et al. 2011) and even volcanic geoparks have been carried out (Errami et al. 2015; Vista and Rosenberger, 2015). This new line of research is fundamental for an adequate protection and conservation of outstanding volcanic landscapes still subjected to multiple aggressions.

So far, the Campo de Calatrava Volcanic Field has been the subject of a study on the geoheritage of magmatic volcanism (Becerra, 2013). Therefore, the objective of this work is focused on the evaluation of different types of hydromagmatic geomorphosites values through the application of qualitative and quantitative methodologies (Pereira and Pereira, 2010; Serrano and Gonzalez-Trueba, 2005).

Following the methodological proposals of Pereira and Pereira (2010) and Marino et al. (2017) an inventory, mapping and classification of hydromagmatic volcanoes were developed a medium scale (1 X 1 km), using the previous works of Poblete (1991, 1994) and Poblete et al. (2016) and GIS. A total of 289 monogenetic volcanoes

were identified, which 110 were maars and three typologies were distinguished: 7 subsided crater rim maars, 31 embedded maars into quartzite lack tuff rings and vertical slopes and finally 72 carved maars into tertiary basins with tuff rings and gentle slopes. Based on its geomorphological features and morphoeruptive singularity, 6 representative hydromagmatic geomorphosites were selected at a rate of two for each typology: Las Higuieruelas and Hoya de los Muertos (subsided crater rim maars); La Posadilla and La Alberquilla (embedded maars); Cuelgaperros y Espejuelos (carved maars).

The identification of potential geomorphosites was based on criteria such as scientific, cultural and use and management values, being the score as follows: a high value when the score obtained was greater than 7, medium value when it was between 7 and 3.5 and the low value when it was less than 3.5 (Serrano and Gonzalez-Trueba, 2005) (Table 1).

According to the results obtained, the maar of La Posadilla is the only hydromagmatic geomorphosite that achieves a global valuation of outstanding, while the

SCIENTIFIC VALUE (Maximum 5 points for each variable, the maximum total score is 50 points and valued over 10)	CULTURAL VALUE (The maximum total score is 70 points and valued over 10)	USE AND MANAGEMENT VALUES (The maximum total score is 20 and valued over 10)
Genesis	Landscape and esthetic (Maximum 10)	Accessability (High: 2; Medium: 1; Low: 0)
Morfostructures	Heritage elements (Max. 10)	Fragility (H: 0; M: 1; L: 2)
Erosional landforms	Cultural content (Max. 10)	Vulnerability (H: 0; M: 1; L: 2)
Accumulation landforms	Historical content (Max. 10)	Intensity of use (H: 0; M: 1; L: 2)
Inherited processes	Educational resources (Max. 5)	Risk of degradation (H: 0; M: 1; L: 2)
Current processes	Educational levels (Max. 5)	Impacts (H: 0; M: 1; L: 2)
Chronology	Scientific value (Max. 5)	Quality of view (H: 2; M: 1; L: 0)
Litology	Scientific representativeness (Max. 5)	Limits of acceptable change (H: 2; M: 1; L: 0)
Geologic structures	Real tourist contents (Max. 5)	Services and equipment (H: 2; M: 1; L: 0)
Sedimentary structures	Potential for tourist attraction (Max. 5)	Economic potential (H: 2; M: 1; L: 0)

Table 1. Scientific, cultural and use and management values assessment of geomorphosites.

rest of the maars obtain a medium rating, without any of them obtaining a low evaluation (Table 2). In effect, La Posadilla maar is the geomorphosite that obtains the highest scientific, cultural and use and management valuation, which makes it the reference more significant of the Campo de Calatrava Volcanic Field not only regionally but also nationally.

Two other notable geomorphosites are Las Higuieruelas and Cuelgaperros, which obtain a good rating and serve by their proximity to La

Posadilla as complement, since they correspond to the other two types of distinguished maars. The potential of use and management of the three sites is elevated due to its good accessibility, low fragility and low vulnerability. In short, the three geomorphosites can serve as a basis to promote the development of emerging sectors such as geotourism fundamental for the sustainable development of depressed rural areas.

Acknowledgements

We are grateful for the help of the Westminster Foundation. Salvador Beato Bergua is supported by the FPU program (MECD-FPU14/03409).

References

Becerra, R. 2013. Geomorfología y geopatrimonio de los volcanes magmáticos de la Región Volcánica del Campo de Calatrava. Doctoral Thesis, Universidad de Castilla-La Mancha, Ciudad Real.

Dóniz, F.J., Becerra, R., González, E., Guillén-Martín, C., Escobar, E. 2011. Geomorphosites and Geotourism in Volcanic Landscapes: the example of La Corona del Lajial cinder cone (El Hierro, Canary Islands, Spain). *Geo. J. Tourism Geosites* 2: 185-197.

Errami, E., Brocx, M., Semeniuk, V. (eds.) 2015. From geoheritage to geoparks: case studies from Africa and beyond. Springer-Verlag, 269 pp. DOI: 10.1007/978-3-319-10708-0.

Henriques, M.H., Neto, K. 2015. Geoheritage at the equator: selected geosites of Sao Tome Island (Cameron Line, Central Africa). *Sustainability* 7: 648-667.

Joyce, B. 2009. Geomorphosites and volcanism, in Reynard E, Coratz P, and, Regolini-Bissing, G., eds., *Geomorphosites*. Verlag Dr. Friedrich Pfeil, München, Germany, 175–188.

Marino, J.L., Poblete, M.A., Beato, S. 2017. Valoración del patrimonio geomorfológico de un sector del Parque Natural de Arribes del Duero (Bajo Sayago, Zamora). *Cuaternario y Geomorfología* 31 (3-4): 27-50.

Martí, J., Planagumà, L. (eds.). 2017. *La Garrotxa Volcanic Field of Northeast Spain: Case Study of Sustainable Volcanic Landscape Management*. Springer, 136 pp. DOI: 10.1007/978-3-319-42080-6.

Pereira, P., Pereira, D. 2010. Methodological guidelines for geomorphosite assessment. *Géomorphologie – Relief, Processus, Environment* 16: 215-222.

Poblete, M.A. 1991. Morfología de los cráteres explosivos pliocenos del Campo de Calatrava (Ciudad Real). *Ería* 26: 179-198.

Poblete, M.A., 1994. El relieve volcánico del Campo de Calatrava (Ciudad Real). Gijón. Junta de Comunidades de Castilla-La Mancha and Departamento de Geografía de la Universidad de Oviedo

Poblete, M.A., Beato, S., Marino, J.L., 2016. “Landforms in the Campo de Calatrava Volcanic Field”, *Journal of Maps* 12: 271-279. DOI: 10.1080/17445647.2016.1195302.

Reolid, M., Sánchez-Gómez, M., Abad, I., Gómez-Sánchez, M.E., de Mora, J. 2013. Natural monument of the volcano Cancarix, Spain: a case of lamproite phreatomagmatic volcanism. *Geoheritage* 5: 35-45.

Serrano, E., González-Trueba, J.J., 2005. Assessment of geomorphosites in natural protectec areas: the Picos de Europa National Park (Spain). *Géomorphologie – Relief, Processus, Environment* 11: 197-208.

Vista, A.B., Rosenberger, R.S. 2015. Estimating the recreational value of Taal Volcano protected landscape, Philippines using benefit transfer. *Journal of Environmental Science and Management* 18: 22-33.

Nº	Name	Evaluation			
		Scientific	Cultural	Use and management	Global
1	La Posadilla maar	6.4	5.7	9.5	7.2
2	Las Higuieruelas maar	4	2.9	9.5	5.5
3	Cuelgaperros maar	6	2.7	7.5	5.4
4	Espejuelos maar	4.6	2.6	8	5.1
5	Hoya de los Muertos maar	4	2.1	7.5	4.5
6	La Alberquilla maar	2.6	3.1	5.5	3.7

Table 2. Results of hydromagmatic geomorphosites assessment in the Campo de Calatrava Volcanic Field.

A geotouristic route to discover the maars of the Medias Lunas Range (Campo de Calatrava Volcanic Field, Central Spain)

Salvador Beato, Miguel Ángel Poblete and José Luis Marino

*Oviedo University, Humanities Faculty, Geography Department. Campus de El Milan, 33011 Oviedo, Asturias, Spain.
beatosalvador@uniovi.es.*

Keywords: Georoute, maars, Central Spain.

In the last years, new lines of research have been opened related to the valuation and conservation of volcanic heritage (Risso et al. 2006; Joyce, 2009), as well as the active role that volcanism can play in the development of geotourism (Erfurt-Cooper, 2011). We must also highlight the role that educational itineraries can play as a resource to boost the development of scientific tourism (Dóniz et al. 2011; Poblete et al. 2014).

The objective of this georoute for the Medias Lunas Range is, on the one hand, to show society the high scientific and landscape value of the volcanic heritage of the Campo de Calatrava and, on the other, to promote a more active and committed scientific and educational tourism based on the principles of conservation and sustainable development.

The itinerary through the Medias Lunas Range consists of six stops in which the characteristics of the most outstanding maars of the Campo de Calatrava are explained. The georoute begins in Ciudad Real capital, surrounded by several maars, where we take the N-420 in the direction of Poblete. Past this village we will visit the Maar of Los Corchuelos, which pierces the anticlinal vault of the Despeñadero. Then, the maars of La Posadilla, El Portillo y El Paso are visited in Valverde. It's advisable to walk up to the top of the range known as Malos Aires (780 m a.s.l.) from which it can be seen a complete view of the whole itinerary. The route ends in Alcolea visiting two of the most important Pliocene maars of the Campo de Calatrava: Galiana y Las Higuieruelas. The feature that characterizes the Pliocene maars is that they lack tephra ring and instead are bordered of Ruscinian limestones.

1^a Stop: Maar of Los Corchuelos. The Despeñadero Range is the eastern prolongation of the Medias Lunas Range where the maars of Peñalagua, Los Corchuelos and Hoya del Arzollar are located. The one of greater geomorphological interest is Los Corchuelos, which abruptly interrupts the continuity of the quartzitic alignment. The opening of this great hole in the anticlinal vault of the Despeñadero was as result of a violent hydromagmatic explosion produced through a strike-slip fault, which crosses said mountainous alignment. The hydromagmatic explosion of great intensity deeply pierced the anticlinal vault of the Despeñadero, carving a subcircular

explosion crater of 500 m in diameter and 80 m of depth. The bottom of the crater has a flat shape because it is filled with explosive breccias and abundant cauliflower bombs that contain a huge amount of quartzitic xenoliths of small size (Fig. 1).

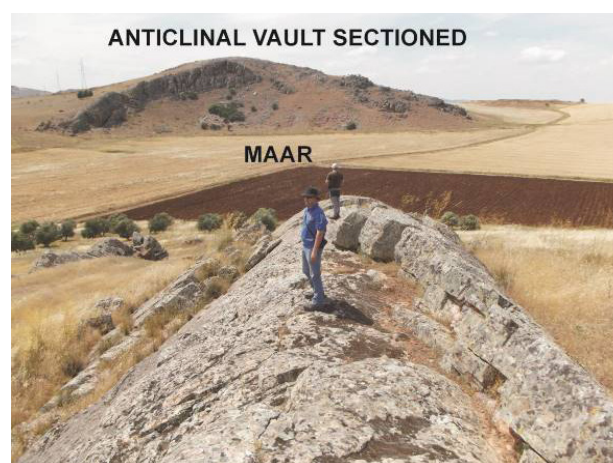


Fig. 1 – Eastern view of the maar of Los Corchuelos (Despeñadero Range).

2^a Stop: Maar of La Posadilla. It is located 5 km to the SSO of Valverde, in the front of the quartzitic crest of the Medias Lunas Range. In this range is, certainly, the most important ensemble of maars excavated in the Paleozoic basement of Campo de Calatrava. A total of five maars are grouped arranged from west to east: Maestras, Medias Lunas, El Paso, La Posadilla y El Portillo. These maars are associated with an important strike-slip fault of about 12 km in length, which crosses the Medias Lunas Range. Of all of them the most interesting from the geomorphological as well as the volcanological point of view is La Posadilla, due to the changes that its eruptive behavior has experienced throughout the volcanic dynamics, distinguishing at least three major phases: a strombolian that constructs the cone of Malos Aires, a hydromagmatic phase that destroys said cone and originates the maar of La Posadilla and finally a phreatic explosion that excavates at the summit of the quartzitic range the maar of El Portillo (Poblete, 1991).

The maar of La Posadilla, formed from a hydromagmatic eruption in the Upper Pleistocene, consist of a circular

crater of 1 km in diameter and 120 m maximum depth, excavated on the northern quartzitic slope of Medias Lunas Range (Fig. 2).

3^a Stop: Maar of El Portillo. At 50 m to the east of La Posadilla, the summit of the Medias Lunas Range is broken by a small gap or pass resulting from a phreatic explosion. It is El Portillo maar that forms a small hole open in the quartzitic crest, whose dimensions are of the order of 100 m in diameter and 5 m deep. This maar is a small crater without tephra ring, from which two very fluid lava flow were subsequently emitted.



Fig. 2 – Southern view of the maar of La Posadilla (Medias Lunas Range).

4^a Stop: El Paso maar. Located 1 km west of La Posadilla maar consists of a horseshoe shape crater of 300 m in diameter and no tephra ring drilled from a steam explosion, followed by an effusive phase in which two lava flow was emitted.

5^a Stop: Maar of Galiana. Unlike the previous ones, this maar is formed in the tertiary sedimentary sub-basin of Alcolea and is Pliocene age. Galiana maar, located between kilometers 227 and 228 of the N-430, is characterized by a circular depression of 750 m wide and 8 m deep. Not only does it lack a tephra ring, but it is formed by a remnant of Ruscinian limestones, whose central part was destroyed by the freatomagmatic explosion, inclined between 25 and 40° with periclinal tip toward the center of the depression. All this as a consequence of the volcano-tectonic subsidence of diatrema, from ring fracture system and the diagenesis (dehydration and compaction) of Pliocene PDC deposits (Poblete, 1991).

6^a Stop: Maar of Las Higuieruelas. It is 3 km east of Alcolea village. It is characterized by a circular depression of 450 m in diameter and 20 m in depth formed from freatomagmatic eruption, no tephra ring and bordered by a remnant or piece of Ruscinian limestones with periclinal and convergent dip between 30 to 40° toward the center of crater. This dislocation is the result of the volcano-tectonic subsidence of the rim of the crater and diatrema, through ring fractures in response to posteruptive distension and diagenesis of the PDC deposits (Poblete, 1991). It houses in the bottom an important Plio-Quaternary paleontological site.

Acknowledgements

This research was supported by the FPU program of Ministerio de Educacion, Cultura y Deportes through doctoral fellowship of Salvador Beato Bergua (grant number MECD-FPU14/03409).

References

- Dóniz, F.J., Becerra, R., González, E., Guillén-Martín, C., Escobar, E. 2011. Geomorphosites and Geotourism in Volcanic Landscapes: the example of La Corona del Lajjal cinder cone (El Hierro, Canary Islands, Spain). *Geo. J. Tourism Geosites* 2: 185-197.
- Erfurt-Cooper, P. 2011. Geotourism in volcanic and geothermal environments: playing with fire? *Geoheritage* 3(3): 187–193.
- Joyce, B. 2009. Geomorphosites and volcanism, in Reynard E, Coratz P., and, Regolini-Bissing, G., eds., *Geomorphosites*. Verlag Dr. Friedrich Pfeil, München, Germany, 175–188.
- Poblete, M.A. 1991. Morfología de los cráteres explosivos pliocenos del Campo de Calatrava (Ciudad Real). *Ería* 26: 179-198.
- Poblete, M. A. 1993. Morfología y secuencia eruptiva del cráter explosivo de La Posadilla (Campo de Calatrava, Ciudad Real). *Ería* 30:51-59.
- Poblete, M.A., Ruiz, J., Beato, S., Marino, J.L. y García, C. 2014. Recorrido didáctico por los lugares de interés geológico del Campo de Calatrava como recurso para la valorización y divulgación de su patrimonio volcánico, in Mata Perelló, J.M., ed., *El patrimonio geológico y minero como motor del desarrollo local*. SEDPGYM, Manresa, 131-150.
- Risso, C., Németh, K., Martin, U. 2006. Proposed geotops on Pliocene to recent pyroclastic cone fields in Mendoza, Argentina. *Z. Dtsch. Geol. Ges.* 157(3): 477–490.

Monte Preto monogenetic volcano (Fogo, Cape Verde) an exceptional volcanic heritage for the geotourism

Javier Dóniz-Páez^{1, 2}, Rafael Becerra-Ramírez^{3, 2}, Elena González-Cárdenas^{3, 2}, Estela Escobar-Lahoz^{3, 2}, Samara Dionis² and Vera Alfama⁴

¹ GeoTurVol-Departamento de Geografía e Historia, Universidad de La Laguna, Campus de Guajara s/n, 38071, La Laguna, Tenerife, Spain. jdoniz@ull.es

² Instituto Volcanológico de Canarias (INVOLCAN), Hotel Tahoro, 38400, Puerto de La Cruz, Tenerife, Spain.

³ GEOVOL-Departamento de Geografía y Ordenación del Territorio, Universidad de Castilla-La Mancha, Avda. Camilo José Cela s/n, 13071, Ciudad Real, Spain.

⁴ Faculdade de Ciências e Tecnologia, Universidade de Cabo Verde, Campus de Palmarejo, CP-279, Praia, Santiago, Cape Verde.

Keywords: Volcanic Heritage, geotourism, Cape Verde

The volcanic landscape is attractive for the general public. Sites with a special tourist interest are created by them Dóniz-Páez, (2017). These geosites or geomorphosites are remarkable forms and processes because of their high scientific values, but also by their social, cultural, aesthetic and economic importance amongst other aspects. The geomorphosites measure the volcanic heritage regarding to geotourism, geoconservation or geoeducation. These aspects related to volcanic heritage are commonly viewed through micro to macro scales Németh et al., (2017). For example, when using the macro scale, it could be possible not to see the volcanic geodiversity. Therefore, once we study volcanoes at micro scale, we can observe all the geodiversity and biodiversity of volcanic landscapes.

The aim of this paper is studying the volcanic heritage of Monte Preto volcano (MPV), a cinder cone with tourism interest. The methodology used in this paper is based on a non-systematic inventory of geomorphosites from MPV with geotourist potential, according to a bibliographical review, an aerial photo and mainly, to the fieldwork made with campaigns in November 2015 and July 2016.

MPV is located in Fogo Natural Park, on the summit of Fogo Island (Fig. 1). Fogo is located in the southern group of Cape Verde archipelago, in the central Atlantic, about 600 km from the western coast of Africa, at 15° N Costa, (2011). MPV takes part of the basaltic monogenetic eruptive complex, in an eruptive fissure of 5 km length whose origin goes back to 1951. The 1951 event is similar to historical eruptions documented in Fogo (1769, 1785, 1816, 1847, 1852, 1995 and 2014-15) Alfama et al., (2008). This eruption emerged in the flank of Pico de Fogo stratovolcano along a NW-SE fissure. In the south flank, multiple volcanoes (Monte Lestisco-Orlando-Rendall) of lapilli, scoria, spatter and bombs with important pahoehoe and aa lava flows with more 6 km length were formed. In the north flank, we can observe two main groups of cones from the eruption of 1951. The first one consists of a four-small scoria cones with pahoehoe and aa lava flows with an altitude of 1,980-2,000 m and the MPV complex. The other one is compounded by two main cinder cones (MPV) and more than 20 small scoria and spatter cones

in the NW-SE fissure eruption. The morphology of volcanoes corresponds to the multiple basaltic monogenetic cones according to Dóniz-Páez, (2015).

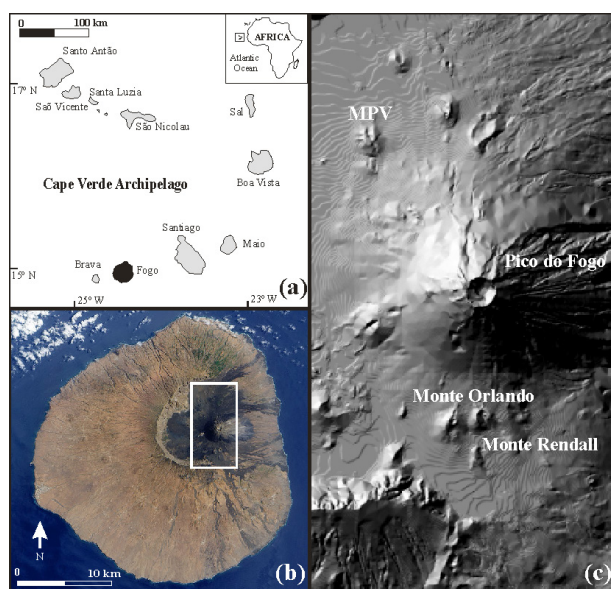


Fig. 1 – Location of Monte Preto volcano, Fogo, Cape Verde Archipelago.

Two important groups of volcanic landforms can be identified in MPV: cones and lava flows. In the MPV, three types of eruptive structures can be distinguished: cinder cones, small scoria cones, and spatter cones or hornitos. The cinder cone constitutes a multiple volcano, formed by lapilli, bombs, scoria and spatter deposits and interstratified lavas. It has various rings and open craters (Fig. 2) with abundant pahoehoe and aa lavas with some lava tubes and channels which flow along several kilometers. The small scoria cones are formed by accumulations of lapilli, and especially by spatter with vent with ring, horseshoe and multiple shapes. The hornitos are the smallest eruptive buildings. They are the most common structures in MPV and they are not more than 10 meters height. They present irregular bases as a consequence of the association of various hornitos formed by spatter de-

posits, and eruptive centers connected to lava tubes and channels. All the eruptive cones are affected by erosional processes. The most important one is a colluvial and torrential landform, but we can also observe the effects of human action on them (paths, crops, livestock, extractions of lapilli, etc.).



Fig. 2 – The main cinder cone of Monte Preto Volcano.

The lava flows are emitted from the cinder and scoria cones and hornitos. The main lava flows are aa, pahoehoe and blocks, but it is possible to admire different morphological forms associated to a lava field: small lava lakes, pond of lavas, lava cascades, lava collapses, lava tubes, lava channels, jameos, etc.

In MPV, we can recognize a wide range of volcanic landforms: cinder cones, scoria cones, spatter cones or hornitos, pahoehoe, aa and blocks lava flows, lava tubes, lava channels, gullies, taluses, etc. The great geodiversity of this volcano is an exceptional heritage for geotourism. The geotourism can be considered as a tourism segment mainly focused on the geodiversity and geoheritage. Nevertheless, the cultural heritage (material and immaterial) of the areas can be considered as pull factor for it Rocha and Ferreras, (2014). Therefore, the geoheritage is the driving force of the geotourism itineraries, but the cultural heritage it is also added to increase the value of the visited regions Rocha and Ferreria, (2014). When we talk about geotourism, we are use to pay attention to two main aspects: the geoheritage site and its administrations and their legal frameworks. In this sense, we propose a geotourist itinerary through the different landforms of MPV in Fogo Natural Park, with a special interest in volcanic heritage and cultural values of Portelas and Bangaieira villages.

Now, in Fogo Natural Park, there are 13 itineraries according to Moreno et al., (2015). Tourists can use path number nine (Portela-Monte Preto), five (Portela-Penedo Rachado-Fernão Gomes) and six (Portela-Pico do Vulcão). However, the first one, number nine, is the best because it crosses the two groups of volcanoes in MPV complex. Therefore, the geotourist potential can be observed and interpreted when we pay attention to all the volcanic heritage of MPV and its culture.

Acknowledgements

This paper has been funded by the project “Fortalecimento del tejido económico y empresarial ligado al sector turístico de Tenerife mediante la potenciación del volcaturismo”, supported by Cabildo de Tenerife, Spain.

References

- Alfama, V., Gomes, A., Brilha, J., 2008. Guia geoturístico da Ilha do Fogo, Cabo Verde. Departamento de Ciências da Terra Universidade de Coimbra.
- Costa, F., 2011. Volcanic geomorphosites assessment of the last eruption, on April to May 1995, within the Natural Park of Fogo Island, Cape Verde. *GeoJournal of Tourism and Geosites* IV, 2(8): 167-177.
- Dóniz-Páez, J., 2015. Volcanic geomorphological classification of the cinder cones of Tenerife (Canary Islands, Spain). *Geomorphology* 228: 432-447 DOI: <http://dx.doi.org/10.1016/j.geomorph.2014.10.004>.
- Dóniz-Páez, J., 2017. Las rocas son atractivas: volcaturismo en Fogo. *Bínter* 176: 38-42.
- Németh, K., Casadevall, T., Moufti, M., Martí, J., 2017. Volcanic Geoheritage. *Geoheritage* 9: 251-254. DOI: 10.1007/s12371-017-0257-9.
- Moreno, C., Bueno, A., Rodríguez, A., Guerra, E., Naranjo, A., Pérez, F., (2015). Carta turística Ilha do Fogo. ULPGC-Direcção Nacional do Ambiente.
- Rocha, F., Ferreira, E., 2014. Geotourism, medical geology and local development: Cape Verde case study. *Journal of African Earth Sciences* 99: 735-742. DOI: doi.org/10.1016/j.jafrearsci.2014.04.015.

Identification, cataloguing, and preservation of outcrops of geological interest in monogenetic volcanic fields: the case La Garrotxa volcanoes Natural Park

Llorenç Planaguma¹, Joan Martí², Xavier Bolós³

¹ Environment group, Girona University. Facultat de Lletres, Campus Barri Vell, Plaça Ferrater Mora, 1, 17071 GIRONA. llplanaguma@gmail.com

² Institute of Earth Sciences Jaume Almera, ICTJA, CSIC, Group of Volcanology, Lluís Sole i Sabaris s/n, 08028 Barcelona, Spain.

³ Institute of Geophysics, UNAM, Campus Morelia, 58190 Morelia, Michoacán, Mexico

Keywords: monogenetic eruption, geological heritage, Natural Park

Volcanic zones have complex and interesting stratigraphic relationships (Cas and Wright, 1987), and constitute substantial geoheritage sites. Active volcanic fields have a special value because they are places with volcanism under activity, soil richness, access to points of geological interest, and beautiful landscapes. The combination of these factors imposes the creation of a network of outcrops to help preserving the geological heritage and the social and economic dynamism of the area. In La Garrotxa volcanic field, part of which is included in a Natural Park, a new methodology was created to identify the points of geological interest, particularly those showing the great diversity of eruptive styles present in the area. The volcanic zone of the Garrotxa has about 55 monogenetic volcanoes located in two main zones (Martí et al., 2011; Bolós et al., 2014). Most of them are located in the upper part of the Fluvià River, the rest in the middle-lower basin of the Ter river. The eruptive dynamics of this volcanism is Strombolian to violent Strombolian and effusive. However, more than half of these monogenetic volcanoes present phreatomagmatism, thus giving rise to a great variety of deposit successions that represent diverse eruptive sequences (Martí et al., 2011).

In 1994, a total of 65 outcrops were classified as points of geological interest to interpret the volcanology of the area, taking into account the main management requirements (conservation and dissemination). Therefore, we applied a specific methodology to choose from this total the most suitable sites for preservation and that represent the main features of the volcanism of this area. In this sense, we filtered the total of 65 outcrops identified in the first step and selected a total of 12, which were the most representative in terms of geological and pedagogical values, as well as the easiest for access and preservation.

These 12 selected outcrops showed several problems that had to be considered: The loss of the geomorphology and the visualization of the outcrops (e.g.: craters), by forests, erosion, urbanism, etc.) and the possible impact of the potential visitors to the outcrops (e.g.: erosion, etc.). For this reason, the following criteria were taken into account while restoring these outcrops: integration into the landscape, strengthening of their geology, regulation of the public visitors, landscapes mitigation risk, and partici-

pation of the local community that lives in the area. The preservation and dissemination of the geological outcrops from this Natural Park seek to generate sustainable economic activity, as it is an area surrounded by over 14 million people with potential interest in the volcanic region. This economic activity consists of a wide offer of high quality guided itineraries, also considering the natural local values such as the volcanic cuisine and the small rural hotels.

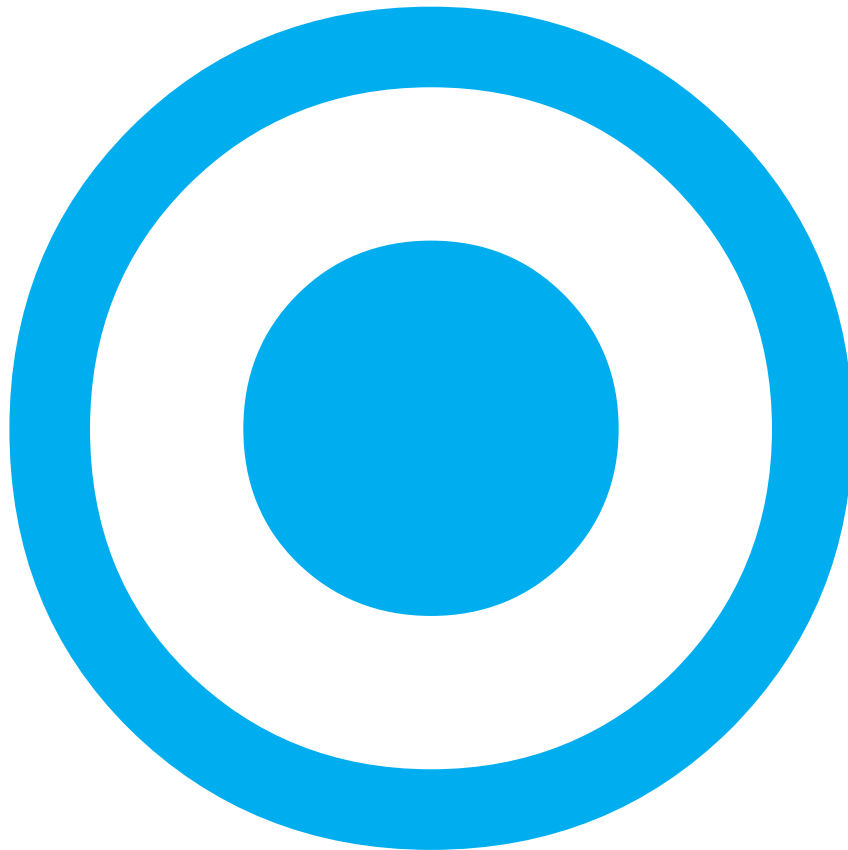


Fig. 1 –Quarry outcrop in the Croscat volcano. This quarry was in operation from the late 1950s to the early 1990s. The quarry on the northern flank of the volcano constitutes an exceptional outcrop that enables us to observe the internal structure of a complex cinder cone including the phreatomagmatic deposits.

References

- Bolós, X., Planagumà, L., Martí, J. 2014. Volcanic stratigraphy of the Quaternary La Garrotxa Volcanic Field (north-east Iberian Peninsula). *J. Quat. Sci.* 29 (6), 547–560.
- Cas R. A. F. & Wright J. V. (eds) 1987. *Volcanic Successions. Modern and Ancient*, xviii + 528 pp. London, Boston, Sydney, Wellington: Allen & Unwin.
- Martí, J., Planagumà, L., Geyer, A., Canal, E., Pedrazzi, D., 2011. Complex interaction between Strombolian and phreatomagmatic eruptions in the Quaternary monogenetic volcanism of the Catalan Volcanic Zone (NE of Spain). *Journal of Volcanology and Geothermal Research* 201, 178–193

7th international
MAAR **C**ONFERENCE



MAY 21 to 25, 2018

OLOT - CATALONIA - SPAIN

